



# Iron, manganese and rhenium-catalyzed (de)hydrogenation and hydroelementation reactions

Duo Wei

## ► To cite this version:

Duo Wei. Iron, manganese and rhenium-catalyzed (de)hydrogenation and hydroelementation reactions. Catalysis. Université de Rennes, 2019. English. NNT : 2019REN1S105 . tel-03510162

**HAL Id: tel-03510162**

**<https://theses.hal.science/tel-03510162>**

Submitted on 4 Jan 2022

**HAL** is a multi-disciplinary open access archive for the deposit and dissemination of scientific research documents, whether they are published or not. The documents may come from teaching and research institutions in France or abroad, or from public or private research centers.

L'archive ouverte pluridisciplinaire **HAL**, est destinée au dépôt et à la diffusion de documents scientifiques de niveau recherche, publiés ou non, émanant des établissements d'enseignement et de recherche français ou étrangers, des laboratoires publics ou privés.

# THESE DE DOCTORAT DE

L'UNIVERSITE DE RENNES 1  
COMUE UNIVERSITE BRETAGNE LOIRE

ECOLE DOCTORALE N° 596  
*Matière Molécules et Matériaux*  
Spécialité : Chimie Moléculaire et Macromoléculaire

Par

**Duo WEI**

## Iron, Manganese and Rhenium-Catalyzed (De)Hydrogenation and Hydroelementation Reactions

Thèse présentée et soutenue à Rennes, le 10 Septembre 2019

Unité de recherche : UMR 6226, CNRS, Université de Rennes 1, Institut des Sciences Chimiques de Rennes

### Rapporteurs avant soutenance :

**Marine DESAGE-EL MURR**  
Professeur, Université de Strasbourg (France)

**Marc PETIT**  
Directeur de Recherche, CNRS,  
Sorbonne Université (France)

### Composition du Jury :

**Jeanne CRASSOUS**  
Directeur de Recherche, CNRS  
Université de Rennes 1 (France)

**Marine DESAGE-EL MURR**  
Professeur, Université de Strasbourg (France)

**Matthias BELLER**  
Professeur, Leibniz-Institut für Katalyse  
Rostock (Germany)

**Marc PETIT**  
Directeur de Recherche, CNRS  
Sorbonne Université (France)

**Christophe DARCEL**  
Professeur, Université de Rennes 1 (France)  
Directeur de thèse

**Jean-Baptiste SORTAIS**  
Professeur, Université Paul Sabatier Toulouse 3 (France)  
Co-directeur de thèse



## *Acknowledgements*

Five years have passed away since my first step in Rennes and I have spent a wonderful life here for the diplomas in Master and also PhD. And the following work presented in this thesis was mainly realized in the team of “Organometallics: Materials and Catalysis (OMC)”, UMR 6226 CNRS-Université de Rennes 1, Institut des Sciences Chimiques de Rennes (ISCR), between Oct. 2016 and Sep. 2019. Part of those work was accomplished in the team of “Molecular design of transition-metal pre-catalysts”, Laboratoire de Chimie de Coordination (LCC), CNRS, Université Paul Sabatier Toulouse 3, between Apr. 2018 and Jun. 2018.

First of all, I would like to express my sincere gratefulness to my two respected PhD and also Master supervisors: *Prof.* Christophe Darcel and *Prof.* Jean-Baptiste Sortais, from whom I benefit a lot, in not only the chemical reasearch but also my daily life. They shared a lot of enthusiasm and knowledge of chemistry to me. They are always encouraging me to explore diverse aspects of chemistry and inspiring me when I was in my dark despair at times. It was also my great pleasure to work with supervisors who has great personality. Without their strong support, practical advice and critical opinions, I am not able to finish my thesis.

Meanwhile, I would like to acknowledge *Dr.* Christian Bruneau, the head of the Centre for catalysis and green chemistry, and *Prof.* Pierre H. Dixneuf, for accepting me as master student to the brilliant CatGreenChem program, “The International Master in Molecular Catalysis and Green Chemistry” in 2014, and *Prof.* Xiao-Feng Wu, *Prof.* Chuan-Ying Li (Zhejiang Sci-Tech University), who encourage and help me to join this master program. Thanks to all of them, I could have the opportunity to meet the well-known chemists in the world, and their spirits in persisting in and discovering chemistry, encourage me all the time and will motivate me forever.

Next, I would like to extend my appreciation to the jury members: *Dr.* Jeanne Crassous, *Prof.* Marine Desage-El Murr, *Prof.* Matthias Beller and *Dr.* Marc Petit, and thank them for spending their valuable time in evaluating my thesis. Even more thanks to the rapporteurs *Prof.* Marine Desage-El Murr and *Dr.* Marc Petit for the time they spent on reading and estimating this manuscript.

Then, I would like to extend my thanks to *Prof.* Matthias Beller and *Dr.* Ralf Jackstell in Leibniz-Institut für Katalyse e. V. (LIKAT), Universität Rostock via “LIA CHEMSUSCAT Germany, 2013-2020, Catalysis for Sustainable Chemistry” program, and thanks to *Prof.* Jean-Baptiste Sortais and *Dr.* Noël Lugan in Laboratoire de Chimie de Coordination (LCC), CNRS,



Université Paul Sabatier Toulouse 3, for providing me the chances to perform the short-term scientific communication. It was really my pleasure to stay in new groups for learning new techniques and also expanding my horizon.

After, I would like to give my thanks to *Dr. Cédric Fischmeister*, *Dr. Henri Doucet*, *Dr. Jean-François Soulé*, *Dr. Rafael Gramage-Doria*, *Dr. Mathieu Achard*, and *Dr. Sylvie Derien* in the team at Rennes, for their great instruction and useful help in my research during the past five years.

In the meantime, I would like to take this opportunity to thank *Prof. Dominique Lorcy*, *Prof. Muriel Hissler*, *Dr. Véronique Guerschais*, *Dr. Florence Geneste*, *Dr. Sophie Guillaume*, *Dr. Lucie Norel*, *Prof. Christophe Darcel*, *Prof. Jean-François Carpentier*, *Dr. Cédric Fischmeister*, *Dr. Jean-François Soulé*, *Prof. Jean-Pierre Bazureau*, *Dr. Jean-Luc Fillaut*, *Dr. Evgueni Kirillov*, *Dr. Yann Sarazin*, and *Prof. Stéphane Rigaut* for their innovative, inspirational and informative teaching during my master and PhD study. Besides, I always feel fortunate to get help from Mrs. Béatrice Mahi, Mrs. Françoise Toupet, Mrs. Anne Tonn and Mrs. Nicole Aulerich, and I would like to give them my cordial gratefulness for those important secretarial work.

It is also my pleasure to thank *Dr. Thierry Roisnel* and *Dr. Vincent Dorcet* (X-Ray diffraction analysis, Université de Rennes 1), *Dr. Muriel Escadeillas* (elemental analysis, CRMPO, Université de Rennes 1), Bertrand Lefeuvre (ICP-OES analysis, Université de Rennes 1). *Dr. Bertrand Carboni* (collaboration intergroup of ISCR), Clément Orionne, *Dr. Elsa Caytan* (NMR service at Rennes), Francis Lacassin, David Paryl (NMR service at Toulouse), Philippe Jéhan, Fabian Lambert (HR-MS analysis at Rennes) and collaboration with *Dr. Eric Clot* (Université de Montpellier), *Dr. Mary Grellier* (LCC, Université Paul Sabatier Toulouse 3), *Dr. Tomoya Ichino*, *Dr. Satoshi Maeda* (Hokkaido University) for DFT calculations.

During 3 months in Toulouse, I also met those researchers: *Dr. Vincent Caesar*, *Dr. Yves Canac*, *Dr. Stephanie Bastin* and *Dr. Dmitry Valyaev*, who are excellent specialists in organometallic chemistry. They are always kind to me, gave me support and usefull talk.

Additionally, I feel very lucky to work with these team members at Rennes: *Dr. Antoine Bruneau-Voisine*, Haoran Li, Ding Wang, Chakkrit Netkaew, *Dr. Jianxia Zheng*, *Dr. Shi Jiang*, Victor Carré, Téo Chauvin, *Dr. Saravanakumar Elangovan*, *Dr. Linus P. Bheeter*, *Dr. Thomas Dombray*, and lab mates: *Dr. Apurba Sahoo*, Hortense Lauwick, Arpan Sasmal, *Dr. Imane*

Idriss, *Dr. Aymen Skhiri, Dr. Meriem Abderrezak, Dr. Paolo Zardi, Julien Hervochon, Katharina Hoff.* At Toulouse: Ruqaya Buhaibeh, Lenka Pallova, Idir Benaissa, Rachid Taakili, Karim Azouzi, Maxime Dubois. At Rostock: *Dr. Jiawang Liu, Rui Sang, Ji Yang, Dr. Deepika Tyagi, Dr. Baoxin Zhang, Dr. Weiping Liu, Xin Liu, Dr. Zechao Wang, Dr. Zhiping Yin, Shaoke Zhang,* I would like to thank all of them for their daily help in the lab and also in my life.

Furthermore, I feel very happy to be friends with the Chinese students team at Rennes: *Dr. Fan Jiang, Dr. Liqin Zhao, Dr. Chenshuo Shen, Dr. Kedong Yuan, Dr. Min Feng, Dr. Xiaoyan He, Dr. Wenyan He, Dr. Xiaolu Ma, Dr. Jiangkun Ouyang, Dr. Feng Yu, Dr. Xiang Liu, Dr. Xu Zhang, Dr. Shengdong Wang, Dr. Chang-Sheng Wang, Yuchao Yuan, Mian He, Yuya Hu, Rui Sang, Jingran Hou, Hong Zhao, Haiyun Huang, Shuxin Mao, Yixuan Cao, Weiheng Huang, Yaoying Lou, Xiaoping Liu, Shizheng Wu, Limiao Shi, Dr. Xingbao Wang, Zijun Xu* and I would like to thank all of them for their comfort and support during my difficult time.

I would like to thank also the Université de Rennes 1 for giving me a “Allocation doctorale” fellowship for my PhD project.

Last but not least, I would like to attribute my immerse gratefulness to my family members: my parents, my sister, and my beloved wife Xinzhe Shi who are always standing beside me and giving me support all the time all the way, and to all of whom I shall always be ready to devote myself.

路漫漫其修远兮，吾将上下而求索。

The road ahead will be long, I shall search high and low.

June, 2019, Rennes



# Table of contents

<b>General Introduction .....</b>	<b>9</b>
<b>Chapter I - General Introduction on Fe-Catalyzed Reductions .....</b>	<b>15</b>
1. Introduction.....	15
2. Hydrogenation and transfer hydrogenation .....	16
2.1. Carbonyl derivatives.....	16
2.2. Imines and reductive amination of carbonyl compounds .....	27
2.3. Carboxylic acid derivatives and carbon dioxide .....	32
3. Hydrosilylation .....	42
3.1. Aldehydes and ketones .....	42
3.2. Imines .....	55
3.3. Hydrosilylation of carboxylic acid derivatives .....	57
4. Hydrogen borrowing reactions .....	62
5. Hydroboration.....	66
5.1. Hydroboration of alkenes and alkynes.....	66
5.2. Dehydrogenative borylation .....	73
6. Conclusion of Chapter I.....	73
7. References.....	75
<b>Chapter II – Fe-Catalyzed Dehydrogenative Borylation Reactions.....</b>	<b>85</b>
Introduction.....	85
II-1 Fe-Catalyzed dehydrogenative borylation of styrenes.....	87
1.1. Introduction .....	87
1.2. Results and discussions .....	88
1.3. Mechanistic insights .....	91
1.4. Conclusion.....	103
II-2 Fe-Catalyzed dehydrogenative borylation of terminal alkynes .....	105
2.1. Results and discussions .....	105
2.2. Mechanistic insights .....	110
2.3. Conclusion.....	112
II-3 Conclusion of Chapter II.....	113
II-4 References.....	114
II-5 Experimental data .....	117
<b>Chapter III - Hydrosilylation Reactions .....</b>	<b>129</b>
Part 1 - Synthesis of cyclic amines <i>via</i> iron-catalyzed hydrosilylation .....	129
Introduction.....	129
III-1 Reductive amination of keto acids derivatives with hydrosilanes catalyzed by Fe-NHC complexes .....	131
1.1. Introduction .....	131
1.2. Results and discussions .....	133
1.3. Mechanistic studies.....	139
1.4. Conclusion.....	139
III-2 Reductive amination of carbonyl derivatives with $\omega$ -amino fatty acids catalyzed by $\text{Fe}(\text{CO})_4(\text{IMes})$ .....	141
2.1. Introduction .....	141

2.2. Results and discussions .....	142
2.3. Mechanistic insights .....	147
2.4. Conclusion.....	151
III-3 Hydrosilylation of diacids in the presence of amines catalyzed by $\text{Fe}(\text{CO})_4(\text{IMes})$ .....	153
3.1. Introduction .....	153
3.2. Results and discussions .....	154
3.3. Mechanistic insights .....	158
3.4. Conclusion.....	158
III-4 Conclusion of the Part 1 dedicated to synthesis of cyclic amines <i>via</i> iron-catalyzed hydrosilylation .....	159
III-5 References .....	160
III-6 Experimental data.....	163
Part 2 – Hydrosilylation catalyzed by Group 7 metal complexes.....	191
III-7 Hydrosilylation of carboxylic acids, esters and amides catalyzed by $\text{Mn}_2(\text{CO})_{10}$ and $\text{Re}_2(\text{CO})_{10}$ .....	191
7.1. Introduction .....	191
7.2. Hydrosilylation reactions catalyzed by manganese and rhenium complexes: a literature survey. ....	191
7.3. Results and discussions .....	208
7.4. Mechanistic insights .....	216
7.5. Conclusion of the Part 2 dedicated to $\text{Mn}_2(\text{CO})_{10}$ and $\text{Re}_2(\text{CO})_{10}$ catalyzed hydrosilylation of carboxylic acids, esters and amides.....	219
7.6. References .....	220
7.7. Experimental data .....	222
<b>Chapter IV - (Transfer)Hydrogenation Reactions Catalyzed by Mn(I) Bidentate Complexes.....</b>	<b>235</b>
Introduction.....	235
IV-1 Hydrogenation of carbonyl derivatives catalyzed by bidentate Mn complexes.....	237
1.1. Results and discussions .....	237
1.2. Conclusion.....	242
IV-2 Reductive amination of aldehydes with $\text{H}_2$ catalyzed by bidentate Mn complexes .....	245
2.1. Introduction .....	245
2.2. Results and discussions .....	245
2.3. Conclusion.....	251
IV-3 Transfer hydrogenation of aldimines catalyzed by bidentate Mn complexes .....	253
3.1. Introduction .....	253
3.2. Results and discussions .....	254
3.3. Mechanistic insights .....	258
3.4. Conclusion.....	259
IV-4 Conclusion of Chapter IV .....	260
IV-5 References .....	261
IV-6 Experimental data.....	263
<b>Chapter V - (De)Hydrogenative Synthesis Catalyzed by Rhenium .....</b>	<b>295</b>
Introduction.....	295
V-1 Hydrogenation of carbonyl derivatives catalyzed by Re PN(H)P complexes .....	299
1.1. Results and discussions .....	299
1.2. Mechanistic insights .....	305
1.3. Conclusion.....	308
V-2 Mono <i>N</i> -methylation of anilines with methanol catalyzed by Re PN(H)P complexes.....	309

2.1. Introduction .....	309
2.2. Results and discussions .....	309
2.3. Mechanistic insights .....	312
2.4. Conclusion.....	318
V-3 Synthesis of quinolines through acceptorless dehydrogenative coupling catalyzed by Re PN(H)P complexes .....	319
3.1. Introduction .....	319
3.2. Results and discussions .....	319
3.3. Conclusion.....	325
V-4 Conclusion of Chapter V .....	326
V-5 References .....	327
V-6 Experimental data .....	332
<b>Chapter VI - Mn-Catalyzed Imine and N-Heteroaromatic Compounds Synthesis via Aerobic Oxidation of Amines.....</b>	<b>371</b>
1. Introduction.....	371
2. Results and discussions.....	372
3. Mechanistic insights .....	383
4. Conclusion of Chapter VI.....	385
5. References.....	386
6. Experimental data .....	389
<b>General Conclusion.....</b>	<b>401</b>
<b>Annex .....</b>	<b>405</b>
List of publications .....	405



## General Introduction

Nowadays, catalysis is the key technology for the synthesis of molecular materials, organic building blocks, fine chemicals, natural products, pharmaceuticals and all kinds of bio-active compounds.<sup>[1]</sup> In general, by the use of catalysts, chemical reactions can be conducted in a safer, more efficient, and environmentally benign manner. Most importantly, catalysts may permit to control the selectivity of a given reaction usually under milder reaction conditions. Furthermore, improved cost-effective and more environmentally benign chemical synthesis will rely on the continuing development of new and more efficient catalyst systems.

In the past few decades, due to their importance especially in pharmaceuticals, much effort has been devoted to the development of the eco-designed catalytic processes for the production of fine chemicals such as alcohols, amines, or *N*-heteroaromatics *via* hydrogenation, transfer hydrogenation, hydrosilylation of the corresponding unsaturated compounds.

Hydrogenation with molecular dihydrogen is a clean, atom-economic and efficient reaction that has drawn a huge interest for more than a century from the Nobel Prize of Sabatier in 1912 for heterogeneous hydrogenation of fatty acid derivatives to the one of Noyori and Knowles in 2001 for asymmetric homogeneous hydrogenation.<sup>[2]</sup> In addition to hydrogenation reactions performed with gaseous hydrogen in appropriate high pressure apparatus, transfer hydrogenation reactions are conducted using easy-to-handle and cheap liquid hydrogen donors such as alcohols and formic acid without special equipment, being thus helpful alternative procedures for the reduction of unsaturated compounds.<sup>[3]</sup> Homogeneous (transfer)hydrogenation catalysts are usually complexes based on late transition metals including ruthenium, rhodium, iridium, palladium and nickel.

Additionally, in reduction area, hydrosilylation<sup>[4]</sup> is another promising alternative for the selective catalytic transformation of organic molecules compared to (transfer)hydrogenation reactions, or the stoichiometric reduction with metal hydrides<sup>[5]</sup> (e.g. aluminium and boron hydride reagents). Thus, the use of hydrosilanes is often interesting owing to its operational simplicity, mild conditions and excellent chemoselectivity notably towards reducible functional groups. Therefore, hydrosilanes can be considered as interesting alternative reductants, even if they produced *in fine* wastes.

Among hydroelementation reactions, (dehydrogenative)hydroboration is one of the most important and efficient methods to prepare alkyl boronic esters which are valuable boron derivatives, widely used in both Suzuki-Miyaura cross-coupling<sup>[6]</sup> and Petasis reactions.<sup>[7]</sup>



On the other hand, there is still less attention devoted to the earth-abundant, low cost and eco-friendly metals in comparison to noble ones. Nevertheless, homogeneous catalysis based on non-noble metals has drawn a huge attention during the last few decades as it offers an abundant, cheap and low-toxic alternative to noble-metal catalysts. Iron, as one of the most abundant and inexpensive transition metals on the Earth, has emerged as a powerful sustainable alternative candidate, notably in catalyzed reduction reactions.<sup>[8]</sup> Actually, the level of the activity, and chemo- and enantio-selectivities obtained by iron catalytic systems can be now compared to the ones involving noble transition metals.

Furthermore, manganese is ranking the third most abundant transition metals after iron and titanium, and has tremendous potential applications in organic synthesis, on account of its numerous oxidation states (-III to +VII). Traditionally, high-valence manganese compounds, represented by  $\text{KMnO}_4$ , are widely used in oxidation reactions. Moreover, in the beginning of this 21<sup>st</sup> century, manganese has been brought to people's attention for catalytic applications. More particularly, until 2016 and the beginning of this PhD thesis, it was scarcely used in catalytic hydrogenation and hydrogen transfer. Nevertheless, since few years, a huge international competition permitted to demonstrate that it can be a suitable transition metal for the design of efficient hydrogenation and hydrogen borrowing catalysts.<sup>[9]</sup> In line with our interest in developing group 7 metals based catalysts for reduction reactions, the well-defined rhenium catalysts for (de)hydrogenative synthesis will be also targeted in this work.

The aim of this PhD work is the use of earth abundant metals such as iron and manganese, and its related Group 7 rhenium in hydrogenation, hydrogen transfer, hydrogen borrowing, hydrosilylation and (dehydrogenative)borylation reactions. The thesis is thus structured into six chapters and each chapter mainly focus on one type of reaction.

The **Chapter I** gives a general introduction on iron catalyzed reduction reactions.

The **Chapter II** describes emerging dehydrogenative borylation reactions, notably the highly selective catalytic direct C-H borylation of styrene derivatives and terminal alkynes with pinacolborane, using  $\text{Fe}(\text{PMe}_3)_4$  and  $\text{Fe}(\text{OTf})_2/\text{DABCO}$  catalytic systems, respectively.

The **Chapter III** will be dedicated to hydrosilylation reactions. It first reports *N*-heterocyclic carbene (NHC) based iron complexes  $\text{Fe}(\text{CO})_4(\text{IMes})$  and  $[\text{CpFe}(\text{CO})_2(\text{IMes})][\text{I}]$  able to efficiently catalyze the catalytic reductive amination reactions with hydrosilanes to access cyclic amines. In a second part, using commercially available  $\text{Mn}_2(\text{CO})_{10}$  and  $\text{Re}_2(\text{CO})_{10}$  as

catalysts and Et<sub>3</sub>SiH as hydrosilane, the reduction of carboxylic acids, esters and amides can be achieved chemo-specifically.

The **Chapter IV** highlights the application of a series of well-defined manganese pre-catalysts featuring readily available bidentate pyridinyl-phosphine and 2-picolylamine ligands in efficient hydrogenation reactions.

The **Chapter V** demonstrates that a series of rhenium pincer catalysts bearing amino-bisphosphino ligands can efficiently promote the hydrogenation of carbonyl derivatives and the selective mono *N*-methylation of anilines with methanol *via* hydrogen borrowing process. Furthermore, acceptorless dehydrogenative synthesis of substituted quinolines can be also performed using such catalysts.

Finally, the **Chapter IV** is devoted to the development of a Mn-catalyzed ligand- and additive-free aerobic oxidation of amines to prepare aldimines, *N*-heteroaromatics and benzoimidazole derivatives.

## References

- [1] P. W. N. M. van Leeuwen, *Homogeneous Catalysis: Understanding the Art*, Kluwer Academic Publishers, **2004**.
- [2] J. G. de Vries, C. J. Elsevier, *The Handbook of Homogeneous Hydrogenation*, Wiley-VCH, Weinheim, **2007**.
- [3] a) K. Sordakis, C. Tang, L. K. Vogt, H. Junge, P. J. Dyson, M. Beller, G. Laurenczy, *Chem. Rev.* **2018**, *118*, 372-433; b) G. Brieger, T. J. Nestruck, *Chem. Rev.* **1974**, *74*, 567-580; c) R. Noyori, S. Hashiguchi, *Acc. Chem. Res.* **1997**, *30*, 97-102; d) A. Matsunami, Y. Kayaki, *Tetrahedron Lett.* **2018**, *59*, 504-513; e) G. Guillena, D. J. Ramón, *Hydrogen Transfer Reactions*, Springer, **2016**.
- [4] I. Ojima, Z. Li, J. Zhu, *Recent Advances in the Hydrosilylation and Related Reactions in The Chemistry of Organic Silicon Compounds* (Eds.: Z. Rappoport, Y. Apeloig), **2003**, pp. 1687-1792.
- [5] G. W. Gribble, *Chem. Soc. Rev.* **1998**, *27*, 395-404.
- [6] D. G. Hall, *Boronic Acids: Preparation and Applications in Organic Synthesis, Medicine and Materials*, 2nd ed., Wiley-VCH, Weinheim, **2011**.
- [7] N. R. Candeias, F. Montalbano, P. M. S. D. Cal, P. M. P. Gois, *Chem. Rev.* **2010**, *110*, 6169-6193.
- [8] a) C. Bolm, J. Legros, J. Le Pailh, L. Zani, *Chem. Rev.* **2004**, *104*, 6217-6254; b) B. Plietker, *Iron Catalysis in Organic Chemistry: Reactions and Applications*, Wiley-VCH, Weinheim, **2008**; c) K. Junge, K. Schröder, M. Beller, *Chem. Commun.* **2011**, *47*, 4849-4859; d) R. M. Bullock, *Science* **2013**, *342*, 1054-1055; e) I. Bauer, H.-J. Knölker, *Chem. Rev.* **2015**, *115*, 3170-3387; f) A. Glüer, S. Schneider, *J. Organomet. Chem.* **2018**, *861*, 159-173; g) D. Wei, C. Darcel, *Chem. Rev.* **2019**, *119*, 2550-2610; h) L. Alig, M. Fritz, S. Schneider, *Chem. Rev.* **2019**, *119*, 2681-2751; i) D. Wei, C. Netkaew, C. Darcel, *Eur. J. Inorg. Chem.* **2019**, 2471-2487.
- [9] a) R. I. Khusnutdinov, A. R. Bayguzina, U. M. Dzhemilev, *Russ. J. Org. Chem.* **2012**, *48*, 309-348; b) D. A. Valyaev, G. Lavigne, N. Lugan, *Coord. Chem. Rev.* **2016**, *308*, 191-235; c) M. Garbe, K. Junge, M. Beller, *Eur. J. Org. Chem.* **2017**, 4344-4362; d) B. Maji, M. K. Barman, *Synthesis* **2017**, *49*, 3377-3393; e) F. Kallmeier, R. Kempe, *Angew. Chem. Int. Ed.* **2018**, *57*, 46-60; f) N. Gorgas, K. Kirchner, *Acc. Chem. Res.* **2018**, *51*, 1558-1569; g) G. A. Filonenko, R. van Putten, E. J. M. Hensen, E. A. Pidko, *Chem. Soc. Rev.* **2018**, *47*, 1459-1483; h) T. Zell, R. Langer, *ChemCatChem* **2018**, *10*, 1930-1940.

## **Chapter I - General Introduction on Fe-Catalyzed Reductions**



## Chapter I - General Introduction on Fe-Catalyzed Reductions

**Contributions in this part:** Literature survey: Duo Wei.

**Adapted from publication:** D. Wei, C. Darcel, *Chem. Rev.*, **2019**, 119, 2550-2610;

D. Wei, C. Netkaew, C. Darcel, *Eur. J. Inorg. Chem.*, **2019**, 20, 2471-2487.

### 1. Introduction

The development of more efficient and sustainable methodologies for the construction of diversely functionalized molecules using homogeneous transition-metal catalysis is nowadays a cornerstone in green chemistry, mainly explained by the outstanding regio-, chemo- and stereoselectivity observed. Indeed, regarding the current important concerns about climate changes and the associated green chemistry principles, the replacement of noble transition metals by more benign ones, such as the first row transition metals is absolutely required and is definitively one of the important challenges of the beginning of this millennium. Thus, the beginning of the 21<sup>st</sup> century has witnessed an interest in the use of iron in homogeneous catalysis which is a highly valuable alternative to classical precious metals such as platinum, rhodium or palladium for catalyzing a wide range of organic transformations, including the efficient and chemoselective reduction processes and hydrofunctionalization of unsaturated C-C or C-heteroatom bonds.<sup>[1]</sup>

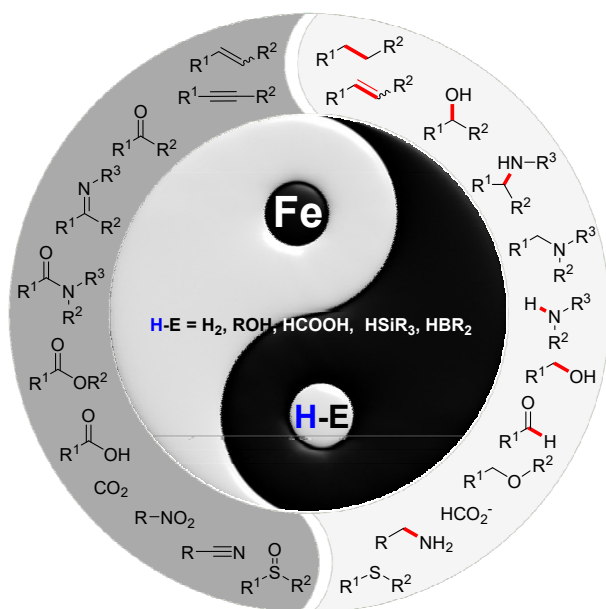


**Figure 1.** Iron catalysis in reduction and hydrometalation reactions.

Although this area of research is now well established, it is amazing that until recently, there were only scarce examples of large-scale applications of iron catalysts, such as the classical

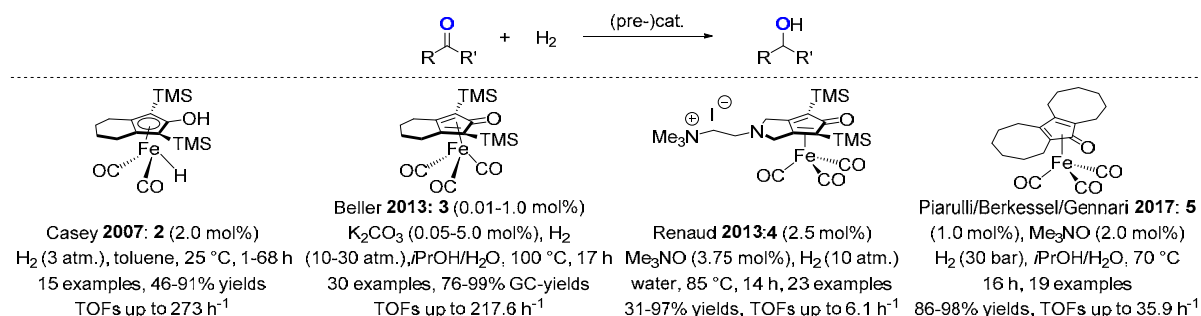
Fischer-Tropsch and Haber-Bosch processes. Thus, the development of new efficient catalytic systems is still attractive and necessary for both academic and industrial applications. Several reviews have treated iron-catalyzed transformations<sup>[2]</sup>, and reduction<sup>[1a, 1b, 3]</sup> in the last decade. In addition, numerous reviews, book chapters, and accounts have been published focusing on thematic aspects of iron catalysis such as hydrogenation,<sup>[4]</sup> and hydrofunctionalization<sup>[5]</sup>. This chapter will summarize the use of iron in hydrogenation, transfer hydrogenation, and hydrosilylation of carbonyl derivatives, imines and carboxylic derivatives. It will also focus on hydroboration and dehydroboration of alkynes and alkenes.

## 2. Hydrogenation and transfer hydrogenation

### 2.1. Carbonyl derivatives

#### 2.1.1. Hydrogenation of aldehydes and ketones.

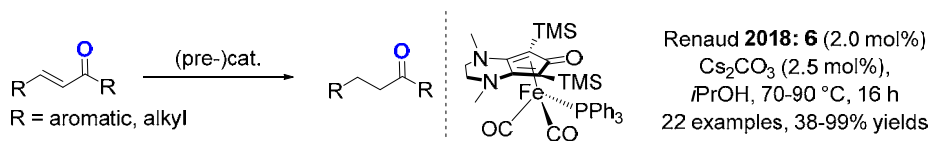
Selective hydrogenation and hydrogen transfer reactions of carbonyl derivatives (aldehydes and ketones) are relevant transformations in both bulk and fine chemistry. For a few decades, there is an increasing interest in an economic and sustainable point of view in the replacement of expensive noble transition-metal catalysts with iron-based ones. In 1983, Markó described the first pioneering report on iron-catalyzed hydrogenation of aldehydes and ketones using 10 mol% of  $\text{Fe}(\text{CO})_5$  (**1**)<sup>[6]</sup> under drastic conditions [triethylamine, at 150 °C under 100 bar of a mixture  $\text{H}_2/\text{CO}$  (98.5/1.5)]. In 2007, Casey<sup>[7]</sup> reported the use of the Knölker complex **2**<sup>[8]</sup> as the catalyst to perform one of the first valuable iron-catalyzed hydrogenation of aldehydes and ketones under mild conditions (3 atm of  $\text{H}_2$  at r.t. for 1–68 h) with TOF up to 273  $\text{h}^{-1}$  (Scheme 1). Noteworthy,  $\text{C}=\text{C}$  and  $\text{C}\equiv\text{C}$  located remotely from the carbonyl were tolerated and unsaturated alcohols were selectively obtained whereas the reduction of  $\alpha,\beta$ -unsaturated ketones led to a mixture of compounds due to the reduction of both the  $\text{C}=\text{O}$  and/or the  $\text{C}=\text{C}$  bond after 6 days. Additionally, **2** can also catalyze the transfer hydrogenation of acetophenone using 2-propanol as the hydrogen donor (87 % isolated yield using 1.0 mol% of catalyst at 75 °C in 16 h).



**Scheme 1.** Knölker type complexes for the hydrogenation of ketones.

Beller *et al.*<sup>[9]</sup> used a series of air-stable Knölker type complexes such as **3**<sup>[10]</sup> able to catalyze the hydrogenation of aldehydes and ketones under 30 atm of H<sub>2</sub> at 100 °C in a mixture of *i*PrOH/water (Scheme 1). It must be underlined that the similar efficiency (TOF up to 217 h<sup>-1</sup>) and the nice functional group tolerance as esters, amides and heterocycles remained intact under such conditions. Furthermore,  $\alpha,\beta$ -unsaturated aldehydes were selectively reduced to the corresponding allylic alcohols. **3** was also an efficient catalyst for the reduction of aldehydes under water-gas shift conditions [10 atm of CO, DMSO/water, 100 °C<sup>[11]</sup> or paraformaldehyde (10 equiv.), Na<sub>2</sub>CO<sub>3</sub> (3 equiv.), DMSO/water, 120 °C, 24 h<sup>[12]</sup>].

Renaud simultaneously designed Knölker type complexes bearing ionic fragments such as ammonium salts **4**<sup>[13]</sup> which were active in the catalytic hydrogenation of carbonyl derivatives in water under 10 atm of H<sub>2</sub> at 85 °C, even if the efficiency decreased as TOF up to 6.1 h<sup>-1</sup> were observed (Scheme 1). Even if cyano moieties were tolerated, by contrast, the hydrogenation of  $\alpha,\beta$ -unsaturated ketones led in the majority of the cases to a mixture of compounds resulting of simultaneous reduction of the C=C and C=O bonds. Additionally, the hydrogenation of C=N bonds of water-soluble imines was also performed in water at 100 °C leading to the corresponding amines with 61–98% isolated yields.



**Scheme 2.** Knölker type complexes for the reduction of  $\alpha,\beta$ -unsaturated ketones.

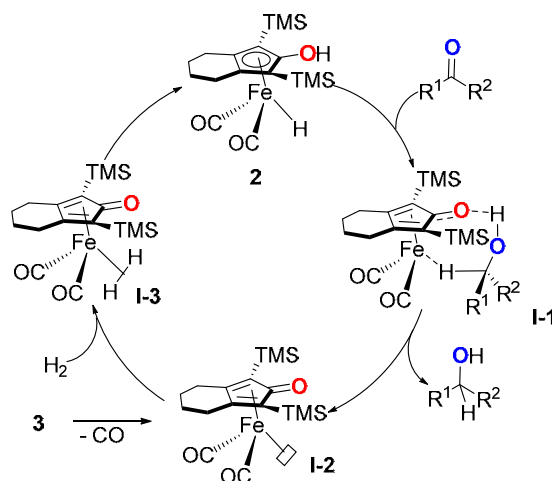
Noticeably, in 2018, the same authors have shown that the nature of the catalytic system have drastic effects on the chemoselectivity of the reduction of  $\alpha,\beta$ -unsaturated ketones into saturated ketones using similar iron complexes. Indeed, using 2.0 mol% of **6** in isopropanol at 70 °C for 16 h in the presence of 2.5 mol% of Cs<sub>2</sub>CO<sub>3</sub>, aromatic unsaturated ketones Ar-CO-C=C-Ar (11 examples, 48–99% yields) (Scheme 2). To promote the reaction with aliphatic unsaturated ketones R-CO-C=C-R, the reaction has to be conducted at 90 °C (11 examples including steroidal derivatives, 38–99% yields).<sup>[14]</sup>

In 2017, Piarulli, Berkessel and Gennari reported the preparation of new [bis(hexamethylene)cyclopentadienone]iron tricarbonyl (**5**) by the reaction of cyclooctyne with [Fe(CO)<sub>5</sub>] (**1**) and showed that upon *in situ* activation with Me<sub>3</sub>NO (2.0 mol%), **5** (1.0 mol%) promoted the catalytic hydrogenation of various ketones and aldehydes at 70 °C under 30 bar of H<sub>2</sub> in a mixture *i*PrOH/H<sub>2</sub>O (5:2) (Scheme 1). Noticeably, **5** exhibited better TOF than the Knölker parent complex **3** under similar conditions (35.9 vs 7.5 h<sup>-1</sup>).<sup>[15]</sup> Interestingly **5** can also



reduce activated trifluoromethyl esters as well as catalyzing the transfer hydrogenation of ketones.

In order to explain the catalytic transformation, an outer-sphere mechanism was proposed (Scheme 3).<sup>[16]</sup> Based on a concerted hydride/proton transfer from the hydroxyl and the iron hydride to the carbonyl moiety, the species (**I-1**) was obtained. (**I-1**) then led to (**I-2**) and the alcohol. The 16 electron species (**I-2**) could be also generated from **3** by the labelization of CO. Finally, the catalytic active species **2** was reformed by heterolytic H<sub>2</sub> cleavage *via* (**I-3**). This mechanism was supported by Density Functional Theory (DFT) calculations and kinetic studies.<sup>[17]</sup>

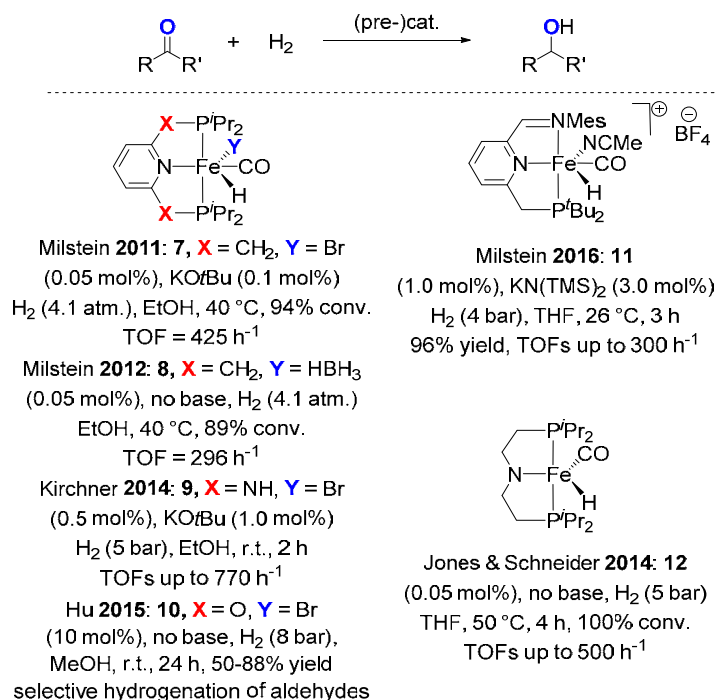


**Scheme 3.** Proposed outer-sphere mechanism for hydrogenation catalyzed by Knölker type catalysts.

In 2011, in the continuation of on his previous work on ruthenium-pincer complexes highlighting an original mode of cooperation ligand-metal center involving aromatization-dearomatization of the ligand,<sup>[18]</sup> Milstein described an elegant contribution on the hydrogenation of ketones catalyzed by a novel iron(II) diphosphino-pyridine pincer complex  $[Fe(Br)(H)(CO)(iPrPNP)]$  (**7**).<sup>[19]</sup> The complex **7** exhibited high activity when the reaction was performed at 40 °C under 4.1 atm of hydrogen in ethanol. 39–97% Conversion, TONs up to 1880 and TOF up to 425 h<sup>-1</sup> were observed for a huge scope of several aromatic and aliphatic ketones (Scheme 4). Noticeably, inhibition of the reaction was observed with cyano, or amino groups and the reduction of  $\alpha,\beta$ -unsaturated ketones was not chemoselective.

Milstein *et al.* also described an iron(II) pincer complex bearing a hydride and a borohydride ligands  $[Fe(\eta^1-BH_4)(H)(CO)(iPrPNP)]$  (**8**) showing catalytic activities comparable to **7** in the hydrogenation of acetophenones, notably with very low catalyst loading (0.05 mol%)<sup>[20]</sup> (Scheme 4). Importantly, the hydrogenation of ketones can be promoted without the use of additional base. The complex **8** is also highly active and exhibited a high TON of 1780 for the

reduction of 2-acetylpyridine in ethanol at 40 °C under 4.1 bar of H<sub>2</sub>. Nevertheless, **8** is less active than the parent complex **7** as the TOF was up to 296 h<sup>-1</sup> (vs 425 h<sup>-1</sup>).

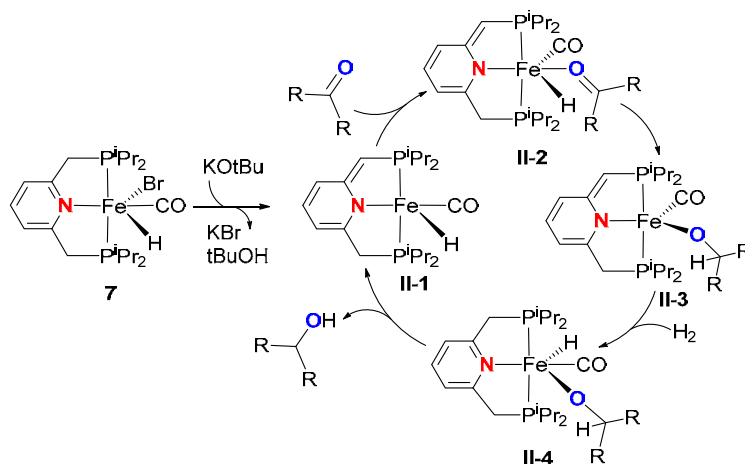


**Scheme 4.** Hydrogenation of ketones catalyzed by iron pincer complexes.

Modifying the backbone and using NH- instead of CH<sub>2</sub>-linkers, Kirchner and co-workers developed a series of complexes such as **9**, which showed rather good activities for the hydrogenation of aldehydes (TOF up to 120 h<sup>-1</sup>) and ketones (0.5 mol% **9**, 1.0 mol% KOtBu, 5 atm H<sub>2</sub>, EtOH, r.t.; TOF up to 770 h<sup>-1</sup>)<sup>[21]</sup> (Scheme 4). Interestingly, the analogous complex bearing a NMe-spacer (X=NMe) led to a drastic loss of activity in ketone hydrogenation activity, but exhibited high activity for the hydrogenation of aldehydes with TON and TOF up to 80000 and 20000 h<sup>-1</sup>, respectively with a very low loading of catalyst (down to 12.5 ppm).<sup>[22]</sup> Notably, this catalyst permitted to perform selective reduction of aldehydes in the presence of ketones, epoxides, and other reducible groups. Noticeably, Kirchner then reported a supported ionic-liquid-phase (SILP) system containing this analogous complex bearing a NMe-spacer used as catalyst in the hydrogenation of aldehydes to alcohols.<sup>[23]</sup> This SILP catalyst was used with low loadings (0.1–0.05 mol%) at 25 °C under 50 bar of hydrogen in heptane in the presence of 5.0 mol% of DBU exhibiting TONs and TOFs of up to 1000 and 4000 h<sup>-1</sup>, respectively. No significant leaching of both the complex and the IL was detected.

In a similar fashion, Hu developed 2,6-bis-(phosphinito)pyridine iron pincer complexes such as **10** as a catalyst (10 mol%) able to selectively hydrogenate aldehydes with 60–90% yields

under 8 bar of H<sub>2</sub> in methanol at r.t. for 24 h<sup>[24]</sup> (Scheme 4). Noticeably, the hydrogenation was accelerated when using 10 mol% of sodium formate as an additive and 5.0 mol% of **10**. Furthermore, it has been shown that the pincer phosphino(imino)pyridine complex **11**<sup>[25]</sup> catalyzed the hydrogenation of ketones at r.t. under 4 atm of H<sub>2</sub> in the presence of a catalytic amount of base with good activities (TOF up to 300 h<sup>-1</sup>, Scheme 4). Jones and Schneider also described an active hydride amido pincer iron complex **12** able to efficiently catalyze the reduction of ketones without an additional base (TOF up to 500 h<sup>-1</sup>)<sup>[26]</sup> (Scheme 4).

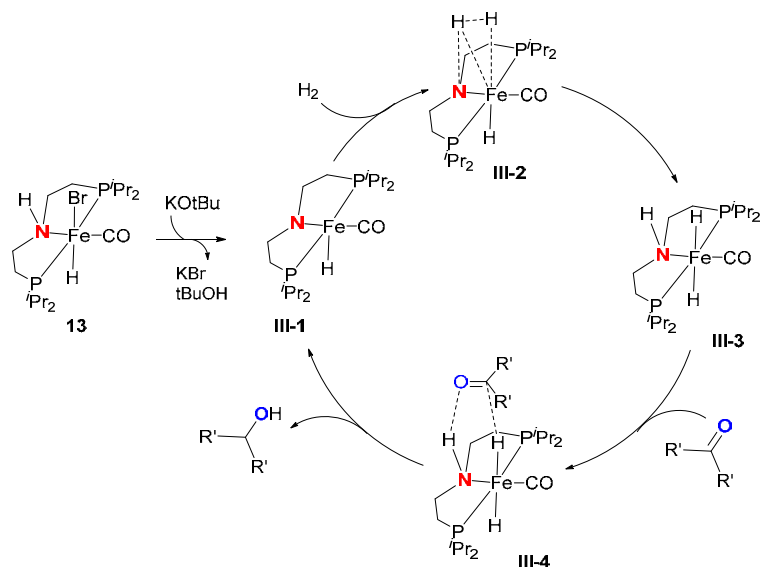


**Scheme 5.** Proposed mechanism for the hydrogenation of ketones catalyzed by diphosphine pyridine iron complexes.

To rationalize the effect of such PNP ligands on the high reactivity of the corresponding iron complexes in hydrogenation, a first plausible mechanism *via* an aromatization-dearomatization process of the diphosphine pyridine ligand, which assisted the activation of dihydrogen in a synergistic metal-ligand fashion was illustrated with the complex **7** (Scheme 5).<sup>[27]</sup> A reactive, dearomatized species (**II-1**) was first produced by action of KO*t*Bu and then coordinated the carbonyl generating the intermediate (**II-2**). Noteworthy the use of *tert*-butoxide is an interesting and general activation pathway of iron halides in order to generate active catalytic species.<sup>[28]</sup> The insertion of the coordinated C=O moiety into the Fe-H bond gave the species (**II-3**) which has then the ability to activate efficiently H<sub>2</sub> leading to the hydrido alkoxo complex (**II-4**). In a last step, the elimination of the alcohol permitted the regeneration of the dearomatized species **II-1**.

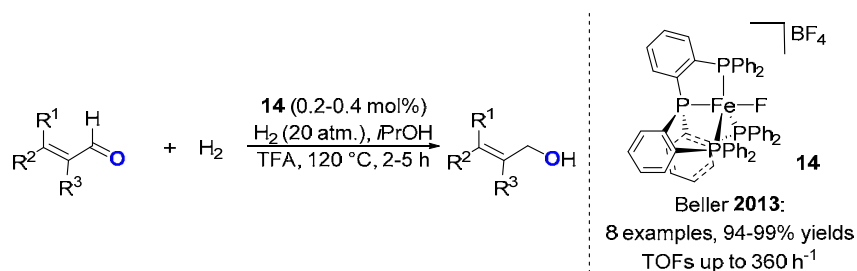
Another plausible mechanism is based on the attack of the hydride on the substrate in the outer sphere process. (Scheme 6). The reaction of the starting complex **13** with a base generates a hydride amide complex (**III-1**) *via* the deprotonation of the NH of ligand. The addition of dihydrogen to **III-1** in *trans* to the hydride leads to the *trans*-dihydride species (**III-3**). **III-3**

transfers then a proton from the nitrogen and a hydride from the iron to the carbonyl of the ketone to lead to the alcohol and regenerate the active amide complex **III-1**.<sup>[29]</sup>



**Scheme 6.** Proposed mechanism for the hydrogenation of ketones catalyzed by diphosphine amino iron complexes.

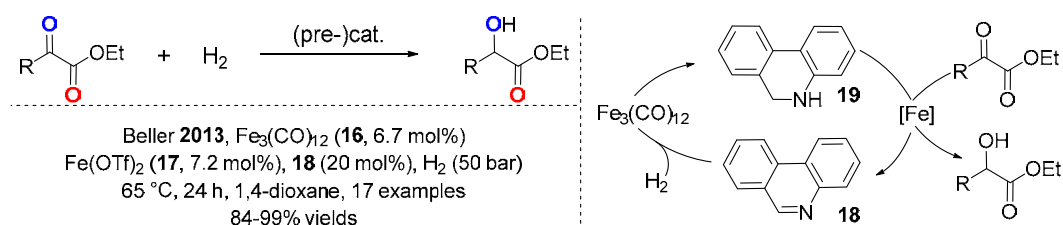
Iron complexes associated to multidentate ligands are also good candidates for hydrogenation of carbonyl compounds. The cationic tetraphosphine iron fluoride complex **14** (0.2–1.0 mol%) promoted the hydrogenation of aromatic and aliphatic aldehydes in the presence of 1.0–5.0 mol% of trifluoroacetic acid (TFA) in isopropanol under 20 atm of H<sub>2</sub> at 120 °C for 2–5 h in 95–99% yields and TOF up to 360 h<sup>-1</sup><sup>[30]</sup> (Scheme 7).



**Scheme 7.** Iron-catalyzed selective hydrogenation of  $\alpha,\beta$ -unsaturated aldehydes.

Interestingly, the transformation tolerated reducible functional substituents such as C=C bonds, esters, and even ketones. Furthermore, allylic alcohols were selectively obtained in 94–99% yields by reduction of  $\alpha,\beta$ -unsaturated aldehydes. Supported by NMR and DFT investigations, a mechanism was proposed suggesting the formation of a catalytically active species [(P<sub>4</sub>)Fe-H][BF<sub>4</sub>] (**15**) generated from the iron fluoride complex **14** *via* an oxidative addition of H<sub>2</sub> followed by a reductive elimination of HF.

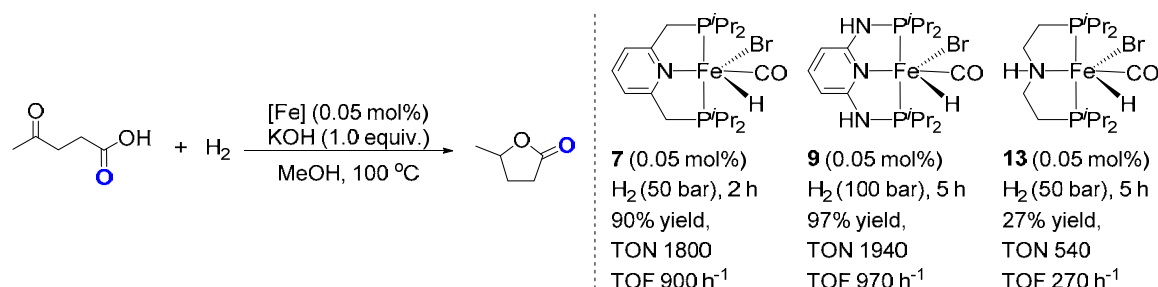
Beller succeeded to reduce selectively  $\alpha$ -ketoesters to produce the corresponding  $\alpha$ -hydroxyesters using in a consecutive way two different iron pre-catalysts,  $\text{Fe}_3(\text{CO})_{12}$  (**16**, 6.7 mol%) and  $\text{Fe}(\text{OTf})_2$  (**17**, 7.2 mol%) in the presence of phenanthridine **18** (20 mol%) (Scheme 8).<sup>[31]</sup>  $\text{Fe}_3(\text{CO})_{12}$  first catalyzed the hydrogenation of **18** to the corresponding hydrogenated reagent **19**, then used as the hydride source to selectively reduce the  $\alpha$ -keto C=O moiety *via* a  $\text{Fe}(\text{OTf})_2$  catalyzed hydrogen transfer reaction.



**Scheme 8.**  $\text{Fe}_3(\text{CO})_{12}$ /  $\text{Fe}(\text{OTf})_2$  catalyzed hydrogenation of  $\alpha$ -ketoesters.

A useful application of the iron-catalyzed hydrogenation is the conversion of levulinic acid to  $\gamma$ -valerolactone. Song *et al.* described an efficient and useful application of the iron-catalyzed hydrogenation for the conversion of both methyl levulinate and levulinic acid (LA) to  $\gamma$ -valerolactone (GVL) (Scheme 9).<sup>[32]</sup>

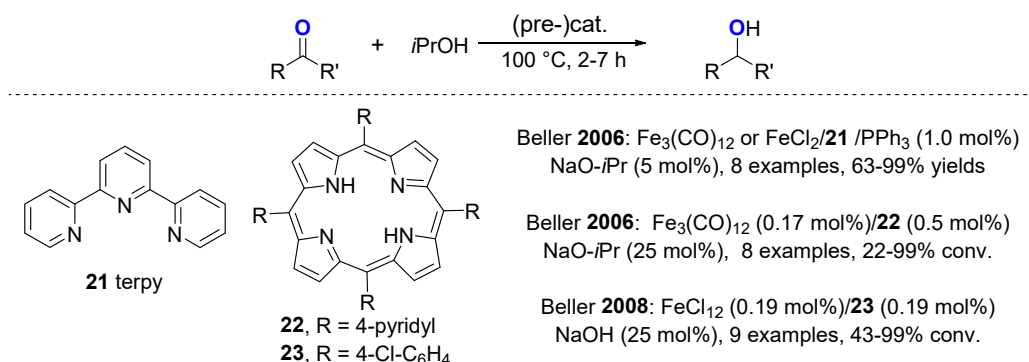
Indeed, using several pincer iron complexes **7**, **9** and **13** in low loading (0.05 mol%), LA was transformed in GVL performing the reaction in methanol at 100 °C for 2–5 h under 50 bar of  $\text{H}_2$  in the presence of 1 equiv. of KOH. The optimized conditions using **9** as the catalyst to produce GVL from levulinic acid in higher efficiency was the use of 0.002 mol% of **9** under 100 bar of  $\text{H}_2$  in methanol at 100 °C for 12 h (TON = 23000; TOF = 1917  $\text{h}^{-1}$  when the reaction was performed on 50 mmol scale). Both methyl levulinate and levulinic acid were transformed in GVL performing the reaction in methanol at 100 °C for 2–12 h under 100 bar of  $\text{H}_2$  in the presence of 1 equiv. of KOH (Scheme 9). GVL was then obtained in high TON and TOF of 23000 and 1917  $\text{h}^{-1}$ , respectively from levulinic acid.



**Scheme 9.** Iron-catalyzed hydrogenation of levulinate derivatives to  $\gamma$ -valerolactone.

### 2.1.2. Transfer hydrogenation of aldehydes and ketones.

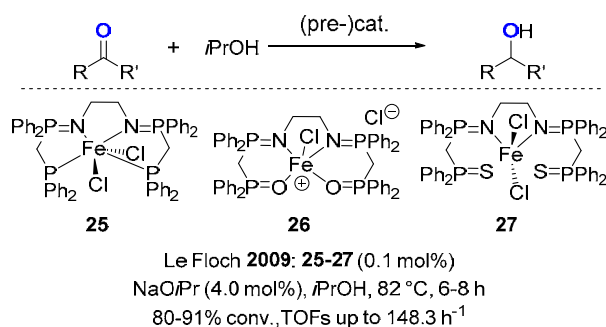
In the 1980's, Vancheesen *et al.* described pioneering contributions dealing with iron-catalyzed transfer hydrogenation of ketones, mainly using iron carbonyl complexes. The most efficient system was based on the use of  $\text{Fe}_3(\text{CO})_{12}$  **16** (4.0 mol%) in the presence of 1-phenylethanol or isopropanol as the hydride source and benzyltriethyl-ammonium chloride and 18-crown-6 as phase transfer agents. The reaction performed at 28 °C for 2.5 h led to the corresponding alcohols with moderate 20–60% conversion and moderate TOFs up to  $13 \text{ h}^{-1}$ .<sup>[33]</sup>



**Scheme 10.** N-containing ligand iron-catalyzed transfer hydrogenation of ketones.

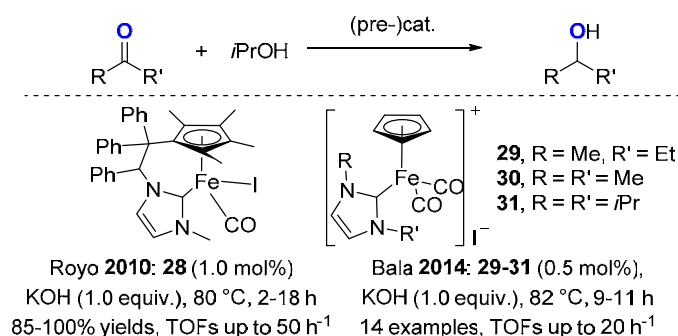
The combination of the commercially available triphenylphosphine, 2,2':6',2''-terpyridine (terpy, **21**) and  $\text{Fe}_3(\text{CO})_{12}$  (**16**) or  $\text{FeCl}_2$  (**20**) led to efficient catalytic systems (1.0 mol%) active for transfer hydrogenation of aliphatic and aromatic ketones, in the presence of NaO*i*Pr (5.0 mol%) in isopropanol at high temperature (100 °C) (Scheme 10).<sup>[34]</sup> In a similar fashion, with *in situ* catalysts prepared from either  $\text{Fe}_3(\text{CO})_{12}$  **16** or  $\text{FeCl}_2$  (**20**) in association with porphyrins (**22-23**), very good activity was obtained in the transfer hydrogenation of numerous ketones including  $\alpha$ -substituted alkoxyketones (22–99% conversion and TOFs up to  $642 \text{ h}^{-1}$ , Scheme 10).<sup>[35]</sup> Noteworthy, in the light of reports demonstrating that simple bases such as NaOH, KOH or KO*t*Bu are able to promote the transfer hydrogenation of aldehydes and ketones at lower temperatures,<sup>[36]</sup> the high reaction temperatures (80–100 °C) and the base-dependent reactivity are the main drawbacks of these catalytic systems.

Le Floch finely designed a series of related iron complexes bearing tetradentate ligands bearing two iminophosphorane moieties with two phosphines, thiophosphino, and phosphine oxide substituents for TH of acetophenone (Scheme 11).<sup>[37]</sup> The versatile coordination of these ligands to iron(II) precursor such as  $[\text{FeCl}_2(\text{THF})_{1.5}]$  (**24**) gave to the corresponding complexes  $[\text{FeCl}_2(\text{P}_2\text{N}_2)]$  (**25**),  $[\text{FeCl}(\text{O}_2\text{N}_2)]$  (**26**) and  $[\text{FeCl}_2(\text{N}_2)]$  (**27**). Using 0.1 mol% of those complexes **25-27**, acetophenone was reduced in 80–91% conversion in the presence of 4.0 mol% NaO*i*Pr in isopropanol at 82 °C for 6–8 h.



**Scheme 11.** Iminophosphorane diorganophosphorus based iron complexes for catalytic TH of acetophenone.

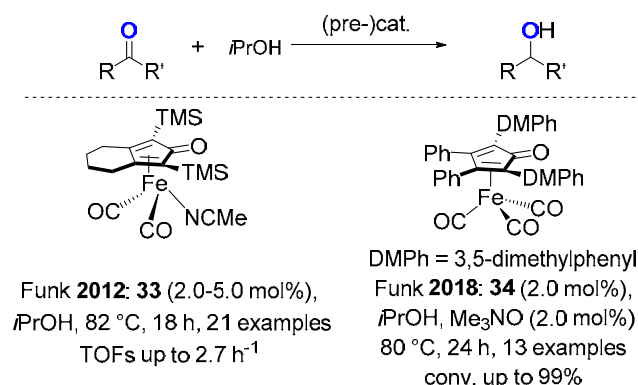
Cyclopentadienyl (Cp) functionalized NHC ligand based iron(II) complexes were also active pre-catalyst for TH of ketones. In 2010, Royo described tethered Cp-NHC iron complexes (e.g. **28**)<sup>[38]</sup> as efficient catalysts for transfer hydrogenation of ketones (e.g. acetophenone, benzophenone and cyclohexanone) in the presence of a stoichiometric amount of KOH in isopropanol at 80 °C for 2–18 h (Scheme 12). [Fe(Cp)(NHC)(CO)<sub>2</sub>][I] complexes (**29-31**)<sup>[39]</sup> with 1,3-dialkylated NHC were also used as efficient catalysts for transfer hydrogenation of cyclohexanone under similar conditions (Scheme 12). Noteworthy, the active species (0.5 mol%) can be obtained *in situ* by reaction of imidazolium salts with the CpFe(CO)<sub>2</sub>I (**32**) precursor and used for the TH of various ketones in 21–99% conversion under similar conditions.



**Scheme 12.** NHC-Fe piano-stool complexes for catalytic TH of ketones.

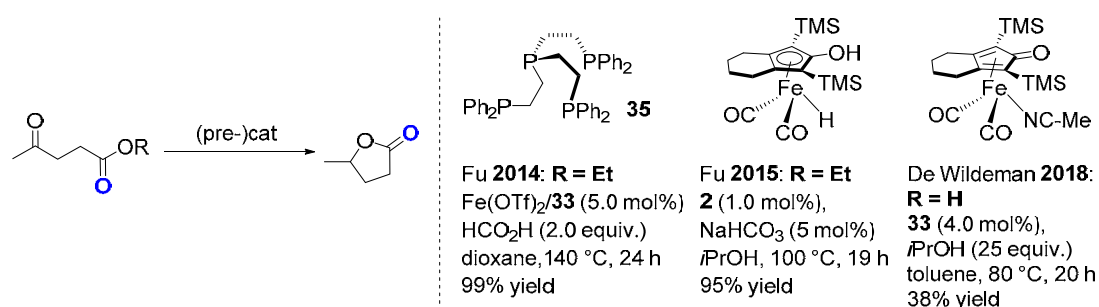
In comparison to hydrogenation reaction, Knölker type complexes were less used in TH of ketones. Nitrile-ligated complexes previously developed by Knölker<sup>[40]</sup> were shown to be efficient catalysts for TH as demonstrated by Funk. The best activity in the TH of aldehydes and ketones was obtained performing the reaction at 80 °C for 18 h using the acetonitrile complex (**33**), (aldehyde, 2.0 mol%; ketones, 5.0 mol%, Scheme 13). Interestingly, the catalyst **33** showed similar activities than the air-sensitive iron hydride complex **2** (1.0 mol%, 75 °C, 16 h).<sup>[41]</sup> The same author reported a [2,5-bis(3,5-dimethylphenyl)-3,4-diphenylcyclopentadienone]iron tricarbonyl (**34**, 2.0 mol%) with Me<sub>3</sub>NO (2.0 mol%) at 80 °C

for 24 h in both transfer hydrogenations and dehydrogenations.<sup>[42]</sup> It is worth mentioning that **34** was as active as or more active than **3** in the carbonyl reductions and alcohol oxidations (Scheme 13).



**Scheme 13.** Knölker type catalysts for TH of ketones.

A useful application of the hydrogen transfer reaction catalyzed by iron catalysts is the conversion of ethyl levulinate to  $\gamma$ -valerolactone (GVL). In 2014, Fu *et al.* reported that using 5.0 mol% of an *in situ* prepared catalyst from Fe(OTf)<sub>2</sub> (**17**) and [P(CH<sub>2</sub>CH<sub>2</sub>PPh<sub>2</sub>)<sub>3</sub>] ligand **35**, GVL was produced in 99% yield by reaction with formic acid (2.0 equiv.) in dioxane at 140 °C for 24 h. Notably, the reaction can be performed without addition of base and with a TON of 24 (Scheme 14).<sup>[43]</sup> In 2015, Metzker and Burtuloso reported the same reaction starting from Fe<sub>3</sub>(CO)<sub>12</sub> catalyst (**16**, 4.0 mol%) in the presence of 4.0 equiv. of formic acid and 4.0 equiv. of imidazole in water at 180 °C for 15 h (92% yield, TON: 23).<sup>[44]</sup>

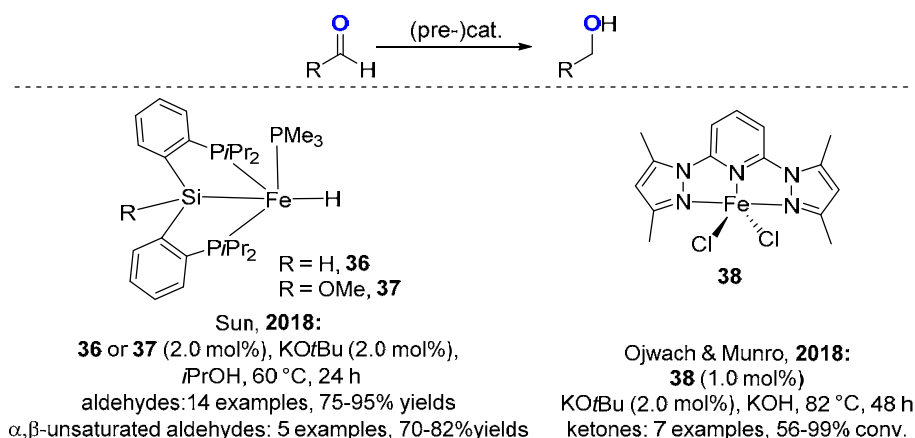


**Scheme 14.** Iron-catalyzed reduction of ethyl levulinate to  $\gamma$ -valerolactone.

The use of Casey's complex **2** permitted to perform the reaction in milder conditions (Scheme 14). Using 1.0 mol% of **2** in the presence of 5.0 mol% of NaHCO<sub>3</sub> in isopropanol at 100 °C for 19 h,  $\gamma$ -valerolactone was obtained in 95% yield and TON of 95 from ethyl levulinate.<sup>[45]</sup> De Wildeman recently described the reduction of levulinic acid using the acetonitrile-ligated Knölker catalyst **33** (4.0 mol%) in the presence of 25 equiv. of isopropanol in toluene at 80 °C for 20 h yielding GVL in 38%. (Scheme 14) Noticeably, **33** (0.1 mol%) can

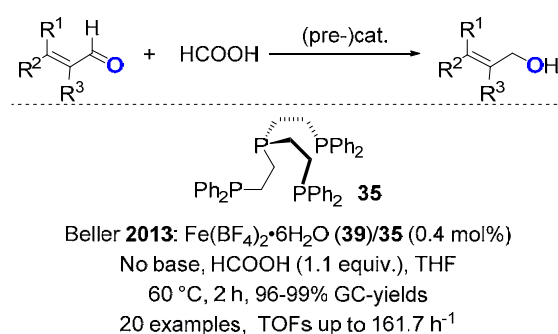


perform the hydrogenation of levulinic acid to GVL in ethanol under 60 bar of H<sub>2</sub> at 100 °C for 20 h with 57% yield (TON: 570).<sup>[46]</sup>



### Scheme 15. Pincer iron catalysts for the TH of aldehydes and ketones

Tridentate PSiP ligand based iron pincer complexes **36** and **37** can be used in transfer hydrogenation of aldehydes (Scheme 15). Sun reported the reduction of aldehydes using 2.0 mol% of catalyst in the presence of 2.0 mol% of KOtBu in isopropanol at 60 °C for 24 h. The reduction can tolerate functional groups such as halides or cyano. Additionally, chemoselective reduction of α,β-unsaturated aldehydes led to the corresponding allylic alcohols in 70–82% yields.<sup>[47]</sup> Noticeably, ketones were not reduced under such conditions. Using another pincer complex, 2,6-bis(pyrazolyl)pyridine iron(II) complex (**38**, 1.0 mol%), TH of ketones can be also achieved using 1 equiv. of KOH as the base in isopropanol at 82 °C for 48 h (Scheme 15). It has a better activity with aromatic ketones than with aliphatic ketones.<sup>[48]</sup>



### Scheme 16. Selective TH of aldehydes catalyzed by Fe(BF<sub>4</sub>)<sub>2</sub>·6H<sub>2</sub>O/**35**.

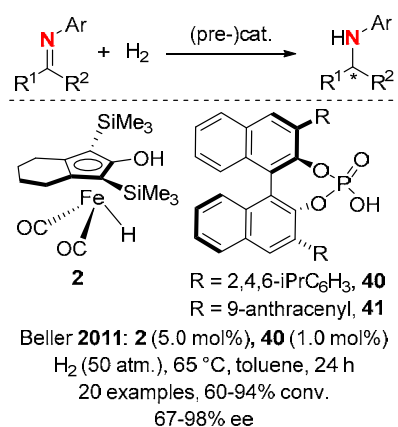
Efficient and highly selective transfer hydrogenation of aromatic, heteroaromatic and aliphatic aldehydes using *in situ* generated catalytically active species (0.4 mol%) from Fe(BF<sub>4</sub>)<sub>2</sub>·6H<sub>2</sub>O (**39**)/tetrakis(diphenylphosphino)methane (**35**) in the presence of 1.1 equiv. of formic acid as the hydrogen source in THF at 60 °C for 2 h (20 examples, GC-yields: 96–99%) were described by Beller

(Scheme 16).<sup>[49]</sup> Chloro, bromo, ketone, ester and styryl functionalities were not reduced under these conditions. Additionally, chemoselective reduction of  $\alpha,\beta$ -unsaturated aldehydes to the corresponding allylic alcohols was conducted under base-free conditions.

## 2.2. Imines and reductive amination of carbonyl compounds

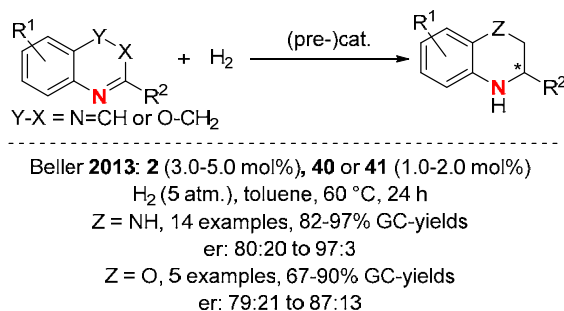
### 2.2.1. Imines.

Up to now, there are only scarce reports on the reduction of imines catalyzed by iron-based species. In 2011, Beller and coworkers developed the first catalytic hydrogenation of imines to amines,<sup>[50]</sup> associating in a synergic manner the Knölker complex **2** and a chiral phosphoric Brønsted acid (**40** and **41**, Scheme 17). The resulting *in situ* catalytic system was active at 50 atm of H<sub>2</sub> at 65 °C resulting in the hydrogenation of numerous *N*-arylketimines to the corresponding amines in 60–94% isolated yields and 67–98% ee. Based on this methodology, chiral amines were prepared from terminal alkynes and primary anilines using consecutive hydroamination/hydrogenation sequence: (i) a gold catalyzed hydroamination of terminal alkynes, using 1.0 mol% of [Au(*o*-BiPh)(*t*-Bu)<sub>2</sub>P][BF<sub>4</sub>] leading to imines, which were then *in situ* involved in (ii) an enantioselective hydrogenation [5.0 mol% of **2**/1.0 mol% of **40** or **41** under the same conditions, yields up to 93%, ee of 70–94%].<sup>[51]</sup>



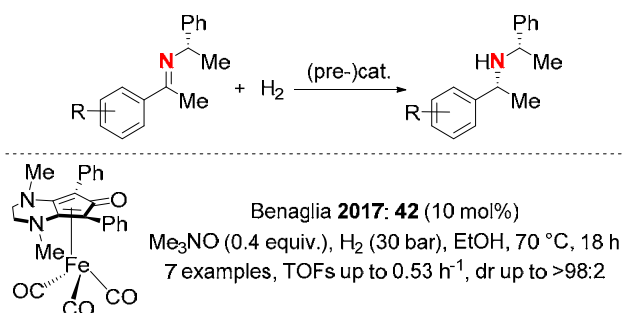
**Scheme 17.** Knölker complex/chiral phosphoric Brønsted acids for the catalytic asymmetric hydrogenation of imines.

The same catalytic system (3.0–5.0 mol% of **2** and 1.0–2.0 mol% of **40** or **41**) was also used to promote the enantioselective hydrogenation of quinoxalines and 2*H*-1,4-benzoxamines, conducting to the corresponding tetrahydroquinoxalines with enantiomeric ratios (er) up to 97:3 and to 3,4-dihydro-2*H*-1,4-benzoxamines with er up to 87:13, respectively (Scheme 18).<sup>[52]</sup>



**Scheme 18.** Knölker complex/chiral phosphoric Brønsted acids for the catalytic asymmetric hydrogenation of C=N bond.

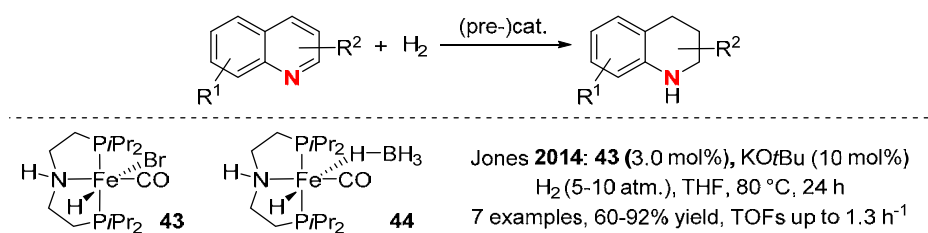
In 2017, Benaglia and co-workers reported an iron-catalyzed diastereoselective reduction of chiral imines, using an achiral cyclopentadienone-based iron complex **42** (10.0 mol%) in the presence of 0.4 equiv. of  $\text{Me}_3\text{NO}$  (Scheme 19). Performing the reduction under 30 bar of  $\text{H}_2$  at 70 °C in EtOH, enantiomerically pure amines were often produced with dr up to 98:2, in moderate conversions, yields and activity (TOF up to  $0.53 \text{ h}^{-1}$ ).<sup>[53]</sup>



**Scheme 19.** Knölker complex for catalyzed diastereoselective reduction of chiral imines.

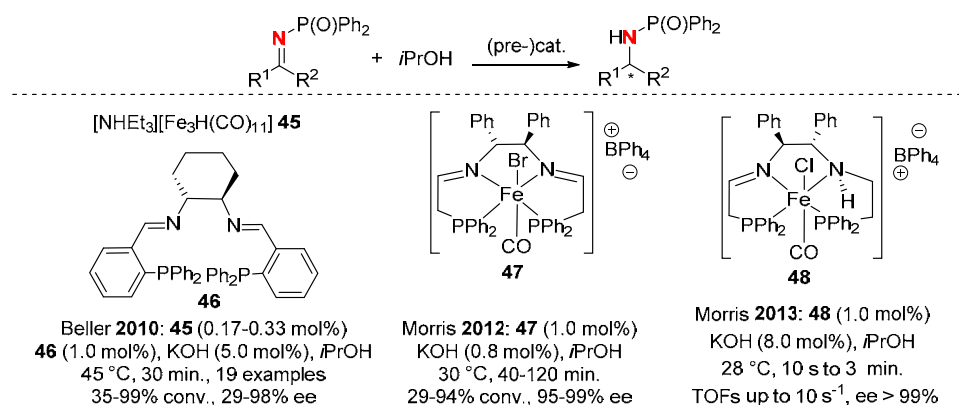
Noteworthy, using a water soluble Knölker type complex **4** (Scheme 1, 2.5 mol%) in the presence of 3.75 mol% of  $\text{Me}_3\text{NO}$  in water under 10 bar of  $\text{H}_2$  at 100 °C for 14 h, Renaud described the reduction of water stable and soluble imines (4 examples) in 50–98% yields.<sup>[13]</sup>

In addition to Knölker type complexes, some other well-defined iron complexes were shown to perform hydrogenation of C=N bonds. Thus, using the bifunctional iron pincer complex **43** as the catalyst (3.0 mol%), Jones has performed the hydrogenation of tetrahydroquinoxaline *N*-heterocycles under 5–10 atm of  $\text{H}_2$ , in the presence of 10 mol% of  $\text{KO}^t\text{Bu}$  in THF at 80 °C for 24 h, and the corresponding reduced derivatives were isolated in 60–92% yields (Scheme 20). Noteworthy, the same type of pincer catalyst [e.g. **44**] also promote the reverse dehydrogenation of *N*-heterocycles when refluxing in xylene for 30 h, whereas **43** was inactive.<sup>[54]</sup>



**Scheme 20.** Pincer iron complexes for the catalytic hydrogenation of *N*-heterocycles.

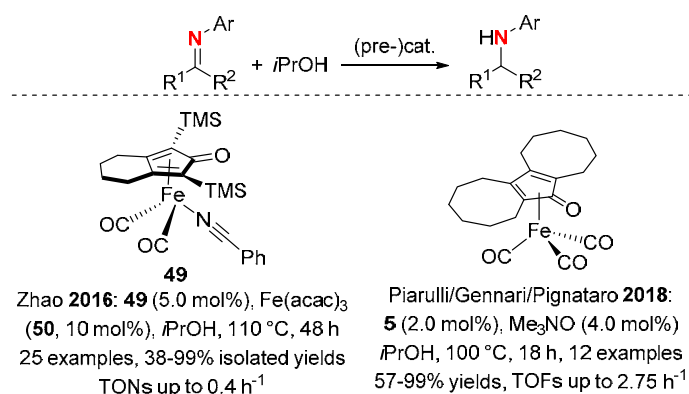
Transfer hydrogenation conditions can be also used for the reduction of imines. In 2011, the first iron-catalyzed enantioselective TH was performed using activated ketimines.<sup>[55]</sup> Thus, using an *in situ* formed catalyst (0.33 mol%) from [NHEt<sub>3</sub>][Fe<sub>3</sub>H(CO)<sub>11</sub>] **45** and the diiminophosphine tetradentate chiral ligand CyN<sub>2</sub>P<sub>2</sub> **46**, aromatic and heteroaromatic *N*-phosphonyl ketimines were reduced in 67–98% yields and 89–98% ee after a reaction in the presence of a catalytic amount of a base at 45 °C for 30 min. in isopropanol (Scheme 21).



**Scheme 21.** ATH of imines promoted by tetradentate chiral ligands.

In a similar manner, using diimino-diphosphine iron complexes, Morris also reported the transfer hydrogenation of *N*-(diphenylphosphinoyl)- and *N*-(tolylsulphonyl)-ketimines. The corresponding amines were then obtained with 29–94% conversion and 95–99% ee using the most efficient complex **47** (1.0 mol%) in combination with 0.8 mol% of KOtBu in *i*PrOH at 40 °C for 40–120 min. (Scheme 21).<sup>[56]</sup> It must be pointed out that the amine(imine)diphosphine analogue **48** exhibited an enhanced activity for transfer hydrogenation of imines with TOF up to 10 s<sup>-1</sup>.<sup>[57]</sup>

Interestingly, Funk's catalyst can also catalyze transfer hydrogenation of *N*-aryl and *N*-alkyl imines. Indeed, Zhao succeeded to perform such a reaction using the combination of the Knölker's nitrile-ligated complex (**49**, 5.0 mol%) and Fe(acac)<sub>3</sub> (**50**) (10 mol%) in isopropanol in the absence of base at 110 °C for 48 h (Scheme 22). The key for the success of this catalytic system is the use of Fe(acac)<sub>3</sub> (**50**) as a Lewis acid, as in its absence, the reaction led to only 9% conversion.<sup>[58]</sup>

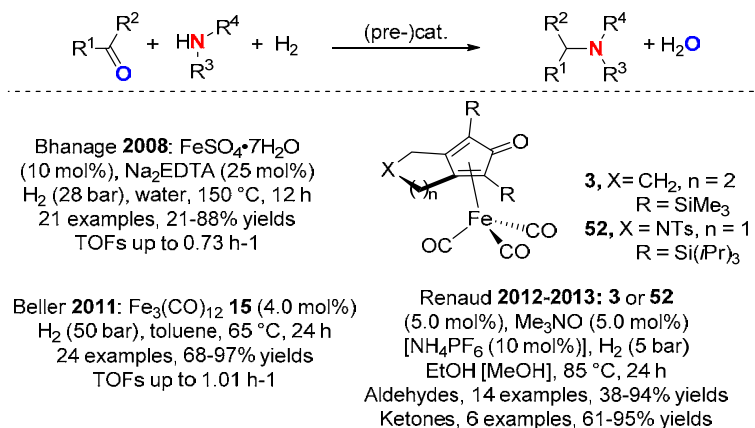


**Scheme 22.** Iron-catalyzed TH of imines.

Recently, Piarulli, Gennari and Pignataro reported TH of non-activated imines promoted by a Knölker complex **5** (2.0 mol%) for the reduction of a number of *N*-aryl and *N*-alkyl imines in the presence of Me<sub>3</sub>NO (4.0 mol%) in *i*PrOH at 100 °C for 18 h (Scheme 22).<sup>[59]</sup>

### 2.2.2. Direct reductive amination (DRA) of carbonyl compounds.

Among the main preparative pathways for the production of amines, DRA is undoubtedly one of the most powerful and useful ones.<sup>[60]</sup> Notwithstanding this reaction has been extensively studied with stoichiometric alkali reducing agents. Over the last decade, applications with iron as a catalyst have been developed.<sup>[61]</sup>



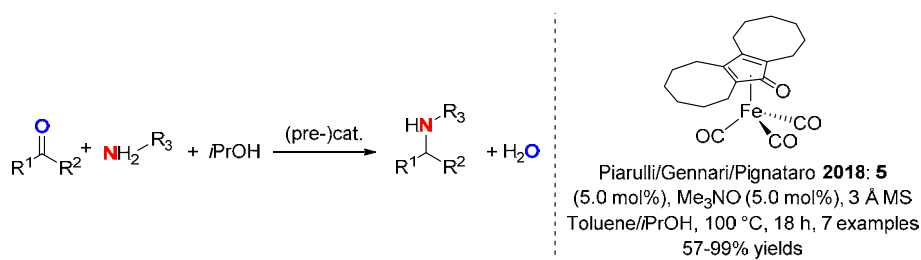
**Scheme 23.** Iron-catalyzed DRA reactions under hydrogenative conditions.

In 2008, using 10 mol% of FeSO<sub>4</sub>·7H<sub>2</sub>O (**51**) and 25 mol% of Na<sub>2</sub>EDTA, Bhanage *et al.* performed the DRA of aldehydes and ketones with primary and secondary amines, in water under 28 bar of hydrogen at 150 °C for 12 h<sup>[62]</sup> (Scheme 23). Under these drastic conditions, small amounts of alcohols due to the reduction of the carbonyl compounds were also detected. DRA can be performed under milder conditions using 4.0 mol% of Fe<sub>3</sub>(CO)<sub>12</sub> **16** under 50 bar of H<sub>2</sub> in toluene at 65 °C for 24 h: by reaction with both aldehydes and ketones, anilines are transformed to the corresponding alkylated anilines in 68–97% yields (Scheme 23). In order to

have a complete condensation between anilines and ketones, the use of molecular sieves is required. Noticeably, the reduction is chemoselective when aldehydes bearing ketone or ester moieties were used.<sup>[63]</sup>

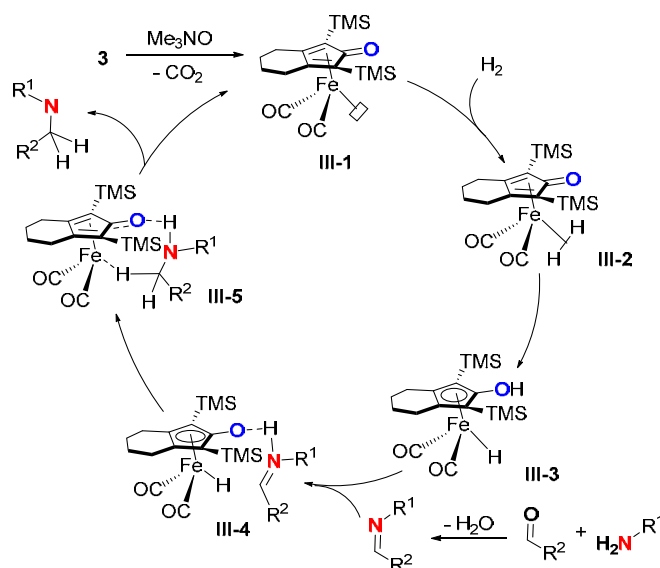
Molecular-defined Knölker complexes **3** and **52** also efficiently catalyzed this transformation under mild conditions: with 5.0 mol% of **3** and 5.0 mol% of Me<sub>3</sub>NO, under low hydrogen pressure (5 bar) at 85 °C in ethanol, aldehydes reacted with alkylamines producing the corresponding alkylated amines in 38–94% yields (Scheme 23). A slight modification of the reaction conditions is required to perform the DRA of ketones: the reaction has to be performed in methanol with a catalytic amount of NH<sub>4</sub>PF<sub>6</sub>.<sup>[64]</sup>

Interestingly the catalyst **5** (5.0 mol%) in combination with Me<sub>3</sub>NO (5.0 mol%) can also promote the transfer hydrogenative reductive amination of aldehydes and ketones in the presence of 3 Å molecular sieves at 100 °C for 18 h, in good yields (Scheme 24).<sup>[59]</sup>



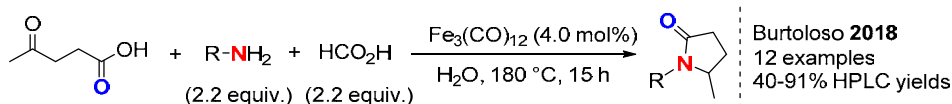
**Scheme 24.** Iron-catalyzed DRA reactions under transfer hydrogenative conditions with isopropanol.

In order to rationalize the catalytic DRA transformation, an outer-sphere mechanism was postulated and supported by DFT calculations (Scheme 25).<sup>[16-17, 65]</sup> The reaction of Me<sub>3</sub>NO on the complex **3** generated the 16 electron species (**III-1**) which can coordinate the dihydrogen leading to the intermediate (**III-2**) then (**III-3**) by heterolytic H<sub>2</sub> cleavage. Based on a concerted hydride/proton transfer from the hydroxyl and the iron hydride to the *in situ* generated imine moiety, the species (**III-4**) then (**III-5**) were produced. Finally, the catalytic active species (**III-1**) is regenerated producing the amine derivative. (Scheme 25)



**Scheme 25.** Plausible outer-sphere mechanism for hydrogenation of imines in DRA catalyzed by Knölker type catalyst **3**.

More recently, reductive amination/cyclization of levulinic acid *via* transfer hydrogenation with  $\text{HCO}_2\text{H}$  (FA) as hydrogen source, was reported by Burtoloso (Scheme 26).<sup>[66]</sup> Using 4.0 mol% of  $\text{Fe}_3(\text{CO})_{12}$  **16** with 2.2 equiv. of amine and 2.2 equiv. of  $\text{HCO}_2\text{H}$  in water at 180 °C, levulinic acid was converted to numerous pyrrolidones in 40–91% yields.



**Scheme 26.** Iron-catalyzed DRA reactions under transfer hydrogenative conditions with  $\text{HCO}_2\text{H}$ .

### 2.3. Carboxylic acid derivatives and carbon dioxide

Iron-catalyzed reduction of polarized  $\text{C}=\text{X}$  bonds such as aldehydes or ketones is a flourishing research area in which some complexes start to compete with the noble metal ones in terms of activity. By contrast, catalytic hydrogenation of less reactive derivatives such as carboxylic acids, amides or esters in the presence of iron complexes is still in its infancy compared to the hydrogenation with noble transition metal complexes such as ruthenium. Nevertheless, some recent results demonstrate the high potential of this chemistry at iron.<sup>[67]</sup>

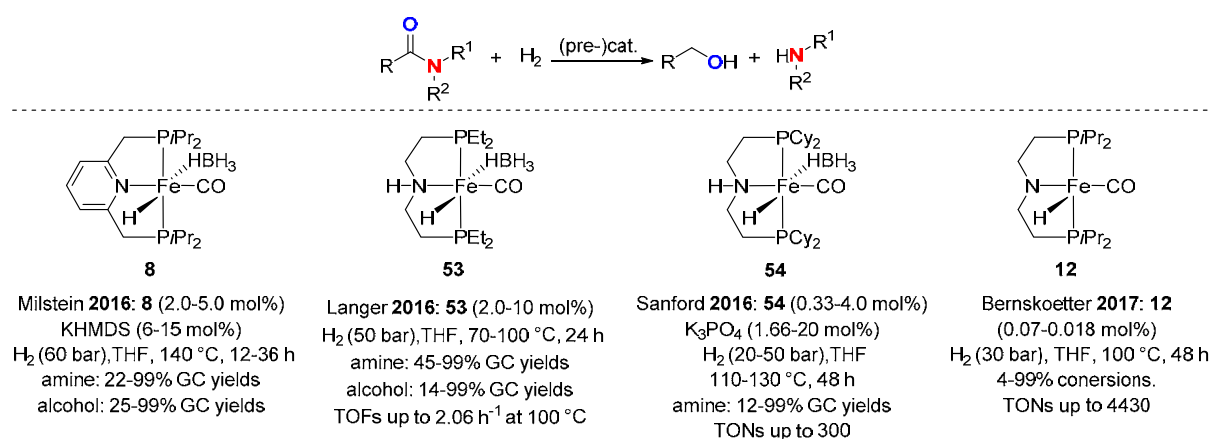
#### 2.3.1. Amides.

In the series of the carboxylic acid derivatives, carboxamides are undoubtedly among the most difficult ones to selectively reduce. Even if numerous transition metals have already efficiently been used for the catalytic reduction of amides, hydrogenations using iron catalysts were

scarcely reported. Additionally, one of the challenges is the selective cleavage the C-N bond leading to alcohols and amines or the C=O bond furnishing the corresponding amines.

In early 2016, Milstein described the first example of homogeneous iron-catalyzed hydrogenation of amides using an iron PNP pincer complex **8** as the catalyst (Scheme 45). The reaction can be performed in the presence of 6.0 mol% of KHMDS (potassium bis(trimethylsilyl)amide) under drastic conditions (60 bar of H<sub>2</sub> at 140 °C) with a range of activated secondary and tertiary *N*-substituted 2,2,2-trifluoroacetamides leading to the corresponding amines and trifluoroethanol with moderate to good yields.<sup>[68]</sup>

In 2016, Langer reported the hydrogenation of non-activated amides and lactams with an iron pincer catalyst (**53**, 2.0–10 mol %, Scheme 45). As a representative example, the treatment of *N*-phenylbenzamide with 50 bar H<sub>2</sub> at 70–100 °C in dry THF after 24 h results in the clean formation of alcohol and amine, whereas the C=O bond cleavage product was not detected by GC analysis.<sup>[69]</sup> Similarly, Sanford used an analogous pincer complex (**54**) bearing PCy<sub>2</sub> moieties to catalyze the hydrogenation of amides (including formamides) in quite harsher conditions (110–130 °C) but at lower hydrogen pressure (20–50 bar) in 3 h (Scheme 45). TON up to 300 can be reached under such conditions. Notably, *N,N*-dimethylformamide was hydrogenated with TON up to 1000.<sup>[70]</sup>



**Scheme 27.** Hydrogenation of amides with iron pincer catalysts

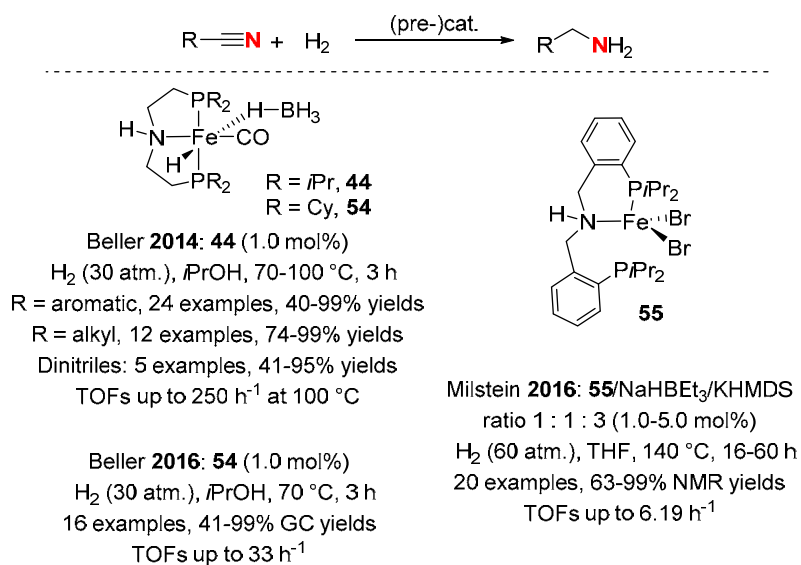
In 2017, Bernskoetter used a PNP iron hydride complex as the catalyst to promote the hydrogenation of amides. The use of 0.07–0.018 mol% of **12** in THF under 30 atm of H<sub>2</sub> for 4 h mainly permitted to hydrogenate secondary formamide derivatives with 4-99% conversion and TON up to 4430 (Scheme 27). Under such conditions, acetamides and benzamides exhibited reduced activities. Interestingly, the addition of co-catalyst such as formanilide



HCON(H)Ph and LiOTf enhanced the productivity of the reaction with acetamide and benzamides derivatives, when performed at 120 °C for 16 h under 60 bar of H<sub>2</sub>.<sup>[71]</sup>

### 2.3.2. Nitriles.

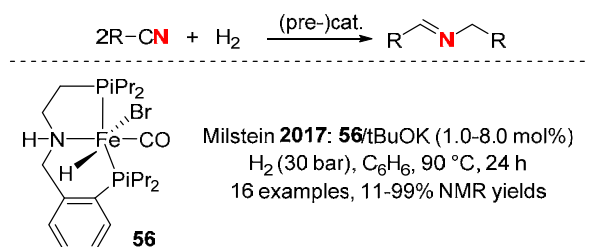
The catalytic hydrogenation of nitriles leading selectively to the corresponding primary amines is still a challenging transformation, mainly with iron catalysts. In his continuous effort to develop new iron-catalyzed transformations, Beller reported the use of 1.0 mol% of the iron PNP pincer complexes **44**<sup>[72]</sup> and **54**<sup>[73]</sup> for the selective hydrogenation of nitriles to primary amines under 30 bar of H<sub>2</sub> in isopropanol at 70–100 °C for 3 h (Scheme 28). Importantly, aromatic, heteroaromatic, alkyl and dinitriles (including the industrial relevant adiponitrile) can be reduced in 40–95% yields with **44**. Notably, TOFs up to 250 h<sup>-1</sup> at 100 °C were obtained. Under such reaction conditions, several functional groups such as halides, esters, ethers, acetamido groups and α,β-unsaturated C=C bonds were tolerated.



**Scheme 28.** Iron PNP complexes in the catalytic hydrogenation of nitriles to primary amines

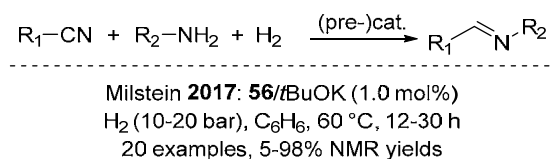
Subsequently, Milstein's group reported the synthesis of a novel complex **55** and its application in the catalytic homogeneous hydrogenation of (hetero)aromatic, benzylic, and aliphatic nitriles to selectively form primary amines (Scheme 28). The catalytic active species (1.0–5.0 mol%) prepared *in situ* by reaction of **55** with 1.0 equiv. of NaHBET<sub>3</sub> and 3.0 equiv. of KHMDS was applied for the reduction of (hetero)aromatic and alkyl nitriles under 60 bar of H<sub>2</sub> in THF at 140 °C for 16–60 h (78–99% conversion, 63–99% NMR-yields).<sup>[74]</sup> Interestingly, they have described an iron-catalyzed hydrogenation of nitriles leading selectively to secondary imines. The reduction proceeded under relatively mild conditions (90 °C, 30 bar H<sub>2</sub>), using 1.0–8.0 mol% of the pincer complex (*i*PrPNP)Fe(H)Br(CO) (**56**) and KO*t*-Bu as a base (in an

equimolar amount to Fe pre-catalyst) leading the corresponding imines in 11–99% NMR-yields (Scheme 29). Noticeably, no products resulting from the full hydrogenation (primary or secondary amines) were observed.<sup>[75]</sup> This reaction resulted from the condensation of the reduced derivatives, the reactive imine intermediate with the amine.



**Scheme 29.** Selective hydrogenation of nitriles to secondary imines catalyzed by **56**.

Using the same catalyst **56**, cross-secondary imines were selectively formed through hydrogenative cross-coupling of nitriles and amines under similar conditions, but at lower temperature (60 °C vs 90 °C) and pressure of  $\text{H}_2$  (10–20 bar vs 30 bar, Scheme 30).<sup>[76]</sup> The reaction was particularly efficient with aromatic nitriles.

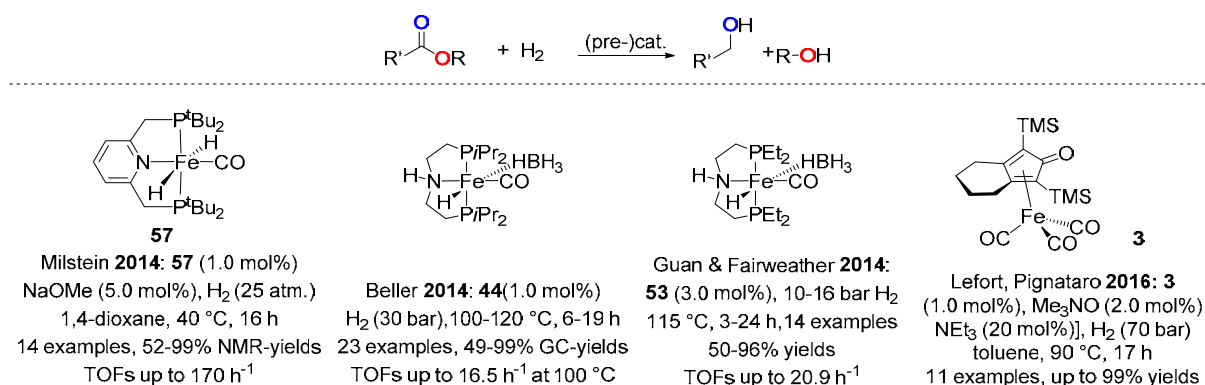


**Scheme 30.** Selective reductive cross-coupling of nitriles and amines to form secondary aldimines catalyzed by **56**.

### 2.3.3. Carboxylic esters.

In organic synthesis, one of the most important, but also the most challenging task is the hydrogenation of carboxylic acids or esters in an efficient and chemoselective manner to obtain alcohols, ethers or aldehydes. In terms of large scale and industrial applications, reduction of esters to alcohols *via* hydrogenation is an important task. In the area of iron catalysis, there are only a few reports until recently, with 2014 being a productive year in this area.

First, Milstein described a selective iron-catalyzed hydrogenation of activated trifluoroacetic acid esters  $\text{F}_3\text{C}-\text{CO}_2\text{R}$  leading to 2,2,2-trifluoroethanol and the corresponding alcohols  $\text{RCH}_2\text{OH}$  in 52–99% NMR-yields. The iron dihydrido pincer complex **57** (1.0 mol%) was used as catalyst in the presence of 5.0 mol% of NaOMe as the base in dioxane under 25 bar of hydrogen at 40 °C for 16 h (Scheme 31).<sup>[77]</sup> It must be pointed out that no reduction activity was observed with difluoroacetic acid ester derivatives.

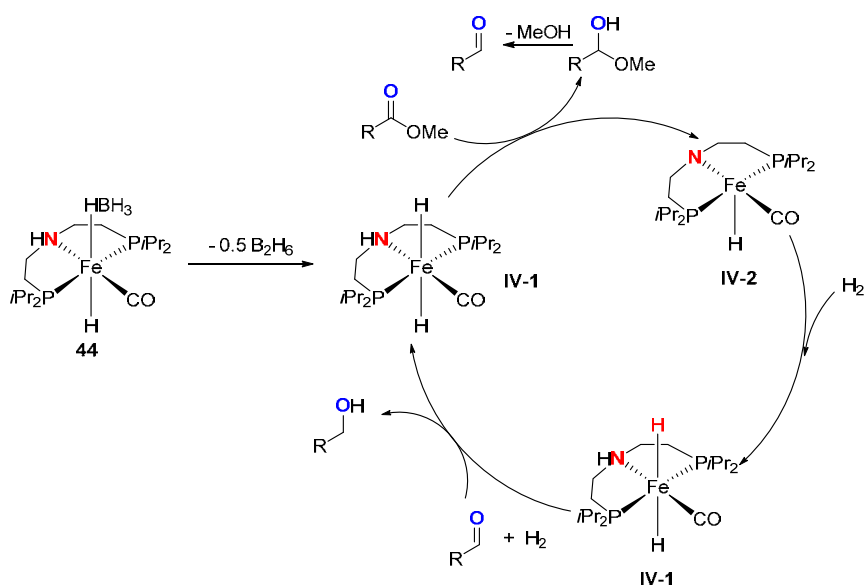


**Scheme 31.** Iron dihydrido pincer complexes for the hydrogenolysis of esters to alcohols

Simultaneously, Beller,<sup>[72]</sup> Guan and Fairweather<sup>[78]</sup> reported the hydrogenation of a wide variety of aliphatic and aromatic esters catalyzed by the bifunctional PNP iron pincer complexes **44** and **53** under base free conditions (Scheme 31). Such PNP ligand was initially described by Gusev in the osmium-catalyzed hydrogenation of esters.<sup>[79]</sup> With this catalytic system, carboxamides, heteroaromatic motifs (e.g. furans, pyridines, benzothiazoles), and remoted alkenyl moieties were well tolerated, whereas cyano functionalities were hydrogenated to the corresponding amines. Noteworthy, lactones led selectively to the corresponding diols. Crude industrial samples of a mixture of C<sub>12</sub>–C<sub>16</sub> esters were also reduced under solvent-free conditions. Beller then have shown that the sterically less hindered <sup>Et</sup>2PNP analogous iron complex **53** gave superior catalytic activity working at lower temperatures (60–100 °C *vs* 100–120 °C).<sup>[80]</sup>

A catalytic cycle was proposed based on DFT calculations and experimental studies including an observation indicating that the –NH moiety on the PNP pincer backbone was an important key as no activity was detected using PNP ligand bearing a *N*-Me substituent (Scheme 32).<sup>[81]</sup>

Thus, after BH<sub>3</sub> elimination from **44**, simultaneous hydrogen transfers from the metal center (**IV-1**) to the carbonyl moiety (without any previous coordination) and from the NH function produced the hemiacetal and an iron-amido complex *via* an outer-sphere mechanism. Hydrogenation of the iron complex (**IV-2**) regenerated the dihydride species **IV-1**. The solvolysis of the acetal led to methanol and aldehydes which is then reduced to alcohol *via* the same catalytic cycle.<sup>[72]</sup>



**Scheme 32.** Proposed mechanism for ester hydrogenolysis catalyzed by **44**.

Apart pincer iron complexes, Lefort and Pignataro reported the use of the (cyclopentadienone)iron complexes **3** for the hydrogenation of activated trifluoroacetate esters (Scheme 31). With 1.0 mol% of **3** in the presence of 2.0 mol% of Me<sub>3</sub>NO and 20 mol% of trimethylamine, the reaction proceeded at 90 °C under 70 bar of H<sub>2</sub> and led quantitatively to the corresponding alcohols, with TON up to 336. One main limitation of this methodology is its substrate dependence as only trifluoroacetate esters could be reduced.<sup>[82]</sup>

### 2.3.4. Carbon dioxide and carbonates.

In terms of sustainability, the use of carbon dioxide as an attractive and abundant C<sub>1</sub> feedstock is nowadays a challenging purpose in bulk chemical industry (methanol, formic acid, formaldehyde, urea, etc.).<sup>[83]</sup> In the field of reductions, the direct hydrogenation of CO<sub>2</sub><sup>[84]</sup> to formaldehyde, methanol, methane, formamides, and amines are crucial but challenging goals, with a particular focus on the CO<sub>2</sub> hydrogenation to afford formic acid (or formate).

Pioneering contribution made by Evans in 1978 using [NR<sub>4</sub>][HFe(CO)<sub>4</sub>] (**58**) demonstrated that iron complexes could be nice candidates for the reduction of CO<sub>2</sub> into formate derivatives, although harsh reaction conditions were used to reach very low yields (up to 6%).<sup>[85]</sup> In 2003, thanks to a high-pressure combinatorial catalyst discovery technique, Jessop *et al.* identified that the combination of FeCl<sub>3</sub> (**59**) and 1,2-bisdicyclohexylphosphinoethane (dcpe) in the presence of 0.5 equiv. of DBU (1,8-diazabicyclo[5.4.0]undec-7-ene) catalyzed the direct hydrogenation of CO<sub>2</sub> to formic acid with a TON of 113 and a TOF of 15.1 h<sup>-1</sup> under 40 bar

H<sub>2</sub> and 60 bar CO<sub>2</sub> at 50 °C for 7.5 h.<sup>[86]</sup> Noticeably, this *in situ* formed catalyst was more active than [NR<sub>4</sub>][HFe(CO)<sub>4</sub>] **58** when used with DBU.

**Table 1.** Iron-catalyzed hydrogenation of carbon dioxide and bicarbonate

<p><b>35</b></p>	<p>Beller &amp; Laurency 2010: Fe(BF<sub>4</sub>)<sub>2</sub>·6H<sub>2</sub>O/<b>35</b> H<sub>2</sub> (60 bar), NaHCO<sub>3</sub>, 80 °C, MeOH, 20 h</p> <p>TONs up to 610 TOFs up to 30 h<sup>-1</sup></p>	<p><b>67</b></p>	<p>Hazari &amp; Bernskoetter 2017: <b>67</b>, CO<sub>2</sub>:H<sub>2</sub> (69 bar) DBU/LiOTf (7.5/1), THF, 80 °C, 24 h</p> <p>TON = 613</p>												
<p><b>63</b></p>	<p>Beller 2012: <b>63</b>, CO<sub>2</sub> (30 bar), H<sub>2</sub> (30–70 bar) 100 °C, 20 h</p> <table border="1"> <thead> <tr> <th>Product (Yield%)</th> <th>HCO<sub>2</sub>H (Yield%)</th> <th>TON</th> </tr> </thead> <tbody> <tr> <td>HCO<sub>2</sub>Me (7)</td> <td>(7.9)</td> <td>1897</td> </tr> <tr> <td>DMF (70)</td> <td>(2.9)</td> <td>2329</td> </tr> <tr> <td>HCONEt<sub>2</sub> (39)</td> <td>(9.1)</td> <td>2114</td> </tr> </tbody> </table>	Product (Yield%)	HCO <sub>2</sub> H (Yield%)	TON	HCO <sub>2</sub> Me (7)	(7.9)	1897	DMF (70)	(2.9)	2329	HCONEt <sub>2</sub> (39)	(9.1)	2114	<p><b>9</b> or <b>68</b></p>	<p>Kirchner &amp; Gonsalvi 2016: <b>9</b> or <b>68</b> (0.1 mol%) CO<sub>2</sub> and NaHCO<sub>3</sub>, H<sub>2</sub></p> <p>TONs up to 10275 TOFs up to 489 h<sup>-1</sup></p>
Product (Yield%)	HCO <sub>2</sub> H (Yield%)	TON													
HCO <sub>2</sub> Me (7)	(7.9)	1897													
DMF (70)	(2.9)	2329													
HCONEt <sub>2</sub> (39)	(9.1)	2114													
<p><b>57</b> X = CH, Y = H, <b>57</b> X = N, Y = Cl, <b>64</b></p>	<p>Milstein 2011 &amp; 2015: <b>57</b> (0.1 mol%), CO<sub>2</sub> and NaHCO<sub>3</sub>, H<sub>2</sub> (8.3 bar), H<sub>2</sub>O/THF (10:1), 80 °C 16 h, TONs up to 788; TOFs up to 156 h<sup>-1</sup></p> <p><b>64</b> (0.1 mol%), CO<sub>2</sub> (3.3 bar) and NaOH (3N) H<sub>2</sub> (6.3 bar), H<sub>2</sub>O/THF (10:1), 55 °C, 16 h TONs up to 388</p>	<p><b>69</b></p>	<p>Peters 2015: <b>69</b> (0.1 mol%) CO<sub>2</sub> (29 atm), H<sub>2</sub> (29 atm), NEt<sub>3</sub>, 100 °C, 20 h</p> <p>TONs up to 200</p>												
<p><b>65</b> R = <i>i</i>Pr, <b>65</b> R = Cy, <b>66</b></p>	<p>Hazari &amp; Bernskoetter 2015: <b>65</b>, CO<sub>2</sub> (69 bar) H<sub>2</sub> (69 bar), DBU/LiOTf (7.5/1), THF, 80 °C, 24 h</p> <p>TONs up to 58990 TOFs up to 2458 h<sup>-1</sup></p>	<p><b>3</b></p>	<p>Zhou 2015: <b>3</b> (0.1 mol%), H<sub>2</sub> (30 bar), NaHCO<sub>3</sub>, 120 °C, EtOH/H<sub>2</sub>O, 24 h</p> <p>TONs up to 447 TOFs up to 19 h<sup>-1</sup></p>												

In 2010, Beller, Laurency and coworkers described the hydrogenation of carbon dioxide and bicarbonates (HCO<sub>3</sub><sup>-</sup>) to formates, alkyl formates and formamides (when the reaction was performed in the presence of alcohols and amines, respectively). Indeed, using an *in situ* formed catalyst [(**35**)FeH][BF<sub>4</sub>] (**60**) from Fe(BF<sub>4</sub>)<sub>2</sub>·6H<sub>2</sub>O (**39**), [P(CH<sub>2</sub>CH<sub>2</sub>PPh<sub>2</sub>)<sub>3</sub>] (**35**) and H<sub>2</sub>, the reduction of sodium bicarbonate led to formate with 88% yield and a TON of 610, when performing the reaction at 80 °C, under 60 bar H<sub>2</sub> for 20 h (Table 1).<sup>[87]</sup> Using the same catalyst, methyl formate was also obtained by hydrogenation of CO<sub>2</sub> in the presence of methanol and an excess of triethylamine, with 56% yield and a TON of 585, and dimethylformamide from dimethylamine with 75% yield and a TON of 727 [P<sub>H<sub>2</sub>/CO<sub>2</sub></sub> = 60/30 bar, 100 °C, 20 h]. When performing the hydrogenation in the presence of ethanol, propanol and diethylamine, ethyl and propyl formates and diethylformamide were produced, respectively, in lower yields (9–28%). Additionally, the *in situ* catalyst obtained from **35** and FeCl<sub>2</sub> (**20**) was also efficient in the hydrogenation of CO<sub>2</sub>.<sup>[88]</sup> Furthermore, the *in situ* catalytic system Fe(BF<sub>4</sub>)<sub>2</sub>·6H<sub>2</sub>O (**39**)/**35** can also promote the reversible reaction by dehydrogenation of formic acid to CO<sub>2</sub> and H<sub>2</sub> without base in high catalytic activity (TOFs up to 9425 h<sup>-1</sup> and TONs up to 92417 at 80 °C with 0.005 mol% of catalyst, Table 1).<sup>[89]</sup> Noticeably, using a *meta*-trisulfonated-tris[2-(diphenylphosphino)ethyl] phosphine sodium salt P[(CH<sub>2</sub>CH<sub>2</sub>P(Ph))(*m*-NaO<sub>3</sub>S-C<sub>6</sub>H<sub>4</sub>)]<sub>3</sub> (**61**) as

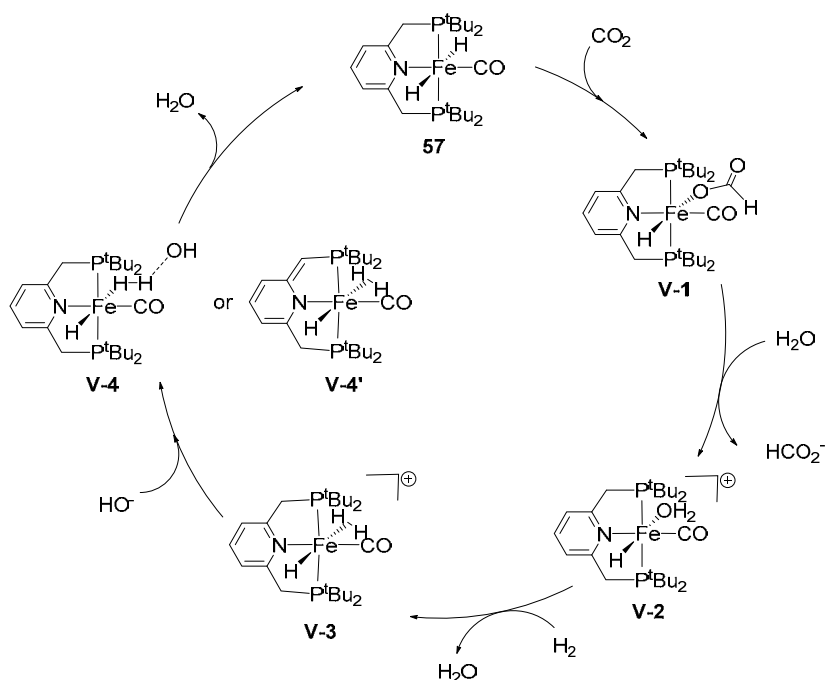
a ligand associated to Fe(II) salts, Laurenczy demonstrated that the hydrogenation of CO<sub>2</sub> can be also promoted in water at r.t.<sup>[90]</sup>

By reaction of the tetradentate tris[2-(diphenylphosphino)phenyl]-phosphine (**62**) and Fe(BF<sub>4</sub>)<sub>2</sub>·6H<sub>2</sub>O (**39**), the air- and thermally stable complex [(**62**)Fe(F)][BF<sub>4</sub>] (**63**), was shown to be one of the most active iron catalysts for the hydrogenation of carbon dioxide and bicarbonates affording formates and formamides with TONs up to 7500 for the hydrogenation of sodium bicarbonate (Table 1).<sup>[91]</sup> Milstein described that *trans*-[Fe(H)<sub>2</sub>(CO) (*t*BuPNP)] (**57**, 0.1 mol% loading) was efficient for the hydrogenation of CO<sub>2</sub> and sodium bicarbonate to formate salts in a 10:1 H<sub>2</sub>O/THF mixture at 80 °C at low pressures (Table 1). The highest TON of 320 (32% formate yield) was obtained for the hydrogenation of bicarbonate performing at 80 °C under 8.3 bar H<sub>2</sub>. The catalytic activity in CO<sub>2</sub> hydrogenation was increased for the reaction under 10 bar pressure (H<sub>2</sub>/CO<sub>2</sub> = 2:1) in an aqueous NaOH/THF solution (TONs up to 788 and TOFs up to 156 h<sup>-1</sup>).<sup>[92]</sup> Similar complex based on the pyrazine backbone [(2,6-bis(di(*tert*-butyl)-phosphinomethyl)pyrazine)Fe(H)(Cl)(CO)] (**64**) was evaluated in the catalytic hydrogenation of CO<sub>2</sub> at 55 °C, but exhibited lower activity (TON = 388, Table 1).<sup>[93]</sup>

Iron PNP pincer complexes (**65**, **66**) which previously shown to exhibit remarkable activities in formic acid dehydrogenation, were also tested for the reverse CO<sub>2</sub> hydrogenation in the presence of a Lewis acid (Table 1).<sup>[94]</sup> The transformation was realized in a DBU/THF solution at 80 °C under 69 bar H<sub>2</sub>/CO<sub>2</sub> (1:1). The addition of lithium triflate (LiOTf) was shown to have a beneficial effect and provided the best results with TON of 58 990. Hazari and Bernskoetter also described similar pincer complexes (**67**) with an aryl isonitrile ligand instead of a carbonyl which exhibited lower activity in the CO<sub>2</sub> hydrogenation (TON = 613, Table 1).<sup>[95]</sup>

Supported by computational, including the initial DFT calculations by Yang,<sup>[96]</sup> and experimental studies with **57**,<sup>[92, 96]</sup> a possible reaction mechanism for the hydrogenation of carbon dioxide was proposed and is outlined in Scheme 33. Resulting from the direct attack of CO<sub>2</sub> on the hydride ligand of **57**, the oxygen-bound formate complex (**V-1**) is obtained. The formate ligand in **V-1** is then easily substituted by a molecule of water, leading to the cationic complex (**V-2**). Under hydrogen pressure, the η<sup>2</sup>-H<sub>2</sub> coordinated species (**V-3**) may be formed. Finally, **V-3**, by reaction with <sup>-</sup>OH, the active species **57** is then regenerated by heterolytic cleavage of the coordinated H<sub>2</sub> in (**V-4**) or by dearomatization and subsequent proton migration in (**V-4'**). Noticeably, theoretical studies showed that the reaction was very dependent on the

choice of the solvent used, protic solvent with a higher ability to solvate the bicarbonate being then best.<sup>[97]</sup>

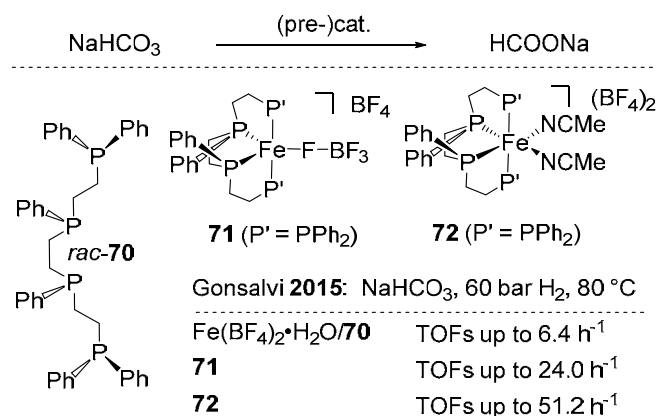


**Scheme 33.** Proposed mechanism for (**57**)-catalyzed CO<sub>2</sub> hydrogenation

Similarly, the groups of Kirchner and Gonsalvi demonstrated that **9** and **68** were good candidates to catalyze the CO<sub>2</sub>/bicarbonate reduction under comparable reaction conditions (Table 1).<sup>[98]</sup> In the case of bicarbonate reduction, a high TON of 1964 (98% conversion) and 4560 (23% conversion) were detected after 24 h under 90 bar of H<sub>2</sub> with catalyst loadings of 0.05 and 0.005 mol%, respectively. The hydrogenation of CO<sub>2</sub> in basic conditions (0.5 M NaOH) proceeded with TONs of up to 1220 and quantitative yields when catalyzed by **9** under 80 bar at 80 °C. The *N*-methylated aminophosphino pincer complex **68** was less active than **9** in the presence of NaOH. Noteworthy, at a lower catalyst loading (0.01 mol%), quantitative formation of formate was still observed at 80 °C, which corresponds to a TON of approximately 10000.

Peters showed that triphosphinoiron chloride complexes including [(SiPR<sub>3</sub>)Fe(Cl)(H)] (**69**, 0.1 mol%) also reacted with CO<sub>2</sub> under elevated pressures of CO<sub>2</sub> (29 atm) and H<sub>2</sub> (29 atm), leading to formate and methylformate (Table 1). When conducting the reaction in the presence of NEt<sub>3</sub> in MeOH at 100 °C for 20 h, (Et<sub>3</sub>NH)(OCHO) and MeOCHO were obtained in 2:1 ratio with TON = 200.<sup>[99]</sup>

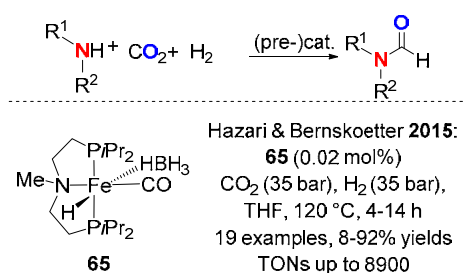
Gonsalvi and co-workers studied both a well-defined iron complex and the *in situ* analogous one prepared from  $\text{Fe}(\text{BF}_4)_2 \cdot 6\text{H}_2\text{O}$  (**39**) bearing the tetradentate 1,1,4,7,10,10-hexaphenyl-1,4,7,10-tetraphosphadecane phosphine (**70**) for bicarbonate hydrogenation (Scheme 34).<sup>[100]</sup> With the catalyst *in situ* prepared from the commercial ligand (**70**) and  $\text{Fe}(\text{BF}_4)_2 \cdot 6\text{H}_2\text{O}$  (**39**), the hydrogenation of sodium bicarbonate in methanol under 60 bar  $\text{H}_2$  at 80 °C for 24 h, was performed leading to the formate in 15% conversion (TON = 154). Under the aforementioned reaction conditions in the presence of propylene carbonate (PC),  $[\text{Fe}(\text{rac-70})\text{BF}_4][\text{BF}_4]$  (**71**), the authors succeeded to obtain the formate in 58% conversion (TON = 575). (**72**) led to an improvement in the bicarbonate conversion up to 76% in the absence of PC, whereas the TON reached a maximum value of 1229 at a higher substrate-to-catalyst ratio of 10000, (12% conversion). High-pressure NMR experiments suggested the formation of  $[\text{Fe}(\text{rac-70})\text{H}]^+$  (**73**) as a key intermediate species whatever the starting complex **71** or **72**.



**Scheme 34.** Structure of **70** and its iron catalysts tested for bicarbonate hydrogenation.

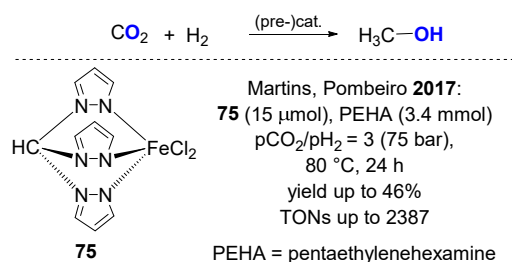
As an alternative to the iron pincer catalyst discussed above, the group of Zhou developed a phosphine-free, air- and moisture-stable iron catalyst **3** active for bicarbonate hydrogenation in basic media (Table 1).<sup>[101]</sup> The highest activity (TON of 447 after 24 h) was obtained for the reduction of sodium bicarbonate in ethanol/water (1:2) under 30 bar  $\text{H}_2$  at 120 °C (yield = 45%). Noticeably, even at lower  $\text{H}_2$  pressure (5 bar), TON of 163 could still be obtained. By contrast, with  $\text{CO}_2$  in the presence of  $\text{NaOH}$ , only traces of sodium formate were formed whatever the pressure applied. It is note mentioning that the complex **3** in association with an iridium complex,  $[\text{Ir}(\text{dF}(\text{CF}_3)\text{ppy})_2(\text{dtbbpy})][\text{PF}_6]$  (IrPS, **74**), used as a photosensitizer and triethanolamine used as a electron/proton donor, can promote the photochemical reduction of  $\text{CO}_2$  to carbon monoxide under visible light at r.t. with initial TOF up to 22.2  $\text{min}^{-1}$ .<sup>[102]</sup> ( $\text{dF}(\text{CF}_3)\text{ppy}$  = cyclometalated 2-(2,4-difluorophenyl)-5-trifluoro-methylpyridine and dtbbpy = 4,4'-di-tert-butyl-2,2'-bipyridyl).





### Scheme 35. Iron-catalyzed *N*-formylation of amines by hydrogen and carbon dioxide

Using the well-defined PNP pincer complex **65** (0.02 mol%), Hazari and Bernskoetter, succeeded recently to perform the selective *N*-formylation of various alkylamine derivatives *via* CO<sub>2</sub> hydrogenation (Scheme 35). Performing the reaction in THF at 120 °C for 4–16 h under 35 bar of CO<sub>2</sub> and 35 bar of H<sub>2</sub>, a large variety of primary and secondary alkylamines led to the corresponding with 8–92% yields and TONs up to 8900.<sup>[103]</sup> Noticeably, mechanistic studies indicated that the transformation proceeded first *via* the reversible reduction of CO<sub>2</sub> to ammonium formate, and then by the its dehydration to formamide.



### Scheme 36. Iron-catalyzed hydrogenation of carbon dioxide to methanol.

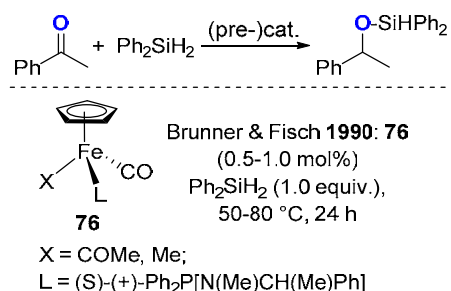
Another interesting target in CO<sub>2</sub> reduction is the production of methanol. Martins and Pombeiro described this reaction using an iron(II) scorpionate catalyst [FeCl<sub>2</sub>{κ<sup>3</sup>-HC(pz)<sub>3</sub>}] (**75**) (pz = 1-pyrazolyl) in solvent-free conditions at 80 °C for 24 h (Scheme 36). Even if the transformation can be promoted in amine free conditions (yields up to 28%), the addition of pentaethylenehexamine increase the efficiency of the transformation. Notably, TONs up to 2.3 × 10<sup>3</sup> were obtained, making this catalyst one of the most efficient for this reaction.<sup>[104]</sup>

## 3. Hydrosilylation

### 3.1. Aldehydes and ketones

Even if the catalyzed hydrogenation or transfer hydrogenation are powerful methodology for the reduction of carbonyl derivatives, for chemoselectivity issues, the hydrosilylation can be an interesting alternative pathway, more particularly when using inexpensive hydrogen sources

such as PMHS and TMDS (1,1,3,3-tetramethyldisiloxane). During the last decade, the area of iron-catalyzed hydrosilylation of aldehydes and ketones has seen an amazing development.

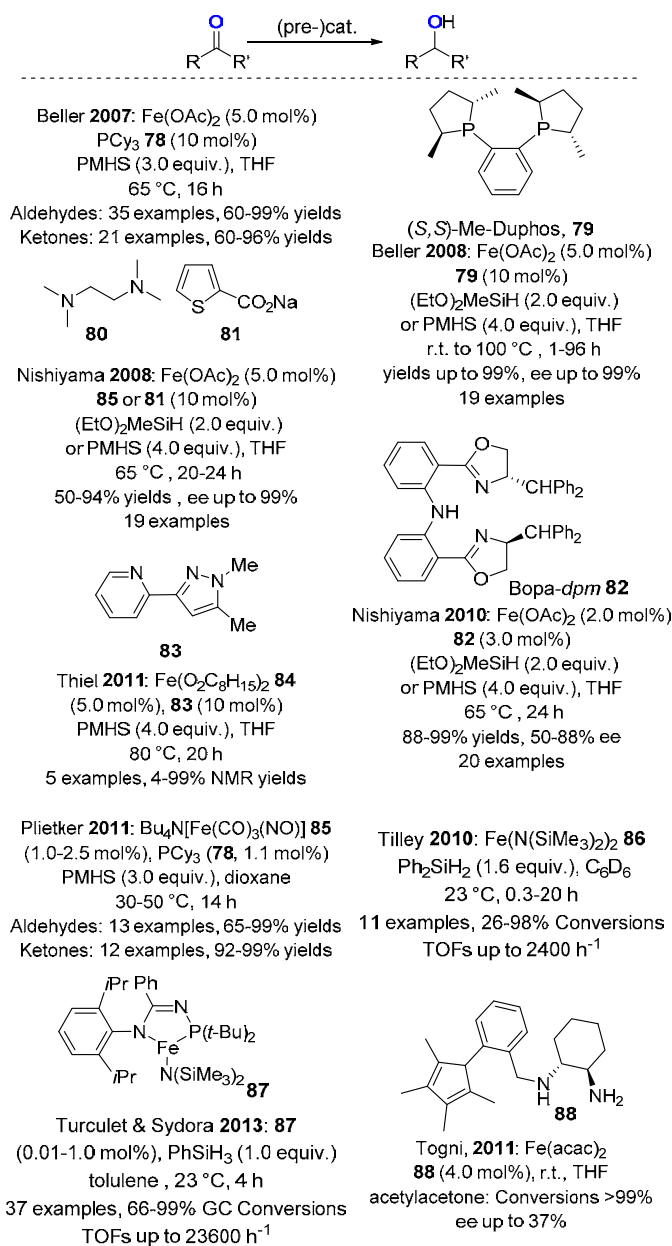


### Scheme 37. Pioneering iron-catalyzed hydrosilylation of acetophenone by Brunner

The early example of the hydrosilylation of ketones catalyzed by iron complexes was reported in 1990 by Brunner and Fisch.<sup>[105]</sup> Indeed, 0.5–1.0 mol% of  $[\text{Fe}(\text{Cp})(\text{CO})(\text{X})(\text{L})]$  (**76**) promoted the reaction of acetophenone with 1.0 equiv. of diphenylsilane at 50–80 °C for 24 h, yielding quantitatively the silylated ether, without the formation of the silylated enol ether (Scheme 37). Two decades later, one of the first efficient and scalable methodology using iron-based catalysts for the hydrosilylation of carbonyl derivatives was described by Beller. Thus, the *in situ* formed catalyst from  $\text{Fe}(\text{OAc})_2$  (**77**, 5.0 mol%) and  $\text{PCy}_3$  (**78**, 10.0 mol%) permitted to conduct the reduction of functionalized (hetero)aromatic and alkyl aldehydes in the presence of 3.0 equiv. of PMHS in THF at 65 °C for 16 h, (35 examples, 60–99% yields, Scheme 38).<sup>[106]</sup> It also catalyzed the reduction of ketones (21 examples, 60–96% yields) after 20 h at 65 °C.<sup>[107]</sup> Interestingly, ester, amino, cyano and  $\alpha,\beta\text{-C}=\text{C}$  moieties were tolerated.

Using the same methodology, an enantioselective version was then developed associating  $\text{Fe}(\text{OAc})_2$  (**77**) and (*S,S*)-Me-Duphos (**79**) as a chiral diphosphine ligand. Thus, using stoichiometric amounts of  $(\text{EtO})_2\text{MeSiH}$  or PMHS at r.t. or 65 °C, aromatic ketones were reduced affording the corresponding alcohols with yields and ee up to 99% (Scheme 38).<sup>[108]</sup> In concomitant contributions, Nishiyama showed that the nitrogen-based ligands such as *N,N,N',N'*-tetramethylethylenediamine (TMEDA, **80**)<sup>[109]</sup> or sodium thiophenecarboxylate (**81**)<sup>[110]</sup> (10 mol%) associated to  $\text{Fe}(\text{OAc})_2$  (**77**, 5.0 mol%) gave an efficient catalyst for the hydrosilylation of ketones under similar conditions (2.0 equiv. of  $(\text{EtO})_2\text{MeSiH}$ ; 65 °C; 20–24 h; 50–94% yields, Scheme 38). Asymmetric hydrosilylation of ketones was experimentally achieved using *N,N,N*-bis(oxazolinyphenyl)-(Bopa) ligands such as Bopa-*dpm* (**82**, 3.0 mol%) in combination with  $\text{Fe}(\text{OAc})_2$  (**77**, 2.0 mol%) and  $(\text{EtO})_2\text{MeSiH}$  as the hydride source (88–99% yields and 50–88% ee, Scheme 38).<sup>[111]</sup> It must be also underlined that when using the preformed complex  $[(\text{77})\text{FeCl}_2]$  (5.0 mol%) in association with zinc powder (6.0 mol%) with

2 equiv. of (EtO)<sub>2</sub>MeSiH under similar conditions, the other enantiomer of the alcohol was obtained.<sup>[112]</sup>



**Scheme 38.** Initial iron based catalysts for hydrosilylation of ketones.

N1-Alkylated 2-(pyrazol-3-yl)pyridines such as (**83**, 10 mol%) by reaction with iron octanoate [Fe(O<sub>2</sub>C<sub>8</sub>H<sub>15</sub>)<sub>2</sub>] (**84**, 5.0 mol%) led also to suitable catalyst precursors for the hydrosilylation of aldehydes and ketones at 80 °C for 20 h in the presence of PMHS with yields up to 99% (Scheme 38).<sup>[113]</sup> Furthermore, Plietker *et al.* described a catalyst prepared *in situ* from PCy<sub>3</sub> (**78**) and the [Bu<sub>4</sub>N][Fe(CO)<sub>3</sub>(NO)] complex<sup>[114]</sup> (**85**), (which is used with success in allylic substitution reactions<sup>[115]</sup>), also highly active for the hydrosilylation of numerous functionalized aldehydes and ketones in the presence of PMHS (Scheme 38). The

corresponding alcohols were produced in moderate to excellent yields [aldehydes (65–99%); ketones (92–99%)], at low catalyst loadings [**85** (1.0–2.5 mol%); PCy<sub>3</sub> (**78**) (1.1 mol%)] at 30–50 °C for 14 h.<sup>[116]</sup>

In terms of activity, Tilley achieved a breakthrough. Indeed, the simple low valent but highly air-sensitive iron silylamide complex [Fe(N(SiMe<sub>3</sub>)<sub>2</sub>)<sub>2</sub>] (**86**, 0.01–2.7 mol%), catalyzed efficiently the hydrosilylation of various aldehydes and ketones in the presence of 1.6 equiv. of Ph<sub>2</sub>SiH<sub>2</sub> at 23 °C for 0.3–20 h (Scheme 38). Remarkably, TOFs up to 2400 h<sup>-1</sup> can be reached for the reduction of 3-pentanone, and the reaction tolerated functional groups such as nitrile, cyclopropyl or C=C bond (Scheme 38).<sup>[117]</sup> The related iron(II) bis-(trimethylsilyl)amido complexes (**87**) coordinated to a *N*-phosphinoamidate ligand (0.015–1.0 mol%) promoted the hydrosilylation of a range of aldehydes and ketones in the presence of 1.0 equiv. of phenylsilane (Scheme 38).<sup>[118]</sup> Noteworthy, a significant beneficial influence of the ligand on the activity was increased with TOFs up to 23600 h<sup>-1</sup> for the reduction of acetophenone (to be compared to 1266 h<sup>-1</sup> with **86**). Togni has shown that an *in situ* formed catalyst from cyclopentadienyl-bearing chiral diamine (**88**) and Fe(acac)<sub>2</sub> (**89**) promoted the reduction of ketones affording the corresponding alcohols with conversion up to 99% but with low to moderate ee up to 37% (Scheme 38).<sup>[119]</sup>

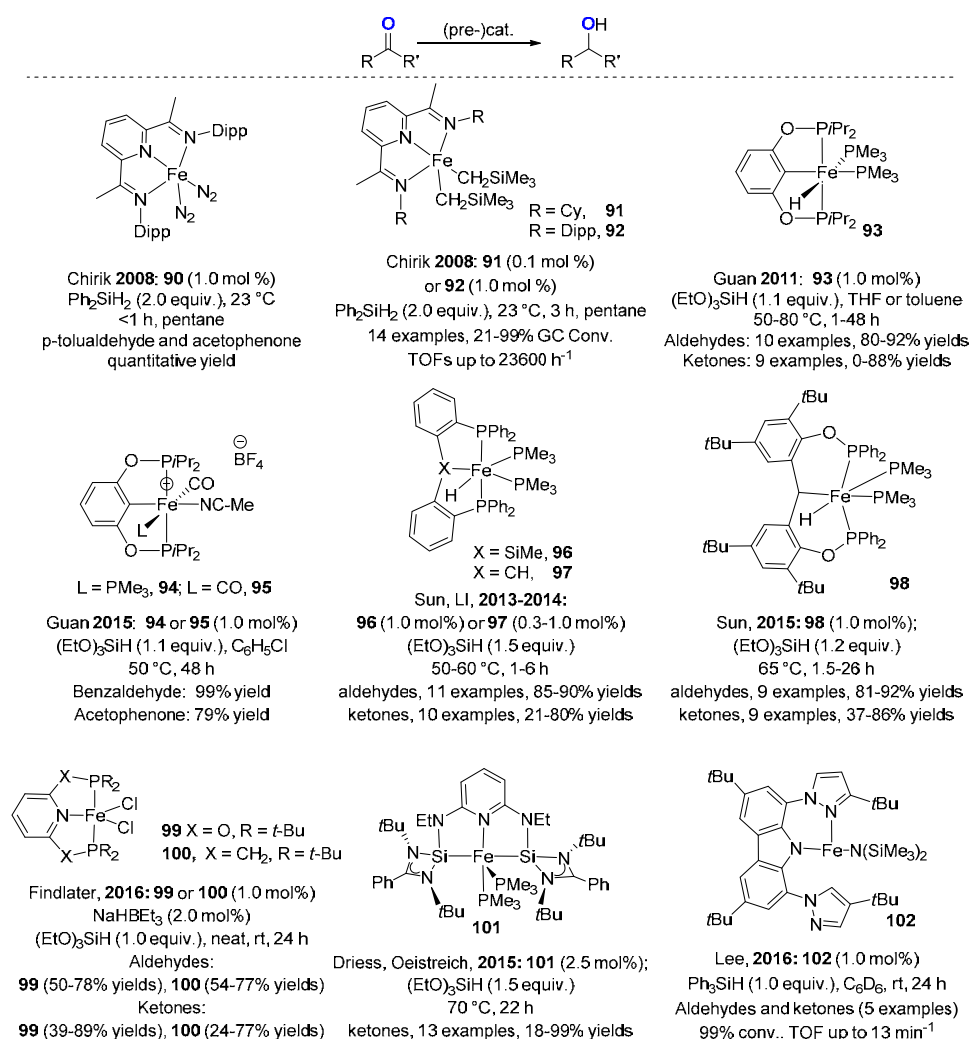
Pincer type iron complexes, which are usually more stable and efficient in hydrogenation, were also extensively reported in hydrosilylation of carbonyl compounds.

The first contribution by Chirik in 2008, described a family of highly active bis(imino)pyridine(PDI) iron complexes such as [Fe(*i*PrPDI)(N<sub>2</sub>)<sub>2</sub>] **90**, already identified as catalysts for the hydrogenation and hydrosilylation of alkenes, was also active in the hydrosilylation of *p*-tolualdehyde and acetophenone with Ph<sub>2</sub>SiH<sub>2</sub> in pentane at 23 °C in 1 h (Scheme 39).<sup>[120]</sup>

Using the iron dialkyl complexes (**91**, 0.1 mol%) or (**92**, 1.0 mol%) under similar conditions (2.0 equiv. Ph<sub>2</sub>SiH<sub>2</sub>, pentane, 23 °C, 3 h), numerous ketones including cyclohexanones were efficiently reduced (Scheme 39).<sup>[120]</sup> Noteworthy, cyclohexenones were chemoselectively reduced to the corresponding unsaturated alcohols, although acyclic enones led to the allylic alcohols in a less selective manner. Furthermore, this catalytic system is highly active exhibiting one of the highest TOF up to 23600 h<sup>-1</sup>.

In 2011, Guan designed new iron hydride complexes coordinated to phosphinite-based pincer ligands (POCOP) such as **93** applicable in the catalytic hydrosilylation of aldehydes and ketones (Scheme 39).<sup>[121]</sup> Full conversion of benzaldehyde was reached at 50 °C for 1 h using

1.0 mol% of catalyst **93** and of 1.1 equiv. of (EtO)<sub>3</sub>SiH. For the hydrosilylation of ketones such as acetophenone, a higher temperature (80 °C for 4.5 h) was necessary to observe full conversion; the corresponding alcohols were then obtained in up to 88% yield. This system was appropriate for the hydrosilylation of aromatic and aliphatic aldehydes (80–92% yields at 50–65 °C for 1–36 h) and aromatic ketones (0–88% yields at 50–80 °C for 4.5–48 h). Noticeably, the decoordination of PMe<sub>3</sub> or CO ligand in an initial step seems to be crucial step in order to generate the active catalytic species. Noticeably, similar activities were obtained with cationic pincer iron complexes (**94** and **99**).<sup>[122]</sup>



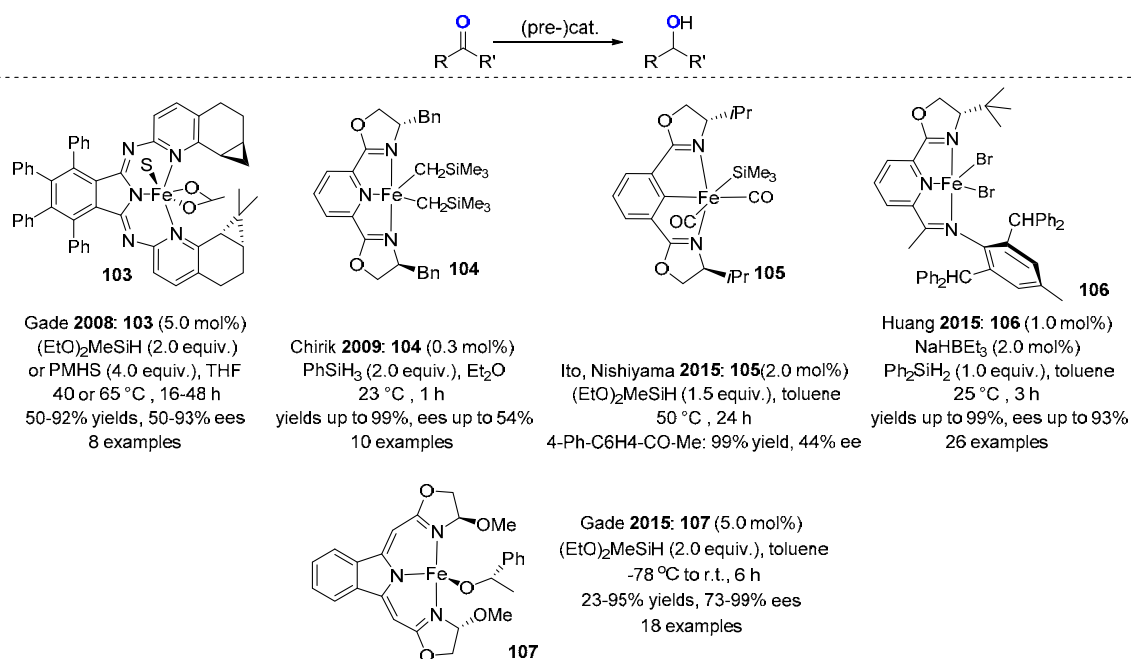
### Scheme 39. Pincer iron catalysts for hydrosilylation of carbonyl derivatives

Similarly, tridentate PSiP (**96**)<sup>[123]</sup> and PCP (**97**)<sup>[124]</sup> and (**98**)<sup>[125]</sup> ligand based iron pincer complexes can be used under mild conditions in hydrosilylation (Scheme 39). Thus, using 1.0 mol% of **96** and 1.5 equiv. of (EtO)<sub>3</sub>SiH, the reduction of aldehydes and ketones can be performed at 60 °C in 1 h and in 6 h, respectively. Slightly higher activities are obtained with the complex **97** at 50 °C (aldehydes: 0.3–1.0 mol% **97**, 1–13 h, 85–90 % yields; ketones:

1.0 mol% **97**, 16 h, 21–90% yields). Findlater prepared similar structural iron complexes, (2,6-bis(di-*tert*-butyl-phosphinito)pyridine) [(*t*BuPONOP)FeCl<sub>2</sub>] (**99**) and (2,6-bis(di-*tert*-butyl-phosphinomethyl)pyridine) [(*t*BuPNP)FeCl<sub>2</sub>] (**100**) complexes which were more active in hydrosilylation of aldehydes and ketones by reaction with 1.5 equiv. of (EtO)<sub>3</sub>SiH at r.t. for 24 h.<sup>[126]</sup>

Noticeably, unusual pincer iron complexes were also reported in catalytic hydrosilylation. Driess and Oestreich reported a disilylene pyridine SiNSi pincer complex (**101**) which exhibited catalytic activity towards the hydrosilylation of ketones (Scheme 39). Noticeably, it was shown that the transition metal in the catalytic species does not seem to be directly involved in the catalytic process. By contrast, the activation of the ketone and silane should happen in the ligand sphere, *i.e.* at silicon.<sup>[127]</sup>

Recently, Lee described the use of a low-coordinate iron(II) complex bearing an NNN-pincer ligand (**102**, 1.0 mol%) for the hydrosilylation of aldehydes and ketones using phenylsilane (1 equiv.) at r.t. for 24 h (Scheme 39). TOFs up to 13 min<sup>-1</sup> were observed showing the good efficiency of such catalyst.<sup>[128]</sup>



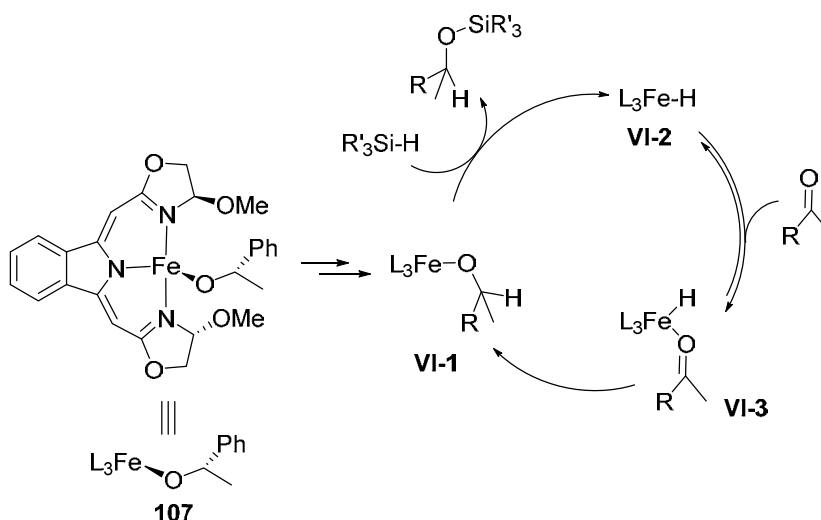
#### Scheme 40. Chiral pincer iron catalysts for asymmetric hydrosilylation of ketones

On the other hand, chiral pincer iron complexes have been developed for asymmetric hydrosilylation of ketones. In 2008, Gade reported a [Fe(tetraphenyl-carbpi)(OAc)] complex (**103** 5.0 mol%), able to promote the reduction using (EtO)<sub>2</sub>MeSiH or PHMS as the hydrosilane at 40–65 °C leading to the corresponding alcohols in 50–93% ee (Scheme 40).<sup>[129]</sup> To date, it is still one of the most efficient catalysts in terms of enantioselectivity and activity.

In 2009, Chirik has described a chiral tridentate bis-(oxazolynyl) ligated  $[(S,S)\text{-}(i^{\text{Pr}}\text{pybox})\text{-Fe}(\text{CH}_2\text{SiMe}_3)_2]$  complex (**104**) (0.3 mol%) able to catalyze the asymmetric hydrosilylation of ketones with 2.0 equiv. of  $\text{PhSiH}_3$  and 0.95 equiv. of  $\text{B}(\text{C}_6\text{F}_5)_3$  at 23 °C for 1 h, exhibiting ee up to 54% (Scheme 40).<sup>[130]</sup>

Similarly, in 2015, Nishiyama and Ito reported a bis-(oxazolynyl) ligated iron complex (**105**) with lower enantioselectivity (up to 44% ee) under relatively similar conditions (Scheme 40).<sup>[131]</sup> Modifying the structure of one arm of the Pybox ligand, Huang designed an unsymmetrical oxazolynyl-imino pyridine iron complex (**106**) able to enhance the enantioselectivity of the hydrosilylation (Scheme 40). Activating the complex **106** (1.0 mol%) with 2.0 mol% of  $\text{NaHBET}_3$ , in the presence of 1.0 equiv. of  $\text{Ph}_2\text{SiH}_2$  at 25 °C for 3 h, ee values increased up to 93%.<sup>[132]</sup>

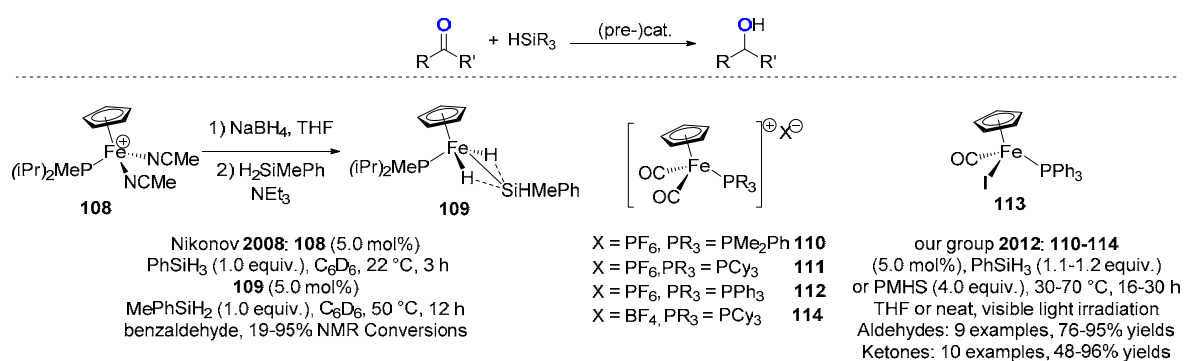
In 2015, Gade described a general and highly efficient asymmetric hydrosilylation of ketones using 5.0 mol% of chiral iron alkoxide pincer complex (**107**) in the presence of 2.0 equiv. of  $(\text{EtO})_2\text{MeSiH}$  in toluene in a temperature range from -78 °C to r.t. for 6 h (Scheme 40). Importantly, unprecedented activities and stereoselectivities were obtained in hydrosilylation area with TOF up  $240\text{ h}^{-1}$  at -40 °C, with 73–99% ee for numerous alkyl aryl ketones.<sup>[133]</sup>



**Scheme 41.** Mechanistic proposal for iron-catalyzed hydrosilylation of ketones

A detailed mechanism study of the catalytic cycle demonstrated that the rate-determining step is a  $\sigma$ -bond metathesis of the alkoxide complex (**VI-1**) with the hydrosilane, leading to an iron hydride species (**VI-2**) and generating the alkoxy silane compounds (Scheme 41). The subsequent coordination then insertion of the ketone to the iron hydride bond then regenerated the catalytic alkoxy species **VI-1**.<sup>[134]</sup>

Cyclopentadienyl piano-stool iron(II) complexes are another family of molecular-defined iron complexes widely studied in hydrosilylation reactions. Following the pioneering work of Brunner in the early 1990s,<sup>[105]</sup> in 2008, Nikonov reported an unusual and new iron silyl dihydride complex (**109**, 5.0 mol%) active for the hydrosilylation of benzaldehyde with H<sub>2</sub>SiMePh at 50 °C for 12 h (Scheme 42).<sup>[135]</sup> Noteworthy, the parent cationic complex (**108**, 5.0 mol%) was also efficient in hydrosilylation of benzaldehyde with PhSiH<sub>3</sub> at 22 °C for 3 h.



#### Scheme 42. Cyclopentadienyl iron phosphine based complexes

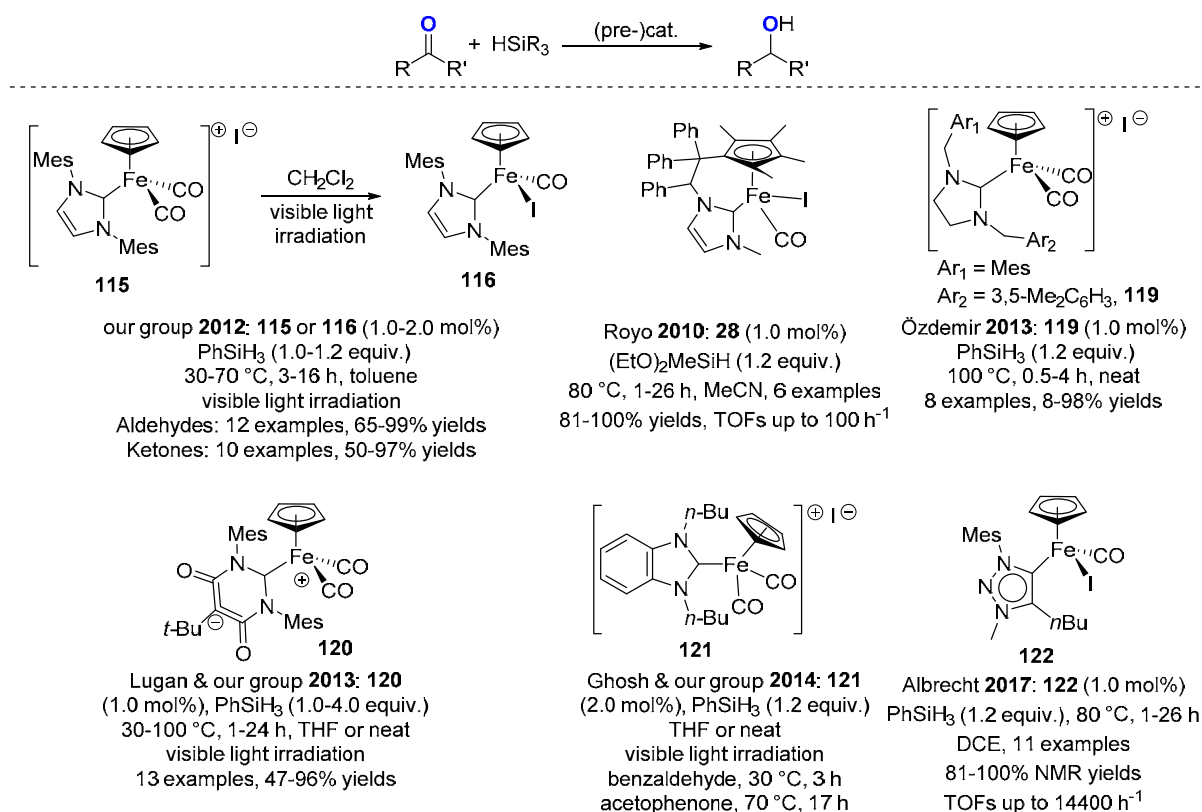
Our group has developed an analogous series of cationic carbonyl complexes [Fe(Cp)(CO)<sub>2</sub>(PR<sub>3</sub>)]<sup>+</sup>[X]<sup>-</sup> (**110-114**, Scheme 42) which successfully catalyzed the hydrosilylation of both aldehydes and ketones. Using 5.0 mol% of catalysts **110-112** and 1.1 equiv. of phenylsilane at 30 °C for 16 h under continuous visible light irradiation, the reduction of benzaldehyde derivatives proceeded with excellent conversions either in THF (92–98%) or under neat conditions (91–97%). Importantly, PMHS (4.0 equiv.) could also be used in the presence of 5.0 mol% of complexes **110-112** under similar conditions in THF: the best conversion reached 95%. In this series, the best catalyst identified for the reduction of acetophenone was the neutral iron complex [CpFe(CO)(I)(PPh<sub>3</sub>)] (**113**) which exhibited higher activity in the presence of 1.2 equiv. of phenylsilane under neat conditions and visible light activation and slightly harsher conditions (70 °C, 30 h). Noticeably, the tetrafluoroborate complex (**114**, 5.0 mol%) exhibited similar or superior activities compared to the iodo- or hexafluorophosphate analogs. (e.g. acetophenone: 98% conversion, visible light activation, 70 °C, 16 h with 1.2 equiv. of PhSiH<sub>3</sub> or 72 h with 4.0 equiv. of PMHS). It is important to notice that visible light activation is required in order to favor the decooordination of one CO ligand and then generate an unsaturated active species.

Cyclopentadienyl piano-stool iron(II) complexes, particularly when associated to *N*-heterocyclic carbene ligands (NHC), are another important series of efficient catalysts extensively developed for the hydrosilylation of carbonyl derivatives.<sup>[137]</sup> Following the pioneering contribution of Brunner, in 2010, Royo reported the activity of tethered Cp-NHC



iron complexes (e.g. **28**, 1.0 mol%) for the hydrosilylation of activated aldehydes (6 examples) with 1.2 equiv. of (EtO)<sub>2</sub>MeSiH in acetonitrile at 80 °C for 1–18 h (Scheme 43).<sup>[38a]</sup>

Our group has designed a series of NHC-piano-stool iron complexes including the cationic complex [Fe(CO)<sub>2</sub>(IMes)][I] (**115**), and the neutral complex [Fe(I)(CO)(IMes)] (**95**), which was selectively obtained by visible photo irradiation of **115** in CH<sub>2</sub>Cl<sub>2</sub> (Scheme 43). They were efficient in the reduction of both aldehydes and ketones using 1.0 equiv. of PhSiH<sub>3</sub> (aldehydes, THF, 30 °C, 3 h, 88–99% conversion; ketones, toluene, 70 °C, 16 h, 50–99% conversion).<sup>[138]</sup> Notably, lower activities were obtained with ketones, electron deficient acetophenone derivatives being easier to reduce.



**Scheme 43.** Representative Cp-NHC iron complexes for catalyzed hydrosilylation reactions

It must be underlined that the visible light activation is required to generate the active catalyst from the cationic complex **115** albeit neutral complex **116** was active at 30 °C without activation. When conducting the transformation under solvent-free conditions and light irradiation, significant rate enhancements were obtained as the reactions proceeded with higher conversions and yields and at lower temperatures (50 °C *versus* 70 °C).<sup>[139]</sup> Interestingly, nitrile, amine and alkene groups were tolerated.

Furthermore, NHC ligands such as IMes exhibited a significant influence on the activity and this effect was clearly demonstrated: when using **115** *versus* [Fe(Cp)(CO)<sub>2</sub>]<sub>2</sub> (**117**) or

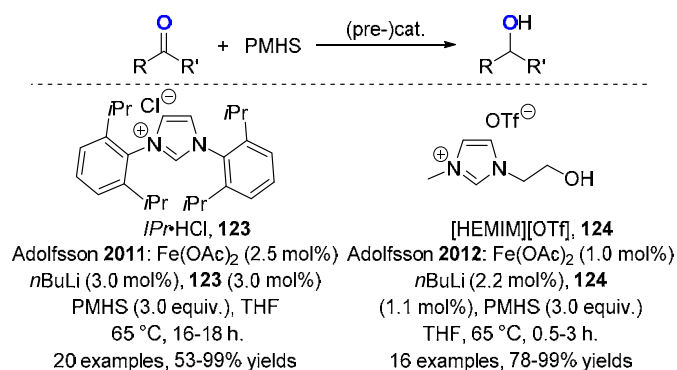
[Fe(Cp)(I)(CO)<sub>2</sub>] (**118**) precursors as the catalysts for benzaldehyde reduction, after 3 h at 30 °C, the conversions are > 97 % for **115** vs <10 % for **117** and **118**. [CpFe(CO)<sub>2</sub>]<sub>2</sub> **117** was shown to catalyze similar hydrosilylations but harsher conditions [5.0 mol% of **117**, 2.0 equiv. of (EtO)<sub>2</sub>MeSiH, 100 °C, 24 h for both aldehydes and ketones, Scheme 43].<sup>[140]</sup>

The architecture of the NHC ligand has also a great influence on the activity of the corresponding [Fe(Cp)(NHC)(CO)<sub>2</sub>][I] precatalyst in the hydrosilylation. Indeed, A series of piano-stool iron complexes coordinated to 1,3-disubstituted imidazolidin-2-ylidene ligands [Fe(Cp)(CO)<sub>2</sub>(NHC)][I] (e.g. **119**) have shown moderate activity as full conversions were obtained only at 100 °C (PhSiH<sub>3</sub>, 0.5–4 h, neat conditions, without light activation) (Scheme 43).<sup>[141]</sup>

By contrast, the complex [Fe(Cp)(NHC)(CO)<sub>2</sub>] (**120**, 1.0 mol%) with a cyclic, six-membered *N*-heterocyclic carbene ligand incorporating a malonate backbone efficiently performed the hydrosilylation of aromatic aldehydes using 1.0 equiv. of diphenylsilane at 30 °C (full conversion after 1–3 h) and for reduction of acetophenone derivatives in the presence of 1.0 equiv. of phenylsilane at 70 °C (37–98% conversions after 16 h), thus exhibiting comparable activity than **115** (Scheme 43).<sup>[142]</sup> Likely, benzimidazole based NHC iron complexes such as **121** (2.0 mol%) showed analogous activity for the hydrosilylation of benzaldehyde at 30 °C within 3 h and acetophenone at 70 °C within 17 h (1.2 equiv. PhSiH<sub>3</sub>, visible light irradiation, neat, Scheme 43).<sup>[143]</sup>

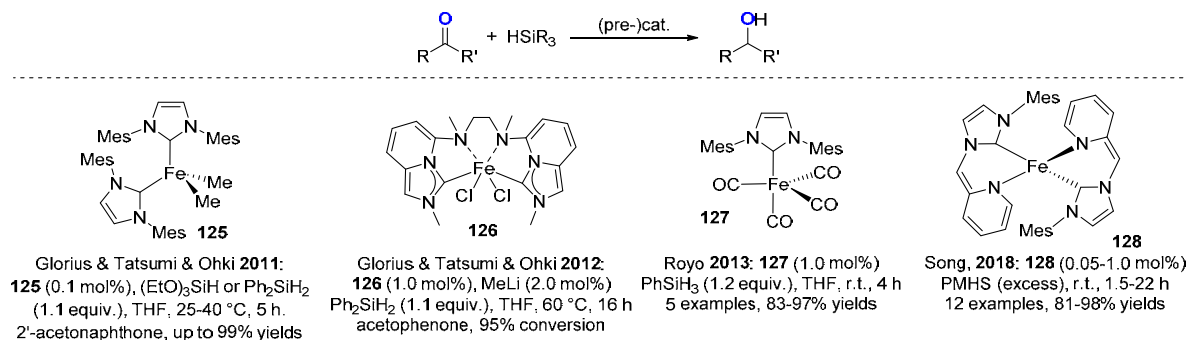
In 2017, Albrecht has developed a new series of 1,2,3-triazolylidene iron(II) piano stool complexes such as **122** which exhibited high activity in the hydrosilylation of aldehydes and ketones: under relatively mild conditions (1,2-dichloroethane, 60 °C), in the presence of 1.2 equiv. of phenylsilane, TOFs up to 14400 h<sup>-1</sup> at 0.1 mol % catalyst loading (for the hydrosilylation of 4-bromobenzaldehyde) were obtained, which notably an induction period of 20–30 minutes (Scheme 43). Preliminary mechanistic investigations suggested the formation of radical species and the involvement of SET type mechanism for the hydrosilanes activation.<sup>[144]</sup>

Adolfsson has shown that an *in situ* prepared iron complexes, starting from iron(II) acetate salt and the imidazolium salt precursors *IPr*·HCl (**123**) or *N*-hydroxyethyl-imidazolium (**124**) in the presence of a base such as *n*-BuLi can be also used efficiently for the hydrosilylation of ketones with 3.0 equiv. of PHMS in THF at 65 °C (Scheme 44).<sup>[145]</sup> Importantly, the exact stoichiometry imidazolium salts / base is crucial, as simple alkoxide salts are also known to promote catalytic hydrosilylations with trisubstituted silanes.



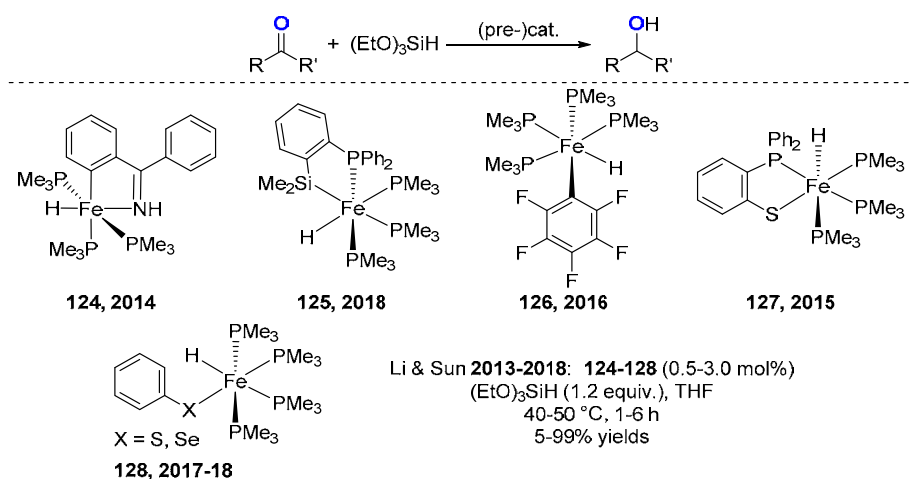
**Scheme 44.** Adolfsen's catalytic system for hydrosilylation of ketones

Alternatively, the square planar low valent NHC iron complex [Fe(Me)<sub>2</sub>(IMes)<sub>2</sub>] (**125**, 0.1 mol%) showed good activity for the hydrosilylation of 2'-acetonaphthone in THF (1.1 equiv. of (EtO)<sub>3</sub>SiH, 25 °C, 5 h or 1.1 equiv. of Ph<sub>2</sub>SiH<sub>2</sub>, 40 °C, 5 h, Scheme 45). Noteworthy, **125** (1.0 mol%) was also efficient in TH at 70 °C in the presence of 1.2 equiv. of *i*PrOLi in *i*PrOH.<sup>[146]</sup> Similarly, hydrosilylation of acetophenone can be performed using the iron complex (**126**) bearing a diamine-bridged bis-NHC (1.0 mol%) in association with MeLi (2.0 mol%, used to generate a Fe-Me species) (THF, 1.1 equiv. of Ph<sub>2</sub>SiH<sub>2</sub>, 60 °C, 16 h, 95% conversion, Scheme 45).<sup>[147]</sup>



**Scheme 45.** Representative NHC-iron based catalysts for hydrosilylation reactions

NHC-Iron(0) can be suitable catalysts for hydrosilylation of carbonyl derivatives. Thus, Royo reported this ability of the [Fe(CO)<sub>4</sub>(IMes)] complex (**127**, 1.0 mol%) to reduce benzaldehyde derivatives with 1.2 equiv. of phenylsilane at r.t. for 4 h, and a good reducible functional group tolerance was shown (e.g. ketones, nitriles, nitro groups) (Scheme 45).<sup>[148]</sup> Song described four coordinate picolyl-functionalized NHC iron complex (**128**) which were able to promote the hydrosilylation of ketones (Scheme 45). Using 0.05–1.0 mol% of **128** in the presence of an excess of PMHS at r.t., ketones such as arylmethylketones, or dialkylketones were reduced to alcohols in 81–98% yields.<sup>[149]</sup>

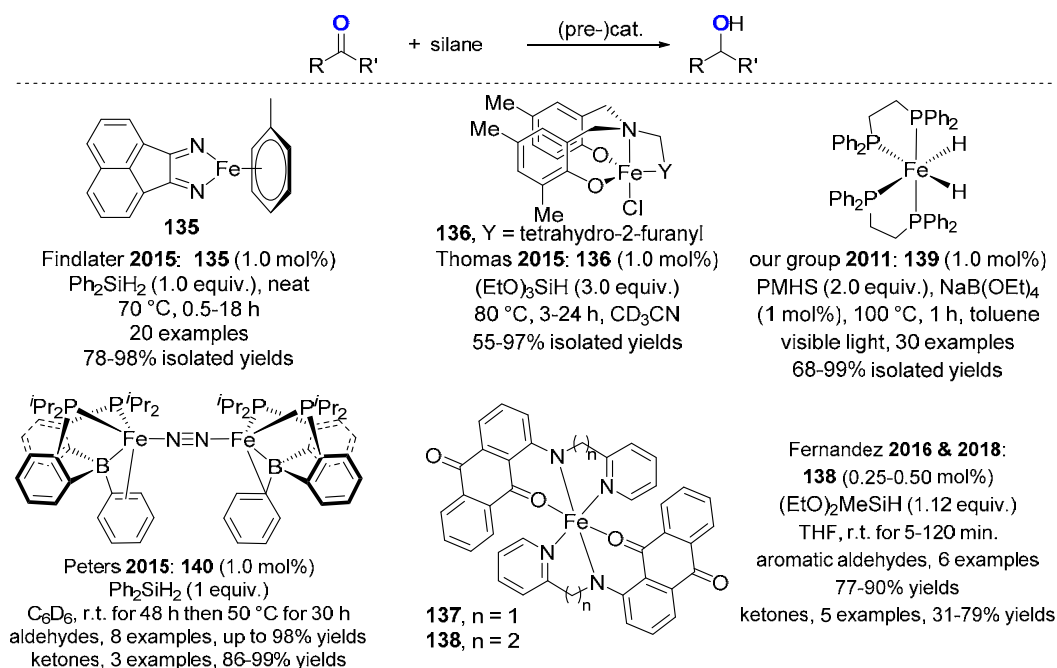


#### Scheme 46. Fe(PMe<sub>3</sub>)<sub>4</sub> based complexes as catalysts in hydrosilylation reactions

Li and Sun's group did intensive work on the design and catalytic use of a series of Fe(PMe<sub>3</sub>)<sub>4</sub> (**129**) based complexes. Thus, they reported the use of cyclometallated iron complexes such as the hydrido iron complex (**130**) as a catalyst (0.3–0.6 mol%) in the presence of 1.2 equiv. of (EtO)<sub>3</sub>SiH in THF at 55 °C for the reduction of aldehydes and ketones yielding the alcohols in 65–92%<sup>[150]</sup> (Scheme 46). Other similar iron hydride complexes like (**128**),<sup>[151]</sup> (**132**),<sup>[152]</sup> (**133**),<sup>[153]</sup> (**134**),<sup>[154]</sup> were also be applied in hydrosilylation reactions under similar conditions giving comparable activities (Scheme 46).

In 2015, another iron(0) complex, the bis(imino)acenaphthene iron arene complex, [BIAN-Fe(C<sub>7</sub>H<sub>8</sub>)] (**135**) (1.0 mol%) was shown to be an active catalyst using Ph<sub>2</sub>SiH<sub>2</sub> (1.0 equiv.) at 70 °C under solvent-free conditions exhibiting broad functional group tolerance (Scheme 47).<sup>[155]</sup> Iron(III) based complexes were identified as good catalysts for hydrosilylation reactions. Thomas has then shown that the amine–bis(phenolate) iron(III) (**136**) (1.0 mol%) with (EtO)<sub>3</sub>SiH (3.0 equiv.) at 80 °C, 3–24 h promoted the hydrosilylation of both ketones and aldehydes with wide functional group tolerance and 55–97% yields (Scheme 47).<sup>[156]</sup>

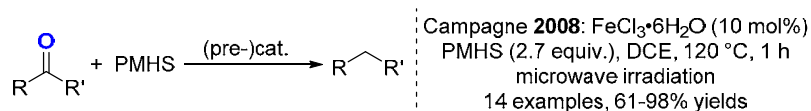
Fernandez described iron complexes based on anthraquinonic ligands (**137**)<sup>[157]</sup> and (**138**)<sup>[158]</sup> which was active in hydrosilylation of aldehydes and ketones. More particularly, the complex (**138** 0.25–0.5 mol%) exhibited TOF up to 63 min<sup>−1</sup> when performing the reaction at r.t. for 5–120 min. in the presence of 1.12 equiv. of (EtO)<sub>2</sub>MeSiH. Both aromatic aldehydes and ketones (such as cyclohexanone or benzophenone) were reduced (Scheme 47).



### Scheme 47. Various iron complexes for the hydrosilylation of carbonyl derivatives

In 2011, our group reported a general and efficient hydrosilylation of aldehydes and ketones to the corresponding alcohols using the well-defined complex [(dppe)<sub>2</sub>Fe(H)<sub>2</sub>] (**139**, 0.1–1.0 mol%) as the pre-catalyst using PMHS (2.0 equiv.) as the reducing agent and NaB(OEt)<sub>4</sub> (1.0 mol%) as a co-catalyst under visible light irradiation (Scheme 47).<sup>[159]</sup> This iron catalyst was tolerant towards numerous functional groups and worked well under various conditions (from 5 h at r.t. to 8 min. at 100 °C, TONs up to 1000 and TOFs up to 600 h<sup>−1</sup>).

In 2015, Peters described a bis(*o*-diisopropylphosphinophenyl)phenylborane iron complex (**140**, 1.0 mol%) able to catalyze hydrosilylation of aldehydes and ketones by reaction with 1 equiv. of diphenylsilane at r.t. for 48 h than at 50 °C for 30 h leading after quench to the corresponding alcohols with 86–99% yields (Scheme 47).<sup>[160]</sup>

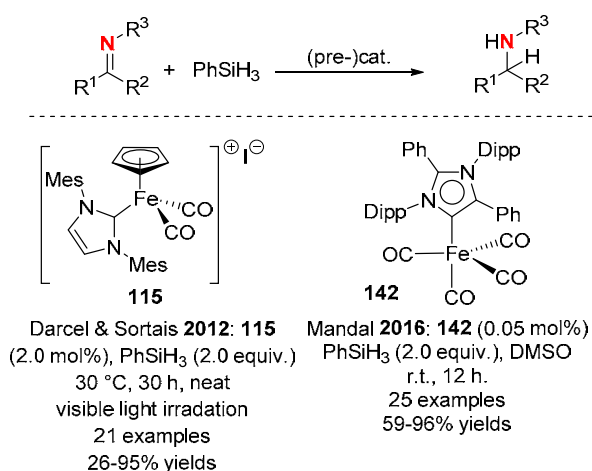


### Scheme 48. Unusual chemoselectivity in hydrosilylation of carbonyl compounds

Finally, in this area, Campagne discovered an unusual reactivity, using the association of PMHS (2.7 equiv.) and FeCl<sub>3</sub>·6H<sub>2</sub>O (**141**, 10 mol%) in 1,2-dichloroethane (DCE) under microwave irradiation: after a reaction at 120 °C for 1 h, aldehydes and ketones were converted to the corresponding methylene derivatives in 62–98% yields (Scheme 48).<sup>[161]</sup>

### 3.2. Imines

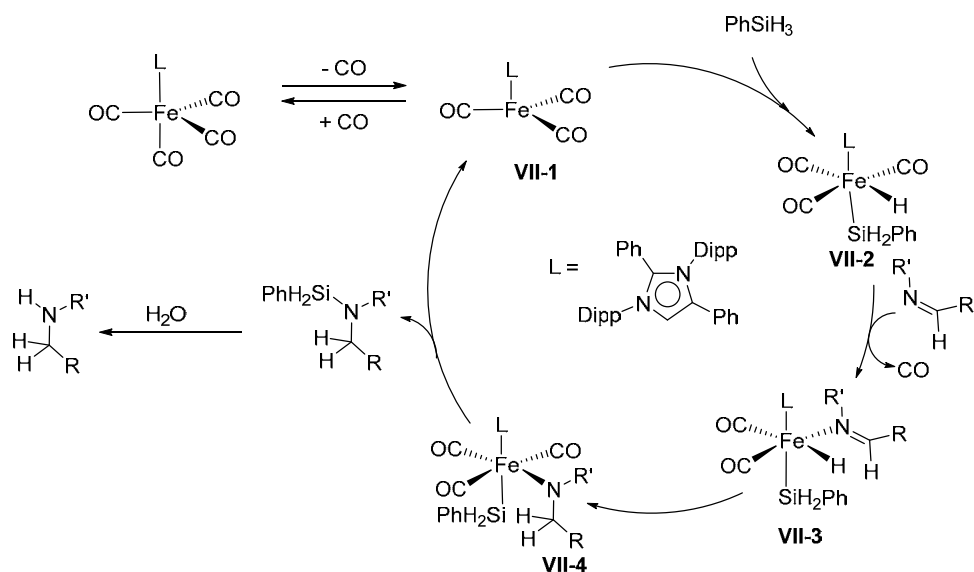
In the field of hydrosilylation of imines, only scarce general methodologies of iron-catalyzed hydrosilylation of aldimines and ketimines were described. The first report was published in 2012 using 2.0 mol% of the complex  $[\text{Fe}(\text{Cp})(\text{IMes})(\text{CO})_2][\text{I}]$  **115** and 2.0 equiv. of phenylsilane, under solvent free conditions and light irradiation at 30 °C for 30 h, a large range of aldimines were reduced leading to the corresponding amines after a basic treatment (Scheme 49).<sup>[162]</sup> Numerous functional groups were tolerated, including halides (I, Br, Cl), ketones, esters and alkenes. Slightly harsher reaction conditions were required to reduce efficiently ketimines: 24 h at 100 °C under neat conditions with higher catalyst loading (5.0 mol%) (57–95% yields).



**Scheme 49.** Iron-catalyzed hydrosilylation of imines.

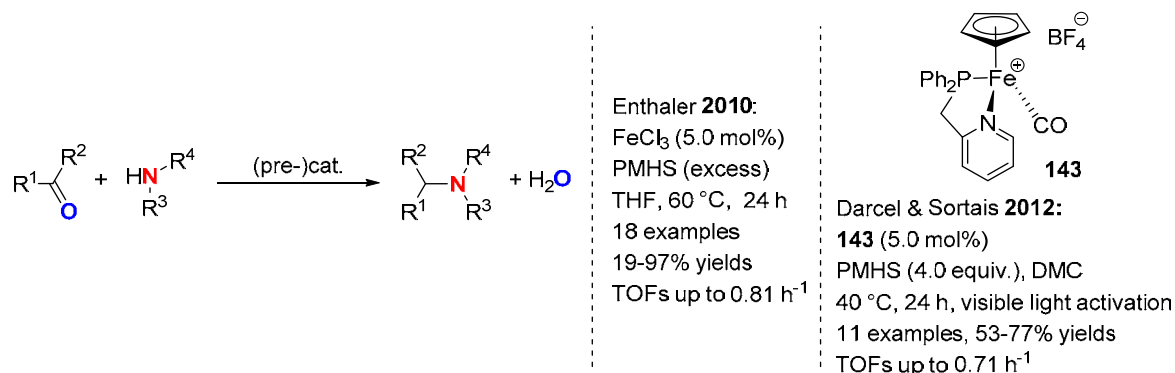
By designing the NHC ligand, Mandal reported a highly active abnormal-NHC–Fe(0) complex (**142**) for reduction of imines (Scheme 49). Using a very low catalyst loading (down to 0.005 mol %) and 2.0 equiv. of phenylsilane in DMSO at r.t., imines were obtained with TON up to 17000.<sup>[163]</sup> Noteworthy, a broad functional group tolerance was shown and interestingly the reduction of imines bearing *N*-alkylated *O*-protected sugars was possible. By contrast, to reduce ketimines, 2.0 mol% of (**142**) was required.

In a mechanistic point of view, the proposed catalytic cycle follows the classic Chalk-Harrod pathway and was supported by DFT calculations. One CO ligand of **142** is released in order to generate a 16 electron species (**VII-1**) able to perform an oxidative addition of PhSiH<sub>3</sub> leading to the iron hydride species (**VII-2**). The intermediates (**VII-3**) is then obtained after decoordination of one CO ligand and coordination of the imine derivative, which is subsequently inserted by a hydride migration leading to (**VII-4**). After reductive elimination, **VII-1** is regenerated and the silylated amine produced (Scheme 50).



**Scheme 50.** Proposed mechanism of an iron-catalyzed hydrosilylation of imines

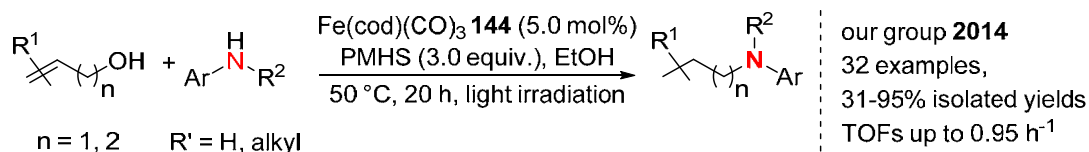
Among methodologies to synthesize amines in a large scale, the direct reductive amination (DRA) of aldehydes and ketones, using stoichiometric alkali reducing agents such as  $\text{LiAlH}_4$  or  $\text{NaBH}_4$  is certainly one of the most efficient. An interesting alternative is the transition metal catalyzed DRA, with a special interest using earth abundant ones, mainly under hydrogenation conditions. Noticeably, iron-catalyzed DRA can also be performed under hydrosilylation conditions. In 2010, Enthaler reported the first DRA of aldehydes by anilines catalyzed by  $\text{FeCl}_3$  (**59**, 5.0 mol%) with a large excess of PMHS in THF at 60 °C for 24 h (Scheme 51).



**Scheme 51.** Iron-catalyzed DRA reactions under hydrosilylation conditions.

By contrast, no reaction occurred with alkylamines such as benzylamine.<sup>[164]</sup> Using PMHS and molecular-defined Cp phosphanyl-pyridine iron complexes such as (**143**, 5.0 mol%), DRA of benzaldehydes and secondary amines in dimethylcarbonate (DMC) at 40 °C for 24 h under visible light irradiation, produced the corresponding tertiary amines in 53–93% yields (Scheme 51). Good functional group tolerance was observed as esters, nitriles, ketones and halides were not reduced.<sup>[165]</sup> In order to highlight the importance of the phosphanyl-pyridine

ligand on the activity, when using monophosphine complexes  $[\text{CpFe}(\text{CO})_2(\text{PR}_3)][\text{BF}_4]$  such as **114**, only moderate conversion (35–58%) were reached.



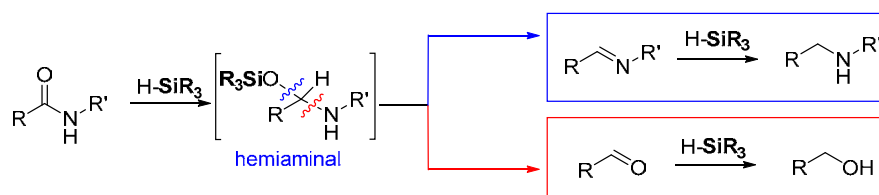
**Scheme 52.** Cascade reaction involving iron-catalyzed DRA.

Iron-catalyzed DRA can be conducted starting from allylic or homoallylic alcohols and secondary or primary anilines; indeed, using  $[\text{Fe}(\text{cod})(\text{CO})_3]$  (**144**, 5.0 mol%) and PMHS in ethanol at 50–70 °C under visible light irradiation, tertiary and secondary aniline compounds were selectively obtained in 31–95% yields (Scheme 52). This transformation is a formal DRA of (homo)allylic alcohols which occurred *via* a tandem isomerization/ condensation/ hydrosilylation process.<sup>[166]</sup>

### 3.3. Hydrosilylation of carboxylic acid derivatives

#### 3.3.1. Carboxamides.

Among the carboxylic acid derivatives, the most difficult ones to reduce are carboxamides. Furthermore, chemoselectivity issues can be also met during the reduction of amides, as the C–N or C=O bond cleavage can occur, depending on the reaction conditions, leading the amine and/or alcohol (Scheme 53).<sup>[167]</sup>



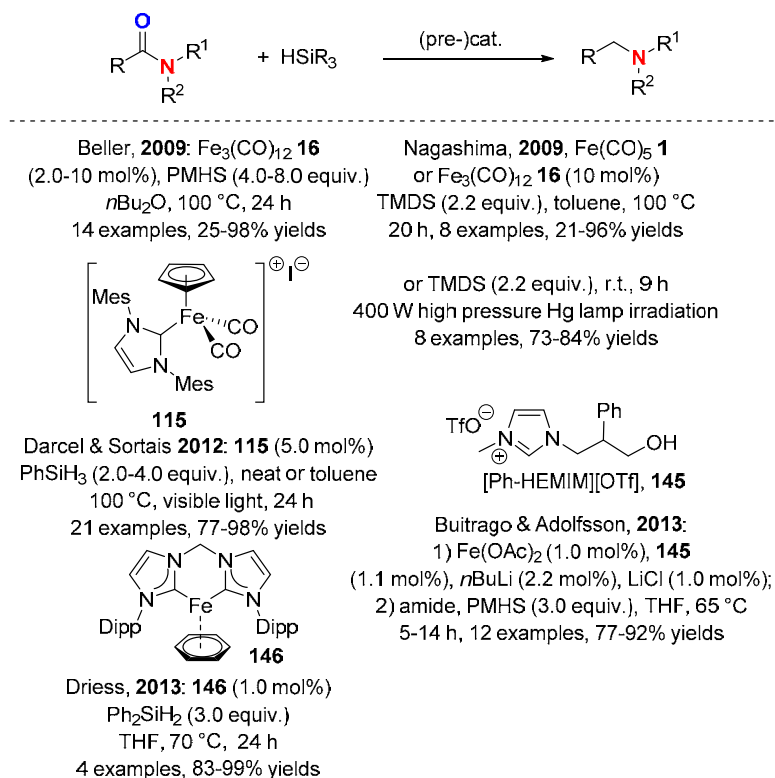
**Scheme 53.** Possible reaction pathways involved in the reduction of carboxamides.

Pioneering contributions were described concomitantly by Beller<sup>[168]</sup> and Nagashima<sup>[169]</sup> on iron-catalyzed hydrosilylation reactions of secondary and tertiary carboxamides yielding specifically the corresponding amines, using  $\text{Fe}_3(\text{CO})_{12}$  **16** or  $\text{Fe}(\text{CO})_5$  **1** as pre-catalysts (2.0–10 mol%), and either PMHS (4.0–10 equiv.) or TMDS (2.2 equiv.) as cheap hydrosilanes at 100 °C for 24 h (Scheme 54). Noticeably, Nagashima highlighted that such transformations were also promoted at r.t. for 9 h when conducted under irradiation conditions using a 400 W high pressure mercury lamp.

The use of molecular defined iron(II) NHC complexes such as  $[\text{CpFe}(\text{CO})_2(\text{IMes})][\text{I}]$  **110** (5.0 mol%) in the presence of 2.0 equiv. of phenylsilane at 100 °C for 24 h also permitted to



reduce both tertiary and secondary amines when the reaction was conducted under visible light irradiation (24 W compact fluorescent lamps) and solvent free conditions (Scheme 54).<sup>[170]</sup>

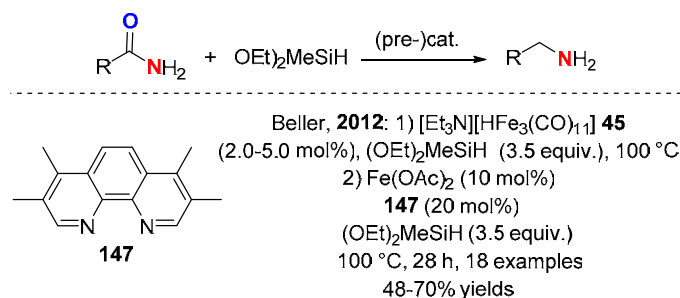


**Scheme 54.** Iron-catalyzed hydrosilylation of tertiary and secondary amides.

By preparing carefully an *in situ* iron/NHC catalytic species from a THF mixture of  $\text{Fe}(\text{OAc})_2$  (**77**, 1.0 mol%), ([Ph-HEMIM][OTf]) (**145**, 1.1 mol%) and  $\text{LiCl}$  (1.0 mol%) and then treated by 2.2 mol% of  $n\text{BuLi}$ , Adolfsson reported the hydrosilylation of tertiary amides using 3.0 equiv. of PMHS at 65 °C for 5–14 h (Scheme 54).<sup>[171]</sup> Importantly, the use of  $\text{LiCl}$  is crucial to increase both the chemoselectivity and activity. The well-defined NHC-Fe(0) complex [bis-(*N*-Dipp-imidazole-2-ylidene)methylene-Fe( $\eta^6$ -benzene)] (**146**, 1.0 mol%) promoted the catalytic reduction of tertiary carboxamides by reaction in THF with 3.0 equiv. of diphenylsilane at 70 °C for 24 h (4 examples, 83–99% yields).<sup>[172]</sup>

By contrast, the reductions of primary amides under hydrosilylation conditions are usually more difficult to conduct. Indeed, under the classical reaction conditions, dehydration of amides to nitrile derivatives is always the major reaction observed.<sup>[170, 173]</sup> To tackle this selectivity issues and efficiently reduce primary amides to primary amines, Beller used two different iron catalytic systems in a sequential way. Thus, using  $[\text{NHEt}_3][\text{Fe}_3\text{H}(\text{CO})_{11}]$  **45** (2.0–5.0 mol%) in the presence of 3.0 equiv. of  $(\text{EtO})_2\text{MeSiH}$  in toluene, the dehydration of primary amides was first performed leading to nitriles (Scheme 55). Then the combination of  $\text{Fe}(\text{OAc})_2$

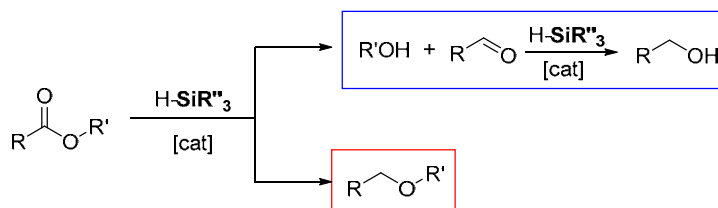
(**77**, 20 mol%) and the terpyridine ligand (**147**, 20 mol%), catalyzed the reduction of nitriles to primary amines at 100 °C for additional 28 h.<sup>[174]</sup>



**Scheme 55.** Iron-catalyzed reduction of primary amides to primary amines.

### 3.3.2. Carboxylic esters.

In organic synthesis, the efficient and chemoselective reduction of carboxylic acid derivatives such as carboxylic acids or esters to alcohols, ethers or aldehydes is a crucial and tedious task. Similarly, to carboxamides, the selective bond cleavage of the esters will direct the selective formation of aldehydes, alcohols or ethers (Scheme 56). All these selective transformations have been already described at iron, even if up to date, there are only scarce reports dealing with that challenging task.

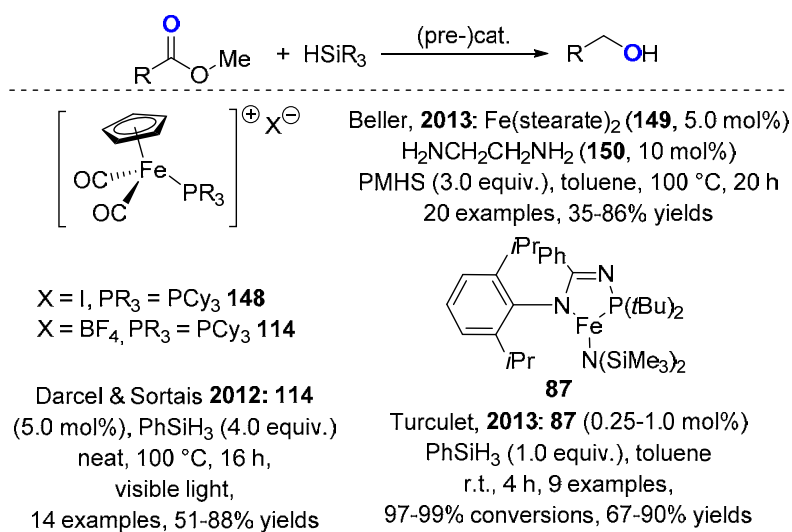


**Scheme 56.** Possible bond cleavages in ester reduction.

The first iron-catalyzed hydrosilylation of esters was reported in 2012, using 5.0 mol% of  $[\text{FeCp}(\text{CO})_2(\text{PCy}_3)][\text{I}]$ <sup>[175]</sup> (**148**) and 4.0 equiv. of  $\text{PhSiH}_3$  under solvent free conditions and visible light activation at 100 °C for 16 h (Scheme 57). As a representative example, methyl phenylacetate was converted in 85% leading to a mixture of 2-phenylethanol and methyl 2-phenylethyl ether (ratio 6:1). The best catalyst identified was  $[\text{Fe}(\text{Cp})(\text{CO})_2(\text{PCy}_3)][\text{BF}_4]$  **114** (5.0 mol%) which led specifically to 2-phenylethanol in 97% conversion and 88% isolated yield. Carboxylic esters such as alkanoates and 2-substituted acetates were then converted to the corresponding primary alcohols in 51–88% isolated yields.

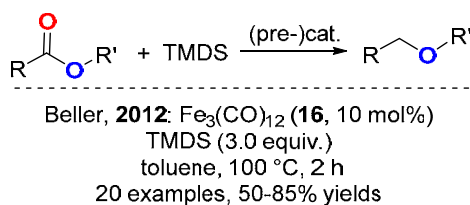
Similar chemoselective catalyzed hydrosilylation reactions of aromatic and aliphatic esters to alcohols were also conducted using an *in situ* catalyst generated from 5.0 mol% of  $\text{Fe}(\text{stearate})_2$  (**149**) and 10 mol% of ethylenediamine (**150**) with 3.0 equiv. of PMHS at 100 °C for 20 h (35–86% yields, Scheme 57).<sup>[176]</sup> Interestingly, Turculet *et al.* described a more active catalytic

system using the three coordinate iron(II) *N*-phosphinoamidinate complex **87** in low catalytic loading (0.25–1.0 mol%) in the presence of 1.0 equiv. of phenylsilane for the reduction of esters to alcohols at r.t. within 4 h (Scheme 57).<sup>[118]</sup>



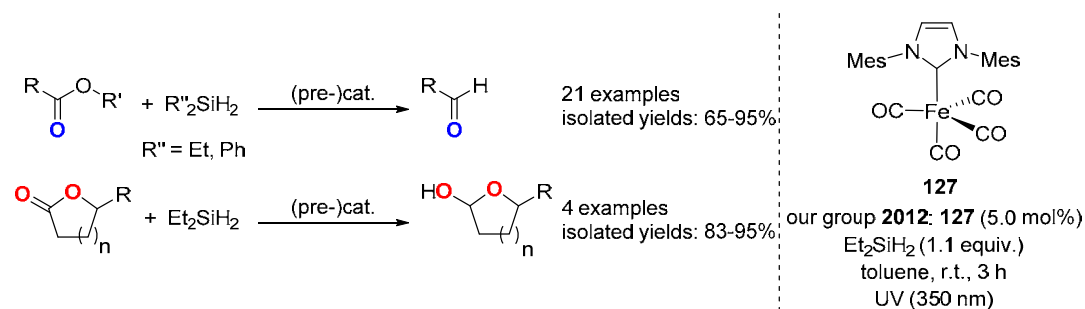
**Scheme 57.** Selective iron-catalyzed hydrosilylation of esters to alcohols.

The chemoselectivity of these hydrosilylations can be finely controlled by a fine design of the catalytic system. Indeed, to obtain selectively ethers from esters, the combination of Fe<sub>3</sub>(CO)<sub>12</sub> (**16**, 10 mol%) and TMDS (3.0 equiv.) in toluene at 100 °C for 2 h permitted to reduce aliphatic and alicyclic esters, even steroid esters<sup>[177]</sup> (Scheme 58).



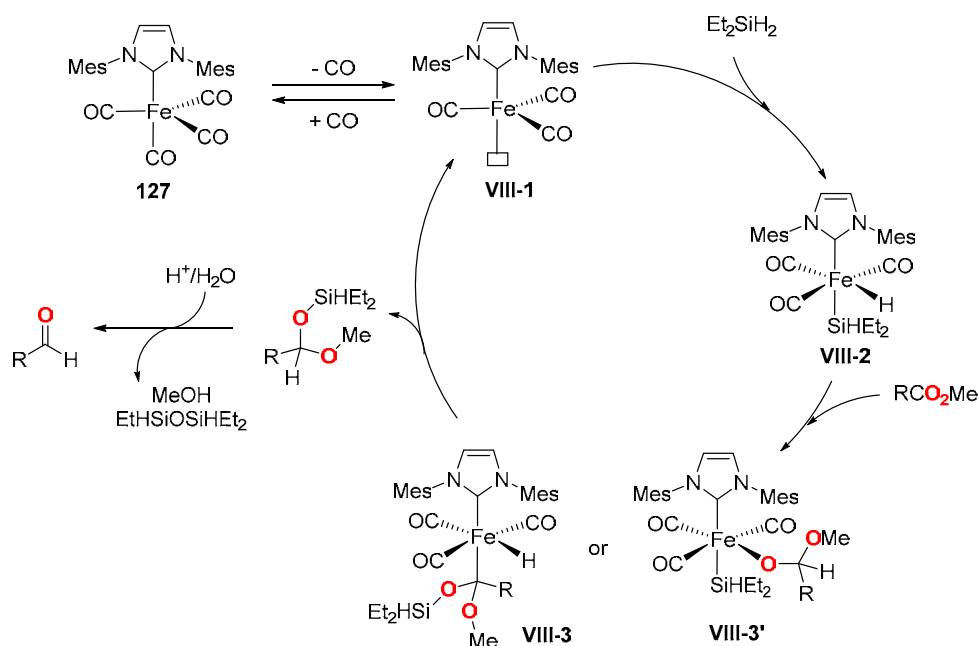
**Scheme 58.** Selective iron-catalyzed hydrosilylation of esters to ethers.

In multi-step synthesis, the reduction of esters furnishing aldehydes is always a tedious step, even if proven procedures with stoichiometric alkali reductant are always efficient. Thus, to produce specifically aldehydes from (hetero)aromatic and aliphatic esters, the association of the complex [Fe(CO)<sub>4</sub>(IMes)] **127** (5.0 mol%) and the hydrosilanes R<sub>2</sub>SiH<sub>2</sub> (R = Et, Ph) permitted the efficient and specific reduction at r.t. under UV irradiation (350 nm)<sup>[178]</sup> (Scheme 59). Et<sub>2</sub>SiH<sub>2</sub> showed the best performance for the reduction of alkanoates, whereas Ph<sub>2</sub>SiH<sub>2</sub> was the most active for benzoates. Noteworthy, this catalytic system was also efficient for the more tedious and chemoselective reduction of lactones to lactols in good isolated yields (83–95%).



**Scheme 59.** Selective iron-catalyzed hydrosilylation of esters to aldehydes and lactones to lactols.

Furthermore, experimental evidence proved that the hydrosilylation proceeded *via* an oxidative addition of various hydrosilanes to unsaturated NHC-Fe species obtained from the complex such as **127** by UV activation, furnishing a hydride-silyl iron complex which was fully characterized by NMR and X-ray analysis.<sup>[179]</sup> Based on these observations, the following mechanism was proposed (Scheme 60): after decooordination of one CO ligand under UV-irradiation, oxidative addition of a hydrosilane led to the hydride iron(II) intermediate (**VIII-2**). Then, insertion of the C=O bond of the ester into either the Fe-H or Fe-Si was postulated. A final reductive elimination produced the silylated acetal and regenerated the unsaturated iron(0) active species.<sup>[178]</sup>

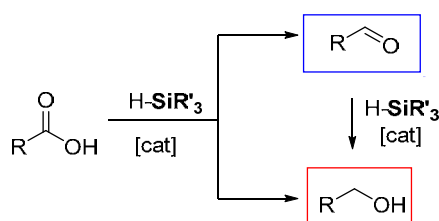


**Scheme 60.** Proposed catalytic cycle for the semi-reduction of esters.

Noticeably, aldehydes were obtained starting from more reactive acyl chlorides, using a catalytic system generated from FeO (**151**, 20 mol%) and tris(2,4,6-trimethoxyphenyl)phosphine (TMPP, **152**, 5.0 mol%) in the presence of PhSiH<sub>3</sub> (1.12 equiv.) in toluene at 60–120 °C for 20 h.<sup>[180]</sup>

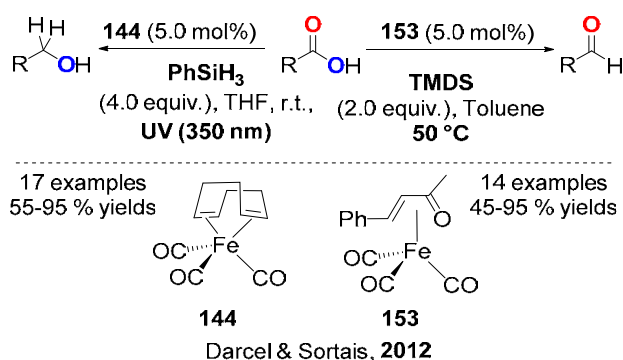
### 3.2.3. Carboxylic acids.

The chemoselective reduction of carboxylic acids leading selectively to alcohols or aldehydes is also an important challenging target. Even if such reactions can be selectively conducted through heterogeneous catalysis using highly drastic conditions, or through homogeneous catalytic hydrogenation, it has been scarcely reported using iron-catalyzed hydrosilylation (Scheme 61).



**Scheme 61.** Carboxylic acid reduction into alcohols or aldehydes.

Such selective hydrosilylation can be conducted using a one pot procedure using well-chosen silane-iron complex association. Indeed, conducting the transformation with 4.0 equiv. of  $PhSiH_3$  and 5.0 mol% of  $[Fe(cod)(CO)_3]$  complex **144** under UV irradiation (350 nm) at r.t. for 24 h, alkanolic and activated benzoic acids were converted to the corresponding alcohols (67–97% yields) after acidic hydrolysis (Scheme 62). By contrast, when the reaction was performed with 5.0 mol% of  $[Fe(t-PBO)(CO)_3]$  (**153**) and 2.0 equiv. of TMDS at 50 °C for 24 h, alkanolic acids were selectively reduced leading to the corresponding aldehydes in 45–95 isolated yields<sup>[181]</sup> (Scheme 62). In order to have insight into the chemoselectivity, a disilylacetal intermediate  $p-Br-C_6H_4-CH[OSi(Me)_2-CH_2-SiH(Me)_2]_2$  was isolated and fully characterized by NMR and MS. This intermediate was stable under the reaction conditions and generated the aldehydes after an acidic hydrolysis step, thus avoiding any over-reduction process.

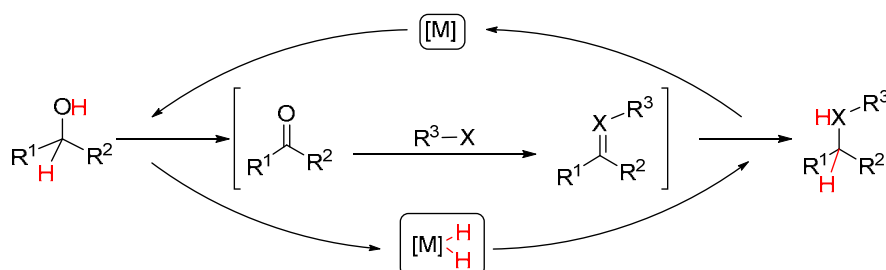


**Scheme 62.** Chemoselective hydrosilylation of carboxylic acids to alcohols and aldehydes.

## 4. Hydrogen borrowing reactions

The hydrogen auto-transfer also called borrowing hydrogen methodology is another important pathway in the area of reduction reactions. It involves a metal promoted hydrogen transfer

mechanism starting from an alcohol which is oxidized to a carbonyl intermediate and a metal hydride species which will be able in the last step to release hydrogen for the reduction of the unsaturated intermediate formed from the carbonyl condensation, the transition metal catalyst playing here the role of hydrogen shuttle (Scheme 63). Such transformations are typically performed with noble metals such as ruthenium, rhodium or iridium.<sup>[182]</sup>



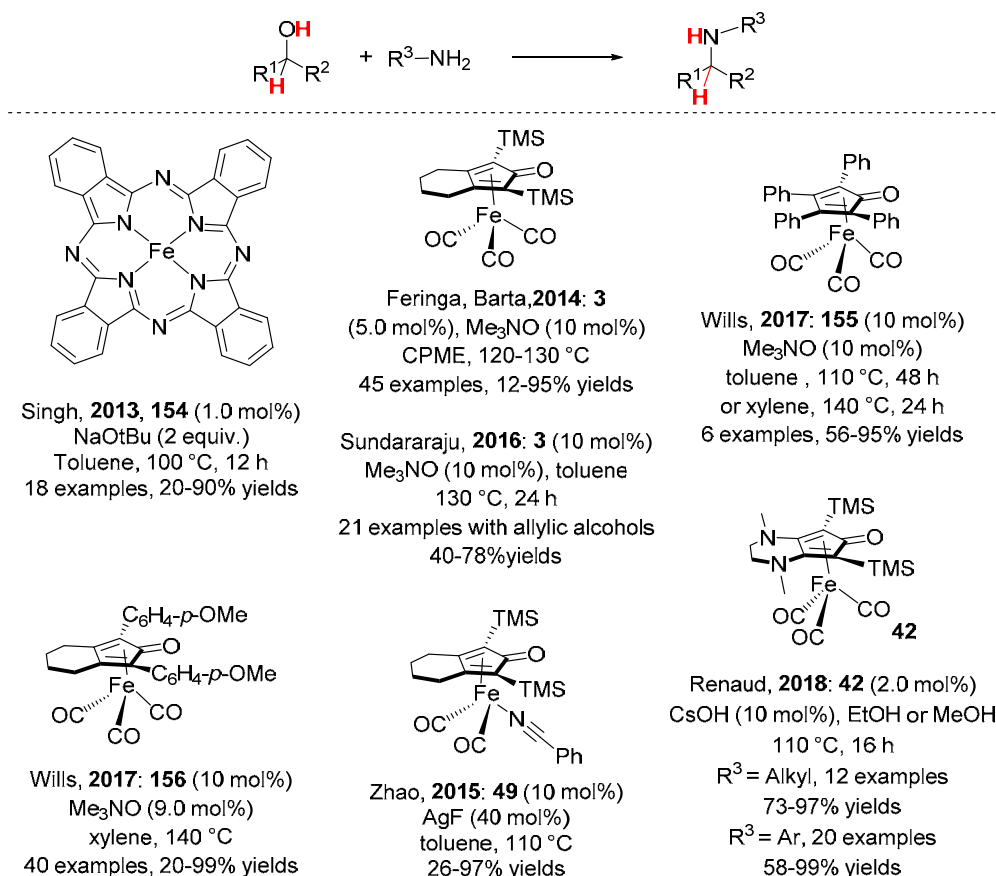
**Scheme 63.** Principle of metal catalyzed borrowing hydrogen methodology

Iron can also perform such transformation mainly using Knölker type complexes as the catalysts. Indeed, direct reductive amination reactions can be efficiently promoted *via* a hydrogen borrowing pathway at rather high temperatures starting from primary alcohols.

In a pioneering contribution, Deng reported the *N*-alkylation of sulfonamides with 5.0 equiv. of benzylic alcohols using a  $\text{FeCl}_2$  (**20**, 5.0 mol%)/ $\text{K}_2\text{CO}_3$  (20 mol%) catalytic system at 135 °C for 20 h leading to the corresponding *N*-alkylated sulfonamides  $\text{R-SO}_2\text{-NR}'$  (21 examples, 89–98% yields).<sup>[183]</sup> In 2013, Singh described an efficient iron phthalocyanine (**154**) catalyzed *N*-alkylation of amines such as aminobenzothiazoles, aminopyridines and aminopyrimidines with benzyl alcohols: using 1.0 mol% of iron phthalocyanine **154** in the presence of 2.0 equiv. of  $\text{NaOtBu}$  in toluene at 100 °C for 12 h, the mono *N*-alkylated derivatives were yielded in 20–90% (Scheme 64).<sup>[184]</sup> Noticeably, starting from *o*-phenylenediamine, 2-aminothiophenol and 2-aminophenol, at 120 °C, under similar conditions, 2-phenylbenzimidazoles, 2-substituted benzothiazoles, and 2-phenylbenzoxazole were produced, respectively, in 41–99% yields.

In 2014, Feringa and Barta described a general methodology using the complex **3** (5.0 mol%) associated to 10 mol% of  $\text{Me}_3\text{NO}$  which catalyzed the auto-transfer hydrogenation of numerous primary alkylalcohols with aniline and benzylamine derivatives in CPME (cyclopentyl methyl ether) at 120–140 °C affording the corresponding monoalkylated amines with yields up to 95% (Scheme 64). The reaction can be also performed with diols leading selectively to the corresponding 5-, 6- and 7-membered heterocycles *via* a *N,N*-dialkylation process and tolerated various functional groups such as halides, hydroxyl, ester, nitrile, nitro. Noticeably, this methodology was applied for the synthesis of two pharmaceutical active molecules, Piribedil,

an anti-Parkinson drug and the Glycine transporter type 1 (GlyT1) inhibitor which exhibited potential in the treatment of schizophrenia.<sup>[185]</sup> This BH reaction was extended to allylic alcohols giving the corresponding allylic amines without isomerization of the C=C bond.<sup>[186]</sup>



**Scheme 64.** Iron-catalyzed RDA reaction *via* hydrogen borrowing.

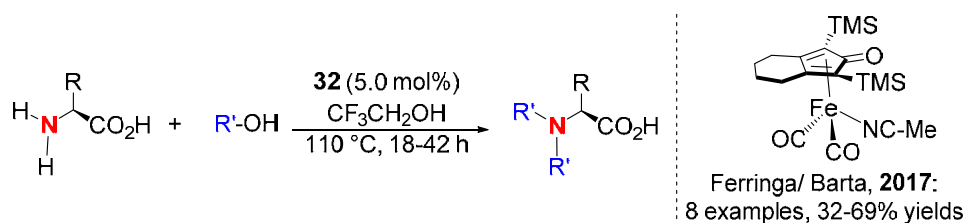
Later, Wills developed a catalytic system prepared *in situ* from the modified Knölker complex (**155**, 10 mol%) and 10 mol% of Me<sub>3</sub>NO which showed the same range of activity in toluene at 110 °C for 48 h or xylene at 140 °C for 24 h (Scheme 64).<sup>[187]</sup> Concomitantly, Zhao reported that the Knölker complex **49** (10 mol%) in combination with 40 mol% of AgF was efficient for the reaction of primary anilines with 5.0 equiv. of secondary alcohols giving the corresponding monoalkylated amines with 26–97% yields (Scheme 64).<sup>[188]</sup> With primary alcohols, its quantity is crucial for the selectivity of the reaction: with 1.2 equiv., monoalkylated anilines were selectively obtained, whereas with 5.0 equiv. mixtures mono- and dialkylated amines were observed.

Wills also designed a series of (cyclopentadienone)iron tricarbonyl complexes by modifying the electronic variation of the aromatic groups neighboring the C=O of the cyclopentadienone, and identified the complex (**156**) as the best catalyst precursor for BH of alcohols with various

amines (Scheme 64). Notably, unsaturated alcohols containing double and triple bonds were applied.<sup>[187]</sup>

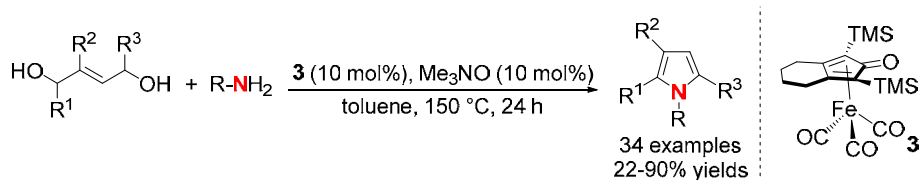
Renaud *et al.* recently reported an efficient way to perform the *N*-ethylation (or *N*-methylation) of amines with ethanol (or methanol), as the solvent, in the presence of 2.0 mol% of iron Knölker type complex **42** and 10 mol% of CsOH at 110 °C for 16 h (Scheme 64).<sup>[189]</sup> With ethanol (or methanol), starting with primary anilines, the mono *N*-alkylation was selectively observed, whereas the primary alkylamines led to the di-*N*-alkylation derivatives.

Noteworthy, starting from fatty alcohols (4.0 equiv.), Barta described the *N*-monoalkylation of unprotected  $\alpha$ -amino acids using 5.0 mol% of Knölker's nitrile-ligated complex **32** in neat conditions or 2,2,2-trifluoroethanol at 110 °C for 18–42 h (8 examples, 32–69% yields, Scheme 65).<sup>[190]</sup>



**Scheme 65.** Iron-catalyzed hydrogen borrowing reaction involving amino acids.

Sundararaju developed an original synthesis of substituted pyrroles using the hydrogen borrowing methodology. Indeed, using 10 mol% of **3** and 10 mol% of Me<sub>3</sub>NO in toluene at 150 °C, the reaction of various anilines and alkylamines with *cis/trans* buten-1,4-diol derivatives lead to substituted pyrroles in 22–90% yields (Scheme 66).<sup>[191]</sup> To explain the formation of pyrroles, a hydrogen auto transfer process–oxidation–intramolecular dehydrative condensation sequence was suggested.

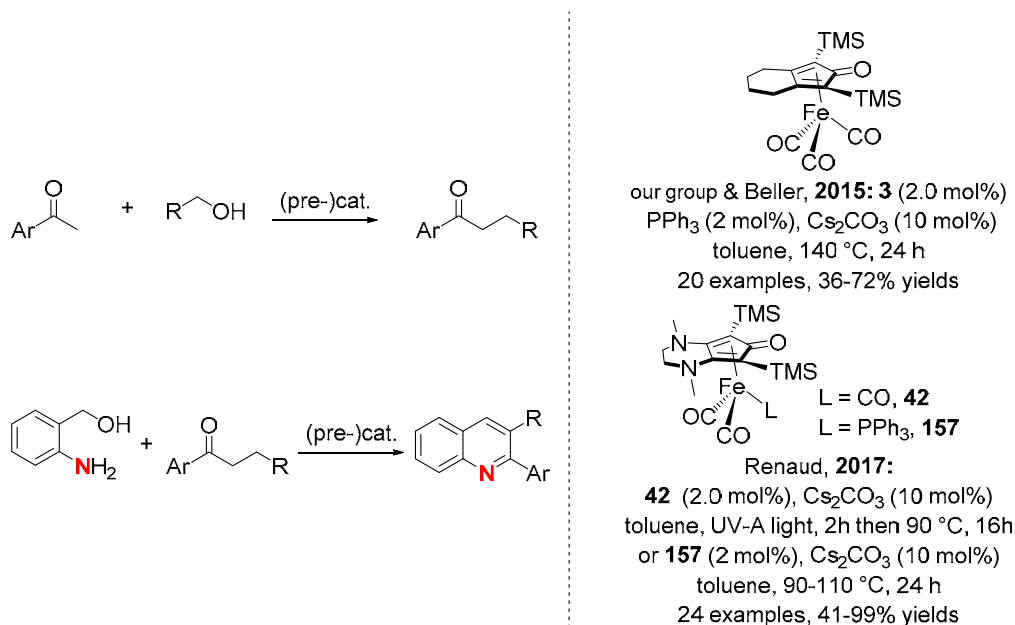


**Scheme 66.** Iron-catalyzed pyrrole synthesis *via* hydrogen borrowing reaction

The hydrogen borrowing methodology can be used to build carbon chains through C–C bond formation. More particularly,  $\alpha$ -alkylation of the ketone using an alcohol as the electrophilic alkylation agent in replacement of alkyl halides/pseudohalides is a strategy which permits to decrease the production of waste. The first report at iron was reported in 2015 by our group



using the complex **3** (2.0 mol%) associated to 2.0 mol% of PPh<sub>3</sub> in the presence of a catalytic amount of base (Cs<sub>2</sub>CO<sub>3</sub>, 10 mol%): various primary alcohols then reacted with acetophenone derivatives in toluene at 140 °C leading to the alkylated products in 36–72% yields (Scheme 67).



**Scheme 67.** Iron-catalyzed  $\alpha$ -alkylation of ketones

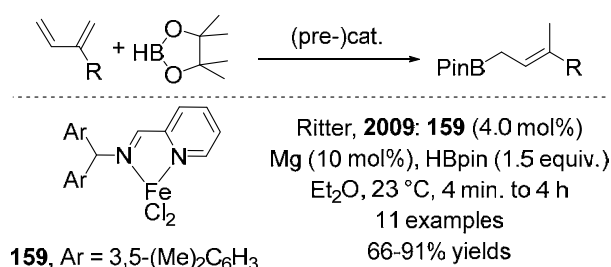
Noteworthy, under similar conditions with 10–30 mol% of KO<sup>*t*</sup>Bu,  $\alpha$ -alkylation of ketones reacted with 2-aminobenzyl alcohol yielding the quinoline derivatives in 55–67% yields.<sup>[192]</sup> Renaud used more active Knölker type complexes bearing an electron rich cyclopentadienone ligand [e.g. **40** or (**157**)] which permitted to perform the same reactions (except quinoline synthesis) at lower temperature (90 °C vs 140 °C, Scheme 67). Noticeably, DFT calculations rationalized the better activity of these catalysts.<sup>[193]</sup>

## 5. Hydroboration

### 5.1. Hydroboration of alkenes and alkynes

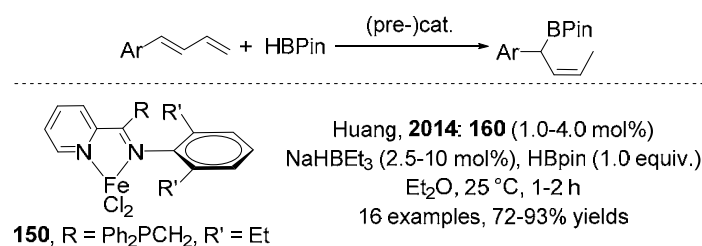
Transition metal catalyzed hydroelementations are efficient and greener transformations for the introduction of boron<sup>[194]</sup> into unsaturated molecules. More particularly, in the area of transition metal catalyzed hydroboration, organoboronates became an important class of reagents, as they are quite stable toward atmospheric oxidation, and widely used as synthons in selective carbon-carbon or carbon-heteroatom bond formations.<sup>[195]</sup> Up to now, rhodium is usually identified as the metal of choice to promote efficiently such reactions.<sup>[196]</sup> By contrast, contributions with iron catalysts are scarce.

In the 1990s, using the  $[\text{FeCp}(\text{Bcat})(\text{CO})_2]$  complex (**158**), Hartwig developed a pioneering stoichiometric activation of arenes giving arylcatecholborane.<sup>[197]</sup> In 2009, Ritter reported the first iron-catalyzed hydroboration of 1,3-dienes by pinacolborane (HBpin, 1.5 equiv.), using a catalyst generated from a well-defined [(iminopyridine)FeCl<sub>2</sub>] complex (**159**, 4.0 mol%) in the presence of 10 mol% of magnesium at r.t. for 4 min.–4 h (Scheme 68).<sup>[198]</sup> Noteworthy, isolated C=C double bonds and esters were tolerated under the reaction conditions. Additionally, even if starting from unsymmetrical dienes, only 1,4-addition adducts and (*E*)-C=C bonds were exclusively obtained, highlighting the high chemo- and regioselectivity of the transformation.



**Scheme 68.** Chemo- and regioselective hydroboration of 1,3-dienes.

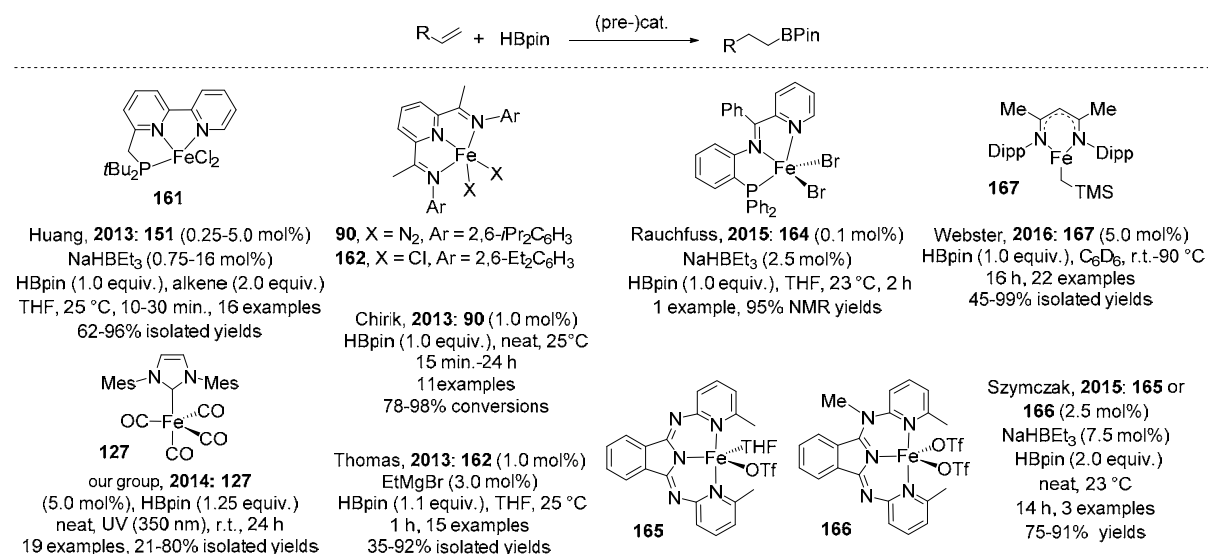
Similarly, Huang prepared a series of new iminopyridine iron complexes in particular bearing bulky diphenylphosphinomethyl-ketimine substituents. The iron complex (**160**, 1.0–4.0 mol%) was identified as the most selective and in association with NaHBEt<sub>3</sub> (2.5–10 mol%), promoted the hydroboration of 1-(hetero)aryl-substituted 1,3-dienes with 1.04 equiv. of HBpin at 25 °C in 1–2 h in Et<sub>2</sub>O leading in a regio- and stereo-selective manner to secondary (*Z*)-allylboronates as the major compounds in 72–93% yields (Scheme 69).<sup>[199]</sup> Importantly, this report constitutes the first example of 1,4 hydroboration of 1-substituted dienes leading to secondary allylboronates.



**Scheme 69.** Chemo- and regioselective hydroboration of 1,3-dienes.

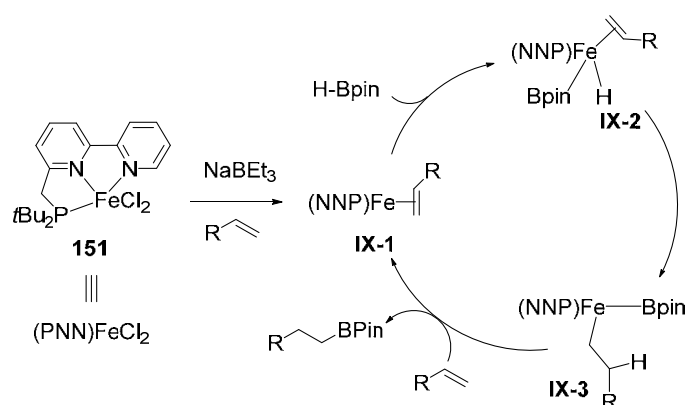
During the last few years, hydroboration of olefins was competitively studied utilizing iron based catalysts. In 2013, Huang described the use of a catalyst *in situ* prepared from the bipyridyl-based phosphine iron complex (**161**, 0.25–5.0 mol%) and NaHBEt<sub>3</sub> (0.75–15 mol%) to perform the hydroborylation of terminal olefins using 0.5 equiv. of HBpin at r.t. for 10–30 min. leading to the alkylboronates with 62–96% yields (Scheme 70). This reaction is

particularly suitable for the hydroboration of linear terminal alkenes and functional groups such as tosylate, tertiary amines, benzylethers and acetals were tolerated. The reaction is chemoselective as only terminal C=C bond of a polyene is hydroborated.<sup>[200]</sup>



### Scheme 70. Iron-catalyzed hydroborylation of alkenes.

Furthermore, this catalytic system was applied for the hydroboration of styrenes. When the reaction was performed in toluene with 2.0 mol% of **161** and 6.0 mol% of NaHBEt<sub>3</sub> at 25 °C for 30 min., a mixture of hydroboration, dehydrogenative borylation and hydrogenation products was obtained (Scheme 70). By contrast, adding 20–40 mol% of acetonitrile, the reaction became selective as only the hydroboration adduct was obtained with 78–96% yields. The quantity of acetonitrile was crucial as the similar reaction performed in acetonitrile led to only 5% of the hydroborated derivative after 30 min.



### Scheme 71. Proposed mechanism for iron-catalyzed hydroborylation of alkenes.

The authors then proposed a mechanism for this reaction (Scheme 71). After reduction of the complex **161** by NaHBEt<sub>3</sub> and coordination of the alkene, the species (**IX-1**) is generated and its oxidative addition of H-Bpin led to the Fe(II) species (**IX-2**). The 1,2-insertion of the C=C

into the Fe-H bond produced the iron alkyl boryl (**IX-3**). The reductive elimination gave the linear boronate and regenerated the species **IX-1** by coordination of an alkene.

Simultaneously, Chirik reported that the bis(imino)pyridine iron dinitrogen complex **90** (1.0 mol%) was also efficient for the hydroboration of terminal and disubstituted alkenes using 1.0 equiv. of H-Bpin under neat conditions at 25 °C for 15 min. to 24 h (Scheme 70). It must be underlined that this catalytic system permitted to hydroborate cyclic alkenes and C=C bond in internal linear olefins such as *cis*-4-octene. In the latter case, a mixture of 1- and 4-octylboronate products in a 5:1 ratio was obtained showing that an isomerization process can also operate. Notably, the reaction also succeeded regioselectively with styrene derivatives. Starting from styrene, the anti-Markovnikov boronate ester, PhCH<sub>2</sub>CH<sub>2</sub>BPin, was exclusively obtained using 1.0 mol% of **90**.

The hydroborations of  $\alpha$ - and *cis*- $\beta$ -methyl styrenes led specifically to 2-phenylpropyl boronate ester and 1-phenylpropyl boronate ester, respectively after 24 h (Scheme 70).<sup>[201]</sup> Using a similar system, generating the active catalyst from EtMgBr (3.0 mol%) and the dichloro iron complex (**162**, 1.0 mol%) or from the complex formed from FeCl<sub>2</sub> (**20**) and the corresponding bis-iminopyridine ligand **163** (1.0 mol%), the hydroboration of functional alkenes was efficiently performed in THF at r.t. for 1 h using 1.1 equiv. of HBpin. Importantly, halides, esters, amides, imines, amines, and alcohols were tolerated (Scheme 70).<sup>[202]</sup> Additionally, the hydroborylation of internal alkenes such as cyclooctene was successfully performed.

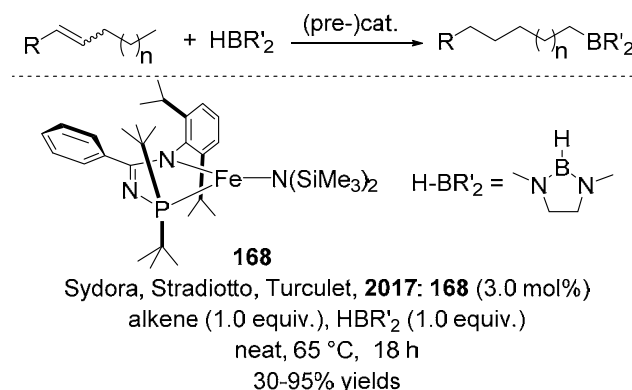
In our group, using a molecular-defined iron-NHC complex, [(IMes)Fe(CO)<sub>4</sub>] **127** (5.0 mol%) under UV irradiation (350 nm) and neat conditions in the presence of 1.25 equiv. of HBpin at r.t. for 24 h, functionalized terminal alkenes can be hydroborated in moderate to good yields. It must be underlined the good functional group tolerance with ester, acetal, ether, silylether, epoxide and nitrile moieties which were not altered (Scheme 70).<sup>[203]</sup>

In 2015, Rauchfuss described the potential of the phosphine-iminopyridine iron complex (**164**) as a catalyst (0.1 mol%) in hydroboration, highlighting the full reaction of 1-octene with 1.0 equiv. of HBpin at r.t. when **164** was treated with 2.5 equiv. of NaHBET<sub>3</sub> (Scheme 70).<sup>[204]</sup> Szymczak designed amidobispyridine Fe(II) complexes (**165**) and (**166**) able to catalyze the hydroboration of alkenes when associated to 3.0 equiv. of NaHBET<sub>3</sub> (Scheme 70). For the reaction of HBpin (2.0 equiv.) at r.t. under neat conditions with terminal linear and cyclic olefins, both complexes exhibited similar reactivity. For the hydroboration of styrene, **166** gave the best result (81% yields), **165** giving a less selective reaction with 11% of by-products resulting from dehydrogenative borylation and hydrogenation reactions. The hydroborylation

of the more challenging *cis*-4-octene led to a mixture of alkylboronates using **166** whereas **165** permitted to obtain specifically the linear boronates, resulting first in the isomerization of the C=C bond followed by hydroborylation.<sup>[205]</sup>

In 2016, Webster reported iron(II)  $\beta$ -diketiminate complexes, such as (**167**) for the hydroboration of alkenes and alkynes (Scheme 70). Using 5.0 mol% of **167**, terminal linear olefins were hydroborylated using 2.0 equiv. of HBpin at r.t. for 16 h in C<sub>6</sub>D<sub>6</sub> leading to the anti-Markovnikov products with 45–99% yields. Noticeably, epoxide, ketone, and substituted C=C bonds were not altered. With styrenes, harsher reaction conditions (60 °C, 2.5–18 h) were necessary, but a mixture of isomers was obtained. By contrast, the hydroborations of  $\alpha$ - and *cis*- $\beta$ -methyl styrenes led specifically to 2-phenylpropyl boronate esters and 1-phenylpropyl boronate esters, respectively (Scheme 70).<sup>[206]</sup>

*N*-phosphinoamidinate-coordinated iron complexes (**168**) was reported to be a useful catalyst for the isomerization/hydroborylation of internal olefins using 1,3-dimethyl-1,3-diaza-2-boracyclopentane as the hydroboron reagent leading to linear terminal alkyl diazaborolanes (Scheme 72). Noticeably, 1,3-dimethyl-1,3-diaza-2-boracyclopentane was a better partner than HBpin for such transformation.<sup>[207]</sup>

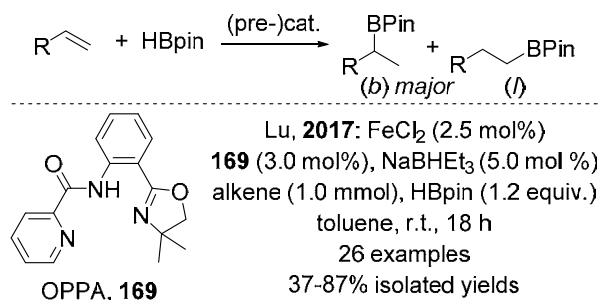


**Scheme 72.** Iron-catalyzed isomerization/hydroborylation of internal olefins.

Using bis(pinacolato)diboron (B<sub>2</sub>pin<sub>2</sub>), Zhou reported a simple system based on FeCl<sub>2</sub> (**20**, 0.1–10 mol%) working in the presence of 1.2 equiv. of KO*t*-Bu and 1.0 equiv. of *t*-BuOH in THF at 65 °C for 12 h. Numerous styrenes and heteroarylalkenes were hydroborylated and led to the anti-Markovnikov products with 64–99% yields (24 examples).<sup>[208]</sup>

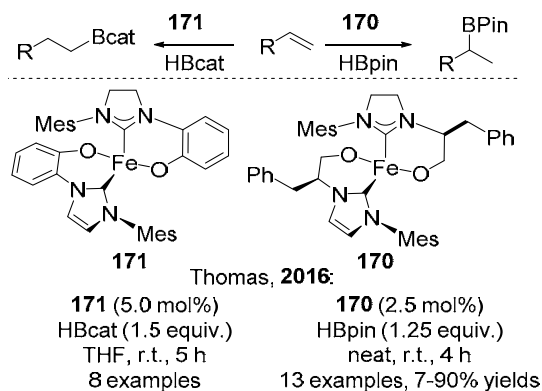
Regioselective hydroboration of styrenes is always a more challenging task. A highly Markovnikov-selective hydroboration of styrenes was described using a catalytic system from FeCl<sub>2</sub> (**20**, 2.5 mol%), an oxazolinylphenyl picolinamide ligand (**169**, 3.0 mol%) and NaBHET<sub>3</sub> (5.0 mol%), affording the branched borylated products with up to >50/1 (b/l) at r.t. in toluene

after 18 h (Scheme 73).<sup>[209]</sup> By contrast, with linear olefins such as 1-octene, 1/1 ratio was obtained.



**Scheme 73.** Iron-catalyzed Markovnikov selective hydroborylation of styrenes.

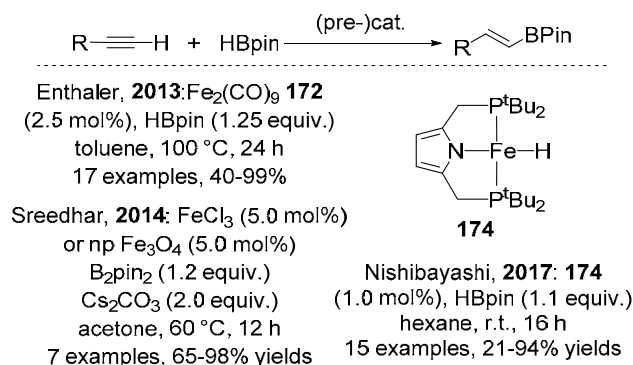
Similarly, Thomas developed alkoxytethered NHC iron(II) complexes able to perform regioselective hydroboration of terminal olefins. Noticeably, using the right hydroboranes associated to the right iron complex permitted to direct the regioselectivity. With 1.25 equiv. of HBpin and 2.5 mol% of (**170**) under neat conditions at r.t., styrene derivatives led to the corresponding branched borylated product with yields up to 90% and selectivity b/l from 5:1 to 37:1 (Scheme 74). By contrast, selecting HBcat (1.5 equiv.) and the complex (**171**, 5.0 mol%) in THF at r.t. a reverse anti-Markovnikov selectivity was observed (Scheme 74). As the catechol boronic esters are sensitive and difficult to purify, to quantify the reaction, they were either oxidized ( $\text{H}_2\text{O}_2$ , NaOH, 0 °C, 0.5 h) or transesterified with pinacol to give the primary alkyl- boronic esters. (44–71% yields).<sup>[210]</sup>



**Scheme 74.** Switchable iron catalyst systems for Markovnikov and anti-Markovnikov hydroborylation of styrenes.

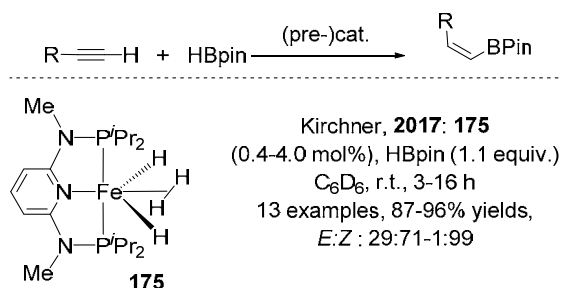
Hydroborylation of alkynes can be also performed using iron-based catalysts. In 2013, Enthaler reported the hydroboration of terminal alkynes using  $\text{Fe}_2(\text{CO})_9$  **172** as the catalyst (2.5 mol%), in the presence of 1.25 equiv. of HBpin at 100 °C for 24 h (Scheme 75). Vinyl boronate esters were then obtained with high stereoselectivity. Starting from terminal alkynes, (*E*)-vinylboronate derivatives were obtained selectively (17 examples, 40–99% yields), whereas

more complex mixtures of regioisomers were obtained with internal non symmetric alkynes.<sup>[211]</sup> Using FeCl<sub>3</sub> (**59**) or iron nanoparticles from Fe<sub>3</sub>O<sub>4</sub> (**173**, 5.0 mol%) in the presence of 1.2 equiv. of B<sub>2</sub>pin<sub>2</sub> and 2.0 equiv. of Cs<sub>2</sub>CO<sub>3</sub> in acetone at 60 °C, terminal alkynes led selectively to (*E*)-vinylboronates in 65–98% yields (Scheme 75). It is interesting to note that NP Fe<sub>3</sub>O<sub>4</sub> can be recycled up to 6 times without significant loss of activity.<sup>[212]</sup>



### Scheme 75. Iron-catalyzed hydroboration of alkynes.

In 2017, Nishibayashi described pyrrolide-based PNP pincer iron complexes (**174**, 1.0 mol%) active in hydroboration of alkynes with HBpin (1.1 equiv.) in hexane at r.t. after 16 h (Scheme 75).<sup>[213]</sup> The corresponding *E*-vinylboronates were obtained selectively in 84–94% yields. Noteworthy, steric hindrance seemed to inhibit the reaction, as *o*-methylphenylacetylene was converted in less than 5%. Furthermore, with internal alkynes such as diphenylacetylene, a lower yield was detected (21%). TONs up 710 were reached when the reaction was performed at 60 °C.

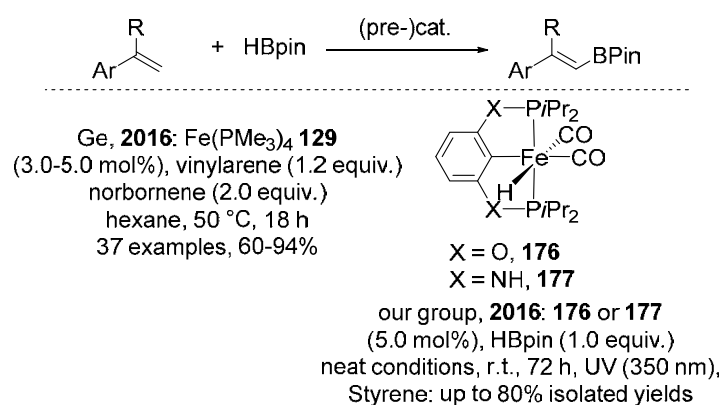


### Scheme 76. Iron-catalyzed hydroboration of alkynes.

Using iron(II) polyhydride complexes containing tridentate PNP pincer-type ligands [Fe(PNP)(H)<sub>2</sub>(η<sup>2</sup>-H<sub>2</sub>)] (**175**, 0.4–4.0 mol%), Kirchner reported a catalytic system able to promote the hydroboration of terminal alkynes in the presence of pinacolborane (1.1 equiv.), leading vinylboronates with high *Z*-selectivity (Scheme 76). When the reaction was performed at r.t. in C<sub>6</sub>D<sub>6</sub> after 3–16 h, vinylboronates were obtained in 87–96% yields, *E*:*Z* ratios of 29:71–1:99.<sup>[214]</sup>

## 5.2. Dehydrogenative borylation

An attractive alternative way of preparation of vinyl boronate esters can be performed by the catalytic dehydrogenative borylation of styrene derivatives. In 2016, Ge,<sup>[215]</sup> our group<sup>[216]</sup> reported such selective dehydrogenative borylation of vinylarenes with pinacolborane catalyzed by molecular defined iron complexes. Thus, using  $[\text{Fe}(\text{PMe}_3)_4]$  (**129**, 3.0–5.0 mol%), in the presence of 1.2 equiv. of monosubstituted and disubstituted vinylarenes and 2.0 equiv. of norbornene in hexane at 50 °C for 18 h, *E*-vinyl boronate esters were selectively produced in high yields of 60–94% (Scheme 77).<sup>[215]</sup> Good functional group tolerance was shown as acetal, imines, furyl, amino, boronate,  $\text{Ph}_2\text{P}$  were not altered. It must be noticed that norbornene is crucial for the success of the transformation: indeed, when the hydroboration was conducted in the absence of hydrogen acceptors, only a trace amount of desired product was detected.



**Scheme 77.** Iron-catalyzed dehydrogenative borylation of alkenes.

Our group has developed the synthesis of a series of dicarbonyl PCP-iron hydride complexes,<sup>[216]</sup> and has shown that they are active and selective catalytic precursors for the dehydrogenative borylation of styrene with HBpin. Using (**176**) or (**177**) (5.0 mol%), HBpin (1.0 equiv.) reacted with styrene at r.t. under neat conditions and UV irradiation (350 nm) for 72 h giving the corresponding vinyl boronate ester with up to 80% isolated yields (Scheme 77). Noticeably, no hydrogen scavenger was required to promote the reaction.

## 6. Conclusion of Chapter I

This chapter highlights the main advances made in the area of iron-catalyzed, chemoselective reduction of carbonyl derivatives, carboxylic compounds and  $\text{CO}_2$ . In particular, it was shown that an accurate design of the catalytic iron system is crucial to perform highly chemoselective transformations. Furthermore, these reported results demonstrate without any doubts the high potential of the earth abundant, inexpensive, benign iron transition metal to realize reduction, hydroelementation and hydrogen borrowing reactions under mild conditions. Since two



decades, a rebirth began in iron-catalyzed transformations which represent an impressive potential for future academic or industrial applications.

In terms of catalyst design, innocent as well as non-innocent redox-active and tri- or tetradentate cooperative ligands have already shown impressive and promising results. NHC, cyclopentadienyl and organophosphorus based complexes have also reveals outstanding activities and selectivities. Notably, in-depth mechanistic studies will be crucial to elucidate reaction pathways, important steps in the elaboration of finely designed iron catalysts able to reach the best activity and selectivity.

These initial achievements, in particular for the challenging reductions of carboxylic acid derivatives and carbon dioxide, have already allowed very impressive advances and should stimulate the utilization of iron-catalyzed methodologies in large-scale synthesis and fine chemistry.

## 7. References

- [1] a) C. Darcel, J.-B. Sortais, *Iron-Catalyzed Reduction and Hydroelementation Reactions in Iron Catalysis II, Vol. 50* (Ed.: E. Bauer), Springer, **2015**, pp. 173-216; b) H. Nakazawa, M. Itazaki, *Fe-H Complexes in Catalysis in Iron Catalysis, Vol. 33* (Ed.: B. Plietker), Springer, Berlin, Heidelberg, **2011**, pp. 27-81; c) L. C. Misal Castro, H. Li, J.-B. Sortais, C. Darcel, *Green Chem.* **2015**, *17*, 2283-2303.
- [2] a) C. Bolm, J. Legros, J. Le Pailh, L. Zani, *Chem. Rev.* **2004**, *104*, 6217-6254; b) E. B. Bauer, *Curr. Org. Chem.* **2008**, *12*, 1341-1369; c) B. Plietker, *Iron Catalysis in Organic Chemistry: Reactions and Applications*, Wiley-VCH, Weinheim, **2008**; d) B. Plietker, *Iron Catalysis: Fundamentals and Applications, Vol. 33*, Springer-Verlag, Berlin Heidelberg, **2011**; e) K. Riener, S. Haslinger, A. Raba, M. P. Högerl, M. Cokoja, W. A. Herrmann, F. E. Kühn, *Chem. Rev.* **2014**, *114*, 5215-5272; f) I. Bauer, H.-J. Knölker, *Chem. Rev.* **2015**, *115*, 3170-3387; g) T. Ollevier, H. Keipour, *Enantioselective Iron Catalysts in Iron Catalysis II, Vol. 50* (Ed.: E. Bauer), Springer-Verlag, Berlin, **2015**, pp. 259-309; h) X. He, X. Hu, J. Tao, G. Han, Y. Shang, *Chin. J. Org. Chem.* **2016**, *36*, 1465-1483; i) H. Dai, H. Guan, *Isr. J. Chem.* **2017**, *57*, 1170-1203.
- [3] a) S. Gaillard, J.-L. Renaud, *ChemSusChem* **2008**, *1*, 505-509; b) K. Junge, K. Schröder, M. Beller, *Chem. Commun.* **2011**, *47*, 4849-4859; c) B. A. F. Le Bailly, S. P. Thomas, *RSC Adv.* **2011**, *1*, 1435-1445; d) G. Bauer, K. A. Kirchner, *Angew. Chem. Int. Ed.* **2011**, *50*, 5798-5800; e) R. Lopes, B. Royo, *Isr. J. Chem.* **2017**, *57*, 1151-1159.
- [4] a) R. H. Morris, *Chem. Soc. Rev.* **2009**, *38*, 2282-2291; b) J. I. van der Vlugt, *Eur. J. Inorg. Chem.* **2012**, 363-375; c) P. E. Sues, K. Z. Demmans, R. H. Morris, *Dalton Trans.* **2014**, *43*, 7650-7667; d) J.-i. Ito, H. Nishiyama, *Tetrahedron Lett.* **2014**, *55*, 3133-3146; e) N. Guo, S. F. Zhu, *Chin. J. Org. Chem.* **2015**, *35*, 1383-1398; f) P. J. Chirik, *Acc. Chem. Res.* **2015**, *48*, 1687-1695; g) R. H. Morris, *Acc. Chem. Res.* **2015**, *48*, 1494-1502; h) Y.-Y. Li, S.-L. Yu, W.-Y. Shen, J.-X. Gao, *Acc. Chem. Res.* **2015**, *48*, 2587-2598; i) D. Wang, D. Astruc, *Chem. Rev.* **2015**, *115*, 6621-6686; j) J.-L. Renaud, S. Gaillard, *Synthesis* **2016**, *48*, 3659-3683; k) B. Štefane, F. Požgan, *Metal-Catalyzed Transfer Hydrogenation of Ketones in Hydrogen Transfer Reactions* (Eds.: G. Guillena, D. Ramón), Springer, **2016**, pp. 1-67; l) A. Mezzetti, *Isr. J. Chem.* **2017**, *57*, 1090-1105; m) N. Gorgas, K. Kirchner, *Acc. Chem. Res.* **2018**, *51*, 1558-1569; n) G. A. Filonenko, R. van Putten, E. J. Hensen, E. A. Pidko, *Chem. Soc. Rev.* **2018**, *47*, 1459-1483; o) T. Zell, R. Langer, *ChemCatChem* **2018**, *10*, 1930-1940; p) Z. Zhang, N. A. Butt, M. Zhou, D. Liu, W. Zhang, *Chin. J. Chem.* **2018**, *36*, 443-454.
- [5] a) M. Zhang, A. Zhang, *Appl. Organomet. Chem.* **2010**, *24*, 751-757; b) Y. Nakajima, S. Shimada, *RSC Adv.* **2015**, *5*, 20603-20616; c) M. D. Greenhalgh, A. S. Jones, S. P. Thomas, *ChemCatChem* **2015**, *7*, 190-222; d) X. Du, Z. Huang, *ACS Catal.* **2017**, *7*, 1227-1243.
- [6] a) L. Markó, M. A. Radhi, I. Ötvös, *J. Organomet. Chem.* **1981**, *218*, 369-376; b) L. Markó, J. Palágyi, *Transition Met. Chem.* **1983**, *8*, 207-209.
- [7] C. P. Casey, H. Guan, *J. Am. Chem. Soc.* **2007**, *129*, 5816-5817.
- [8] H.-J. Knölker, E. Baum, H. Goesmann, R. Klauss, *Angew. Chem. Int. Ed.* **1999**, *38*, 2064-2066.
- [9] S. Fleischer, S. Zhou, K. Junge, M. Beller, *Angew. Chem. Int. Ed.* **2013**, *52*, 5120-5124.
- [10] a) H.-J. Knölker, J. Heber, C. H. Mahler, *Synlett* **1992**, 1002-1004; b) H.-J. Knölker, J. Heber, *Synlett* **1993**, 924-926; c) H.-J. Knölker, E. Baum, J. Heber, *Tetrahedron Lett.* **1995**, *36*, 7647-7650.
- [11] A. Tlili, J. Schranck, H. Neumann, M. Beller, *Chem. Eur. J.* **2012**, *18*, 15935-15939.
- [12] K. Natte, W. Li, S. Zhou, H. Neumann, X.-F. Wu, *Tetrahedron Lett.* **2015**, *56*, 1118-1121.
- [13] D. S. Mérel, M. Elie, J. F. Lohier, S. Gaillard, J. L. Renaud, *ChemCatChem* **2013**, *5*, 2939-2945.
- [14] A. Lator, S. Gaillard, A. Poater, J. L. Renaud, *Chem. Eur. J.* **2018**, *24*, 5770-5774.
- [15] S. Vailati Facchini, J. M. Neudörfl, L. Pignataro, M. Cettolin, C. Gennari, A. Berkessel, U. Piarulli, *ChemCatChem* **2017**, *9*, 1461-1468.
- [16] a) C. P. Casey, H. Guan, *J. Am. Chem. Soc.* **2009**, *131*, 2499-2507; b) R. M. Bullock, *Angew. Chem. Int. Ed.* **2007**, *46*, 7360-7363.
- [17] H. Zhang, D. Chen, Y. Zhang, G. Zhang, J. Liu, *Dalton Trans.* **2010**, *39*, 1972-1978.

- [18] a) J. Zhang, G. Leitus, Y. Ben-David, D. Milstein, *J. Am. Chem. Soc.* **2005**, *127*, 10840-10841; b) J. Zhang, G. Leitus, Y. Ben-David, D. Milstein, *Angew. Chem. Int. Ed.* **2006**, *45*, 1113-1115; c) E. Balaraman, B. Gnanaprakasam, L. J. Shimon, D. Milstein, *J. Am. Chem. Soc.* **2010**, *132*, 16756-16758; d) C. Gunanathan, D. Milstein, *Acc. Chem. Res.* **2011**, *44*, 588-602; e) T. Zell, D. Milstein, *Acc. Chem. Res.* **2015**, *48*, 1979-1994.
- [19] R. Langer, G. Leitus, Y. Ben-David, D. Milstein, *Angew. Chem. Int. Ed.* **2011**, *50*, 2120-2124.
- [20] R. Langer, M. A. Iron, L. Konstantinovski, Y. Diskin-Posner, G. Leitus, Y. Ben-David, D. Milstein, *Chem. Eur. J.* **2012**, *18*, 7196-7209.
- [21] a) N. Gorgas, B. Stöger, L. F. Veiros, E. Pittenauer, G. Allmaier, K. Kirchner, *Organometallics* **2014**, *33*, 6905-6914; b) C. Schröder-Holzhacker, N. Gorgas, B. Stöger, K. Kirchner, *Monatsh. Chem.* **2016**, *147*, 1023-1030.
- [22] N. Gorgas, B. Stöger, L. F. Veiros, K. Kirchner, *ACS Catal.* **2016**, *6*, 2664-2672.
- [23] J. Brünig, Z. Csendes, S. Weber, N. Gorgas, R. W. Bittner, A. Limbeck, K. Bica, H. Hoffmann, K. Kirchner, *ACS Catal.* **2018**, *8*, 1048-1051.
- [24] S. Mazza, R. Scopelliti, X. Hu, *Organometallics* **2015**, *34*, 1538-1545.
- [25] B. Butschke, M. Feller, Y. Diskin-Posner, D. Milstein, *Catal. Sci. Technol.* **2016**, *6*, 4428-4437.
- [26] S. Chakraborty, P. O. Lagaditis, M. Förster, E. A. Bielinski, N. Hazari, M. C. Holthausen, W. D. Jones, S. Schneider, *ACS Catal.* **2014**, *4*, 3994-4003.
- [27] X. Yang, *Inorg. Chem.* **2011**, *50*, 12836-12843.
- [28] J. H. Docherty, J. Peng, A. P. Dominey, S. P. Thomas, *Nat. Chem.* **2017**, *9*, 595-600.
- [29] J. F. Sonnenberg, K. Y. Wan, P. E. Sues, R. H. Morris, *ACS Catal.* **2016**, *7*, 316-326.
- [30] G. Wienhoefer, F. A. Westerhaus, K. Junge, R. Ludwig, M. Beller, *Chem. Eur. J.* **2013**, *19*, 7701-7707.
- [31] L. Q. Lu, Y. Li, K. Junge, M. Beller, *Angew. Chem. Int. Ed.* **2013**, *52*, 8382-8386.
- [32] Y. Yi, H. Liu, L.-P. Xiao, B. Wang, G. Song, *ChemSusChem* **2018**, *11*, 1474-1478.
- [33] a) K. Jothimony, S. Vancheesan, *J. Mol. Catal.* **1989**, *52*, 301-304; b) K. Jothimony, S. Vancheesan, J. Kuriacose, *J. Mol. Catal.* **1985**, *32*, 11-16.
- [34] S. Enthaler, B. Hagemann, G. Erre, K. Junge, M. Beller, *Chem. Asian J.* **2006**, *1*, 598-604.
- [35] a) S. Enthaler, G. Erre, M. K. Tse, K. Junge, M. Beller, *Tetrahedron Lett.* **2006**, *47*, 8095-8099; b) S. Enthaler, B. Spilker, G. Erre, K. Junge, M. K. Tse, M. Beller, *Tetrahedron* **2008**, *64*, 3867-3876.
- [36] a) V. Polshettiwar, R. S. Varma, *Green Chem.* **2009**, *11*, 1313-1316; b) A. Ouali, J.-P. Majoral, A.-M. Caminade, M. Taillefer, *ChemCatChem* **2009**, *1*, 504-509.
- [37] A. Buchard, H. Heuclin, A. Auffrant, X. F. Le Goff, P. Le Floch, *Dalton Trans.* **2009**, 1659-1667.
- [38] a) V. V. K. M. Kandepi, J. M. S. Cardoso, E. Peris, B. Royo, *Organometallics* **2010**, *29*, 2777-2782; b) J. M. S. Cardoso, A. Fernandes, B. D. P. Cardoso, M. D. Carvalho, L. P. Ferreira, M. J. Calhorda, B. Royo, *Organometallics* **2014**, *33*, 5670-5677.
- [39] M. D. Bala, M. I. Ikhile, *J. Mol. Catal. A: Chem.* **2014**, *385*, 98-105.
- [40] H.-J. Knölker, H. Goesmann, R. Klaus, *Angew. Chem. Int. Ed.* **1999**, *38*, 702-705.
- [41] a) T. N. Plank, J. L. Drake, D. K. Kim, T. W. Funk, *Adv. Synth. Catal.* **2012**, *354*, 597-601; b) T. N. Plank, J. L. Drake, D. K. Kim, T. W. Funk, *Adv. Synth. Catal.* **2012**, *354*, 1179-1179.
- [42] T. W. Funk, A. R. Mahoney, R. A. Sponenburg, K. P. Zimmerman, D. K. Kim, E. E. Harrison, *Organometallics* **2018**, *37*, 1133-1140.
- [43] M.-C. Fu, R. Shang, Z. Huang, Y. Fu, *Synlett* **2014**, 2748-2752.
- [44] G. Metzker, A. C. B. Burtoloso, *Chem. Commun.* **2015**, *51*, 14199-14202.
- [45] N. Dai, R. Shang, M. Fu, Y. Fu, *Chin. J. Chem.* **2015**, *33*, 405-408.
- [46] C. A. M. R. van Slagmaat, S. M. A. De Wildeman, *Eur. J. Inorg. Chem.* **2018**, 694-702.
- [47] P. Zhang, X. Li, X. Qi, H. Sun, O. Fuhr, D. Fenske, *RSC Adv.* **2018**, *8*, 14092-14099.
- [48] M. N. Magubane, G. S. Nyamato, S. O. Ojwach, O. Q. Munro, *RSC Adv.* **2016**, *6*, 65205-65221.
- [49] G. Wienhöfer, F. A. Westerhaus, K. Junge, M. Beller, *J. Organomet. Chem.* **2013**, *744*, 156-159.
- [50] S. Zhou, S. Fleischer, K. Junge, M. Beller, *Angew. Chem.* **2011**, *123*, 5226-5230.
- [51] S. Fleischer, S. Werkmeister, S. Zhou, K. Junge, M. Beller, *Chem. Eur. J.* **2012**, *18*, 9005-9010.

- [52] S. Fleischer, S. Zhou, S. Werkmeister, K. Junge, M. Beller, *Chem. Eur. J.* **2013**, *19*, 4997-5003.
- [53] D. Brenna, S. Rossi, F. Cozzi, M. Benaglia, *Org. Biomol. Chem.* **2017**, *15*, 5685-5688.
- [54] S. Chakraborty, W. W. Brennessel, W. D. Jones, *J. Am. Chem. Soc.* **2014**, *136*, 8564-8567.
- [55] S. Zhou, S. Fleischer, K. Junge, S. Das, D. Addis, M. Beller, *Angew. Chem. Int. Ed.* **2010**, *49*, 8121-8125.
- [56] A. A. Mikhailine, M. I. Maishan, R. H. Morris, *Org. Lett.* **2012**, *14*, 4638-4641.
- [57] W. Zuo, A. J. Lough, Y. F. Li, R. H. Morris, *Science* **2013**, *342*, 1080-1083.
- [58] H.-J. Pan, T. W. Ng, Y. Zhao, *Org. Biomol. Chem.* **2016**, *14*, 5490-5493.
- [59] S. V. Facchini, M. Cettolin, X. Bai, G. Casamassima, L. Pignataro, C. Gennari, U. Piarulli, *Adv. Synth. Catal.* **2018**, *360*, 1054-1059.
- [60] R. V. Jagadeesh, K. Murugesan, A. S. Alshammari, H. Neumann, M.-M. Pohl, J. Radnik, M. Beller, *Science* **2017**, *358*, 326-332.
- [61] Y. Watanabe, M. Yamashita, T.-A. Mitsudo, M. Tanaka, Y. Takegami, *Tetrahedron Lett.* **1974**, *15*, 1879-1880.
- [62] M. D. Bhor, M. J. Bhanushali, N. S. Nandurkar, B. M. Bhanage, *Tetrahedron Lett.* **2008**, *49*, 965-969.
- [63] S. Fleischer, S. Zhou, K. Junge, M. Beller, *Chem. Asian J.* **2011**, *6*, 2240-2245.
- [64] a) A. Pagnoux-Ozherelyeva, N. Pannetier, M. D. Mbaye, S. Gaillard, J. L. Renaud, *Angew. Chem. Int. Ed.* **2012**, *51*, 4976-4980; b) S. Moulin, H. Dentel, A. Pagnoux-Ozherelyeva, S. Gaillard, A. Poater, L. Cavallo, J. F. Lohier, J. L. Renaud, *Chem. Eur. J.* **2013**, *19*, 17881-17890.
- [65] a) A. Pagnoux-Ozherelyeva, N. Pannetier, M. D. Mbaye, S. Gaillard, J.-L. Renaud, *Angew. Chem. Int. Ed.* **2012**, *51*, 4976-4980; b) S. Moulin, H. Dentel, A. Pagnoux-Ozherelyeva, S. Gaillard, A. Poater, L. Cavallo, J. F. Lohier, J. L. Renaud, *Chem. Eur. J.* **2013**, *19*, 17881-17890.
- [66] G. Metzker, R. M. Dias, A. C. Burtoloso, *ChemistrySelect* **2018**, *3*, 368-372.
- [67] D. S. Mérel, M. L. T. Do, S. Gaillard, P. Dupau, J.-L. Renaud, *Coord. Chem. Rev.* **2015**, *288*, 50-68.
- [68] J. A. Garg, S. Chakraborty, Y. Ben-David, D. Milstein, *Chem. Commun.* **2016**, *52*, 5285-5288.
- [69] F. Schneck, M. Assmann, M. Balmer, K. Harms, R. Langer, *Organometallics* **2016**, *35*, 1931-1943.
- [70] N. M. Rezayee, D. C. Samblanet, M. S. Sanford, *ACS Catal.* **2016**, *6*, 6377-6383.
- [71] U. Jayarathne, Y. Zhang, N. Hazari, W. H. Bernskoetter, *Organometallics* **2017**, *36*, 409-416.
- [72] C. Bornschein, S. Werkmeister, B. Wendt, H. Jiao, E. Alberico, W. Baumann, H. Junge, K. Junge, M. Beller, *Nat. Commun.* **2014**, *5*, 4111.
- [73] S. Lange, S. Elangovan, C. Cordes, A. Spannenberg, H. Jiao, H. Junge, S. Bachmann, M. Scalone, C. Topf, K. Junge, *Catal. Sci. Technol.* **2016**, *6*, 4768-4772.
- [74] S. Chakraborty, G. Leitus, D. Milstein, *Chem. Commun.* **2016**, *52*, 1812-1815.
- [75] S. Chakraborty, D. Milstein, *ACS Catal.* **2017**, *7*, 3968-3972.
- [76] S. Chakraborty, G. Leitus, D. Milstein, *Angew. Chem. Int. Ed.* **2017**, *56*, 2074-2078.
- [77] T. Zell, Y. Ben-David, D. Milstein, *Angew. Chem. Int. Ed.* **2014**, *53*, 4685-4689.
- [78] a) S. Chakraborty, H. Dai, P. Bhattacharya, N. T. Fairweather, M. S. Gibson, J. A. Krause, H. Guan, *J. Am. Chem. Soc.* **2014**, *136*, 7869-7872; b) N. T. Fairweather, M. S. Gibson, H. Guan, *Organometallics* **2014**, *34*, 335-339.
- [79] a) D. Spasyuk, D. G. Gusev, *Organometallics* **2012**, *31*, 5239-5242; b) A. Acosta-Ramirez, M. Bertoli, D. G. Gusev, M. Schlaf, *Green Chem.* **2012**, *14*, 1178-1188.
- [80] S. Elangovan, B. Wendt, C. Topf, S. Bachmann, M. Scalone, A. Spannenberg, H. Jiao, W. Baumann, K. Junge, M. Beller, *Adv. Synth. Catal.* **2016**, *358*, 820-825.
- [81] S. Qu, H. Dai, Y. Dang, C. Song, Z.-X. Wang, H. Guan, *ACS Catal.* **2014**, *4*, 4377-4388.
- [82] P. Gajewski, A. Gonzalez-de-Castro, M. Renom-Carrasco, U. Piarulli, C. Gennari, J. G. de Vries, L. Lefort, L. Pignataro, *ChemCatChem* **2016**, *8*, 3431-3435.
- [83] a) E. A. Quadrelli, G. Centi, J. L. Duplan, S. Perathoner, *ChemSusChem* **2011**, *4*, 1194-1215; b) W. Wang, S. Wang, X. Ma, J. Gong, *Chem. Soc. Rev.* **2011**, *40*, 3703-3727.
- [84] a) P. G. Jessop, T. Ikariya, R. Noyori, *Chem. Rev.* **1995**, *95*, 259-272; b) W. Leitner, *Angew. Chem. Int. Ed.* **1995**, *34*, 2207-2221; c) P. G. Jessop, F. Joó, C.-C. Tai, *Coord. Chem. Rev.* **2004**, *248*, 2425-2442; d) C. Federsel, R. Jackstell, M. Beller, *Angew. Chem. Int. Ed.* **2010**, *49*, 6254-

- 6257; e) K. Sordakis, C. Tang, L. K. Vogt, H. Junge, P. J. Dyson, M. Beller, G. Laurenczy, *Chem. Rev.* **2018**, *118*, 372-433; f) K. Dong, R. Razzaq, Y. Hu, K. Ding, *Top. Curr. Chem.* **2017**, *375*, 23; g) W.-H. Wang, X. Feng, M. Bao, *Transformation of Carbon Dioxide to Formic Acid and Methanol*, Springer, Singapore, **2018**; h) B. Li, J.-B. Sortais, C. Darcel, *RSC Adv.* **2016**, *6*, 57603-57625.
- [85] G. Evans, C. Newell, *Inorg. Chim. Acta* **1978**, *31*, L387-L389.
- [86] C.-C. Tai, T. Chang, B. Roller, P. G. Jessop, *Inorg. Chem.* **2003**, *42*, 7340-7341.
- [87] C. Federsel, A. Boddien, R. Jackstell, R. Jennerjahn, P. J. Dyson, R. Scopelliti, G. Laurenczy, M. Beller, *Angew. Chem. Int. Ed.* **2010**, *49*, 9777-9780.
- [88] J. L. Drake, C. M. Manna, J. A. Byers, *Organometallics* **2013**, *32*, 6891-6894.
- [89] a) A. Boddien, D. Mellmann, F. Gärtner, R. Jackstell, H. Junge, P. J. Dyson, G. Laurenczy, R. Ludwig, M. Beller, *Science* **2011**, *333*, 1733-1736; b) X. Yang, *Dalton Trans.* **2013**, *42*, 11987-11991.
- [90] M. Montandon-Clerc, G. Laurenczy, *J. Catal.* **2018**, *362*, 78-84.
- [91] C. Ziebart, C. Federsel, P. Anbarasan, R. Jackstell, W. Baumann, A. Spannenberg, M. Beller, *J. Am. Chem. Soc.* **2012**, *134*, 20701-20704.
- [92] R. Langer, Y. Diskin-Posner, G. Leitus, L. J. Shimon, Y. Ben-David, D. Milstein, *Angew. Chem., Int. Ed.* **2011**, *50*, 9948-9952.
- [93] O. Rivada-Wheelaghan, A. Dauth, G. Leitus, Y. Diskin-Posner, D. Milstein, *Inorg. Chem.* **2015**, *54*, 4526-4538.
- [94] Y. Zhang, A. D. MacIntosh, J. L. Wong, E. A. Bielinski, P. G. Williard, B. Q. Mercado, N. Hazari, W. H. Bernskoetter, *Chem. Sci.* **2015**, *6*, 4291-4299.
- [95] N. E. Smith, W. H. Bernskoetter, N. Hazari, B. Q. Mercado, *Organometallics* **2017**, *36*, 3995-4004.
- [96] X. Yang, *ACS Catal.* **2011**, *1*, 849-854.
- [97] R. Marcos, L. Xue, R. Sanchez-de-Armas, M. S. G. Ahlquist, *ACS Catal.* **2016**, *6*, 2923-2929.
- [98] F. Bertini, N. Gorgas, B. Stöger, M. Peruzzini, L. F. Veiros, K. Kirchner, L. Gonsalvi, *ACS Catal.* **2016**, *6*, 2889-2893.
- [99] H. Fong, J. C. Peters, *Inorg. Chem.* **2014**, *54*, 5124-5135.
- [100] a) F. Bertini, I. Mellone, A. Ienco, M. Peruzzini, L. Gonsalvi, *ACS Catal.* **2015**, *5*, 1254-1265; b) R. Marcos, F. Bertini, Z. Rinkevicius, M. Peruzzini, L. Gonsalvi, M. S. Ahlquist, *Chem. Eur. J.* **2018**, *24*, 5366-5372.
- [101] F. Zhu, L. Zhu-Ge, G. Yang, S. Zhou, *ChemSusChem* **2015**, *8*, 609-612.
- [102] A. Rosas-Hernández, P. G. Alsabeh, E. Barsch, H. Junge, R. Ludwig, M. Beller, *Chem. Commun.* **2016**, *52*, 8393-8396.
- [103] U. Jayarathne, N. Hazari, W. H. Bernskoetter, *ACS Catal.* **2018**, *8*, 1338-1345.
- [104] A. P. C. Ribeiro, L. M. D. Martins, A. J. L. Pombeiro, *Green Chem.* **2017**, *19*, 4811-4815.
- [105] H. Brunner, K. Fisch, *Angew. Chem. Int. Ed.* **1990**, *29*, 1131-1132.
- [106] N. S. Shaikh, K. Junge, M. Beller, *Org. Lett.* **2007**, *9*, 5429-5432.
- [107] D. Addis, N. Shaikh, S. Zhou, S. Das, K. Junge, M. Beller, *Chem. Asian J.* **2010**, *5*, 1687-1691.
- [108] N. S. Shaikh, S. Enthaler, K. Junge, M. Beller, *Angew. Chem. Int. Ed.* **2008**, *47*, 2497-2501.
- [109] H. Nishiyama, A. Furuta, *Chem. Commun.* **2007**, 760-762.
- [110] A. Furuta, H. Nishiyama, *Tetrahedron Lett.* **2008**, *49*, 110-113.
- [111] c.
- [112] T. Inagaki, A. Ito, J.-i. Ito, H. Nishiyama, *Angew. Chem. Int. Ed.* **2010**, *49*, 9384-9387.
- [113] K. Muller, A. Schubert, T. Jozak, A. Ahrens-Botzong, V. Schünemann, W. R. Thiel, *ChemCatChem* **2011**, *3*, 887-892.
- [114] B. Plietker, A. Dieskau, *Eur. J. Org. Chem.* **2009**, 775-787.
- [115] M. Holzwarth, A. Dieskau, M. Tabassam, B. Plietker, *Angew. Chem. Int. Ed.* **2009**, *48*, 7251-7255.
- [116] A. P. Dieskau, J. M. Begouin, B. Plietker, *Eur. J. Org. Chem.* **2011**, 5291-5296.
- [117] J. Yang, T. D. Tilley, *Angew. Chem. Int. Ed.* **2010**, *49*, 10186-10188.
- [118] A. J. Ruddy, C. M. Kelly, S. M. Crawford, C. A. Wheaton, O. L. Sydora, B. L. Small, M. Stradiotto, L. Turculet, *Organometallics* **2013**, *32*, 5581-5588.

- [119] M. Flückiger, A. Togni, *Eur. J. Org. Chem.* **2011**, 4353-4360.
- [120] A. M. Tondreau, E. Lobkovsky, P. J. Chirik, *Org. Lett.* **2008**, *10*, 2789-2792.
- [121] P. Bhattacharya, J. A. Krause, H. Guan, *Organometallics* **2011**, *30*, 4720-4729.
- [122] a) P. Bhattacharya, J. A. Krause, H. Guan, *Organometallics* **2014**, *33*, 6113-6121; b) S. Chakraborty, P. Bhattacharya, H. Dai, H. Guan, *Acc. Chem. Res.* **2015**, *48*, 1995-2003.
- [123] S. Wu, X. Li, Z. Xiong, W. Xu, Y. Lu, H. Sun, *Organometallics* **2013**, *32*, 3227-3237.
- [124] H. Zhao, H. Sun, X. Li, *Organometallics* **2014**, *33*, 3535-3539.
- [125] S. Huang, H. Zhao, X. Li, L. Wang, H. Sun, *RSC Adv.* **2015**, *5*, 15660-15667.
- [126] A. D. Smith, A. Saini, L. M. Singer, N. Phadke, M. Findlater, *Polyhedron* **2016**, *114*, 286-291.
- [127] a) T. T. Metsänen, D. Gallego, T. Szilvási, M. Driess, M. Oestreich, *Chem. Sci.* **2015**, *6*, 7143-7149; b) D. Gallego, S. Inoue, B. Blom, M. Driess, *Organometallics* **2014**, *33*, 6885-6897.
- [128] H.-J. Lin, S. Lutz, C. O'Kane, M. Zeller, C.-H. Chen, T. Al Assil, W.-T. Lee, *Dalton Trans.* **2018**, *47*, 3243-3247.
- [129] B. K. Langlotz, H. Wadepohl, L. H. Gade, *Angew. Chem. Int. Ed.* **2008**, *47*, 4670-4674.
- [130] a) A. M. Tondreau, J. M. Darmon, B. M. Wile, S. K. Floyd, E. Lobkovsky, P. J. Chirik, *Organometallics* **2009**, *28*, 3928-3940; b) S. Hosokawa, J.-i. Ito, H. Nishiyama, *Organometallics* **2010**, *29*, 5773-5775.
- [131] Z. Zuo, L. Zhang, X. Leng, Z. Huang, *Chem. Commun.* **2015**, *51*, 5073-5076.
- [132] J.-i. Ito, S. Hosokawa, H. B. Khalid, H. Nishiyama, *Organometallics* **2015**, *34*, 1377-1383.
- [133] T. Bleith, H. Wadepohl, L. H. Gade, *J. Am. Chem. Soc.* **2015**, *137*, 2456-2459.
- [134] T. Bleith, L. H. Gade, *J. Am. Chem. Soc.* **2016**, *138*, 4972-4983.
- [135] D. V. Gutsulyak, L. G. Kuzmina, J. A. Howard, S. F. Vyboishchikov, G. I. Nikonov, *J. Am. Chem. Soc.* **2008**, *130*, 3732-3733.
- [136] J. Zheng, L. C. Misal Castro, T. Roisnel, C. Darcel, J.-B. Sortais, *Inorg. Chim. Acta* **2012**, *380*, 301-307.
- [137] D. Bézier, J.-B. Sortais, C. Darcel, *Adv. Synth. Catal.* **2013**, *355*, 19-33.
- [138] F. Jiang, D. Bézier, J.-B. Sortais, C. Darcel, *Adv. Synth. Catal.* **2011**, *353*, 239-244.
- [139] D. Bézier, F. Jiang, T. Roisnel, J.-B. Sortais, C. Darcel, *Eur. J. Inorg. Chem.* **2012**, 1333-1337.
- [140] T. C. Jung, G. Argouarch, P. van de Weghe, *Catal. Commun.* **2016**, *78*, 52-54.
- [141] S. Demir, Y. Gökçe, N. Kaloğlu, J.-B. Sortais, C. Darcel, İ. Özdemir, *Appl. Organomet. Chem.* **2013**, *27*, 459-464.
- [142] V. César, L. C. Misal Castro, T. Dombray, J.-B. Sortais, C. Darcel, S. Labat, K. Miqueu, J.-M. Sotiropoulos, R. Brousses, N. Lugan, *Organometallics* **2013**, *32*, 4643-4655.
- [143] D. Kumar, A. Prakasham, L. P. Bheeter, J.-B. Sortais, M. Gangwar, T. Roisnel, A. C. Kalita, C. Darcel, P. Ghosh, *J. Organomet. Chem.* **2014**, *762*, 81-87.
- [144] C. Johnson, M. Albrecht, *Organometallics* **2017**, *36*, 2902-2913.
- [145] a) E. Buitrago, L. Zani, H. Adolfsson, *Appl. Organomet. Chem.* **2011**, *25*, 748-752; b) E. Buitrago, F. Tinnis, H. Adolfsson, *Adv. Synth. Catal.* **2012**, *354*, 217-222.
- [146] T. Hashimoto, S. Urban, R. Hoshino, Y. Ohki, K. Tatsumi, F. Glorius, *Organometallics* **2012**, *31*, 4474-4479.
- [147] C. Grohmann, T. Hashimoto, R. Fröhlich, Y. Ohki, K. Tatsumi, F. Glorius, *Organometallics* **2012**, *31*, 8047-8050.
- [148] S. Warratz, L. Postigo, B. Royo, *Organometallics* **2013**, *32*, 893-897.
- [149] Q. Liang, N. J. Liu, D. Song, *Dalton Trans.* **2018**, *47*, 9889-9896.
- [150] Z. Zuo, H. Sun, L. Wang, X. Li, *Dalton Trans.* **2014**, *43*, 11716-11722.
- [151] S. Ren, S. Xie, T. Zheng, Y. Wang, S. Xu, B. Xue, X. Li, H. Sun, O. Fuhr, D. Fenske, *Dalton Trans.* **2018**, *47*, 4352-4359.
- [152] T. Zheng, J. Li, S. Zhang, B. Xue, H. Sun, X. Li, O. Fuhr, D. Fenske, *Organometallics* **2016**, *35*, 3538-3545.
- [153] B. Xue, H. Sun, X. Li, *RSC Adv.* **2015**, *5*, 52000-52006.
- [154] a) B. Xue, H. Sun, Q. Niu, X. Li, O. Fuhr, D. Fenske, *Catal. Commun.* **2017**, *94*, 23-28; b) Y. Wang, S. Ren, W. Zhang, B. Xue, X. Qi, H. Sun, X. Li, O. Fuhr, D. Fenske, *Catal. Commun.* **2018**, *115*, 1-5.

- [155] F. S. Wekesa, R. Arias-Ugarte, L. Kong, Z. Sumner, G. P. McGovern, M. Findlater, *Organometallics* **2015**, *34*, 5051-5056.
- [156] K. Zhu, M. P. Shaver, S. P. Thomas, *Eur. J. Org. Chem.* **2015**, *2015*, 2119-2123.
- [157] Á. Raya-Barón, M. A. Ortuño, P. Oña-Burgos, A. Rodríguez-Diéguez, R. Langer, C. J. Cramer, I. Kuzu, I. Fernández, *Organometallics* **2016**, *35*, 4083-4089.
- [158] Á. Raya-Barón, C. P. Galdeano-Ruano, P. Oña-Burgos, A. Rodríguez-Diéguez, R. Langer, R. López-Ruiz, R. Romero-González, I. Kuzu, I. Fernández, *Dalton Trans.* **2018**, *47*, 7272-7281.
- [159] L. C. Misal Castro, D. Bézier, J.-B. Sortais, C. Darcel, *Adv. Synth. Catal.* **2011**, *353*, 1279-1284.
- [160] M. A. Nesbit, D. L. Suess, J. C. Peters, *Organometallics* **2015**, *34*, 4741-4752.
- [161] C. Dal Zotto, D. Virieux, J.-M. Campagne, *Synlett* **2009**, 276-278.
- [162] L. C. Misal Castro, J.-B. Sortais, C. Darcel, *Chem. Commun.* **2012**, *48*, 151-153.
- [163] M. Bhunia, P. K. Hota, G. Vijaykumar, D. Adhikari, S. K. Mandal, *Organometallics* **2016**, *35*, 2930-2937.
- [164] S. Enthaler, *ChemCatChem* **2010**, *2*, 1411-1415.
- [165] H. Jaafar, H. Li, L. C. Misal Castro, J. Zheng, T. Roisnel, V. Dorcet, J.-B. Sortais, C. Darcel, *Eur. J. Inorg. Chem.* **2012**, 3546-3550.
- [166] H. Li, M. Achard, C. Bruneau, J.-B. Sortais, C. Darcel, *RSC Adv.* **2014**, *4*, 25892-25897.
- [167] S. Werkmeister, K. Junge, M. Beller, *Org. Process Res. Dev.* **2014**, *18*, 289-302.
- [168] S. Zhou, K. Junge, D. Addis, S. Das, M. Beller, *Angew. Chem. Int. Ed.* **2009**, *48*, 9507-9510.
- [169] a) Y. Sunada, H. Kawakami, T. Imaoka, Y. Motoyama, H. Nagashima, *Angew. Chem. Int. Ed.* **2009**, *48*, 9511-9514; b) H. Tsutsumi, Y. Sunada, H. Nagashima, *Chem. Commun.* **2011**, *47*, 6581-6583.
- [170] D. Bézier, G. T. Venkanna, J.-B. Sortais, C. Darcel, *ChemCatChem* **2011**, *3*, 1747-1750.
- [171] A. Volkov, E. Buitrago, H. Adolfsson, *Eur. J. Org. Chem.* **2013**, 2066-2070.
- [172] B. Blom, G. Tan, S. Enthaler, S. Inoue, J. D. Epping, M. Driess, *J. Am. Chem. Soc.* **2013**, *135*, 18108-18120.
- [173] a) S. Zhou, D. Addis, S. Das, K. Junge, M. Beller, *Chem. Commun.* **2009**, 4883-4885; b) B. Xue, H. Sun, Y. Wang, T. Zheng, X. Li, O. Fuhr, D. Fenske, *Catal. Commun.* **2016**, *86*, 148-150.
- [174] S. Das, B. Wendt, K. Möller, K. Junge, M. Beller, *Angew. Chem. Int. Ed.* **2012**, *51*, 1662-1666.
- [175] D. Bézier, G. T. Venkanna, L. C. Misal Castro, J. Zheng, T. Roisnel, J.-B. Sortais, C. Darcel, *Adv. Synth. Catal.* **2012**, *354*, 1879-1884.
- [176] K. Junge, B. Wendt, S. Zhou, M. Beller, *Eur. J. Org. Chem.* **2013**, 2061-2065.
- [177] S. Das, Y. Li, K. Junge, M. Beller, *Chem. Commun.* **2012**, *48*, 10742-10744.
- [178] H. Li, L. C. Misal Castro, J. Zheng, T. Roisnel, V. Dorcet, J.-B. Sortais, C. Darcel, *Angew. Chem., Int. Ed.* **2013**, *52*, 8045-8049.
- [179] S. Quintero-Duque, H. Li, L. C. Misal Castro, V. Dorcet, T. Roisnel, E. Clot, M. Grellier, J.-B. Sortais, C. Darcel, *Isr. J. Chem.* **2017**, *57*, 1216-1221.
- [180] C. Cong, T. Fujihara, J. Terao, Y. Tsuji, *Catal. Commun.* **2014**, *50*, 25-28.
- [181] L. C. Misal Castro, H. Li, J.-B. Sortais, C. Darcel, *Chem. Commun.* **2012**, *48*, 10514-10516.
- [182] A. Corma, J. Navas, M. J. Sabater, *Chem. Rev.* **2018**, *118*, 1410-1459.
- [183] X. Cui, F. Shi, Y. Zhang, Y. Deng, *Tetrahedron Lett.* **2010**, *51*, 2048-2051.
- [184] M. Bala, P. K. Verma, U. Sharma, N. Kumar, B. Singh, *Green Chem.* **2013**, *15*, 1687-1693.
- [185] a) T. Yan, B. L. Feringa, K. Barta, *Nat. Commun.* **2014**, *5*, 5602; b) T. Yan, B. L. Feringa, K. Barta, *ACS Catal.* **2015**, *6*, 381-388.
- [186] B. Emayavaramban, M. Roy, B. Sundararaju, *Chem. Eur. J.* **2016**, *22*, 3952-3955.
- [187] T. J. Brown, M. Cumbes, L. J. Diorazio, G. J. Clarkson, M. Wills, *J. Org. Chem.* **2017**, *82*, 10489-10503.
- [188] H.-J. Pan, T. W. Ng, Y. Zhao, *Chem. Commun.* **2015**, *51*, 11907-11910.
- [189] A. Lator, S. Gaillard, A. Poater, J.-L. Renaud, *Org. Lett.* **2018**, *20*, 5985-5990.
- [190] T. Yan, B. L. Feringa, K. Barta, *Sci. Adv.* **2017**, *3*, eaao6494.
- [191] B. Emayavaramban, M. Sen, B. Sundararaju, *Org. Lett.* **2016**, *19*, 6-9.
- [192] S. Elangovan, J.-B. Sortais, M. Beller, C. Darcel, *Angew. Chem. Int. Ed.* **2015**, *54*, 14483-14486.

- [193] C. Seck, M. D. Mbaye, S. Coufourier, A. Lator, J. F. Lohier, A. Poater, T. R. Ward, S. Gaillard, J. L. Renaud, *ChemCatChem* **2017**, *9*, 4410-4416.
- [194] a) K. Burgess, M. J. Ohlmeyer, *Chem. Rev.* **1991**, *91*, 1179-1191; b) J. F. Hartwig, *Chem. Soc. Rev.* **2011**, *40*, 1992-2002; c) N. Miyaura, *Hydroboration, Diboration, Silylboration, and Stannylboration in Catalytic Heterofunctionalization* (Eds.: A. Togni, H. Grützmacher), Wiley-VCH Verlag GmbH, Weinheim, **2001**, pp. 1-45; d) I. Mkhaliid, J. Barnard, T. Marder, J. Murphy, J. Hartwig, *Chem. Rev.* **2010**, *110*, 890-931.
- [195] a) H. Doucet, *Eur. J. Org. Chem.* **2008**, 2013-2030; b) D. G. Hall, *Boronic Acids: Preparation, Applications in Organic Synthesis and Medicine*, Wiley-VCH Verlag GmbH & Co. KGaA, Weinheim, **2006**; c) R. Jana, T. P. Pathak, M. S. Sigman, *Chem. Rev.* **2011**, *111*, 1417-1492; d) N. Miyaura, A. Suzuki, *Chem. Rev.* **1995**, *95*, 2457-2483.
- [196] a) J. M. Brown, *Rhodium-Catalyzed Hydroborations and Related Reactions in Modern Rhodium-Catalyzed Organic Reactions* (Ed.: P. A. Evans), Wiley-VCH, Weinheim, **2005**, pp. 33-54; b) A. Coyne, P. Guiry, *The Development and Application of Rhodium-Catalyzed Hydroboration of Alkenes in Modern Reduction Methods* (Eds.: P. G. Andersson, I. J. Munslow), Wiley-VCH, Weinheim, **2008**, pp. 65-86.
- [197] a) J. F. Hartwig, S. Huber, *J. Am. Chem. Soc.* **1993**, *115*, 4908-4909; b) K. M. Waltz, X. He, C. Muhoro, J. F. Hartwig, *J. Am. Chem. Soc.* **1995**, *117*, 11357-11358.
- [198] J. Y. Wu, B. Moreau, T. Ritter, *J. Am. Chem. Soc.* **2009**, *131*, 12915-12917.
- [199] Y. Cao, Y. Zhang, L. Zhang, D. Zhang, X. Leng, Z. Huang, *Org. Chem. Front.* **2014**, *1*, 1101-1106.
- [200] L. Zhang, D. Peng, X. Leng, Z. Huang, *Angew. Chem.* **2013**, *125*, 3764-3768.
- [201] J. V. Obligation, P. J. Chirik, *Org. Lett.* **2013**, *15*, 2680-2683.
- [202] M. D. Greenhalgh, S. P. Thomas, *Chem. Commun.* **2013**, *49*, 11230-11232.
- [203] J. Zheng, J.-B. Sortais, C. Darcel, *ChemCatChem* **2014**, *6*, 763-766.
- [204] R. Gilbert-Wilson, W.-Y. Chu, T. B. Rauchfuss, *Inorg. Chem.* **2015**, *54*, 5596-5603.
- [205] K.-N. T. Tseng, J. W. Kampf, N. K. Szymczak, *ACS Catal.* **2014**, *5*, 411-415.
- [206] M. Espinal-Viguri, C. R. Woof, R. L. Webster, *Chem. Eur. J.* **2016**, *22*, 11605-11608.
- [207] T. Ogawa, A. J. Ruddy, O. L. Sydora, M. Stradiotto, L. Turculet, *Organometallics* **2016**, *36*, 417-423.
- [208] Y. Liu, Y. Zhou, H. Wang, J. Qu, *RSC Adv.* **2015**, *5*, 73705-73713.
- [209] X. Chen, Z. Cheng, Z. Lu, *Org. Lett.* **2017**, *19*, 969-971.
- [210] A. J. MacNair, C. R. Millet, G. S. Nichol, A. Ironmonger, S. P. Thomas, *ACS Catal.* **2016**, *6*, 7217-7221.
- [211] M. Haberberger, S. Enthaler, *Chem. Asian J.* **2013**, *8*, 50-54.
- [212] V. S. Rawat, B. Sreedhar, *Synlett* **2014**, *25*, 1132-1136.
- [213] K. Nakajima, T. Kato, Y. Nishibayashi, *Org. Lett.* **2017**, *19*, 4323-4326.
- [214] N. Gorgas, L. G. Alves, B. Stöger, A. M. Martins, L. F. Veiros, K. Kirchner, *J. Am. Chem. Soc.* **2017**, *139*, 8130-8133.
- [215] C. Wang, C. Wu, S. Ge, *ACS Catal.* **2016**, *6*, 7585-7589.
- [216] S. Jiang, S. Quintero-Duque, T. Roisnel, V. Dorcet, M. Grellier, S. Sabo-Etienne, C. Darcel, J.-B. Sortais, *Dalton Trans.* **2016**, *45*, 11101-11108.





## **Chapter II – Fe-Catalyzed Dehydrogenative Borylation Reactions**



## Chapter II – Fe-Catalyzed Dehydrogenative Borylation Reactions

### Introduction

Thanks to the impressive progress made in Suzuki-Miyaura coupling reactions,<sup>[1]</sup> the selective preparation of organoboron compounds has attracted broad interest over the last two decades.<sup>[2]</sup> In particular, alkenyl and alkynyl boronic esters are nowadays valuable boron derivatives, using in both Suzuki cross-couplings<sup>[2a]</sup> or Petasis reactions<sup>[3]</sup>. This family of compounds is traditionally prepared through the (dehydrogenative)hydroboration of alkynes and alkenes,<sup>[4]</sup> cross-metathesis,<sup>[5]</sup> Miyaura borylation<sup>[6]</sup> or boryl-Heck reactions.<sup>[7]</sup> More particularly, there has recently been intense interest in developing first row transition metal complexes for catalytic hydroboration of alkenes (with iron<sup>[8]</sup>, cobalt<sup>[9]</sup>, nickel<sup>[10]</sup> and manganese<sup>[11]</sup> catalysts) alkynes (with iron<sup>[8d, 12]</sup>, cobalt<sup>[13]</sup> and copper<sup>[14]</sup> catalysts), and enynes.<sup>[15]</sup> As an alternative, the selective C-H borylation of alkenes and alkynes is far less developed.<sup>[16]</sup> While the dehydrogenative borylation of styrenes or alkynes is often encountered and considered as a side reaction of their hydroboration to form organoboranes,<sup>[17]</sup> achieving a selective dehydrogenation of styrenes remains challenging.<sup>[18]</sup> However, an accurate design of the catalytic system can be performed to favor such pathway, then yielding alkenyl- or alkynylboronates from terminal alkenes or alkynes, respectively.<sup>[18]</sup>

In this chapter, we describe the use of iron based catalysts for the selective dehydrogenative borylation of styrenes giving styrylboronates (paragraph II-1) and of terminal alkynes leading to the corresponding alkynylboronates (Paragraph II-2).

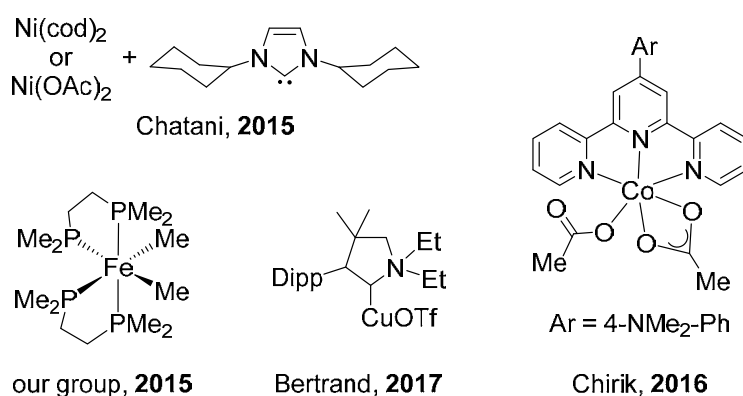


## II-1 Fe-Catalyzed dehydrogenative borylation of styrenes

**Contributions in this part:** Optimization and scope: Duo Wei, Thomas Dombray; DFT calculations: Mary Grellier, Tomoya Ichino, Satoshi Maeda.

### 1.1. Introduction

The direct C-H borylation of C<sub>sp2</sub>-H bonds of arenes has attracted a lot of attention,<sup>[19]</sup> notably lately with catalysts based on first row transition metals, due to (i) the importance of organoborate derivatives in organic synthesis,<sup>[20]</sup> (ii) the great advantages of direct C-H bond functionalization in terms of atom and step economic synthesis compared with classical synthetic methods<sup>[21]</sup> and (iii) the challenge of replacing traditional precious transition metals by abundant ones.<sup>[22]</sup> Several efficient catalytic systems based on nickel,<sup>[23]</sup> cobalt,<sup>[24]</sup> iron,<sup>[25]</sup> iron-zinc or iron-copper,<sup>[26]</sup> copper,<sup>[27]</sup> manganese,<sup>[28]</sup> titanium<sup>[29]</sup> and even metal-free Frustrated Lewis Pair (FLP)<sup>[30]</sup> have been developed (Scheme 1).

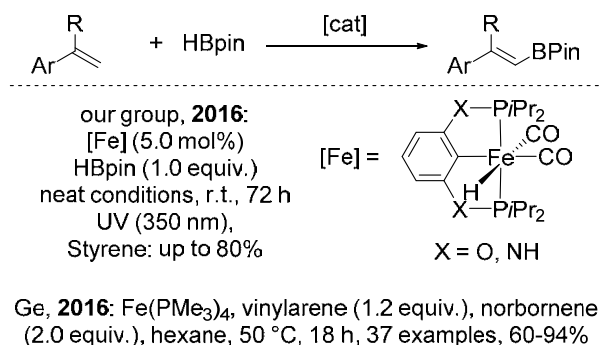


**Scheme 1.** Representative organometallic catalysts for C-H borylation reactions.

On the other hand, alkenyl boronic esters are also valuable boron derivatives, using in Suzuki cross-couplings<sup>[2a]</sup> or Petasis reactions.<sup>[3]</sup> As an alternative preparation method, the selective C-H borylation of C<sub>sp2</sub>-H of alkenes is far less developed. While the dehydrogenative borylation of styrenes is often encountered and considered as a side reaction of the hydroboration of alkenes to form organoboranes,<sup>[17]</sup> achieving a selective dehydrogenation of styrenes remains challenging.<sup>[18]</sup> Moreover, the rare examples of selective dehydrogenative borylation have been performed either in the presence of an excess of styrenes as hydrogen acceptor<sup>[31]</sup> or of boron precursors.<sup>[32]</sup>

In the case of iron, our group<sup>[33]</sup> and others<sup>[34]</sup> have observed the formation of vinylboronates, in the course of our studies on hydroboration of alkenes. Furthermore, using POCOP-iron hydride complexes, we have demonstrated for the first time that in the presence of

pinacolborane and an excess of styrene (3 equiv.), the corresponding vinyl boronate could be obtained with satisfying selectivity and good yield.<sup>[16a]</sup> In the course of our study, the group of Ge, reported that  $\text{Fe}(\text{PMe}_3)_4$  is an efficient catalyst for the borylation of styrenes in the presence of norbornene (2 equiv.), as an hydrogen acceptor (Scheme 2).<sup>[16b]</sup>



**Scheme 2.** Fe-catalyzed dehydrogenative borylation of styrenes.

In this chapter, following our strategy of C-H borylation of arenes in the absence of hydrogen acceptor<sup>[35]</sup>, we present an iron catalyzed selective dehydrogenative coupling of styrenes in the presence of a stoichiometric amount of HBpin, with the formation of  $\text{H}_2$  as the sole by-product.

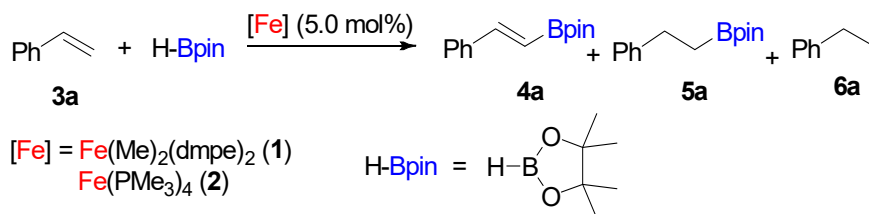
## 1.2. Results and discussions

### 1.2.1. Optimization of the parameters of the reaction

Based on our previous contribution on dehydrogenative borylation of arenes,<sup>[25d]</sup> we have first selected  $[\text{Fe}(\text{Me})_2(\text{dmpe})_2]$  complex **1** as the catalyst (5.0 mol%) to perform the first tests for the dehydroborylation of styrene **3a** (3 equiv.) with HBpin (1 equiv.) under UV irradiation at 350 nm at room temperature for 72 h under neat conditions (Table 1, entry 1); under such conditions, a full consumption of HBpin was observed by  $^{11}\text{B}$  NMR and the converted styrene lead to a mixture of styrylboronate **4a** (62%), 2-phenylethylboronate **5a** (19%) and ethylbenzene **6a** (19%) (Table 1). With this catalyst **1**, bearing two dmpe ligands, the selectivity couldn't be improved further. As iron(0) complex  $[\text{Fe}(\text{dmpe})_2]$  was postulated as a key intermediate in the course of the borylation of arenes, we turned our attention towards the parent iron (0) complex bearing monodentate phosphines, namely tetrakis(trimethylphosphine)-iron(0). To our delight, using  $\text{Fe}(\text{PMe}_3)_4$  (**2**) as the catalyst under similar conditions (Table 1, entry 2), after 18h, a full conversion of HBpin was detected by  $^{11}\text{B}$  NMR and styrylboronate **4a** was obtained in 87% isolated yield; It is important to note that: (i) more than 1 equiv. of styrene has reacted; (ii) in the crude mixture, only 2% of 2-phenylethylboronate **5a** was detected by CG; and (iii) the quantity of ethylbenzene **6a** formed

(34 %), resulting from the hydrogenation of styrene, is lower than the one of styrylboronate **4a** (64 %).

**Table 1.** Optimization of the Iron catalyzed dehydroborylation of styrene<sup>[a]</sup>



Entry	3a (equiv.)	Conditions <sup>[a]</sup>	Conv. (%) <sup>[b]</sup>	Select. (%) <sup>[b,c]</sup> 4a : 5a : 6a	Yield 4a (%) <sup>[d]</sup>
1 <sup>[e]</sup>	3.0	Neat, UV, 18 h	>98	62:19:19	83 <sup>f</sup>
2 <sup>[g]</sup>	3.0	Neat, UV, 18 h	>98	64:2:34	87
3 <sup>[g]</sup>	2.0	Neat, UV, 18 h	>98	64:5:31	80
4 <sup>[g]</sup>	1.0	Neat, UV, 18 h	>98	40:36:24	37
5 <sup>[g]</sup>	3.0	Neat, 50 °C, 18 h	>98	74:1:25	85
6 <sup>[g]</sup>	3.0	MeCN, 50 °C, 18 h	8	-	-
7 <sup>[g]</sup>	3.0	THF, 50 °C, 18 h	>98	68:1:31	81
8 <sup>[g]</sup>	3.0	pentane, 50 °C, 18 h	>98	71:2:27	81
9 <sup>[g]</sup>	3.0	Toluene, 50 °C, 18 h	>98	71:1:28	83
10 <sup>[g]</sup>	2.0	Toluene, 50 °C, 18 h	>98	77:1:22	78
11 <sup>[g]</sup>	1.0	Toluene, 50 °C, 18 h	>98	80:5:15	76
12	1.0	Toluene, 50 °C, 18 h	>98 <sup>[i]</sup>	85:5:15	76
13	1.0	Toluene, 50 °C, 6 h	90 <sup>[i]</sup>	86:11:3	64
14 <sup>[h]</sup>	1.0	Toluene, 50 °C, 18 h	47 <sup>[i]</sup>	86:9:5	34
15	1.0	Toluene, 30 °C, 18 h	84 <sup>[i]</sup>	84:4:12	35
16 <sup>[j]</sup>	1.0	Toluene, 50 °C, 18h	46	94:3:3	28

<sup>[a]</sup> Typical conditions: 5.0 mol% of [Fe] catalyst, 0.5 mmol of HBpin, neat or 0.5 mL of toluene, 18 h;

<sup>[b]</sup> Conversion based on HBpin detected by <sup>11</sup>B NMR;

<sup>[c]</sup> product distribution determined by GC based on converted styrene. N.B.: more than 1.0 equiv. of styrene may be consumed;

<sup>[d]</sup> Isolated yield based on HBpin;

<sup>[e]</sup> [Fe(dmpe)<sub>2</sub>Me<sub>2</sub>] as the catalyst, 72 h;

<sup>[f]</sup> 83% isolated yield, mixture of **4a** (77%) and **5a** (23%) (by <sup>1</sup>H NMR);

<sup>[g]</sup> [Fe(PMe<sub>3</sub>)<sub>4</sub>] as the catalyst.

<sup>[h]</sup> 2.5 mol% of catalyst was used instead of 5.0 mol%.

<sup>[i]</sup> Determined by GC based on styrene.

<sup>[j]</sup> With 20 mol% PMe<sub>3</sub>

More importantly, compared to the borylation of arenes, the irradiation is not mandatory for the borylation to occur as the reaction can be also performed at 50 °C without any UV irradiation, leading to similar activity and selectivity (entry 5). Interestingly, under thermal conditions, with Fe(PMe<sub>3</sub>)<sub>4</sub> **2** as the catalyst (5.0 mol%), the borylation of styrene can be performed in organic solvents (entries 6-9). Whereas no reaction was observed in acetonitrile, toluene was identified to be the best solvent, with an excellent selectivity and notably without the concomitant borylation of the aromatic solvent (entry 9). Finally, in neat conditions and in



toluene, the quantity of styrene can be decreased from 3 to 1 equiv.: in toluene, with a slightly lower yield based on HBpin (76 % vs 83%) but a yield based on styrene increasing from 27 to 76% (Entries 2-4 and 9-11). Finally, lowering the temperature to 30 °C, the catalyst loading to 2.5 mol% or the reaction time to 6 h has a deleterious effect on the activity (entries 12-15).

Thus the optimized conditions to obtain the dehydroborated styryl boronate derivatives is the use of 5.0 mol% of the catalyst  $\text{Fe}(\text{PMe}_3)_4$  **2** in the presence of 1 equiv. of styrene derivative, 1 equiv. of H-Bpin in toluene at 50 °C for 18h (Table 1, entry 11).

### 1.2.2. Scope of the dehydrogenative borylation of styrene derivatives

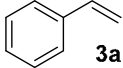
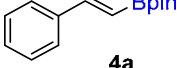
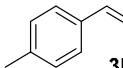
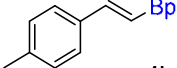
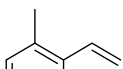
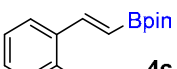
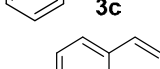
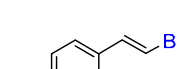
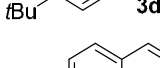
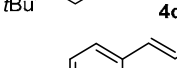
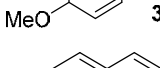
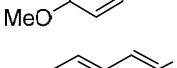
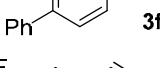
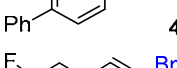
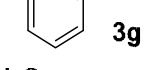
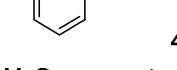
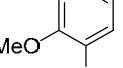
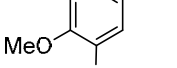
Then, we probed the scope of the reaction with  $\text{Fe}(\text{PMe}_3)_4$  **2** as the catalyst precursor (Table 2). Good isolated yields for alkyl substituted styrenes were obtained (**4a-d**, 79-90%). In the case of *p*-methylstyrene **3b**, in addition to the styrylboronate **4b**, 20% of 2-(4'-methylphenyl)ethylboronate **5b** were also obtained. Styrenes bearing *para*-electron donating substituents such as methoxy **3e** and phenyl **3f** led to the corresponding borylated styryl derivatives **4e-f** with 70-90% yields. Starting with 3,4,5-trimethoxyphenylethene **3h**, under similar conditions, only 70% of conversion was observed and the expected borylated styryl derivative **4h** was obtained in 31% NMR-yield, in addition of 38% of 1-ethyl-3,4,5-trimethoxybenzene **6h**.

Noticeably,  $\alpha$ -methylstyrene **3i** can be also dehydroborylated and the expected borylated styryl derivative **4i** was isolated in 68% yield. However, with (*E*)- $\beta$ -methylstyrene, bearing an internal C=C bond, under similar conditions, no reaction occurred.

With 4-chloro-styrene, under similar conditions, low conversions were observed (21 %), and a mixture was obtained including the products resulting of the dehalogenation of the starting material. Noticeably, it must be also pointed out that in the cases of functionalized styrenes such as 4-cyanostyrene or vinyl-pyridine, no reaction of dehydrogenative borylation occurred due to polymerization of the starting materials.

**Table 2.** Functionalized styrene dehydroborylation catalyzed by Fe(PMe<sub>3</sub>)<sub>4</sub> **2**.

$\text{3 (1.0 equiv.)} + \text{H-Bpin} \xrightarrow[\text{toluene (0.5 mL), 50 }^\circ\text{C}]{\text{Fe(PMe}_3)_4 \text{ (5 mol\%)}}$ 
 $\boxed{\text{4}} + \text{5} + \text{6}$

Entry	Substrate	Time (h)	Conv. (%) <sup>[a]</sup>	4:5:6	Borylated styrene	Yield of 4 (%) <sup>[b]</sup>
1	 <b>3a</b>	18	>98	80:5:15	 <b>4a</b>	76
2	 <b>3b</b>	40	>98	88:7:5	 <b>4b</b>	80 <sup>[c]</sup>
3	 <b>3c</b>	40	>98	89:6:5	 <b>4c</b>	79 <sup>[d]</sup>
4	 <b>3d</b>	20	>98	76:9:15	 <b>4d</b>	90 <sup>[e]</sup>
5	 <b>3e</b>	72	>98	77:3:20	 <b>4e</b>	77
6	 <b>3f</b>	40	>98	73:3:24	 <b>4f</b>	70
7	 <b>3g</b>	86	>98	89:5:6	 <b>4g</b>	81 <sup>[f]</sup>
8	 <b>3h</b>	86	70	43:3:54	 <b>4h</b>	31 <sup>[g]</sup>
9 <sup>[h]</sup>	 <b>3i</b>	86	>98	91:6:3	 <b>4i</b>	68

<sup>[a]</sup> Detected by <sup>1</sup>H NMR of crude mixture;<sup>[b]</sup> Isolated yield;<sup>[c]</sup> Isolated as mixture of **4b** and **5b** in 1:0.20;<sup>[d]</sup> Isolated as mixture of **4c** and **5c** in 1:0.10;<sup>[e]</sup> Isolated as mixture of **4d** and **5d** in ratio of 1:0.12.;<sup>[f]</sup> Isolated as mixture of **4g**, **5g** and **6g** in ratio of 1:0.06:0.07<sup>[g]</sup> Yield determined by NMR<sup>[h]</sup> 2.0 equiv. of α-methylstyrene (**3i**) were used

### 1.3. Mechanistic insights

In order to determine theoretically the reaction pathway for the reaction of **3a** with H-Bpin catalyzed by Fe(PMe<sub>3</sub>)<sub>4</sub>, an automated reaction path search method, artificial force induced reaction (AFIR)<sup>[36]</sup> has been used and performed by Mary Grellier (LCC Toulouse). All structures discussed below were optimized by a spin-unrestricted DFT method with the B3LYP

functional<sup>[37]</sup>, the 6-31G\* basis set and the empirical dispersion correction<sup>[38]</sup>. Transition states (TSs) were confirmed to be first-order saddle points by normal mode analysis, and path connections were determined by intrinsic reaction coordinate calculations starting from TSs. The analysis of the different reaction pathways has been done on iron complexes at singlet, triplet, and quintet spin states multiplicities.

### 1.3.1. Structure of the ground spin state of Fe(PMe<sub>3</sub>)<sub>4</sub> catalyst

Optimized structures of the Fe(PMe<sub>3</sub>)<sub>4</sub> catalyst in the three spin multiplicities are shown in Figure 1. Coordination number of singlet and triplet states is four, while that of quintet state is three. The quintet structure is identified as Fe(PMe<sub>3</sub>)<sub>3</sub>. The expectation value of spin-squared operator  $\langle \hat{S}^2 \rangle$  indicates that the singlet structure corresponds to open-shell-singlet. Relative electronic energies and Gibbs free energies of these spin states are summarized in Figure 1. The quintet state is the most unstable of the three spin states, showing that the quintet state is excluded from the ground spin state of Fe(PMe<sub>3</sub>)<sub>4</sub>. It is found that the triplet state is more stable than the singlet state. Therefore, the ground spin state of Fe(PMe<sub>3</sub>)<sub>4</sub> is triplet.

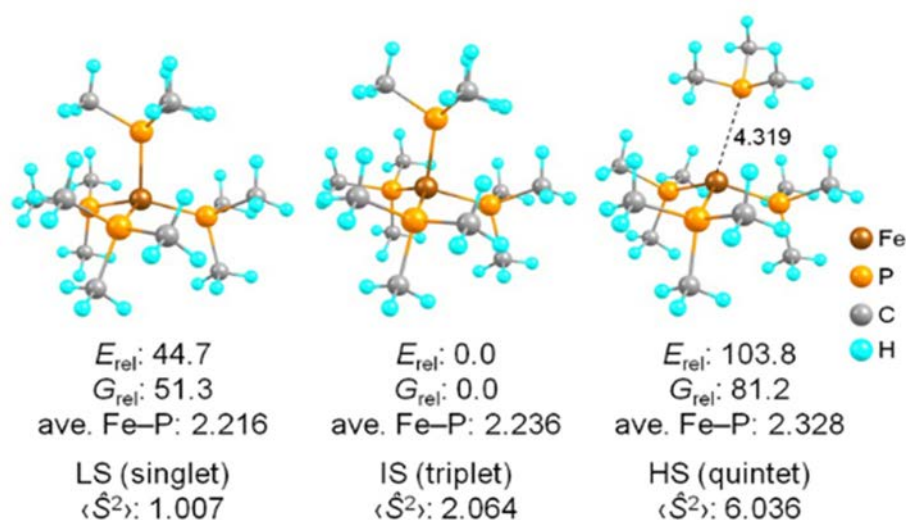


**Figure. 1.** Optimized structures of Fe(PMe<sub>3</sub>)<sub>4</sub> in singlet, triplet, and quintet states. Electronic and free energy values ( $E_{\text{rel}}$  and  $G_{\text{rel}}$ ) relative to the starting point in unit of kJ/mol, averaged Fe-P bond length (ave. Fe-P) in unit of Å, and the expectation value of spin-squared operator ( $\langle \hat{S}^2 \rangle$ ) are shown.

### 1.3.2. Substrate coordination

The possibilities of coordination of styrene or HBpin to  $\text{Fe}(\text{PMe}_3)_4$ , and the dissociation of  $\text{PMe}_3$  ligand from the iron complex **2** at the first reaction step have been examined. Energy profiles in triplet state are shown in Figure 2. The barrier energy for the  $\text{PMe}_3$  dissociation step is 59.4 kJ/mol, which is the lowest in the possible reaction steps. The alternatives for the first reaction step involving styrene or HBpin approaches to the catalyst **2** lead to a  $\text{PMe}_3$  spontaneous dissociation from the Fe atom. The energy of simple  $\text{PMe}_3$  dissociation is lower than the energy found for the transition states involving the coordination of styrene **3a** (TS1/2) or HBpin (TS3/4) (e.g. 104.0 and 109.6 kJ/mol respectively). For the two coordination steps to the catalyst, spin dependence has been studied. These energy barriers in singlet state are higher than those in triplet state. For the structural change of coordination of styrene, spontaneous dissociation of  $\text{PMe}_3$  occurs, which is same as that in triplet. Therefore, a styrene-bound  $\text{Fe}(\text{PMe}_3)_4$  complex does not exist at the present computational level. The dissociation of  $\text{PMe}_3$  in the triplet state is then the first reaction step, and the possibilities of coordination of styrene and HBpin can be ruled out.

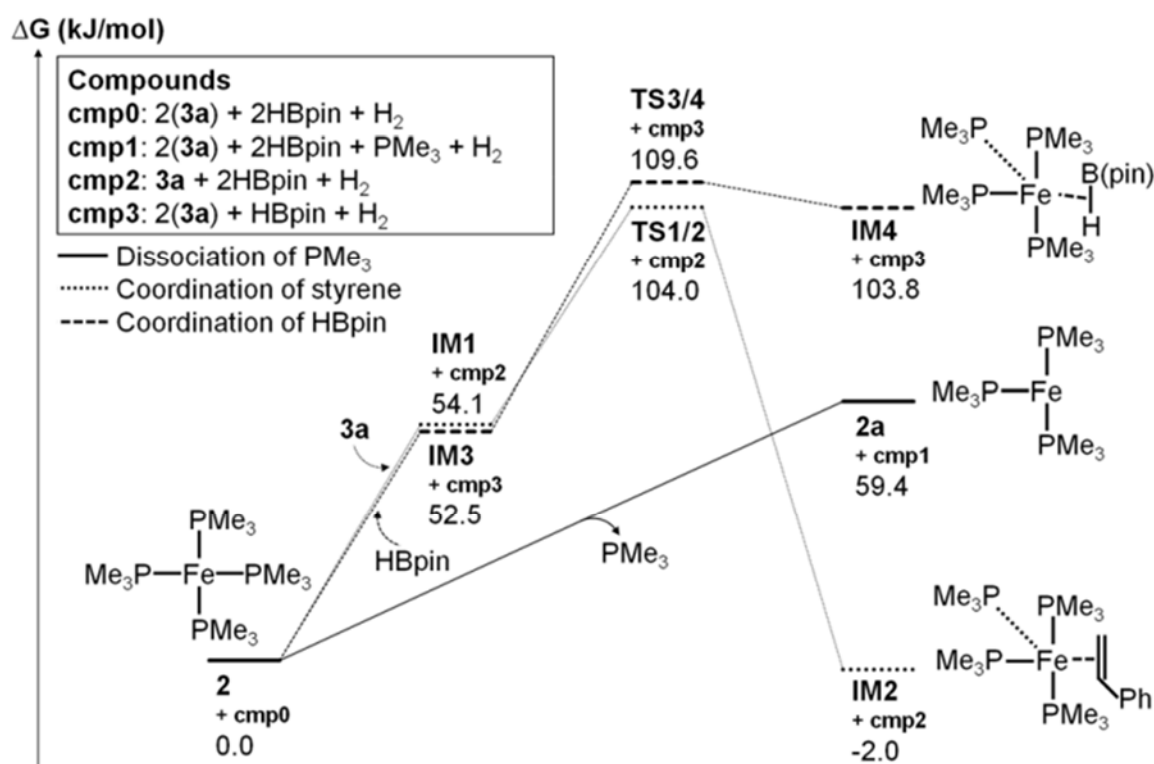


**Figure 2.** Energy profiles at first reaction step in triplet state. Dissociation step of  $\text{PMe}_3$ , and coordination steps of styrene and HBpin are represented in solid, dotted, and dashed lines, respectively. Gibbs free energy was estimated at 323.15 K and 1.0 atm. Energy reference is sum of  $\text{Fe}(\text{PMe}_3)_4$  in triplet state, two styrenes, HBpin, and H<sub>2</sub>. **2** and **3a** are  $\text{Fe}(\text{PMe}_3)_4$  and styrene, respectively.

Possibilities of coordination of styrene or HBpin to **2a**, and dissociation of  $\text{PMe}_3$  from **2a** have been investigated and compared at second reaction step. Energy profiles for the three possible steps are shown in Figure 3. It is clear that the coordination of styrene is energetically preferable step. Furthermore, the coordination of styrene would kinetically proceed than that of HBpin since the concentration of styrene is higher than that of HBpin at initial condition of the catalytic reaction (see entry 4–6 in Table1). The possibility of dissociation step is ruled out since this step is only endothermic reaction, and has the highest barrier. Therefore, the coordination of styrene to  $\text{Fe}(\text{PMe}_3)_3$  is the second reaction step.

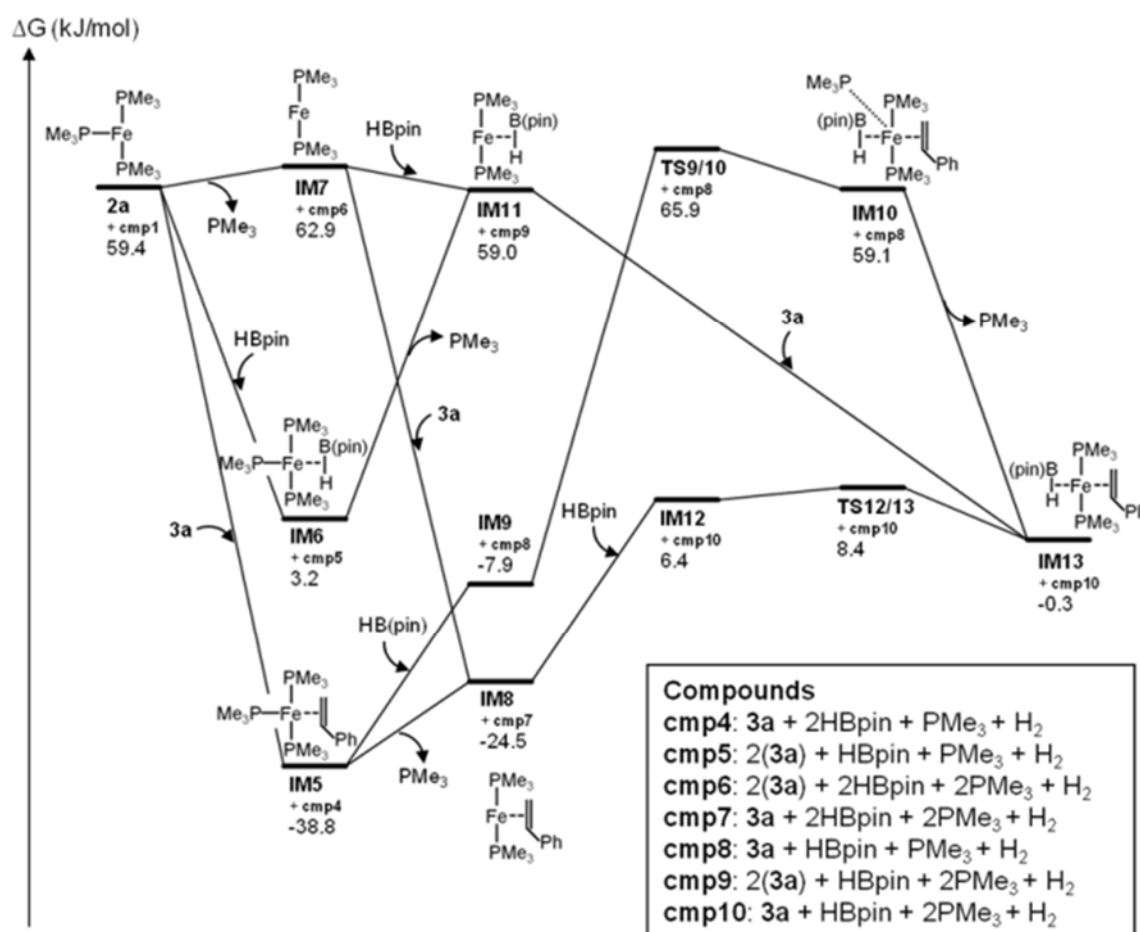


**Figure 3.** Energy profiles at second reaction step in triplet state. Gibbs free energy was estimated at 323.15 K and 1.0 atm. Energy reference is sum of  $\text{Fe}(\text{PMe}_3)_4$  in triplet state, two styrenes, HBpin, and  $\text{H}_2$ . **3a** is styrene (see in scheme 1).

The coordination of HBpin to **IM5** and the dissociation of  $\text{PMe}_3$  from **IM5** have been investigated at the third reaction step. Energy profiles for the two possible steps are shown in Fig. 3. **IM9** corresponds to a weak complex between **IM5** and HBpin. As HBpin approaches **IM5**, a  $\text{PMe}_3$  spontaneously dissociates from the Fe atom through **TS9/10** with a high barrier. The dissociation of  $\text{PMe}_3$  to generate **IM8** is energetically more preferred and thus is the third

reaction step. **IM12** is a weak complex between **IM8** and HBpin, and it generates **IM13** through a tiny barrier **TS12/13**. Overall, the coordination of substrates occurs in the following sequence: (i)  $\text{PMe}_3$  dissociation, (ii) styrene coordination, (iii) another  $\text{PMe}_3$  dissociation, and (iv) HBpin coordination.

It was also shown that the singlet state is not favorable at any of intermediate along the best path. At **2a**, quintet is 12.5 kJ/mol lower than triplet. A spin-crossover may take place at **2a**, although its impact on the reaction kinetics would be small because quintet is not favorable at any other intermediate.

### 1.3.3. Styrylboronate formation

Figure 4 shows a reaction profile for the formation of styrylboronate. Along the path of triplet state, a B-H bond cleavage occurs at **TS13/14<sub>IS</sub>**. Then, conformational rearrangements and pseudo rotation around the Fe atom take place in the area between **IM14<sub>IS</sub>** and **IM17<sub>IS</sub>**. The C-H bond activation takes place at **TS17/18<sub>IS</sub>**, and this TS is the highest energy point along this path. There is a tiny barrier at **TS18/19<sub>IS</sub>** to form an H-H bond. Subsequent  $\text{H}_2$  dissociation, styrene coordination, and dissociation of the styrylboronate product reproduces **IM8<sub>IS</sub>**.

Along the path of triplet state, the hydride transfer step through **TS17/18<sub>IS</sub>** corresponds to the rate-determining step. TSs of the same step for singlet and quintet paths are both much higher in free energy than the triplet one. Therefore, we conclude that **TS17/18<sub>IS</sub>** is the rate-determining step of this reaction. As seen in Figure 4, a spin-crossover may take place between **IM13** and **IM14** and also between **IM17** and **IM18**. The lowest energy point before the rate-determining step is **IM14<sub>HS</sub>**. The overall barrier for this reaction would thus be the energy difference between **TS17/18<sub>IS</sub>** and **IM14<sub>HS</sub>** ~89.1 kJ/mol. The experimental temperature 50°C is enough to overcome this barrier.

Another remarkable point is that the reverse reaction from **IM21<sub>IS</sub>** to **IM14<sub>HS</sub>** is also possible at the experimental temperature. Its overall barrier (the energy gap between **TS17/18<sub>IS</sub>** and **IM21<sub>IS</sub>**) is ~107.6 kJ/mol. This allows the system to access byproducts that are preferred thermodynamically, as discussed below.

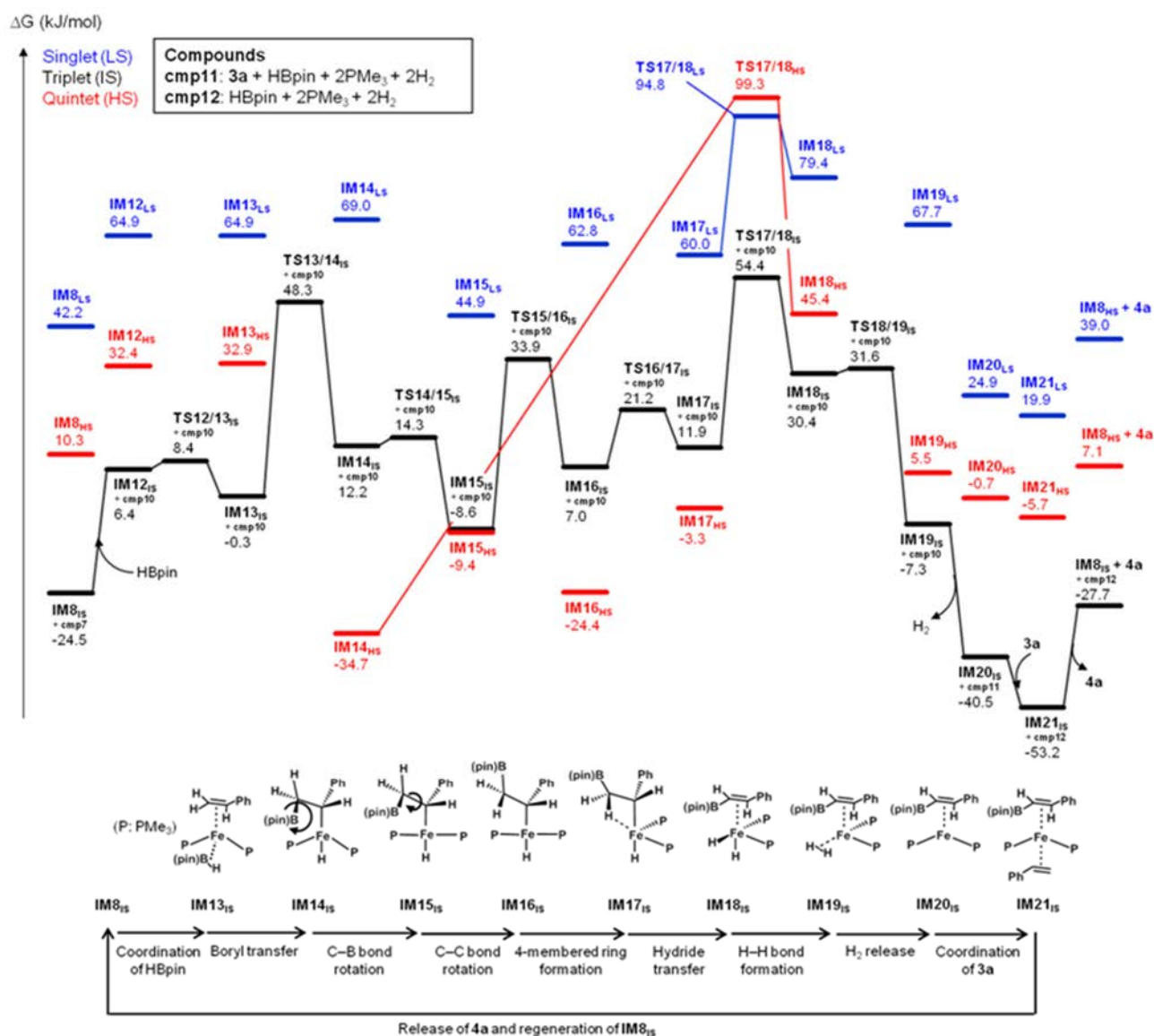


**Figure 4.** A reaction profile for the formation of styrylboronate in singlet (LS: low spin), triplet (IS: intermediate spin), and quintet (HS: high spin) states. For LS and HS, only local minima and the rate determining transition state are shown. Energy values relative to the starting point are shown in unit of kJ/mol.

### 1.3.4. 2-Phenylethylboronate formation

In Figure 5, a reaction profile for the formation of 2-phenylethylboronate is given. The B-H activation part is identical to the one for styrylboronate formation in Figure 4. The branching between formation of styrylboronate or 2-phenylethylboronate occurs at  $\text{IM15}_{\text{IS}}$ . A pseudo rotation takes place through a relatively high barrier  $\text{TS15/22}_{\text{IS}}$  to take a form in which a subsequent hydride transfer can happen. The hydride transfer TS ( $\text{TS22/23}_{\text{IS}}$ ) is the highest energy point along this profile. Finally, a coordination of styrene and a subsequent dissociation of 2-phenylethylboronate give  $\text{IM8}_{\text{IS}}$ .

Singlet and quintet TSs for the hydride transfer step are much higher in energy than the one in the triplet state. This confirms that the hydride transfer step through **TS22/23<sub>IS</sub>** is the rate-determining step. The lowest energy point before **TS22/23<sub>IS</sub>** is **IM14<sub>HS</sub>**. The overall barrier can therefore be estimated to be ~98.9 kJ/mol as the energy difference between **TS22/23<sub>IS</sub>** and **IM14<sub>HS</sub>**. The overall barrier is bigger than the one in the styrylboronate formation. This explains the dominant formation of the styrylboronate product.

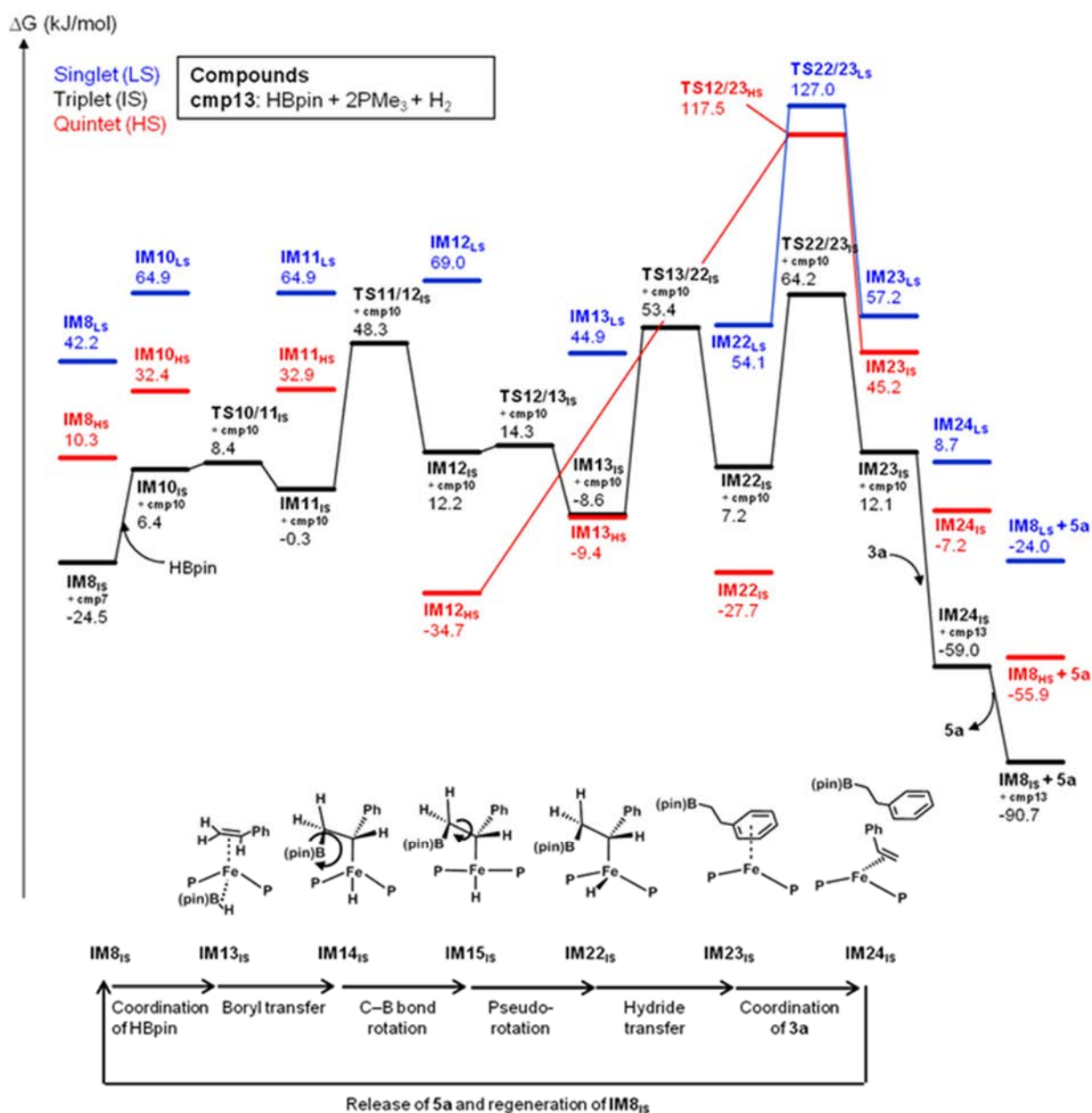


**Figure 5.** A reaction profile for the formation of 2-phenylethylboronate in singlet (LS: low spin), triplet (IS: intermediate spin), and quintet (HS: high spin) states. For LS and HS, only local minima and the rate determining transition state are shown. Energy values relative to the starting point are shown in unit of kJ/mol.



On the other hand, styrylboronate is thermodynamically less preferred than 2-phenylethylboronate. In other words, it is expected that the amount of 2-phenylethylboronate formation changes depending on reaction conditions. This point is discussed below in more detail.

### 1.3.5. Ethylbenzene formation

As shown experimentally, ethylbenzene is one of significant byproducts. We therefore studied the formation path of ethylbenzene *via* a hydrogenation of styrene. In this path, H<sub>2</sub> produced as byproduct of the styrylboronate formation is the hydrogen source. Figure 6 shows its reaction profile. Along the triplet path, H-H dissociation occurs on the Fe center through **TS25/26<sub>IS</sub>**. Then, the hydride transfer occurs from Fe to C *via* **TS26/27<sub>IS</sub>**, where this TS is the highest energy point along the profile. After pseudo rotations in the area from **IM27<sub>IS</sub>** to **IM30<sub>IS</sub>**, the second hydride transfer takes place *via* **TS30/31<sub>IS</sub>**. Then, a styrene coordination and H<sub>2</sub> dissociation reproduces **IM8<sub>IS</sub>**.

The overall barrier in the reaction from **IM8<sub>IS</sub>** to **IM27<sub>IS</sub>** or **IM27<sub>HS</sub>** can be estimated as the energy gap between **TS26/27<sub>IS</sub>** and **IM8<sub>IS</sub>** ~68.6 kJ/mol. On the other hand, the overall barrier for the second hydride transfer can be estimated as the energy gap between **TS30/31<sub>IS</sub>** and **IM29<sub>HS</sub>** ~94.2 kJ/mol. Therefore, the second hydride transfer through **TS30/31<sub>IS</sub>** is the rate-determining step of this reaction. In singlet and quintet states, **TS26/27<sub>LS</sub>**, **TS30/31<sub>LS</sub>**, and **TS30/31<sub>HS</sub>** were found to be higher in free energy than those in triplet state (see Figure 6). However, TS in quintet corresponding to **TS26/27<sub>IS</sub>** was not be obtained at the computational level used.

Along this profile, once the system goes over the highest TS (**TS26/27<sub>IS</sub>**), the reverse reaction generating styrene and H<sub>2</sub> is unlikely to proceed because the forward reaction is preferred both kinetically and thermodynamically. Therefore, the overall barrier ~68.6 kJ/mol for the first hydride transfer is compared to those in styrylboronate (~89.1 kJ/mol) and 2-phenylethylboronate (~98.9 kJ/mol); the overall barrier is smallest in the ethylbenzene formation. However, it is kinetically unfavorable, because concentration of H<sub>2</sub>, which is a byproduct of styrylboronate formation, is expected to be low especially in the initial stage of the reaction. Its concentration increases as the reaction proceeds is not negligible. This would explain generation of ethylbenzene of 15-34% in the present experiments (see Table 1).

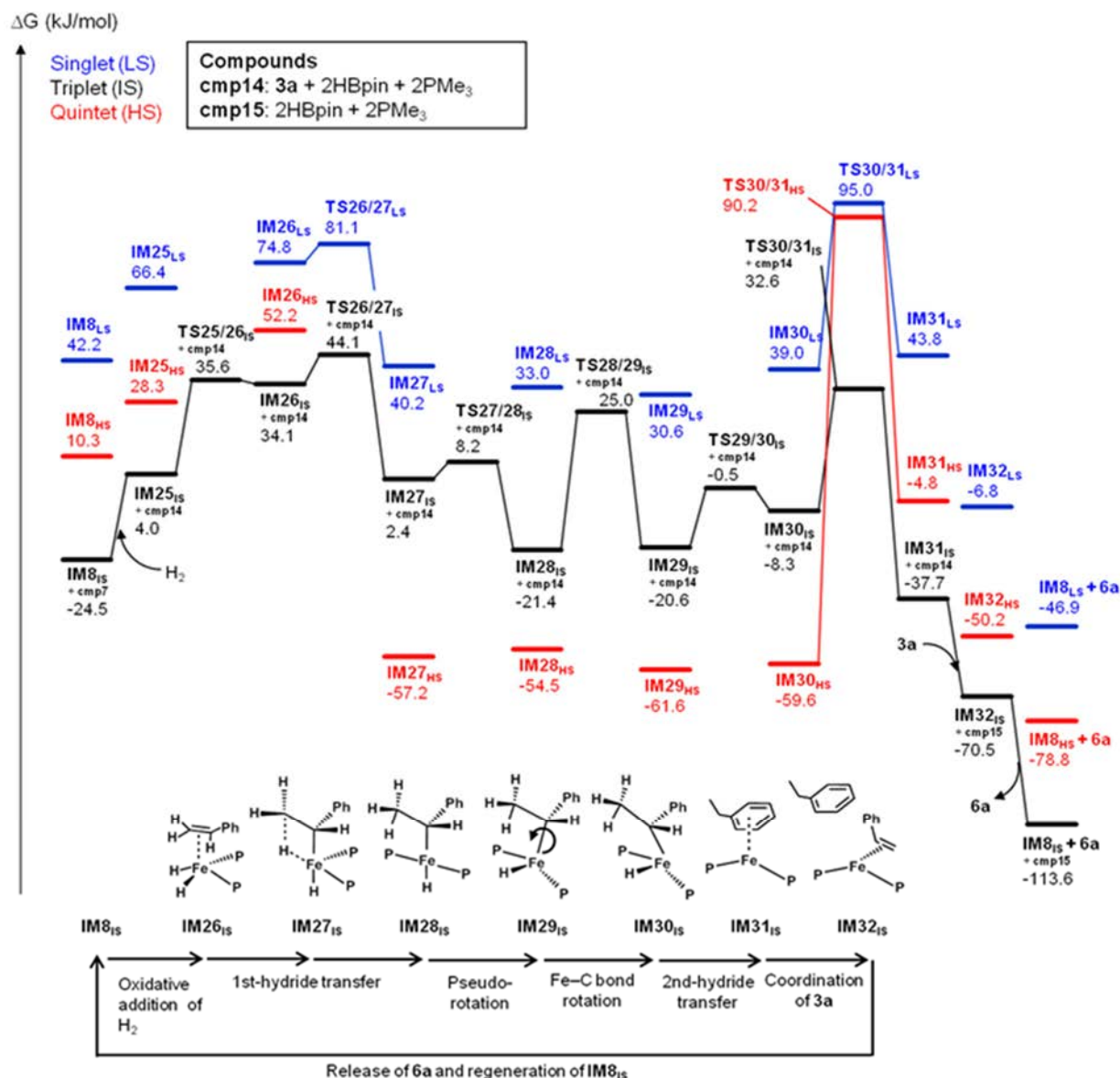


**Figure 6.** A reaction profile for the formation of ethylbenzene in singlet (LS: low spin), triplet (IS: intermediate spin), and quintet (HS: high spin) states. For LS and HS, only local minima and the rate determining transition state are shown. Energy values relative to the starting point are shown in unit of kJ/mol.

### 1.3.6. Competition among three pathways

Competition among dehydrogenative borylation, hydroboration, and hydrogenation is discussed. At first, profiles of the three pathways are compared in Figure 7. Energetically, hydrogenation (green line) is most preferable. Kinetically, dehydrogenative borylation (black line) is more favorable than hydroboration (orange line). Thermodynamically, in contrast, hydroboration is more favorable than dehydrogenative borylation.

The change in the final product ratio among **4a**, **5a**, and **6a**, depending on the initial concentration of **3a**, can be discussed based on Figure 7. In the final stage of the reaction, the

concentration of **3a** should be very low. In contrast, conversion of **4a** to **5a** via hydrogenation of **4a** can occur gradually, since the concentration of **4a** should be large enough and its barrier 104.8 kJ/mol is moderate. This process affords **5a** and therefore increases the yield of **5a** a little. On the other hand, this process also consumes H<sub>2</sub> and reduces its concentration. Consequently, the contribution of hydrogenation giving **6a** should decrease slightly. These happened in the entry 6 in Table 1. In this entry, the yield of **4a** increased a little bit due to the decrease of the contribution of hydrogenation.

To gain further insights, a kinetic simulation is done using a simplified reaction profile. It is known to be difficult to solve the kinetic equation with the full reaction profile including fast reaction steps. The simplification was therefore done assuming local equilibria among local minima that quickly interconvert to each other.

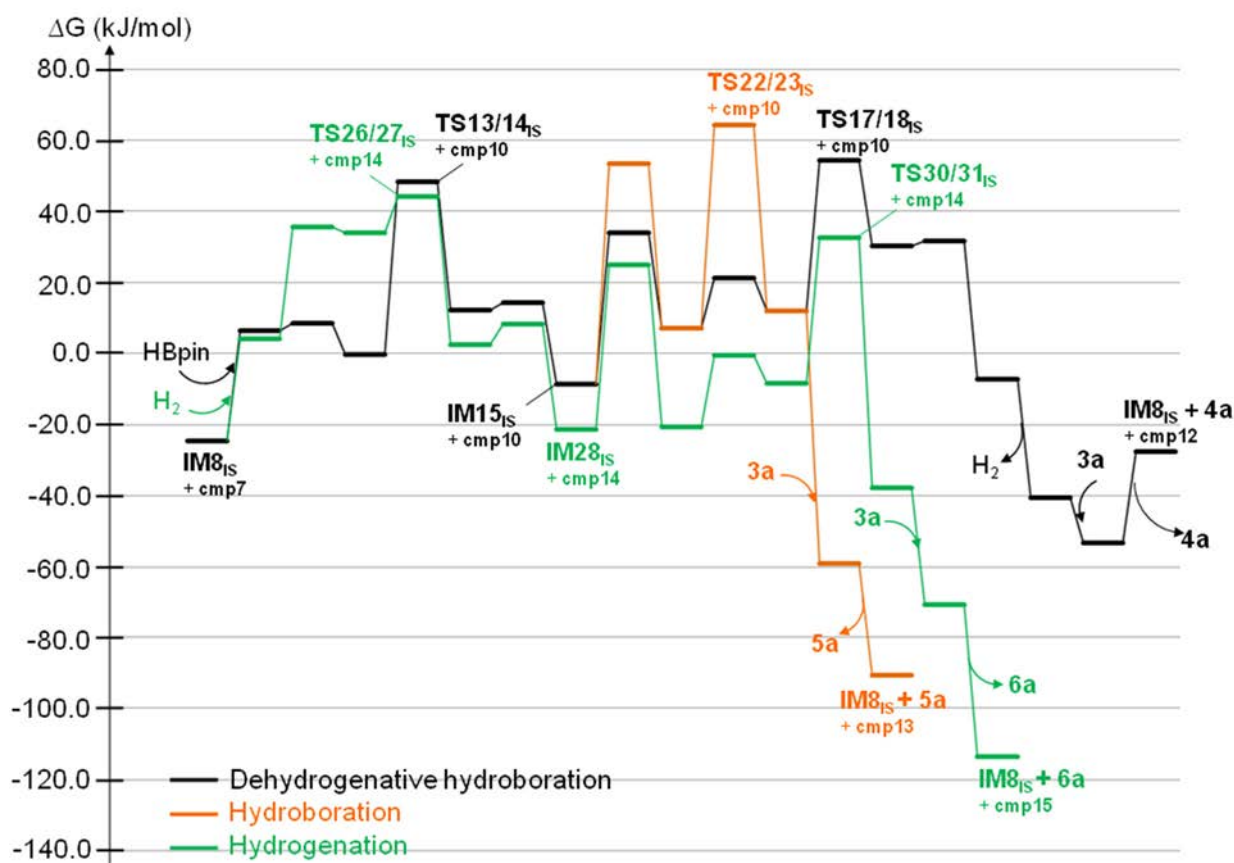


**Figure 7.** Comparison of energy profiles for dehydrogenative borylation (black), hydroboration (orange), and hydrogenation (green).

The simulation without consideration of disappearance of H<sub>2</sub> from the system gave **4a** and **6a** with nearly the same amount. This result can easily be expected from Figure 7; in the middle to final stage, styrene is most likely to react with H<sub>2</sub> generated through the dehydrogenative

borylation because of the high thermodynamic stability of **6a** and the low barrier. We therefore introduced a disappearance process of H<sub>2</sub> in the simulation. That is, the term  $-k_v[\text{H}_2]$  was added to the equation of the concentration of H<sub>2</sub>, assuming that H<sub>2</sub> gradually disappeared from the system *via* its vaporization. The rate constant for H<sub>2</sub> vaporization  $k_v$  ( $= 3.32 \text{ s}^{-1}$ ) was determined empirically so that the simulation with the condition of entry 6 in Table 1 reproduced the experimental products' ratio.

Figure 8 shows the variation of concentrations of styrene and the three products as a function of time, with the reaction condition of Entry 9, Table 1, where **IM5<sub>IS</sub>** and **IM20<sub>IS</sub>** are regarded to be equivalent to styrene and styrylboronate, respectively. As seen in Figure 8, the concentration of styrene decreased gradually in the early stage, and the concentration of styrylboronate started to increase a short time later. The other two products, **5a** and **6a**, started to be formed in the later stage. This is because styrylboronate is kinetically the most preferred product and is formed first. The final products' ratio 81:2:17 (evaluated at 4.3 hour) of the present simulation, which included single empirical parameter, reproduced the experimental ratio well.

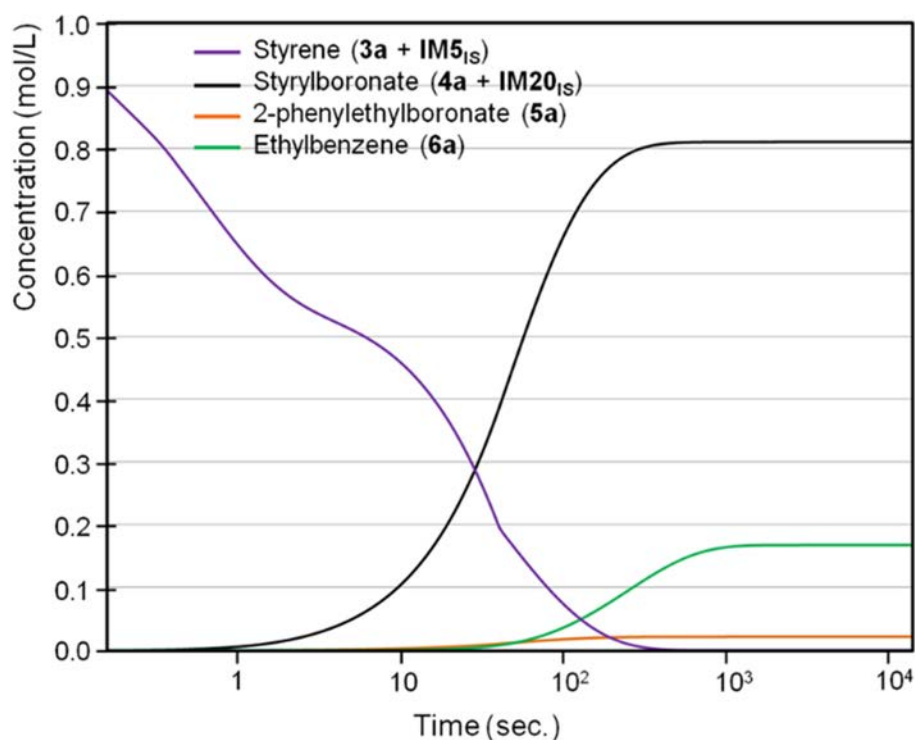


**Figure 8.** Concentration of **3a**, **4a**, **5a**, and **6a** as a function of time in Entry 9, Table 1.

Table 3 presents the calculated products' ratio by simulations for entries 9-11 (Table 1), where  $k_v = 3.32 \text{ s}^{-1}$  was adopted in all the three simulations. (The rate constant for H<sub>2</sub> vaporization  $k_v$  ( $= 3.32 \text{ s}^{-1}$ ) was determined empirically) As seen in Table 3, the ratio of **4a** was smallest in

Entry 1, increased in Entry 2, and largest in Entry 3. This trend qualitatively is consistent with the experimental data in Table 1. These results support the above discussion on the initial styrene concentration dependence of the products' ratio based on the energy profiles in Figure 7.

**Table 3.** Product distribution obtained by the kinetic simulation.

Entry	<b>3a</b> (equiv.)	Select. (%) <b>4a:5a:6a</b>	Observed Select. (%) <b>4a:5a:6a</b> <sup>[a]</sup>
1	3.0	72:2:26	71:1:28
2	2.0	73:2:25	77:1:22
3	1.0	81:2:17	80:5:15

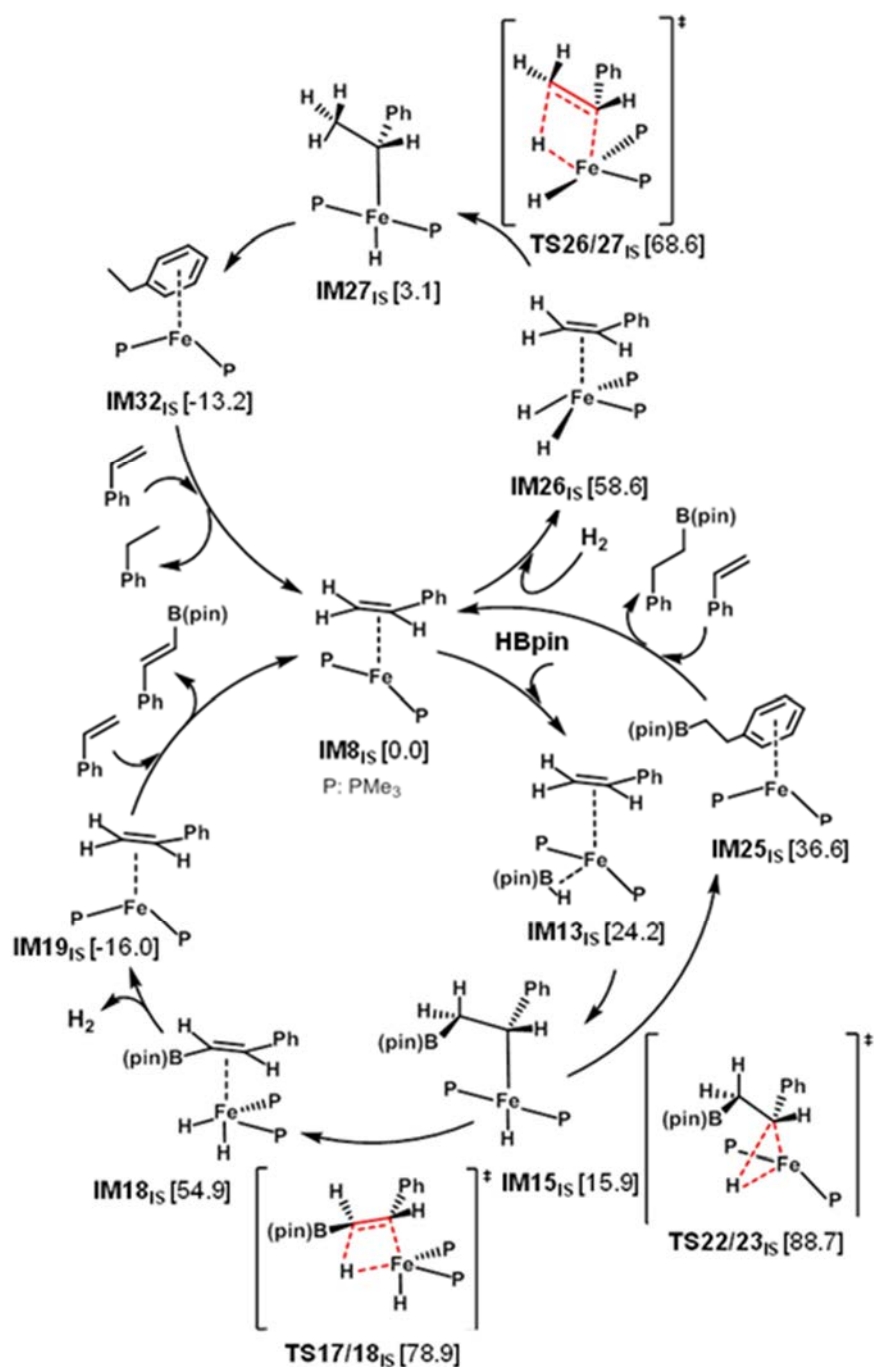
<sup>[a]</sup> Results from Table 1, entries 9-11

### 1.3.7. Proposed mechanism

Scheme 3 summarizes most favorable catalytic cycles for the three products **4a**, **5a**, and **6a**. Only selected intermediates (IMs) and TSs for the rate-determining steps are shown. It was found that **IM8<sub>IS</sub>** was the active species in all the three cycles. As discussed above, generation of **IM8<sub>IS</sub>** occurs in three steps: (i)  $\text{PMe}_3$  dissociation, (ii) styrene coordination, and (iii) another  $\text{PMe}_3$  dissociation. In all the three cycles, the spin multiplicity of TSs for their rate-determining step is triplet. In some intermediates, quintet is more stable than triplet. Singlet is always unstable and has negligible contribution.

All the IMs in Scheme 3 have only two  $\text{PMe}_3$ . As discussed with Figures 1-3, coordination of styrene, HBpin, or  $\text{PMe}_3$  to tetra-coordinate Fe species results in dissociation one of their ligands. It is thus concluded that five-coordinate Fe intermediates are not stable at the present computational level.

The catalytic cycles in Scheme 3 are consistent to the trend seen in Table 1. Dehydroborylation is kinetically more favorable than borylation. The energy difference 9.8 kJ/mol between **TS17/18<sub>IS</sub>** and **TS22/23<sub>IS</sub>** is large enough to selectively afford the dehydroborylation product **4a**. Although **TS26/27<sub>IS</sub>** is the lowest in free energy among the three TSs, hydrogenation requires  $\text{H}_2$  generated through dehydroborylation and occurs only after dehydroborylation proceeds sufficiently. The selectivity **4a** > **6a** > **5a** can thus be explained from Scheme 3.



**Scheme 3.** Catalytic cycles for generation of **4a**, **5a** and **6a**.

#### 1.4. Conclusion

In summary, we have reported a highly selective direct C-H borylation of styrene derivatives with pinacolborane (1.0 equiv.), using  $\text{Fe(PMe}_3)_4$  as catalyst in the absence of any hydrogen acceptor. A detailed mechanism study allowed us to rationalize the observed high chemo- and regio-selectivity of this reaction.



## II-2 Fe-Catalyzed dehydrogenative borylation of terminal alkynes

**Contributions in this part:** Optimization, scope and mechanistic studies: Duo Wei; ICP-OES analyses: Bertrand Lefeuvre

**Publication:** D. Wei, B. Carboni, J.-B. Sortais, C. Darcel, *Adv. Synth. Catal.* **2018**, *360*, 3649-3654.

Alkynylboronates are useful building blocks and are classically prepared by deprotonation of the corresponding alkynes by *n*-BuLi, then reaction with a boric ester and finally quench with anhydrous acid.<sup>[39]</sup> Transition metal catalyzed dehydrogenative borylation of terminal alkynes was only scarcely reported: the known catalytic systems are SiNN and PNP pincer iridium complexes,<sup>[40]</sup> silver<sup>[41]</sup> or NHC-copper<sup>[4b, 42]</sup> well defined complexes.

To continue with our investigation of the previous section, we firstly selected Fe(Me)<sub>2</sub>(dmpe)<sub>2</sub> (**1**) and Fe(PMe<sub>3</sub>)<sub>4</sub> (**2**) as the catalysts and phenylacetylene as the substrate, under similar conditions as shown in § 1.2, Table 1, entry 11. It was disappointing to observe that only styrylboronate **4a** was detected in ca. 20% yield, resulting from hydroboration of phenylacetylene, without any formation of the desired phenylethynylboronates product. A quick literature survey shown that the combination of simple zinc Lewis acid, for example Zn(OTf)<sub>2</sub>, and an organic base could promote the dehydrogenative borylation of alkynes.<sup>[42]</sup> So we turned our attention to seek suitable iron salts which could act as efficient catalysts for the selective dehydrogenative borylation of terminal alkynes leading to the corresponding alkynylboronates.

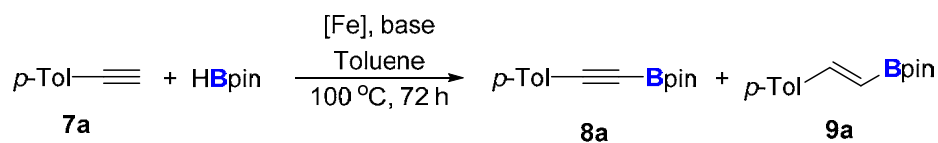
### 2.1. Results and discussions

#### 2.1.1. Optimization of reaction conditions

Our initial studies showed that the dehydrogenative borylation of *p*-tolylacetylene **7a** could be achieved in 67% conversion in toluene solution at 100 °C for 72 h with 1 equiv. of HBpin in the presence of 10 mol% of Fe(OTf)<sub>2</sub><sup>[43]</sup> as precatalyst, and 10 mol% of pyridine. The borylated *p*-tolylacetylene **8a** was obtained as the major product (87%) along with trace amounts of the hydroborated derivative **9a** (7%) and of 4-methylstyrene **10a** (5%) (Table 4, entry 1). The chemoselectivity decreased significantly when 2,6-lutidine, 2,2'-bipyridine or Et<sub>3</sub>N (10 mol%) was used as the base (entries 2-4). Upon screening various bases, DABCO was found to lead to both high conversion (84%) and selectivity towards the formation of the borylated *p*-tolylacetylene **8a** (87%) besides trace amounts of the alkenyl derivative **9a** (10%) and of 4-methylstyrene **10a** (3%) (Entry 5).



**Table 4.** Optimization of the reaction parameters for *p*-tolylacetylene.<sup>[a]</sup>



Entry	[Fe] (mol%)	Base (mol%)	Conv. (%)	8a/9a	Yield (%) 8a
1	Fe(OTf) <sub>2</sub> (10)	Pyridine (10)	76	87/7	66
2	Fe(OTf) <sub>2</sub> (10)	2,6-lutidine (10)	93	43/36	40
3	Fe(OTf) <sub>2</sub> (10)	2,2'-bipyr (10)	85	44/43	37
4	Fe(OTf) <sub>2</sub> (10)	Et <sub>3</sub> N (10)	57	54/20	31
5	Fe(OTf) <sub>2</sub> (10)	DABCO (10)	84	87/10	73
6	Fe(OTf) <sub>2</sub> (2.5)	DABCO (2.5)	99	84/8	83
7	Fe(OTf) <sub>2</sub> (2.5)	DABCO (2.5)	90	85/9	77 <sup>[b]</sup>
8	Fe(OTf) <sub>2</sub> (2.5)	DABCO (1.0)	99	81/11	80
9	Fe(OTf) <sub>2</sub> (1.0)	DABCO (1.0)	90	45/47	41
10	Fe(OTf) <sub>2</sub> (2.5)	DABCO (1.0)	88	59/12	52 <sup>[c]</sup>
11	Fe(OTf) <sub>2</sub> (2.5)	DABCO (1.0)	91	76/17	69 <sup>[d]</sup>
12	None	DABCO (5.0)	<1	-	<1
13	Fe(OTf) <sub>2</sub> (5.0)	None	80	34/29	27
14	FeF <sub>2</sub> (2.5)	DABCO (2.5)	99	24/58	24
15	FeCl <sub>2</sub> (2.5)	DABCO (2.5)	59	11/9	6
16	FeBr <sub>2</sub> (2.5)	DABCO (2.5)	99	42/24	42
17	Fe(OAc) <sub>2</sub> (2.5)	DABCO (2.5)	98	33/44	33

[a] Reaction conditions: Fe(OTf)<sub>2</sub> (2.5-10 mol%), toluene (1 M), alkyne **7** (0.5 mmol), HBpin (0.5 mmol) and base (1.0-10 mol%) at 100 °C for 72 h. Conversion and yield were measured by <sup>1</sup>H NMR analysis of the crude product, based on **7a**, and the identity of the products **8a** and **9a** was confirmed by GC-MS. Bipy: bipyridine; DABCO: 1,4-diazabicyclo[2.2.2]octane.

[b] 48 h.

[c] with 2 equiv. of norbornadiene.

[d] with 2 equiv. of cyclooctene.

Fe(OTf)<sub>2</sub> and DABCO loadings can be efficiently decreased to 2.5 mol% as full conversion was obtained after 72 h at 100 °C, **8a** being produced selectively in 84% NMR yield (entry 6). Decreasing the reaction time to 48 h led to lower conversion (90%, entry 7). However, with only 1.0 mol% of Fe(OTf)<sub>2</sub> and DABCO, even with 90% conversion, the selectivity dropped (**8a/9a** = 45:47, entry 9). Noticeably, the addition of hydrogen scavengers such as norbornadiene or cyclooctene has a deleterious effect on the chemoselectivity of the reaction (entries 10 and 11).

Notably, using DABCO, without iron precursor, resulted in no activity (entry 12). By contrast, a low yield and selectivity was obtained using  $\text{Fe}(\text{OTf})_2$  (2.5 mol%) without base, even if the conversion can reach 80%, thus showing the crucial role of the DABCO catalytic additive on the efficiency and chemoselectivity of this transformation (entry 13).

The influence of the nature of the iron precursors was also investigated. FeF<sub>2</sub>, FeBr<sub>2</sub> and Fe(OAc)<sub>2</sub> (2.5 mol%) in association with DABCO (2.5 mol%) led to full conversion under standard conditions but with a lower selectivity towards **8a** (24-42%, entries 14-17), whereas FeCl<sub>2</sub> was less active (entry 15).

The influence of the solvent was also studied using the system Fe(OTf)<sub>2</sub>/pyridine. (Table 5) Even if the conversion is less important in toluene in comparison to dimethylcarbonate or 2-methyl-THF, the selectivity towards **8a** is higher, which makes toluene the most appropriate solvent for the reaction.

**Table 5.** Fe(OTf)<sub>2</sub> catalyzed dehydrogenative borylation of **7a**: influence of the solvent.<sup>[a]</sup>

$p\text{-Tol}\text{---}\equiv + \text{HBpin} \xrightarrow[\text{Solvent, 100 }^\circ\text{C, 72 h}]{\text{Fe(OTf)}_2 \text{ (10 mol\%)} \\ \text{Pyridine (20 mol\%)}} p\text{-Tol}\text{---}\equiv\text{---Bpin} + p\text{-Tol}\text{---}\text{CH=CH}\text{---Bpin}$				
<b>7a</b>			<b>8a</b>	<b>9a</b>
Entry	Solvent (1 M)	Conv. (%)	8a/9a	Yield (%) 8a
1	Toluene	63	84/10	53
2	2-Methyl-THF	69	67/34	46
3	Bu <sub>2</sub> O	63	46/54	29
4	DMC	66	24/68	16

<sup>[a]</sup> Conditions: a 20 mL Schlenk tube was charged in a glove box, with Fe(OTf)<sub>2</sub> (10 mol%), solvent (1 M), **7a** (0.5 mmol), HBpin (0.5 mmol) and pyridine (20 mol%) in this order, and stirred at 100 °C for 72 h. Yields are measured on the crude product by NMR based on **7a**. DMC = dimethylcarbonate

Hence, the optimal conditions selected to probe the substrate scope of the reaction are 2.5 mol% of Fe(OTf)<sub>2</sub>, 1.0 mol% of DABCO, in toluene (1 M) at 100 °C for 72 h (Table 4).

As Fe(OTf)<sub>2</sub> exhibited the best activity in this transformation, in order to exclude any controversies about transition metal traces responsible of the observed catalytic activity, ICP-OES analyses were performed and are summarized in the Table 6 showing that the higher amounts of metals are 0.19% of silver, 0.04% of ruthenium, 0.02% of nickel (in mass%).

**Table 6.** ICP-OES analysis of Fe(OTf)<sub>2</sub> in mass%

Element	Ag (%)	Ru (%)	Ni (%)	Mn (%)	Pd (%)	Zn (%)	Cu (%)	Co (%)	Cd (%)
Percentage	0.18968	0.039	0.0156	0.00615	0.0039	0.00375	0.0032	0.00175	0.00072

In order to check that silver, nickel and ruthenium in such level are not responsible of the catalytic activity, few reactions of dehydrogenative borylation of *p*-tolylacetylene involving 2.5 mol% of Ag(OTf)<sub>2</sub>, Ni(OAc)<sub>2</sub> or RuCl<sub>3</sub>•xH<sub>2</sub>O were performed in standard conditions (Table 7). With Ag(OTf)<sub>2</sub>, Ni(OAc)<sub>2</sub>, no reaction occurred. By contrast, with RuCl<sub>3</sub>•xH<sub>2</sub>O,

58% of conversion was detected, with the selective production of *p*-tolylstyrylboronate **9a**.

**Table 7.** Dehydrogenative borylation of **7a** catalyzed by metal based salts present in trace amount in the iron salt.<sup>[a]</sup>

$p\text{-Tol}-\text{C}\equiv\text{C}-\text{H} + \text{HBpin} \xrightarrow[\text{toluene (1 M), 100 }^\circ\text{C, 72 h}]{\text{metal catalyst (2.5 mol\%), DABCO (2.5 mol\%)}} p\text{-Tol}-\text{C}\equiv\text{C}-\text{Bpin} + p\text{-Tol}-\text{CH}=\text{CH}-\text{Bpin}$				
	<b>7a</b>		<b>8a</b>	<b>9a</b>
Entry	Metal catalyst	Conv. (%)	<b>8a/9a</b>	Yield(%) <b>8a</b>
1	Ag(OTf) <sub>2</sub>	<1	-	<1
2	Ni(OAc) <sub>2</sub>	<1	-	<1
3	RuCl <sub>3</sub> ·xH <sub>2</sub> O (36.70% Ru)	58	1/95	0

<sup>[a]</sup> Conditions: a 20 mL Schlenk tube was charged in a glove box, with metal catalyst (2.5 mol%), toluene (1 M), **7a** (0.5 mmol), HBpin (0.5 mmol) and DABCO (1.0 mol%, stock solution in toluene) in this order, and stirred at 100 °C for 72 h. Yields are detected by crude NMR based on **7a**.

### 2.1.2. Scope of the reaction for alkynes

Phenylacetylene and arylacetylene derivatives bearing *para*-electron-donating substituents, e.g. *p*-methyl, *p*-*tert*-butyl or *p*-methoxy, led selectively to the corresponding borylated arylacetylene compounds **8a-8d** with isolated yields up to 85% (Table 8, entries 1-4).

It is worth noting that electron-withdrawing substituted arylacetylene derivatives such as *p*-trifluoromethylphenylacetylene, required shorter reaction times (24 h instead of 72 h at 100 °C, entry 5) to lead to the corresponding borylated acetylenic derivative **8e** specifically obtained with 87% isolated yield. Interestingly, the extension of the reaction time to 72 h permitted to only obtain specifically pinacol (*E*)-styrylborane **9e** in 92 % yield (entry 6). This result suggests that the production of the hydroborylated compounds **9e** could occur through the hydrogenation of the borylated acetylenic derivative **8e**. Noteworthy, the bis(ethynyl)benzene afforded selectively the bis(pinacolborylethynyl)-benzene **8f** in 93% yield (entry 7).

In addition, the reaction can be also efficiently performed with 1-dodecyne or terminal alkynes bearing a benzyloxy group, leading to the corresponding borylated alkynes **8g-8i** in 78-93% isolated yields (entries 8-10). Trimethylsilylacetylene is also a suitable starting material as the corresponding borylated compound **8j** was isolated in 89% yield (entry 11).

Using alkadiynes such as 1,7-octadiyne or 1,6-heptadiyne, the monofunctionalization was only observed in the presence of 2 equiv. of HBpin and the corresponding monoborylated derivatives **8k** and **8l** were obtained selectively in 70-72% isolated yields (entries 12 and 13). Noticeably, no trace of diborylated compounds was detected, the only by-products observed in



A prolonged 72 h of reaction permitted to switch the chemoselectivity as pinacol (*E*)-2-*tert*-butylvinyl-borate **9m** and pinacol (*E*)-2-cyclopropylvinyl-borate **9n** were selectively isolated in 85 and 90% yields, respectively (entries 15 and 17). Notably, cyclopropylacetylene furnished **8n** and **9n** in good yields (63 and 85%, respectively), which seem to indicate that the reaction did not proceed *via* stable radical intermediates. Starting from methyl hex-6-ynoate or 3-bromo-1-propyne, only the hydroborated derivative **9o** and **9p** were obtained in high yields, 95 and 92%, respectively, whatever the reaction time, 9 or 72 h (entries 18 and 19).

Additionally, under the optimized reaction conditions, no reaction was observed with terminal alkynes bearing primary amine, alcohol or carboxylic acid substituents (Figure 9).

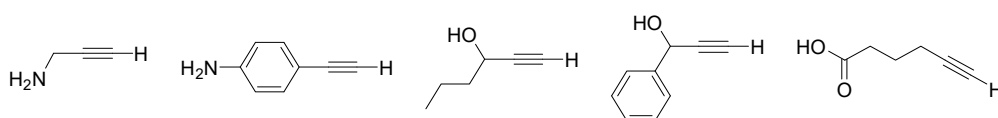


**Figure 9.** Non-working substrates in dehydrogenative borylation reactions.

## 2.2. Mechanistic insights

Preliminary experiments aimed at gaining an insight into the reaction course were then performed. The reaction outlined in Table 4, entry 8, was achieved in a Young NMR tube, charged under argon atmosphere with 2.5 mol% of Fe(OTf)<sub>2</sub> in C<sub>6</sub>D<sub>6</sub> (1.0 mol/L), 0.5 mmol of **7b**, 0.5 mmol of HBpin and DABCO (1.0 mol%) at 100 °C for indicated time.

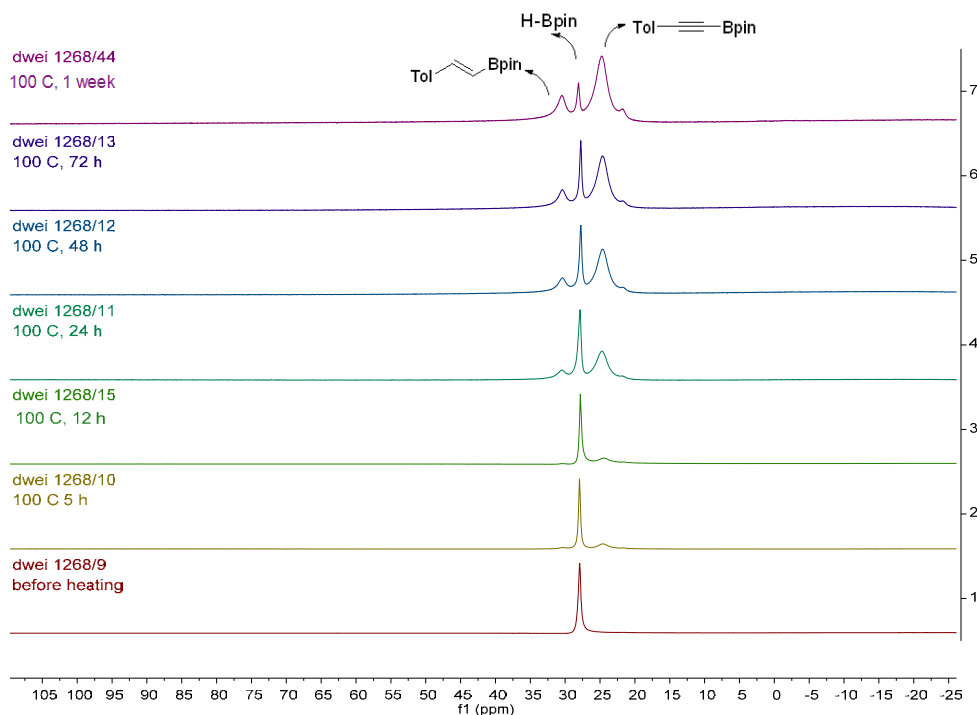


**Figure 10:** <sup>11</sup>B NMR spectra recorded at 96 MHz of the reaction of *p*-tolylacetylene **a2** with HBpin in C<sub>6</sub>D<sub>6</sub> at 100 °C leading to the compounds **8b** and **9b**.

Analysis of  $^{11}\text{B}$  NMR spectra showed that the dehydroborylated and the borylated compound **8b** and **9b** were formed simultaneously, **8b** being always the major product (Figure 10). Additionally, the results described in Table 4, entries 6, 15 and 17 indicated that the formation of the alkenyl boronates results from the reduction of the corresponding alkynylboronates. On the other hand, the evolution of the  $\text{H}_2$  gas was also identified in  $^1\text{H}$  NMR at 4.47 ppm (Figure 11).

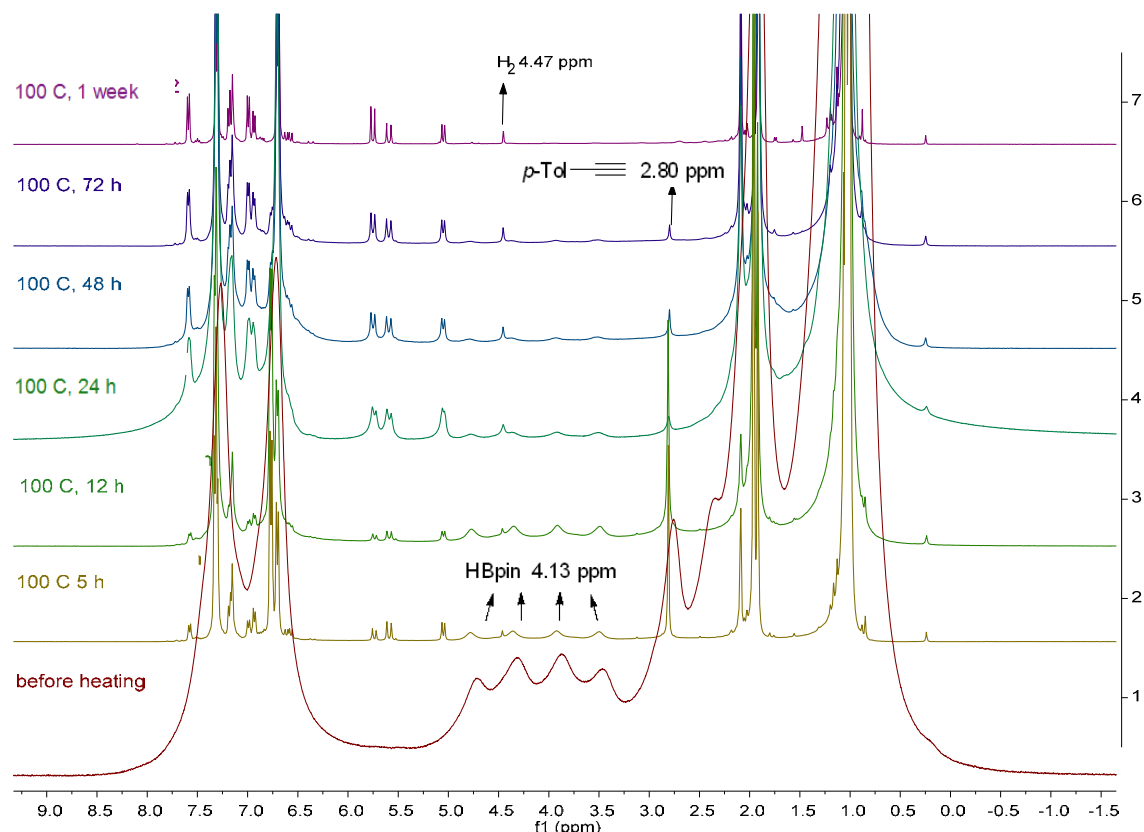
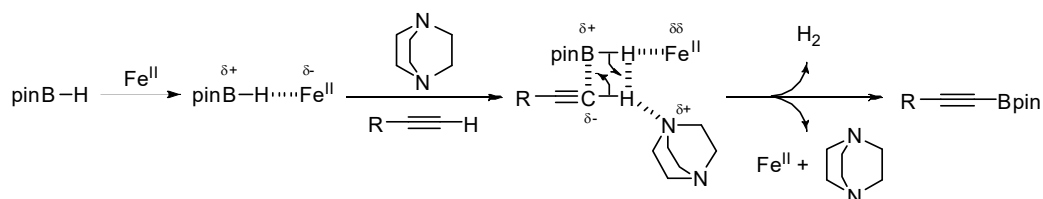


**Figure 11:**  $^1\text{H}$  NMR spectra recorded at 400 MHz of the reaction of *p*-tolylacetylene **7b** with HBpin in  $\text{C}_6\text{D}_6$  at 100 °C leading to the formation of  $\text{H}_2$ .

From a mechanistic point of view, as a Lewis acid,  $\text{Fe}(\text{OTf})_2$  should be able to activate the B-H bond, thus enhancing the electrophilic capacity of the boron center to react with acetylenic derivative. This process would be accelerated by the presence of DABCO which increases the nucleophilicity of the terminal acetylenic carbon (Scheme 4).<sup>[42]</sup>



**Scheme 4.** Possible reaction mechanism of dehydrogenative borylation reactions.

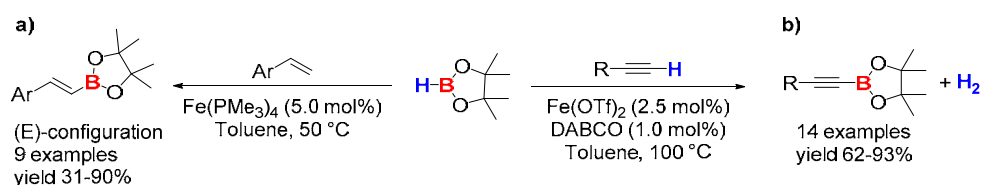
### 2.3. Conclusion

In summary, we have reported the first example of a highly selective catalytic dehydrogenative borylation of terminal alkynes with pinacolborane, using  $\text{Fe}(\text{OTf})_2$  as an inexpensive catalyst and DABCO as a co-catalyst. Both aryl and alkyl substituted alkynes were borylated (14 examples, yield: 62-93%) at 100 °C in toluene.

## II-3 Conclusion of Chapter II

In summary, we reported the first examples of highly selective catalytic direct C-H borylation of **a)** styrene derivatives and **b)** terminal alkynes with pinacolborane (1.0 equiv.), using  $\text{Fe}(\text{PMe}_3)_4$  and  $\text{Fe}(\text{OTf})_2/\text{DABCO}$  as catalyst system, respectively.

For C-H borylation of terminal alkynes, both aryl and alkyl substituted alkynes were applied in the substrate scope with 14 examples (yields: 62-93%) at 100 °C in toluene. In the case of the dehydrogenative borylation of styrene derivatives, the substrate scope was developed with 9 examples (yields: 31-90%) at 50 °C in toluene. The detailed mechanism study showed that the dehydroborylation is kinetically more favorable than the hydroboration.





## II-4 References

- [1] a) N. Miyaura, A. Suzuki, *Chem. Rev.* **1995**, *95*, 2457-2483; b) A. Suzuki, *Angew. Chem. Int. Ed.* **2011**, *50*, 6722-6737; c) N. Miyaura, *Top. Curr. Chem.* **2002**, *219*, 11-59; d) E. M. Beck, R. Hatley, M. J. Gaunt, *Angew. Chem. Int. Ed.* **2008**, *47*, 3004-3007; e) A. D. Finke, J. S. Moore, *Org. Lett.* **2008**, *10*, 4851-4854.
- [2] a) D. G. Hall, *Boronic Acids: Preparation, Applications in Organic Synthesis and Medicine*, Wiley-VCH, Weinheim, **2011**; b) A. Coca, *Boron Reagents in Synthesis*, ACS Symposium, Series 1236; American Chemical Society, Washington, DC, **2016**; c) E. Fernández, A. Whiting, *Synthesis and Application of Organoboron Compound*, Springer, New York, **2015**.
- [3] N. R. Candeias, F. Montalbano, P. M. S. D. Cal, P. M. P. Gois, *Chem. Rev.* **2010**, *110*, 6169-6193.
- [4] a) R. Barbeyron, E. Benedetti, J. Cossy, J.-J. Vasseur, S. Arseniyadis, M. Smietana, *Tetrahedron* **2014**, *70*, 8431-8452; b) E. A. Romero, R. Jazzar, G. Bertrand, *Chem. Sci.* **2016**, *8*, 165-168.
- [5] a) C. Morrill, T. W. Funk, R. H. Grubbs, *Tetrahedron Lett.* **2004**, *45*, 7733-7736; b) R. Hemelaere, F. Carreaux, B. Carboni, *J. Org. Chem.* **2013**, *78*, 6786-6792; c) E. T. Kiesewetter, R. V. O'Brien, E. C. Yu, S. J. Meek, R. R. Schrock, A. H. Hoveyda, *J. Am. Chem. Soc.* **2013**, *135*, 6026-6029.
- [6] T. Ishiyama, N. Miyaura, *Chem. Rec.* **2004**, *3*, 271-280.
- [7] W. B. Reid, J. J. Spillane, S. B. Krause, D. A. Watson, *J. Am. Chem. Soc.* **2016**, *138*, 5539-5542.
- [8] a) J. Y. Wu, B. Moreau, T. Ritter, *J. Am. Chem. Soc.* **2009**, *131*, 12915-12917; b) M. Haberberger, S. Enthaler, *Chem. Asian J.* **2013**, *8*, 50-54; c) J. V. Obligacion, P. J. Chirik, *Org. Lett.* **2013**, *15*, 2680-2683; d) M. D. Greenhalgh, S. P. Thomas, *Chem. Commun.* **2013**, *49*, 11230-11232; e) J. Zheng, J.-B. Sortais, C. Darcel, *ChemCatChem* **2014**, *6*, 763-766; f) V. S. Rawat, B. Sreedhar, *Synlett* **2014**, *25*, 1132-1136; g) M. Espinal-Viguri, C. R. Woof, R. L. Webster, *Chem. Eur. J.* **2016**, *22*, 11605-11608; h) A. J. MacNair, C. R. Millet, G. S. Nichol, A. Ironmonger, S. P. Thomas, *ACS Catal.* **2016**, *6*, 7217-7221; i) C. Chen, X. Shen, J. Chen, X. Hong, Z. Lu, *Org. Lett.* **2017**, *19*, 5422-5425; j) X. Chen, Z. Cheng, Z. Lu, *Org. Lett.* **2017**, *19*, 969-971.
- [9] a) J. V. Obligacion, P. J. Chirik, *J. Am. Chem. Soc.* **2013**, *135*, 19107-19110; b) L. Zhang, Z. Zuo, X. Leng, Z. Huang, *Angew. Chem. Int. Ed.* **2014**, *53*, 2696-2700; c) A. J. Ruddy, O. L. Sydora, B. L. Small, M. Stradiotto, L. Turculet, *Chem. Eur. J.* **2014**, *20*, 13918-13922; d) L. Zhang, Z. Zuo, X. Wan, Z. Huang, *J. Am. Chem. Soc.* **2014**, *136*, 15501-15504; e) J. Chen, T. Xi, X. Ren, B. Cheng, J. Guo, Z. Lu, *Org. Chem. Front.* **2014**, *1*, 1306-1309; f) W. N. Palmer, T. Diao, I. Pappas, P. J. Chirik, *ACS Catal.* **2015**, *5*, 622-626; g) M. L. Scheuermann, E. J. Johnson, P. J. Chirik, *Org. Lett.* **2015**, *17*, 2716-2719; h) Y. Liu, Y. Zhou, H. Wang, J. Qu, *RSC Adv.* **2015**, *5*, 73705-73713.
- [10] a) M. Zaidlewicz, J. Meller, *Tetrahedron Lett.* **1997**, *38*, 7279-7282; b) R. J. Ely, J. P. Morken, *J. Am. Chem. Soc.* **2010**, *132*, 2534-2535; c) Z. Yu, R. J. Ely, J. P. Morken, *Angew. Chem. Int. Ed.* **2014**, *53*, 9632-9636; d) E. E. Touney, R. Van Hoveln, C. T. Buttke, M. D. Freidberg, I. A. Guzei, J. M. Schomaker, *Organometallics* **2016**, *35*, 3436-3439.
- [11] G. Zhang, H. Zeng, J. Wu, Z. Yin, S. Zheng, J. C. Fettinger, *Angew. Chem. Int. Ed.* **2016**, *55*, 14369-14372.
- [12] J. V. Obligacion, P. J. Chirik, *Org. Lett.* **2013**, *15*, 2680-2683.
- [13] J. V. Obligacion, J. M. Neely, A. N. Yazdani, I. Pappas, P. J. Chirik, *J. Am. Chem. Soc.* **2015**, *137*, 5855-5858.
- [14] E. A. Romero, R. Jazzar, G. Bertrand, *J. Organomet. Chem.* **2017**, *829*, 11-13.
- [15] a) N. Cabrera-Lobera, P. Rodríguez-Salamanca, J. C. Nieto-Carmona, E. Buñuel, D. J. Cárdenas, *Chem. Eur. J.* **2018**, *24*, 784-788; b) T. Xi, Z. Lu, *ACS Catal.* **2017**, *7*, 1181-1185; c) S. Yu, C. Wu, S. Ge, *J. Am. Chem. Soc.* **2017**, *139*, 6526-6529.

- [16] a) S. Jiang, S. Quintero-Duque, T. Roisnel, V. Dorcet, M. Grellier, S. Sabo-Etienne, C. Darcel, J.-B. Sortais, *Dalton Trans.* **2016**, 45, 11101-11108; b) C. Wang, C. Wu, S. Ge, *ACS Catal.* **2016**, 6, 7585-7589.
- [17] a) S. A. Westcott, T. B. Marder, R. T. Baker, *Organometallics* **1993**, 12, 975-979; b) J. M. Brown, G. C. Lloyd-Jones, *J. Am. Chem. Soc.* **1994**, 116, 866-878; c) R. T. Baker, J. C. Calabrese, S. A. Westcott, T. B. Marder, *J. Am. Chem. Soc.* **1995**, 117, 8777-8784.
- [18] S. J. Geier, S. A. Westcott, *Rev. Inorg. Chem.* **2015**, 35, 69-79.
- [19] a) I. A. I. Mkhalid, J. H. Barnard, T. B. Marder, J. M. Murphy, J. F. Hartwig, *Chem. Rev.* **2010**, 110, 890-931; b) M. A. Larsen, J. F. Hartwig, *J. Am. Chem. Soc.* **2014**, 136, 4287-4299; c) T. Furukawa, M. Tobisu, N. Chatani, *J. Am. Chem. Soc.* **2015**, 137, 12211-12214; d) C. B. Bheeter, A. D. Chowdhury, R. Adam, R. Jackstell, M. Beller, *Org. Biomol. Chem.* **2015**, 13, 10336-10340; e) L. P. Press, A. J. Kosanovich, B. J. McCulloch, O. V. Ozerov, *J. Am. Chem. Soc.* **2016**, 138, 9487-9497.
- [20] a) D. G. Hall, 2nd ed., Wiley-VCH, Weinheim, **2011**; b) R. Shang, L. Ilies, S. Asako, E. Nakamura, *J. Am. Chem. Soc.* **2014**, 136, 14349-14352.
- [21] a) V. Ritleng, C. Sirlin, M. Pfeffer, *Chem. Rev.* **2002**, 102, 1731-1770; b) J. Wencel-Delord, F. Glorius, *Nat. Chem.* **2013**, 5, 369-375.
- [22] a) M. Bullock, *Catalysis without Precious Metals*, Wiley-VCH, Weinheim, **2010**; b) S. Enthaler, K. Junge, M. Beller, *Angew. Chem. Int. Ed.* **2008**, 47, 3317-3321; c) R. M. Bullock, *Science* **2013**, 342, 1054-1055; d) A. Fürstner, *ACS Central Sci.* **2016**, 2, 778-789.
- [23] T. Furukawa, M. Tobisu, N. Chatani, *Chem. Commun.* **2015**, 51, 6508-6511.
- [24] a) N. G. Léonard, M. J. Bezdek, P. J. Chirik, *Organometallics* **2016**; b) W. N. Palmer, J. V. Obligation, I. Pappas, P. J. Chirik, *J. Am. Chem. Soc.* **2016**, 138, 766-769; c) J. V. Obligation, S. P. Semproni, I. Pappas, P. J. Chirik, *J. Am. Chem. Soc.* **2016**, 138, 10645-10653.
- [25] a) K. M. Waltz, X. He, C. Muhoro, J. F. Hartwig, *J. Am. Chem. Soc.* **1995**, 117, 11357-11358; b) Y. Ohki, T. Hatanaka, K. Tatsumi, *J. Am. Chem. Soc.* **2008**, 130, 17174-17186; c) V. S. Rawat, B. Sreedhar, *Synlett* **2014**, 25, 1132-1136, 1135 pp; d) T. Dombay, G. C. Werncke, S. Jiang, M. Grellier, L. Vendier, S. Bontemps, J.-B. Sortais, S. Sabo-Etienne, C. Darcel, *J. Am. Chem. Soc.* **2015**, 137, 4062-4065; e) T. Hatanaka, Y. Ohki, K. Tatsumi, *Chem. Asian J.* **2010**, 5, 1657-1666.
- [26] a) T. J. Mazzacano, N. P. Mankad, *J. Am. Chem. Soc.* **2013**, 135, 17258-17261; b) F. Labre, Y. Gimbert, P. Bannwarth, S. Olivero, E. Duñach, P. Y. Chavant, *Org. Lett.* **2014**, 16, 2366-2369; c) S. R. Parmelee, T. J. Mazzacano, Y. Zhu, N. P. Mankad, J. A. Keith, *ACS Catal.* **2015**, 5, 3689-3699.
- [27] E. A. Romero, R. Jazzar, G. Bertrand, *Chem. Sci.* **2017**
- [28] a) T. C. Atack, S. P. Cook, *J. Am. Chem. Soc.* **2016**, 138, 6139-6142; b) H. Chen, J. F. Hartwig, *Angew. Chem. Int. Ed.* **1999**, 38, 3391-3393.
- [29] D. H. Motry, M. R. Smith, *J. Am. Chem. Soc.* **1995**, 117, 6615-6616.
- [30] a) M.-A. Légaré, M.-A. Courtemanche, É. Rochette, F.-G. Fontaine, *Science* **2015**, 349, 513; b) K. Chernichenko, M. Lindqvist, B. Kótai, M. Nieger, K. Sorochkina, I. Pápai, T. Repo, *J. Am. Chem. Soc.* **2016**, 138, 4860-4868; c) M.-A. Legare, E. Rochette, J. Legare Lavergne, N. Bouchard, F.-G. Fontaine, *Chem. Commun.* **2016**, 52, 5387-5390.
- [31] a) M. Murata, S. Watanabe, Y. Masuda, *Tetrahedron Lett.* **1999**, 40, 2585-2588; b) M. Murata, K. Kawakita, T. Asana, S. Watanabe, Y. Masuda, *Bull. Chem. Soc. Jpn.* **2002**, 75, 825-829; c) A. Caballero, S. Sabo-Etienne, *Organometallics* **2007**, 26, 1191-1195; d) N. Selander, B. Willy, K. J. Szabó, *Angew. Chem. Int. Ed.* **2010**, 49, 4051-4053; e) I. Noriyuki, S. Michinori, *Chem. Lett.* **2010**, 39, 558-560.
- [32] a) T.-J. Hu, G. Zhang, Y.-H. Chen, C.-G. Feng, G.-Q. Lin, *J. Am. Chem. Soc.* **2016**, 138, 2897-2900; b) R. B. Coapes, F. E. S. Souza, R. L. Thomas, J. J. Hall, T. B. Marder, *Chem. Commun.* **2003**, 614-615; c) I. A. I. Mkhalid, R. B. Coapes, S. N. Edes, D. N. Coventry, F. E. S. Souza, R. L. Thomas, J. J. Hall, S.-W. Bi, Z. Lin, T. B. Marder, *Dalton Trans.* **2008**, 1055-1064; d) J. Takaya, N. Kirai, N. Iwasawa, *J. Am. Chem. Soc.* **2011**, 133, 12980-12983; e) N. Kirai, S. Iguchi, T. Ito, J. Takaya, N. Iwasawa, *Bull. Chem. Soc. Jpn.* **2013**, 86, 784-799; f) M. Morimoto, T. Miura, M. Murakami, *Angew. Chem. Int. Ed.* **2015**, 54, 12659-12663.

- [33] J. Zheng, J.-B. Sortais, C. Darcel, *ChemCatChem* **2014**, *6*, 763-766.
- [34] a) L. Zhang, Z. Huang, *Synlett* **2013**, *24*, 1745-1747; b) L. Zhang, D. Peng, X. Leng, Z. Huang, *Angew. Chem. Int. Ed.* **2013**, *52*, 3676-3680; c) L. Zhang, Z. Zuo, X. Leng, Z. Huang, *Angew. Chem. Int. Ed.* **2014**, *53*, 2696-2700.
- [35] T. Dombray, C. G. Werncke, S. Jiang, M. Grellier, L. Vendier, S. Bontemps, J.-B. Sortais, S. Sabo-Etienne, C. Darcel, *J. Am. Chem. Soc.* **2015**, *137*, 4062-4065.
- [36] a) S. Maeda, Y. Harabuchi, M. Takagi, T. Taketsugu, K. Morokuma, *Chem. Rec.* **2016**, *16*, 2232-2248; b) S. Maeda, K. Morokuma, *J. Chem. Phys.* **2010**, *132*, 241102; c) S. Maeda, K. Morokuma, *J. Chem. Theory. Comput.* **2011**, *7*, 2335-2345; d) S. Maeda, K. Ohno, K. Morokuma, *Phys. Chem. Chem. Phys.* **2013**, *15*, 3683-3701; e) S. Maeda, T. Taketsugu, K. Morokuma, *J. Comput. Chem.* **2014**, *35*, 166-173; f) S. Maeda, S. Komagawa, M. Uchiyama, K. Morokuma, *Angew. Chem. Int. Ed.* **2011**, *50*, 644-649; g) S. Maeda, K. Morokuma, *J. Chem. Theory. Comput.* **2012**, *8*, 380-385; h) M. Hatanaka, S. Maeda, K. Morokuma, *J. Chem. Theory. Comput.* **2013**, *9*, 2882-2886; i) R. Uematsu, E. Yamamoto, S. Maeda, H. Ito, T. Taketsugu, *J. Am. Chem. Soc.* **2015**, *137*, 4090-4099.
- [37] A. D. Becke, *J. Chem. Phys.* **1993**, *98*, 5648-5652.
- [38] S. Grimme, J. Antony, S. Ehrlich, H. Krieg, *J. Chem. Phys.* **2010**, *132*, 154104.
- [39] H. C. Brown, N. Bhat, M. Srebnik, *Tetrahedron Lett.* **1988**, *29*, 2631-2634.
- [40] a) C.-I. Lee, J. Zhou, O. V. Ozerov, *J. Am. Chem. Soc.* **2013**, *135*, 3560-3566; b) C.-I. Lee, J. C. DeMott, C. J. Pell, A. Christopher, J. Zhou, N. Bhuvanesh, O. V. Ozerov, *Chem. Sci.* **2015**, *6*, 6572-6582; c) J. Zhou, C.-I. Lee, O. V. Ozerov, *ACS Catal.* **2018**, *8*, 536-545.
- [41] J.-R. Hu, L.-H. Liu, X. Hu, H.-D. Ye, *Tetrahedron* **2014**, *70*, 5815-5819.
- [42] T. Tsuchimoto, H. Utsugi, T. Sugiura, S. Horio, *Adv. Synth. Catal.* **2015**, *357*, 77-82.
- [43] Iron(II) trifluoromethanesulfonate, 98% purchased from Strem was used for this study. ICP-OES analysis was performed on this complex. For a critical review about impurities in catalysis see: I. Thom  , A. Nijs, C. Bolm, *Chem. Soc. Rev.* **2012**, *41*, 979-987.

## II-5 Experimental data

### 5.1. General information.

All reactions were carried out with oven-dried glassware using standard Schlenk techniques under an inert atmosphere of dry argon or in an argon-filled glove-box. Toluene, THF, diethyl ether (Et<sub>2</sub>O), and CH<sub>2</sub>Cl<sub>2</sub> were dried over Braun MB-SPS-800 solvent purification system and degassed by thaw-freeze cycles. Technical grade petroleum ether, diethyl ether were used for chromatography column. Analytical TLC was performed on Merck 60F<sub>254</sub> silica gel plates (0.25 mm thickness). Column chromatography was performed on Across Organics Ultrapure silica gel (mesh size 40-60 μm, 60 Å). All reagents were obtained from commercial sources and liquid reagents were dried on molecular sieves and degassed prior to use.

<sup>1</sup>H, <sup>13</sup>C, <sup>19</sup>F, <sup>31</sup>P and <sup>11</sup>B NMR spectra were recorded in CDCl<sub>3</sub>, C<sub>6</sub>D<sub>6</sub>, C<sub>7</sub>D<sub>8</sub> at 298 K unless otherwise stated, on Bruker, AVANCE 400 and AVANCE 300 spectrometers at 400.1 and 300.1 MHz, respectively. (<sup>1</sup>H: CDCl<sub>3</sub> 7.26 ppm, C<sub>6</sub>D<sub>6</sub> 7.16 ppm, C<sub>7</sub>D<sub>8</sub> 2.08 ppm, <sup>13</sup>C: CDCl<sub>3</sub>, central peak is 77.0 ppm, C<sub>6</sub>D<sub>6</sub>, central peak is 128.1 ppm, C<sub>7</sub>D<sub>8</sub>, central peak is 20.4 ppm). <sup>31</sup>P NMR spectra were calibrated against an external H<sub>3</sub>PO<sub>4</sub> and <sup>11</sup>B NMR spectra against an external BF<sub>3</sub>•OEt<sub>2</sub> standard. Chemical shift (δ) and coupling constants (*J*) are given in ppm and in Hz, respectively. The peak patterns are indicated as follows: (s, singlet; d, doublet; t, triplet; q, quartet; quin, quintet; m, multiplet, and br. for broad).

GCMS were measured by GCMS-QP2010S (Shimadzu) with GC-2010 equipped with a 30-m capillary column (Supelco, SLBTM-5ms, fused silica capillary column, 30 M × 0.25 mm × 0.25 mm film thickness), which was used with helium as vector gas. The following GC-MS conditions were used: Initial temperature 100 °C, for 2 minutes, then rate 10 °C/min. until 250 °C and 250 °C for 10 minutes.

### 5.2. - Part II-1- Dehydrogenative borylation of styrenes

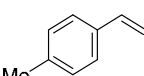
#### 5.2.1. Preparation of the catalysts (1) and (2)

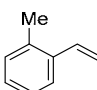
[Fe(Me)<sub>2</sub>(dmpe)<sub>2</sub>] and Fe(PMe<sub>3</sub>)<sub>4</sub> were prepared according to described methods.<sup>[1,2]</sup>

#### 5.2.2. Preparation of styrene derivatives

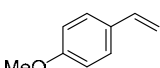
A solution of the aldehyde (6.36 mmol, 1.0 equiv.) in anhydrous THF (30 mL) was cooled at 0 °C then triphenylmethylphosphonium bromide (2.50 g, 6.97 mmol, 1.1 equiv.) was added followed by potassium *t*-butoxyde (0.78 g, 6.97 mmol, 1.1 equiv.) in small portions. The mixture was then stirred at room temperature until completion (TLC monitored). The reaction was then quenched with water (20 mL). The product was extracted with dichloromethane (3×30 mL). The organic layer was washed with brine, then dried with anhydrous Na<sub>2</sub>SO<sub>4</sub> and evaporated. The crude residue was dissolved in the minimum amount of dichloromethane and packed on 2.5 g of silica and purified by column chromatography (petroleum ether/ Et<sub>2</sub>O) to give the desired compound

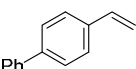
#### 5.2.3. Characterization of the styrene derivatives

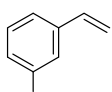
**3b:**  <sup>1</sup>H NMR (400 MHz, C<sub>6</sub>D<sub>6</sub>) δ 7.21 (d, *J* = 8.2 Hz, 2H), 6.95 (d, *J* = 8.0 Hz, 2H), 6.62 (dd, *J* = 17.6, 10.9 Hz, 1H), 5.62 (dd, *J* = 17.6, 1.2 Hz, 1H), 5.07 (dd, *J* = 10.9, 1.1 Hz, 1H), 2.09 (s, 3H).

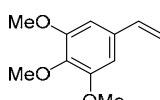
**3c:**  <sup>1</sup>H NMR (400 MHz, CDCl<sub>3</sub>) δ 7.54 – 7.42 (m, 1H), 7.22 – 7.12 (m, 3H), 6.95 (dd,

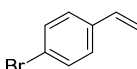
$J = 17.4, 11.0$  Hz, 1H), 5.64 (dd, 1H), 5.30 (dd, 1H), 2.36 (s, 3H).

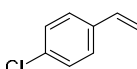
**3e:**   $^1\text{H NMR}$  (400 MHz,  $\text{CDCl}_3$ )  $\delta$  7.35 (d,  $J = 8.6$  Hz, 2H), 6.86 (d,  $J = 8.6$  Hz, 2H), 6.67 (dd,  $J = 17.6, 10.9$  Hz, 1H), 5.61 (d,  $J = 17.6$  Hz, 1H), 5.13 (d,  $J = 10.9$  Hz, 1H), 3.82 (s, 3H).

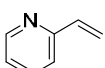
**3f:**   $^1\text{H NMR}$  (400 MHz,  $\text{CDCl}_3$ )  $\delta$  7.69 – 7.56 (m, 4H), 7.55 – 7.42 (m, 4H), 7.41 – 7.32 (m, 1H), 6.78 (dd,  $J = 17.6, 10.9$  Hz, 1H), 5.81 (dd,  $J = 17.7, 0.9$  Hz, 1H), 5.29 (dd,  $J = 10.9, 0.8$  Hz, 1H).

**3g:**   $^1\text{H NMR}$  (400 MHz,  $\text{CDCl}_3$ )  $\delta$  7.36 – 7.26 (m, 1H), 7.14 (dd,  $J = 20.9, 8.9$  Hz, 2H), 6.95 (td,  $J = 8.3, 1.9$  Hz, 1H), 6.69 (dd,  $J = 17.6, 10.9$  Hz, 1H), 5.76 (d,  $J = 17.6$  Hz, 1H), 5.31 (d,  $J = 10.9$  Hz, 1H).

**3h:**   $^1\text{H NMR}$  (400 MHz,  $\text{C}_6\text{D}_6$ )  $\delta$  6.80 – 6.29 (m, 3H), 5.61 (d,  $J = 17.5$  Hz, 1H), 5.13 (d,  $J = 10.8$  Hz, 1H), 3.83 (s, 3H), 3.39 (s, 6H).

  $^1\text{H NMR}$  (400 MHz,  $\text{CDCl}_3$ )  $\delta$  7.47 (d,  $J = 8.4$  Hz, 2H), 7.30 (d,  $J = 8.9$  Hz, 2H), 6.68 (dd,  $J = 17.6, 10.9$  Hz, 1H), 5.77 (d,  $J = 17.6$  Hz, 1H), 5.31 (d,  $J = 10.9$  Hz, 1H).

  $^1\text{H NMR}$  (400 MHz,  $\text{C}_6\text{D}_6$ )  $\delta$  7.04 (d,  $J = 8.4$  Hz, 2H), 6.88 (d,  $J = 8.4$  Hz, 2H), 6.36 (dd,  $J = 17.6, 10.9$  Hz, 1H), 5.42 (d,  $J = 17.6$  Hz, 1H), 5.00 (d,  $J = 10.9$  Hz, 1H).

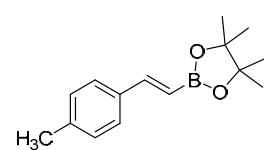
  $^1\text{H NMR}$  (400 MHz,  $\text{CDCl}_3$ )  $\delta$  8.73 – 8.39 (m, 1H), 7.65 (td,  $J = 7.7, 1.9$  Hz, 1H), 7.36 (d,  $J = 7.9$  Hz, 1H), 7.20 – 7.11 (m, 1H), 6.83 (dd,  $J = 17.5, 10.8$  Hz, 1H), 6.20 (dd,  $J = 17.4, 1.3$  Hz, 1H), 5.49 (dd,  $J = 10.9, 1.2$  Hz, 1H).

#### 5.2.4. General procedure for dehydrogenative borylation of styrene derivatives catalyzed by $[\text{Fe}(\text{PMe}_3)_4]$

In an argon filled glove box, a Schlenk flask was charged with  $\text{Fe}(\text{PMe}_3)_4$  (9.0 mg, 5.0 mol%), followed by toluene (0.5 mL), styrene (0.5 mmol) and pinacol borane (0.5 mmol). The mixture was stirred for 18 h at 50 °C. The solution was then diluted with diethyl ether (5.0 mL) and filtered through a small pad of silica (2 cm in a Pasteur pipette). The silica was washed with diethyl ether. The filtrate was evaporated and the crude residue was purified by column chromatography ( $\text{SiO}_2$ , petroleum ether/ $\text{Et}_2\text{O}$  as eluent).

#### 5.2.5. Characterization of the borylated products

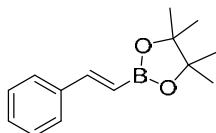
(*E*)-4,4,5,5-Tetramethyl-2-(4-methyl)-styryl-1,3,2-dioxaborolane **4a**<sup>[5]</sup>



According to general procedure, 4-methylstyrene (64  $\mu\text{L}$ , 0.5 mmol, 1.0 equiv.) gave the title compound as a pale-yellow oil after column chromatography ( $\text{SiO}_2$ ,

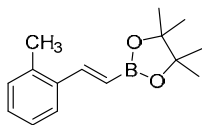
petroleum ether/ Et<sub>2</sub>O 9:1) (97 mg, 80%). <sup>1</sup>H NMR (400 MHz, CDCl<sub>3</sub>): δ 7.41 (m, 3H), 7.15 (d, *J* = 8.1 Hz, 2H), 6.12 (d, *J* = 18.5 Hz, 1H), 2.35 (s, 3H), 1.32 (s, 12H). <sup>13</sup>C{<sup>1</sup>H} NMR (101 MHz, CDCl<sub>3</sub>, the carbon attached to quadrupole B was not observed due to low intensity): δ 149.6, 139.1, 134.9, 129.4, 127.1, 83.4, 25.0, 21.5. <sup>11</sup>B NMR (96 MHz, CDCl<sub>3</sub>): δ 30.2. Spectral data were in good agreement with literature values. GC-MS, *m/z*(%) = 244([M]<sup>+</sup>, 78), 229(22), 171(11), 158(65), 143(100), 117(51), 105(11), 91(18), 77(7), 57(8).

**(*E*)-4,4,5,5-Tetramethyl-2-styryl-1,3,2-dioxaborolane 4b<sup>[3]</sup>**



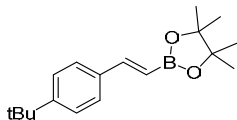
According to the general procedure, styrene (57 μL, 0.5 mmol, 1.0 equiv.) gave the title compound as a colorless oil after column chromatography (SiO<sub>2</sub>, petroleum ether/ Et<sub>2</sub>O 9:1) (87 mg, 76%). <sup>1</sup>H NMR (300 MHz, CDCl<sub>3</sub>): δ 7.51-7.48 (m, 2H), 7.40 (d, *J* = 18.4 Hz, 1H), 7.36-7.29 (m, 3H), 6.17 (d, *J* = 18.4 Hz, 1H), 1.32 (s, 12H). <sup>13</sup>C{<sup>1</sup>H} NMR (75 MHz, CDCl<sub>3</sub>, the carbon attached to quadrupole B was not observed due to low intensity): δ 149.7, 137.7, 129.0, 128.7, 127.2, 83.5, 25.0. <sup>11</sup>B NMR (96 MHz, CDCl<sub>3</sub>): δ 30.6. Spectral data were in good agreement with literature values. GC-MS, *m/z*(%) = 230([M]<sup>+</sup>, 61), 215(28), 173(10), 157(14), 130(100), 118(23), 105(41), 85(26), 77(29), 51(9).

**(*E*)-4,4,5,5-Tetramethyl-2-(2-methyl)-styryl-1,3,2-dioxaborolane 4c<sup>[4]</sup>**



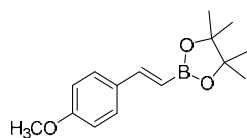
According to general procedure, 2-methystyrene (65 μL, 0.5 mmol, 1.0 equiv.) gave the title compound as a colorless needle crystal after column chromatography (SiO<sub>2</sub>, petroleum ether/ Et<sub>2</sub>O 9:1) (96 mg, 79%). <sup>1</sup>H NMR (300 MHz, CDCl<sub>3</sub>): δ 7.65 (d, *J* = 18.4 Hz, 1H), 7.57-7.54 (m, 1H), 7.20-7.13 (m, 3H), 6.08 (d, *J* = 18.4 Hz, 1H), 2.42 (s, 3H), 1.32 (s, 12H). <sup>13</sup>C{<sup>1</sup>H} NMR (75 MHz, CDCl<sub>3</sub>, the carbon attached to quadrupole B was not observed due to low intensity): δ 147.3, 136.9, 136.4, 130.5, 128.7, 126.2, 125.9, 83.4, 25.0, 20.0. <sup>11</sup>B NMR (96 MHz, CDCl<sub>3</sub>): δ 30.7. Spectral data were in good agreement with literature values. GC-MS, *m/z*(%) = 244([M]<sup>+</sup>, 62), 229(13), 171(9), 158(23), 144(100), 128(39), 116(93), 105(9), 84(26), 77(7), 57(10).

**(*E*)-4,4,5,5-Tetramethyl-2-(4-*t*-butyl)-styryl-1,3,2-dioxaborolane 4d<sup>[6]</sup>**



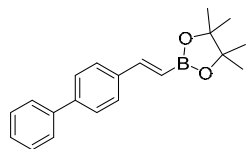
According to general procedure, 4-*t*-butylstyrene (89 μL, 0.5 mmol, 1.0 equiv.) gave the title compound as a pale-yellow needle crystal after column chromatography (SiO<sub>2</sub>, petroleum ether/ Et<sub>2</sub>O 9:1) (136 mg, 95%). <sup>1</sup>H NMR (300 MHz, CDCl<sub>3</sub>): δ 7.45-7.35 (m, 5H), 6.13 (d, *J* = 18.4 Hz, 1H), 1.32 (s, 21H). <sup>13</sup>C{<sup>1</sup>H} NMR (75 MHz, CDCl<sub>3</sub>, the carbon attached to quadrupole B was not observed due to low intensity): δ 152.3, 149.5, 134.9, 127.0, 125.6, 83.4, 34.8, 31.4, 25.0. <sup>11</sup>B NMR (96 MHz, CDCl<sub>3</sub>): δ 30.9. Spectral data were in good agreement with literature values. GC-MS, *m/z*(%) = 286([M]<sup>+</sup>, 87), 271(100), 213(10), 185(22), 171(48), 155(18), 143(86), 128(34), 101(15), 91(9), 83(18), 57(78), 55(14).

**(E)-4,4,5,5-Tetramethyl-2-(4-methoxy)-styryl-1,3,2-dioxaborolane 4e<sup>[7]</sup>**



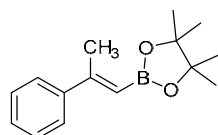
According to general procedure, 4-methoxystyrene (67  $\mu$ L, 0.5 mmol, 1.0 equiv.) gave the title compound as a pale-yellow needle crystal after column chromatography ( $\text{SiO}_2$ , petroleum ether/  $\text{Et}_2\text{O}$  9:1) (72 mg, 55%).  $^1\text{H}$  NMR (400 MHz,  $\text{CDCl}_3$ ):  $\delta$  7.43 (d,  $J$  = 8.5 Hz, 2H), 7.36 (d,  $J$  = 18.5 Hz, 1H), 6.86 (d,  $J$  = 8.5 Hz, 2H), 6.02 (d,  $J$  = 18.5 Hz, 1H), 3.80 (s, 3H), 1.30 (s, 12H).  $^{13}\text{C}\{^1\text{H}\}$  NMR (101 MHz,  $\text{CDCl}_3$ , the carbon attached to quadrupole B was not observed due to low intensity):  $\delta$  160.4, 149.2, 130.5, 128.6, 114.1, 83.3, 55.4, 25.0.  $^{11}\text{B}$  NMR (96 MHz,  $\text{CDCl}_3$ ):  $\delta$  30.4. Spectral data were in good agreement with literature values. GC-MS,  $m/z(\%)$  = 260( $[\text{M}]^+$ , 100), 245(24), 187(10), 175(35), 160(80), 144(98), 135(19), 117(31), 91(11), 77(26), 65(12), 55(9).

**(E)-4,4,5,5-Tetramethyl-2-(4-phenyl)-styryl-1,3,2-dioxaborolane 4f<sup>[7]</sup>**



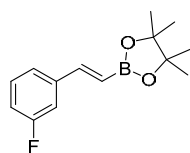
According to general procedure, 4-phenylstyrene (90 mg, 0.5 mmol, 1.0 equiv.) gave the title compound as a colorless solid after column chromatography ( $\text{SiO}_2$ , petroleum ether/  $\text{Et}_2\text{O}$  9:1) (107 mg, 70%).  $^1\text{H}$  NMR (300 MHz,  $\text{CDCl}_3$ ):  $\delta$  7.63-7.55 (m, 6H), 7.49-7.43 (m, 3H), 7.38-7.38 (m, 1H), 6.23 (d,  $J$  = 18.4 Hz, 1H), 1.34 (s, 12H).  $^{13}\text{C}\{^1\text{H}\}$  NMR (75 MHz,  $\text{CDCl}_3$ , the carbon attached to quadrupole B was not observed due to low intensity):  $\delta$  149.1, 141.7, 140.7, 136.6, 128.9, 127.7, 127.6, 127.4, 127.1, 83.5, 25.0.  $^{11}\text{B}$  NMR (96 MHz,  $\text{CDCl}_3$ ):  $\delta$  29.4. Spectral data were in good agreement with literature values. GC-MS,  $m/z(\%)$  = 306( $[\text{M}]^+$ , 100), 291(15), 220(40), 206(66), 190(48), 179(36), 165(23), 152(16), 77(7), 57(8).

**(E)-4,4,5,5-Tetramethyl-2-( $\alpha$ -methyl)-styryl-1,3,2-dioxaborolane 4i<sup>[8]</sup>**



According to general procedure,  $\alpha$ -methylstyrene (130  $\mu$ L, 1.0 mmol, 2.0 equiv.) gave the title compound as a pale-yellow oil after column chromatography ( $\text{SiO}_2$ , petroleum ether/  $\text{Et}_2\text{O}$  9:1) (17 mg, 21%).  $^1\text{H}$  NMR (400 MHz,  $\text{CDCl}_3$ ):  $\delta$  7.51 (m, 3H), 7.34-7.27 (m, 2H), 5.76 (s, 1H), 2.41 (s, 3H), 1.32 (s, 12H).  $^{13}\text{C}\{^1\text{H}\}$  NMR (101 MHz,  $\text{CDCl}_3$ , the carbon attached to quadrupole B was not observed due to low intensity):  $\delta$  158.0, 144.0, 128.3, 128.1, 126.0, 83.1, 25.1, 20.3.  $^{11}\text{B}$  NMR (96 MHz,  $\text{CDCl}_3$ ):  $\delta$  30.9. Spectral data were in good agreement with literature values. GC-MS,  $m/z(\%)$  = 244( $[\text{M}]^+$ , 89), 229(24), 187(56), 171(23), 158(71), 128(100), 116(41), 105(96), 85(13), 77(28), 55(12).

**(E)-4,4,5,5-Tetramethyl-2-(3-fluoro)-styryl-1,3,2-dioxaborolane 4g<sup>[3]</sup>**



According to general procedure, 3-fluoro-styrene (60  $\mu$ L, 1.0 mmol, 1.0 equiv.) gave the title compound as a pale-yellow oil after column chromatography ( $\text{SiO}_2$ , petroleum ether/  $\text{Et}_2\text{O}$  9:1) (100 mg, 81%).  $^1\text{H}$  NMR (400 MHz,  $\text{CDCl}_3$ ):  $\delta$  7.36 (d,  $J$  = 18.4 Hz, 1H),

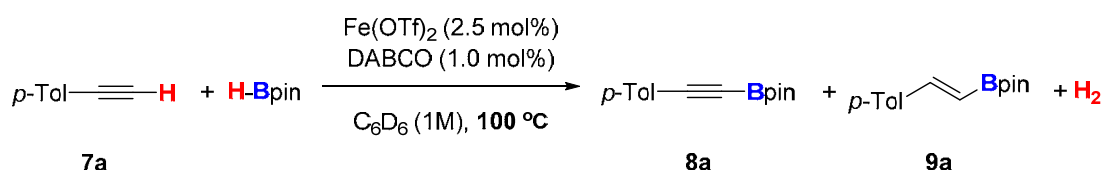
7.32-7.28 (m, 1H), 7.26-7.22 (m, 1H), 7.20-7.18 (m, 1H), 7.02-6.98 (m, 1H), 6.18 (d,  $J = 18.4$  Hz, 1H), 1.33 (s, 12H).  $^{13}\text{C}\{^1\text{H}\}$  NMR (101 MHz,  $\text{CDCl}_3$ , the carbon attached to quadrupole B was not observed due to low intensity):  $\delta$  163.3 (d,  $J_{\text{CF}} = 245$ ), 148.2 (d,  $J_{\text{CF}} = 2.7$ ), 140.0 (d,  $J_{\text{CF}} = 7.1$ ), 130.2 (d,  $J_{\text{CF}} = 8.3$ ), 123.1 (d,  $J_{\text{CF}} = 2.7$ ), 115.8 (d,  $J_{\text{CF}} = 21.6$ ), 113.4 (d,  $J_{\text{CF}} = 21.6$ ), 83.7, 25.0.  $^{11}\text{B}$  NMR (96 MHz,  $\text{CDCl}_3$ ):  $\delta$  31.0.  $^{19}\text{F}$  NMR (376 MHz,  $\text{CDCl}_3$ )  $\delta$  -113.47. Spectral data were in good agreement with literature values. GC-MS,  $m/z(\%) = 248([\text{M}]^+, 48)$ , 233(27), 205(17), 175(8), 162(60), 147(100), 123(17), 103(21), 85(23), 77(10), 59(15), 55(7)

### 5.3. Part II-2- Dehydrogenative borylation of alkynes

#### 5.3.1. General procedure for $\text{Fe}(\text{OTf})_2$ catalyzed dehydrogenative borylation of terminal alkynes

In an argon filled glove box, a 20 mL Schlenk tube was charged with  $\text{Fe}(\text{OTf})_2$  (2.5 mol%), toluene (1.0 mol/L), alkyne (0.5 mmol), HBpin (0.5 mmol) and DABCO (1.0 mol%, stock solution in toluene) in this order. Then the reaction mixture was stirred at 100 °C for 72 h. After cooling the mixture to room temperature, the solution was diluted with pentane (2.0 mL) and filtered through a small pad of celite (2 cm in a Pasteur pipette). The celite was washed with pentane (2.0 mL $\times$ 2). The filtrate was evaporated and the crude residue was then purified either by recrystallization (slow evaporation from pentane) or bulb to bulb distillation.

#### 5.3.2. General procedure for kinetic study of $\text{Fe}(\text{OTf})_2$ catalyzed dehydrogenative borylation of terminal alkynes

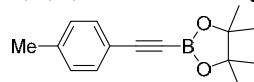


In an argon filled glove box, a Young NMR tube was charged with  $\text{Fe}(\text{OTf})_2$  (2.5 mol%),  $\text{C}_6\text{D}_6$  (1.0 mol/L), **a2** (0.5 mmol), HBpin (0.5 mmol) and DABCO (1.0 mol%, stock solution in  $\text{C}_6\text{D}_6$ ) in this order. Then the reaction mixture was heated at 100 °C for indicated time. After cooling the mixture to room temperature, crude NMRs were done *in situ*.

#### 5.3.3. Characterization of the products of dehydrogenative borylation reactions

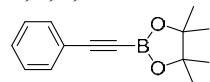
NMR spectra of these products are in accordance with literature reports (see references accordingly). As noted by those references, the signals of quaternary carbon atoms bound to boron were not observed due to low intensity.

#### 4,4,5,5-Tetramethyl-2-(*p*-tolylethynyl)-1,3,2-dioxaborolane **8a**<sup>[9]</sup>



Recrystallization from pentane gave the title compound (102.9 mg, 85% yield) as a white solid.  $^1\text{H}$  NMR (400 MHz,  $\text{C}_6\text{D}_6$ )  $\delta$  7.35 (d,  $J = 8.0$ , 2H), 6.66 (d,  $J = 8.0$ , 2H), 1.88 (s, 3H), 1.03 (s, 12H).  $^{11}\text{B}$  NMR (128 MHz,  $\text{C}_6\text{D}_6$ )  $\delta$  24.87.  $^{13}\text{C}\{^1\text{H}\}$  NMR (101 MHz,  $\text{C}_6\text{D}_6$ )  $\delta$  139.5, 132.8, 129.4, 119.8, 102.3, 84.0, 24.7, 21.3.

#### 4,4,5,5-Tetramethyl-2-(phenylethynyl)-1,3,2-dioxaborolane **8b**<sup>[9]</sup>

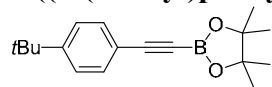


Bulb to bulb distillation (120 °C/2 Torr) gave the title compound (91.2 mg, 80% yield) as a white solid.  $^1\text{H}$  NMR (400 MHz,  $\text{C}_6\text{D}_6$ )  $\delta$  7.41 – 7.38 (m, 2H), 6.91 – 6.82 (m, 3H), 1.03 (s,



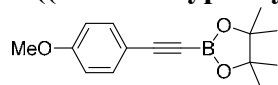
12H).  $^{11}\text{B}$  NMR (128 MHz,  $\text{C}_6\text{D}_6$ )  $\delta$  24.79.  $^{13}\text{C}\{^1\text{H}\}$  NMR (101 MHz,  $\text{C}_6\text{D}_6$ )  $\delta$  132.7, 129.3, 128.5, 122.7, 101.9, 84.1, 24.7.

### 2-((4-(*t*-Butyl)phenyl)ethynyl)-4,4,5,5-tetramethyl-1,3,2-dioxaborolane **8c**



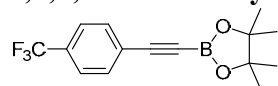
Recrystallization from pentane gave the title compound (120.8 mg, 85% yield) as a white solid.  $^1\text{H}$  NMR (400 MHz,  $\text{C}_6\text{D}_6$ )  $\delta$  7.45 (d,  $J$  = 8.4, 2H), 6.97 (d,  $J$  = 8.4, 2H), 1.04 (s, 9H), 1.03 (s, 12H).  $^{11}\text{B}$  NMR (128 MHz,  $\text{C}_6\text{D}_6$ )  $\delta$  24.90.  $^{13}\text{C}\{^1\text{H}\}$  NMR (101 MHz,  $\text{C}_6\text{D}_6$ )  $\delta$  152.5, 132.7, 125.7, 119.9, 100.9, 84.0, 34.7, 31.0, 24.7. GC-MS,  $m/z$ (%) = 284 ( $[\text{M}]^+$ , 39), 269(100), 199(29), 169(28), 141(19), 57(16).

### 2-((4-Methoxyphenyl)ethynyl)-4,4,5,5-tetramethyl-1,3,2-dioxaborolane **8d**<sup>[10]</sup>



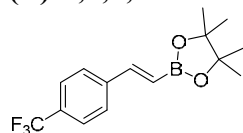
Bulb to bulb distillation (130 °C/2 Torr) gave the title compound (96.8 mg, 75% yield) as a pale yellow solid.  $^1\text{H}$  NMR (400 MHz,  $\text{C}_6\text{D}_6$ )  $\delta$  7.36 (d,  $J$  = 8.8, 2H), 6.43 (d,  $J$  = 8.8, 2H), 3.08 (s, 3H), 1.05 (s, 12H).  $^{11}\text{B}$  NMR (128 MHz,  $\text{C}_6\text{D}_6$ )  $\delta$  25.01.  $^{13}\text{C}\{^1\text{H}\}$  NMR (101 MHz,  $\text{C}_6\text{D}_6$ )  $\delta$  160.8, 134.5, 114.3, 114.3, 102.4, 84.0, 54.7, 24.8.

### 4,4,5,5-Tetramethyl-2-((4-(trifluoromethyl)phenyl)ethynyl)-1,3,2-dioxaborolane **8e**<sup>[10]</sup>



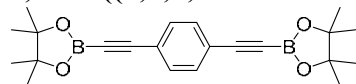
Recrystallization from pentane gave the title compound (128.8 mg, 87% yield) as a white solid.  $^1\text{H}$  NMR (400 MHz,  $\text{C}_6\text{D}_6$ )  $\delta$  7.11 (d,  $J$  = 8.2, 2H), 6.97 (d,  $J$  = 8.2, 2H), 1.02 (s, 12H).  $^{11}\text{B}$  NMR (128 MHz,  $\text{C}_6\text{D}_6$ )  $\delta$  24.63.  $^{19}\text{F}$  NMR (376 MHz,  $\text{C}_6\text{D}_6$ )  $\delta$  -62.81.  $^{13}\text{C}\{^1\text{H}\}$  NMR (101 MHz,  $\text{C}_6\text{D}_6$ )  $\delta$  132.4, 130.4 (q,  $J$  = 32.6), 125.7, 125.0 (q,  $J$  = 3.8), 124.04 (q,  $J$  = 272.4 Hz), 99.7, 84.0, 24.3.

### (E)-4,4,5,5-Tetramethyl-2-(4-(trifluoromethyl)styryl)-1,3,2-dioxaborolane **9e**<sup>[4]</sup>

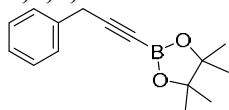


Recrystallization from pentane gave the title compound (137.1 mg, 92% yield) as a white solid.  $^1\text{H}$  NMR (400 MHz,  $\text{C}_6\text{D}_6$ )  $\delta$  7.55 (d,  $J$  = 18.4, 1H), 7.19 (d,  $J$  = 8.1, 2H), 7.05 (d,  $J$  = 8.1, 2H), 6.35 (d,  $J$  = 18.4, 1H), 1.13 (s, 13H).  $^{11}\text{B}$  NMR (128 MHz,  $\text{C}_6\text{D}_6$ )  $\delta$  30.19.  $^{19}\text{F}$  NMR (376 MHz,  $\text{C}_6\text{D}_6$ )  $\delta$  -62.37.  $^{13}\text{C}\{^1\text{H}\}$  NMR (101 MHz,  $\text{C}_6\text{D}_6$ )  $\delta$  148.3, 141.1, 130.4 (q,  $J$  = 32.2), 127.5, 125.7 (q,  $J$  = 3.8), 124.9 (d,  $J$  = 271.9 Hz), 83.5, 25.0.

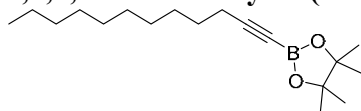
### 1,4-Bis((4,4,5,5-tetramethyl-1,3,2-dioxaborolan-2-yl)ethynyl)benzene **8f**



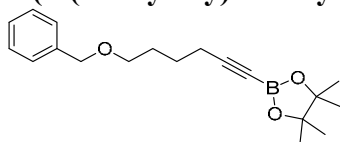
Recrystallization from pentane gave the title compound (175.8 mg, 93% yield) as a white solid.  $^1\text{H}$  NMR (400 MHz,  $\text{C}_6\text{D}_6$ )  $\delta$  7.35 (s, 4H), 1.21 (s, 24H).  $^{11}\text{B}$  NMR (128 MHz,  $\text{C}_6\text{D}_6$ )  $\delta$  24.53.  $^{13}\text{C}\{^1\text{H}\}$  NMR (101 MHz,  $\text{C}_6\text{D}_6$ )  $\delta$  132.5, 123.3, 101.1, 84.2, 24.7. GC-MS,  $m/z$ (%) = 378 ( $[\text{M}]^+$ , 0.5), 252(49), 237(22), 194(25), 167(63), 152(100), 124(12), 77(12).

**4,4,5,5-Tetramethyl-2-(3-phenylprop-1-yn-1-yl)-1,3,2-dioxaborolane 8g<sup>[9]</sup>**

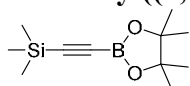
Bulb to bulb distillation (130 °C/2 Torr) gave the title compound (98.1 mg, 81% yield) as a pale yellow liquid. <sup>1</sup>H NMR (400 MHz, C<sub>6</sub>D<sub>6</sub>) δ 7.15 (d, *J* = 7.1, 2H), 7.06 – 6.95 (m, 3H), 3.28 (s, 2H), 1.00 (s, 12H). <sup>11</sup>B NMR (128 MHz, C<sub>6</sub>D<sub>6</sub>) δ 24.29. <sup>13</sup>C{<sup>1</sup>H} NMR (101 MHz, C<sub>6</sub>D<sub>6</sub>) δ 135.9, 128.7, 128.29 (overlap with C<sub>6</sub>D<sub>6</sub> peak), 126.9, 101.6, 83.8, 25.9, 24.7.

**4,4,5,5-Tetramethyl-2-(dodec-1-yn-1-yl)-1,3,2-dioxaborolane 8h<sup>[11]</sup>**

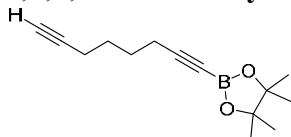
Bulb to bulb distillation (130 °C/2 Torr) gave the title compound (114.0 mg, 78% yield) as a white solid. <sup>1</sup>H NMR (400 MHz, C<sub>6</sub>D<sub>6</sub>) δ 2.01 (t, *J* = 6.9, 2H), 1.39 – 1.06 (m, 16H), 1.00 (s, 12H), 0.92 (t, *J* = 7.0, 3H). <sup>11</sup>B NMR (128 MHz, C<sub>6</sub>D<sub>6</sub>) δ 24.28. <sup>13</sup>C{<sup>1</sup>H} NMR (101 MHz, C<sub>6</sub>D<sub>6</sub>) δ 104.6, 83.7, 32.3, 30.0, 29.9, 29.8, 29.5, 29.1, 28.5, 24.7, 23.1, 19.8, 14.4.

**2-(6-(Benzyloxy)hex-1-yn-1-yl)-4,4,5,5-tetramethyl-1,3,2-dioxaborolane 8i**

Bulb to bulb distillation (130 °C/2 Torr) gave the title compound (146.1 mg, 93% yield) as a colorless liquid. <sup>1</sup>H NMR (400 MHz, C<sub>6</sub>D<sub>6</sub>) δ 7.25 (d, *J* = 7.3, 2H), 7.18 (d, *J* = 7.3, 2H), 7.10 (t, *J* = 7.3, 1H), 4.23 (s, 2H), 3.14 (t, *J* = 6.1, 2H), 1.99 (t, *J* = 6.9, 2H), 1.58 – 1.40 (m, 4H), 1.00 (s, 12H). <sup>11</sup>B NMR (128 MHz, C<sub>6</sub>D<sub>6</sub>) δ 24.24. <sup>13</sup>C{<sup>1</sup>H} NMR (101 MHz, C<sub>6</sub>D<sub>6</sub>) δ 139.5, 128.5, 127.7, 127.5, 83.7, 72.9, 69.7, 29.1, 25.3, 24.7, 19.5. GC-MS, *m/z*(%) = 313 ([M]<sup>+</sup>, 6), 231(18), 214(12), 165(18), 142(17), 101(27), 91(100), 79(43), 55(14).

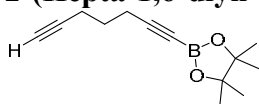
**Trimethyl((4,4,5,5-tetramethyl-1,3,2-dioxaborolan-2-yl)ethynyl)silane 8j<sup>[9]</sup>**

Bulb to bulb distillation (100 °C/2 Torr) gave the title compound (99.8 mg, 89% yield) as a white solid. <sup>1</sup>H NMR (400 MHz, C<sub>6</sub>D<sub>6</sub>) δ 0.96 (s, 12H), 0.08 (s, 9H). <sup>11</sup>B NMR (128 MHz, C<sub>6</sub>D<sub>6</sub>) δ 23.55. <sup>13</sup>C{<sup>1</sup>H} NMR (101 MHz, C<sub>6</sub>D<sub>6</sub>) δ 110.7, 84.1, 24.6, -0.5.

**4,4,5,5-Tetramethyl-2-(octa-1,7-diyn-1-yl)-1,3,2-dioxaborolane 8k**

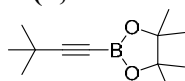
Bulb to bulb distillation (120 °C/2 Torr) gave the title compound (81.2 mg, 70% yield) as a white solid. <sup>1</sup>H NMR (400 MHz, C<sub>6</sub>D<sub>6</sub>) δ 1.89 – 1.86 (m, 2H), 1.79 – 1.76 (m, 2H), 1.71 (t, *J* = 2.6, 1H), 1.32 – 1.29 (m, 4H), 1.00 (s, 12H). <sup>11</sup>B NMR (128 MHz, C<sub>6</sub>D<sub>6</sub>) δ 24.25. <sup>13</sup>C{<sup>1</sup>H} NMR (101 MHz, C<sub>6</sub>D<sub>6</sub>) δ 103.9, 83.9, 83.7, 69.0, 27.6, 27.3, 24.7, 19.1, 18.0. GC-MS, *m/z*(%) = 231 ([M]<sup>+</sup>, 0.5), 217(28), 189(11), 145(30), 131(100), 118(42), 105(83), 91(51), 79(42), 67(32), 55(28).

## 2-(Hepta-1,6-diyn-1-yl)-4,4,5,5-tetramethyl-1,3,2-dioxaborolane **8l**



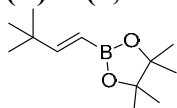
Bulb to bulb distillation (120 °C/2 Torr) gave the title compound (78.5 mg, 72% yield) as a white solid.  $^1\text{H NMR}$  (400 MHz,  $\text{C}_6\text{D}_6$ )  $\delta$  2.02 (t,  $J = 7.1$ , 2H), 1.93 (td,  $J = 7.0$ , 6.6, 2.2, 2H), 1.66 (t,  $J = 2.6$ , 1H), 1.36 (p,  $J = 7.0$ , 2H), 0.99 (s, 12H).  $^{11}\text{B NMR}$  (128 MHz,  $\text{C}_6\text{D}_6$ )  $\delta$  24.06.  $^{13}\text{C}\{^1\text{H}\}$  NMR (101 MHz,  $\text{C}_6\text{D}_6$ )  $\delta$  103.2, 83.7, 83.2, 69.4, 27.3, 24.7, 18.6, 17.6. **GC-MS**,  $m/z(\%) = 218$  ( $[\text{M}]^+$ , 2), 203(28), 175(15), 161(20), 131(35), 117(100), 105(24), 91(48), 79(28), 57(21), 53(16).

## 2-(3,3-Dimethylbut-1-yn-1-yl)-4,4,5,5-tetramethyl-1,3,2-dioxaborolane **8m**<sup>[11,12]</sup>



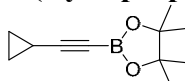
Bulb to bulb distillation (100 °C/2 Torr) gave the title compound (64.5 mg, 62% yield) as a white solid.  $^1\text{H NMR}$  (400 MHz,  $\text{C}_6\text{D}_6$ )  $\delta$  1.09 (s, 9H), 0.99 (s, 12H).  $^{11}\text{B NMR}$  (128 MHz,  $\text{C}_6\text{D}_6$ )  $\delta$  24.30.  $^{13}\text{C}\{^1\text{H}\}$  NMR (101 MHz,  $\text{C}_6\text{D}_6$ )  $\delta$  112.2, 83.6, 30.6, 28.1, 24.7.

## (*E*)-2-(3,3-Dimethylbut-1-en-1-yl)-4,4,5,5-tetramethyl-1,3,2-dioxaborolane **9m**<sup>[13]</sup>



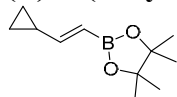
Bulb to bulb distillation (100 °C/2 Torr) gave the title compound (94.6 mg, 90% yield) as colorless liquid.  $^1\text{H NMR}$  (400 MHz,  $\text{C}_6\text{D}_6$ )  $\delta$  7.02 (d,  $J = 18.2$ , 1H), 5.72 (d,  $J = 18.2$ , 1H), 1.10 (s, 12H), 0.94 (s, 9H).  $^{11}\text{B NMR}$  (128 MHz,  $\text{C}_6\text{D}_6$ )  $\delta$  30.67.  $^{13}\text{C}\{^1\text{H}\}$  NMR (101 MHz,  $\text{C}_6\text{D}_6$ )  $\delta$  164.6, 82.9, 35.0, 28.9, 25.0.

## 2-(Cyclopropylethynyl)-4,4,5,5-tetramethyl-1,3,2-dioxaborolane **8n**



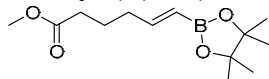
Bulb to bulb distillation (100 °C/2 Torr) gave the title compound (60.5 mg, 63% yield) as a white solid.  $^1\text{H NMR}$  (400 MHz,  $\text{C}_6\text{D}_6$ )  $\delta$  0.99 (s, 12H), 0.92 (tt,  $J = 8.4$ , 5.0, 1H), 0.59 – 0.52 (m, 2H), 0.30 – 0.20 (m, 2H).  $^{11}\text{B NMR}$  (128 MHz,  $\text{C}_6\text{D}_6$ )  $\delta$  24.09.  $^{13}\text{C}\{^1\text{H}\}$  NMR (101 MHz,  $\text{C}_6\text{D}_6$ )  $\delta$  107.2, 83.2, 24.3, 8.3, 0.2. **GC-MS**,  $m/z(\%) = 192$  ( $[\text{M}]^+$ , 13), 177(58), 149(49), 135(35), 119(10), 106(40), 93(100), 79(18), 67(19), 53(13).

## (*E*)-2-(2-Cyclopropylvinyl)-4,4,5,5-tetramethyl-1,3,2-dioxaborolane **9n**



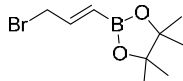
Bulb to bulb distillation (100 °C/2 Torr) gave the title compound (82.5 mg, 85% yield) as colorless liquid.  $^1\text{H NMR}$  (400 MHz,  $\text{C}_6\text{D}_6$ )  $\delta$  6.38 (dd,  $J = 17.7$ , 9.3, 1H), 5.85 (d,  $J = 17.7$ , 1H), 1.10 (s, 12H), 0.49 – 0.44 (m, 2H), 0.43 (s, 1H), 0.31 – 0.27 (m, 2H).  $^{11}\text{B NMR}$  (128 MHz,  $\text{C}_6\text{D}_6$ )  $\delta$  30.22.  $^{13}\text{C}\{^1\text{H}\}$  NMR (101 MHz,  $\text{C}_6\text{D}_6$ )  $\delta$  159.0, 82.8, 25.0, 17.3, 8.0. **GC-MS**,  $m/z(\%) = 194$  ( $[\text{M}]^+$ , 29), 179(30), 150(15), 121(20), 101(100), 95(75), 83(54), 67(85), 55(38).

**Methyl (*E*)-6-(4,4,5,5-tetramethyl-1,3,2-dioxaborolan-2-yl)hex-5-enoate 9o<sup>[14]</sup>**



Filtration through Al<sub>2</sub>O<sub>3</sub> with pentane gave the title compound (120.7 mg, 95% yield) as a colorless liquid. <sup>1</sup>H NMR (400 MHz, C<sub>6</sub>D<sub>6</sub>) δ 6.81 (dt, *J* = 17.9, 6.5, 1H), 5.71 (dt, *J* = 17.9, 1.6, 1H), 3.30 (s, 3H), 2.04 – 1.90 (m, 4H), 1.57 (p, *J* = 7.5, 2H), 1.09 (s, 12H). <sup>11</sup>B NMR (128 MHz, C<sub>6</sub>D<sub>6</sub>) δ 29.96. <sup>13</sup>C{<sup>1</sup>H} NMR (101 MHz, C<sub>6</sub>D<sub>6</sub>) δ 173.0, 153.5, 83.0, 50.9, 35.2, 33.3, 25.0, 23.8.

**(*E*)-2-(3-bromoprop-1-en-1-yl)-4,4,5,5-tetramethyl-1,3,2-dioxaborolane 9p<sup>[14]</sup>**



Filtration through Al<sub>2</sub>O<sub>3</sub> with pentane gave the title compound (113.6 mg, 92% yield) as a colorless liquid. <sup>1</sup>H NMR (400 MHz, C<sub>6</sub>D<sub>6</sub>) δ 6.78 (dt, *J* = 17.5, 7.1, 1H), 5.67 (dt, *J* = 17.5, 1.2, 1H), 3.41 (dd, *J* = 7.1, 1.2, 2H), 1.02 (s, 12H). <sup>11</sup>B NMR (128 MHz, C<sub>6</sub>D<sub>6</sub>) δ 29.62. <sup>13</sup>C{<sup>1</sup>H} NMR (101 MHz, C<sub>6</sub>D<sub>6</sub>) δ 147.5, 83.4, 33.5, 24.8.

## 5.4. References

- [1] (a) Girolami, G. S.; Wilkinson, G.; Galas, A. M. R.; Thornton-Pett, M.; Hursthouse, M. B. *Dalton Trans.* **1985**, 1339. (b) Allen, A. R.; Dalgarno, S. J.; Field, L. D.; Jensen, P.; Turnbull, A. J.; Willis, A. C. *Organometallics* **2008**, 27, 2092.
- [2] Karsch, H. H.; Klein, H.-F.; Schmidbaur, H., *Chem. Ber.* **1977**, 110, 2200-2212.
- [3] Zhao, J.; Niu, Z.; Fu, H.; Li, Y., *Chem. Commun.* **2014**, 50, 2058-2060.
- [4] Jang, H.; Zhugralin, A. R.; Lee, Y.; Hoveyda, A. H., *J. Am. Chem. Soc.* **2011**, 133, 7859-7871.
- [5] Stewart, S. K.; Whiting, A., *J. Organomet. Chem.* **1994**, 482, 293-300.
- [6] Feng, Q.; Yang, K.; Song, Q., *Chem. Commun.* **2015**, 51, 15394-15397.
- [7] Ho, H. E.; Asao, N.; Yamamoto, Y.; Jin, T., *Org. Lett.* **2014**, 16, 4670-4673.
- [8] Mkhaliid, I. A. I.; Coapes, R. B.; Edes, S. N.; Coventry, D. N.; Souza, F. E. S.; Thomas, R. L.; Hall, J. J.; Bi, S.-W.; Lin, Z.; Marder, T. B., *Dalton Trans.* **2008**, 1055-1064.
- [9] Romero, E. A.; Jazzar, R.; Bertrand, G. *Chem. Sci.* **2016**, 8, 165-168.
- [10] Nishihara, Y.; Miyasaka, M.; Okamoto, M.; Takahashi, H.; Inoue, E.; Tanemura, K.; Takagi, K. *J. Am. Chem. Soc.* **2007**, 129, 12634-12635.
- [11] Nishihara, Y.; Okada, Y.; Jiao, J.; Suetsugu, M.; Lan, M. T.; Kinoshita, M.; Iwasaki, M.; Takagi, K. *Angew. Chem. Int. Ed.* **2011**, 50, 8660-8664.
- [12] Cheesman, B. V.; Deloux, L.; Srebnik, M. *Magn. Reson. Chem.* **1995**, 33, 724-728.
- [13] Pietruszka, J.; Rieche, A. C. M.; Wilhelm, T.; Witt, A. *Adv. Synth. Catal.* **2003**, 345, 1273-1286.
- [14] Hoffmann, R. W.; Landmann, B. *Eur. J. Inorg. Chem.* **1986**, 119, 1039-1053.

## **Chapter III - Hydrosilylation Reactions**

### **Part I - Synthesis of Cyclic Amines *via* Iron-Catalyzed Hydrosilylation**



## Chapter III - Hydrosilylation Reactions

### Part 1 - Synthesis of cyclic amines *via* iron-catalyzed hydrosilylation

#### Introduction

*N*-Heterocycles are one of the most important compounds due to their widely potential applications in agrochemical, natural products, pharmaceutical chemistry, biologically valuable fine chemicals, as well as material chemistry.<sup>[1]</sup> Particularly, cyclic amines (such as pyrrolidines, piperidines and azepanes) are present in a large class of natural products and biologically active molecules.<sup>[2]</sup> Noticeably, as a representative example, the pyrrolidine ring motif is present in numerous natural alkaloids (e.g. nicotine and hygrine). It is also found in many pharmaceuticals such as procyclidine and bepridil (Figure 1a). Piperidine motif can be present in Mefloquine, an important anti-malarial drug and azepane in Cetiedil, a vasodilator and anti-sickling agent. Furthermore, pyrrolidones are usually substructure in the drug racetams such as piracetam, levetiracetam and aniracetam (Figure 1b).

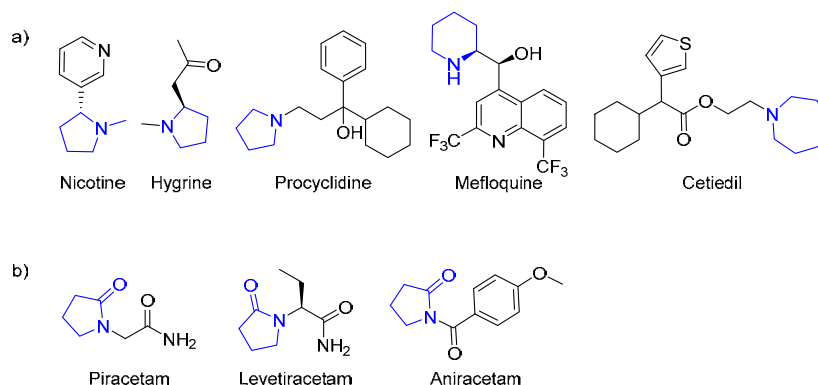
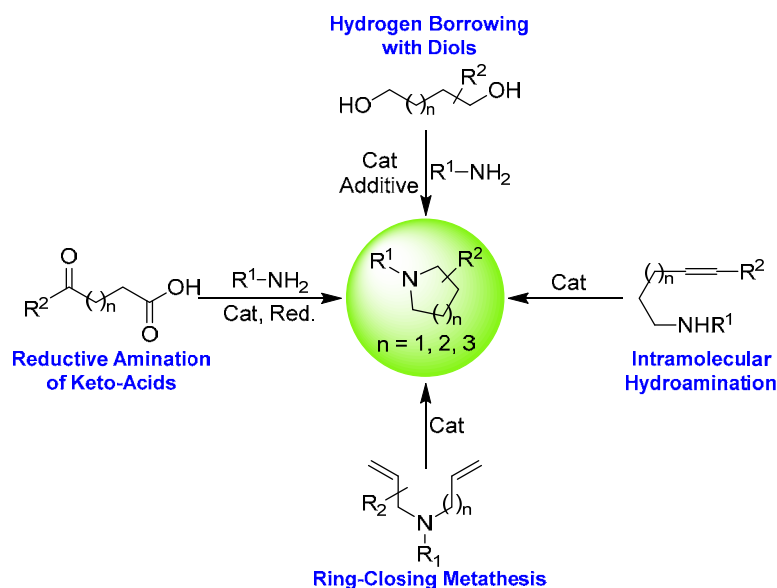


**Figure 1.** Selected examples for **a)** pyrrolidine, piperidine and azepane functionalities in natural alkaloids and pharmaceuticals and **b)** pyrrolidone structures in racetam drugs.

Among the numerous synthetic methodologies, the conventional double alkylation of primary amines with dihalides<sup>[3]</sup> seems to be a convenient pathway, however the utilization of stoichiometric amount of base additives is unavoidable. In the past few decades, huge efforts have been devoted to the development of efficient methods for the synthesis of cyclic amines,<sup>[4]</sup> including hydrogen borrowing,<sup>[5]</sup> intramolecular hydroamination reactions,<sup>[6]</sup> ring-closing metathesis<sup>[7]</sup> and reductive amination of keto acids (especially levulinic acid, Scheme 1).<sup>[8]</sup>

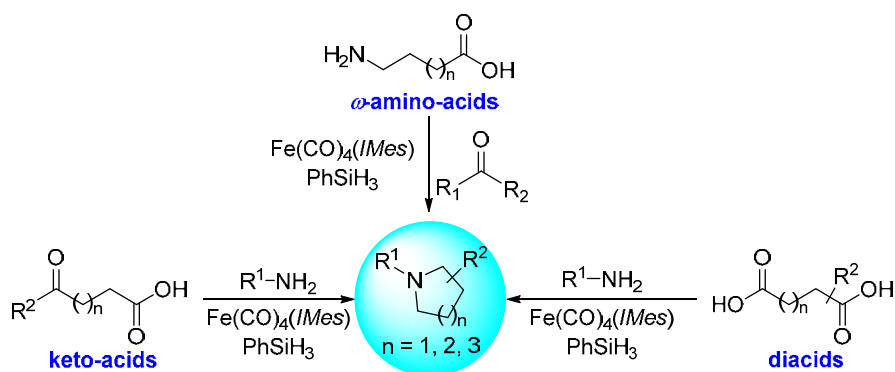
In addition, those synthetic routes have been dominated by noble metals as the catalysts, for examples Ir, Ru, Rh and also Pd. In comparison, Earth-abundant metals are relatively less applied in such transformations.





**Scheme 1.** Representative catalytic synthetic routes to *N*-substituted cyclic amines.

This first part of the chapter will be devoted to iron-catalyzed efficient and selective one-pot pathways involving a reductive amination step *via* hydrosilylation for the selective preparation of (i) pyrrolidines *vs* pyrrolidinones from levulinic acid derivatives, (ii) pyrrolidines, piperidines and azepanes from  $\omega$ -amino fatty acids and (iii) from dicarboxylic acids. (Scheme 2).



**Scheme 2.** Iron-catalyzed synthesis of cyclic amines *via* iron catalyzed one pot sequence involving a reductive amination step.

### III-1 Reductive amination of keto acids derivatives with hydrosilanes catalyzed by Fe-NHC complexes

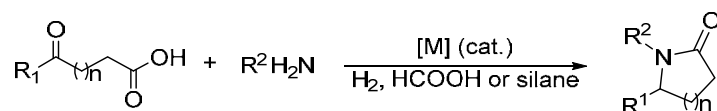
**Contributions in this part:** Optimization and scope: Duo Wei, Chakkrit Netkaew;  
Mechanistic studies: Duo Wei.

**Publication:** D. Wei, C. Netkaew, C. Darcel, *Adv. Synth. Catal.* **2019**, *361*, 1781-1786.

#### 1.1. Introduction

The selective and efficient production of inedible biomass or biomass platform derived fine chemicals, such as ethanol, hydroxymethylfurfural (HMF), furfural, and levulinic acid (LA), has drawn much attention with the huge development of green and sustainable chemistry in the past two decades.<sup>[9]</sup> Levulinic acid or levulinate derivatives, which are easily accessible from acidic hydrolysis of carbohydrates such as lignocellulose,<sup>[10]</sup> have been extensively studied. Indeed, they are valuable fine chemicals for access to platform molecules, such as  $\gamma$ -valerolactone (GVL), *N*-substituted-5-methyl-2-pyrrolidones, 2-methyl-tetrahydrofuran, and 1,4-pentanediol.<sup>[11]</sup>

The combination of a reductive amination of levulinic acid and a subsequent intramolecular cyclization is one of the most atom economic and sustainable approaches to access pyrrolidines and pyrrolidinones (Scheme 3).



**Scheme 3.** General methodology involving transition metal catalyzed reductive amination of levulinic acid and keto-acids for the synthesis of lactams

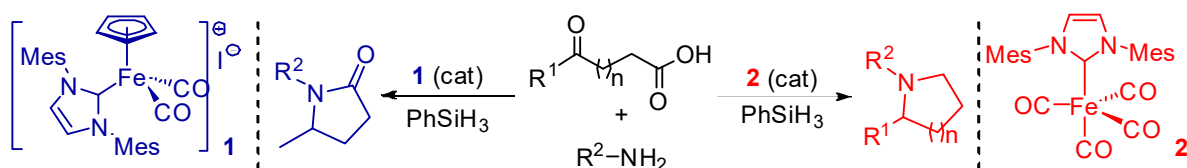
In the area of homogeneous catalysis, in 2011, Fu *et al.*<sup>[12]</sup> reported the first example of transformation of levulinic acid to pyrrolidines with formic acid as the hydrogen source. A ruthenium catalyst generated *in situ* from  $[ \{ RuCl_2(p\text{-cymene}) \}_2 ]$  and *t*Bu<sub>3</sub>P was efficiently used at 80 °C with alkylamines, and 120 °C with arylamines. Afterwards, Xiao<sup>[13]</sup>, Zhang<sup>[14]</sup> and Fischmeister<sup>[15]</sup> developed efficient Cp\*Ir based catalysts which operated in water or neat conditions at 80-110 °C, with either formic acid or H<sub>2</sub> as the reductants. It is also important to underline that the selective production of lactams *versus* cyclic amines starting from levulinic acid and amines in the presence of PhSiH<sub>3</sub> were reported by either switching from In(OAc)<sub>3</sub> to InI<sub>3</sub><sup>[8a]</sup>, or from AlCl<sub>3</sub>•6H<sub>2</sub>O to RuCl<sub>3</sub>•3H<sub>2</sub>O<sup>[8b]</sup>, respectively. Furthermore, organoboron-catalyzed reductive aminations of LA with silanes as reducing reagents has also been

reported.<sup>[16]</sup> Additionally, reductive aminase from *Aspergillus oryzae* was also able to promote the enantioselective formation of *N*-alkylpyrrolidinones from ethyl levulinate.<sup>[17]</sup>

At iron, few reports deal with catalysts able to reduce levulinic acid or levulinate derivatives to  $\gamma$ -valerolactone under transfer hydrogenation: (i) using formic acid,  $\text{Fe}(\text{OTf})_2$  and  $[\text{P}(\text{CH}_2\text{CH}_2\text{PPh}_2)_3]$  ligand (140 °C, 24 h),<sup>[19]</sup> and  $\text{Fe}_3(\text{CO})_{12}$  (water, 180 °C, 15 h),<sup>[20]</sup> and (ii) using isopropanol, Casey type complex ( $\text{NaHCO}_3$ , 100 °C, 19 h)<sup>[21]</sup> and Knölker type complexes (80-100 °C, 19-20 h).<sup>[22]</sup> Additionally, the hydrogenation of levulinic acid to GVL was performed using Knölker type complexes with TON up to 570 (EtOH, 60 bar  $\text{H}_2$ , 100 °C, 20 h). Recently, PNNNP pincer iron complex catalyzed the hydrogenation of both methyl levulinate and levulinic acid leading to GVL with TOF up to 1900  $\text{h}^{-1}$  (100 bar  $\text{H}_2$ , 100 °C).<sup>[23]</sup>

Besides hydrogenation, hydrosilanes are mild and higher selective reducing agents in terms of chemoselectivity and functional-group tolerance for the production of fine chemicals. They can be considered as interesting alternative reductants, although siloxane waste is an unavoidable by-product. To the best of our knowledge, the use of well-defined iron complexes as catalysts for transformation of levulinic acid derivatives to pyrrolidines and pyrrolidinones was scarcely explored. Only one recent contribution of Burtoloso reported the use of  $\text{Fe}_3(\text{CO})_{12}$  for catalyzed transfer hydrogenation of levulinic acid using 2.2 equiv. of a mixture 1:1 of formic acid and amine in water in drastic conditions (180 °C) leading to pyrrolidones.<sup>[24]</sup>

This paragraph will be devoted to the efficient and selective one-pot methodology for the switchable reductive amination of levulinic acid or levulinates *via* hydrosilylation for the selective preparation of pyrrolidines vs pyrrolidinones by the right choice of iron catalysts (Scheme 1b).



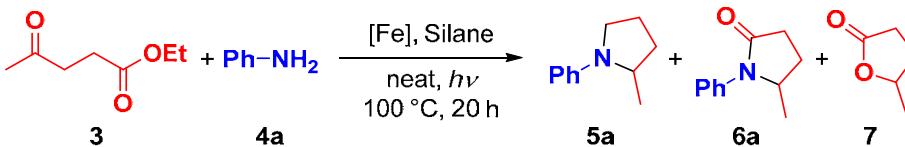
**Scheme 4.** Reductive amination of levulinic acid using well-defined iron catalysts.

## 1.2. Results and discussions

### 1.2.1. Optimization of reaction conditions for the reductive amination of ethyl levulinate with aniline

In our group, a series of *N*-heterocyclic carbene (NHC) based iron complexes have been previously developed, including [CpFe(CO)<sub>2</sub>(*IMes*)]<sup>[I]</sup> **1** and [Fe(CO)<sub>4</sub>(*IMes*)] **2** [Scheme 4, *IMes* = 1,3-bis (2,4,6-trimethylphenyl)imidazol-2-ylidene], for catalytic hydrosilylation of carbonyl derivatives<sup>[25]</sup>, imines<sup>[26]</sup>, amides<sup>[27]</sup>, esters<sup>[28]</sup> and also methylation of secondary amines.<sup>[29]</sup> Inspired by recent reports on the catalytic transformation of biomass and of bio-based synthons, we began our initial investigation using ethyl levulinate **3**, aniline **2a**, phenylsilane in the absence of solvent, combined with **1** or **2** as catalysts. The preliminary experiment using **1** (5.0 mol%) in the presence of 4 equiv. of PhSiH<sub>3</sub> at 100 °C upon visible light irradiation (using 24 watt compact fluorescent lamp) under neat conditions exhibited a promising result for reductive amination of **3** with **4a**: 2-methyl-1-phenyl-pyrrolidine **5a** was obtained in 94% yield (Table 1, entry 1).

**Table 1** Optimization for the reductive amination of ethyl levulinate **3** with aniline **4a**<sup>[a]</sup>



Entry	[Fe] (mol%)	Silane (equiv.)	Conv. (%) <sup>[b]</sup>	Yield (%) <sup>[b]</sup>		
				5a	6a	7
1	<b>1</b> (5.0)	PhSiH <sub>3</sub> (4)	99	94	0	0
2	<b>1</b> (5.0)	Ph <sub>2</sub> SiH <sub>2</sub> (6)	99	0	46	47
3	<b>1</b> (5.0)	Et <sub>3</sub> SiH (12)	99	0	0	0
4 <sup>[c]</sup>	<b>1</b> (5.0)	PhSiH <sub>3</sub> (4)	99	37	21	17
5	<b>1</b> (5.0)	PhSiH <sub>3</sub> (2)	99	50	27	23
6	<b>1</b> (5.0)	PhSiH <sub>3</sub> (1)	99	27	29	28
7 <sup>[d]</sup>	<b>1</b> (5.0)	PhSiH <sub>3</sub> (4)	99	32	35	11
8	<b>2</b> (5.0)	PhSiH <sub>3</sub> (4)	99	90	0	6
9	<b>2</b> (2.5)	PhSiH <sub>3</sub> (4)	99	99	0	0
10	<b>2</b> (1.0)	PhSiH <sub>3</sub> (4)	99	92	0	2
11	<b>2</b> (2.5)	PhSiH <sub>3</sub> (2)	99	75	0	13
12 <sup>[d]</sup>	<b>2</b> (2.5)	PhSiH <sub>3</sub> (4)	89	13	19	0

<sup>[a]</sup> Conditions: **1** or **2** (1.0-5.0 mol%), **3** (0.25 mmol), **4a** (0.25 mmol) and silane, visible light irradiation (24 watt compact fluorescent lamp), 100 °C, 20 h; then hydrolysis (THF/NaOH 2 N).

<sup>[b]</sup> Conversion and yield determined by <sup>1</sup>H NMR of the crude mixture. The condensation imine product from **3** and **2a** was also detected.

<sup>[c]</sup> Reaction performed at 60 °C.

<sup>[d]</sup> Reaction conducted in the absence of visible light irradiation.

The nature of the silanes was also crucial for the selectivity of the reaction. While TMDS (1,1,3,3- tetramethyldisiloxane, 6 equiv.) and PMHS (polymethylhydrosiloxane, 12 equiv.)

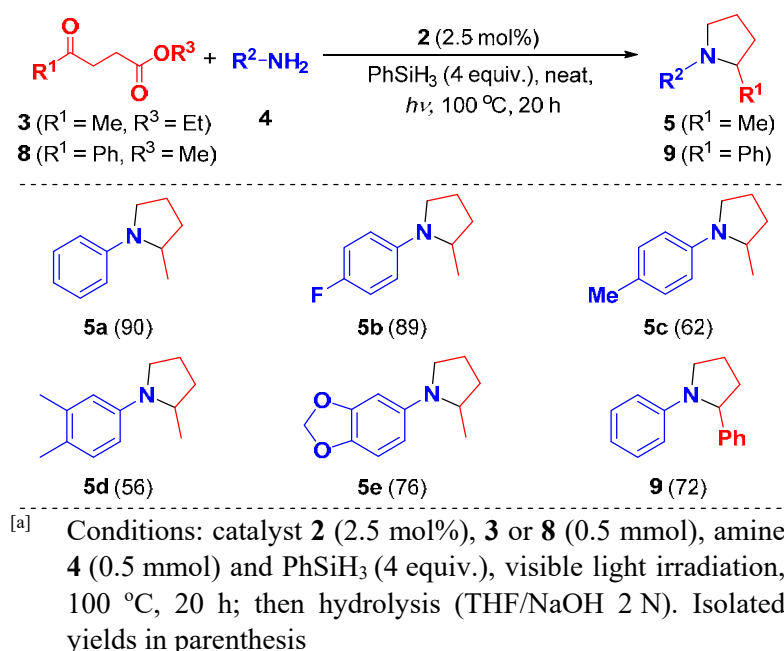
were totally inactive, diphenylsilane (6 equiv.) led to a mixture of pyrrolidinone (**6a**, 46%) and GVL (**7**, 47%) (Table 1, entry 2). Using 12 equiv. of Et<sub>3</sub>SiH led only to the condensation imine product generated from **3** and **4a** (Table 1, entry 3). Decreasing the temperature to 60 °C or the amount of PhSiH<sub>3</sub> led to a deteriorative selectivity (entries 4-6) as **5a** was obtained in mixture with **6a** and **7**.

Compared to **1**, **2** exhibited a better activity. Indeed, at lower catalyst loading of **2** (2.5 mol% and even at 1.0 mol%), excellent yields of **5a**, 99 and 92%, respectively, were achieved (entries 8-10). Furthermore, lowering the PhSiH<sub>3</sub> amount to 2 equiv. led to a mixture of **5a** and **7**. Noticeably, the catalytic reaction performed in the absence of visible light irradiation led to unsatisfactory selectivity under catalysis of **1** or **2** (entries 7 and 12). In absence of catalyst, no reduction reaction occurs, as only the condensation imine product from **3** and **4a** was detected.

### 1.2.2. Scope for reductive amination of levulinates into pyrrolidines

The substrate scope for the catalyzed reductive amination of levulinate into pyrrolidines was then explored using 2.5 mol% of **2** in the presence of 4 equiv. of phenylsilane in solvent-free conditions at 100 °C for 20 h (Table 2).

**Table 2.** Scope of reductive amination of levulinates into pyrrolidines catalyzed by complex **2**.<sup>[a]</sup>



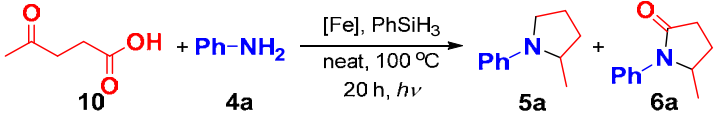
Aromatic amines bearing substituents such as methyl, methoxy or fluoro **4b-4d**, as well as aniline **4a**, were smoothly converted into corresponding pyrrolidines in moderate to good isolated yields (56-90%). Notably, important building blocks for pharmaceuticals such as

5-amino-1,3-benzodioxole was effectively transformed to **5e** in 76%. Additionally, methyl 3-benzoylpropanoate **8** can be also transformed into 1,2-diphenylpyrrolidine **9** in 72% yield.

### 1.2.3. Optimization of reaction conditions for reductive amination of levulinic acid

The direct transformation of levulinic acid to pyrrolidines and pyrrolidinones is also another interesting target. The feasibility of the catalytic reductive amination of levulinic acid with aniline **4a** was conducted with the catalyst **1** (5.0 mol%) under similar conditions: 4 equiv. of PhSiH<sub>3</sub>, 100 °C, 24 h upon visible light irradiation. Levulinic acid **10** was quantitatively converted to a mixture with pyrrolidinone **6a** as the major product (**5a**:**6a** = 28:72, Table 3, entry 1). Increasing the quantity of PhSiH<sub>3</sub> to 6 equiv. gave a 7:3 mixture of **5a** and **6a** (entry 2). Noticeably, lowering the amount of PhSiH<sub>3</sub> to 2 equiv. led to a remarkable improvement in selectivity as **6a** was obtained specifically with 99% yield (entry 3).

**Table 3.** Optimization for reductive amination of levulinic acid.**10**<sup>[a]</sup>



Entry	[Fe] (mol%)	PhSiH <sub>3</sub> (equiv.)	Conv. (%) <sup>[b]</sup>	Yield (%) <sup>[b]</sup>	
				<b>5a</b>	<b>6a</b>
1	<b>1</b> (5.0)	4	99	28	72
2	<b>1</b> (5.0)	6	99	69	31
3	<b>1</b> (5.0)	2	99	0	99
4	<b>1</b> (2.5)	4	99	18	82
5	<b>2</b> (5.0)	5	99	90	9
6	<b>2</b> (5.0)	6	99	99	0
7	<b>2</b> (2.5)	6	99	72	27
8	<b>2</b> (5.0)	2	82	0	80
9	<b>2</b> (2.5)	2	80	0	75

<sup>[a]</sup> Conditions: **1** or **2** (2.5-5.0 mol%), **10** (0.25 mmol), **2a** (0.25 mmol) and PhSiH<sub>3</sub> (2-6 equiv.), visible light irradiation, 100 °C, 20 h; then hydrolysis (THF/NaOH 2 N).

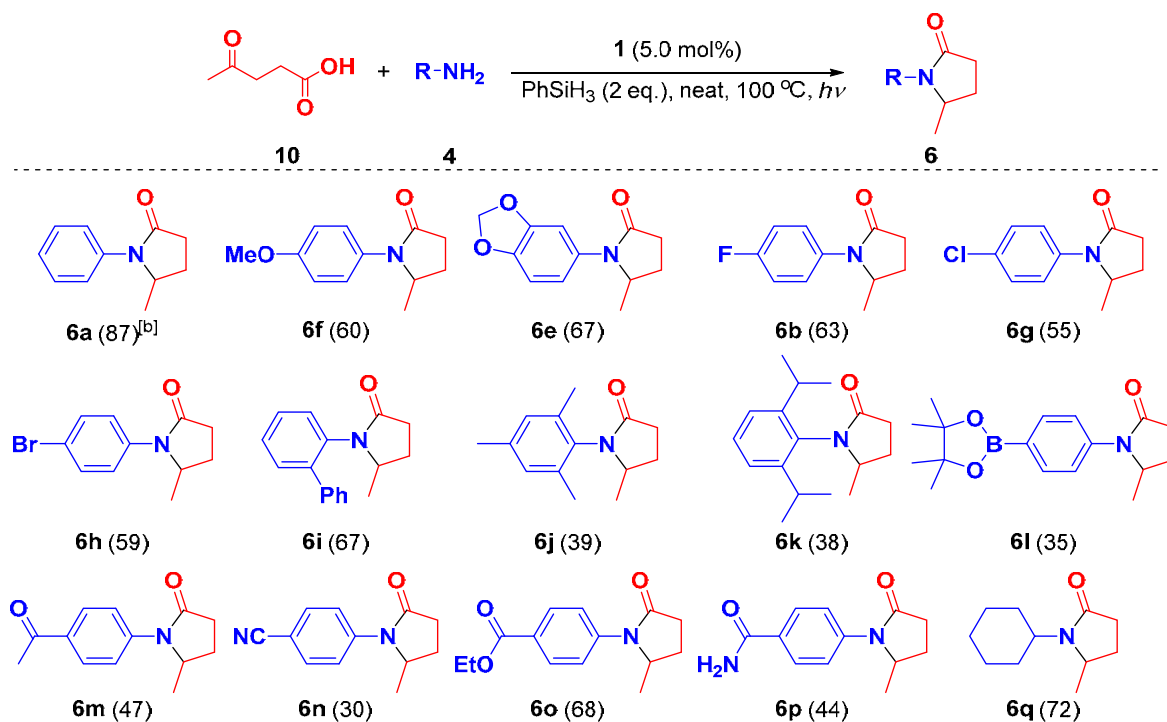
<sup>[b]</sup> Conversion and yield determined by <sup>1</sup>H NMR of the crude mixture. GVL **7** was not observed under these conditions.

The use of **2** as the catalyst permitted to switch the selectivity of the reaction. Indeed, using 5.0 mol% of **2** led to **5a** as the sole product (99%) when the reaction was conducted with 6 equiv. of PhSiH<sub>3</sub> (Table 3, entry 6). Further lowering the catalyst loading of **1** or **2** from 5.0 to 2.5 mol% result in the drop of the selectivity with mixtures of **5a** and **6a** (entries 4 and 7). Furthermore, with 2 equiv. of PhSiH<sub>3</sub>, **6a** can be formed in lower yield 80% and 75% with 5% and 2.5% of **2** respectively (Table 3, entry 8, 9). Similarly, to methyl levulinate, the reaction did not proceed using 6 equiv. of TMDS or PMHS.

### 1.2.4. Scope for reductive amination of levulinic acid into pyrrolidinones

We then explored the substrates scope in regard of levulinic acid. To prepare pyrrolidinones **6**, a variety of anilines **4** were employed for the annulation of levulinic acid catalyzed by **1** (5.0 mol%), with PhSiH<sub>3</sub> (2 equiv.) at 100 °C under visible light irradiation (Table 4).

**Table 4.** Scope of reductive amination of levulinic acid into pyrrolidinones catalyzed by complex **1**.<sup>[a]</sup>



<sup>[a]</sup> Conditions: **1** (5.0 mol%), **10** (0.5 mmol), **4** (0.5 mmol) and PhSiH<sub>3</sub> (2 equiv.), visible light irradiation, 100 °C, 20 h; then hydrolysis (THF/NaOH 2 N). Isolated yields in parenthesis.

<sup>[b]</sup> 84% isolated yield on gram scale (10 mmol) reaction.

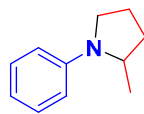
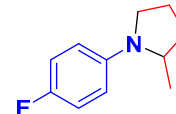
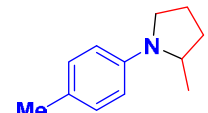
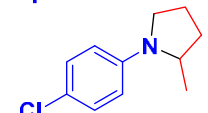
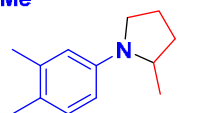
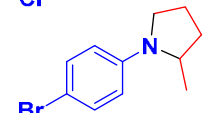
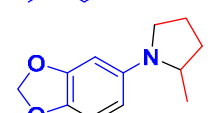
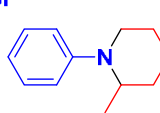
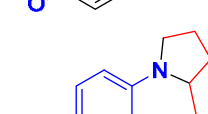
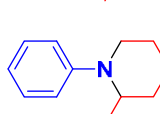
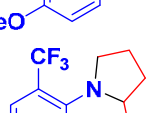
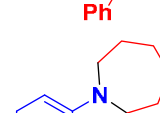
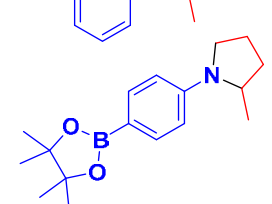
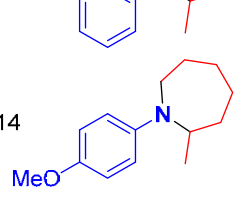
The reactions of aniline **4a**, 3,4-(methylenedioxy) aniline **4e** as well as 4-methoxyaniline **4f** afforded the corresponding *N*-arylpyrrolidinones **6a**, **6e** and **6f** in 60–87% yields. Notably, anilines bearing reducible functional group such as halogen substituents, boronate ester, acetyl, cyano, carboxylic ester and primary amide also provided the corresponding products **6b**, **6g–h**, **6l–6p** in 30–68% yields, highlighting the good group tolerance of the transformation. Noticeably, the reaction can be performed with hindered amines leading to the pyrrolidinones **6i–6k** in moderate yields up to 67%. Indeed, alkylamines such as cyclohexylamine can be used giving the pyrrolidinone **6q** in 72% yield (Table 4).

### 1.2.5. Scope for reductive amination of keto acids into cyclic amines

On the other hand, the reaction scope can be extended to pyrrolidines **5** using **2** (5.0 mol%) as the catalyst: indeed, the reaction of various keto acids with amines to give cyclic amines were

performed in the presence of PhSiH<sub>3</sub> (6 equiv.) at 100 °C for 20 h under visible light irradiation (Table 5).

**Table 5.** Scope of reductive amination of keto acids into cyclic amines catalyzed by complex **2**.<sup>[a]</sup>

$  \begin{array}{c}  \text{R}^1-\text{C}(=\text{O})-\text{CH}_2-\text{CH}_2-\text{C}(=\text{O})\text{OH} + \text{R}-\text{NH}_2 \xrightarrow[\text{PhSiH}_3 (6 \text{ eq.}), \text{ neat}, 100^\circ\text{C}, h\nu]{\text{2 (5.0 mol\%)}} \\  \text{10 (n = 1, R}^1 = \text{Me)} \quad \text{4} \qquad \qquad \qquad \text{5 (n = 1, R}^1 = \text{Me)} \\  \text{11 (n = 2, R}^1 = \text{Me)} \qquad \qquad \qquad \text{12 (n = 2, R}^1 = \text{Me)} \\  \text{13 (n = 2, R}^1 = \text{Ph)} \qquad \qquad \qquad \text{14 (n = 2, R}^1 = \text{Ph)} \\  \text{15 (n = 3, R}^1 = \text{Me)} \qquad \qquad \qquad \text{16 (n = 3, R}^1 = \text{Me)}  \end{array}  $					
Entry	Product	(Yield, %)	Entry	Product	(Yield, %)
1		<b>5a</b> (91) <sup>[b]</sup>	8		<b>5b</b> (86)
2		<b>5c</b> (73)	9		<b>5g</b> (93)
3		<b>5d</b> (62)	10		<b>5h</b> (84)
4		<b>5e</b> (80)	11		<b>12</b> (89)
5		<b>5f</b> (92)	12		<b>14</b> (83)
6		<b>5r</b> (89)	13		<b>16a</b> (92)
7		<b>3l</b> (90)	14		<b>16f</b> (90)

<sup>[a]</sup> Conditions: **2** (5.0 mol%), **10**, **11**, **13** or **15** (0.5 mmol), **4** (0.5 mmol) and PhSiH<sub>3</sub> (4 equiv.), visible light irradiation, 100 °C, 20 h; then hydrolysis (THF/NaOH 2 N). Isolated yields in parenthesis.

<sup>[b]</sup> 89% isolated yield on gram scale (10 mmol) reaction.

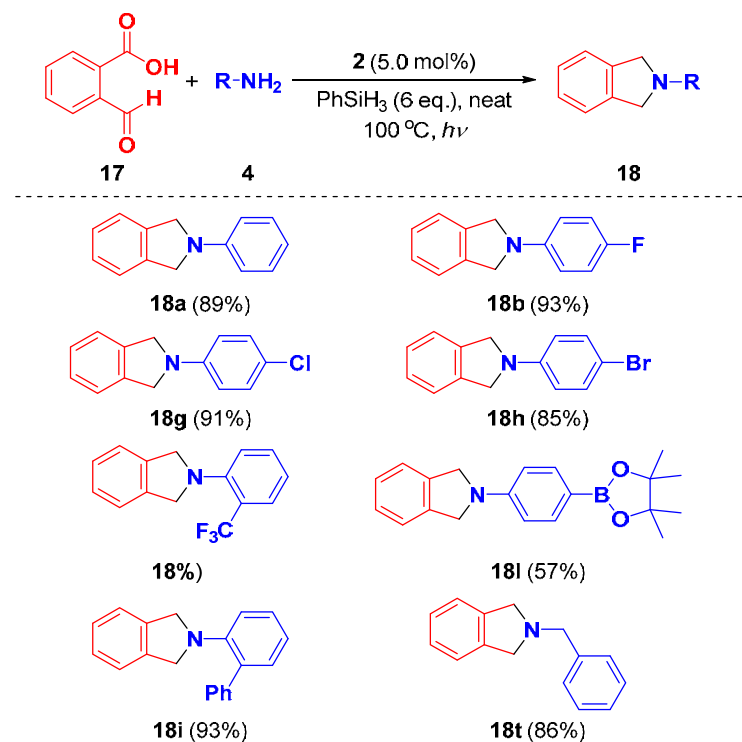
Interestingly, by reaction with levulinic acid, aniline **4a**, methyl-substituted anilines **4c-4d**, 3,4-(methylenedioxy)aniline **4e**, as well as 4-methoxyaniline **4f** afforded the corresponding pyrrolidines **5a**, **5c-f** in 62%-92% yields. Notably, the boronate ester **4l** and trifluoromethyl **4r** substituted anilines led also to **5l** and **5r** in 90% and 89% yields, respectively. Additionally, halogen-containing anilines **4b**, **4g-4h** were converted to the corresponding pyrrolidines **5b**,



**5g-5h** in yields up to 93% (Table 5, entries 8-10). Even if the reaction showed a broad functional group tolerance including reducible functional groups, no reaction occurred with 4-nitroaniline. It must be underlined that this methodology can be extended to the synthesis of cyclic amines like piperidines **12**, **14** and azepane (**16a** and **16f**) which can be obtained efficiently by reaction of anilines with 1,5- or 1,6-keto acids with yields up to 92%.

### 1.2.6. Scope for reductive amination of 2-formylbenzoic acid into isoindolines

**Table 6.** Scope of reductive amination of **17** into isoindolines catalyzed by complex **2**.<sup>[a]</sup>

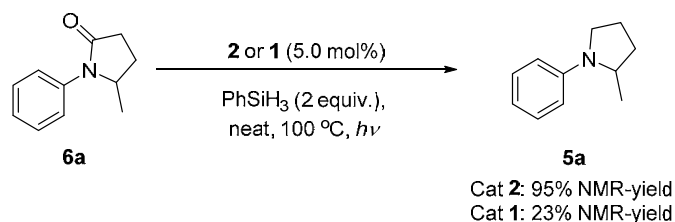


<sup>[a]</sup> Conditions: **2** (5.0 mol%), **17** (0.5 mmol), **4** (0.5 mmol) and PhSiH<sub>3</sub> (6 equiv.) visible light irradiation, 100 °C, 24 h; then hydrolysis (THF/NaOH 2 N). Isolated yields in parenthesis.

In order to show the generality of the catalyzed transformation, the use of 2-formylbenzoic acid **17** rather than keto acids for this transformation was next investigated under similar conditions (Scheme 5). Several *N*-arylisoinidoline derivatives **18** were then synthesized starting from anilines bearing halogen atoms **4b**, **4g-4h**, trifluoromethyl **4r**, boronate ester **4l**, as well as *o*-phenyl group **4i** (57-93% isolated yields). Notably, under similar conditions, benzylamine **4t** gave also the 2-benzylisoinidoline **18t** in a good yield (86%). It is particularly worth mentioning that this methodology permitted to tolerate halogen and boronate ester functionality and the corresponding products could be applied for further elaboration of complex molecules *via* catalyzed cross-coupling reactions.

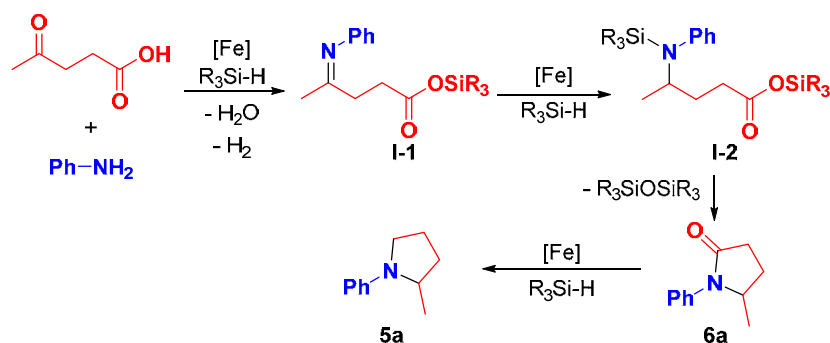
### 1.3. Mechanistic studies

In order to have evidences of the pathway of the transformation, the reduction of pyrrolidinone **6a** with 2 equiv. of PhSiH<sub>3</sub> was then carried out in the presence of [Fe(CO)<sub>4</sub>(*IMes*)] **2** (5.0 mol%) at 100 °C for 20 h upon visible light irradiation: the 2-methyl-1-phenylpyrrolidine **5a** was then obtained in 95% NMR-yield (Scheme 5). This result indicates that in the reaction process of aniline with levulinic acid, the resulting pyrrolidinone **6a** could be further converted into pyrrolidine **5a** catalyzed by **2** under similar reductive conditions.



**Scheme 5.** Iron-catalyzed reduction of pyrrolidinone **6a** to pyrrolidine **5a**

In a mechanism point of view, based on the previous reaction pathway proposed with indium,<sup>[8a]</sup> an imine intermediate **I-1** could be firstly generated from the condensation of levulinic acid with amine and dehydrogenative silylation of carboxylic acid with hydrosilanes. (Scheme 6) Then the imine moiety of **I-1** was reduced under catalytic hydrosilylation conditions leading to silylamine species **I-2**<sup>[26, 30]</sup> which underwent transamidation generating **6a** (Scheme 6). Finally, **6a** could be further reduced into **5a** under catalytic hydrosilylation conditions.<sup>[28, 31]</sup>



**Scheme 6.** Proposed reaction pathway.

### 1.4. Conclusion

In summary, in this paragraph, a switchable and efficient iron catalyzed synthesis of *N*-substituted pyrrolidinones and pyrrolidines starting from renewable sources such as levulinic acid and esters and a variety of amines, was described *via* a reductive amination using phenylsilane as the reducing agent. It must be underlined that two well-defined NHC iron complexes were employed, each of them being able to conduct specifically to a single

derivative: pyrrolidones or pyrrolidines. Interestingly, using similar conditions, cyclic amines such as piperidines and azepanes were efficiently prepared by reaction of anilines with 1,5- or 1,6-keto acids, respectively. Additionally, this methodology can be applied for the preparation of isoindolines starting from 2-formylbenzoic acid.

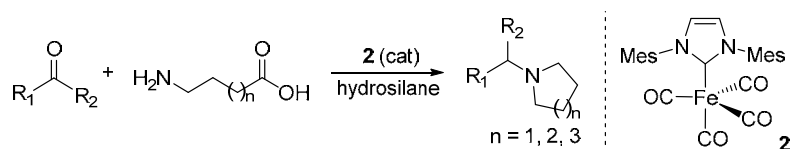
### III-2 Reductive amination of carbonyl derivatives with $\omega$ -amino fatty acids catalyzed by $\text{Fe}(\text{CO})_4(\text{IMes})$

**Contributions in this part:** Optimization and scope: Duo Wei, Chakkrit Netkaew, Victor Carré; Mechanistic studies: Duo Wei, Chakkrit Netkaew.

**Publication:** D. Wei, C. Netkaew, V. Carré, C. Darcel, *ChemSusChem* **2019**, 12, 3008-3012.

#### 2.1. Introduction

In III-1-1, we have already described an iron-catalyzed reductive amination of keto-acids such as levulinic acid, 1,5- and 1,6-keto acids leading to cyclic amines such as pyrrolidines, piperidines and azepanes, respectively, under hydrosilylation conditions.<sup>[32]</sup> From a sustainable organic synthesis point of view, iron-catalyzed reductive amination of aldehydes and ketones with  $\omega$ -amino fatty acids should be another attractive method to prepare *N*-substituted cyclic amine derivatives in one step (Scheme 7). Indeed,  $\omega$ -amino fatty acids are widely present in plants and animal species: as a representative example, 4-aminobutanoic acid (GABA) is the chief inhibitory neurotransmitter in the mammalian central nervous system and GABA is also sold as a dietary supplement.<sup>[33]</sup> Furthermore, 5-aminopentanoic acid is a normal metabolite present in human saliva, with a tendency to elevated concentration in patients with chronic periodontitis,<sup>[34]</sup> and 6-aminohexanoic acid is effective in treatment of certain bleeding disorders (for instance postoperative bleeding), marketed as Amicar.<sup>[35]</sup>



**Scheme 7.** Iron-catalyzed reductive amination of carbonyl derivatives with  $\omega$ -amino fatty acids. This paragraph will be dedicated to an iron-catalyzed efficient and selective one-pot preparation of *N*-substituted cyclic amines (including pyrrolidines, piperidines and azepanes) *via* reductive amination of carbonyl derivatives with  $\omega$ -amino fatty acids by hydrosilylation (Scheme 7).

## 2.2. Results and discussions

### 2.2.1. Optimization of reaction conditions

We thus began our initial optimization work with benzaldehyde **18a**, 5-aminopentanoic acid **19** and phenylsilane in toluene, in the presence of **2** as the catalyst. The preliminary experiment using 5.0 mol% of **2** associated to 4 equiv. of PhSiH<sub>3</sub> at 100 °C upon visible light irradiation (using 24 watt compact fluorescent lamp) showed an interesting result for reductive amination of **18a** and **19**: thus, *N*-benzylpiperidine **20a** was produced in 96% yield (Table 7, entry 1) with only trace amounts of benzyl alcohol **22** (3%) resulting from the reduction of the benzaldehyde, underlining the remarkable selectivity with respect to **18a**.

**Table 7.** Optimization of the reaction parameters.<sup>[a]</sup>

Entry	Catalyst [mol%]	Silane [equiv.]	T [°C]	Conv. [%]	Yield [%]		
					20a	21	22
1	<b>2</b> [5.0]	PhSiH <sub>3</sub> [4]	100	99	96	0	3
2	<b>2</b> [5.0]	Ph <sub>2</sub> SiH <sub>2</sub> [6]	100	99	0	59	40
3	<b>2</b> [5.0]	TMDS [6]	100	0	-	-	-
4	<b>2</b> [5.0]	PMHS [12]	100	0	-	-	-
5 <sup>[b]</sup>	<b>2</b> [5.0]	PhSiH <sub>3</sub> [4]	100	98	67	31	0
6 <sup>[c]</sup>	<b>2</b> [5.0]	PhSiH <sub>3</sub> [4]	100	99	87	12	0
7	<b>2</b> [5.0]	PhSiH <sub>3</sub> [4]	80	97	47	50	0
8	<b>2</b> [5.0]	PhSiH <sub>3</sub> [4]	50	97	32	65	0
9	<b>2</b> [5.0]	PhSiH <sub>3</sub> [4]	30	96	7	25	64
10	<b>2</b> [5.0]	PhSiH <sub>3</sub> [5]	100	99	84	1	14
11	<b>2</b> [5.0]	PhSiH <sub>3</sub> [3]	100	99	30	69	0
12	<b>2</b> [5.0]	PhSiH <sub>3</sub> [2]	100	95	20	71	4
13	<b>2</b> [2.5]	PhSiH <sub>3</sub> [4]	100	86	71	13	2
14	Fe(CO) <sub>5</sub> [5.0]	PhSiH <sub>3</sub> [4]	100	99	40	0	59
15	Fe <sub>3</sub> (CO) <sub>12</sub> [5.0]	PhSiH <sub>3</sub> [4]	100	99	-	-	99

<sup>[a]</sup> General reaction conditions: **2** (5.0 mol%), **19** (0.5 mmol), **18a** (0.5 mmol), PhSiH<sub>3</sub> and toluene (0.5 mL), visible light irradiation (using 24 watt compact fluorescent lamp), 100 °C, 20 h; then hydrolysis (THF/NaOH 2 N). The conversions and yields were determined by <sup>1</sup>H NMR spectroscopy.

<sup>[b]</sup> neat condition.

<sup>[c]</sup> In the absence of visible light irradiation.

Afterwards, different hydrosilanes were evaluated in order to study the selectivity of the reaction. Using diphenylsilane (6 equiv.) led to a mixture of 1-benzylpiperidin-2-one (**21**, 59%) and benzyl alcohol (**22**, 40%) with no expected piperidine **20a**, entry 2). By contrast, with TMDS (6 equiv.) and PMHS (12 equiv.) no reaction occurred (entries 3 and 4). The absence of toluene or visible light irradiation resulted in deteriorative selectivity (entries 5 and 6) as

**20a** was obtained in mixture with **21**. Decreasing the temperature to 80 or 50 °C led to a mixture of **20a** and **21** with **21** as the major product (50% and 65%, respectively, entries 7 and 8). Nevertheless, when the reaction was conducted at 30 °C, even if the conversion reached 96%, benzyl alcohol **22** was the major product (64%, entry 9). The quantity of hydrosilanes has also a crucial effect on the selectivity; indeed, increasing the amount of phenylsilane to 5 equiv. or decreasing to 3 or 2 equiv. lowered the selectivity of the reaction (entries 10-12 vs 1). Finally, with a lower catalyst loading of **2** (2.5 mol%), a lower conversion (86%) was obtained, with **20a** being the major product (71%, entry 13). Additionally, using Fe(CO)<sub>5</sub> or Fe<sub>3</sub>(CO)<sub>12</sub> under the optimized conditions, even if full conversions were observed, benzyl alcohol resulting from the reduction of benzaldehyde was the major product obtained (59 and 99% respectively), showing the crucial role of the IMes ligand for the selectivity of the reaction (Table 7, Entries 14 and 15).

It must be also mentioned that this transformation using the catalyst **2** (5.0 mol%) at 100°C for 20 h, under hydrogenation conditions (2 bar of H<sub>2</sub> under visible light irradiation or 50 bar of H<sub>2</sub> in an autoclave in the absence of light irradiation) or hydrogen transfer conditions (4 equiv. of HCO<sub>2</sub>H / 2 equiv. of NEt<sub>3</sub>) did not succeed, as no conversion of benzaldehyde **18a** was detected.

**Table 8.** Control experiments in iron-free catalytic conditions.<sup>[a]</sup>

Entry	PhSiH <sub>3</sub> [equiv.]	T [°C]	Time [h]	Conv. [%] <sup>a</sup>	Yields [%] <sup>a</sup>		
					20a	21	22
1	5.0	100	3	95	0	99	0
2	4.0	100	3	66	0	99	0
3	2.0	50	4	82	0	97	3
4	2.0	30	4	78	0	93	7

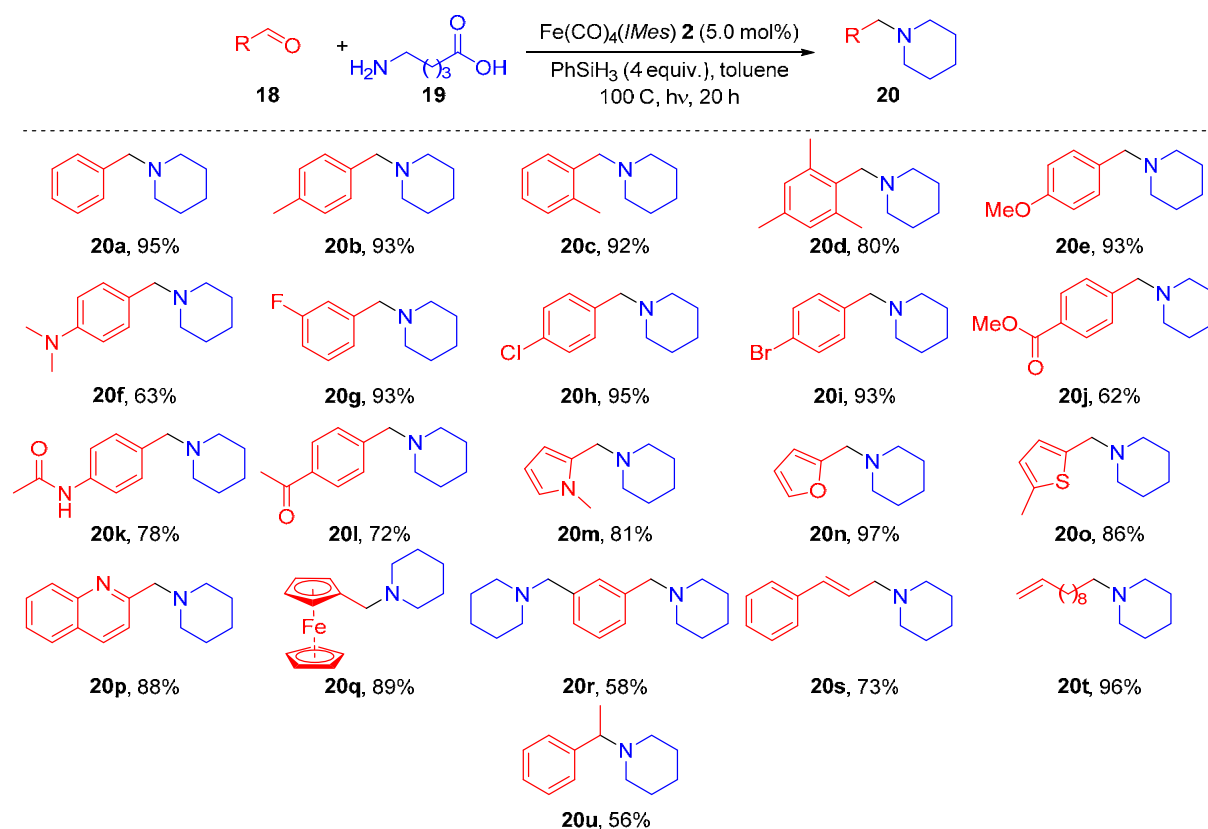
<sup>[a]</sup> General reaction conditions: **19** (0.5 mmol), **18a** (0.5 mmol), PhSiH<sub>3</sub> and toluene (0.5 mL); then hydrolysis (THF/NaOH 2 N). The conversions and yields were determined by <sup>1</sup>H NMR spectroscopy.

It must be underlined that in the absence of iron catalyst, the piperidinone **21** can be detected in quantitative yield using 5, 4 or 2 equiv. of phenylsilane at 100, 50 or 30 °C in 4 h. Noticeably, the piperidine **20a** was not detected (Table 8). More detailed experiments were performed and explained in the mechanistic studies (Schemes 9 and 10).

### 2.2.2. Scope for the preparation of piperidines

With our optimized conditions in hand (5.0 mol% of **2**, 4 equiv. of PhSiH<sub>3</sub>, toluene, 100 °C, 20 h, visible light irradiation, Table 7, entry 1), we then explored the substrate scope and limitation for the catalyzed reductive amination of carbonyl derivatives with  $\omega$ -amino fatty acids into *N*-substituted cyclic amines (Tables 9, 10 and 11). Benzaldehyde, *o*- and *p*-tolualdehyde were smoothly converted into the corresponding *N*-substituted piperidines isolated in 92-95% yields (**20a-20c**, Table 9). Starting from the more hindered mesitaldehyde, the corresponding product **20d** was isolated in good yield (80%), showing that the steric hinderance did not inhibit the reactivity. The reactions of *p*-methoxy or *p*-*N,N*-dimethylamino benzaldehyde afforded the corresponding piperidines **20e-20f** in 93 and 63% yields, respectively.

**Table 9.** Scope of the synthesis of piperidines by reductive amination of carbonyl derivatives with 5-aminopentanoic acid **19**.<sup>[a]</sup>



<sup>[a]</sup> General reaction conditions: **2** (5.0 mol%), **19** (0.5 mmol), **18** (0.5 mmol), PhSiH<sub>3</sub> (4 equiv.) and toluene (0.5 mL), visible light irradiation, 100 °C, 20 h; then hydrolysis (THF/NaOH 2 N). Isolated yields of **20** are shown.

The reaction also tolerated halides (chloro, bromo and fluoro) giving **20g-20i** in 93-95% yields. Importantly, piperidines bearing reducible functional groups such as carboxylic ester (**20j**) and amide (**20k**), were prepared in 62% and 78% yields, respectively highlighting the good group

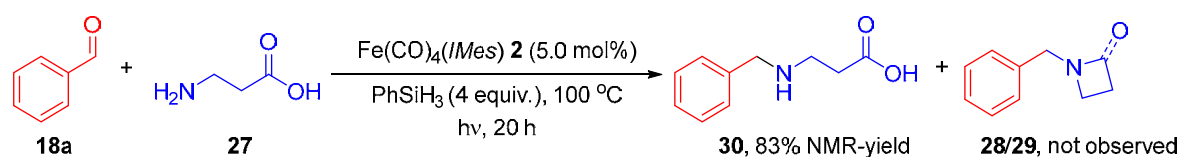






In order to show the generality of this cyclic amine preparation, 4-aminobutanoic acid (**25**, GABA) was employed with different aldehydes to prepare pyrrolidines **26** as shown in Table 11. Thus, *p*-fluorobenzaldehyde furnished **26a** in 93% yield. Heteroaromatic aldehydes containing quinoline, thiophene and furan groups can be effectively transformed to **26b-26d** in good yields (87-90%). Similar to piperidine **20t** and azepane **24h**, pyrrolidine **26e** was prepared in 95% yield starting from 10-undecenal and **25**, again without alteration of the remoted C=C bond.

Even though this method is quite general for the synthesis of 5, 6 and 7 membered cyclic amines, in a similar fashion, the reaction of  $\beta$ -alanine (3-aminopropanoic acid) **27** with benzaldehyde **18a** under the optimized conditions in the presence of 5.0 mol% of **2**, did not furnish the desired azetidine product **28** (or even the corresponding *N*-benzyl- $\beta$ -lactam **29**). Indeed, the 3-(*N*-benzylamino)propanoic acid **30** was the sole product obtained with 83% NMR-yield. It resulted from the simple reductive amination of  $\beta$ -alanine with benzaldehyde, showing that the transamidation leading to the 4-membered ring is the limiting step of the reaction (Scheme 8).



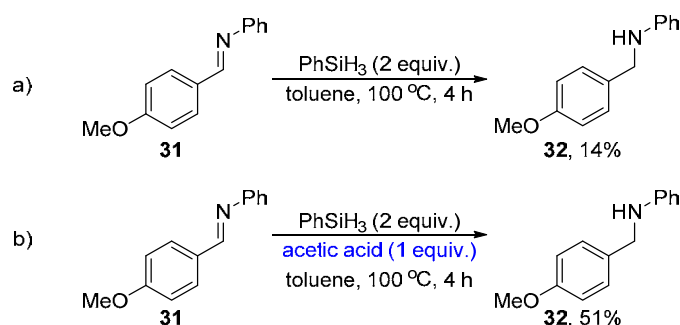
**Scheme 8.** Reductive amination of  $\beta$ -alanine with benzaldehyde.

### 2.3. Mechanistic insights

Summarising the results described above, 5-, 6- and 7-membered cyclic amines can be efficiently formed *via* an iron catalyzed hydrosilylation of  $\omega$ -amino fatty acids in the presence of aldehydes. Importantly, it was shown that the first steps of the transformation generating specifically piperidinone **20** (*i.e.* (i) imine formation, (ii) its reduction then (iii) transamidation) can be performed in the absence of iron catalyst, as shown for the reaction of benzaldehyde with 5-aminopentanoic acid **19** leading quite exclusively to the piperidinone **21** with only trace amount of benzyl alcohol **22** and no piperidine **20a**, whatever the quantity of phenylsilane (2-5 equiv.) or the temperature (30-100 °C) (Table 8). Additionally, this transformation seems to be specific to  $\omega$ -amino fatty acids used as with methyl 4-aminobutyric ester, no reduction reaction occurred.

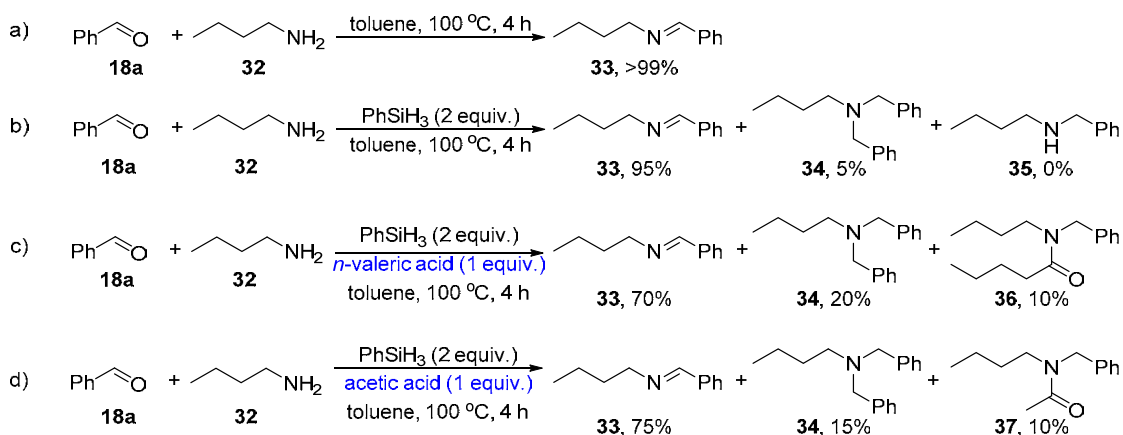
Noticeably, the ability of carboxylic acid to promote the hydrosilylation of aldimines was evaluated. Indeed, carboxylic acid such as acetic acid can promote the hydrosilylation of aldimines: the aldimine **31** can be hydrosilylated leading to the corresponding amine **32**, but in

very low yield (14% NMR-yield) when the reaction was conducted with 2 equiv. phenylsilane in toluene at 100 °C for 4 h (Scheme 9-a). Noticeably, the addition of 1 equiv. of acetic acid permitted to promote the hydrosilylation of the imine **31** in 51% NMR-yield (Scheme 9-b).



**Scheme 9.** Controlled experiments for acetic acid promoted aldimine hydrosilylation.

Furthermore, carboxylic acids also seem to promote the reductive amination of aldehydes with primary amines for the formation of imines in the presence of hydrosilanes (Scheme 10).<sup>[36]</sup> In the case of the reductive amination of benzaldehyde with butylamine, in the absence of any additive, the reaction gave the corresponding aldimine **33** in quantitative yield when conducting in toluene at 100 °C (Scheme 10-a). When the reaction was performed in the presence of 2 equiv. of phenylsilane, the major product obtained still was the aldimine **33** (95%), with trace amounts of the product resulting from a double reductive amination of benzaldehyde (**34**, 5% yield) and no product from the direct reductive amination product **35** (Scheme 10-b).



**Scheme 10.** Controlled experiments for carboxylic acid promoted reductive amination of benzaldehyde.

When *n*-valeric acid or acetic acid (1 equiv.) were used as additives, the aldimine **33** was the major compound (70-75%), but a significant increase of the amount of the product resulting from a double reductive amination of benzaldehyde, **34**, was obtained (15-20%, Scheme 10c-d). In addition, the compound produced by reductive amination of benzaldehyde then

intermolecular amidation with carboxylic acid, **36**, was detected in 10% yield. **36** was generated by (i) reductive amination of benzaldehyde, then (ii) intermolecular amidation with carboxylic acid.

These results seem to prove that the carboxylic moiety of  $\omega$ -amino fatty acids promote the reductive amination of the amino part with the carbonyl derivative under hydrosilylation. By contrast, the reduction of the formed piperidinones with phenylsilane has to be performed in the presence of an iron catalyst.

On another hand, to gain information on the nature of the iron active species, a reductive amination of **18a** with **19** using 5.0 mol% of **2** in the presence of 4 equiv. of PhSiH<sub>3</sub> was conducted in a Young NMR tube at 100 °C under visible light irradiation and the evolution of the reaction was checked by NMR. It is important to underline that the signal of H<sub>2</sub> and Fe-H species were observed at 4.46 ppm and – 9.13 ppm, respectively, after 3 h of reaction at 100 °C (Figures 2 and 3). The shift of the Fe-H signal is very close to the one observed in hydrosilylation of esters.<sup>[18]</sup>

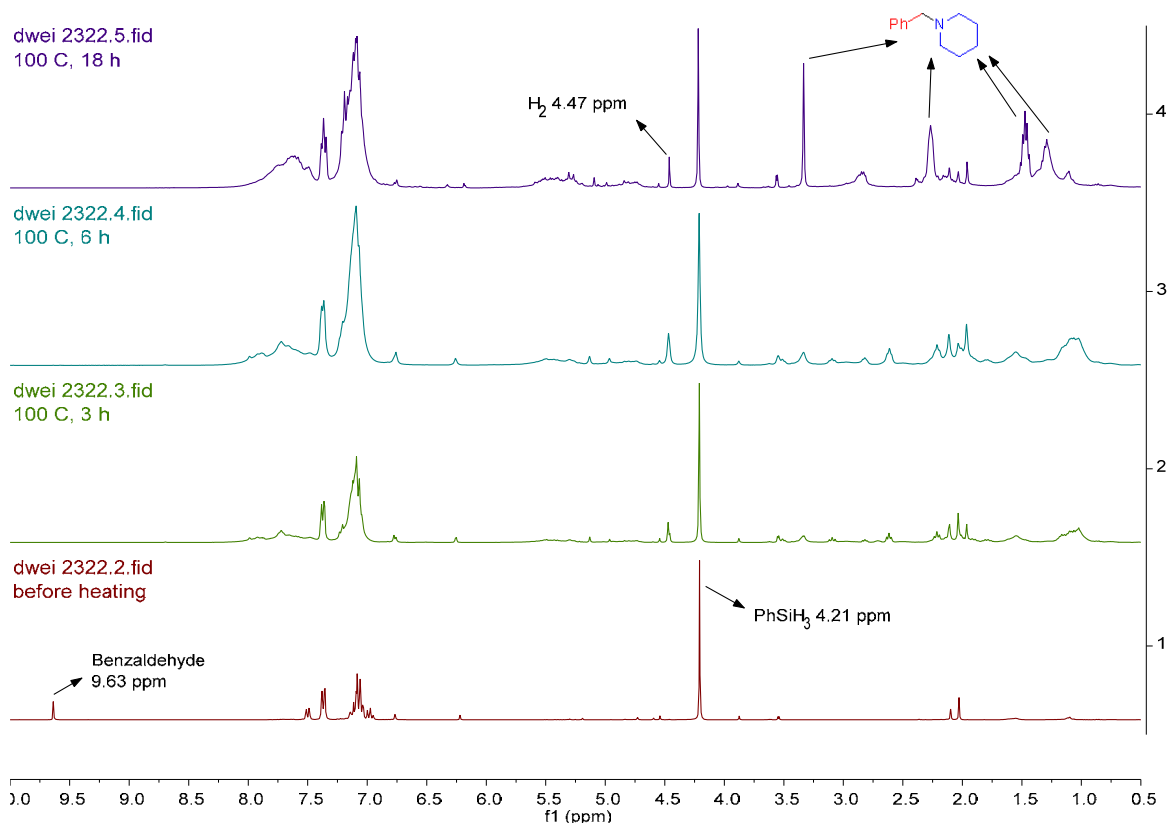


**Figure 2:** <sup>1</sup>H NMR spectrum between 0 and 10 ppm.

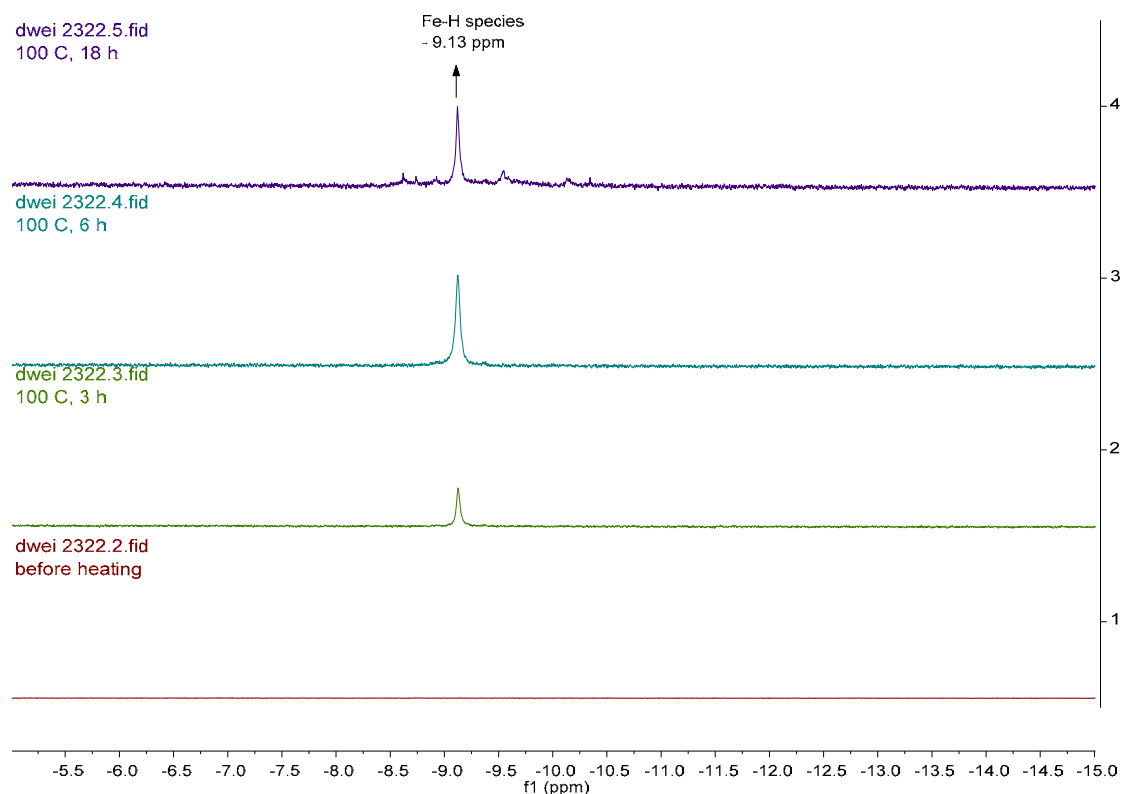
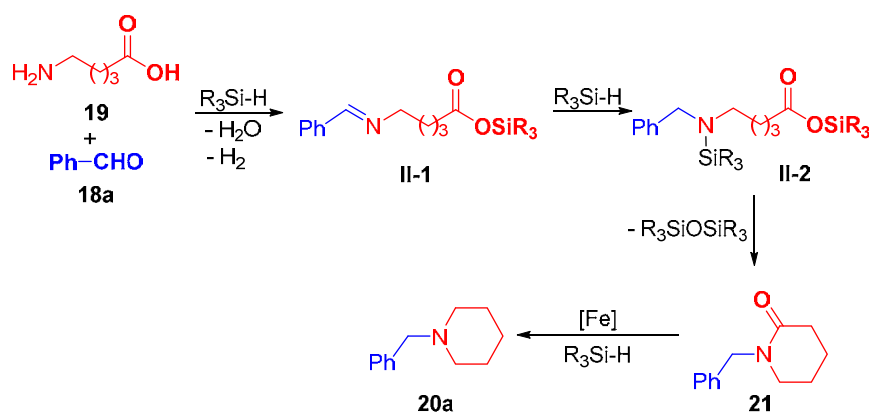


**Figure 3:**  $^1\text{H}$  NMR spectrum in the hydride area.

Based on these observations and on the previous reaction proposed pathways,<sup>[8, 32]</sup> an imine intermediate **II-1** is first produced by condensation of **18a** with **19** and dehydrogenative silylation of the carboxylic acid moiety with phenylsilane, then generating  $\text{H}_2$ . The reduction of the imine moiety of **II-1** under hydrosilylation conditions generated the silylamine intermediate **II-2**, then the piperidinone **21** via intramolecular transamidation (Scheme 11). The final step is an iron-catalyzed reduction of **21** into **20a** under hydrosilylation conditions.<sup>[28, 31, 37]</sup>



**Scheme 11.** Possible reaction pathway.

## 2.4. Conclusion

This paragraph described an unprecedented efficient method for the preparation of *N*-substituted cyclic amines (including pyrrolidines, piperidines and azepanes) starting from  $\omega$ -amino fatty acids and aldehydes or ketones, *via* reductive amination. The reaction proceeds with a notably high functional group tolerance as reducible groups such as carboxylic ester, amide, cyano and even acetyl, are well tolerated. Nevertheless, 4-membered cyclic amines or  $\beta$ -lactams can not be produced starting from  $\beta$ -alanine under these conditions.



### III-3 Hydrosilylation of diacids in the presence of amines catalyzed by $\text{Fe}(\text{CO})_4(\text{IMes})$

**Contributions in this part:** Optimization and scope: Duo Wei, Chakkrit Netkaew.

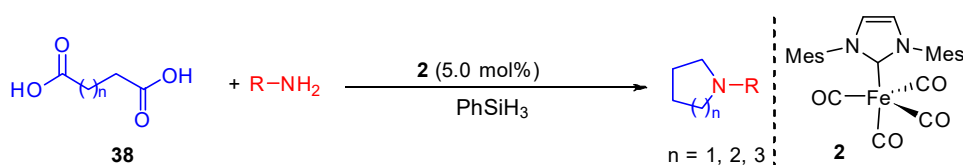
#### 3.1. Introduction

In the two first paragraph of this part, we have described iron-catalyzed access to cyclic amines amines such as pyrrolidines, piperidines and azepanes, *via* reductive amination of keto-acids with amines and of  $\omega$ -amino fatty acids with carbonyl derivatives under hydrosilylation conditions. Over the other alternatives methods involving such iron-catalyzed reductive amination sequences, diols and diacids can be envisaged as starting materials. In this area, significant breakthrough has been made in the development of milder and greener methods for the *N*-heterocyclization of primary amines starting from diols *via* hydrogen borrowing catalyzed with noble metals<sup>[5b, 38]</sup>, base metals<sup>[39]</sup>,  $\gamma\text{-Al}_2\text{O}_3$ <sup>[40]</sup> as well as organic catalysts<sup>[41]</sup>. The advantages of such methodology are clearly the reaction at ambient conditions without generation of harmful by-products (only water as a by-product) even if most of these systems require high reaction temperature.

On the other hand, carboxylic acids can be interesting starting materials for reductive amination. Indeed, an interesting straightforward catalytic *N*-alkylation of amines with carboxylic acids was reported by Beller *et al.* in 2014 using Karstedt's catalyst associated to dppe as a ligand and hydrosilanes as reducing agents under mild reaction conditions.<sup>[42]</sup> Furthermore, dicarboxylic acids are well-known starting materials in the preparation of copolymers such as polyamides and polyesters, including the most widely used adipic acid in the production of Nylon 6-6. Other representative examples of dicarboxylic acids include aspartic acid and glutamic acid, two amino acids in the human body. Even if diacids are also stable and readily available, to the best of our knowledge, the direct reductive amination of diacids with amines yielding *N*-substituted cyclic amines is unknown to date. It must be noticed that the reaction of diesters in the presence of anilines under hydrogenation conditions leading to *N*-aromatic heterocycles catalyzed by ruthenium complex was developed in 2017.<sup>[43]</sup> However harsh reaction conditions (220 °C) was generally required and its scope is limited to aniline.

This third paragraph of this part is dedicated to the first hydrosilylation of diacids in the presence of amines as a novel route to *N*-substituted cyclic amines. (Scheme 12)





**Scheme 12.** Novel route to *N*-substituted cyclic amines *via* iron-catalyzed reductive amination of diacids with amine under hydrosilylation conditions.

## 3.2. Results and discussions

### 3.2.1. Optimization of reaction conditions

In classical organic synthesis, the synthesis of cyclic imides starting from diacids (or from the corresponding cyclic anhydrides) and amine always requires ancillary reagents such as carboxylic acids,<sup>[44]</sup> acid chlorides,<sup>[45]</sup> anhydrides,<sup>[46]</sup> SOCl<sub>2</sub><sup>[47]</sup> or dramatically harsh conditions (such as high temperature up to 330 °C).<sup>[48]</sup>

To find a more sustainable pathway starting from diacids, we began our initial optimization work with glutaric acid **39**, cyclohexylamine **40** and PhSiH<sub>3</sub> (6.0 equiv.) in dimethyl carbonate (DMC), catalyzed by Fe(CO)<sub>4</sub>(*IMes*) **2** (using classical conditions already developed in the previous paragraphs).<sup>[28-29, 32, 49]</sup> After 20 h at 110 °C using 3.0 mol% of **2**, the fully reduced product *N*-cyclohexylpiperidine **20v** was generated in quantitative yield (Table 12, entry 1), notably without production of the other two intermediates *N*-cyclohexylglutarimide **41a** and *N*-cyclohexyl-2-piperidone **42a**. The amount of PhSiH<sub>3</sub> can be decreased to 4.0 equiv. without any loss of activity and selectivity, as **20v** was still obtained quantitatively and exclusively. (Table 12, entry 2) However, the selectivity dropped when decreasing the amount of PhSiH<sub>3</sub> into 2 equiv. or the catalyst loading to 2.5 mol% (Table 12, entries 3 and 4).

**Table 12.** Reductive amination of glutaric acid with cyclohexylamine<sup>[a]</sup>

Entry	Cat. [mol%]	PhSiH <sub>3</sub> [equiv]	T [°C]	Conv. [%] <sup>a</sup>	NMR-yield [%]		
					41a	42a	20v
1	5.0	6	110	>99	0	0	>99
2	<b>5.0</b>	<b>4</b>	<b>110</b>	<b>&gt;99</b>	<b>0</b>	<b>0</b>	<b>&gt;99</b>
3	5.0	2	110	>99	0	40	60
4	2.5	4	90	98	0	4	92

<sup>[a]</sup> General reaction conditions: Fe catalyst **2**, **39** (0.5 mmol), **40** (0.5 mmol), PhSiH<sub>3</sub> and DMC (0.5 mL), visible light irradiation (using 24 watt compact fluorescent lamp), 110 °C, 20 h; then hydrolysis (THF/NaOH 2 N). The conversions and yields were determined by <sup>1</sup>H NMR spectroscopy.

It should be noted that the two steps of reduction of succimide **41a** to pyrrolidinone **42a** and the reduction of pyrrolidinone **42a** to pyrrolidine **20v** were shown to be catalyzed by the catalyst **2** under hydrosilylation conditions.

**Table 13.** Reductive amination of glutaric acid with aniline<sup>[a]</sup>

Reaction scheme: Glutaric acid (**39**) + Aniline (**4a**)  $\xrightarrow[\text{DMC, 110 } ^\circ\text{C, hv, 20 h}]{\text{2, PhSiH}_3}$  Mixture of **41b**, **42b**, and **20w**.

Entry	Cat [mol%]	PhSiH <sub>3</sub> [equiv.]	Additive [mol%]	Conv. [%] <sup>a</sup>	NMR-yield [%] <sup>a</sup>		
					<b>41b</b>	<b>42b</b>	<b>20w</b>
1	5.0	6	-	70	0	0	70
2	5.0	4	-	40	12	4	24
3	5.0	6	Fe(OTf) <sub>2</sub> [10]	83	0	0	83
4	5.0	6	Fe(OTf) <sub>3</sub> [10]	26	26	0	0
5	5.0	6	FeCl <sub>3</sub> [10]	32	32	0	0
6	<b>5.0</b>	<b>6</b>	<b>Fe(OTf)<sub>2</sub> [20]</b>	<b>90</b>	<b>0</b>	<b>0</b>	<b>90</b>
7	5.0	6	Fe(OTf) <sub>2</sub> [30]	84	17	0	67
8	None	None	-	0	0	0	0
9	None	6	-	50	50	0	0
10	5.0	None	-	0	0	0	0

<sup>[a]</sup> General reaction conditions: Fe catalyst **2**, **39** (0.5 mmol), **4a** (0.5 mmol), PhSiH<sub>3</sub> and DMC (0.5 mL), visible light irradiation (using 24 watt compact fluorescent lamp), 110 °C, 20 h; then hydrolysis (THF/NaOH 2 N). The conversions and yields were determined by <sup>1</sup>H NMR spectroscopy.

To evaluate the transformation of diacid with aromatic amines, aniline **4a** was selected as annulation partner instead of cyclohexylamine **40** in the hydrosilylation of glutaric acid **39** (Table 13). When the reaction was performed with 6.0 equiv. of PhSiH<sub>3</sub> under the previous optimized conditions, only 70 % conversion was observed but with an excellent selectivity as 70% yield of the full reduced cyclic amine **20w** was obtained (Table 13, entry 1). Reducing the amount of phenylsilane to 4.0 equiv. led to a mixture of **41b**, **42b** and **20w** with a moderate conversion (40%) (Table 13, entry 2). Interestingly, the addition of a catalytic amount of Lewis acid like 10 mol% of Fe(OTf)<sub>2</sub> in the presence of 6 equiv. of phenylsilane resulted in the increase of both conversion and yield of **20w** (83%, Table 13, entry 3). The use of other Fe Lewis acids such as FeCl<sub>3</sub> or Fe(OTf)<sub>3</sub> gave only partial conversions of **39** into imide **41b** (26 and 32%, respectively, Table 13, entries 4 and 5). Increasing the Fe(OTf)<sub>2</sub> amount to 20 mol% permitted to obtain **20w** in 90% yield, while the use of 30 mol% of Fe(OTf)<sub>2</sub> has a detrimental effect on the reaction as a mixture of **41b** and **20w** was observed in a ratio 17:67 (84% conversion, Table 13, entries 6 and 7). Notably, in the absence of both the Fe catalyst **2** and PhSiH<sub>3</sub>, no product can be produced. Nevertheless, using 6.0 equiv. of PhSiH<sub>3</sub> in the absence of catalyst **2** and Lewis acid 50% of the amidation product **41b** can be detected, indicating that

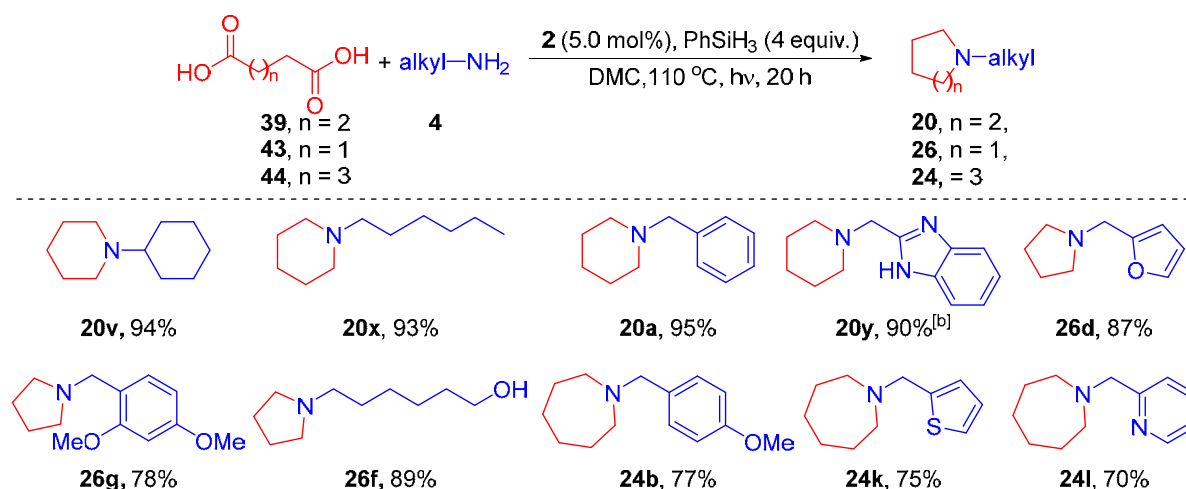
PhSiH<sub>3</sub> promotes the formation of **41b**. Finally, the presence of the catalyst **2** in the absence of silane led to no conversion (Table 13, entries 8-10). The role of the Lewis acid should be to increase the electrophilicity of the carbon of the C=O moiety in order to make the addition of softer nucleophilic aniline more easy.

### 3.2.2. Scope for the preparation of cyclic amines starting from linear diacids

With the optimized conditions found for the condensation of alkylamines and anilines (Table 12, entry 2, and Table 13, entry 6 for anilines, respectively), we then explored the substrate scope for the catalyzed reductive amination of diacids in the presence of various amines (alkylamines, Table 14; anilines, Table 15).

Starting from glutaric acid **39**, various alkylamines such as benzylamine, cyclohexylamine, or 1-hexylamine can be used leading to the corresponding piperidines in very good isolated yields: 89-94% (**20a**, **20v**, and **20x**, Table 14). Additionally, 2-aminomethylbenzimidazole can be used conducting to the corresponding piperidine **20y** in 90% NMR yield.

**Table 14.** Reductive amination of diacids with aliphatic amines <sup>[a]</sup>



<sup>[a]</sup> General reaction conditions: **2** (5.0 mol%), **39**, **43** or **44** (0.5 mmol), amine (0.5 mmol), PhSiH<sub>3</sub> (4 equiv.) and DMC (0.5 mL), visible light irradiation, 110 °C, 20 h; then hydrolysis (THF/NaOH 2 N). Isolated yields of the products are shown.

<sup>[b]</sup> NMR yield.

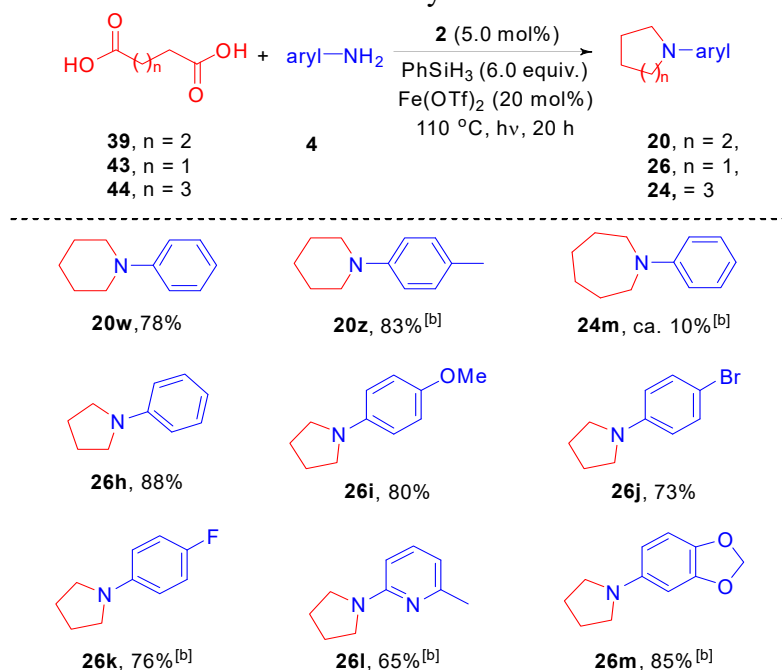
Pyrrolidines **26d** and **26g** can be also efficiently prepared from succinic acid **43** by reaction with the corresponding amines, furfurylamine and 2,4-dimethoxybenzylamine, in 87 and 78% yield, respectively. Remarkably, using an amino-alcohol such as 6-aminohexan-1-ol, a chemoselective transformation occurred as the pyrrolidine **26f** the pending hydroxyl group was produced in 89% yield.

Finally, when starting from adipic acid **44**, azepanes were obtained in good yields when reacting with *p*-methoxybenzylamine, 2-thienylmethylamine and 2-picolylamine (70-77% yields)

To reach good conversions, when working with aniline derivatives, 20 mol% of Fe(OTf)<sub>2</sub> had to be used as an additive. The scope of aromatic amines was thus investigated (Table 15). By reaction of glutaric acid **39** with aniline and 4-methoxyaniline, the corresponding *N*-arylpyrrolidines **20w** and **20z** were obtained in 78% and 83% yields, respectively.

The reaction of succinic acid **43** with aniline, *p*-methoxy, *p*-bromo and *p*-fluoroanilines led to the corresponding pyrrolidines **26h-k** in 73-88% yields. Additionally, heteroaromatic amine such as 6-amino-2-picoline was successfully converted in the corresponding piperidine **26l** in 76% yield. Notably, an important building block for pharmaceuticals such as 5-amino-1,3-benzodioxole was effectively transformed to piperidine **26m** in 85% yield. It must be underlined that anilines bearing an electron-withdrawing substituent did not permit to obtain cyclic amines. When adipic acid **44** was used in association with aniline, the desired product *N*-phenylazepane **24m** was detected with ca. 10% NMR-yield.

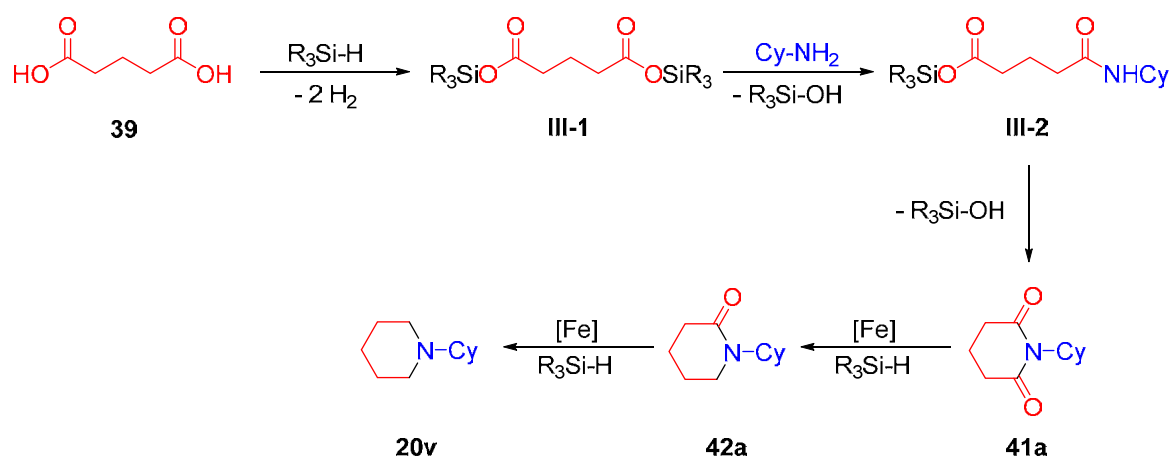
**Table 15.** Reductive amination of diacids with arylamines<sup>[a]</sup>



<sup>[a]</sup> General reaction conditions: **2** (5.0 mol%), **39**, **43** or **44** (0.5 mmol), amine (0.5 mmol), PhSiH<sub>3</sub> (6 equiv.) and DMC (0.5 mL), visible light irradiation, 110 °C, 20 h; then hydrolysis (THF/NaOH 2 N). Isolated yields of the products are shown. <sup>[b]</sup> NMR yield.

### 3.3. Mechanistic insights

A possible reaction pathway was purposed (Scheme 13). **III-1** and hydrogen gas were generated as the result of dehydrogenative silylation of glutaric acid. Then, a transamidation reaction took place in the presence of a primary amine, generating **III-2**. Cyclization of **III-2** led to **41a** and liberated a silanol. Noticeably, these 3 first steps were not catalyzed by the iron complex as **41a** and **41b** can be produced in the absence of the complex **2**. The first reduction of **41a** into **42a** *via* hydrosilylation catalyzed by the iron catalyst **2** took place. Finally, **42a** was reduced to **20v** under the same condition.



**Scheme 13.** Possible reaction pathway.

### 3.4. Conclusion

In summary, in this paragraph, we have shown that for the first time, linear diacids such as glutaric, succinic and adipic acids can be good starting materials to prepare cyclic amines (including piperidines, pyrrolidines and azepanes) *via* a sequence involving reduction steps under hydrosilylation conditions. Noticeably, both alkylamines and anilines are suitable partners in such transformation generating the cyclic amines in good isolated yields. It must be underlined that the reaction with anilines is more difficult and required the use of a catalytic amount of a Lewis acid to increase the electrophilicity of the carboxylic moiety towards the attack of the aniline. Nevertheless, *N*-arylazepanes are more difficult to obtain. Further optimization, scopes and mechanism studies have to be done.

### III-4 Conclusion of the Part 1 dedicated to synthesis of cyclic amines *via* iron-catalyzed hydrosilylation

In this first part dedicated to iron-catalyzed hydrosilylation reactions, it was shown that cyclic amines such as pyrrolidines, piperidines and azepanes can be selectively prepared using a sequential procedure involving a reductive amination of carbonyl derivatives under hydrosilylation. Three procedures were described:

- (i) The first one starting from keto-acid derivatives (including the bio-based levulinic acid and methyl levulinate) by reaction with various amines derivatives. In particular, we have shown that depending on the nature of the iron catalyst used, either cyclic amines or cyclic amides were selectively produced.
- (ii) The second one starting from  $\omega$ -amino fatty acids in the presence of carbonyl derivatives (aldehydes, ketones) and a catalytic amount of  $\text{Fe}(\text{CO})_4(\text{IMes})$  under hydrosilylation conditions.
- (iii) The last one by reaction of diacids such as glutaric, succinic and adipic acids with alkylamines or aniline derivatives. In the latter case, an additional Lewis acid was necessary to promote efficiently the production of cyclic amines. This last methodology is particularly interesting as it permitted to access efficiently to *N*-arylpiperidines and *N*-arylpyrrolidines.

It must also be underline that these three methods tolerated numerous functional groups such halides, hydroxyl, cyano, remoted C=C, ester, boronic esters, etc.

### III-5 References

- [1] a) C. W. Bird, *Comprehensive Heterocyclic Chemistry II*, Pergamon, Oxford, **1996**; b) J. A. Joule, K. Mills, *Heterocyclic Chemistry*, 5th ed., Wiley-Blackwell, Chichester, **2010**.
- [2] a) D. O'Hagan, *Nat. Prod. Rep.* **1997**, *14*, 637-651; b) D. O'Hagan, *Nat. Prod. Rep.* **2000**, *17*, 435-446.
- [3] a) Y. Ju, R. S. Varma, *J. Org. Chem.* **2006**, *71*, 135-141; b) H. He, Q. Lin, X. Liu, Y. Yang, Y. Zhou, Y. Jia, X. Gao, *Synth. Commun.* **2012**, *42*, 2512-2525.
- [4] I. Nakamura, Y. Yamamoto, *Chem. Rev.* **2004**, *104*, 2127-2198.
- [5] a) Y. Tsuji, K. T. Huh, Y. Ohsugi, Y. Watanabe, *J. Org. Chem.* **1985**, *50*, 1365-1370; b) K.-i. Fujita, T. Fujii, R. Yamaguchi, *Org. Lett.* **2004**, *6*, 3525-3528; c) K. Yuan, F. Jiang, Z. Sahli, M. Achard, T. Roisnel, C. Bruneau, *Angew. Chem. Int. Ed.* **2012**, *51*, 8876-8880.
- [6] T. E. Müller, M. Beller, *Chem. Rev.* **1998**, *98*, 675-704.
- [7] F.-X. Felpin, J. Lebreton, *Eur. J. Org. Chem.* **2003**, 3693-3712.
- [8] a) Y. Ogiwara, T. Uchiyama, N. Sakai, *Angew. Chem. Int. Ed.* **2016**, *55*, 1864-1867; b) C. Wu, X. Luo, H. Zhang, X. Liu, G. Ji, Z. Liu, Z. Liu, *Green Chem.* **2017**, *19*, 3525-3529.
- [9] a) G. W. Huber, S. Iborra, A. Corma, *Chem. Rev.* **2006**, *106*, 4044-4098; b) A. Corma, S. Iborra, A. Velty, *Chem. Rev.* **2007**, *107*, 2411-2502; c) P. Gallezot, *Catal. Today* **2007**, *121*, 76-91; d) L. D. Schmidt, P. J. Dauenhauer, *Nature* **2007**, *447*, 914; e) J. C. Serrano-Ruiz, J. A. Dumesic, *Energy Environ. Sci.* **2011**, *4*, 83-99; f) P. Gallezot, *Chem. Soc. Rev.* **2012**, *41*, 1538-1558; g) M. I. Besson, P. Gallezot, C. Pinel, *Chem. Rev.* **2013**, *114*, 1827-1870; h) D. M. Alonso, S. G. Wettstein, M. A. Mellmer, E. I. Gurbuz, J. A. Dumesic, *Energy Environ. Sci.* **2013**, *6*, 76-80.
- [10] a) B. Girisuta, L. Janssen, H. Heeres, *Green Chem.* **2006**, *8*, 701-709; b) B. Kamm, *Angew. Chem. Int. Ed.* **2007**, *46*, 5056-5058; c) G. M. G. Maldonado, R. S. Assary, J. Dumesic, L. A. Curtiss, *Energy Environ. Sci.* **2012**, *5*, 6981-6989; d) R. Weingarten, J. Cho, R. Xing, W. C. Conner, G. W. Huber, *ChemSusChem* **2012**, *5*, 1280-1290; e) R.-J. van Putten, J. C. van der Waal, E. De Jong, C. B. Rasrendra, H. J. Heeres, J. G. de Vries, *Chem. Rev.* **2013**, *113*, 1499-1597; f) C. Li, X. Zhao, A. Wang, G. W. Huber, T. Zhang, *Chem. Rev.* **2015**, *115*, 11559-11624.
- [11] a) C.-H. Zhou, X. Xia, C.-X. Lin, D.-S. Tong, J. Beltramini, *Chem. Soc. Rev.* **2011**, *40*, 5588-5617; b) K. Yan, C. Jarvis, J. Gu, Y. Yan, *Renew. Sust. Energ. Rev.* **2015**, *51*, 986-997.
- [12] Y. B. Huang, J. J. Dai, X. J. Deng, Y. C. Qu, Q. X. Guo, Y. Fu, *ChemSusChem* **2011**, *4*, 1578-1581.
- [13] Y. Wei, C. Wang, X. Jiang, D. Xue, J. Li, J. Xiao, *Chem. Commun.* **2013**, *49*, 5408-5410.
- [14] Z. Xu, P. Yan, H. Jiang, K. Liu, Z. C. Zhang, *Chin. J. Chem.* **2017**, *35*, 581-585.
- [15] S. Wang, H. Huang, C. Bruneau, C. Fischmeister, *ChemSusChem* **2017**, *10*, 4150-4154.
- [16] M. C. Fu, R. Shang, W. M. Cheng, Y. Fu, *Angew. Chem. Int. Ed.* **2015**, *54*, 9042-9046.
- [17] G. A. Aleku, S. P. France, H. Man, J. Mangas-Sanchez, S. L. Montgomery, M. Sharma, F. Leipold, S. Hussain, G. Grogan, N. J. Turner, *Nat. Chem.* **2017**, *9*, 961-969.
- [18] a) C. Bolm, J. Legros, J. Le Paih, L. Zani, *Chem. Rev.* **2004**, *104*, 6217-6254; b) B. Plietker, *Iron Catalysis in Organic Chemistry: Reactions and Applications*, Wiley-VCH, Weinheim, **2008**; c) C.-L. Sun, B.-J. Li, Z.-J. Shi, *Chem. Rev.* **2010**, *111*, 1293-1314; d) H. Nakazawa, M. Itazaki, *Fe-H Complexes in Catalysis in Iron Catalysis, Vol. 33* (Ed.: B. Plietker), Springer, Berlin, Heidelberg, **2011**, pp. 27-81; e) C. Darcel, J.-B. Sortais, *Iron-Catalyzed Reduction and Hydroelementation Reactions in Iron Catalysis II, Vol. 50* (Ed.: E. Bauer), Springer, Cham, **2015**, pp. 173-216; f) R. Lopes, B. Royo, *Isr. J. Chem.* **2017**, *57*, 1151-1159; g) I. Bauer, H.-J. Knölker, *Chem. Rev.* **2015**, *115*, 3170-3387; h) N. Guo, S. F. Zhu, *Chin. J. Org. Chem.* **2015**, *35*, 1383-1398; i) K. Junge, K. Schröder, M. Beller, *Chem. Commun.* **2011**, *47*, 4849-4859; j) B. A. F. Le Bailly, S. P. Thomas, *RSC Adv.* **2011**, *1*, 1435-1445; k) M. Zhang, A. Zhang, *Appl. Organometal. Chem.* **2010**, *24*, 751-757; l) R. H. Morris, *Chem. Soc. Rev.* **2009**, *38*, 2282-2291.
- [19] M.-C. Fu, R. Shang, Z. Huang, Y. Fu, *Synlett* **2014**, *25*, 2748-2752.
- [20] G. Metzker, A. C. B. Burtoloso, *Chem. Commun.* **2015**, *51*, 14199-14202.
- [21] N. Dai, R. Shang, M. Fu, Y. Fu, *Chin. J. Chem.* **2015**, *33*, 405-408.
- [22] C. A. M. R. van Slagmaat, S. M. A. De Wildeman, *Eur. J. Inorg. Chem.* **2018**, 694-702.
- [23] Y. Yi, H. Liu, L.-P. Xiao, B. Wang, G. Song, *ChemSusChem* **2018**, *11*, 1474-1478.

- [24] G. Metzker, R. M. Dias, A. C. B. Burtoloso, *ChemistrySelect* **2018**, *3*, 368-372.
- [25] F. Jiang, D. Bézier, J.-B. Sortais, C. Darcel, *Adv. Synth. Catal.* **2011**, *353*, 239-244.
- [26] L. C. Misal Castro, J.-B. Sortais, C. Darcel, *Chem. Commun.* **2012**, *48*, 151-153.
- [27] D. Bézier, G. T. Venkanna, J.-B. Sortais, C. Darcel, *ChemCatChem* **2011**, *3*, 1747-1750.
- [28] H. Li, L. C. Misal Castro, J. Zheng, T. Roisnel, V. Dorcet, J.-B. Sortais, C. Darcel, *Angew. Chem. Int. Ed.* **2013**, *52*, 8045-8049.
- [29] J. Zheng, C. Darcel, J.-B. Sortais, *Chem. Commun.* **2014**, *50*, 14229-14232.
- [30] M. Bhunia, P. K. Hota, G. Vijaykumar, D. Adhikari, S. K. Mandal, *Organometallics* **2016**, *35*, 2930-2937.
- [31] S. Quintero-Duque, H. Li, L. C. Misal Castro, V. Dorcet, T. Roisnel, E. Clot, M. Grellier, J.-B. Sortais, C. Darcel, *Isr. J. Chem.* **2017**, *57*, 1216-1221.
- [32] D. Wei, C. Netkaew, C. Darcel, *Adv. Synth. Catal.* **2019**, *361*, 1781-1786.
- [33] M. Watanabe, K. Maemura, K. Kanbara, T. Tamayama, H. Hayasaki, *GABA and GABA Receptors in the Central Nervous System and Other Organs in International Review of Cytology, Vol. 213* (Ed.: K. W. Jeon), Academic Press, **2002**, pp. 1-47.
- [34] S. Syrjänen, P. Piironen, H. Markkanen, *Arch. Oral. Biol.* **1987**, *32*, 607-610.
- [35] a) N. Alkjaersig, A. P. Fletcher, S. Sherry, *J. Biol. Chem.* **1959**, *234*, 832; b) J. Lu, H. Meng, Z. Meng, Y. Sun, J. P. Pribis, C. Zhu, Q. Li, *Int. J. Clin. Exp. Pathol.* **2015**, *8*, 7978-7987.
- [36] a) Y. Li, J. A. Molina de La Torre, K. Grabow, U. Bentrup, K. Junge, S. Zhou, A. Brückner, M. Beller, *Angew. Chem. Int. Ed.* **2013**, *52*, 11577-11580; b) M. P. Doyle, D. J. DeBruyn, D. A. Kooistra, *J. Am. Chem. Soc.* **1972**, *94*, 3659-3661; c) X.-H. Chen, Y. Deng, K. Jiang, G.-Q. Lai, Y. Ni, K.-F. Yang, J.-X. Jiang, L.-W. Xu, *Eur. J. Org. Chem.* **2011**, 1736-1742; d) Y. Li, L.-Q. Lu, S. Das, S. Pisiewicz, K. Junge, M. Beller, *J. Am. Chem. Soc.* **2012**, *134*, 18325-18329.
- [37] a) S. Das, B. Wendt, K. Möller, K. Junge, M. Beller, *Angew. Chem. Int. Ed.* **2012**, *51*, 1662-1666; b) D. Bézier, G. T. Venkanna, J.-B. Sortais, C. Darcel, *ChemCatChem* **2011**, *3*, 1747-1750; c) Y. Sunada, H. Kawakami, T. Imaoka, Y. Motoyama, H. Nagashima, *Angew. Chem. Int. Ed.* **2009**, *48*, 9511-9514; d) S. Zhou, K. Junge, D. Addis, S. Das, M. Beller, *Angew. Chem. Int. Ed.* **2009**, *48*, 9507-9510.
- [38] a) A. J. A. Watson, A. C. Maxwell, J. M. J. Williams, *J. Org. Chem.* **2011**, *76*, 2328-2331; b) S.-I. Murahashi, K. Kondo, T. Hakata, *Tetrahedron Lett.* **1982**, *23*, 229-232; c) T. Naota, H. Takaya, S.-I. Murahashi, *Chem. Rev.* **1998**, *98*, 2599-2660; d) R. A. Abbenhuis, J. Boersma, G. van Koten, *J. Org. Chem.* **1998**, *63*, 4282-4290; e) Y. Tsuji, Y. Yokoyama, K.-T. Huh, Y. Watanabe, *Bull. Chem. Soc. Jpn.* **1987**, *60*, 3456-3458; f) K. Yuan, F. Jiang, Z. Sahli, M. Achard, T. Roisnel, C. Bruneau, *Angew. Chem. Int. Ed.* **2012**, *51*, 8876-8880; g) Q. Zou, C. Wang, J. Smith, D. Xue, J. Xiao, *Chem. Eur. J.* **2015**, *21*, 9656-9661; h) W. He, L. Wang, C. Sun, K. Wu, S. He, J. Chen, P. Wu, *Z. Yu Chem. Eur. J.* **2011**, *17*, 13308-13317; i) M. H. S. A. Hamid, C. L. Allen, G. W. Lamb, A. C. Maxwell, H. C. Maytum, A. J. A. Watson, J. M. J. Williams, *J. Am. Chem. Soc.* **2009**, *131*, 1766-1774.
- [39] a) R. I. Khusnutdinov, A. R. Bayguzina, R. S. Asylbaeva, R. I. Aminov, U. M. Dzhemilev, *ARKIVOC* **2014**, 341-350; b) A. Afanasenko, S. Elangovan, M. C. A. Stuart, G. Bonura, F. Frusteri, K. Barta, *Catal. Sci. Technol.* **2018**, *8*, 5498-5505.
- [40] W. Tan, C. Li, J. Zheng, L. Shi, Q. Sun, Y. He, *J. Nat. Gas Chem.* **2008**, *17*, 383-386.
- [41] Y. Du, S. Oishi, S. Saito, *Chem. Eur. J.* **2011**, *17*, 12262-12267.
- [42] I. Sorribes, K. Junge, M. Beller, *J. Am. Chem. Soc.* **2014**, *136*, 14314-14319.
- [43] Y. Shi, P. C. J. Kamer, D. J. Cole-Hamilton, M. Harvie, E. F. Baxter, K. J. C. Lim, P. Pogorzelec, *Chem. Sci.* **2017**, *8*, 6911-6917.
- [44] Y.-C. Yuan, R. Kamaraj, C. Bruneau, T. Labasque, T. Roisnel, R. Gramage-Doria, *Org. Lett.* **2017**, *19*, 6404-6407.
- [45] a) R. Dhivare, S. Rajput, R. Yadav, *Int. J. Chem. Stud.* **2016**, *4*, 61-63; b) I. U. Kutama, S. Jones, *J. Org. Chem.* **2015**, *80*, 11468-11479.
- [46] Y. Wang, S. Xu, T. R. Hoye, *J. Polym. Sci., Part A: Polym. Chem.* **2018**, *56*, 1020-1027.
- [47] a) A. P. Rajput, P. O. Girase, *Indian J. Heterocycl. Chem.* **2012**, *21*, 201-208; b) A. P. Rajput, P. D. Girase, *J. Pharm. Chem. Biol. Sci.* **2014**, *4*, 556-561; c) A. P. Rajput, A. R. Kankhare, *Der Pharma Chemica* **2015**, *7*, 143-148.



- [48] a) S. Sen, S. Sarker, A. Ghosh, S. Mishra, A. Saha, D. Goswami, J. K. Gupta, A. U. De, *Asian. J. Chem.* **2012**, *24*, 1872-1878; b) J. Fraga-Dubreuil, G. Çomak, A. W. Taylor, M. Poliakoff, *Green Chem.* **2007**, *9*, 1067-1072.
- [49] a) S. Warratz, L. Postigo, B. Royo, *Organometallics* **2013**, *32*, 893-897; b) D. Wei, C. Netkaew, V. Carré, C. Darcel, *ChemSusChem* **2019**, *12*, 3008-3012.

## III-6 Experimental data

### 6.1. General information.

$^1\text{H}$ ,  $^{13}\text{C}\{^1\text{H}\}$ ,  $^{19}\text{F}\{^1\text{H}\}$  and  $^{11}\text{B}\{^1\text{H}\}$  NMR spectra were recorded in  $\text{CDCl}_3$  at 298 K unless otherwise stated, on Bruker, AVANCE 400 and AVANCE 300 spectrometers at 400.1, 300.1, 376.5 and 128.4 MHz, respectively.  $^1\text{H}$  and  $^{13}\text{C}\{^1\text{H}\}$  NMR spectra were calibrated using the residual solvent signal as internal standard ( $^1\text{H}$ :  $\text{CDCl}_3$  7.26 ppm,  $^{13}\text{C}$ :  $\text{CDCl}_3$ , central peak is 77.16 ppm). Chemical shift ( $\delta$ ) and coupling constants ( $J$ ) are given in ppm and in Hz, respectively. The peak patterns are indicated as follows: (s, singlet; d, doublet; t, triplet; q, quartet; quin, quintet; m, multiplet, and br. for broad).

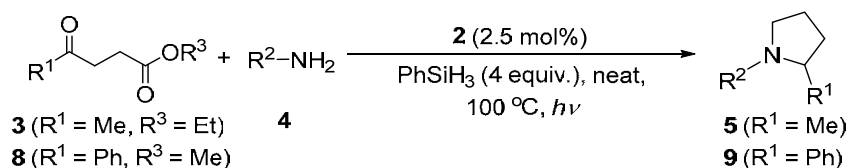
HR-MS were recorded on a Waters Q-ToF 2 mass spectrometer at the corresponding facilities of the CRMPO, Centre Régional de Mesures Physiques de l'Ouest, Université de Rennes 1.

### 6.2. Synthesis of complexes

The complexes  $[\text{CpFe}(\text{CO})_2(\text{IMes})][\text{I}]$  **1** and  $[\text{Fe}(\text{CO})_4(\text{IMes})]$  **2** were prepared according to the published procedure.

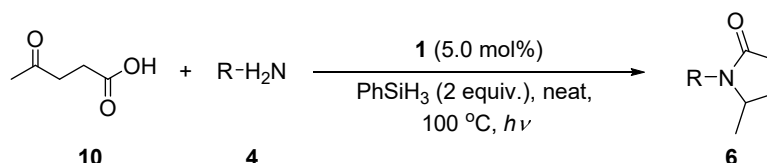
### 6.3. - Part III-1- Reductive amination of keto acids

#### 6.3.1. Typical procedure for the reductive amination of ethyl levulinate into pyrrolidines catalyzed by $[\text{Fe}(\text{CO})_4(\text{IMes})]$ **2**



In an argon filled glove box, a 20 mL Schlenk tube was charged with  $[\text{Fe}(\text{CO})_4(\text{IMes})]$  **2** (2.5 mol%), ethyl levulinate (0.5 mmol), aniline (0.5 mmol) and  $\text{PhSiH}_3$  (4 equiv.) in this order. Then the reaction mixture was stirred upon visible light irradiation (using 24 watt compact fluorescent lamp) at 100 °C for 20 h. After cooling to room temperature, the reaction was quenched by adding 2 mL THF and 2 mL NaOH (aq.) 2 N, stirred for 2 h at room temperature and then extracted with  $3 \times 10$  mL of ethyl acetate. The combined fractions were dried over anhydrous  $\text{Na}_2\text{SO}_4$  for 0.5 h. After filtration through degreasing cotton, the crude mixture was dried under reduced pressure. The residue was then purified by silica gel column chromatography using a mixture of heptane/ethyl acetate as the eluent to afford the desired product.

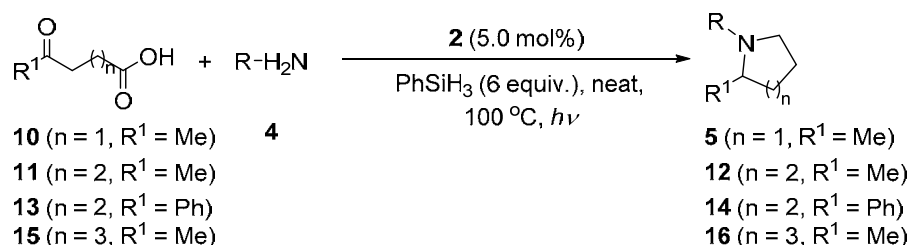
#### 6.3.2. Typical procedure for the reductive amination of levulinic acid into pyrrolidinones catalyzed by $[\text{CpFe}(\text{CO})_2(\text{IMes})][\text{I}]$ **1**



In an argon filled glove box, a 20 mL Schlenk tube was charged with  $[\text{CpFe}(\text{CO})_2(\text{IMes})][\text{I}]$  **1** (5.0 mol%), levulinic acid (0.5 mmol), aniline (0.5 mmol) and  $\text{PhSiH}_3$  (2 equiv.) in this order. Then the reaction mixture was stirred upon visible light irradiation (using 24 watt compact fluorescent lamp) at 100 °C for 20 h. After cooling to room temperature, the reaction was quenched by adding 2 mL THF and 2 mL NaOH (aq.) 2 N, stirred for 2 h at room temperature and then extracted with  $3 \times 10$  mL of ethyl acetate. The combined fractions were dried over

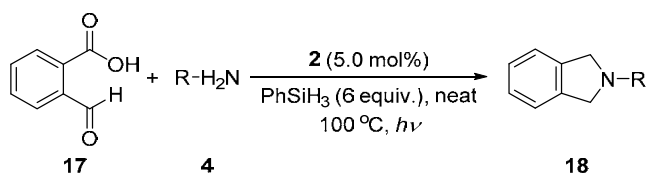
anhydrous Na<sub>2</sub>SO<sub>4</sub> for 0.5 h. After filtration through degreasing cotton, the crude mixture was dried under reduced pressure. The residue was then purified by silica gel column chromatography using a mixture of heptane/ethyl acetate as the eluent to afford the desired product.

### 6.3.3. Typical procedure for the reductive amination of keto acids into cyclic amines catalyzed by [Fe(CO)<sub>4</sub>(*IMes*)] **2**



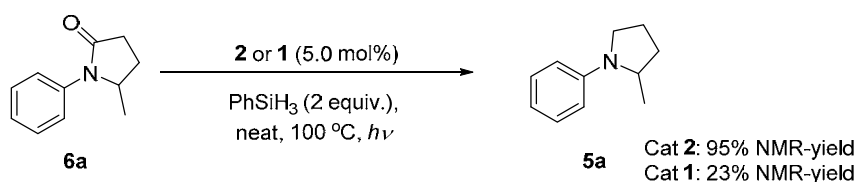
In an argon filled glove box, a 20 mL Schlenk tube was charged with [Fe(CO)<sub>4</sub>(*IMes*)] **2** (5.0 mol%), keto acid (0.5 mmol), aniline (0.5 mmol) and PhSiH<sub>3</sub> (6 equiv.) in this order. Then the reaction mixture was stirred upon visible light irradiation (using 24 watt compact fluorescent lamp) at 100 °C for 20 h. After cooling to room temperature, the reaction was quenched by adding 2 mL THF and 2 mL NaOH (aq.) 2 N, stirred for 2 h at room temperature and then extracted with 3×10 mL of ethyl acetate. The combined fractions were dried over anhydrous Na<sub>2</sub>SO<sub>4</sub> for 0.5 h. After filtration through degreasing cotton, the crude mixture was dried under reduced pressure. The residue was then purified by silica gel column chromatography using a mixture of heptane/ethyl acetate as the eluent to afford the desired product.

### 6.3.4. Typical procedure for the reductive amination of 2-formylbenzoic acid into isoindolines catalyzed by [Fe(CO)<sub>4</sub>(*IMes*)] **2**



In an argon filled glove box, a 20 mL Schlenk tube was charged with [Fe(CO)<sub>4</sub>(*IMes*)] **2** (5.0 mol%), 2-formylbenzoic acid (0.5 mmol), aniline (0.5 mmol) and PhSiH<sub>3</sub> (6 equiv.) in this order. Then the reaction mixture was stirred upon visible light irradiation (using 24 watt compact fluorescent lamp) at 100 °C for 20 h. After cooling to room temperature, the reaction was quenched by adding 2 mL THF and 2 mL NaOH (aq.) 2 N, stirred for 2 h at room temperature and then extracted with 3×10 mL of ethyl acetate. The combined fractions were dried over anhydrous Na<sub>2</sub>SO<sub>4</sub> for 0.5 h. After filtration through degreasing cotton, the crude mixture was dried under reduced pressure. The residue was then purified by silica gel column chromatography using a mixture of heptane/ethyl acetate as the eluent to afford the desired product.

### 6.3.5. Reduction of 5-methyl-1-phenylpyrrolidin-2-one **6a** to 2-methyl-1-phenylpyrrolidine **5a**



In an argon filled glove box, a 20 mL Schlenk tube was charged with  $[\text{Fe}(\text{CO})_4(\text{IMes})]$  **2** (5.0 mol%) or  $[\text{CpFe}(\text{CO})_2(\text{IMes})][\text{I}]$  **1** (5.0 mol%), 5-methyl-1-phenylpyrrolidin-2-one **6a** (0.25 mmol) and  $\text{PhSiH}_3$  (2 equiv.) in this order. Then the reaction mixture was stirred upon visible light irradiation (using 24 watt compact fluorescent lamp) at 100 °C for 20 h. After cooling to room temperature, the reaction was quenched by adding 2 mL THF and 2 mL NaOH (aq.) 2 N, stirred for 2 h at room temperature and then extracted with 3×10 mL of ethyl acetate. The combined fractions were dried over anhydrous  $\text{Na}_2\text{SO}_4$  for 0.5 h. After filtration through degreasing cotton, the crude mixture was dried under reduced pressure. The product yield was determined by  $^1\text{H}$  NMR of the crude mixture.

### 6.3.6. General procedure for gram scale reactions

#### Preparation of 2-methyl-1-phenyl-pyrrolidine **5a**

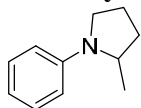
In an argon filled glove box, a 100 mL Schlenk tube was charged with  $[\text{Fe}(\text{CO})_4(\text{IMes})]$  **2** (5.0 mol%, 240 mg), levulinic acid (10 mmol, 1.16 g), aniline (10 mmol, 0.93 g) and  $\text{PhSiH}_3$  (60 mmol, 6.49 g) in this order. Then the reaction mixture was stirred upon visible light irradiation (using 24 watt compact fluorescent lamp) at 100 °C for 48 h. After cooling to room temperature, the reaction was quenched by adding 20 mL THF and 30 mL NaOH (aq.) 2 N, stirred for 2 h at room temperature and then extracted with 3×20 mL of ethyl acetate. The combined fractions were dried over anhydrous  $\text{Na}_2\text{SO}_4$  for 0.5 h. After filtrate through degreasing cotton, the crude mixture was dried under reduced pressure. The residue was then purified by silica gel column chromatography using a mixture of heptane/ethyl acetate as the eluent to afford **5a** in 89% isolated yield.

#### Preparation of 5-methyl-1-phenylpyrrolidin-2-one **6a**

In an argon filled glove box, a 100 mL Schlenk tube was charged with  $[\text{CpFe}(\text{CO})_2(\text{IMes})][\text{I}]$  **1** (5.0 mol%, 312 mg), levulinic acid (10 mmol, 1.16 g), aniline (10 mmol, 0.93 g) and  $\text{PhSiH}_3$  (20 mmol, 2.16 g) in this order. Then the reaction mixture was stirred upon visible light irradiation (using 24 watt compact fluorescent lamp) at 100 °C for 18 h. After cooling to room temperature, the reaction was quenched by adding 20 mL THF and 20 mL NaOH (aq.) 2 N, stirred for 2 h at room temperature and then extracted with 3×20 mL of ethyl acetate. The combined fractions were dried over anhydrous  $\text{Na}_2\text{SO}_4$  for 0.5 h. After filtrate through degreasing cotton, the crude mixture was dried under reduced pressure. The residue was then purified by silica gel column chromatography using a mixture of heptane/ethyl acetate as the eluent to afford **6a** in 84% isolated yield.

### 6.3.7. Characterization data for cyclic amines obtained from keto-acid derivatives

#### 2-Methyl-1-phenylpyrrolidine **5a**<sup>[3]</sup>



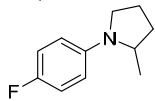
Ethyl levulinate (70.9  $\mu\text{L}$ , 0.5 mmol) and aniline (45.6  $\mu\text{L}$ , 0.5 mmol) gave the title compound **5a** (72.6 mg) in 99% conversion and 90% yield.

Levulinic acid (51.2  $\mu\text{L}$ , 0.5 mmol) and aniline (45.6  $\mu\text{L}$ , 0.5 mmol) gave the title compound **5a** (73.4 mg) in 99% conversion and 91% yield.

$^1\text{H}$  NMR (400 MHz,  $\text{CDCl}_3$ )  $\delta$  7.26 (td,  $J = 7.3, 2.0$  Hz, 2H), 6.70 – 6.61 (m, 3H), 3.95 – 3.87 (m, 1H), 3.49 – 3.43 (m, 1H), 3.23 – 3.15 (m, 1H), 2.15 – 1.97 (m, 3H), 1.79 – 1.68 (m, 1H), 1.21 (d,  $J = 6.2$  Hz, 3H).  $^{13}\text{C}\{^1\text{H}\}$  NMR (101 MHz,  $\text{CDCl}_3$ )  $\delta$  147.3, 129.3, 115.2, 111.9, 53.7,

48.3, 33.2, 23.4, 19.5. **GC-MS**,  $m/z(\%) = 161([M]^+, 18), 146(100), 104(19), 91(10), 77(33), 51(13)$ .

### 1-(4-Fluorophenyl)-2-methylpyrrolidine **5b**<sup>[3]</sup>

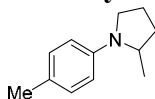


Ethyl levulinate (70.9  $\mu$ L, 0.5 mmol) and 4-fluoroaniline (47.4  $\mu$ L, 0.5 mmol) gave the title compound **5b** (79.8 mg) in 99% conversion and 89% yield.

Levulinic acid (51.2  $\mu$ L, 0.5 mmol) and 4-fluoroaniline (47.4  $\mu$ L, 0.5 mmol) gave the title compound **5b** (77.1 mg) in 99% conversion and 86% yield.

**<sup>1</sup>H NMR** (400 MHz, CDCl<sub>3</sub>)  $\delta$  6.99 – 6.90 (m, 2H), 6.52 – 6.47 (m, 2H), 3.81 (qt,  $J = 6.4, 3.2$  Hz, 1H), 3.45 – 3.35 (m, 1H), 3.15 – 3.09 (m, 1H), 2.14 – 1.93 (m, 3H), 1.75 – 1.66 (m, 1H), 1.16 (d,  $J = 6.2$  Hz, 3H). **<sup>13</sup>C{<sup>1</sup>H} NMR** (101 MHz, CDCl<sub>3</sub>)  $\delta$  154.8 (d,  $J = 233.1$  Hz), 144.1, 115.6 (d,  $J = 22.0$  Hz), 112.3 (d,  $J = 7.1$  Hz), 54.2, 48.9, 33.4, 23.5, 19.5. **<sup>19</sup>F{<sup>1</sup>H} NMR** (376 MHz, CDCl<sub>3</sub>)  $\delta$  -131.2. **GC-MS**,  $m/z(\%) = 179([M]^+, 22), 164(100), 122(29), 109(13), 95(25), 75(10)$ .

### 2-Methyl-1-(*p*-tolyl)pyrrolidine **5c**<sup>[3]</sup>

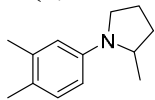


Ethyl levulinate (70.9  $\mu$ L, 0.5 mmol) and *p*-toluidine (55.1  $\mu$ L, 0.5 mmol) gave the title compound **5c** (54.3 mg) in 86% conversion and 62% yield.

Levulinic acid (51.2  $\mu$ L, 0.5 mmol) and *p*-toluidine (55.1  $\mu$ L, 0.5 mmol) gave the title compound **5c** (64.0 mg) in 90% conversion and 73% yield.

**<sup>1</sup>H NMR** (400 MHz, CDCl<sub>3</sub>)  $\delta$  7.08 – 7.05 (m, 2H), 6.57 – 6.53 (m, 2H), 3.90 – 3.83 (m, 1H), 3.46 – 3.42 (m, 1H), 3.19 – 3.13 (m, 1H), 2.28 (s, 3H), 2.15 – 1.92 (m, 3H), 1.75 – 1.67 (m, 1H), 1.20 (d,  $J = 6.2$  Hz, 3H). **<sup>13</sup>C{<sup>1</sup>H} NMR** (101 MHz, CDCl<sub>3</sub>)  $\delta$  145.4, 129.8, 124.3, 112.0, 53.9, 48.6, 33.3, 23.5, 20.4, 19.6. **GC-MS**,  $m/z(\%) = 175([M]^+, 33), 160(100), 118(16), 91(23), 65(10)$ .

### 1-(3,4-Dimethylphenyl)-2-methylpyrrolidine **5d**

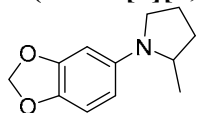


Ethyl levulinate (70.9  $\mu$ L, 0.5 mmol) and 3,4-dimethylaniline (60.6 mg, 0.5 mmol) gave the title compound **5d** (53.0 mg) in 62% conversion and 56% yield.

Levulinic acid (51.2  $\mu$ L, 0.5 mmol) and 3,4-dimethylaniline (60.6 mg, 0.5 mmol) gave the title compound **5d** (58.7 mg) in 78% conversion and 62% yield.

**<sup>1</sup>H NMR** (400 MHz, CDCl<sub>3</sub>)  $\delta$  6.99 (d,  $J = 8.2$  Hz, 1H), 6.43 (d,  $J = 2.6$  Hz, 1H), 6.38 (dd,  $J = 8.2, 2.7$  Hz, 1H), 3.84 (qt,  $J = 6.4, 3.0$  Hz, 1H), 3.44 – 3.40 (m, 1H), 3.17 – 3.11 (m, 1H), 2.24 (s, 3H), 2.17 (s, 3H), 2.11 – 1.91 (m, 3H), 1.70 – 1.64 (m, 1H), 1.17 (d,  $J = 6.2$  Hz, 3H). **<sup>13</sup>C{<sup>1</sup>H} NMR** (101 MHz, CDCl<sub>3</sub>) 145.9, 137.2, 130.4, 123.2, 113.6, 109.5, 53.8, 48.6, 33.3, 23.5, 20.5, 19.7, 18.7. **GC-MS**,  $m/z(\%) = 189([M]^+, 35), 174(100), 132(10), 105(15), 77(10)$ . **HR-MS (ESI)** calcd. for  $[M+H]^+ C_{13}H_{20}N$  190.1590, found 190.1592 (1 ppm).

### 1-(Benzo[d][1,3]dioxol-5-yl)-2-methylpyrrolidine **5e**

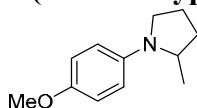


Ethyl levulinate (70.9  $\mu$ L, 0.5 mmol) and benzo[d][1,3]dioxol-5-amine (68.6 mg, 0.5 mmol) gave the title compound **5e** (78.0 mg) in 99% conversion and 76% yield.

Levulinic acid (51.2  $\mu$ L, 0.5 mmol) and benzo[d][1,3]dioxol-5-amine (68.6 mg, 0.5 mmol) gave the title compound **5e** (82.1 mg) in 99% conversion and 80% yield.

**$^1\text{H}$  NMR** (400 MHz,  $\text{CDCl}_3$ )  $\delta$  6.72 (d,  $J$  = 8.5 Hz, 1H), 6.25 (d,  $J$  = 2.4 Hz, 1H), 5.98 (dd,  $J$  = 8.4, 2.4 Hz, 1H), 5.85 – 5.83 (m, 2H), 3.80 – 3.73 (m, 1H), 3.39 – 3.34 (m, 1H), 3.13 – 3.07 (m, 1H), 2.12 – 1.90 (m, 3H), 1.71 – 1.64 (m, 1H), 1.15 (d,  $J$  = 6.2 Hz, 3H).  **$^{13}\text{C}\{^1\text{H}\}$  NMR** (101 MHz,  $\text{CDCl}_3$ )  $\delta$  148.5, 143.9, 138.0, 108.9, 103.4, 100.5, 94.8, 54.4, 49.2, 33.3, 23.5, 19.6. **GC-MS**,  $m/z(\%)$  = 205([M]<sup>+</sup>, 40), 190(100), 148(12). **HR-MS (ESI)** calcd. for [M+H]<sup>+</sup>  $\text{C}_{12}\text{H}_{16}\text{NO}_2$  206.1176, found 206.1177 (1 ppm).

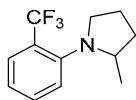
### 1-(4-Methoxyphenyl)-2-methylpyrrolidine **5f**<sup>[3]</sup>



Levulinic acid (51.2  $\mu$ L, 0.5 mmol) and 4-methoxyaniline (61.6 mg, 0.5 mmol) gave the title compound **5f** (88.0 mg) in 99% conversion and 92% yield.

**$^1\text{H}$  NMR** (400 MHz,  $\text{CDCl}_3$ )  $\delta$  6.85 (d,  $J$  = 9.0 Hz, 2H), 6.55 (d,  $J$  = 9.0 Hz, 2H), 3.76 (s, 3H), 3.43 – 3.38 (m, 1H), 3.14 – 3.08 (m, 1H), 2.12 – 1.91 (m, 4H), 1.72 – 1.64 (m, 1H), 1.16 (d,  $J$  = 6.2 Hz, 3H).  **$^{13}\text{C}\{^1\text{H}\}$  NMR** (101 MHz,  $\text{CDCl}_3$ )  $\delta$  150.7, 142.5, 115.2, 112.9, 56.2, 54.2, 49.1, 33.4, 23.6, 19.8. **GC-MS**,  $m/z(\%)$  = 191([M]<sup>+</sup>, 33), 176(100), 134(12), 77(10).

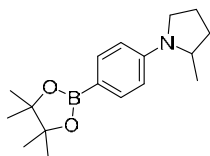
### 2-Methyl-1-(2-(trifluoromethyl)phenyl)pyrrolidine **5r**



Levulinic acid (51.2  $\mu$ L, 0.5 mmol) and 2-(trifluoromethyl)aniline (62.8  $\mu$ L, 0.5 mmol) gave the title compound **5r** (102.0 mg) in 99% conversion and 89% yield.

**$^1\text{H}$  NMR** (400 MHz,  $\text{CDCl}_3$ )  $\delta$  7.61 – 7.57 (m, 1H), 7.46 – 7.41 (m, 1H), 7.22 (d,  $J$  = 8.2 Hz, 1H), 7.04 (t,  $J$  = 7.6 Hz, 1H), 3.66 – 3.51 (m, 2H), 2.94 – 2.88 (m, 1H), 2.16 – 2.09 (m, 1H), 1.97 – 1.88 (m, 1H), 1.85 – 1.74 (m, 1H), 1.63 – 1.55 (m, 1H), 1.01 (d,  $J$  = 6.0 Hz, 3H).  **$^{13}\text{C}\{^1\text{H}\}$  NMR** (101 MHz,  $\text{CDCl}_3$ )  $\delta$  149.3, 136.0, 132.4, 127.7 (q,  $J$  = 5.7 Hz), 125.3 (q,  $J$  = 29.0 Hz), 124.6 (q,  $J$  = 272.9 Hz), 122.0 (d,  $J$  = 42.9 Hz), 57.2, 55.9 (q,  $J$  = 2.3 Hz), 33.8, 24.0, 19.1.  **$^{19}\text{F}\{^1\text{H}\}$  NMR** (376 MHz,  $\text{CDCl}_3$ )  $\delta$  -59.4. **GC-MS**,  $m/z(\%)$  = 229([M]<sup>+</sup>, 25), 214(100), 172(20), 145(25). **HR-MS (ESI)** calcd. for [M+H]<sup>+</sup>  $\text{C}_{12}\text{H}_{15}\text{NF}_3$  230.1151, found 230.1150 (1 ppm).

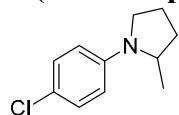
### 2-Methyl-1-(4-(4,4,5,5-tetramethyl-1,3,2-dioxaborolan-2-yl)phenyl)pyrrolidine **5l**



Levulinic acid (51.2  $\mu$ L, 0.5 mmol) and 4-(4,4,5,5-tetramethyl-1,3,2-dioxaborolan-2-yl)aniline (109.5 mg, 0.5 mmol) gave the title compound **5i** (129.2 mg) in 99% conversion and 90% yield.

**$^1\text{H}$  NMR** (400 MHz,  $\text{CDCl}_3$ )  $\delta$  7.67 (d,  $J$  = 8.6 Hz, 2H), 6.55 (d,  $J$  = 8.6 Hz, 2H), 3.97 – 3.91 (m, 1H), 3.46 – 3.41 (m, 1H), 3.23 – 3.17 (m, 1H), 2.11 – 1.95 (m, 3H), 1.72 – 1.69 (m, 1H), 1.32 (s, 12H), 1.17 (d,  $J$  = 6.3 Hz, 3H).  **$^{13}\text{C}\{^1\text{H}\}$  NMR** (101 MHz,  $\text{CDCl}_3$ , the carbon attached to quadrupole boron was not observed due to low intensity)  $\delta$  149.4, 136.4, 111.2, 83.2, 53.5, 48.0, 33.1, 25.0, 23.3, 19.2.  **$^{11}\text{B}\{^1\text{H}\}$  NMR** (128 MHz,  $\text{CDCl}_3$ )  $\delta$  31.7. **GC-MS**,  $m/z(\%)$  = 287([M]<sup>+</sup>, 25), 272(100), 214(10), 172(15). **HR-MS (ESI)** calcd. for  $[\text{M}+\text{H}]^+$   $\text{C}_{17}\text{H}_{27}\text{NO}_2^{11}\text{B}$  288.2129, found 288.2134 (2 ppm).

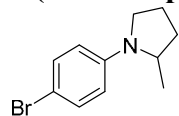
### 1-(4-Chlorophenyl)-2-methylpyrrolidine **5g**<sup>[3]</sup>



Levulinic acid (51.2  $\mu$ L, 0.5 mmol) and 4-chloroaniline (44.6  $\mu$ L, 0.5 mmol) gave the title compound **5g** (91.0 mg) in 99% conversion and 93% yield.

**$^1\text{H}$  NMR** (400 MHz,  $\text{CDCl}_3$ )  $\delta$  7.16 – 7.12 (m, 2H), 6.50 – 6.46 (m, 2H), 3.86 – 3.79 (m, 1H), 3.41 – 3.36 (m, 1H), 3.16 – 3.09 (m, 1H), 2.14 – 1.93 (m, 3H), 1.72 – 1.68 (m, 1H), 1.15 (d,  $J$  = 6.2 Hz, 3H).  **$^{13}\text{C}\{^1\text{H}\}$  NMR** (126 MHz,  $\text{CDCl}_3$ )  $\delta$  145.9, 129.0, 120.0, 112.9, 53.9, 48.4, 33.3, 23.4, 19.3. **GC-MS**,  $m/z(\%)$  = 195([M]<sup>+</sup>, 25), 180(100), 138(22), 111(19), 75(11).

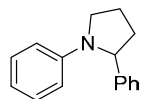
### 1-(4-Bromophenyl)-2-methylpyrrolidine **5h**<sup>[3]</sup>



Levulinic acid (51.2  $\mu$ L, 0.5 mmol) and 4-bromoaniline (86.9 mg, 0.5 mmol) gave the title compound **5h** (100.8 mg) in 99% conversion and 84% yield.

**$^1\text{H}$  NMR** (400 MHz,  $\text{CDCl}_3$ )  $\delta$  7.31 – 7.28 (m, 2H), 6.48 – 6.45 (m, 2H), 3.87 – 3.83 (m, 1H), 3.43 – 3.37 (m, 1H), 3.18 – 3.11 (m, 1H), 2.14 – 1.98 (m, 3H), 1.74–1.72 (m, 1H), 1.18 (d,  $J$  = 6.2 Hz, 3H).  **$^{13}\text{C}\{^1\text{H}\}$  NMR** (126 MHz,  $\text{CDCl}_3$ )  $\delta$  146.2, 131.9, 113.5, 107.0, 53.9, 48.3, 33.2, 23.4, 19.2. **GC-MS**,  $m/z(\%)$  = 239([M]<sup>+</sup>, 25), 224(100), 182(11), 117(10), 76(13).

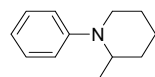
### 1,2-Diphenylpyrrolidine **9**<sup>[4]</sup>



Methyl 3-benzoylpropionate (84.3  $\mu$ L, 0.5 mmol) and aniline (45.6  $\mu$ L, 0.5 mmol) gave the title compound **9** (80.4 mg) in 85% conversion and 72% yield.

**$^1\text{H}$  NMR** (400 MHz,  $\text{CDCl}_3$ )  $\delta$  7.31 – 7.27 (m, 2H), 7.23 – 7.21 (m, 3H), 7.16 – 7.12 (m, 2H), 6.65 – 6.61 (m, 1H), 6.49 (d,  $J$  = 8.0 Hz, 2H), 4.72 (dd,  $J$  = 8.2, 2.2 Hz, 1H), 3.73 – 3.68 (m, 1H), 3.44–3.38 (m, 1H), 2.43–2.34 (m, 1H), 2.10 – 1.91 (m, 3H).  **$^{13}\text{C}\{^1\text{H}\}$  NMR** (101 MHz,  $\text{CDCl}_3$ )  $\delta$  147.3, 144.8, 129.1, 128.6, 126.7, 126.1, 115.9, 112.5, 63.1, 49.2, 36.2, 23.2. **GC-MS**,  $m/z(\%)$  = 223([M]<sup>+</sup>, 51), 194(15), 146(100), 117(10), 91(13), 77(28).

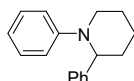
### 2-Methyl-1-phenylpiperidine **12**<sup>[5]</sup>



5-Oxohexanoic acid (59.7  $\mu$ L, 0.5 mmol) and aniline (45.6  $\mu$ L, 0.5 mmol) gave the title compound **12** (78.0 mg) in 99% conversion and 89% yield.

**$^1\text{H}$  NMR** (400 MHz,  $\text{CDCl}_3$ )  $\delta$  7.34 – 7.27 (m, 2H), 7.00 (d,  $J$  = 7.9 Hz, 2H), 6.88 (t,  $J$  = 7.3 Hz, 1H), 3.99 – 3.92 (m, 1H), 3.27 (m, 1H), 3.06 – 2.99 (m, 1H), 1.97 – 1.59 (m, 6H), 1.05 (d,  $J$  = 6.6 Hz, 3H).  **$^{13}\text{C}\{^1\text{H}\}$  NMR** (126 MHz,  $\text{CDCl}_3$ )  $\delta$  151.5, 129.1, 119.3, 117.8, 51.6, 45.3, 32.0, 26.3, 20.0, 14.0. **GC-MS**,  $m/z(\%)$  = 175( $[\text{M}]^+$ , 28), 160(100), 132(23), 119(10), 104(30), 77(31), 51(10).

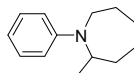
### 1,2-Diphenylpiperidine **14**<sup>[6]</sup>



5-Oxo-5-phenylpentanoic acid (96.1 mg, 0.5 mmol) and aniline (45.6  $\mu$ L, 0.5 mmol) gave the title compound **14** (98.5 mg) in 99% conversion and 83% yield.

**$^1\text{H}$  NMR** (400 MHz,  $\text{CDCl}_3$ )  $\delta$  7.32 – 7.24 (m, 4H), 7.20 – 7.16 (m, 3H), 6.93 (d,  $J$  = 7.9 Hz, 2H), 6.79 (t,  $J$  = 7.3 Hz, 1H), 4.54 (dd,  $J$  = 6.7, 4.5 Hz, 1H), 3.48 – 3.42 (m, 1H), 3.33 – 3.27 (m, 1H), 2.08 – 1.54 (m, 6H).  **$^{13}\text{C}\{^1\text{H}\}$  NMR** (126 MHz,  $\text{CDCl}_3$ )  $\delta$  151.9, 143.7, 128.9, 128.4, 127.3, 126.3, 119.7, 118.9, 61.1, 50.6, 33.6, 25.8, 22.2. **GC-MS**,  $m/z(\%)$  = 237( $[\text{M}]^+$ , 54), 180(15), 160(100), 132(12), 104(24), 91(14), 77(32).

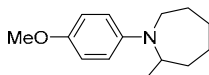
### 2-Methyl-1-phenylazepane **16a**<sup>[7]</sup>



6-Oxoheptanoic acid (72.1 mg, 0.5 mmol) and aniline (45.6  $\mu$ L, 0.5 mmol) gave the title compound **16a** (87.1 mg) in 99% conversion and 92% yield.

**$^1\text{H}$  NMR** (400 MHz,  $\text{CDCl}_3$ )  $\delta$  7.24 – 7.19 (m, 2H), 6.68 (d,  $J$  = 8.2 Hz, 2H), 6.60 (t,  $J$  = 7.2 Hz, 1H), 3.79 – 3.70 (m, 1H), 3.44 – 3.40 (m, 1H), 3.22 – 3.15 (m, 1H), 2.14 – 2.07 (m, 1H), 1.85 – 1.58 (m, 3H), 1.48 – 1.22 (m, 4H), 1.13 (d,  $J$  = 6.3 Hz, 3H).  **$^{13}\text{C}\{^1\text{H}\}$  NMR** (126 MHz,  $\text{CDCl}_3$ )  $\delta$  148.6, 129.5, 114.5, 110.4, 52.6, 42.6, 37.8, 30.2, 27.8, 25.7, 18.1. **GC-MS**,  $m/z(\%)$  = 189 ( $[\text{M}]^+$ , 35), 174(100), 160(15), 146(41), 119(15), 104(30), 91(15), 77(30).

### 2-Methyl-1-(4-methoxyphenyl)azepane **16f**



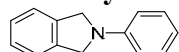
6-Oxoheptanoic acid (72.1 mg, 0.5 mmol) and 4-methoxyaniline (61.6 mg, 0.5 mmol) gave the title compound **16f** (98.7 mg) in 99% conversion and 90% yield.

**$^1\text{H}$  NMR** (400 MHz,  $\text{CDCl}_3$ )  $\delta$  6.87 – 6.80 (m, 2H), 6.66 – 6.58 (m, 2H), 3.76 (s, 3H), 3.73 – 3.62 (m, 1H), 3.43 – 3.30 (m, 1H), 3.23 – 3.11 (m, 1H), 2.16 – 2.00 (m, 1H), 1.87 – 1.51 (m, 3H), 1.47 – 1.18 (m, 4H), 1.12 (d,  $J$  = 6.3 Hz, 3H).  **$^{13}\text{C}\{^1\text{H}\}$  NMR** (101 MHz,  $\text{CDCl}_3$ )  $\delta$  149.9, 143.7, 115.4, 111.0, 56.2, 52.8, 43.0, 37.9, 30.2, 28.0, 25.8, 18.1. **GC-MS**,  $m/z(\%)$  = 219 ( $[\text{M}]^+$ , 55), 204(100), 190(15), 176(25), 150(90), 134(25), 121(15), 77(10). **HR-MS (ESI)** calcd. for  $[\text{M}+\text{H}]^+$   $\text{C}_{14}\text{H}_{22}\text{NO}$  220.1696, found 220.1696 (0 ppm).



### 6.3.8. Characterization data for isoindolines 18

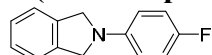
#### 2-Phenylisoindoline 18a<sup>[8]</sup>



2-Formylbenzoic acid (75.1 mg, 0.5 mmol) and aniline (45.6  $\mu$ L, 0.5 mmol) gave the title compound **18a** (86.9 mg) in 99% conversion and 89% yield.

**<sup>1</sup>H NMR** (400 MHz, CDCl<sub>3</sub>)  $\delta$  7.37 – 7.30 (m, 6H), 6.76 (t,  $J$  = 7.3 Hz, 1H), 6.70 (d,  $J$  = 8.1 Hz, 2H), 4.67 (s, 4H). **<sup>13</sup>C{<sup>1</sup>H} NMR** (101 MHz, CDCl<sub>3</sub>)  $\delta$  147.3, 138.1, 129.5, 127.3, 122.7, 116.3, 111.7, 53.9. **GC-MS**,  $m/z$ (%) = 194([M]<sup>+</sup>, 100), 165(11), 116(15), 77(27), 51(12).

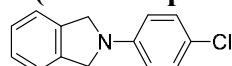
#### 2-(4-Fluorophenyl)isoindoline 18b<sup>[8]</sup>



2-Formylbenzoic acid (75.1 mg, 0.5 mmol) and 4-fluoroaniline (47.4  $\mu$ L, 0.5 mmol) gave the title compound **18b** (99.2 mg) in 99% conversion and 93% yield.

**<sup>1</sup>H NMR** (400 MHz, CDCl<sub>3</sub>)  $\delta$  7.36 – 7.29 (m, 4H), 7.05 – 7.00 (m, 2H), 6.61 – 6.57 (m, 2H), 4.62 (s, 4H). **<sup>13</sup>C{<sup>1</sup>H} NMR** (101 MHz, CDCl<sub>3</sub>)  $\delta$  155.4 (d,  $J$  = 234.0 Hz), 144.0 (d,  $J$  = 1.3 Hz), 138.1, 127.4, 122.7, 115.9 (d,  $J$  = 22.1 Hz), 112.1 (d,  $J$  = 7.3 Hz), 54.3. **<sup>19</sup>F{<sup>1</sup>H} NMR** (376 MHz, CDCl<sub>3</sub>)  $\delta$  -130.1. **GC-MS**,  $m/z$ (%) = 212([M]<sup>+</sup>, 100), 116(14), 95(15).

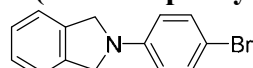
#### 2-(4-Chlorophenyl)isoindoline 18g<sup>[8]</sup>



2-Formylbenzoic acid (75.1 mg, 0.5 mmol) and 4-chloroaniline (44.6  $\mu$ L, 0.5 mmol) gave the title compound **18g** (104.5 mg) in 99% conversion and 91% yield.

**<sup>1</sup>H NMR** (400 MHz, CDCl<sub>3</sub>)  $\delta$  7.35 – 7.29 (m, 4H), 7.25 – 7.22 (m, 2H), 6.61 – 6.57 (m, 2H), 4.63 (s, 4H). **<sup>13</sup>C{<sup>1</sup>H} NMR** (101 MHz, CDCl<sub>3</sub>)  $\delta$  145.9, 137.8, 129.3, 127.4, 122.8, 121.2, 112.7, 54.1. **GC-MS**,  $m/z$ (%) = 228([M]<sup>+</sup>, 100), 193(12), 111(13), 75(11).

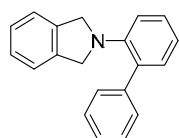
#### 2-(4-Bromophenyl)isoindoline 18h<sup>[9]</sup>



2-Formylbenzoic acid (75.1 mg, 0.5 mmol) and 4-bromoaniline (86.9 mg, 0.5 mmol) gave the title compound **18h** (116.5 mg) in 99% conversion and 85% yield.

**<sup>1</sup>H NMR** (400 MHz, CDCl<sub>3</sub>)  $\delta$  7.39 – 7.30 (m, 6H), 6.56 – 6.52 (m, 2H), 4.61 (s, 4H). **<sup>13</sup>C{<sup>1</sup>H} NMR** (101 MHz, CDCl<sub>3</sub>)  $\delta$  146.2, 137.7, 132.1, 127.4, 122.7, 113.3, 108.3, 54.0. **GC-MS**,  $m/z$ (%) = 274([M]<sup>+</sup>, 100), 193(29), 165(10), 116(13), 97(11), 76(14).

#### 2-([1,1'-Biphenyl]-2-yl)isoindoline 18i

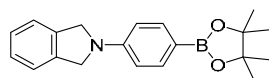


2-Formylbenzoic acid (75.1 mg, 0.5 mmol) and 2-aminobiphenyl (84.6 mg, 0.5 mmol) gave the title compound **18i** in (126.2 mg) 99% conversion and 93% yield.

**<sup>1</sup>H NMR** (400 MHz, CDCl<sub>3</sub>)  $\delta$  7.55 – 7.52 (m, 2H), 7.44 – 7.40 (m, 2H), 7.38 – 7.34 (m, 2H), 7.27 – 7.16 (m, 5H), 7.07 (d,  $J$  = 8.1 Hz, 1H), 6.97 (td,  $J$  = 7.4, 1.1 Hz, 1H), 4.34 (s, 4H). **<sup>13</sup>C{<sup>1</sup>H} NMR** (101 MHz, CDCl<sub>3</sub>) 146.7, 143.2, 138.5, 132.8, 130.7, 129.3, 128.3, 128.2, 126.9,

126.7, 122.2, 118.9, 115.5, 56.3. **GC-MS**,  $m/z(\%) = 270$  ( $[M]^+$ , 100), 254(18), 193(17), 152(30), 133(30), 118(15).

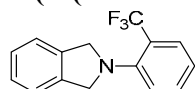
### 2-(4-(4,4,5,5-Tetramethyl-1,3,2-dioxaborolan-2-yl)phenyl)isoindoline **18l**



2-Formylbenzoic acid (75.1 mg, 0.5 mmol) and 4-(4,4,5,5-tetramethyl-1,3,2-dioxaborolan-2-yl)aniline (109.5 mg, 0.5 mmol) gave the title compound **18l** (91.6 mg) in 82% conversion and 57% yield.

**<sup>1</sup>H NMR** (400 MHz, CDCl<sub>3</sub>)  $\delta$  7.80 – 7.75 (m, 2H), 7.37 – 7.29 (m, 4H), 6.67 (d,  $J = 8.6$  Hz, 2H), 4.69 (s, 4H), 1.34 (s, 12H). **<sup>13</sup>C{<sup>1</sup>H} NMR** (101 MHz, CDCl<sub>3</sub>, the carbon attached to quadrupole boron was not observed due to low intensity)  $\delta$  149.4, 137.7, 136.6, 127.4, 122.8, 111.1, 83.3, 53.8, 25.0. **<sup>11</sup>B{<sup>1</sup>H} NMR** (128 MHz, CDCl<sub>3</sub>)  $\delta$  31.2. **GC-MS**,  $m/z(\%) = 320$  ( $[M]^+$ , 100), 262(15), 220(25). **HR-MS (ESI)** calcd. For  $[M+Na]^+ C_{20}H_{24}NO_2^{11}BNa$  344.1792, found 344.1800 (2 ppm).

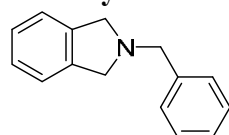
### 2-(2-(Trifluoromethyl)phenyl)isoindoline **18r**



2-Formylbenzoic acid (75.1 mg, 0.5 mmol) and 2-(trifluoromethyl)aniline (62.8  $\mu$ L, 0.5 mmol) gave the title compound **18r** (81.6 mg) in 87% conversion and 62% yield.

**<sup>1</sup>H NMR** (400 MHz, CDCl<sub>3</sub>)  $\delta$  7.68 – 7.65 (m, 1H), 7.49 – 7.45 (m, 1H), 7.32 – 7.27 (m, 4H), 7.20 (d,  $J = 8.4$  Hz, 1H), 7.00 (t,  $J = 7.7$  Hz, 1H), 4.72 (s, 4H). **<sup>13</sup>C{<sup>1</sup>H} NMR** (101 MHz, CDCl<sub>3</sub>) 148.3, 138.4, 136.0, 132.9, 128.2 (q,  $J = 6.2$  Hz), 127.3, 124.9 (q,  $J = 272.4$  Hz), 122.3, 120.6, 120.2, 58.2. **<sup>19</sup>F{<sup>1</sup>H} NMR** (376 MHz, CDCl<sub>3</sub>)  $\delta$  -56.8. **GC-MS**,  $m/z(\%) = 262$  ( $[M]^+$ , 100), 222(13), 145(15), 111(15). **HR-MS (ESI)** calcd. For  $[M+Na]^+ C_{15}H_{12}NF_3Na$  286.0819, found 286.0807 (4 ppm).

### 2-Benzylisoindoline **18t**<sup>[10]</sup>

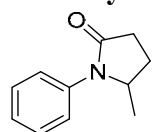


2-Formylbenzoic acid (75.1 mg, 0.5 mmol) and benzylamine (54.6  $\mu$ L, 0.5 mmol) gave the title compound **18t** (90.0 mg) in 99% conversion and 86% yield.

**<sup>1</sup>H NMR** (400 MHz, CDCl<sub>3</sub>)  $\delta$  7.46 – 7.43 (m, 2H), 7.40 – 7.36 (m, 2H), 7.32 – 7.30 (m, 1H), 7.20 (s, 4H), 3.96 (s, 4H), 3.94 (s, 2H). **<sup>13</sup>C{<sup>1</sup>H} NMR** (101 MHz, CDCl<sub>3</sub>)  $\delta$  140.4, 139.3, 128.9, 128.5, 127.2, 126.8, 122.4, 60.4, 59.1. **GC-MS**,  $m/z(\%) = 208$  ( $[M]^+$ , 45), 118(62), 91(100), 65(18).

## 6.3.9. Characterization data for pyrrolidones **6**

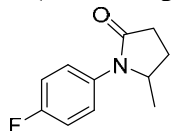
### 5-Methyl-1-phenylpyrrolidin-2-one **6a**<sup>[3]</sup>



Levulinic acid (51.2  $\mu$ L, 0.5 mmol) and aniline (45.6  $\mu$ L, 0.5 mmol) gave the title compound **6a** (76.2 mg) in 99% conversion and 87% yield.

**<sup>1</sup>H NMR** (400 MHz, CDCl<sub>3</sub>): δ 7.41 – 7.35 (m, 4H), 7.22 – 7.18 (m, 1H), 4.33 – 4.25 (m, 1H), 2.64 – 2.49 (m, 2H), 2.41 – 2.32 (m, 1H), 1.79 – 1.71 (m, 1H), 1.20 (d, *J* = 6.2 Hz, 1H). **<sup>13</sup>C NMR** (101 MHz, CDCl<sub>3</sub>): δ 174.3, 137.7, 129.1, 125.8, 124.1, 55.7, 31.4, 26.9, 20.3. **GC-MS**, *m/z*(%) = 175([M]<sup>+</sup>, 43), 160(100), 132(14), 120(31), 104(19), 91(10), 77(43), 51(21).

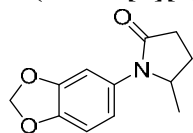
#### 1-(4-Fluorophenyl)-5-methylpyrrolidin-2-one **6b**<sup>[11]</sup>



Levulinic acid (51.2 μL, 0.5 mmol) and 4-fluoroaniline (47.4 μL, 0.5 mmol) gave the title compound **6b** (60.9 mg) in 99% conversion and 63% yield.

**<sup>1</sup>H NMR** (400 MHz, CDCl<sub>3</sub>): δ 7.33 – 7.28 (m, 2H), 7.10 – 7.04 (m, 2H), 4.26 – 4.18 (m, 1H), 2.66 – 2.48 (m, 2H), 2.41 – 2.32 (m, 1H), 1.79 – 1.70 (m, 1H), 1.18 (d, *J* = 6.2 Hz, 3H). **<sup>13</sup>C{<sup>1</sup>H} NMR** (101 MHz, CDCl<sub>3</sub>): δ 174.4, 160.5 (d, *J* = 245.4 Hz), 133.6 (d, *J* = 3.1 Hz), 126.1 (d, *J* = 8.2 Hz), 115.9 (d, *J* = 22.5 Hz), 56.0, 31.3, 26.9, 20.3. **<sup>19</sup>F{<sup>1</sup>H} NMR** (471 MHz, CDCl<sub>3</sub>) δ -116.1. **GC-MS**, *m/z*(%) = 193([M]<sup>+</sup>, 54), 178(100), 150(11), 138(48), 122(25), 109(12), 95(31), 75(12), 55(10).

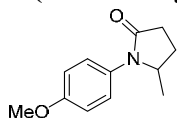
#### 1-(Benzo[d][1,3]dioxol-5-yl)-5-methylpyrrolidin-2-one **6e**<sup>[12]</sup>



Levulinic acid (51.2 μL, 0.5 mmol) and benzo[d][1,3]dioxol-5-amine (68.6 mg, 0.5 mmol) gave the title compound **6e** (73.4 mg) in 96% conversion and 67% yield.

**<sup>1</sup>H NMR** (400 MHz, CDCl<sub>3</sub>): δ 6.85 (s, 1H), 6.80 (d, *J* = 8.2 Hz, 1H), 6.70 (d, *J* = 8.0 Hz, 1H), 5.96 (s, 2H), 4.17 – 4.09 (m, 1H), 2.59 – 2.46 (m, 2H), 2.39 – 2.30 (m, 1H), 1.76 – 1.67 (m, 1H), 1.17 (d, *J* = 6.2 Hz, 3H). **<sup>13</sup>C{<sup>1</sup>H} NMR** (101 MHz, CDCl<sub>3</sub>): δ 174.5, 148.1, 145.9, 131.6, 118.3, 108.3, 106.9, 101.5, 56.5, 31.2, 26.9, 20.4. **GC-MS**, *m/z*(%) = 219([M]<sup>+</sup>, 92), 204(100), 174(10), 164(49), 132(17), 106(10), 55(10).

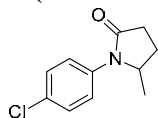
#### 1-(4-Methoxyphenyl)-5-methylpyrrolidin-2-one **6f**<sup>[12]</sup>



Levulinic acid (51.2 μL, 0.5 mmol) and 4-methoxyaniline (61.6 mg, 0.5 mmol) gave the title compound **6f** (61.6 mg) in 99% conversion and 60% yield.

**<sup>1</sup>H NMR** (400 MHz, CDCl<sub>3</sub>): δ 7.22 (d, *J* = 8.8 Hz, 2H), 6.91 (d, *J* = 8.7 Hz, 2H), 4.20 – 4.12 (m, 1H), 3.79 (s, 3H), 2.64 – 2.47 (m, 2H), 2.39 – 2.31 (m, 1H), 1.77 – 1.64 (m, 1H), 1.16 (d, *J* = 6.2 Hz, 3H). **<sup>13</sup>C{<sup>1</sup>H} NMR** (126 MHz, CDCl<sub>3</sub>): δ 174.4, 157.8, 130.5, 126.2, 114.4, 56.2, 55.5, 31.3, 26.9, 20.4. **GC-MS**, *m/z*(%) = 205([M]<sup>+</sup>, 66), 190(100), 150(34), 134(25), 122(14), 77(13), 55(15).

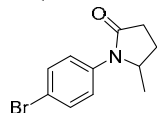
#### 1-(4-Chlorophenyl)-5-methylpyrrolidin-2-one **6g**<sup>[11]</sup>



Levulinic acid (51.2  $\mu$ L, 0.5 mmol) and 4-chloroaniline (44.6  $\mu$ L, 0.5 mmol) gave the title compound **6g** (57.7 mg) in 75% conversion and 55% yield.

**$^1\text{H}$  NMR** (400 MHz,  $\text{CDCl}_3$ ):  $\delta$  7.36 – 7.31 (m, 4H), 4.31 – 4.23 (m, 1H), 2.67 – 2.48 (m, 2H), 2.41 – 2.32 (m, 1H), 1.79 – 1.70 (m, 1H), 1.20 (d,  $J$  = 6.1 Hz, 3H).  **$^{13}\text{C}\{^1\text{H}\}$  NMR** (101 MHz,  $\text{CDCl}_3$ ):  $\delta$  174.3, 136.3, 131.0, 129.2, 125.0, 55.6, 31.4, 26.7, 20.1. **GC-MS**,  $m/z(\%)$  = 209( $[\text{M}]^+$ , 53), 194(100), 154(41), 138(20), 111(28), 75(25), 55(14).

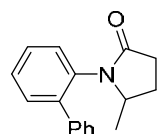
#### 1-(4-Bromophenyl)-5-methylpyrrolidin-2-one **6h**<sup>[11]</sup>



Levulinic acid (51.2  $\mu$ L, 0.5 mmol) and 4-bromoaniline (86.9 mg, 0.5 mmol) gave the title compound **6h** (75.0 mg) in 97% conversion and 59% yield.

**$^1\text{H}$  NMR** (400 MHz,  $\text{CDCl}_3$ ):  $\delta$  7.49 (d,  $J$  = 8.7 Hz, 2H), 7.28 (d,  $J$  = 8.7 Hz, 2H), 4.31 – 4.23 (m, 1H), 2.67 – 2.47 (m, 2H), 2.40 – 2.31 (m, 1H), 1.79 – 1.70 (m, 1H), 1.20 (d,  $J$  = 6.2 Hz, 3H).  **$^{13}\text{C}\{^1\text{H}\}$  NMR** (101 MHz,  $\text{CDCl}_3$ ):  $\delta$  174.3, 136.8, 132.1, 125.3, 118.8, 55.5, 31.4, 26.7, 20.1. **GC-MS**,  $m/z(\%)$  = 255 ( $[\text{M}]^+$ , 60), 238(100), 198(28), 159(32), 130(30), 119(20), 90(15), 76(24), 63(13), 55(18), 50(13).

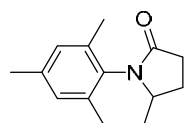
#### 1-([1,1'-biphenyl]-2-yl)-5-methylpyrrolidin-2-one **6i**<sup>[12]</sup>



Levulinic acid (51.2  $\mu$ L, 0.5 mmol) and 2-aminobiphenyl (84.6 mg, 0.5 mmol) gave the title compound **6i** (84.2 mg) in 83% conversion and 67% yield.

**$^1\text{H}$  NMR** (400 MHz,  $\text{CDCl}_3$ )  $\delta$  7.43 – 7.33 (m, 8H), 7.25 – 7.23 (m, 1H), 2.54 – 2.46 (m, 1H), 2.41 – 2.32 (m, 1H), 2.00 – 1.92 (m, 1H), 1.57 – 1.48 (m, 1H), 1.30 – 1.24 (m, 1H), 0.87 (d,  $J$  = 6.3 Hz, 3H).  **$^{13}\text{C}\{^1\text{H}\}$  NMR** (101 MHz,  $\text{CDCl}_3$ )  $\delta$  175.9, 140.3, 139.4, 135.0, 130.9, 130.4, 128.6, 128.5, 128.3, 127.7, 56.0, 31.0, 27.8, 20.1. **GC-MS**,  $m/z(\%)$  = 251( $[\text{M}]^+$ , 89), 236(100), 193(16), 180(33), 167(15), 152(34), 76(11).

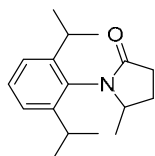
#### 1-Mesityl-5-methylpyrrolidin-2-one **6j**<sup>[13]</sup>



Levulinic acid (51.2  $\mu$ L, 0.5 mmol) and 2,4,6-trimethylaniline (70.2  $\mu$ L, 0.5 mmol) gave the title compound **6j** (42.4 mg) in 46% conversion and 39% yield.

**$^1\text{H}$  NMR** (400 MHz,  $\text{CDCl}_3$ )  $\delta$  6.92 (s, 1H), 6.89 (s, 1H), 4.07 – 3.98 (m, 1H), 2.65 – 2.49 (m, 2H), 2.45 – 2.36 (m, 1H), 2.26 (s, 3H), 2.17 (s, 3H), 2.14 (s, 3H), 1.86 – 1.76 (m, 1H), 1.09 (d,  $J$  = 6.4 Hz, 3H).  **$^{13}\text{C}\{^1\text{H}\}$  NMR** (101 MHz,  $\text{CDCl}_3$ )  $\delta$  174.4, 137.7, 137.1, 135.2, 132.1, 129.54, 129.47, 56.3, 30.8, 28.4, 21.0, 19.7, 18.7, 18.2. **GC-MS**,  $m/z(\%)$  = 217( $[\text{M}]^+$ , 84), 202(100), 158(19), 146(23), 135(27), 120(49), 98(15), 91(20), 77(10), 55(10).

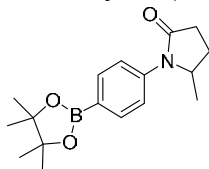
### 1-(2,6-Diisopropylphenyl)-5-methylpyrrolidin-2-one **6k**<sup>[13]</sup>



Levulinic acid (51.2  $\mu$ L, 0.5 mmol) and 2,6-diisopropylaniline (94.3  $\mu$ L, 0.5 mmol) gave the title compound **6k** (49.3 mg) in 50% conversion and 38% yield.

**<sup>1</sup>H NMR** (400 MHz, CDCl<sub>3</sub>)  $\delta$  7.31 (t,  $J$  = 7.7 Hz, 1H), 7.21 – 7.16 (m, 2H), 3.97 – 3.89 (m, 1H), 3.03 – 2.93 (m, 1H), 2.84 – 2.73 (m, 1H), 2.67 – 2.53 (m, 2H), 2.46 – 2.38 (m, 1H), 1.87 – 1.78 (m, 1H), 1.24 – 1.17 (m, 12H), 1.09 (d,  $J$  = 6.4 Hz, 3H). **<sup>13</sup>C{<sup>1</sup>H} NMR** (101 MHz, CDCl<sub>3</sub>)  $\delta$  175.2, 148.2, 146.5, 131.7, 128.8, 124.11, 124.08, 57.8, 30.9, 28.9, 28.8, 28.5, 25.4, 24.7, 24.2, 23.5, 19.8. **GC-MS**,  $m/z$ (%) = 259([M]<sup>+</sup>, 87), 244(100), 226(18), 202(10), 159(29), 145(21), 117(10), 91(14), 55(20).

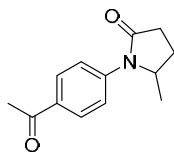
### 5-Methyl-1-(4-(4,4,5,5-tetramethyl-1,3,2-dioxaborolan-2-yl)phenyl)pyrrolidin-2-one **6l**



Levulinic acid (51.2  $\mu$ L, 0.5 mmol) and 4-(4,4,5,5-tetramethyl-1,3,2-dioxaborolan-2-yl)aniline (109.5 mg, 0.5 mmol) gave the title compound **6l** (52.7 mg) in 80% conversion and 35% yield.

**<sup>1</sup>H NMR** (400 MHz, CDCl<sub>3</sub>):  $\delta$  7.83 (d,  $J$  = 8.0 Hz, 2H), 7.43 (d,  $J$  = 8.0 Hz, 2H), 4.39 – 4.34 (m, 1H), 2.69 – 2.49 (m, 2H), 2.41 – 2.32 (m, 1H), 1.79 – 1.72 (m, 1H), 1.34 (s, 12H), 1.22 (d,  $J$  = 6.0 Hz, 3H). **<sup>13</sup>C{<sup>1</sup>H} NMR** (101 MHz, CDCl<sub>3</sub>):  $\delta$  174.3, 140.4, 135.7, 129.9, 122.6, 83.9, 55.4, 31.7, 26.8, 25.0, 20.2. **<sup>11</sup>B{<sup>1</sup>H} NMR** (128 MHz, CDCl<sub>3</sub>):  $\delta$  31.1. **GC-MS**,  $m/z$ (%) = 301 ([M]<sup>+</sup>, 58), 286(100), 202(25), 186(30), 146(20), 103(10), 55(15). **HR-MS (ESI)** calcd. for [M+Na]<sup>+</sup> C<sub>17</sub>H<sub>24</sub>NO<sub>3</sub><sup>11</sup>BNa 324.1741, found 324.1745 (1 ppm).

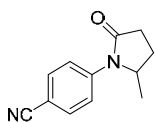
### 1-(4-Acetylphenyl)-5-methylpyrrolidin-2-one **6m**<sup>[13]</sup>



Levulinic acid (51.2  $\mu$ L, 0.5 mmol) and 4'-aminoacetophenone (67.6 mg, 0.5 mmol) gave the title compound **6m** (51.1 mg) in 60% conversion and 47% yield.

**<sup>1</sup>H NMR** (400 MHz, CDCl<sub>3</sub>):  $\delta$  7.99 (d,  $J$  = 8.4 Hz, 2H), 7.59 (d,  $J$  = 8.4 Hz, 2H), 4.46 – 4.38 (m, 1H), 2.74 – 2.65 (m, 1H), 2.59 (s, 3H), 2.56 – 2.50 (m, 1H), 2.44 – 2.35 (m, 1H), 1.84 – 1.75 (m, 1H), 1.27 (d,  $J$  = 6.1 Hz, 3H). **<sup>13</sup>C{<sup>1</sup>H} NMR** (126 MHz, CDCl<sub>3</sub>):  $\delta$  197.2, 174.5, 142.2, 133.7, 129.5, 122.1, 55.1, 31.6, 26.65, 26.58, 20.0. **GC-MS**,  $m/z$ (%) = 217([M]<sup>+</sup>, 53), 202(100), 146(13), 118(13), 91(10).

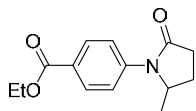
### 4-(2-Methyl-5-oxopyrrolidin-1-yl)benzonitrile **6n**<sup>[13]</sup>



Levulinic acid (51.2  $\mu$ L, 0.5 mmol) and 4-aminobenzonitrile (59.1 mg, 0.5 mmol) gave the title compound **6n** (30.0 mg) in 48% conversion and 30% yield.

**$^1\text{H}$  NMR** (400 MHz,  $\text{CDCl}_3$ ):  $\delta$  7.67 – 7.62 (m, 4H), 4.44 – 4.36 (m, 1H), 2.74 – 2.66 (m, 1H), 2.60 – 2.51 (m, 1H), 2.43 – 2.34 (m, 1H), 1.84 – 1.76 (m, 1H), 1.27 (d,  $J$  = 6.1 Hz, 3H).  **$^{13}\text{C}\{^1\text{H}\}$  NMR** (101 MHz,  $\text{CDCl}_3$ ):  $\delta$  174.6, 142.0, 133.1, 122.3, 118.9, 108.0, 54.9, 31.5, 26.4, 19.8. **GC-MS**,  $m/z(\%)$  = 200( $[\text{M}]^+$ , 45), 185(100), 157(10), 145(54), 129(19), 102(28).

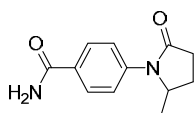
#### Ethyl 4-(2-methyl-5-oxopyrrolidin-1-yl)benzoate **6o**<sup>[14]</sup>



Levulinic acid (51.2  $\mu$ L, 0.5 mmol) and 4-aminobenzoate (82.6 mg, 0.5 mmol) gave the title compound **6o** (84.1 mg) in 75% conversion and 68% yield.

**$^1\text{H}$  NMR** (400 MHz,  $\text{CDCl}_3$ )  $\delta$  8.03 (d,  $J$  = 8.6 Hz, 2H), 7.52 (d,  $J$  = 8.6 Hz, 2H), 4.41 – 4.31 (m, 3H), 2.68 – 2.60 (m, 1H), 2.55 – 2.46 (m, 1H), 2.38 – 2.29 (m, 1H), 1.78 – 1.70 (m, 1H), 1.35 (t,  $J$  = 7.1 Hz, 3H), 1.21 (d,  $J$  = 6.2 Hz, 3H).  **$^{13}\text{C}\{^1\text{H}\}$  NMR** (101 MHz,  $\text{CDCl}_3$ )  $\delta$  174.4, 166.1, 141.9, 130.4, 126.8, 122.0, 60.9, 55.1, 31.5, 26.4, 19.8, 14.4. **GC-MS**,  $m/z(\%)$  = 247 ( $[\text{M}]^+$ , 50), 232(100), 202(20), 192(10).

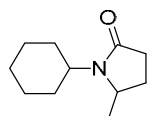
#### 4-(2-Methyl-5-oxopyrrolidin-1-yl)benzamide **6p**<sup>[13]</sup>



Levulinic acid (51.2  $\mu$ L, 0.5 mmol) and ethyl 4-aminobenzamide (68.1 mg, 0.5 mmol) gave the title compound **6p** (48.0 mg) in 53% conversion and 44% yield.

**$^1\text{H}$  NMR** (400 MHz,  $\text{CD}_3\text{OD}$ )  $\delta$  7.92 (d,  $J$  = 8.6 Hz, 2H), 7.55 (d,  $J$  = 8.6 Hz, 2H), 4.53 – 4.45 (m, 1H), 2.71 – 2.62 (m, 1H), 2.58 – 2.50 (m, 1H), 2.46 – 2.37 (m, 1H), 1.84 – 1.76 (m, 1H), 1.22 (d,  $J$  = 6.3 Hz, 3H).  **$^{13}\text{C}\{^1\text{H}\}$  NMR** (101 MHz,  $\text{CD}_3\text{OD}$ )  $\delta$  177.0, 171.6, 142.1, 132.0, 129.5, 124.6, 57.2, 32.2, 27.4, 20.0. **GC-MS**,  $m/z(\%)$  = 218( $[\text{M}]^+$ , 70), 203(100), 163(24), 146(17), 120(16), 103(10), 55(10).

#### 1-cyclohexyl-5-methylpyrrolidin-2-one **6q**<sup>[13]</sup>

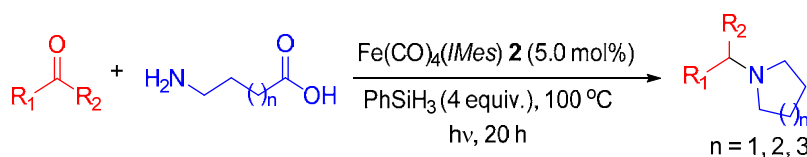


Levulinic acid (51.2  $\mu$ L, 0.5 mmol) and cyclohexylamine (57.2  $\mu$ L, 0.5 mmol) gave the title compound **6q** (65.3 mg) in 99% conversion and 72% yield.

**$^1\text{H}$  NMR** (400 MHz,  $\text{CDCl}_3$ )  $\delta$  3.80 – 3.65 (m, 2H), 2.51 – 2.35 (m, 1H), 2.27 – 2.20 (m, 1H), 2.16 – 2.06 (m, 1H), 1.82 – 1.44 (m, 8H), 1.39 – 1.25 (m, 2H), 1.22 (d,  $J$  = 6.3 Hz, 3H), 1.18 – 1.04 (m, 1H).  **$^{13}\text{C}\{^1\text{H}\}$  NMR** (101 MHz,  $\text{CDCl}_3$ )  $\delta$  174.6, 53.0, 52.6, 32.0, 30.5, 30.2, 27.6, 26.1, 26.0, 25.7, 22.5. **GC-MS**,  $m/z(\%)$  = 181( $[\text{M}]^+$ , 28), 138(64), 100(100), 84(28), 55(25).

## 6.4.- Part III-2- Reductive amination of carbonyl derivatives with $\omega$ -amino fatty acids

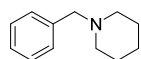
### 6.4.1. Typical procedure for the reductive amination of carbonyl derivatives with $\omega$ -amino fatty acids



A 20 mL Schlenk tube was charged with  $[\text{Fe(CO)}_4(\text{IMes})]$  **2** (5.0 mol%),  $\omega$ -amino fatty acids **19**, **23** or **25** (0.5 mmol), aldehyde **18** (0.5 mmol),  $\text{PhSiH}_3$  (4 equiv.), and toluene (0.5 mL) under argon in this order. Then the reaction mixture was stirred upon visible light irradiation (using 24 watt compact fluorescent lamp) at 100 °C for 20 h. After cooling to room temperature, the reaction was quenched by adding 2 mL THF and 2 mL NaOH (aq.) 2 N, stirred for 2 h at room temperature and then extracted with 3×2 mL of ethyl acetate. The combined organic fractions were dried over anhydrous  $\text{Na}_2\text{SO}_4$  for 0.5 h. After filtrate through degreasing cotton, the crude mixture was dried under reduced pressure. The residue was then purified by silica gel column chromatography using a mixture of heptane/ethyl acetate (60:1 to 5:1) as the eluent to afford the desired product.

### 6.4.2. Characterization of cyclic amines

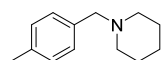
#### 1-Benzylpiperidine **20a**<sup>[15]</sup>



The title compound was prepared as described in the general procedure in 99% conversion and 95% isolated yield (83.3 mg).

**$^1\text{H}$  NMR** (400 MHz,  $\text{CDCl}_3$ )  $\delta$  7.37 – 7.29 (m, 4H), 7.29 – 7.21 (m, 1H), 3.49 (s, 2H), 2.39 (s, br, 4H), 1.62 – 1.56 (m, 4H), 1.47 – 1.41 (m, 2H).  **$^{13}\text{C}\{^1\text{H}\}$  NMR** (101 MHz,  $\text{CDCl}_3$ )  $\delta$  138.8, 129.3, 128.2, 126.9, 64.0, 54.6, 26.1, 24.5. **GC-MS**,  $m/z(\%) = 174([\text{M}]^+, 50)$ , 98(56), 91(100), 65(18), 55(10).

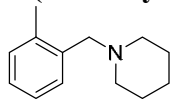
#### 1-(4-Methylbenzyl)piperidine **20b**<sup>[16]</sup>



The title compound was prepared as described in the general procedure in 99% conversion and 93% isolated yield (88.0 mg).

**$^1\text{H}$  NMR** (400 MHz,  $\text{CDCl}_3$ )  $\delta$  7.22 (d,  $J = 7.9$  Hz, 2H), 7.14 (d,  $J = 7.9$  Hz, 2H), 3.46 (s, 2H), 2.38 (s, br, 4H), 2.35 (s, 3H), 1.62 – 1.56 (m, 4H), 1.47 – 1.41 (m, 2H).  **$^{13}\text{C}\{^1\text{H}\}$  NMR** (101 MHz,  $\text{CDCl}_3$ )  $\delta$  136.4, 135.6, 129.3, 128.9, 63.7, 54.6, 26.1, 24.6, 21.2. **GC-MS**,  $m/z(\%) = 189([\text{M}]^+, 50)$ , 105(100), 84(82), 77(18), 55(10).

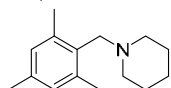
### 1-(2-Methylbenzyl)piperidine 20c<sup>[16]</sup>



The title compound was prepared as described in the general procedure in 99% conversion and 92% isolated yield (87.1 mg).

**<sup>1</sup>H NMR** (400 MHz, CDCl<sub>3</sub>) δ 7.33 – 7.29 (m, 1H), 7.21 – 7.14 (m, 3H), 3.44 (s, br, 2H), 2.43 – 2.41 (m, 4H), 2.39 (s, 3H), 1.62 – 1.56 (m, 4H), 1.50 – 1.44 (m, 2H). **<sup>13</sup>C{<sup>1</sup>H} NMR** (101 MHz, CDCl<sub>3</sub>) δ 137.5, 137.3, 130.2, 129.8, 126.8, 125.5, 61.7, 54.9, 26.3, 24.7, 19.4. **GC-MS**, m/z(%) = 189([M]<sup>+</sup>, 42), 174(10), 105(83), 84(100), 77(21), 55(10).

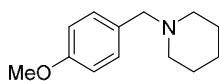
### 1-(2,4,6-Trimethylbenzyl)piperidine 20d<sup>[17]</sup>



The title compound was prepared as described in the general procedure in 99% conversion and 80% isolated yield (86.9 mg).

**<sup>1</sup>H NMR** (400 MHz, CDCl<sub>3</sub>) δ 6.84 (s, 2H), 3.39 (s, 2H), 2.37 (s, 9H), 2.28 (s, 4H), 1.54 – 1.48 (m, 4H), 1.46 – 1.41 (m, 2H). **<sup>13</sup>C{<sup>1</sup>H} NMR** (101 MHz, CDCl<sub>3</sub>) δ 138.3, 136.1, 132.7, 128.9, 56.8, 54.4, 26.5, 24.9, 21.0, 20.2. **GC-MS**, m/z(%) = 217([M]<sup>+</sup>, 28), 132(100), 117(17), 98(14), 84(29).

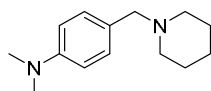
### 1-(4-Methoxybenzyl)piperidine 20e<sup>[16]</sup>



The title compound was prepared as described in the general procedure in 99% conversion and 93% isolated yield (95.5 mg).

**<sup>1</sup>H NMR** (400 MHz, CDCl<sub>3</sub>) δ 7.23 (d, *J* = 8.6 Hz, 2H), 6.85 (d, *J* = 8.6 Hz, 2H), 3.79 (s, 3H), 3.41 (s, 2H), 2.36 (s, br, 4H), 1.59 – 1.54 (m, 4H), 1.45 – 1.39 (m, 2H). **<sup>13</sup>C{<sup>1</sup>H} NMR** (101 MHz, CDCl<sub>3</sub>) δ 158.7, 130.7, 130.5, 113.5, 63.4, 55.3, 54.5, 26.1, 24.6. **GC-MS**, m/z(%) = 205([M]<sup>+</sup>, 25), 121(100), 98(18), 84(32), 77(10).

### *N,N*-Dimethyl-4-(piperidin-1-ylmethyl)aniline 20f<sup>[17]</sup>

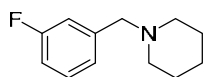


The title compound was prepared as described in the general procedure in 99% conversion and 63% isolated yield (68.8 mg).

**<sup>1</sup>H NMR** (400 MHz, CDCl<sub>3</sub>) δ 7.19 (d, *J* = 8.6 Hz, 2H), 6.72 (d, *J* = 8.6 Hz, 2H), 3.41 (s, 2H), 2.95 (s, 6H), 2.38 (s, br, 4H), 1.61 – 1.56 (m, 4H), 1.46 – 1.40 (m, 2H). **<sup>13</sup>C{<sup>1</sup>H} NMR** (101 MHz, CDCl<sub>3</sub>) δ 149.8, 130.4, 126.3, 112.4, 63.5, 54.4, 40.8, 26.1, 24.6. **GC-MS**, m/z(%) = 218([M]<sup>+</sup>, 18), 134(100), 118(10).



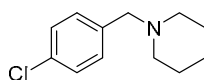
### 1-(3-Fluorobenzyl)piperidine 20g<sup>[18]</sup>



The title compound was prepared as described in the general procedure in 99% conversion and 93% isolated yield (89.9 mg).

**<sup>1</sup>H NMR** (400 MHz, CDCl<sub>3</sub>) δ 7.28 – 7.21 (m, 1H), 7.09 – 7.06 (m, 2H), 6.95 – 6.90 (m, 1H), 3.46 (s, br, 2H), 2.39 – 2.36 (m, 4H), 1.61 – 1.55 (m, 4H), 1.47 – 1.41 (m, 2H). **<sup>13</sup>C{<sup>1</sup>H} NMR** (101 MHz, CDCl<sub>3</sub>) δ 163.1 (d, *J* = 245.1 Hz), 141.8 (d, *J* = 7.0 Hz), 129.6 (d, *J* = 8.2 Hz), 124.6 (d, *J* = 2.7 Hz), 115.8 (d, *J* = 21.2 Hz), 113.8 (d, *J* = 21.2 Hz), 63.4 (d, *J* = 1.9 Hz), 54.7, 26.1, 24.5. **<sup>19</sup>F{<sup>1</sup>H} NMR** (376 MHz, CDCl<sub>3</sub>) δ -114.05. **GC-MS**, *m/z*(%) = 192([M]<sup>+</sup>, 50), 109(100), 84(78), 55(12).

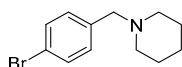
### 1-(4-Chlorobenzyl)piperidine 20h<sup>[16]</sup>



The title compound was prepared as described in the general procedure in 99% conversion and 95% isolated yield (99.6 mg).

**<sup>1</sup>H NMR** (400 MHz, CDCl<sub>3</sub>) δ 7.31 – 7.26 (m, 4H), 3.44 (s, 2H), 2.37 (s, br, 4H), 1.62 – 1.56 (m, 4H), 1.48 – 1.43 (m, 2H). **<sup>13</sup>C{<sup>1</sup>H} NMR** (101 MHz, CDCl<sub>3</sub>) δ 137.4, 132.6, 130.5, 128.3, 63.2, 54.6, 26.1, 24.5. **GC-MS**, *m/z*(%) = 208([M]<sup>+</sup>, 50), 125(100), 98(71), 84(55), 55(11).

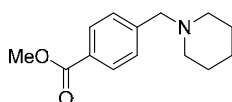
### 1-(4-Bromobenzyl)piperidine 20i<sup>[15]</sup>



The title compound was prepared as described in the general procedure in 99% conversion and 93% isolated yield (118.2 mg).

**<sup>1</sup>H NMR** (400 MHz, CDCl<sub>3</sub>) δ 7.42 (d, *J* = 8.3 Hz, 2H), 7.19 (d, *J* = 8.3 Hz, 2H), 3.40 (s, 2H), 2.35 (m, br, 4H), 1.59 – 1.53 (m, 4H), 1.45 – 1.40 (m, 2H). **<sup>13</sup>C{<sup>1</sup>H} NMR** (101 MHz, CDCl<sub>3</sub>) δ 137.9, 131.3, 130.9, 120.7, 63.2, 54.6, 26.1, 24.5. **GC-MS**, *m/z*(%) = 254([M]<sup>+</sup>, 46), 169(50), 98(100), 84(89), 55(15).

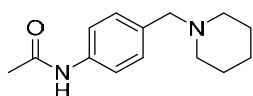
### Methyl 4-(piperidin-1-ylmethyl)benzoate 20j<sup>[17]</sup>



The title compound was prepared as described in the general procedure in 99% conversion and 62% isolated yield (72.3 mg).

**<sup>1</sup>H NMR** (400 MHz, CDCl<sub>3</sub>) δ 7.98 – 7.96 (m, 2H), 7.40 – 7.38 (m, 2H), 3.90 (s, 3H), 3.50 (s, 2H), 2.38 – 2.33 (m, 4H), 1.60 – 1.54 (m, 4H), 1.46 – 1.40 (m, 2H). **<sup>13</sup>C NMR** (101 MHz, CDCl<sub>3</sub>) δ 167.3, 144.6, 129.6, 129.1, 128.9, 63.6, 54.7, 52.1, 26.1, 24.4. **GC-MS**, *m/z*(%) = 232([M]<sup>+</sup>, 80), 202(10), 149(75), 121(23), 98(100), 84(98), 55(13).

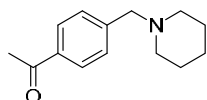
### ***N*-(4-(Piperidin-1-ylmethyl)phenyl)acetamide 20k<sup>[17]</sup>**



The title compound was prepared as described in the general procedure in 99% conversion and 78% isolated yield (90.6 mg).

**<sup>1</sup>H NMR** (300 MHz, CDCl<sub>3</sub>)  $\delta$  7.43 (d,  $J$  = 8.3 Hz, 2H), 7.25 (d,  $J$  = 8.3 Hz, 2H), 3.42 (s, 2H), 2.45 – 2.23 (m, 4H), 2.16 (s, 3H), 1.64 – 1.48 (m, 4H), 1.48 – 1.31 (m, 2H). **<sup>13</sup>C NMR** (101 MHz, CDCl<sub>3</sub>)  $\delta$  168.4, 136.7, 134.7, 129.9, 119.8, 63.4, 54.5, 26.1, 24.7, 24.5. **GC-MS**,  $m/z(\%)$  = 232([M]<sup>+</sup>, 38), 148(40), 106(100), 84(93), 78(10).

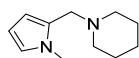
### **1-(4-(Piperidin-1-ylmethyl)phenyl)ethan-1-one 20l<sup>[19]</sup>**



The title compound was prepared as described in the general procedure in 99% conversion and 72% isolated yield (78.2 mg).

**<sup>1</sup>H NMR** (400 MHz, CDCl<sub>3</sub>)  $\delta$  7.90 (d,  $J$  = 8.3 Hz, 2H), 7.42 (d,  $J$  = 8.3 Hz, 2H), 3.51 (s, 2H), 2.59 (s, 3H), 2.37 (m, br, 4H), 1.61 – 1.55 (m, 4H), 1.46 – 1.43 (m, 2H). **<sup>13</sup>C NMR** (101 MHz, CDCl<sub>3</sub>)  $\delta$  198.1, 144.8, 136.1, 129.3, 128.4, 63.6, 54.8, 26.8, 26.1, 24.4. **GC-MS**,  $m/z(\%)$  = 216([M]<sup>+</sup>, 71), 133(62), 118(10), 98(100), 84(81), 55(15).

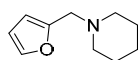
### **1-((1-Methyl-1*H*-pyrrol-2-yl)methyl)piperidine 20m<sup>[20]</sup>**



The title compound was prepared as described in the general procedure in 99% conversion and 81% isolated yield (72.2 mg).

**<sup>1</sup>H NMR** (400 MHz, CDCl<sub>3</sub>)  $\delta$  6.63 – 6.57 (m, 1H), 6.07 – 6.03 (m, 1H), 6.02 – 5.98 (m, 1H), 3.67 (s, 3H), 3.40 (s, 2H), 2.38 (s, br, 4H), 1.59 – 1.51 (m, 4H), 1.48 – 1.40 (m, 2H). **<sup>13</sup>C NMR** (101 MHz, CDCl<sub>3</sub>)  $\delta$  129.6, 122.4, 109.3, 106.1, 55.2, 54.3, 34.0, 26.2, 24.7. **GC-MS**,  $m/z(\%)$  = 178([M]<sup>+</sup>, 11), 94(100).

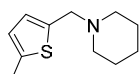
### **1-(Furan-2-ylmethyl)piperidine 20n<sup>[21]</sup>**



The title compound was prepared as described in the general procedure in 99% conversion and 97% isolated yield (80.1 mg).

**<sup>1</sup>H NMR** (400 MHz, CDCl<sub>3</sub>)  $\delta$  7.35 (m, 1H), 6.29 (m, 1H), 6.16 (m, 1H), 3.49 (s, 2H), 2.40 – 2.37 (m, 4H), 1.61 – 1.55 (m, 4H), 1.43 – 1.37 (m, 2H). **<sup>13</sup>C NMR** (101 MHz, CDCl<sub>3</sub>)  $\delta$  152.2, 142.0, 110.0, 108.6, 55.7, 54.3, 25.9, 24.3. **GC-MS**,  $m/z(\%)$  = 165([M]<sup>+</sup>, 32), 81(100), 53(18).

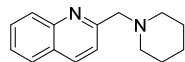
### **1-((5-Methylthiophen-2-yl)methyl)piperidine 20o<sup>[21]</sup>**



The title compound was prepared as described in the general procedure in 99% conversion and 86% isolated yield (84.0 mg).

**<sup>1</sup>H NMR** (400 MHz, CDCl<sub>3</sub>) δ 6.67 – 6.66 (m, 1H), 6.58 – 6.57 (m, 1H), 3.61 (s, br, 2H), 2.45 (s, 3H), 2.42 – 2.40 (m, 4H), 1.61 – 1.56 (m, 4H), 1.45 – 1.39 (m, 2H). **<sup>13</sup>C{<sup>1</sup>H} NMR** (101 MHz, CDCl<sub>3</sub>) δ 139.6, 139.3, 125.9, 124.4, 58.2, 54.2, 26.1, 24.5, 15.5. **GC-MS**, m/z(%) = 195([M]<sup>+</sup>, 20), 111(100), 84(32).

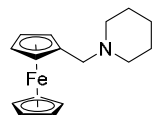
## 2-)Piperidin-1-ylmethyl)quinoline 20p<sup>[22]</sup>



The title compound was prepared as described in the general procedure in 99% conversion and 88% isolated yield (99.6 mg).

**<sup>1</sup>H NMR** (400 MHz, CDCl<sub>3</sub>) δ 8.08 (t, *J* = 9.1 Hz, 2H), 7.77 (dd, *J* = 8.1, 1.4 Hz, 1H), 7.69 – 7.64 (m, 2H), 7.50 – 7.46 (m, 1H), 3.79 (s, br, 2H), 2.48 – 2.46 (m, 4H), 1.62 – 1.57 (m, 4H), 1.48 – 1.42 (m, 2H). **<sup>13</sup>C{<sup>1</sup>H} NMR** (101 MHz, CDCl<sub>3</sub>) δ 160.4, 147.7, 136.3, 129.3, 129.1, 127.6, 127.5, 126.1, 121.3, 66.2, 55.0, 26.1, 24.4. **GC-MS**, m/z(%) = 225([M]<sup>+</sup>, 13), 143(100), 125(14), 98(12), 84(18), 55(8).

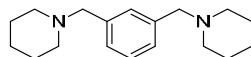
## (1-Piperidinylmethyl)ferrocene 20q<sup>[23]</sup>



The title compound was prepared as described in the general procedure in 99% conversion and 89% isolated yield (126.0 mg).

**<sup>1</sup>H NMR** (400 MHz, CDCl<sub>3</sub>) δ 4.16 – 4.15 (m, 2H), 4.09 (s, 7H), 3.35 (s, 2H), 2.32 (s, br, 4H), 1.55 – 1.49 (m, 4H), 1.37 – 1.33 (m, 2H). **<sup>13</sup>C{<sup>1</sup>H} NMR** (101 MHz, CDCl<sub>3</sub>) δ 82.8, 70.6, 68.6, 68.0, 59.1, 53.8, 25.9, 24.3. **GC-MS**, m/z(%) = 283([M]<sup>+</sup>, 95), 200(100), 186(13), 134(20), 121(64), 56(24).

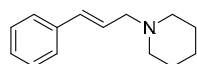
## 1,3-Bis(piperidin-1-ylmethyl)benzene 20r<sup>[24]</sup>



The title compound was prepared as described in the general procedure in 99% conversion and 58% isolated yield (79.0 mg).

**<sup>1</sup>H NMR** (400 MHz, CDCl<sub>3</sub>) δ 7.26 – 7.15 (m, 4H), 3.46 (s, 4H), 2.57 – 2.22 (m, 8H), 1.63 – 1.51 (m, 8H), 1.49 – 1.33 (m, 4H). **<sup>13</sup>C NMR** (101 MHz, CDCl<sub>3</sub>) δ 138.5, 130.3, 127.96, 127.95, 64.0, 54.6, 26.1, 24.6. **GC-MS**, m/z(%) = 271([M]<sup>+</sup>, 12), 189(100), 135(13), 105(68), 84(39), 79(16), 55(10).

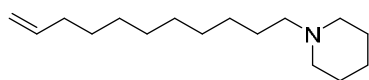
## 1-Cinnamylpiperidine 20s<sup>[25]</sup>



The title compound was prepared as described in the general procedure in 99% conversion and 73% isolated yield (73.5 mg).

**<sup>1</sup>H NMR** (400 MHz, CDCl<sub>3</sub>) δ 7.39 – 7.36 (m, 2H), 7.32 – 7.28 (m, 2H), 7.24 – 7.19 (m, 1H), 6.50 (d, *J* = 15.7 Hz, 1H), 6.31 (dt, *J* = 15.7, 6.8 Hz, 1H), 3.12 (m, 2H), 2.44 (s, br, 4H), 1.64 – 1.58 (m, 4H), 1.48 – 1.43 (m, 2H). **<sup>13</sup>C{<sup>1</sup>H} NMR** (101 MHz, CDCl<sub>3</sub>) δ 137.2, 132.7, 128.7, 127.5, 127.4, 126.4, 62.0, 54.8, 26.1, 24.5. **GC-MS**, m/z(%) = 201([M]<sup>+</sup>, 19), 117(42), 110(100), 91(14).

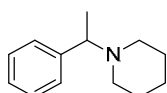
### 1-(Undec-10-en-1-yl)piperidines 20t<sup>[26]</sup>



The title compound was prepared as described in the general procedure in 99% conversion and 96% isolated yield (114.0 mg).

**<sup>1</sup>H NMR** (400 MHz, CDCl<sub>3</sub>) δ 5.81 (ddt, *J* = 17.0, 10.2, 6.7 Hz, 1H), 5.02 – 4.91 (m, 2H), 2.35 – 2.24 (m, 4H), 2.06 – 2.01 (m, 2H), 1.61 – 1.27 (m, 22H). **<sup>13</sup>C NMR** (101 MHz, CDCl<sub>3</sub>) δ 139.4, 114.2, 59.9, 54.8, 34.0, 29.8, 29.7, 29.6, 29.3, 29.1, 27.9, 27.2, 26.2, 24.7. **GC-MS**, *m/z*(%) = 237([M]<sup>+</sup>, 2), 98(100), 55(5).

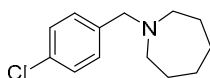
### 1-(1-Phenylethyl)piperidine 20u<sup>[27]</sup>



The title compound was prepared as described in the general procedure in 70% conversion and 56% isolated yield (53.0 mg).

**<sup>1</sup>H NMR** (400 MHz, CDCl<sub>3</sub>) δ 7.36 – 7.17 (m, 5H), 3.39 (q, *J* = 6.8 Hz, 1H), 2.49 – 2.22 (m, 4H), 1.61 – 1.49 (m, 4H), 1.41 – 1.40 (m, 2H), 1.37 (d, *J* = 6.8 Hz, 3H). **<sup>13</sup>C NMR** (101 MHz, CDCl<sub>3</sub>) δ 144.1, 128.2, 127.9, 126.8, 65.3, 51.7, 26.4, 24.8, 19.6. **GC-MS**, *m/z*(%) = 189([M]<sup>+</sup>, 8), 174(100), 112(30), 105(25), 91(19), 77(10).

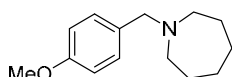
### 1-(4-Chlorobenzyl)azepane 24a<sup>[28]</sup>



The title compound was prepared as described in the general procedure in 99% conversion and 95% isolated yield (106.3 mg).

**<sup>1</sup>H NMR** (400 MHz, CDCl<sub>3</sub>) δ 7.30 – 7.25 (m, 4H), 3.59 (s, 2H), 2.61 – 2.58 (m, 4H), 1.65 – 1.61 (m, 8H). **<sup>13</sup>C NMR** (101 MHz, CDCl<sub>3</sub>) δ 138.9, 132.4, 130.1, 128.4, 62.2, 55.7, 28.4, 27.1. **GC-MS**, *m/z*(%) = 223([M]<sup>+</sup>, 38), 194(25), 180(15), 125(100), 98(53), 89(21), 69(13), 55(10).

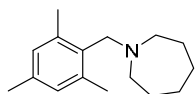
### 1-(4-Methoxybenzyl)azepane 24b<sup>[29]</sup>



The title compound was prepared as described in the general procedure in 99% conversion and 90% isolated yield (98.7 mg).

**<sup>1</sup>H NMR** (400 MHz, CDCl<sub>3</sub>) δ 7.27 – 7.23 (m, 2H), 6.87 – 6.83 (m, 2H), 3.80 (s, 3H), 3.57 (s, 2H), 2.62 – 2.59 (m, 4H), 1.66 – 1.59 (m, 8H). **<sup>13</sup>C NMR** (101 MHz, CDCl<sub>3</sub>) δ 158.6, 132.2, 130.0, 113.6, 62.2, 55.6, 55.4, 28.3, 27.2. **GC-MS**, *m/z*(%) = 219([M]<sup>+</sup>, 30), 121(100), 98(49), 77(11).

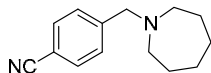
### 1-(2,4,6-Trimethylbenzyl)azepane 24c



The title compound was prepared as described in the general procedure in 89% conversion and 75% isolated yield (86.8 mg).

**<sup>1</sup>H NMR** (400 MHz, CDCl<sub>3</sub>) δ 6.82 (s, 2H), 3.52 (s, 2H), 2.56 – 2.53 (m, 4H), 2.37 (s, 6H), 2.26 (s, 3H), 1.57 (s, 8H). **<sup>13</sup>C NMR** (101 MHz, CDCl<sub>3</sub>) δ 138.2, 136.1, 133.5, 128.9, 56.1, 54.9, 28.7, 27.3, 21.0, 20.3. **GC-MS**, m/z(%) = 231([M]<sup>+</sup>, 28), 132(100), 117(15), 98(45), 91(11).

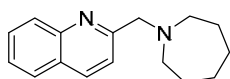
#### 4-(Azepan-1-ylmethyl)benzonitrile **24d**<sup>[29]</sup>



The title compound was prepared as described in the general procedure in 93% conversion and 82% isolated yield (87.9 mg).

**<sup>1</sup>H NMR** (400 MHz, CDCl<sub>3</sub>) δ 7.59 (d, *J* = 8.3 Hz, 2H), 7.46 (d, *J* = 8.3 Hz, 2H), 3.67 (s, 2H), 2.67 – 2.49 (m, 4H), 1.73 – 1.51 (m, 8H). **<sup>13</sup>C NMR** (101 MHz, CDCl<sub>3</sub>) δ 146.4, 132.1, 129.2, 119.3, 110.6, 62.5, 55.9, 28.5, 27.1. **GC-MS**, m/z(%) = 214([M]<sup>+</sup>, 48), 199(10), 185(55), 171(31), 145(15), 116(100), 89(30), 69(15), 55(12).

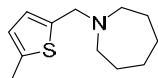
#### 2-(Azepan-1-ylmethyl)quinoline **24e**



The title compound was prepared as described in the general procedure in 99% conversion and 91% isolated yield (109.4 mg).

**<sup>1</sup>H NMR** (400 MHz, CDCl<sub>3</sub>) δ 8.11 (d, *J* = 8.5 Hz, 1H), 8.05 (d, *J* = 8.4 Hz, 1H), 7.79 (dd, *J* = 8.2, 1.4 Hz, 1H), 7.73 (d, *J* = 8.5 Hz, 1H), 7.68 (ddd, *J* = 8.4, 6.8, 1.5 Hz, 1H), 7.49 (ddd, *J* = 8.1, 6.8, 1.2 Hz, 1H), 3.97 (s, 2H), 2.73 – 2.71 (m, 4H), 1.69 – 1.62 (m, 8H). **<sup>13</sup>C NMR** (101 MHz, CDCl<sub>3</sub>) δ 161.6, 147.7, 136.3, 129.3, 129.1, 127.6, 127.5, 126.0, 121.2, 65.2, 56.1, 28.5, 27.2. **GC-MS**, m/z(%) = 241([M]<sup>+</sup>, 1), 143(100), 115(10), 98(45).

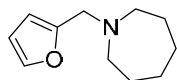
#### 1-((5-Methylthiophen-2-yl)methyl)azepane **24f**



The title compound was prepared as described in the general procedure in 99% conversion and 93% isolated yield (97.3 mg).

**<sup>1</sup>H NMR** (400 MHz, CDCl<sub>3</sub>) δ 6.65 (d, *J* = 3.4 Hz, 1H), 6.59 – 6.53 (m, 1H), 3.76 (s, 2H), 2.74 – 2.57 (m, 4H), 2.45 (s, 3H), 1.74 – 1.51 (m, 8H). **<sup>13</sup>C NMR** (101 MHz, CDCl<sub>3</sub>) δ 141.4, 139.0, 125.2, 124.3, 57.6, 55.3, 28.4, 27.1, 15.5. **GC-MS**, m/z(%) = 209([M]<sup>+</sup>, 18), 111(100), 96(35).

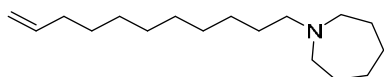
#### 1-(Furan-2-ylmethyl)azepane **24g**<sup>[30]</sup>



The title compound was prepared as described in the general procedure in 99% conversion and 95% isolated yield (85.1 mg).

**<sup>1</sup>H NMR** (400 MHz, CDCl<sub>3</sub>) δ 7.36 – 7.34 (m, 1H), 6.30 (dd, *J* = 3.2, 1.8 Hz, 1H), 6.16 (d, *J* = 3.1 Hz, 1H), 3.66 (s, 2H), 2.67 – 2.64 (m, 4H), 1.67 – 1.56 (m, 8H). **<sup>13</sup>C NMR** (101 MHz, CDCl<sub>3</sub>) δ 153.4, 141.9, 110.1, 108.1, 55.5, 54.9, 28.0, 27.1. **GC-MS**, m/z(%) = 179([M]<sup>+</sup>, 28), 150(10), 98(37), 81(100), 69(10), 53(24).

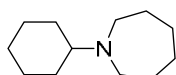
### 1-(Undec-10-en-1-yl)azepane 24h



The title compound was prepared as described in the general procedure in 99% conversion and 94% isolated yield (118.2 mg).

**<sup>1</sup>H NMR** (400 MHz, CDCl<sub>3</sub>) δ 5.81 (ddt, *J* = 17.0, 10.2, 6.7 Hz, 1H), 5.02 – 4.90 (m, 2H), 2.62 – 2.60 (m, 4H), 2.45 – 2.39 (m, 2H), 1.66 – 1.57 (m, 8H), 1.49 – 1.23 (m, 16H). **<sup>13</sup>C NMR** (101 MHz, CDCl<sub>3</sub>) δ 139.4, 114.2, 58.6, 55.8, 34.0, 29.8, 29.7, 29.6, 29.3, 29.1, 28.1, 27.8, 27.7, 27.2. **GC-MS**, *m/z*(%) = 251([M]<sup>+</sup>, 1), 112(100), 55(8).

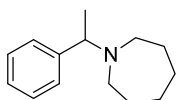
### 1-Cyclohexylazepane 24i<sup>[31]</sup>



The title compound was prepared as described in the general procedure in 91% conversion and 87% isolated yield (78.9 mg).

**<sup>1</sup>H NMR** (400 MHz, CDCl<sub>3</sub>) δ 2.68 – 2.65 (m, 4H), 2.44 – 2.36 (m, 1H), 1.89 – 1.69 (m, 4H), 1.63 – 1.57 (m, 10H), 1.23 – 1.16 (m, 4H). **<sup>13</sup>C NMR** (101 MHz, CDCl<sub>3</sub>) δ 64.4, 51.7, 29.5, 29.4, 27.2, 26.6, 26.3. **GC-MS**, *m/z*(%) = 181([M]<sup>+</sup>, 11), 138(100), 110(10), 55(11).

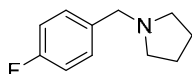
### 1-(1-Phenylethyl)azepane 24j<sup>[32]</sup>



The title compound was prepared as described in the general procedure in 76% conversion and 47% isolated yield (40.7 mg).

**<sup>1</sup>H NMR** (400 MHz, CDCl<sub>3</sub>) δ 7.36 (d, *J* = 7.1 Hz, 2H), 7.30 (t, *J* = 7.4 Hz, 2H), 7.26 – 7.17 (m, 1H), 3.76 (q, *J* = 6.7 Hz, 1H), 2.70 – 2.54 (m, 4H), 1.58 (s, 3H), 1.35 (d, *J* = 6.7 Hz, 3H). **<sup>13</sup>C NMR** (101 MHz, CDCl<sub>3</sub>) δ 145.2, 128.1, 127.7, 126.6, 63.3, 52.2, 29.1, 27.2, 18.4. **GC-MS**, *m/z*(%) = 203([M]<sup>+</sup>, 10), 188(100), 126(22), 105(38), 91(14), 79(12), 55(10).

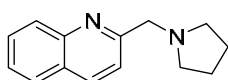
### 1-(4-Fluorobenzyl)pyrrolidine 26a



The title compound was prepared as described in the general procedure in 99% conversion and 93% isolated yield (83.3 mg).

**<sup>1</sup>H NMR** (400 MHz, CDCl<sub>3</sub>) δ 7.31 – 7.26 (m, 2H), 7.02 – 6.96 (m, 2H), 3.57 (s, 2H), 2.51 – 2.46 (m, 4H), 1.83 – 1.74 (m, 4H). **<sup>13</sup>C NMR** (101 MHz, CDCl<sub>3</sub>) δ 162.0 (d, *J* = 244.3 Hz), 135.3 (d, *J* = 3.1 Hz), 130.5 (d, *J* = 8.0 Hz), 115.1 (d, *J* = 21.2 Hz), 60.1, 54.2, 23.6. **<sup>19</sup>F NMR** (376 MHz, CDCl<sub>3</sub>) δ -116.33. **GC-MS**, *m/z*(%) = 178([M]<sup>+</sup>, 43), 109(100), 84(49), 70(39).

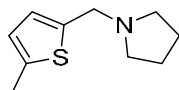
### 2-(Pyrrolidin-1-ylmethyl)quinoline 26b<sup>[22]</sup>



The title compound was prepared as described in the general procedure in 99% conversion and 87% isolated yield (92.4 mg).

**<sup>1</sup>H NMR** (400 MHz, CDCl<sub>3</sub>) δ 8.12 (d, *J* = 8.5 Hz, 1H), 8.08 (d, *J* = 8.5 Hz, 1H), 7.79 (dd, *J* = 8.1, 1.5 Hz, 1H), 7.69 (ddd, *J* = 8.4, 6.9, 1.5 Hz, 1H), 7.61 (d, *J* = 8.5 Hz, 1H), 7.51 (ddd, *J* = 8.1, 6.9, 1.2 Hz, 1H), 3.97 (s, 2H), 2.65 – 2.60 (m, 4H), 1.84 – 1.81 (m, 4H). **<sup>13</sup>C NMR** (101 MHz, CDCl<sub>3</sub>) δ 160.4, 147.8, 136.5, 129.5, 129.3, 127.6, 127.5, 126.2, 121.3, 63.2, 54.6, 23.8. **GC-MS**, *m/z*(%) = 211([M]<sup>+</sup>, 1), 143(100), 115(11).

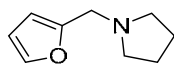
### 1-((5-Methylthiophen-2-yl)methyl)pyrrolidine **26c**<sup>[33]</sup>



The title compound was prepared as described in the general procedure in 99% conversion and 89% isolated yield (80.7 mg).

**<sup>1</sup>H NMR** (400 MHz, CDCl<sub>3</sub>) δ 6.68 (d, *J* = 3.3 Hz, 1H), 6.57 – 6.56 (m, 1H), 3.74 (s, 2H), 2.56 – 2.53 (m, 4H), 2.45 (s, 3H), 1.80 – 1.77 (m, 4H). **<sup>13</sup>C NMR** (101 MHz, CDCl<sub>3</sub>) δ 140.5, 139.2, 125.4, 124.5, 54.9, 53.9, 23.6, 15.5. **GC-MS**, *m/z*(%) = 181([M]<sup>+</sup>, 18), 111(100), 70(20).

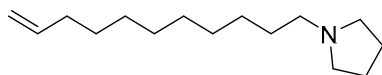
### 1-(Furan-2-ylmethyl)pyrrolidine **26d**<sup>[34]</sup>



The title compound was prepared as described in the general procedure in 99% conversion and 90% isolated yield (68.0 mg).

**<sup>1</sup>H NMR** (400 MHz, CDCl<sub>3</sub>) δ 7.36 – 7.35 (m, 1H), 6.30 (dd, *J* = 3.1, 1.9 Hz, 1H), 6.18 (d, *J* = 3.1 Hz, 1H), 3.63 (s, 2H), 2.56 – 2.52 (m, 4H), 1.80 – 1.77 (m, 4H). **<sup>13</sup>C NMR** (101 MHz, CDCl<sub>3</sub>) δ 153.2, 142.0, 110.1, 107.7, 54.0, 52.2, 23.6. **GC-MS**, *m/z*(%) = 151([M]<sup>+</sup>, 39), 108(10), 81(100), 53(20).

### 1-(Undec-10-en-1-yl)pyrrolidine **26e**<sup>[35]</sup>

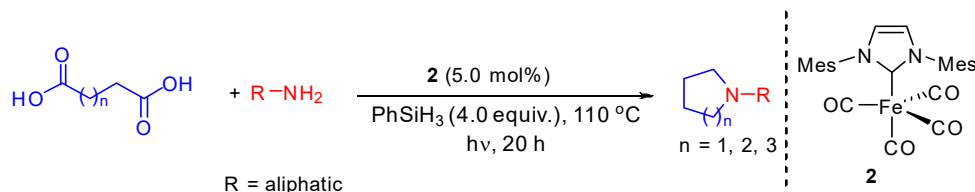


The title compound was prepared as described in the general procedure in 99% conversion and 95% isolated yield (106.1 mg).

**<sup>1</sup>H NMR** (400 MHz, CDCl<sub>3</sub>) δ 5.80 (ddt, *J* = 16.9, 10.2, 6.7 Hz, 1H), 5.01 – 4.90 (m, 2H), 2.49 – 2.45 (m, 4H), 2.42 – 2.38 (m, 2H), 1.78 – 1.75 (m, 4H), 1.53 – 1.25 (m, 16H). **<sup>13</sup>C NMR** (101 MHz, CDCl<sub>3</sub>) δ 139.4, 114.2, 56.9, 54.4, 33.9, 29.8, 29.7, 29.6, 29.3, 29.3, 29.1, 27.9, 23.5. **GC-MS**, *m/z*(%) = 233([M]<sup>+</sup>, 3), 84(100), 55(7).

## 6.5.- Part III-3- Hydrosilylation of diacids in the presence of amines

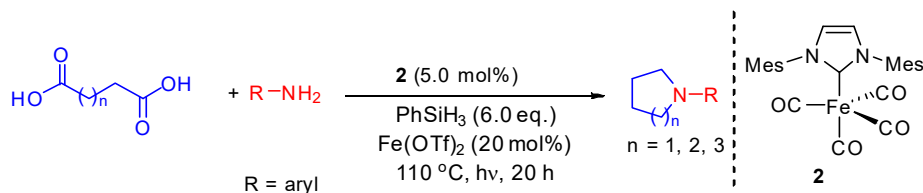
### 6.5.1. Typical procedure for the reductive amination of diacids with aliphatic amines catalyzed by Fe(CO)<sub>4</sub>(*IMes*) **2**



A 20 mL Schlenk tube was charged with [Fe(CO)<sub>4</sub>(*IMes*)] **2** (5.0 mol%), diacids (0.5 mmol), aliphatic amine (0.5 mmol), PhSiH<sub>3</sub> (4.0 equiv.), and dimethyl carbonate (0.5 mL) under argon in this order. Then the reaction mixture was stirred upon visible light irradiation (using 24 watt

compact fluorescent lamp) at 110 °C for 20 h. After cooling to room temperature, the reaction was quenched by adding 2 mL THF and 2 mL NaOH (aq.) 2 N, stirred for 2 h at room temperature and then extracted with 3×2 mL of ethyl acetate. The combined organic fractions were dried over anhydrous Na<sub>2</sub>SO<sub>4</sub> for 0.5 h. After filtrate through degreasing cotton, the crude mixture was dried under reduced pressure. The residue was then purified by silica gel column chromatography using a mixture of heptane/ethyl acetate (60:1 to 5:1) as the eluent to afford the desired product.

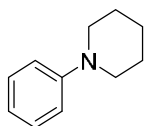
### 6.5.2. Typical procedure for the reductive amination of diacids with arylamines catalyzed by Fe(CO)<sub>4</sub>(*IMes*) 2.



A 20 mL Schlenk tube was charged with [Fe(CO)<sub>4</sub>(*IMes*)] **2** (5.0 mol%), diacids (0.5 mmol), Fe(OTf)<sub>2</sub> (20 mol%), arylamine (0.5 mmol), PhSiH<sub>3</sub> (6.0 equiv.), and dimethyl carbonate (0.5 mL) under argon in this order. Then the reaction mixture was stirred upon visible light irradiation (using 24 watt compact fluorescent lamp) at 110 °C for 20 h. After cooling to room temperature, the reaction was quenched by adding 2 mL THF and 2 mL NaOH (aq.) 2 N, stirred for 2 h at room temperature and then extracted with 3×2 mL of ethyl acetate. The combined organic fractions were dried over anhydrous Na<sub>2</sub>SO<sub>4</sub> for 0.5 h. After filtrate through degreasing cotton, the crude mixture was dried under reduced pressure. The residue was then purified by silica gel column chromatography using a mixture of heptane/ethyl acetate (60:1 to 5:1) as the eluent to afford the desired product.

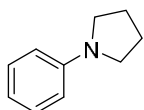
### 6.5.3. Characterization of cyclic amines

#### 1-phenylpiperidine **20w**<sup>[36]</sup>



Glutaric acid (66.1 mg, 0.5 mmol) and aniline (45.7 μL, 0.5 mmol) gave the title compound in 78% (62.9 mg) yield. <sup>1</sup>H NMR (400 MHz, CDCl<sub>3</sub>) δ 7.27 – 7.23 (m, 2H), 6.95 (d, *J* = 7.9 Hz, 2H), 6.82 (t, *J* = 7.3 Hz, 1H), 3.16 (t, 4H), 1.75 – 1.69 (m, 4H), 1.61 – 1.55 (m, 2H). <sup>13</sup>C{<sup>1</sup>H} NMR (101 MHz, CDCl<sub>3</sub>) δ 152.4, 129.1, 119.3, 116.7, 50.8, 26.0, 24.5.

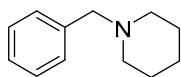
#### 1-phenylpyrrolidines **26h**<sup>[37]</sup>



Succinic acid (59.0 mg, 0.5 mmol) and aniline (45.7 μL, 0.5 mmol) gave the title compound in 88% yield (64.7 mg). <sup>1</sup>H NMR (400 MHz, CDCl<sub>3</sub>) δ 7.27 – 7.23 (m, 2H), 6.68 (t, *J* = 7.3 Hz, 1H), 6.59 (d, *J* = 7.9 Hz, 2H), 3.30 (t, *J* = 6.6 Hz, 4H), 2.04 – 2.00 (m, 4H). <sup>13</sup>C{<sup>1</sup>H} NMR (101 MHz, CDCl<sub>3</sub>) δ 148.1, 129.2, 115.5, 111.8, 47.7, 25.6.

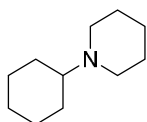


### 1-benzylpiperidine 20a<sup>[38]</sup>



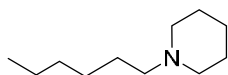
Glutaric acid (66.1 mg, 0.5 mmol) and benzylamine (54.6  $\mu$ L, 0.5 mmol) gave the title compound in 95% yield (83.3 mg).  $^1\text{H NMR}$  (400 MHz,  $\text{CDCl}_3$ )  $\delta$  7.33 – 7.31 (m, 4H), 7.29 – 7.21 (m, 1H), 3.48 (s, 2H), 2.40 – 2.37 (m, 4H), 1.62 – 1.55 (m, 4H), 1.47 – 1.42 (m, 2H).  $^{13}\text{C}\{^1\text{H}\}$  NMR (101 MHz,  $\text{CDCl}_3$ )  $\delta$  138.8, 129.3, 128.2, 126.9, 64.0, 54.6, 26.1, 24.5.

### 1-benzylpiperidine 20v<sup>[39]</sup>



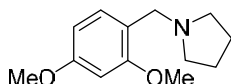
Glutaric acid (66.1 mg, 0.5 mmol) and cyclohexylamine (57.2  $\mu$ L, 0.5 mmol) gave the title compound in 94% yield (78.6 mg).  $^1\text{H NMR}$  (400 MHz,  $\text{CDCl}_3$ )  $\delta$  2.50 – 2.48 (m, 4H), 2.26 – 2.20 (m, 1H), 1.88 – 1.73 (m, 4H), 1.60 – 1.53 (m, 5H), 1.44 – 1.38 (m, 2H), 1.27 – 1.15 (m, 4H), 1.13 – 1.02 (m, 1H).  $^{13}\text{C}\{^1\text{H}\}$  NMR (101 MHz,  $\text{CDCl}_3$ )  $\delta$  64.5, 50.2, 28.9, 26.7, 26.6, 26.3, 25.1.

### 1-hexylpiperidine 20x<sup>[40]</sup>



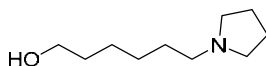
Glutaric acid (66.1 mg, 0.5 mmol) and hexylamine (66.1  $\mu$ L, 0.5 mmol) gave the title compound in 93% yield (78.6 mg).  $^1\text{H NMR}$  (400 MHz,  $\text{CDCl}_3$ )  $\delta$  2.36 – 2.33 (m, 4H), 2.27 – 2.23 (m, 2H), 1.60 – 1.54 (m, 4H), 1.50 – 1.40 (m, 4H), 1.28 – 1.26 (m, 6H), 0.87 (t,  $J$  = 6.8 Hz, 3H).  $^{13}\text{C}\{^1\text{H}\}$  NMR (101 MHz,  $\text{CDCl}_3$ )  $\delta$  59.9, 54.8, 32.0, 27.6, 27.1, 26.2, 24.7, 22.8, 14.2.

### 1-(2,4-dimethoxybenzyl)pyrrolidine 26g



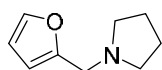
Succinic acid (59.0 mg, 0.5 mmol) and 2,4-dimethoxybenzylamine (75.1  $\mu$ L, 0.5 mmol) gave the title compound in 78% yield (86.2 mg).  $^1\text{H NMR}$  (400 MHz,  $\text{CDCl}_3$ )  $\delta$  7.21 (d,  $J$  = 8.9 Hz, 1H), 6.46 (d,  $J$  = 2.3 Hz, 1H), 6.45 (d,  $J$  = 2.2 Hz, 1H), 3.80 (s, 6H), 3.60 (s, 2H), 2.55 – 2.52 (m, 4H), 1.78 – 1.75 (m, 4H).  $^{13}\text{C}\{^1\text{H}\}$  NMR (101 MHz,  $\text{CDCl}_3$ )  $\delta$  159.9, 158.7, 131.3, 120.0, 103.9, 98.5, 55.6, 55.5, 54.2, 53.5, 23.6.

### 6-(pyrrolidin-1-yl)hexan-1-ol 26f



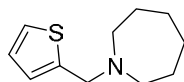
Succinic acid (59.0 mg, 0.5 mmol) and 6-amino-1-hexanol (58.6 mg, 0.5 mmol) gave the title compound in 89% yield (76.1 mg).  $^1\text{H NMR}$  (400 MHz,  $\text{CDCl}_3$ )  $\delta$  3.63 (t,  $J$  = 6.5 Hz, 2H), 2.50 – 2.46 (m, 4H), 2.44 – 2.39 (m, 2H), 1.79 – 1.75 (m, 4H), 1.61 – 1.48 (m, 4H), 1.39 – 1.34 (m, 4H).  $^{13}\text{C}\{^1\text{H}\}$  NMR (101 MHz,  $\text{CDCl}_3$ )  $\delta$  63.0, 56.7, 54.4, 32.8, 29.1, 27.5, 25.7, 23.5.

### 1-(furan-2-ylmethyl)pyrrolidine 26d<sup>[39]</sup>



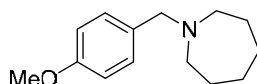
Succinic acid (59.0 mg, 0.5 mmol) and furfurylamine (44.2  $\mu$ L, 0.5 mmol) gave the title compound in 87% yield (65.8 mg). <sup>1</sup>H NMR (400 MHz, CDCl<sub>3</sub>)  $\delta$  7.36 – 7.35 (m, 1H), 6.31 – 6.30 (m, 1H), 6.18 (d,  $J$  = 2.9 Hz, 1H), 3.64 (s, 2H), 2.57 – 2.52 (m, 4H), 1.84 – 1.74 (m, 4H). <sup>13</sup>C{<sup>1</sup>H} NMR (101 MHz, CDCl<sub>3</sub>)  $\delta$  153.1, 142.0, 110.1, 107.7, 54.0, 52.2, 23.6.

### 1-(thiophen-2-ylmethyl)azepane 24k



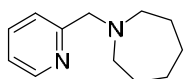
Adipic acid (73.0 mg, 0.5 mmol) and 2-thiophenemethylamine (51.3  $\mu$ L, 0.5 mmol) gave the title compound in 75% (73.2 mg) yield. <sup>1</sup>H NMR (400 MHz, CDCl<sub>3</sub>)  $\delta$  7.20 (dd,  $J$  = 5.1, 1.1 Hz, 1H), 6.94 – 6.92 (m, 1H), 6.89 – 6.88 (m, 1H), 3.85 (s, 2H), 2.68 – 2.65 (m, 2H), 1.67 – 1.60 (m, 8H). <sup>13</sup>C{<sup>1</sup>H} NMR (101 MHz, CDCl<sub>3</sub>)  $\delta$  144.1, 126.4, 125.2, 124.6, 57.4, 55.4, 28.5, 27.1.

### 1-(4-methoxybenzyl)azepanes 24b<sup>[38]</sup>



Succinic acid (59.0 mg, 0.5 mmol) and 4-methoxybenzylamine (65.3  $\mu$ L, 0.5 mmol) gave the title compound in 77% yield (84.3 mg). <sup>1</sup>H NMR (400 MHz, CDCl<sub>3</sub>)  $\delta$  7.25 (d,  $J$  = 8.3 Hz, 2H), 6.85 (d,  $J$  = 8.6 Hz, 2H), 3.80 (s, 3H), 3.57 (s, 2H), 2.61 – 2.59 (m, 4H), 1.61 (s, br, 8H). <sup>13</sup>C{<sup>1</sup>H} NMR (101 MHz, CDCl<sub>3</sub>)  $\delta$  158.6, 132.2, 130.1, 113.6, 62.2, 55.6, 55.4, 28.3, 27.2.

### 1-(pyridin-2-ylmethyl)azepane 24l



Succinic acid (59.0 mg, 0.5 mmol) and 2-picolylamine (51.5  $\mu$ L, 0.5 mmol) gave the title compound in 70% yield (66.5 mg). <sup>1</sup>H NMR (400 MHz, CDCl<sub>3</sub>)  $\delta$  8.53 – 8.52 (m, 1H), 7.64 (td,  $J$  = 7.7, 1.7 Hz, 1H), 7.49 (d,  $J$  = 7.8 Hz, 1H), 7.15 – 7.12 (m, 1H), 3.80 (s, 2H), 2.70 – 2.67 (m, 4H), 1.64 (s, br, 8H). <sup>13</sup>C{<sup>1</sup>H} NMR (101 MHz, CDCl<sub>3</sub>)  $\delta$  148.9, 136.3, 122.8, 121.7, 105.0, 64.4, 55.9, 28.2, 27.1.

## 6.6. References

- [1] H. Li, L. C. Misal Castro, J. Zheng, T. Roisnel, V. Dorcet, J.-B. Sortais, C. Darcel, *Angew. Chem. Int. Ed.* **2013**, *52*, 8045-8049.
- [2] D. Bézier, G. T. Venkanna, J.-B. Sortais, C. Darcel, *ChemCatChem* **2011**, *3*, 1747-1750.
- [3] C. Wu, X. Luo, H. Zhang, X. Liu, G. Ji, Z. Liu, Z. Liu, *Green Chem.* **2017**, *19*, 3525-3529.
- [4] B. Sezen, D. Sames, *J. Am. Chem. Soc.* **2005**, *127*, 5284-5285.
- [5] Y. Ogiwara, T. Uchiyama, N. Sakai, *Angew. Chem. Int. Ed.* **2016**, *55*, 1864-1867.
- [6] F. D. Lewis, J. M. Wagner-Brennan, A. M. Miller, *Can. J. Chem.* **1999**, *77*, 595-604.
- [7] T. Mahdi, D. W. Stephan, *Chem. Eur. J.* **2015**, *21*, 11134-11142.
- [8] T. M. Barnard, G. S. Vanier, M. J. Collins, *Org. Process Res. Dev.* **2006**, *10*, 1233-1237.
- [9] G. Ding, X. Wu, B. Lu, W. Lu, Z. Zhang, X. Xie, *Tetrahedron* **2018**, *74*, 1144-1150.
- [10] R. W. Hoffmann, B. Landmann, *Eur. J. Inorg. Chem.*, **1986**, 1039-1053.
- [11] M. Guyonnet, O. Baudoin, *Org. Lett.* **2011**, *14*, 398-401.
- [12] P. Gao, L. Liu, Z. Shi, Y. Yuan, *Org. Biomol. Chem.* **2016**, *14*, 7109-7113.
- [13] S. Wang, H. Huang, C. Bruneau, C. Fischmeister, *ChemSusChem* **2017**, *10*, 4150-4154.
- [14] B. L. Korbad, S.-H. Lee, *Chem. Commun.* **2014**, *50*, 8985-8988.
- [15] M. T. Peruzzi, Q. Q. Mei, S. J. Lee, M. R. Gagné, *Chem. Commun.* **2018**, *54*, 5855-5858.
- [16] H. Seo, M. H. Katcher, T. F. Jamison, *Nat. Chem.* **2017**, *9*, 453.
- [17] G. A. Molander, D. L. Sandrock, *Org. Lett.* **2007**, *9*, 1597-1600.
- [18] Y. He, F. Wang, X. Zhang, X. Fan, *Chem. Commun.* **2017**, *53*, 4002-4005.
- [19] F. Tinnis, A. Volkov, T. Slagbrand, H. Adolfsson, *Angew. Chem. Int. Ed.* **2016**, *55*, 4562-4566.
- [20] H. Heaney, G. Papageorgiou, R. F. Wilkins, *Tetrahedron* **1997**, *53*, 13361-13372.
- [21] J. Boulos, J. Jakubik, A. Randakova, C. Avila, *J. Heterocycl. Chem.* **2013**, *50*, 1363-1367.
- [22] M. Liman, Y. E. Türkmen, *Tetrahedron Lett.* **2018**, *59*, 1723-1727.
- [23] D.-W. Gao, Q. Gu, S.-L. You, *J. Am. Chem. Soc.* **2016**, *138*, 2544-2547.
- [24] M. J. Saif, M. Zuber, J. Anwar, M. A. Munawar, *Pol. J. Microbiol.* **2012**, *61*, 223-225.
- [25] J. B. Sweeney, A. K. Ball, P. A. Lawrence, M. C. Sinclair, L. J. Smith, *Angew. Chem. Int. Ed.* **2018**, *57*, 10202-10206.
- [26] J. A. Fernández-Salas, S. Manzini, S. P. Nolan, *Chem. Commun.* **2013**, *49*, 9758-9760.
- [27] X. Tao, G. Kehr, C. G. Daniliuc, G. Erker, *Angew. Chem. Int. Ed.* **2017**, *56*, 1376-1380.
- [28] S. Mandal, S. Mahato, C. K. Jana, *Org. Lett.* **2015**, *17*, 3762-3765.
- [29] C. Remeur, C. B. Kelly, N. R. Patel, G. A. Molander, *ACS Catal.* **2017**, *7*, 6065-6069.
- [30] S. C. Shim, C. H. Doh, B. W. Woo, H. S. Kim, K. T. Huh, W. H. Park, H. Lee, *J. Mol. Catal.* **1990**, *62*, L11-L15.
- [31] S. Westhues, M. Meuresch, J. Klankermayer, *Angew. Chem. Int. Ed.* **2016**, *55*, 12841-12844.
- [32] Y. Miki, K. Hirano, T. Satoh, M. Miura, *Angew. Chem. Int. Ed.* **2013**, *52*, 10830-10834.
- [33] S. Bhattacharyya, A. Chatterjee, J. S. Williamson, *Synth. Commun.* **1997**, *27*, 4265-4274.
- [34] A. J. Watson, A. C. Maxwell, J. M. Williams, *J. Org. Chem.* **2011**, *76*, 2328-2331.
- [35] S. B. Coan, D. Papa, *J. Am. Chem. Soc.* **1955**, *77*, 2402-2404.
- [36] T. J. Barker, E. R. Jarvo, *J. Am. Chem. Soc.* **2009**, *131*, 15598-15599.
- [37] D. Hollmann, S. Bähn, A. Tillack, R. Parton, R. Altink, M. Beller, *Tetrahedron Lett.* **2008**, *49*, 5742-5745.
- [38] D. Wei, C. Netkaew, V. Carré, C. Darcel, *ChemSusChem* **2019**, *12*, 3008-3012.
- [39] M. H. S. Hamid, C. L. Allen, G. W. Lamb, A. C. Maxwell, H. C. Maytum, A. J. Watson, J. M. Williams, *J. Am. Chem. Soc.* **2009**, *131*, 1766-1774.
- [40] Z. Sahli, B. Sundararaju, M. Achard, C. Bruneau, *Org. Lett.* **2011**, *13*, 3964-3967.

## **Chapter III - Hydrosilylation Reactions**

### **Part II - Hydrosilylation catalyzed by Group 7 metal complexes**



## Part 2 – Hydrosilylation catalyzed by Group 7 metal complexes

### III-7 Hydrosilylation of carboxylic acids, esters and amides catalyzed by $\text{Mn}_2(\text{CO})_{10}$ and $\text{Re}_2(\text{CO})_{10}$

**Contributions in this part:** Optimization, scope and mechanistic studies: Duo Wei, R. Buhaibeh.

**Publication:** D. Wei, R. Buhaibeh, Y. Canac, J.-B. Sortais, *Org. Lett.* **2019**, *in press*, doi: 10.1021/acs.orglett.9b02449.

#### 7.1. Introduction

The formation of silylated compounds catalyzed by transition-metal complexes *via* hydrosilylation reactions of unsaturated compounds have been investigated extensively in the past few decades due to the potential use of such molecules in organic synthesis and silicon industry.<sup>[1]</sup>

Manganese, the third most abundant transition metals on the Earth, is widely used in oxidation reactions, both in stoichiometric (e.g.  $\text{KMnO}_4$ ) and catalytic versions (e.g. Katsuki-Jacobsen epoxidation<sup>[2]</sup>). By contrast, compared with the well-studied Fe catalysts (see Chapter I), the development of manganese-catalyzed hydrosilylation reactions is less investigated.<sup>[3]</sup> However, more and more attention is currently being paid to its development.

On the other hand, the rhenium chemistry has been studied extensively in part due to the major interest for rhenium compounds' applications as catalysts, particularly in oxidation and oxygen atom transfer reactions.<sup>[4]</sup> Such reactivity is highlighted by organometallic complexes organorhenium(VII) trioxide, and more particularly methyltrioxorhenium ( $\text{MeReO}_3$ , abbreviated as MTO), arguably one of the most versatile transition metal catalysts known to date. Another area of the potential application of  $^{186/188}\text{rhenium}$  radioisotopes is in nuclear medicine and bio-medical chemistry.<sup>[5]</sup> Indeed, the application of organometallic rhenium compounds in the area of catalytic reaction<sup>[6]</sup>, was unveiled since the discovery of Toste for the hydrosilylation reactions in 2003.<sup>[7]</sup>

#### 7.2. Hydrosilylation reactions catalyzed by manganese and rhenium complexes: a literature survey

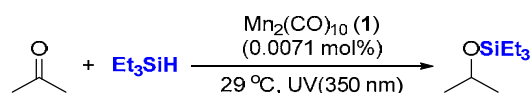
In this part, we would like to summarize the development of manganese and rhenium catalysis in hydrosilylation of unsaturated bonds, including  $\text{C}=\text{O}$ ,  $\text{C}=\text{N}$ ,  $\text{C}\equiv\text{N}$  and  $\text{NO}_2$  functional groups.

### 7.2.1. Hydrosilylation of carbonyl derivatives

The hydride reduction of a carbonyl group followed by the protection of the resulting alcohol as a silyl ether is one of the most prevalent sequences in organic chemistry. Indeed, the direct catalytic hydrosilylation of carbonyl compounds represents a one-step alternative to these procedures, yielding the silyl ether compounds.

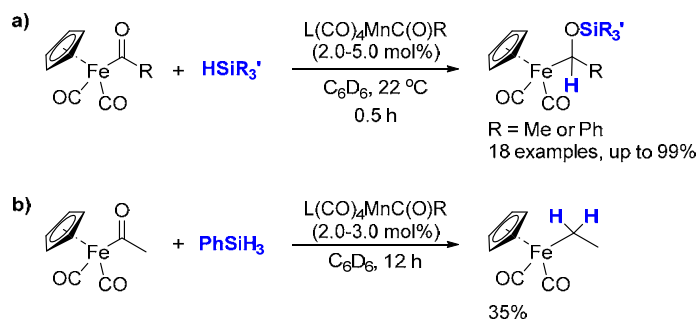
#### 7.2.1-1. Manganese catalyzed hydrosilylation of carbonyl derivatives

In 1982, Yates reported the first manganese-catalyzed hydrosilylation of acetone with  $\text{Mn}_2(\text{CO})_{10}$  **1** under UV irradiation conditions (350 nm)<sup>[8]</sup> (Scheme 1). However, the desired hydrosilylated product was detected in only 5% yield.



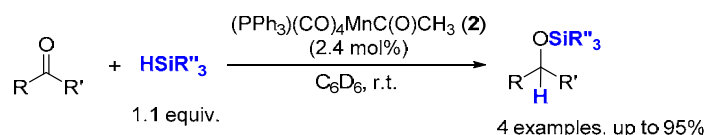
**Scheme 1.** First examples of manganese-catalyzed hydrosilylation of acetone.

In the nineties, Cutler investigated thoroughly hydrosilylation with Mn carbonyl complexes<sup>[9]</sup>  $\text{L}(\text{CO})_4\text{MnC}(\text{O})\text{R}$  ( $\text{L} = \text{CO}$ ,  $\text{R} = \text{CH}_3$ ,  $\text{Ph}$ ;  $\text{L} = \text{PPh}_3$ ,  $\text{PEt}_3$ ,  $\text{R} = \text{CH}_3$ ) (2.0-5.0 mol%) which were effective catalysts for the hydrosilylation of iron acyl compounds  $\text{FpCOR}$  [ $\text{R} = \text{CH}_3$ ,  $\text{Ph}$ ;  $\text{Fp} = (\eta\text{-C}_5\text{H}_5)\text{Fe}(\text{CO})_2$ ] with monohydro-, dihydro-, and trihydrosilanes (Scheme 2a).<sup>[9b]</sup> Phosphine-substituted manganese acetyl complex  $(\text{PPh}_3)(\text{CO})_4\text{MnCOCH}_3$  **2**, was an extremely active and selective catalyst that quantitatively transformed  $\text{FpCOCH}_3$  with  $\text{Et}_2\text{SiH}_2$  or  $\text{Ph}_2\text{SiH}_2$  into solely mono-Fp  $\alpha$ -siloxyalkyl compounds  $\text{FpCH}(\text{CH}_3)\text{OSiHR}'_2$ , with TOF up to  $83 \text{ h}^{-1}$  at r.t. (Scheme 2a). Later, they showed that the same type of manganese carbonyl complexes can catalyze the deoxygenative hydrosilylation of iron acetyl compounds  $\text{Cp}(\text{CO})_2\text{FeC}(\text{O})\text{CH}_3$  to  $\text{Cp}(\text{CO})_2\text{FeCH}_2\text{CH}_3$  with a longer reaction time (Scheme 2b).<sup>[9f]</sup>



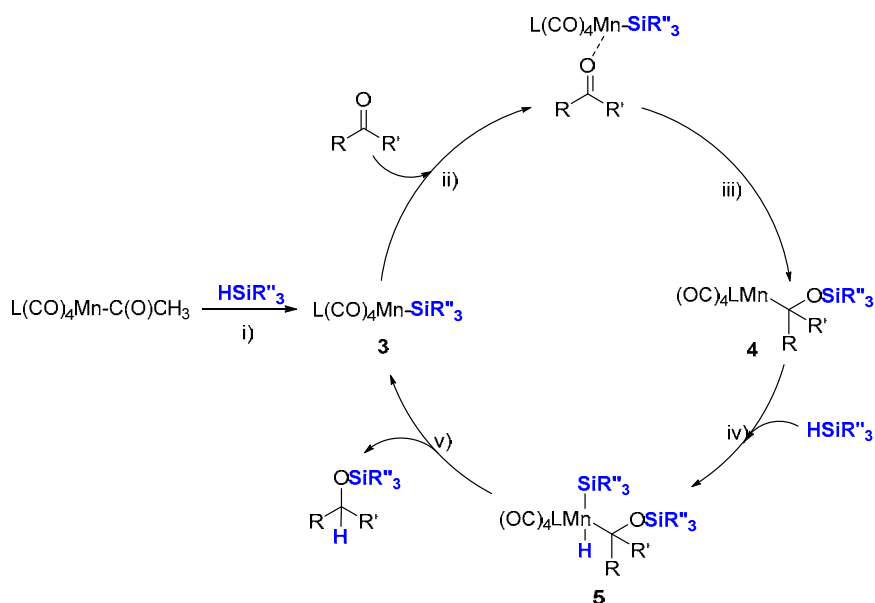
**Scheme 2.** Hydrosilylation of organoiron-carbonyl complexes catalyzed by manganese-acyl complexes

Simple ketones were also amenable in this catalytic system (Scheme 3).<sup>[9i]</sup> The hydrosilylation of acetone, acetophenone, cyclohexanone, and 2-cyclohexen-1-one was achieved with 2.4 mol% of  $(\text{PPh}_3)(\text{CO})_4\text{MnCOCH}_3$  and 1.1 equiv. of  $\text{HSiMe}_2\text{Ph}$  or  $\text{Ph}_2\text{SiH}_2$  in  $\text{C}_6\text{D}_6$  at room temperature, affording the corresponding alkoxy silanes in good yields (80-95% yields, TOF up to  $625\text{ h}^{-1}$ , Scheme 3). Notably, the hydrosilylation of 2-cyclohexen-1-one was more difficult, requiring 4 h to achieve 85% yield of (cyclohex-2-en-1-yloxy)diphenylsilane.



**Scheme 3.** Hydrosilylation of simple ketones catalyzed by manganese-acyl complexes.

The proposed mechanism is shown in Scheme 4: **i)** the catalytic active species Mn silyl complex  $\text{L}(\text{CO})_4\text{MnSiR}_3$  **3** was generated from manganese-acyl complex through ligand metathesis with the silane; **ii)** the  $\text{C}=\text{O}$  bond coordinated to the manganese center and **iii)** inserted into the  $\text{Mn-Si}$  bond of to give a manganese alkyl complex **4**; **iv)** oxidative addition of the  $\text{Si-H}$  bond to the manganese center leading to  $\text{Mn-H}$  complex **5**, which underwent **v)** reductive elimination to access the desired hydrosilylated product and regenerate the catalytic active species **3**.

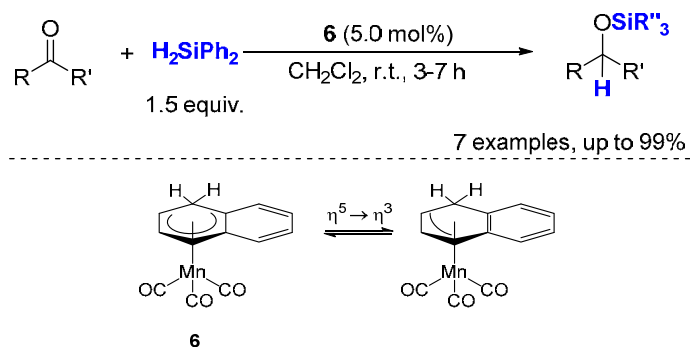


**Scheme 4.** Proposed mechanism for the hydrosilylation of ketones.

In 1999, Chung demonstrated that  $(1H\text{-hydronaphthalene})\text{-Mn}(\text{CO})_3[(\eta^5\text{-C}_{10}\text{H}_9)\text{Mn}(\text{CO})_3]$  **6** can catalyze the hydrosilylation of ketones at r.t. The activity was explained by the facile ring-slippage  $\eta^5 \rightarrow \eta^3$  of the  $1H$ -hydronaphthalene ligand (Scheme 5),<sup>[10]</sup> as neither the

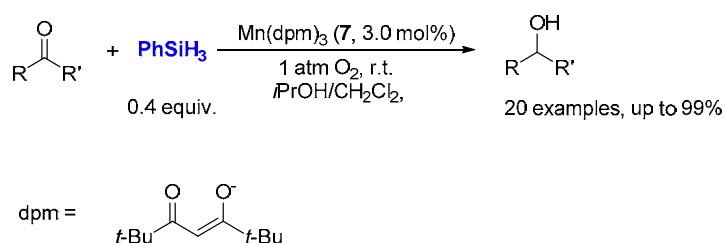


cyclohexadienyl complex ( $\eta^5\text{-C}_6\text{H}_7$ )Mn(CO)<sub>3</sub> nor the indenyl complex ( $\eta^5\text{-C}_9\text{H}_7$ )Mn(CO)<sub>3</sub> was active. As the electron-donating ability of the substituent on the substrate decreased, the yields dropped, and no reaction occurred with a strong electron-withdrawing substituent such as cyano and nitro or with the coordinating substrates such as tetrahydrofuran. This system was also sensitive to the steric hindrance as no reaction took place with 1-acetonaphthone.



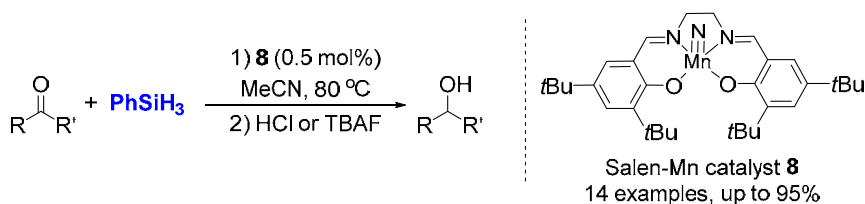
**Scheme 5.** Manganese complex in hydrosilylation reactions and its ring slippage.

In 2000, Magnus reported the hydrosilylation of aldehydes and ketones with Mn(dpm)<sub>3</sub> **7** /PhSiH<sub>3</sub>/*i*PrOH (dpm = dipivaloylmethanato) catalytic system (reaction conditions: 3.0 mol% Mn(dpm)<sub>3</sub>, 0.4 equiv. PhSiH<sub>3</sub> at r.t. under 1 atm of O<sub>2</sub>, Scheme 6).<sup>[11]</sup> Notably, aromatic aldehydes, medium ring ketones, and hindered ketones were slowly reduced.



**Scheme 6.** Hydrosilylation of ketones to alcohols catalyzed by Mn(dpm)<sub>3</sub> in the presence of PhSiH<sub>3</sub>/*i*PrOH/O<sub>2</sub>.

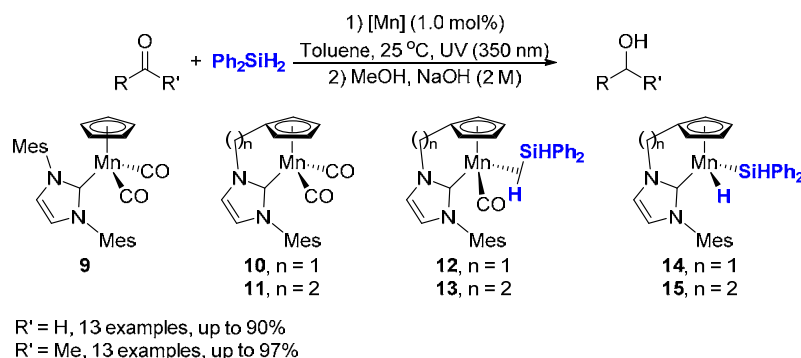
In 2013, Du developed a high valent manganese salen complex **8** for the hydrosilylation of carbonyl compounds (Scheme 7).<sup>[12]</sup> Under the optimized conditions (0.5 mol% catalyst loading, 0.5 equiv. of PhSiH<sub>3</sub> in CH<sub>3</sub>CN at 80 °C), good to excellent isolated yields of the produced alcohols were achieved within less than 3 h. Notably, tertiary silane, namely Et<sub>3</sub>SiH, was unable to serve as the reducing agent. For the  $\alpha,\beta$ -unsaturated ketone, 1,3-diphenyl-2-propen-1-one, 45% yield of saturated ketone 1,3-diphenyl-propan-1-one was isolated.



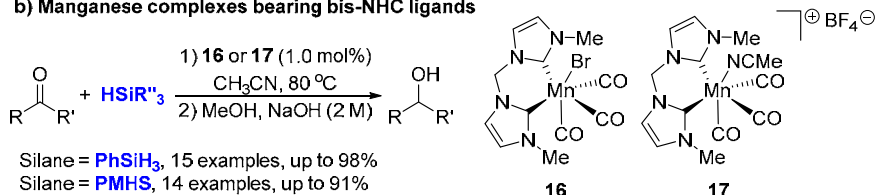
**Scheme 7.** Hydrosilylation of ketones catalyzed by the Salen–Mn complex **8**.

Interestingly, NHC–Mn complexes **9–15** were developed by our group for the hydrosilylation of carbonyl compounds under UV irradiation (350 nm) (Scheme 8a).<sup>[13]</sup> Compared with the initial half-sandwich complex **9**, the reactivity of two tethered complexes **10** and **11** were relatively low so that the Mn-silane  $\sigma$ -complexes **12** and **13** were isolated successfully. Based on the mechanistic study, a traditional Ojima mechanism<sup>[14]</sup> was proposed for the reaction with formation of active noncarbonyl Mn(III) **14** and **15** as the key intermediates. Very recently, Royo's group developed bis-NHC-Mn complexes **16** and **17**, which were shown to be effective catalysts for the hydrosilylation of carbonyl compounds with a wide substrate scope.<sup>[15]</sup> It is worth mentioning that this reaction worked well even with the inexpensive silane PMHS (polymethylhydrosiloxane) (Scheme 8b).

**a) Half-sandwich Mn complexes bearing NHC ligands**



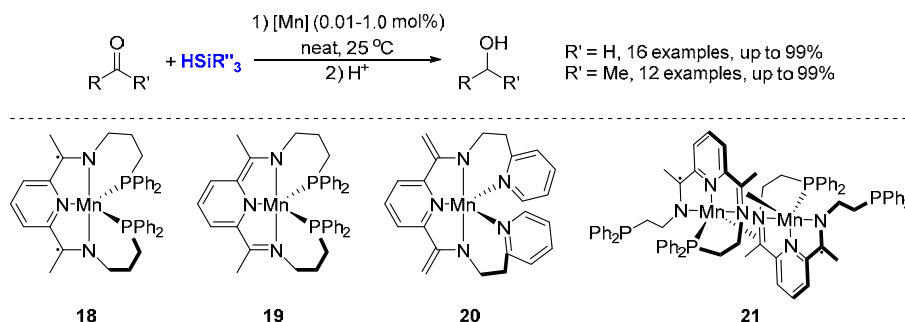
**b) Manganese complexes bearing bis-NHC ligands**



**Scheme 8.** Hydrosilylation of aldehydes and ketones catalyzed by NHC–Mn complexes.

Since 2014, Trovitch's group has developed a series of manganese complexes **18–20**,<sup>[16]</sup> with a pentadentate ligand. The extremely high reactive complex for the hydrosilylation of ketones (TOF up to 1280 min<sup>−1</sup>)<sup>[16a]</sup> and aldehydes (TOF up to 4900 min<sup>−1</sup>)<sup>[16d, 16e]</sup> is (Ph<sub>2</sub>PPrPDI)Mn (**18**) (PDI=pyridine diimine). The dimer complex **21** gave a TOF of 4950 min<sup>−1</sup> for the

hydrosilylation of aldehydes, which is the highest TOF so far for all the base-metal catalysts (Scheme 9).



**Scheme 9.** PDI-Mn complexes catalyzed hydrosilylation of carbonyl compounds.

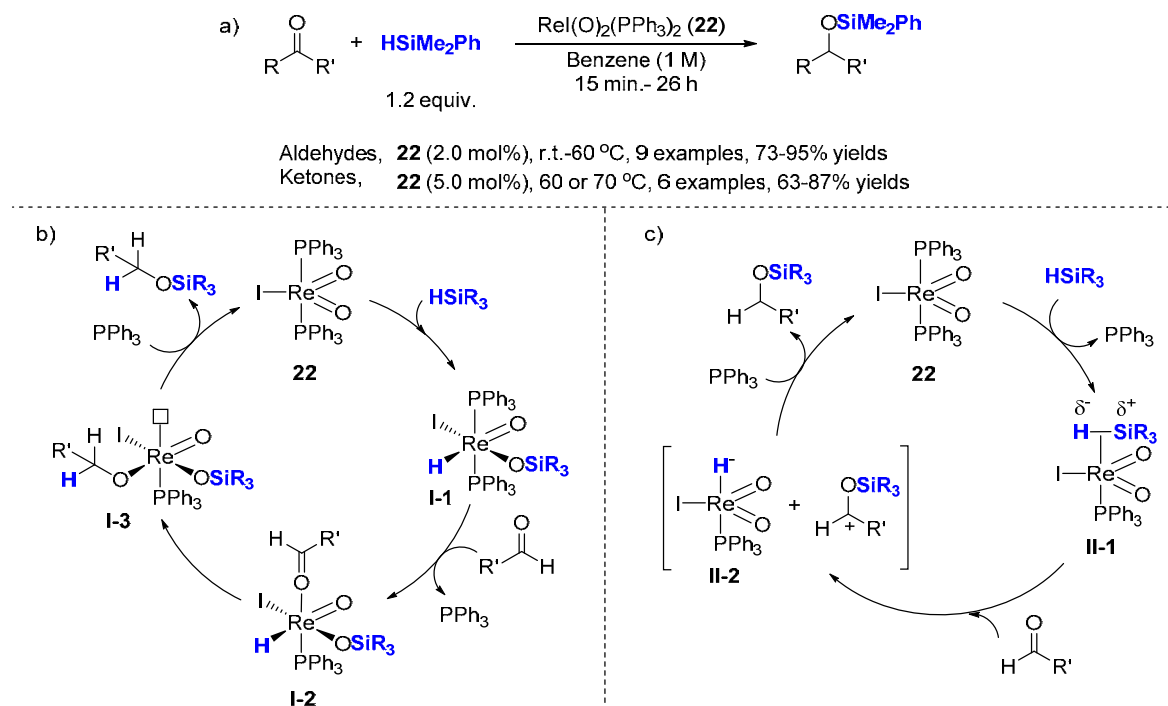
### 7.2.1-2. Rhenium-catalyzed hydrosilylation of carbonyl derivatives

The high-oxidation state rhenium catalysts have been examined in reductions in the last 16 years.<sup>[6, 17]</sup> The first rhenium-catalyzed hydrosilylation, (which is also the first example for a hydrosilylation catalyst with high-valent rhenium species and bearing two terminal oxo ligands) was described in 2003 by Toste *et al* (Scheme 10a). This novel reactivity represents a complete reversal from the traditional role of these complexes as oxidation catalysts. The hydrosilylation of aldehydes and ketones were catalyzed by the readily available iododioxo(bistriphenylphosphine)rhenium(V) [(PPh<sub>3</sub>)<sub>2</sub>Re(O)<sub>2</sub>I] **22**.<sup>[7]</sup> The substrates scope was readily extended to aromatic or aliphatic ketones and aldehydes with a good tolerance towards numerous functional groups (amino, nitro, halides, ester, cyano, cyclopropyl and alkenyl groups are left untouched). This reaction provides an efficient and practical one-step reduction-protection method, showing also tolerance to air and moisture.

A detailed mechanism, confirmed by computational study (DFT calculations) by Wu *et al.* in 2006,<sup>[18]</sup> was proposed by the same group based on experimental studies (Scheme 10b).<sup>[7a, 19]</sup> The first step involved a formal [2+2] addition of silane to the Re=O bond in **22** to produce metal hydride **I-1**, which was isolated and characterized by X-ray diffraction. Alkoxy-metal intermediate **I-3** was produced by addition of the rhenium hydride to the carbonyl group. Transfer of the silyl group to the alkoxy ligand, formally a *retro*-[2+2] reaction, produced the silyl ether product and regenerates dioxo catalyst **22**.

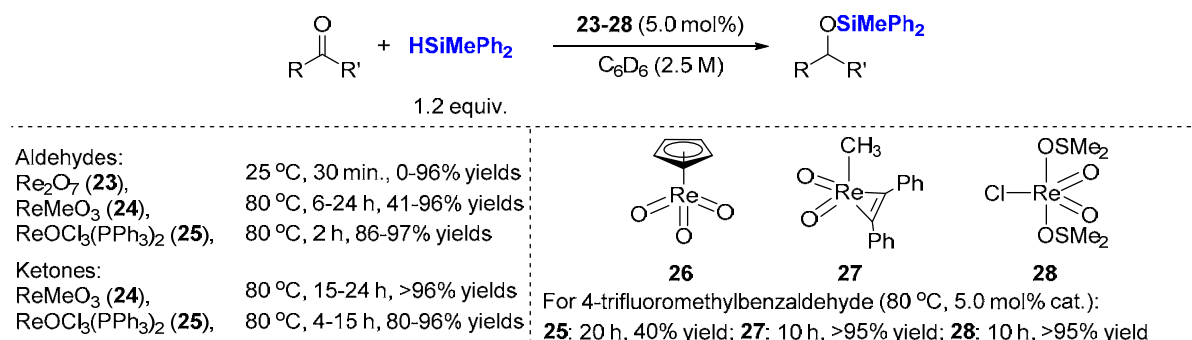
However, the computational study by Wei<sup>[20]</sup> supported that an ionic outer-sphere mechanistic pathway was the preferable route for the **22** catalyzed hydrosilylation of carbonyl compounds and imines (Scheme 10c). The ionic outer-sphere mechanism involved the activation of Si-H

through  $\eta^1$ -bonding of silane to the metal center and subsequent nucleophilic attack on  $\eta^1$ -silane *via* organic substrates to promote the heterolytic cleavage of the Si–H bond. Along the ionic outer-sphere mechanistic catalytic cycle, the metal center acted as a Lewis acid to render the Si–H bond more polarized and more susceptible to the nucleophilic attack by organic substrates.<sup>[21]</sup>



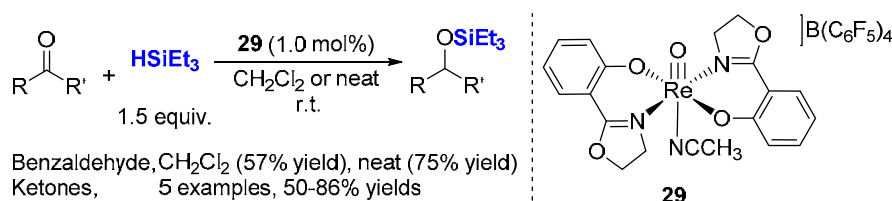
**Scheme 10.**  $\text{ReI(O)}_2(\text{PPh}_3)_2$  **22** catalyzed hydrosilylation of carbonyl compounds and its mechanism studies.

Following the work of Toste, the oxo-rhenium complexes were extended to **23-28** which showed similar activity in the hydrosilylation of aliphatic and aromatic aldehydes (6 examples) and ketones (4 examples) by Romão *et al* in 2005 with  $\text{HSiMePh}_2$  in  $\text{C}_6\text{D}_6$  solution (Scheme 11).<sup>[22]</sup> **23** catalyzed the hydrosilylation of aldehydes at r.t. within 30 min. affording the corresponding silyl ethers in good yield, but was ineffective as ketone hydrosilylation catalyst (even at 80 °C). **26-28** (5.0 mol%) were active for hydrosilylation of 4-trifluoromethylbenzaldehyde at 80 °C, giving the corresponding alcohol with 40% yield (**26**, 20 h), >95% yield (**27**, 10 h) and >95% yield (**28**, 10 h) respectively.



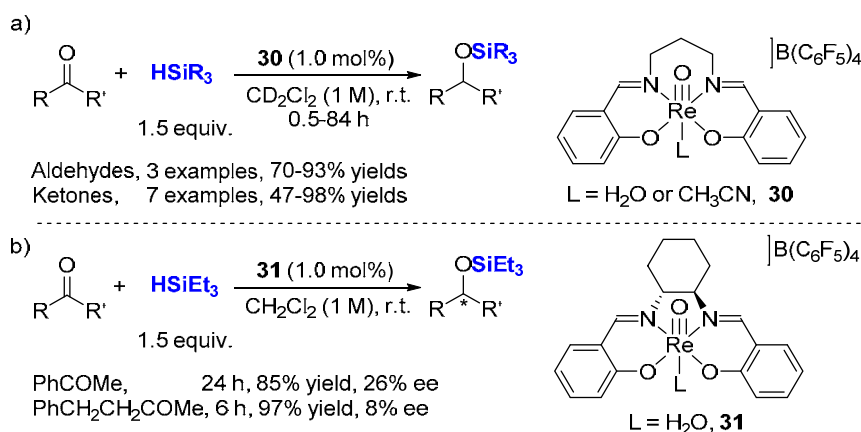
**Scheme 11.** Reduction of carbonyl derivatives by high-valent rhenium oxides **23-28**.

In the same year, Abu-Omar and co-workers reported a new system for the hydrosilylation of aldehydes and ketones using a monooxorhenium(V) catalyst **29** containing an oxazoline ligand (Scheme 12).<sup>[23]</sup> The reaction proceeded efficiently under ambient temperature with a low catalyst loading (0.1 mol %), 1.5 equiv. HSiEt<sub>3</sub> and the reaction could be performed without solvent. The catalyst retained activity after being recycled, for 2-butanone 80% NMR yield (1<sup>st</sup> cycle) and 50% NMR yield (2<sup>nd</sup> cycle).



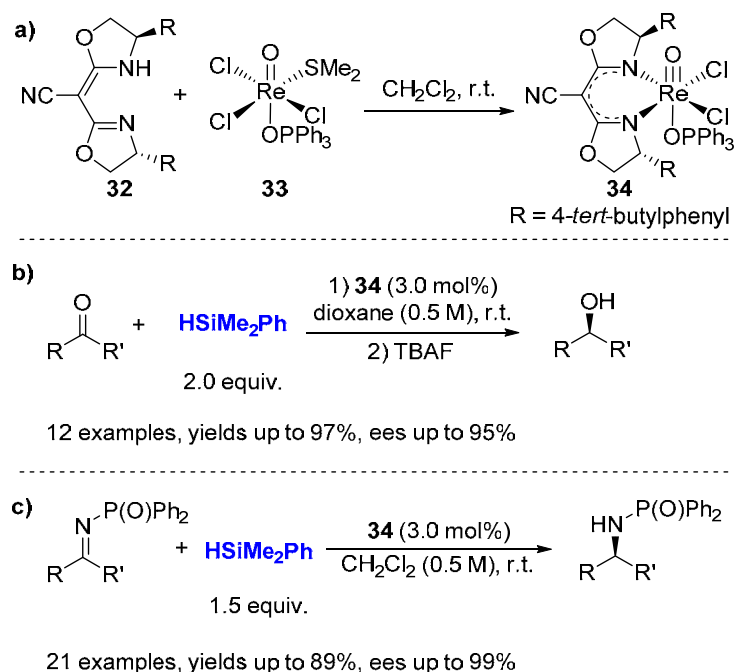
**Scheme 12.** Reduction of carbonyl derivatives by rhenium oxide containing oxazoline.

Then, the same group prepared a number of cationic oxorhenium(V) salen based complexes such as [Re(O)(salpn)(Solv)][B(C<sub>6</sub>F<sub>5</sub>)<sub>4</sub>] **30**<sup>[24]</sup> in 2006 (Scheme 13a) and [ReO(saldach)(H<sub>2</sub>O)][B(C<sub>6</sub>F<sub>5</sub>)<sub>4</sub>] **31**<sup>[25]</sup> in 2008 incorporating a chiral environment, (Scheme 13b). **30** and **31** serve as good catalysts for hydrosilylation of carbonyl compounds (1.0 mol% cat. loading, 1.5 equiv. silane, r.t.). Although, asymmetric versions (**30**) of these reactions afforded poor enantioselectivity even with bulky silanes.



**Scheme 13.** Hydrosilylation of carbonyl compounds with cationic oxorhenium(V) salen based complexes.

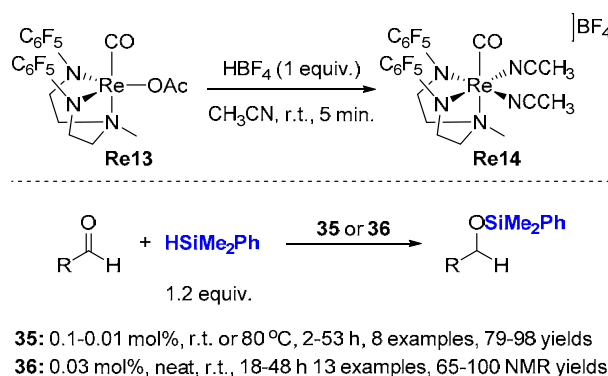
Another application of chiral (CN-box)Re(V)-oxo complexes [3.0 mol%, CN-Box = cyanobis(oxazoline)] in enantioselective reduction of prochiral ketones<sup>[26]</sup> and imines<sup>[27]</sup> with 2 equiv. of HSiMe<sub>2</sub>Ph was reported by Toste and his colleagues in 2010 (Scheme 14). Stirring **32** with Re(O)Cl<sub>3</sub>(OPPh<sub>3</sub>)(SMe<sub>2</sub>) **33** in CH<sub>2</sub>Cl<sub>2</sub> at r.t. yielded (CN-box)ReV-oxo **34** as a green solid. These reductions proceeded under an ambient air atmosphere with highly functional group tolerance with ees up to 99%. The (CNbox)ReV-oxo complexes can be pre-formed and isolated as benchtop stable solids or generated *in situ*.



**Scheme 14.** Enantioselective reduction of ketones and imines catalyzed by (CN-Box)ReV-oxo complexes.

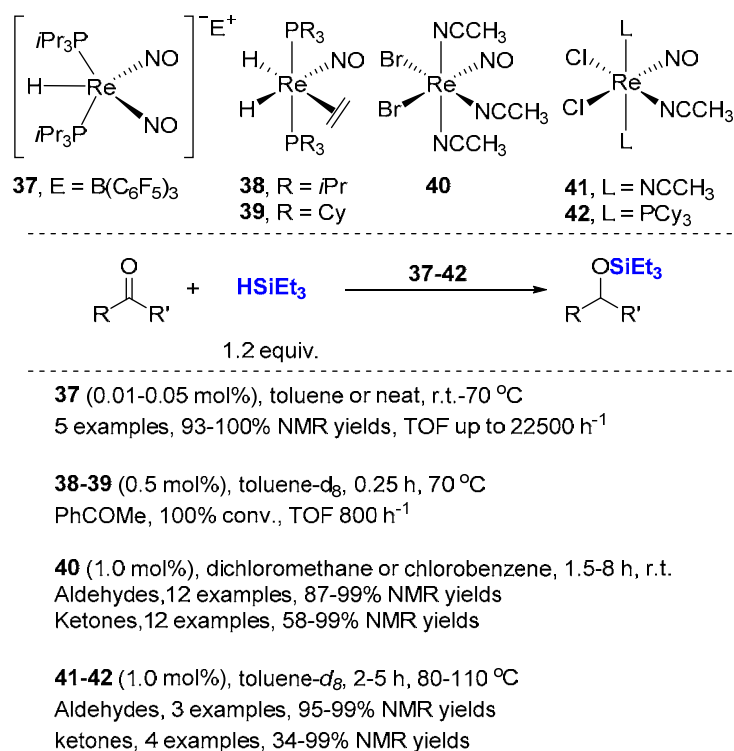
Besides these oxorhenium complexes, a series of novel low-valent Re(III) complexes were synthesized by Ison *et al.*, such as **35**<sup>[28]</sup> in 2012 and **36**<sup>[29]</sup> in 2017 (Scheme 15). **36** (0.03 mol%,

r.t.) was more reactive than **35** (0.1 mol%, 80 °C) for the hydrosilylation of aldehydes. Good to excellent NMR yields (65-100%, 13 examples) were achieved at ambient temperature under neat conditions using HSiMe<sub>2</sub>Ph with **36**. The reaction afforded TON up to 9200 and TOF up to 126 h<sup>-1</sup> (Scheme 15).



**Scheme 15.** Cationic rhenium complexes catalyzed hydrosilylation of aldehydes.

Berke and co-workers reported several easily available rhenium complexes, for example, Re(H)(PiPr<sub>3</sub>)<sub>2</sub>(NO)(NOB(C<sub>6</sub>F<sub>5</sub>)<sub>3</sub>) **37**<sup>[30]</sup> in 2004, Re(H)<sub>2</sub>(η<sup>2</sup>-C<sub>2</sub>H<sub>4</sub>)<sub>3</sub>(NO)(PR<sub>3</sub>)<sub>2</sub> **38** (R = *i*Pr), **39** (R = Cy)<sup>[31]</sup> in 2008, Re(CH<sub>3</sub>CN)<sub>3</sub>Br<sub>2</sub>(NO) **40**<sup>[32]</sup> in 2009, Re(CH<sub>3</sub>CN)<sub>3</sub>Cl<sub>2</sub>(NO) **41**<sup>[33]</sup> and Re(CH<sub>3</sub>CN)Cl<sub>2</sub>(NO)(PCy<sub>3</sub>)<sub>2</sub> **42**<sup>[33]</sup> in 2011. Those nitrosyl rhenium complexes were employed in the catalytic hydrosilylation of a variety of carbonyl compounds (Scheme 16). Hydrosilylations of carbonyl compounds were carried out with the catalyst **37**, HSiR<sub>3</sub> (1 equiv., R = Et or Ph) at r.t.-70 °C. Either toluene or no solvent was applied. TONs up to 9000 and TOFs up to 22500 h<sup>-1</sup> were observed. **38** and **39** exhibited similar activity in hydrosilylation of acetophenone with 0.5 mol% cat. loading at 70 °C in toluene-*d*<sub>8</sub>, giving full conversion and TOF up to 800 h<sup>-1</sup>.

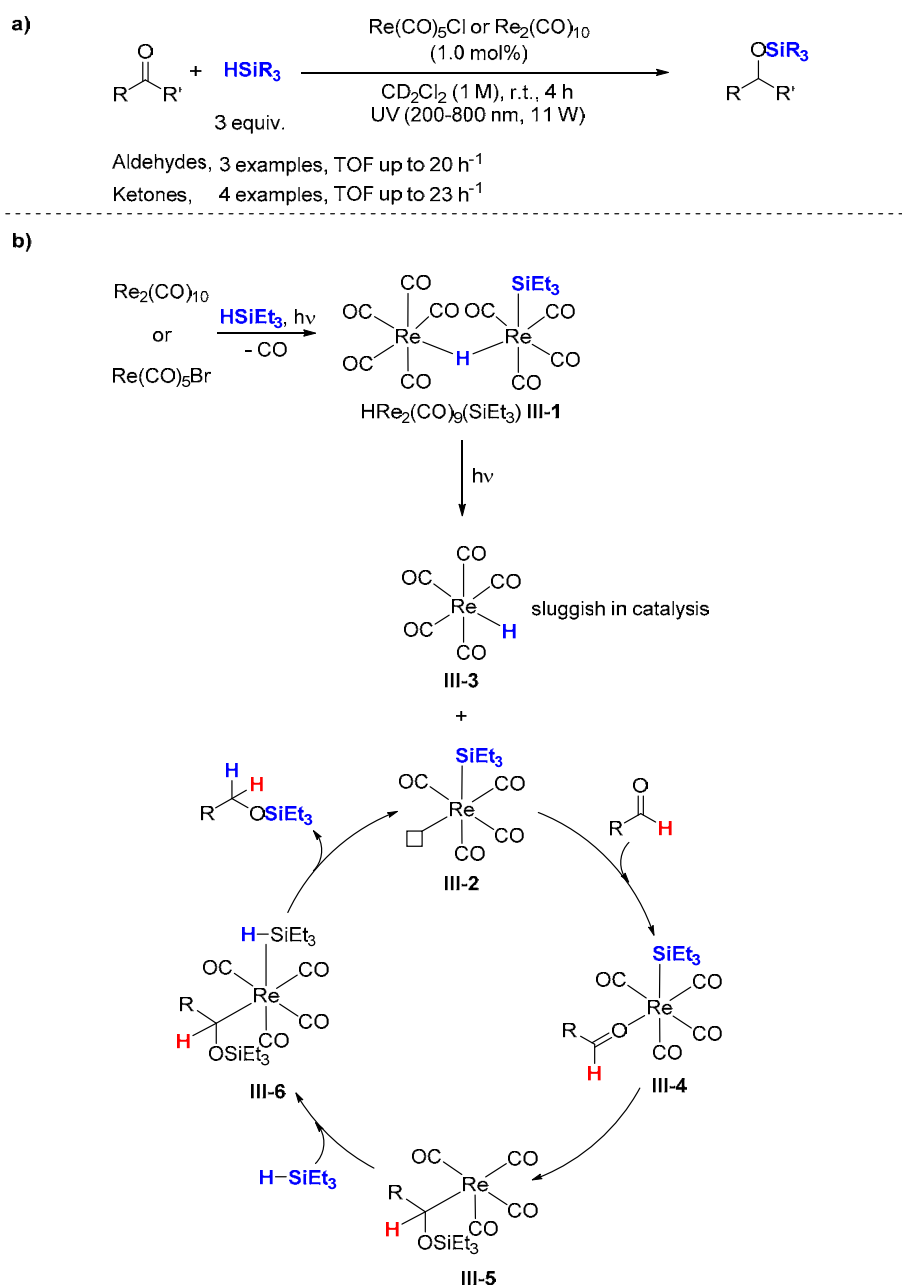


**Scheme 16.** Nitrosyl-rhenium complexes catalyzed hydrosilylation of carbonyl compounds.

For **40**, chlorobenzene was found to be superior over all the other solvents used. Various aliphatic and aromatic silanes were tested. Excellent yields were achieved at r.t. in dichloromethane using triethylsilane, the reaction affording TOF values of up to 495 h<sup>-1</sup>. Phosphine-free complex **41** proved to be less effective than the bisphosphine derivatives **42**, as when the reaction of benzophenone and Et<sub>3</sub>SiH (1.12 equiv.) with 1.0 mol% of **42** was carried out at 80 °C, a conversion of less than 10% was achieved within 4 h, while in the same condition **42** gave 99% yield (Scheme 16).

In 2012, Re(CO)<sub>5</sub>Cl **43** and Re<sub>2</sub>(CO)<sub>10</sub> **44** have been found by Fan and co-workers<sup>[34]</sup> to be effective catalysts for the hydrosilylation of carbonyl substrates with various silanes and with TOF of 20-25 h<sup>-1</sup> for aldehydes (Scheme 17a). In this methodology, 1.0 mol% catalyst and a Et<sub>3</sub>SiH:carbonyl derivative ratio of 3:1 has been used. When different silanes such as Ph<sub>2</sub>SiH<sub>2</sub> and Ph<sub>3</sub>SiH were used, a decrease in the corresponding silyl ether yield was observed.





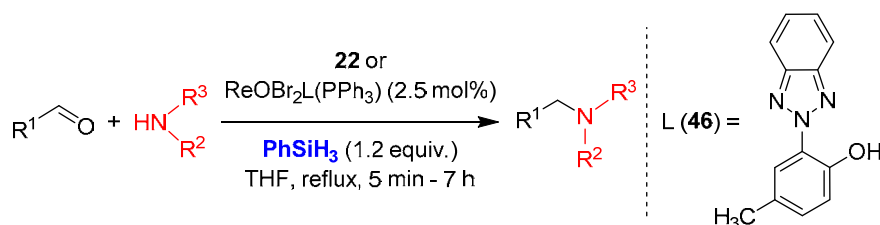
**Scheme 17.** Catalyzed hydrosilylation of carbonyl derivatives *via* Re(CO)<sub>5</sub>Cl photolysis.

A detailed mechanism for the hydrosilylation of carbonyl compounds was proposed by this group to account for the experimental observations (Scheme 17b). Upon photolysis of Et<sub>3</sub>SiH with Re(CO)<sub>5</sub>Cl or Re<sub>2</sub>(CO)<sub>10</sub>, a dimeric rhenium carbonyl species **III-1** with a bridging hydride has been identified in the mixture. When **III-1** was isolated and tested for aldehyde hydrosilylation, the silyl ether was generated about 2–3 times faster in comparison to Re(CO)<sub>5</sub>Cl.

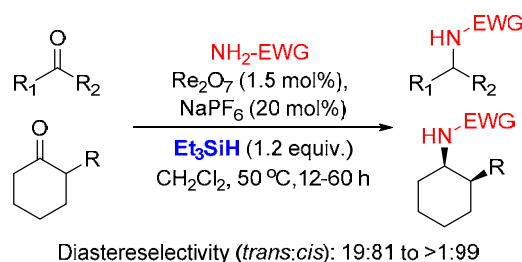
Upon photolysis, the dimer **III-1** dissociated to afford Et<sub>3</sub>SiRe(CO)<sub>4</sub> **III-2** and HRe(CO)<sub>5</sub> **III-3**. Notably, the authors have shown that HRe(CO)<sub>5</sub> **III-3** was sluggish in catalysis. So the

catalytic active species could be  $\text{Et}_3\text{SiRe}(\text{CO})_4$  **III-2**. Starting from **III-2**, the carbonyl substrate underwent coordination onto the vacant site and facilitated the silyl ligand shift onto the oxygen atom. This process resulted in the formation of an alkyl ligand bound to the Re center **III-5**. Another silane underwent coordination *via* a  $\eta^2$ -silyl complex or a  $\sigma$ -silyl ( $\sigma_{\text{H}}$ ) complex. The H atom migrated from the silane to the alkyl group, thus regenerating the catalyst **III-2** and releasing the silyl ether product. When either the carbonyl or silane has been depleted, the  $\text{Et}_3\text{SiRe}(\text{CO})_4$  **III-2** coordinated back to  $\text{HRe}(\text{CO})_5$  **III-3** and became part of the resting state **III-1** (Scheme 17b).

Interestingly, the direct reductive amination of aldehydes with primary and secondary anilines, using the same oxorhenium complex  $\text{ReI}(\text{O})_2(\text{PPh}_3)_2$  **22**, was achieved by the group of Fernandes. Under refluxing THF for 5 min to 7 h, the corresponding amines were prepared with 72–90% yields (Scheme 18). Noticeably, nitro, sulfone, ester, nitrile, amide, halides including iodide can be tolerated.<sup>[35]</sup> The same group have also developed a series of oxorhenium complexes bearing heterocyclic ligands to perform this transformation, for instance, the oxo-rhenium complex  $[\text{ReOBr}_2(\text{L})(\text{PPh}_3)]$  **45** ( $\text{L} = 2$ -(2'-hydroxy-5'-methylphenyl)benzotriazole, **46**) was used as a catalyst (2.5 mol%) with the same efficiency and chemoselectivity in refluxing THF (Scheme 18).<sup>[36]</sup>



**Scheme 18.** Direct reductive amination of aldehydes using silane/oxorhenium catalytic system. Furthermore, in 2013 Ghorai reported a direct reductive amination of ketones such as alkanones and cycloalkanones with electron-deficient amines using  $\text{Re}_2\text{O}_7$  (**23**, 1.5 mol%) and  $\text{NaPF}_6$  (20 mol%) as the catalytic system and triethylsilane (1.2 equiv.) as the reductant in dichloromethane at 50 °C for 12–60 h (Scheme 19).<sup>[37]</sup> The diastereoselective reductive amination of 2-alkyl cyclohexanones were studied and excellent formation of *cis*-selective 2-alkyl amines (up to >1:99) were observed.

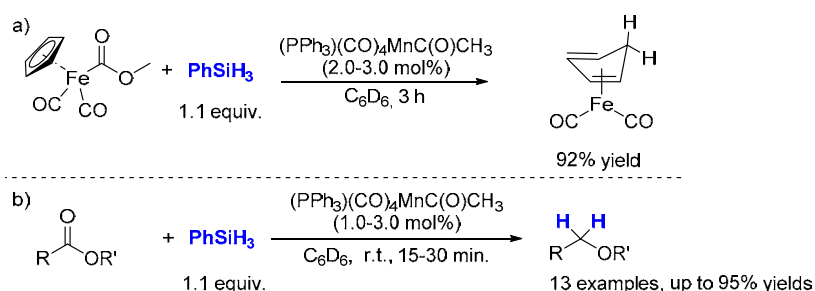


**Scheme 19.** Direct reductive amination of ketones with electron-deficient amines using  $\text{Re}_2\text{O}_7/\text{NaPF}_6$  catalyst system.

## 7.2.2. Hydrosilylation of carboxylic acid derivatives

### 7.2.2-1 Manganese-catalyzed hydrosilylation of carboxylic acid derivatives

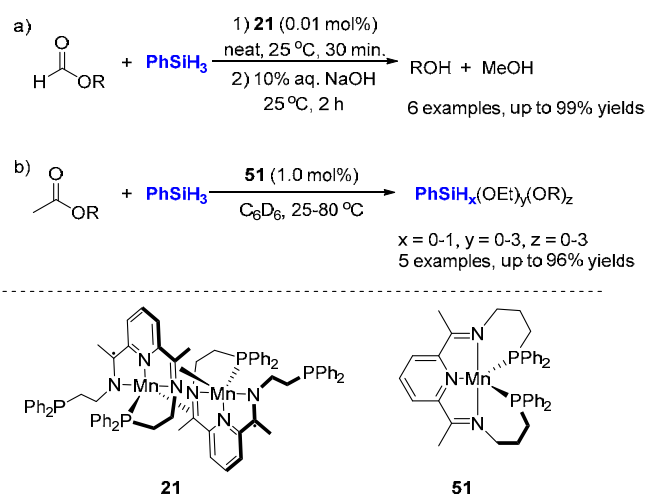
In continuation of the hydrosilylation of metal acyl complexes by Cutler, manganese acyl complexes were thereafter tested in hydrosilylation of esters.<sup>[9e]</sup> With 2.0-3.0 mol% of  $(\text{PPh}_3)(\text{CO})_4\text{MnC}(\text{O})\text{CH}_3$  **2** and 1.1 equiv. of  $\text{PhSiH}_3$  in  $\text{C}_6\text{D}_6$ ,  $\text{Cp}(\text{CO})_2\text{FeC}(\text{O})\text{OCH}_3$  was converted to  $(\eta^4\text{-C}_5\text{H}_6)\text{Fe}(\text{CO})_3$  in 92% yield (Scheme 20a). This catalytic system was then utilized in the hydrosilylation of simple esters to ethers catalyzed by the same manganese-acyl complex **2** (Scheme 20b).<sup>[9h]</sup> All the esters were consumed within 1 h, but only the linear alkanoate esters cleanly yielded the corresponding ethers. The other aromatic or cyclic esters gave mixtures of their ethers and alkoxy silanes, resulting from further reduction of silyl acetal intermediates.  $(\text{CO})_5\text{MnCH}_3$  **47** and  $(\text{CO})_5\text{MnBr}$  **48** were less effective, as 85% and 55% yields were obtained respectively after 4 h under similar conditions. In contrast,  $\text{Mn}(\text{CO})_5(\text{SiMe}_2\text{Ph})$  **49**,  $\text{Mn}(\text{CO})_5(\text{SiHPh}_2)$  **50**, and  $\text{Mn}_2(\text{CO})_{10}$  **1** were inactive. The proposed mechanism for the hydrosilylation of esters is similar to the one for ketones (see Scheme 4). The first hydrosilylation intermediate, alkyl silyl acetal, was further reduced by manganese hydride to afford the final ether product.



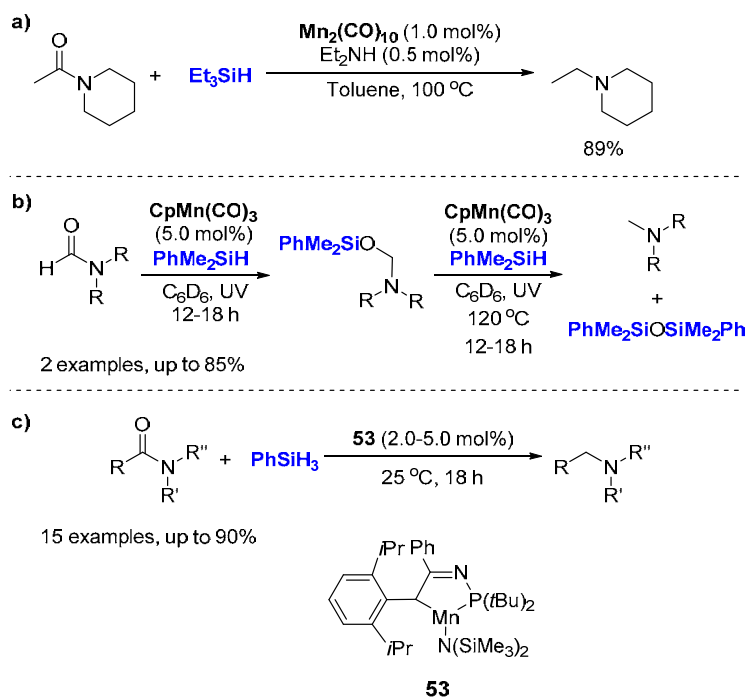
**Scheme 20.** Hydrosilylation of an organoiron-ester complex and simple esters catalyzed by manganese-acyl complexes

PDI-Mn complexes were also used for the hydrosilylation of esters (Scheme 21). The (PDI)Mn dimer complex **21** could catalyze the hydrosilylation of formates to corresponding alcohols with

0.01 mol% catalyst loading (Scheme 21a).<sup>[14d]</sup> The hydrosilylation of esters with **51** proceeded through acyl C-O bond cleavage which was confirmed by the deuterium labeling (Scheme 21b).<sup>[16a]</sup> This reaction gave relatively modest TOFs (**21**: 14 h<sup>-1</sup> and **51**: 18 h<sup>-1</sup>) compared to the case of ketones.



**Scheme 21.** Hydrosilylation of esters with PDI-Mn complexes.

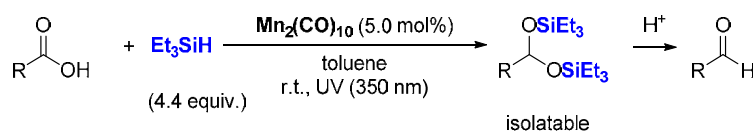


**Scheme 22.** Manganese-catalyzed reduction of amides *via* hydrosilylation.

So far, only a few examples of manganese-catalyzed amide reduction with silanes have been reported. With the co-catalytic system of  $\text{Mn}_2(\text{CO})_{10}$  **1** and  $\text{Et}_2\text{NH}$ , the substrate *N*-acetylpiperidine was readily reduced to *N*-ethylpiperidine in 89% yield (Scheme 22a)<sup>[38]</sup>. Similarly,  $\text{CpMn}(\text{CO})_3$  **52** was shown to be an active catalyst in the reduction of DMF and *N,N*-

diethylformamide (DEF) under UV irradiation conditions (Scheme 22b).<sup>[39]</sup> Moreover, Turculet developed a manganese complex **53**, in 2017, which was a competent catalyst for reduction of challenging tertiary amides to amines (Scheme 22c).<sup>[40]</sup> The reduction of aldehydes, ketones, and esters occurred smoothly by using this protocol. However, the underlying reaction mechanism was not clear.

Finally, our group has successfully developed the first reduction of carboxylic acids to aldehydes catalyzed by commercially available and inexpensive manganese carbonyl complex  $\text{Mn}_2(\text{CO})_{10}$  **1**, in the presence of triethylsilane as an affordable and stable reducing agent (Scheme 23).<sup>[41]</sup> The reaction proceeds at room temperature under UV irradiation. Of notable interest was the isolation of the stable disilylacetals as their protected aldehyde forms, which can be then hydrolyzed to the corresponding aldehydes. Another advantage of this system is the good tolerance of a variety of functional groups, such as halides, amino, furyl, pyridyl and internal double bond. However, the steric hindered substrates and benzoic acid derivatives did not lead to satisfactory results.

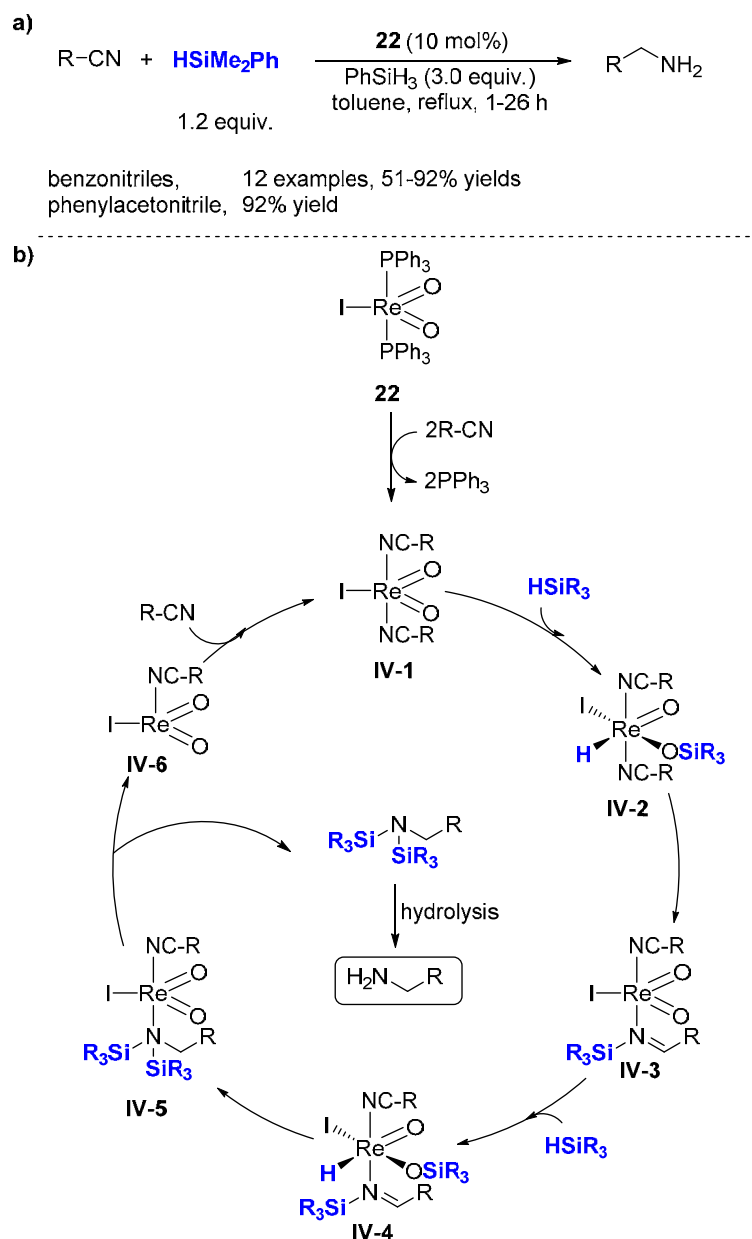


**Scheme 23.** Manganese-catalyzed hydrosilylation of carboxylic acids.

#### 7.2.2-2 Rhenium-catalyzed hydrosilylation of carboxylic acid derivatives

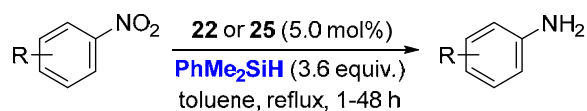
The reduction of carboxylic acid derivatives using rhenium are rare. In 2011, Fernandes reported the reduction of nitriles to the corresponding primary amines with silanes catalyzed by the oxo-rhenium complexes **22** or  $\text{ReOCl}_3(\text{PPh}_3)_2$  **25**. The catalytic system **22** (10 mol%) in the presence of 3 equiv. of  $\text{PhSiH}_3$  reduced efficiently a series of benzonitriles in the presence of a wide range of functional groups such as halides,  $\text{CF}_3$ ,  $\text{SO}_2\text{CH}_3$  and NHTs and also phenylacetone nitrile (Scheme 24a).<sup>[42]</sup>

The catalytic cycle was proposed by the same authors (Scheme 24b): coordination of two nitriles to the rhenium with liberation of two phosphines, affording the complex  $\text{ReIO}_2(\text{nitrile})_2$  **IV-1**; formation of the hydride species  $(\text{nitrile})_2(\text{O})\text{IRe}(\text{H})\text{OSiR}_3$  **IV-2** as the result of the addition of the Si-H bond to one of the oxo-rhenium bond; dihydrosilylation of the nitrile to the corresponding N-disilylamine **IV-5**; formation of the amine by hydrolysis of the N-disilylamine, probably, due to the presence of a trace of water in the reaction mixture.



**Scheme 24.** Proposed catalytic cycle for the reduction of nitriles with **22**/silane.

In 2009, the same group has also reported the reduction of nitroarene compounds to the corresponding amines catalyzed by **22** or **25** in the presence of 3.6 equiv. of PhMe<sub>2</sub>SiH in refluxing toluene for 1-48 h (Scheme 25).<sup>[43]</sup> Aniline derivatives were then isolated in moderate to good yields (31-96%). It is noticeable that this catalytic transformation tolerated a huge variety of functional groups such as halides, esters, amides, sulfones, and nitriles. By contrast, the hydrosilylation of nitroalkanes such as 2-nitroethylbenzene led to the corresponding nitrile in 38% yield.



## Scheme 25. Reduction of nitroarene compounds with **22** or **25**.

In summary, the utilization of manganese and rhenium catalysts in hydrosilylation of carbonyl and carboxylic acid derivatives has been developed since their pioneering examples in 1982 and 2003, respectively. However, carboxylic acid derivatives were far less explored as substrates compared with carbonyl compounds. In the next paragraphs, our results for the chemoselective reduction of carboxylic acids, esters and amides will be discussed.

### 7.3. Results and discussions

Following the study of the hydrosilylation of various carboxylic acids catalyzed by  $\text{Mn}_2(\text{CO})_{10}$ , which is previously developed in our group,<sup>[41]</sup> we describe herein the same reaction but catalyzed by  $\text{Re}_2(\text{CO})_{10}$  and also hydrosilylation of carboxylic esters and amides under the catalysis of  $\text{Mn}_2(\text{CO})_{10}$  and  $\text{Re}_2(\text{CO})_{10}$ .

#### 7.3.1. Optimization of reaction conditions for $\text{Re}_2(\text{CO})_{10}$ catalyzed hydrosilylation of carboxylic acids

We firstly performed the hydrosilylation of 2-naphthaleneacetic acid **54a** catalyzed by  $\text{Re}_2(\text{CO})_{10}$  **44** (0.5 mol%) with 4 equiv. of  $\text{Et}_3\text{SiH}$  under irradiation of UV-LED (395-400 nm, 45 W) in toluene at r.t. within 3 h (Table 1). To our delight, 97% conversion of **54a** was achieved and the disilyl acetal product **55a** was detected in 88% NMR-yield, along with 9% of the fully reduced product silyl ether **56a**, resulting from firstly decomposition of **55a** to 2-naphthaldehyde followed by further hydrosilylation with  $\text{Et}_3\text{SiH}$  (entry 1). A low conversion (44%) was observed when decreased the catalyst loading to 0.2 mol% (entry 2). Theoretically, only 2 equiv. of  $\text{Et}_3\text{SiH}$  are required to reduce 1 equiv. of carboxylic acid; we thus conducted the reaction with 2.2 equiv. of  $\text{Et}_3\text{SiH}$ , and 89% yield of **55a** was observed using 0.5 mol% of  $\text{Re}_2(\text{CO})_{10}$  in 6 h at r.t. (entry 3). Extension the reaction time to 9 h with 2.2 equiv. of  $\text{Et}_3\text{SiH}$  increased the yield to 94% yield of **55a** (entry 4). The nature of the silanes was also crucial for the selectivity of the reaction. The use of  $\text{Et}_2\text{SiH}_2$  and  $\text{PhSiH}_3$  (4 equiv.) led to low conversion of **54a**, while the use of  $\text{Ph}_2\text{SiH}_2$  reversed the selectivity, as 80% yield of silylether **56a** was observed in 3 h. The utilization of TMDS (1,1,3,3- tetramethyldisiloxane, 4 equiv.) led to a full conversion but a mixture of **55a** and **56a**. (entries 5-8). In the absence of any light, under thermal conditions, or with visible light irradiation, no conversion of **54a** was detected after 9 h (entries 9-11). The highest yield of **55a** (98%) was observed when the reaction was performed under UV irradiations (350 nm) in a Rayonet RPR100 apparatus (entry 12). However, when a medium pressure UV mercury lamp (150 W) was used, after only 1 hour, 41% conversion

was obtained with a good selectivity (entry 13). Notably, a comparable yield of **55a** (90%) can be obtained, when  $\text{Re}(\text{CO})_5\text{Br}$  **57** (1.0 mol%) were employed as catalyst under UV irradiations (350 nm) (entry 14). Finally, in the absence of Re catalyst, no conversion of the 2-naphthaleneacetic **1a** can be detected (entry 15).

**Table 1.** Hydrosilylation of 2-naphthaleneacetic acid catalyzed by  $\text{Re}_2(\text{CO})_{10}$

Entry	$\text{Re}_2(\text{CO})_{10}$ (mol%)	Silane (equiv.)	Time (h)	Conv. (%)	Yield (%) <sup>[a]</sup>	
					<b>55a</b>	<b>56a</b>
1	0.5	$\text{Et}_3\text{SiH}$ (4)	3	97	88	9
2	0.2	$\text{Et}_3\text{SiH}$ (4)	3	44	42	2
3	0.5	$\text{Et}_3\text{SiH}$ (2.2)	6	69	67	2
4	<b>0.5</b>	<b><math>\text{Et}_3\text{SiH}</math> (2.2)</b>	<b>9</b>	<b>97</b>	<b>94</b>	<b>3</b>
5	0.5	$\text{Et}_2\text{SiH}_2$ (4)	3	16	12	4
6	0.5	$\text{PhSiH}_3$ (4)	3	52	45	7
7	0.5	$\text{Ph}_2\text{SiH}_2$ (4)	3	81	1	80
8	0.5	TMDS (4)	3	>99	55	45
9 <sup>[b]</sup>	0.5	$\text{Et}_3\text{SiH}$ (2.2)	9	0	-	-
10 <sup>[c]</sup>	0.5	$\text{Et}_3\text{SiH}$ (2.2)	9	0	-	-
11 <sup>[d]</sup>	0.5	$\text{Et}_3\text{SiH}$ (2.2)	9	0	-	-
12 <sup>[e]</sup>	<b>0.5</b>	<b><math>\text{Et}_3\text{SiH}</math> (2.2)</b>	<b>9</b>	<b>&gt;99</b>	<b>98</b>	<b>2</b>
13 <sup>[f]</sup>	0.5	$\text{Et}_3\text{SiH}$ (2.2)	1	41	37	4
14 <sup>[e,g]</sup>	1.0	$\text{Et}_3\text{SiH}$ (2.2)	9	95	90	5
15	None	$\text{Et}_3\text{SiH}$ (2.2)	9	0	-	-

General conditions: a 20 mL Schlenk tube was charged with  $\text{Re}_2(\text{CO})_{10}$  and **54a** followed by toluene (0.5 M) and  $\text{Et}_3\text{SiH}$  under argon atmosphere then stirred at r.t. for indicated hours.

<sup>[a]</sup> Conversion and selectivity were detected by  $^1\text{H}$  NMR of the crude mixture;

<sup>[b]</sup> In the dark;

<sup>[c]</sup> Visible light irradiation (400-800 nm, 30 W);

<sup>[d]</sup> at 100 °C without light;

<sup>[e]</sup> UV irradiations (350 nm) in a Rayonet RPR100 apparatus;

<sup>[f]</sup> With medium pressure UV lamp (150 W)

<sup>[g]</sup>  $\text{Re}(\text{CO})_5\text{Br}$  **57** (1.0 mol%) as catalyst.

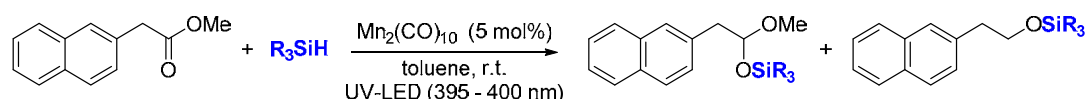
### 7.3.2. Optimization of reaction conditions for $\text{Mn}_2(\text{CO})_{10}$ and $\text{Re}_2(\text{CO})_{10}$ catalyzed hydrosilylation of carboxylic esters

We then performed the hydrosilylation of methyl 2-(2-naphthalenyl)acetate **57a** catalyzed by  $\text{Mn}_2(\text{CO})_{10}$  **1** (5.0 mol%) with 4 equiv. of  $\text{Et}_3\text{SiH}$  under irradiation of UV-LED (395-400 nm, 45 W) in toluene, within 3 h (Table 2). To our delight, 92% conversion of **57a** was observed and the alkyl silyl acetal product **58a** was detected in 75% yield, while 17% of the by-product silyl ether **56a** was produced simultaneously (entry 1). The conversion dropped from 92% to 73%, when reducing the amount of  $\text{Et}_3\text{SiH}$  to 3.0 and 2.0 equiv. (entries 2 and 3). Prolonging



the reaction time from 3 h to 6 h with 2.0 equiv. of Et<sub>3</sub>SiH gave a better yield of **58a** (91%), (entry 4). As shown in entries 5-7, with only 1.1 equiv. of Et<sub>3</sub>SiH, the conversion increased from 60% to 90%, when prolonging the reaction time from 3 h to 9 h, giving **58a** in 89% yield. The use of Et<sub>2</sub>SiH<sub>2</sub> (3 equiv.) led to partial conversion of **57a** (41%) and mixture of **58a** and **56a** (entry 8). While the use of Ph<sub>2</sub>SiH<sub>2</sub>, PhSiH<sub>3</sub> and TMDS (3 equiv.) reversed the selectivity of the reaction with **56a** as the sole obtained product in 99% yield in 3 h, for all cases (entries 9-11).

**Table 2.** Hydrosilylation of methyl 2-(2-naphthalenyl)acetate catalyzed by Mn<sub>2</sub>(CO)<sub>10</sub>



Entry	Silane (equiv.)	Time (h)	Conv. (%)	Yield (%) <sup>[a]</sup>	
				58a	56a
1	Et <sub>3</sub> SiH (4)	3	92	75	17
2	Et <sub>3</sub> SiH (3)	3	82	81	1
3	Et <sub>3</sub> SiH (2)	3	73	66	7
4	Et <sub>3</sub> SiH (2)	6	92	91	1
5	Et <sub>3</sub> SiH (1.1)	3	60	53	7
6	Et <sub>3</sub> SiH (1.1)	6	70	69	1
7	<b>Et<sub>3</sub>SiH (1.1)</b>	<b>9</b>	<b>90</b>	<b>89</b>	<b>1</b>
8	Et <sub>2</sub> SiH <sub>2</sub> (3)	3	41	20	21
9	Ph <sub>2</sub> SiH <sub>2</sub> (3)	3	>99	1	99
10	PhSiH <sub>3</sub> (3)	3	>99	1	99
11	TMDS (3)	3	>99	1	99
12 <sup>[b]</sup>	Et <sub>3</sub> SiH (2)	6	0	-	-
13 <sup>[c]</sup>	Et <sub>3</sub> SiH (2)	6	0	-	-
14 <sup>[d]</sup>	Et <sub>3</sub> SiH (2)	9	92	91	1
15 <sup>[e]</sup>	Et <sub>3</sub> SiH (2)	6	56	55	1
16 <sup>[f]</sup>	Et <sub>3</sub> SiH (2)	1	86	73	13
17 <sup>[g]</sup>	Et <sub>3</sub> SiH (1.1)	9	0	-	-
18 <sup>[h]</sup>	Et <sub>3</sub> SiH (1.1)	9	0	-	-

General conditions: a 20 mL Schlenk tube was charged with Mn<sub>2</sub>(CO)<sub>10</sub> and **57a** followed by toluene (0.5 M) and Et<sub>3</sub>SiH under argon atmosphere then stirred at r.t. for indicated hours.

<sup>[a]</sup> Conversion and selectivity were detected by <sup>1</sup>H NMR of the crude mixture;

<sup>[b]</sup> In the dark;

<sup>[c]</sup> At 100 °C;

<sup>[d]</sup> UV irradiations (350 nm) in a Rayonet RPR100 apparatus;

<sup>[e]</sup> Visible light irradiation (400-800 nm, 30 W);

<sup>[f]</sup> With medium pressure mercury UV lamp (150 W)

<sup>[g]</sup> Mn(CO)<sub>5</sub>Br **48** (10 mol%) as catalyst;

<sup>[h]</sup> CpMn(CO)<sub>3</sub> **52** (10 mol%) as catalyst;

In the absence of any light, or under thermal conditions, no conversion of **57a** was detected after 6 h (Table 2, entries 12 and 13). Notably, **58a** was obtained in a slightly better yield (91%)

when the reaction was performed under UV irradiation (350 nm) in a Rayonet RPR100 apparatus (entry 14). However, when the visible light irradiation (400-800 nm, 30 W) and medium pressure mercury UV lamp (150 W) was used, low selectivity was observed (entries 15 and 16). Noticeably, there is no detectable conversion of **57a**, when  $\text{Mn}(\text{CO})_5\text{Br}$  **48** (10 mol%) and  $\text{CpMn}(\text{CO})_3$  **52** (10 mol%) were employed as catalysts (entries 17 and 18).

Afterwards,  $\text{Re}_2(\text{CO})_{10}$  **44** was tested as the catalyst for the reduction of same ester substrate **57a** (Table 3). Using 4.0 equiv.  $\text{Et}_3\text{SiH}$ , and 0.5 mol%  $\text{Re}_2(\text{CO})_{10}$ , full conversion of **57a** was observed and **58a** was obtained in 85% yield after 6 h of reaction (entry 1). Lower conversions were obtained with a decrease of the reaction time to 3 h or of the amount of  $\text{Et}_3\text{SiH}$  to 1.1 equiv. (entries 2 and 3). However, prolonging the reaction time to 9 h with only 1.1 equiv. of  $\text{Et}_3\text{SiH}$ , 84% yield of **58a** was observed. Similar results can be observed with 1.0 mol%  $\text{Re}_2(\text{CO})_{10}$  **44** in 6 h (entry 5). The utilization of  $\text{Re}(\text{CO})_5\text{Br}$  (1.0 mol%) gave a partial conversion of **57a** (72%) (entry 6). Additionally, in the absence of catalyst, no reaction took place (entry 7).

**Table 3.** Hydrosilylation of ester with  $\text{Re}_2(\text{CO})_{10}$

Entry	$\text{Re}_2(\text{CO})_{10}$ (mol%)	Silane (equiv.)	Time (h)	Conv. (%) <sup>[a]</sup>	Yield (%) <sup>[a]</sup>	
					<b>58a</b>	<b>56a</b>
1	0.5	$\text{Et}_3\text{SiH}$ (4)	6	>99	85	15
2	0.5	$\text{Et}_3\text{SiH}$ (4)	3	75	72	3
3	0.5	$\text{Et}_3\text{SiH}$ (1.1)	6	86	82	4
4	<b>0.5</b>	<b><math>\text{Et}_3\text{SiH}</math> (1.1)</b>	<b>9</b>	<b>91</b>	<b>84</b>	<b>7</b>
5	1.0	$\text{Et}_3\text{SiH}$ (1.1)	6	92	87	5
6 <sup>[b]</sup>	1.0	$\text{Et}_3\text{SiH}$ (1.1)	9	72	63	9
7	None	$\text{Et}_3\text{SiH}$ (1.1)	9	0	-	-

General conditions: a 20 mL Schlenk tube was charged with  $\text{Re}_2(\text{CO})_{10}$  and **57a** followed by toluene (0.5 M) and  $\text{Et}_3\text{SiH}$  under argon atmosphere then stirred at r.t. for indicated hours.

<sup>[a]</sup> Conversion and selectivity were detected by  $^1\text{H}$  NMR of the crude mixture;

<sup>[b]</sup>  $\text{Re}(\text{CO})_5\text{Br}$  (1.0 mol%) as the catalyst

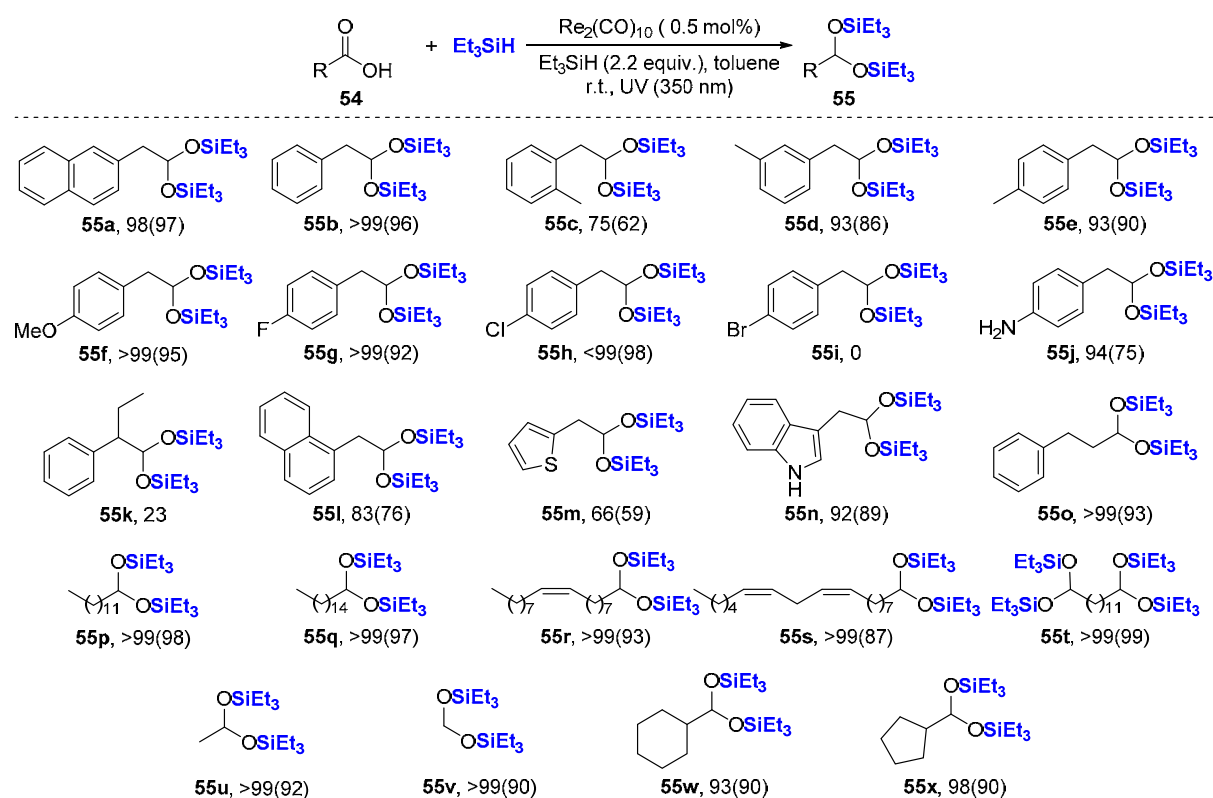
With these optimized conditions in hand for the reduction of acids [0.5 mol% of  $\text{Re}_2(\text{CO})_2$ , 2.2 equiv. of  $\text{Et}_3\text{SiH}$ , toluene, r.t., 9 h, UV-LED (395-400 nm) or UV (350 nm) irradiation, (Table 1, entries 4 and 12)] and for reduction of esters [5.0 mol% of  $\text{Mn}_2(\text{CO})_{10}$  (method A, Table 2, entry 7) or 0.5 mol% of  $\text{Re}_2(\text{CO})_{10}$  (method B, Table 3, entry 4), 1.1 equiv. of  $\text{Et}_3\text{SiH}$ , toluene, r.t., 9 h, UV-LED (395-400 nm, 45 W) irradiation], we then explored the substrate

scope for the catalyzed hydrosilylation of acids with  $\text{Re}_2(\text{CO})_{10}$  (Table 4) and of esters with  $\text{Mn}_2(\text{CO})_{10}$  or  $\text{Re}_2(\text{CO})_{10}$  (Table 5).

### 7.3.3. Scope for the hydrosilylation of carboxylic acids

As shown in Table 4, 2-naphthaleneacetic acid **54a**, 2-phenylacetic acid **54b**, methyl substituted 2-phenylacetic acids in *ortho*, *meta*, *para* positions **54c-e** and 2-(4-methoxyphenyl)acetic acid **54f** were smoothly converted in the corresponding disilyl acetal products in good yields (up to 97%), although 2-(*o*-tolyl)acetic acid led to **54c** in 62% isolated yield. Halogens like fluorine and chlorine can be tolerated, while 2-(4-bromophenyl)acetic acid **54i** cannot be converted to the desired product, but the debromination of **54i** was detected. Amino group was not altered, as 75% of **55j** was isolated, without the formation of silylamine species.

**Table 4.** Scope of hydrosilylation of carboxylic acids with  $\text{Re}_2(\text{CO})_{10}$ <sup>[a]</sup>



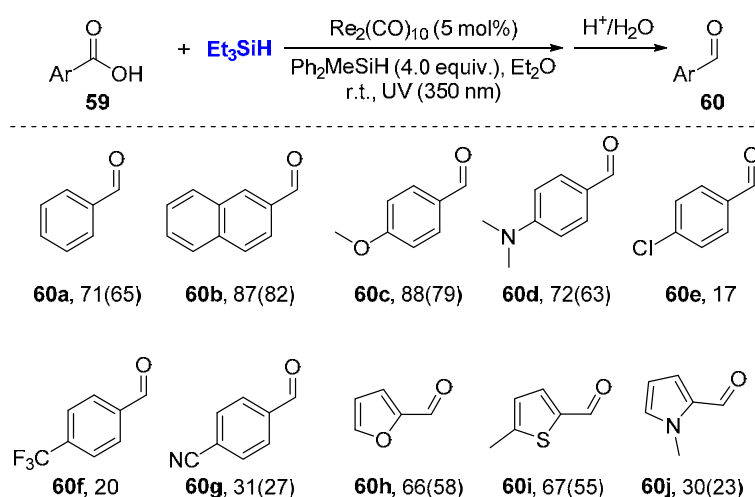
<sup>[a]</sup> General conditions: carboxylic acid (0.5 mmol),  $\text{Et}_3\text{SiH}$  (176  $\mu\text{L}$ , 1.1 mmol, 2.2 equiv.),  $\text{Re}_2(\text{CO})_{10}$  (1.6 mg, 0.5 mol%), r.t., toluene (1 mL), UV (350 nm), 9 h; Conversion of **54** was detected by  $^1\text{H}$  NMR of the crude mixture; and isolated yields of **2** were shown in parentheses;

Steric hindered acids like 2-phenylbutanoic acid **54k** cut down the conversion to 23%. 2-(naphthalen-1-yl)acetic acid **54l** gave the corresponding acetal **55l** in lower yield (76%) compared with **54a**. Interestingly heteroaromatic substituted acetic acids based on thiophene

**54m** and 1*H*-indole **54n** can also be tolerated, giving **55m** and **55n** in 59% and 89% yields, respectively. Carboxylic acids with longer carbon chains (**55o-55t**) gave the corresponding products in excellent isolated yields up to 98%. Notably, dicarboxylic acid **54t** led to the corresponding diacetal **55t** in 99% yield. The internal C=C in **54r** and **55r** can be tolerated while conjugated C=C was reduced, as the saturated product **55o** was detected starting from cinnamic acid. It is worth mentioning that acetic acid and formic acid were also reactive in the current reaction, producing ca. 90% yield of **55u** and **55v**. Finally, good yields (90%) can be obtained with cyclic acids like cyclohexanecarboxylic acid **54w** and cyclopentanecarboxylic acid **54x**.

### 7.3.4. Scope for the hydrosilylation of benzoic acids

**Table 5.** Scope of hydrosilylation of benzoic acids with  $\text{Re}_2(\text{CO})_{10}$ <sup>[a]</sup>



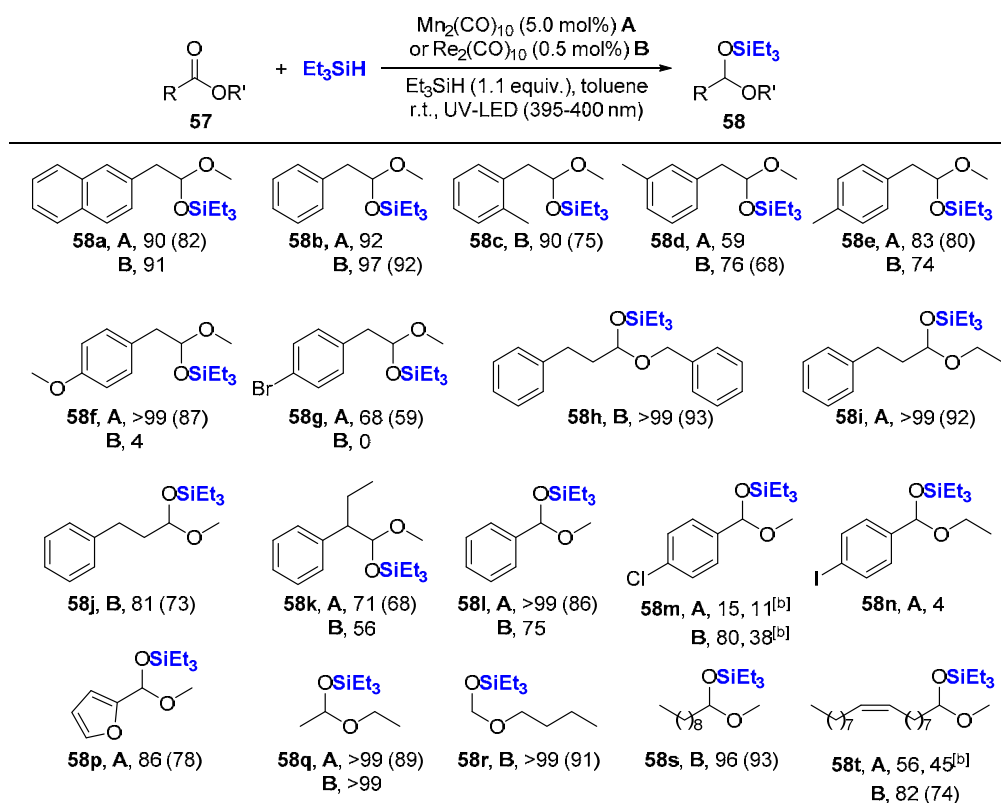
<sup>[a]</sup> General conditions: carboxylic acid (0.5 mmol),  $\text{Ph}_2\text{MeSiH}$  (200  $\mu\text{L}$ , 1.0 mmol, 4.0 equiv.),  $\text{Re}_2(\text{CO})_{10}$  (8.2 mg, 5.0 mol%), r.t.,  $\text{Et}_2\text{O}$  (1 mL), UV irradiation (350 nm), 48 h, then hydrolysed at r.t. with trifluoroacetic acid (99%, 0.25 mL) for 3 h. NMR-yield of **60** are given, and isolated yields of **60** were shown in parentheses;

Benzoic acid derivatives are usually challenging substrates in reduction and particularly in hydrosilylation.<sup>[41]</sup> When benzoic acid **59a** was tested as substrate under the standard conditions shown in Table 5, a mixture of disilyl acetal product and benzaldehyde was detected by  $^1\text{H}$  NMR of the crude mixture, indicating that the disilyl acetal product may be hydrolysed to aldehyde during the reaction process. Thus, a hydrolysis was performed in the end of the reaction to afford aldehydes from the hydrosilylation of aromatic acids. Selected substrate scope is shown in Table 5 using  $\text{Ph}_2\text{MeSiH}$  (4.0 equiv.) as reducing reagent,  $\text{Re}_2(\text{CO})_{10}$  (5.0 mol%) as the catalyst, at r.t., in  $\text{Et}_2\text{O}$ , under UV irradiation (350 nm) in 48 h. Benzoic acid **59a** and 2-naphthoic acid **59b** gave good isolated yield of the corresponding aldehydes in 65%

and 82% respectively. Aromatic acids bearing electron donating groups such as methoxy **59c** and dimethylamino **59d** groups led also to the corresponding aldehydes with good yields. However, low conversion was observed with 4-chlorobenzoic acid **59e** and 4-(trifluoromethyl)benzoic acid **59f** after 48 h. Heteroaromatic acid with furane, thiophene and pyrrole moieties led to the aldehydes in moderate yields (23-58%).

### 7.3.5. Scope for the hydrosilylation of carboxylic esters

**Table 6.** Scope of hydrosilylation of carboxylic esters with  $\text{Mn}_2(\text{CO})_{10}$  and  $\text{Re}_2(\text{CO})_{10}$ <sup>[a]</sup>



<sup>[a]</sup> General conditions: carboxylic ester (0.5 mmol),  $\text{Et}_3\text{SiH}$  (88  $\mu\text{L}$ , 0.55 mmol, 1.1 equiv.),  $\text{Mn}_2(\text{CO})_{10}$  (9.7 mg, 5.0 mol%, method A) or  $\text{Re}_2(\text{CO})_{10}$  (1.6 mg, 0.5 mol%, method B), r.t., toluene (1 mL), UV-LED irradiation (395-400 nm, 45 W), 9 h; Conversion of **57** was detected by  $^1\text{H}$  NMR of the crude mixture; and isolated yields of **58** were shown in parentheses;

<sup>[b]</sup> NMR yield of **58**.

On the other hand, under UV-LED irradiation (395-400 nm, 45 W), methyl 2-(2-naphthalenyl)acetate **57a**, methyl 2-phenylacetate **57b**, *o*-, *m*-, *p*-methyls and *p*-methoxyl substituted methyl 2-phenylacetate **57c-57f** were smoothly converted into the corresponding alkyl silyl acetals in 68-92% isolated yields (Table 6), catalyzed either by  $\text{Mn}_2(\text{CO})_{10}$  (5.0 mol%) or  $\text{Re}_2(\text{CO})_{10}$  (0.5 mol%). Starting from methyl 2-(4-bromo)phenylacetate **57g**, the corresponding product **57g** was isolated in moderate isolated yield (59%) under the catalysis

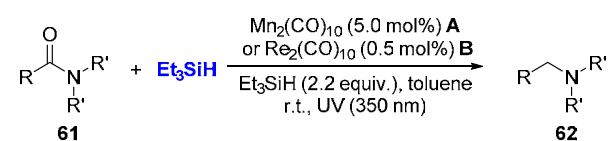
of  $\text{Mn}_2(\text{CO})_{10}$  (5.0 mol%), while  $\text{Re}_2(\text{CO})_{10}$  (0.5 mol%) gave no conversion of the starting ester **57g**.

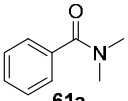
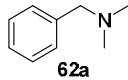
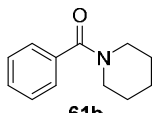
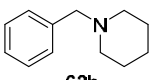
The reactions between  $\text{Et}_3\text{SiH}$  and benzyl 3-phenylpropanoate **57h**, ethyl 3-phenylpropanoate **57i**, methyl 3-phenylpropanoate **57j** afforded the corresponding acetals in 93%, 92% and 73% yields, respectively. By contrast, methyl 2-phenylbutanoate **57k** was converted into **5k** in lower yield certainly due to the increasing steric hindrance which may inhibit the reactivity. Good isolated yield was also obtained with benzoates derivatives, as methyl benzoate **57l** led to the acetal **57l** in 86% yield when catalyzed by  $\text{Mn}_2(\text{CO})_{10}$  (5.0 mol%), although  $\text{Re}_2(\text{CO})_{10}$  (0.5 mol%) gave a slightly lower conversion (75%). Nevertheless, methyl 4-chlorobenzoate **57m** were reduced in 15% and 80% conversion when catalyzed by  $\text{Mn}_2(\text{CO})_{10}$  and  $\text{Re}_2(\text{CO})_{10}$ , respectively. Noticeably, iodo group seems to be problematic to the reaction, as only 4% of the conversion was detected starting with the substrate **58n**. Heteroaromatic containing substrates such as methyl furan-2-carboxylate **57p** can be transformed into **58p** in 78 isolated yield. Simple ethyl acetate **57q**, butyl formate **57r** and methyl decanoate **58s** gave full conversion and led to the compounds **58p-58q** in 89, 91 and 93% isolated yields, respectively. The internal C=C bond in methyl oleate **57t** can be tolerated, leading the acetal **58t** in 74% yield using  $\text{Re}_2(\text{CO})_{10}$  (0.5 mol%).

### 7.3.6. Extension of the methodology to the hydrosilylation of carboxylic amides

This methodology can be extended to carboxylic amides by  $\text{Mn}_2(\text{CO})_{10}$  and  $\text{Re}_2(\text{CO})_{10}$  catalyzed hydrosilylation under UV irradiation (350 nm). Thus, in two selected examples depicted in Table 7, using 2.2 equiv. of  $\text{Et}_3\text{SiH}$ , *N,N*-dimethylbenzamide **61a** and *N*-benzoylpiperidine **61b** afforded the corresponding amines **62a** and **62b** in full conversion using 0.5 mol% of  $\text{Re}_2(\text{CO})_{10}$  or 5.0 mol% of  $\text{Mn}_2(\text{CO})_{10}$ . Using  $\text{Mn}_2(\text{CO})_{10}$  as the catalyst, **62a** and **62b** were isolated in 82% and 90% yields, respectively.

It is worth mentioning that the above results obtained with the irradiation using UV-LED (395-400 nm, 45 W), are quite similar with those using UV (350 nm) in a Rayonet RPR100 apparatus. So the choice of the irradiation device was based on a practical point of view (Rayonet in Rennes, UV-LEDs in Toulouse) more than on a chemical requirement.

**Table 7.** Hydrosilylation of carboxylic amides with  $\text{Mn}_2(\text{CO})_{10}$  and  $\text{Re}_2(\text{CO})_{10}$ <sup>[a]</sup>

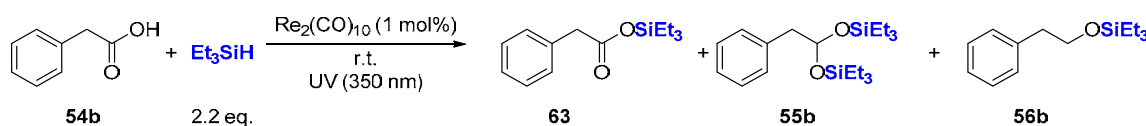
Entry	substrate <b>61</b>	Product <b>62</b>	Conv. (Yield) [%]
1			A, >99 B, >99 (82)
2			A, >99 (90) B, >99

<sup>[a]</sup> General conditions: carboxylic amide (0.5 mmol),  $\text{Et}_3\text{SiH}$  (176  $\mu\text{L}$ , 1.1 mmol, 2.2 equiv.),  $\text{Mn}_2(\text{CO})_{10}$  (9.7 mg, 5.0 mol%, method A) or  $\text{Re}_2(\text{CO})_{10}$  (1.6 mg, 0.5 mol%, method B), r.t., toluene (1 mL), UV irradiation (350 nm), 9 h; Conversion of the **61** was detected by  $^1\text{H}$  NMR of the crude mixture; and isolated yields of **62** were shown in parentheses;

#### 7.4. Mechanistic insights

Kinetic studies were carried out for the hydrosilylation of 2-phenylacetic acid **54b** (Figure 1) and of methyl 2-phenylacetate **57b** (Figure 2) catalyzed by 1.0 mol% of  $\text{Re}_2(\text{CO})_{10}$  performed in the presence of 2.2 and 1.1 equiv. of  $\text{Et}_3\text{SiH}$ , respectively at r.t. in toluene under UV (350 nm) irradiation.

2-Phenylacetic acid **57b** was consumed completely in 4 h. Interestingly, 10% of silyl ester **63** was observed in 20 min. resulting from the dehydrogenative silylation between **54b** and  $\text{Et}_3\text{SiH}$ . After 4 h of reaction, its yield increased to 95%, the disilyl acetal product **55b** being detected in 5%. After 24 h of reaction, 98% yield of **55b** and 1% yield of **56b** were observed. (Figure 1).

				
Time/h	Acid <b>54b</b> /%	Silyl Ester <b>63</b> /%	disilyl acetal <b>55b</b> /%	Silyl ether <b>56b</b> /%
0	100	0	0	0
0.3	90	10	0	0
1	58	41	1	0
2	13	85	2	0
4	0	95	5	0
5	0	81	19	0
10	0	17	83	0
24	0	1	98	1

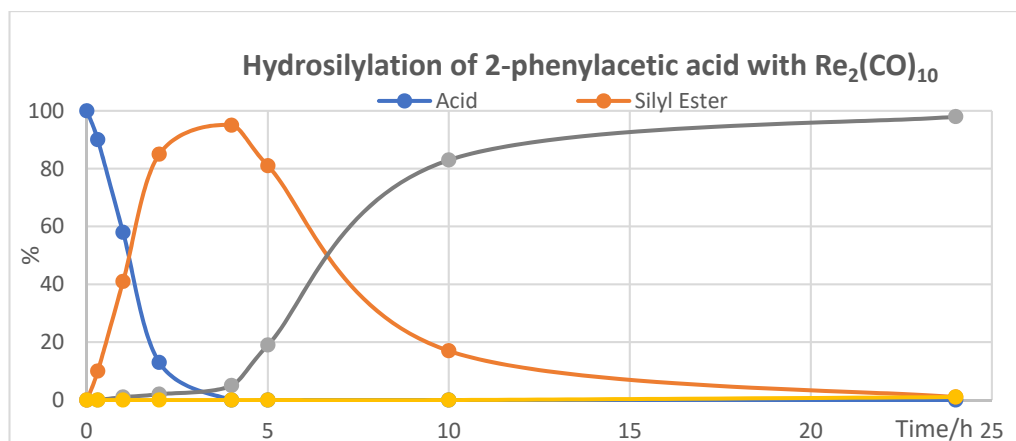


**Figure 1.** Kinetic profile of the hydrosilylation of 2-phenylacetic acid **55b** catalyzed by  $\text{Re}_2(\text{CO})_{10}$  performed with 1.1 equiv. of  $\text{Et}_3\text{SiH}$  at r.t. in toluene under UV (350 nm) irradiation.

In the case of methyl 2-phenylacetate **57b**, it was observed 9% of alkyl silyl acetal product **58b** after 20 min. of reaction. Prolonging the time to 4 h, the acetal was obtained in 78%. At 10 h of reaction, only 5% of silyl ether by-product **56b**, was detected. Finally, after 24 h, 97% conversion of **57b** was reached and the acetal **5b** was obtained in 88% yield. (Figure 2).

<chem>CCOC(=O)Cc1ccccc1</chem> + $\text{Et}_3\text{SiH}$		$\xrightarrow[\text{UV (350 nm)}]{\text{Re}_2(\text{CO})_{10} (1 \text{ mol\%}), \text{r.t., C}_6\text{D}_6}$	<chem>CCOC(=O)C(C)Cc1ccccc1</chem> + <chem>CCOC(C)Cc1ccccc1OSi(C)(C)C</chem>
<b>57b</b>	1.1 eq.		<b>58b</b> <b>56b</b>
Time/h	Ester <b>57b</b> /%	Acetal <b>58b</b> /%	Silyl ether <b>56b</b> /%
0	100	0	0
0.3	91	9	0
1	68	32	0
2	44	56	0
3	29	71	0
4	22	78	0
10	8	87	5
24	3	88	9

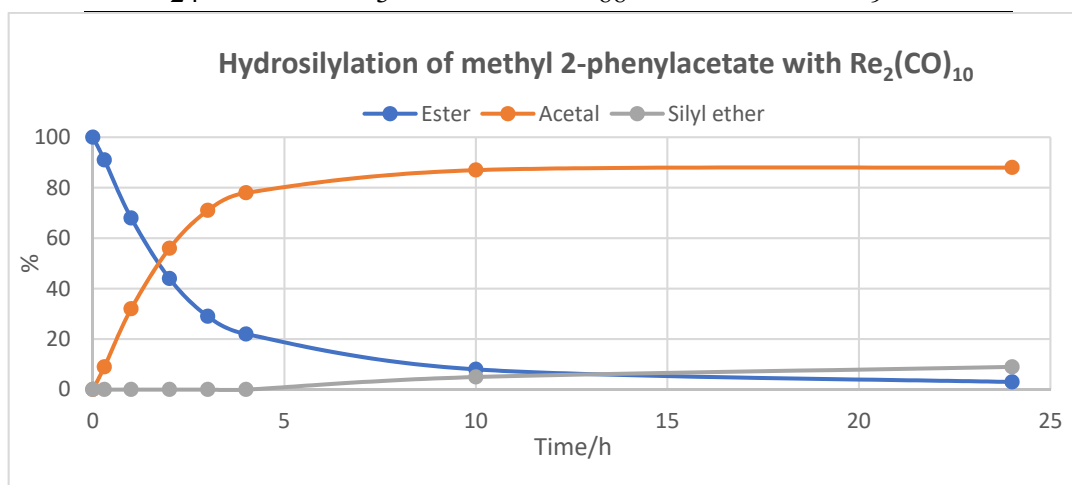
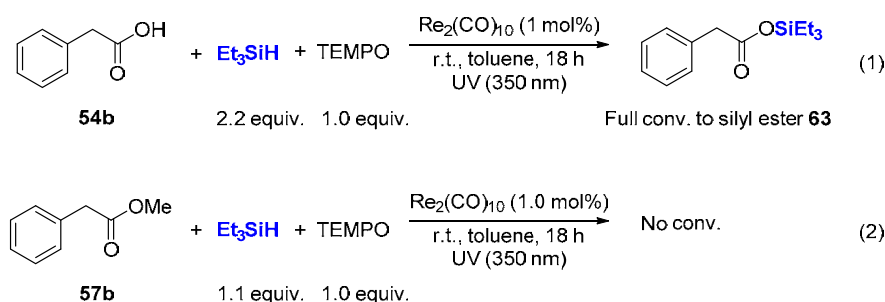


**Figure 2.** Kinetic profile of the hydrosilylation of methyl 2-phenylacetate **57b** catalyzed by  $\text{Re}_2(\text{CO})_{10}$  performed with 1.1 equiv. of  $\text{Et}_3\text{SiH}$  at r.t. in toluene with UV (350 nm) irradiation.



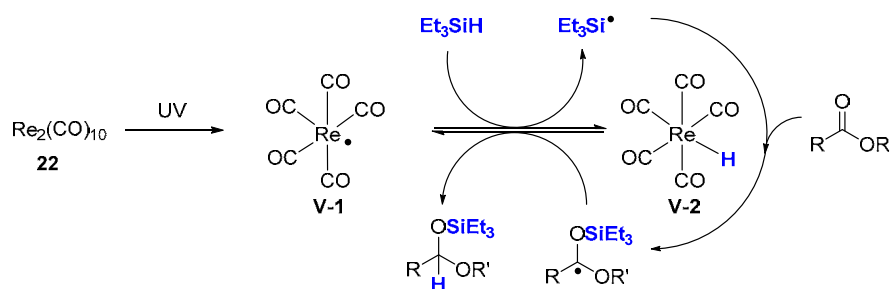
Interestingly, when adding 1.0 equiv. of a radical scavenger, TEMPO (2,2,6,6-tetramethylpiperidin-1-yl)oxyl to the reaction mixture, full conversion of 2-phenylacetic acid **54b** to silyl ester **63** was observed without any formation of the reduction products **55b** or **56b** (equation 1), while methyl 2-phenylacetate **57b** was not converted into any product, (equation 2). These results seem to indicate that the reduction of carboxylic acids and esters catalyzed by  $\text{Mn}_2(\text{CO})_{10}$  and  $\text{Re}_2(\text{CO})_{10}$  involved free radical processes.



**Scheme 26.** TEMPO addition experiment

### Proposed catalytic cycle

Based on our mechanistic study above, and those previously published by Wang<sup>[45]</sup> and Fan<sup>[34]</sup>, we propose here a radical mechanism (Scheme 27). It was reported that  $(\text{CO})_5\text{Re}\cdot$  (**V-1**) was generated *via* the metal–metal bond cleavage of  $\text{Re}_2(\text{CO})_{10}$  under photo-irradiation conditions.<sup>[44]</sup> Then a hydrogen transfer reaction occurred between  $(\text{CO})_5\text{Re}\cdot$  and  $\text{Et}_3\text{SiH}$ , leading to silyl radical and  $\text{HRe}(\text{CO})_5$  (**V-2**).<sup>[44]</sup> The silyl radical  $\text{Et}_3\text{Si}\cdot$  then added to the  $\text{C}=\text{O}$  moiety in the ester substrate to afford alkyl radicals, which underwent hydrogenolysis with  $\text{HRe}(\text{CO})_5$  to form the desired product **58** and regenerate the  $(\text{CO})_5\text{Re}\cdot$  species.



**Scheme 27.** Proposed radical mechanism of the  $\text{Re}_2(\text{CO})_{10}$  catalyzed hydrosilylation of ester.

### **7.5. Conclusion of the Part 2 dedicated to $\text{Mn}_2(\text{CO})_{10}$ and $\text{Re}_2(\text{CO})_{10}$ catalyzed hydrosilylation of carboxylic acids, esters and amides**

In summary, with the commercially available  $\text{Mn}_2(\text{CO})_{10}$  (5.0 mol%) and  $\text{Re}_2(\text{CO})_{10}$  (0.5 mol%) as catalysts and  $\text{Et}_3\text{SiH}$  as an inexpensive silane source, three substrates, namely carboxylic acids, esters and amides can be chemospecifically reduced to the corresponding protected aldehydes (namely acetals) and amines directly, in moderate to good yields at r.t. under UV-LED (395-400 nm) or UV (350 nm) irradiation. Functional groups, such as amino, furyl, thienyl, pyridyl and internal C=C double bond, can be well tolerated. Interestingly,  $\text{Re}_2(\text{CO})_{10}$  seems to be a more active catalyst as it allowed to reduce the catalyst loading by a factor of ten compared with  $\text{Mn}_2(\text{CO})_{10}$ . However, despite that, some bromide substrate were not tolerated with  $\text{Re}_2(\text{CO})_{10}$

## 7.6. References

- [1] B. Marciniec, *Silicon Chem.* **2002**, *1*, 155-174.
- [2] K. K. Krishnan, A. M. Thomas, K. S. Sindhu, G. Anilkumar, *Tetrahedron* **2016**, *72*, 1-16.
- [3] X. Yang, C. Wang, *Chem. Asian J.* **2018**, *13*, 2307-2315.
- [4] a) R. G. Harms, W. A. Herrmann, F. E. Kühn, *Coord. Chem. Rev.* **2015**, *296*, 1-23; b) G. S. Owens, J. Arias, M. M. Abu-Omar, *Catal. Today* **2000**, *55*, 317-363; c) C. C. Romão, F. E. Kühn, W. A. Herrmann, *Chem. Rev.* **1997**, *97*, 3197-3246; d) J. H. Espenson, *Chem. Commun.* **1999**, 479-488.
- [5] a) W. A. Volkert, T. J. Hoffman, *Chem. Rev.* **1999**, *99*, 2269-2292; b) J. R. Dilworth, S. J. Parrott, *Chem. Soc. Rev.* **1998**, *27*, 43-55.
- [6] G. Du, M. M. Abu-Omar, *Curr. Org. Chem.* **2008**, *12*, 1185-1198.
- [7] a) J. J. Kennedy-Smith, K. A. Nolin, H. P. Gunterman, F. D. Toste, *J. Am. Chem. Soc.* **2003**, *125*, 4056-4057; b) W. R. Thiel, *Angew. Chem. Int. Ed.* **2003**, *42*, 5390-5392.
- [8] R. L. Yates, *J. Catal.* **1982**, *78*, 111-115.
- [9] a) B. T. Gregg, P. K. Hanna, E. J. Crawford, A. R. Cutler, *J. Am. Chem. Soc.* **1991**, *113*, 384-385; b) P. K. Hanna, B. T. Gregg, A. R. Cutler, *Organometallics* **1991**, *10*, 31-33; c) B. T. Gregg, A. R. Cutler, *Organometallics* **1993**, *12*, 2006-2009; d) B. T. Gregg, A. R. Cutler, *J. Am. Chem. Soc.* **1996**, *118*, 10069-10084; e) M. D. Cavanaugh, B. T. Gregg, R. Chiulli, A. R. Cutler, *J. Organomet. Chem.* **1997**, *547*, 173-182; f) Z. Mao, B. T. Gregg, A. R. Cutler, *Organometallics* **1998**, *17*, 1993-2002; g) B. T. Gregg, A. R. Cutler, *Organometallics* **1994**, *13*, 1039-1043; h) Z. Mao, B. T. Gregg, A. R. Cutler, *J. Am. Chem. Soc.* **1995**, *117*, 10139-10140; i) M. DiBiase Cavanaugh, B. T. Gregg, A. R. Cutler, *Organometallics* **1996**, *15*, 2764-2769.
- [10] S. U. Son, S.-J. Paik, I. S. Lee, Y.-A. Lee, Y. K. Chung, W. K. Seok, H. N. Lee, *Organometallics* **1999**, *18*, 4114-4118.
- [11] P. Magnus, M. R. Fielding, *Tetrahedron Lett.* **2001**, *42*, 6633-6636.
- [12] V. K. Chidara, G. Du, *Organometallics* **2013**, *32*, 5034-5037.
- [13] a) J. Zheng, S. Elangovan, D. A. Valyaev, R. Brousses, V. César, J.-B. Sortais, C. Darcel, N. Lugan, G. Lavigne, *Adv. Synth. Catal.* **2014**, *356*, 1093-1097; b) D. A. Valyaev, D. Wei, S. Elangovan, M. Cavailles, V. Dorcet, J.-B. Sortais, C. Darcel, N. Lugan, *Organometallics* **2016**, *35*, 4090-4098.
- [14] a) I. Ojima, M. Nihonyanagi, T. Kogure, M. Kumagai, S. Horiuchi, K. Nakatsugawa, Y. Nagai, *J. Organomet. Chem.* **1975**, *94*, 449-461; b) K. Riener, M. P. Högerl, P. Gigler, F. E. Kühn, *ACS Catal.* **2012**, *2*, 613-621.
- [15] M. Pinto, S. Friães, F. Franco, J. Lloret-Fillol, B. Royo, *ChemCatChem* **2018**, *10*, 2734-2740.
- [16] a) T. K. Mukhopadhyay, M. Flores, T. L. Groy, R. J. Trovitch, *J. Am. Chem. Soc.* **2014**, *136*, 882-885; b) R. J. Trovitch, *Synlett* **2014**, *25*, 1638-1642; c) C. Ghosh, T. K. Mukhopadhyay, M. Flores, T. L. Groy, R. J. Trovitch, *Inorg. Chem.* **2015**, *54*, 10398-10406; d) T. K. Mukhopadhyay, C. Ghosh, M. Flores, T. L. Groy, R. J. Trovitch, *Organometallics* **2017**, *36*, 3477-3483; e) T. K. Mukhopadhyay, C. L. Rock, M. Hong, D. C. Ashley, T. L. Groy, M.-H. Baik, R. J. Trovitch, *J. Am. Chem. Soc.* **2017**, *139*, 4901-4915; f) R. J. Trovitch, *Acc. Chem. Res.* **2017**, *50*, 2842-2852.
- [17] Y. Kobayashi, *J. Synth. Org. Chem Jpn.* **2010**, *68*, 866-867.
- [18] L. W. Chung, H. G. Lee, Z. Lin, Y.-D. Wu, *J. Org. Chem.* **2006**, *71*, 6000-6009.
- [19] K. A. Nolin, J. R. Krumper, M. D. Pluth, R. G. Bergman, F. D. Toste, *J. Am. Chem. Soc.* **2007**, *129*, 14684-14696.
- [20] L. Huang, W. Wang, X. Wei, H. Wei, *J. Phys. Chem. A* **2015**, *119*, 3789-3799.
- [21] S. Rendler, M. Oestreich, *Angew. Chem. Int. Ed.* **2008**, *47*, 5997-6000.
- [22] B. Royo, C. C. Romão, *J. Mol. Catal. A: Chem.* **2005**, *236*, 107-112.
- [23] E. A. Ison, E. R. Trivedi, R. A. Corbin, M. M. Abu-Omar, *J. Am. Chem. Soc.* **2005**, *127*, 15374-15375.
- [24] a) G. Du, M. M. Abu-Omar, *Organometallics* **2006**, *25*, 4920-4923; b) E. A. Ison, J. E. Cessarich, G. Du, P. E. Fanwick, M. M. Abu-Omar, *Inorg. Chem.* **2006**, *45*, 2385-2387.
- [25] G. Du, P. E. Fanwick, M. M. Abu-Omar, *Inorg. Chim. Acta* **2008**, *361*, 3184-3192.
- [26] K. A. Nolin, R. W. Ahn, Y. Kobayashi, J. J. Kennedy-Smith, F. D. Toste, *Chem. Eur. J.* **2010**, *16*, 9555-9562.

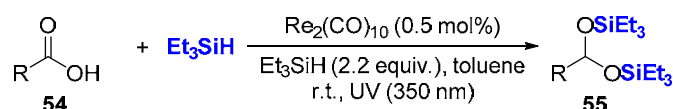
- [27] K. A. Nolin, R. W. Ahn, F. D. Toste, *J. Am. Chem. Soc.* **2005**, *127*, 12462-12463.
- [28] J. L. Smeltz, P. D. Boyle, E. A. Ison, *Organometallics* **2012**, *31*, 5994-5997.
- [29] D. E. Perez, J. L. Smeltz, R. D. Sommer, P. D. Boyle, E. A. Ison, *Dalton Trans.* **2017**, *46*, 4609-4616.
- [30] W. Huang, H. Berke, *Chimia* **2005**, *59*, 113-115.
- [31] A. Choualeb, E. Maccaroni, O. Blacque, H. W. Schmalle, H. Berke, *Organometallics* **2008**, *27*, 3474-3481.
- [32] H. Dong, H. Berke, *Adv. Synth. Catal.* **2009**, *351*, 1783-1788.
- [33] Y. Jiang, O. Blacque, H. Berke, *Dalton Trans.* **2011**, *40*, 2578-2587.
- [34] C. K. Toh, Y. N. Sum, W. K. Fong, S. G. Ang, W. Y. Fan, *Organometallics* **2012**, *31*, 3880-3887.
- [35] S. C. Sousa, A. C. Fernandes, *Adv. Synth. Catal.* **2010**, *352*, 2218-2226.
- [36] J. R. Bernardo, S. C. A. Sousa, P. R. Florindo, M. Wolff, B. Machura, A. C. Fernandes, *Tetrahedron* **2013**, *69*, 9145-9154.
- [37] B. G. Das, P. Ghorai, *Org. Biomol. Chem.* **2013**, *11*, 4379-4382.
- [38] M. Igarashi, T. Fuchikami, *Tetrahedron Lett.* **2001**, *42*, 1945-1947.
- [39] R. Arias-Ugarte, H. K. Sharma, A. L. C. Morris, K. H. Pannell, *J. Am. Chem. Soc.* **2012**, *134*, 848-851.
- [40] C. M. Kelly, R. McDonald, O. L. Sydora, M. Stradiotto, L. Turculet, *Angew. Chem. Int. Ed.* **2017**, *56*, 15901-15904.
- [41] J. Zheng, S. Chevance, C. Darcel, J.-B. Sortais, *Chem. Commun.* **2013**, *49*, 10010-10012.
- [42] I. Cabrita, A. C. Fernandes, *Tetrahedron* **2011**, *67*, 8183-8186.
- [43] R. G. de Noronha, C. C. Romão, A. C. Fernandes, *J. Org. Chem.* **2009**, *74*, 6960-6964.
- [44] M. A. Tehfe, J. Lalevée, D. Gigmes, J. P. Fouassier, *J. Polym. Sci., Part A: Polym. Chem.* **2010**, *48*, 1830-1837.
- [45] X. Yang, C. Wang, *Angew. Chem. Int. Ed.* **2018**, *57*, 923-928.

## 7.7. Experimental data

### 7.7.1. General information.

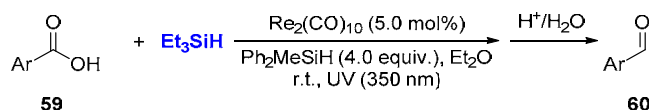
$^1\text{H}$ ,  $^{13}\text{C}\{^1\text{H}\}$ ,  $^{19}\text{F}\{^1\text{H}\}$  and  $^{29}\text{Si}\{^1\text{H}\}$  NMR spectra were recorded in  $\text{CDCl}_3$  at 298 K unless otherwise stated, on Bruker, AVANCE 400 and AVANCE 300 spectrometers at 400.1, and 300.1 MHz, respectively.  $^1\text{H}$  and  $^{13}\text{C}\{^1\text{H}\}$  NMR spectra were calibrated using the residual solvent signal as internal standard ( $^1\text{H}$ :  $\text{CDCl}_3$  7.26 ppm,  $\text{C}_6\text{D}_6$   $^{13}\text{C}$ :  $\text{CDCl}_3$ , central peak is 77.16 ppm  $\text{C}_6\text{D}_6$  128.06 ppm). Chemical shift ( $\delta$ ) and coupling constants ( $J$ ) are given in ppm and in Hz, respectively. The peak patterns are indicated as follows: (s, singlet; d, doublet; t, triplet; q, quartet; quin, quintet; m, multiplet, and br. for broad).

### 7.7.2. Typical procedure for $\text{Re}_2(\text{CO})_{10}$ catalyzed hydrosilylation of acids to disilyl acetals



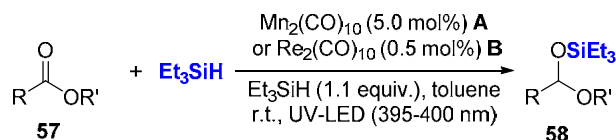
$\text{Re}_2(\text{CO})_{10}$  (1.6 mg, 0.5 mol%) and carboxylic acid **54** (0.5 mmol) were charged in a 20 mL Schlenk tube under argon atmosphere, followed by toluene (1 mL),  $\text{Et}_3\text{SiH}$  (176  $\mu\text{L}$ , 1.1 mmol, 2.2 equiv.), then the Schlenk tube was stirred at room temperature under UV-LED irradiation (395–400 nm, 45 W) for 9 h. The crude solution was then diluted with ethyl acetate (2.0 mL) and filtered through a small pad of celite (2 cm in a Pasteur pipette). The celite was washed with ethyl acetate (2 $\times$ 2.0 mL). The filtrate was evaporated and the crude residue was purified by column chromatography ( $\text{SiO}_2$ , mixture of petroleum ether/ethyl acetate as eluent) to afford the desired product **55**.

### 7.7.3. Typical procedure for $\text{Re}_2(\text{CO})_{10}$ catalyzed hydrosilylation of acids to aldehydes



$\text{Re}_2(\text{CO})_{10}$  (8.2 mg, 5.0 mol%) and carboxylic acid **59** (0.25 mmol) was charged in a 20 mL Schlenk tube under argon atmosphere, followed by  $\text{Et}_2\text{O}$  (0.5 mL),  $\text{Ph}_2\text{MeSiH}$  (200  $\mu\text{L}$ , 1.0 mmol, 4.0 equiv.), then the Schlenk tube was stirred at room temperature under UV irradiations (350 nm) in a Rayonet RPR100 apparatus for 48 h. The crude solution was then hydrolysed at r.t. with trifluoroacetic acid (99%, 0.25 mL) for 3 h. Then the mixture was evaporated and the crude residue was purified by column chromatography ( $\text{SiO}_2$ , mixture of petroleum ether/ethyl acetate as eluent) to afford the desired product **60**.

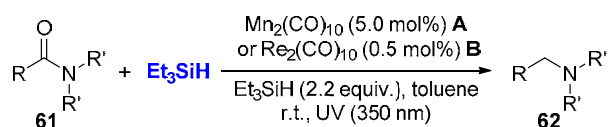
### 7.7.4. Typical procedure for $\text{Mn}_2(\text{CO})_{10}$ or $\text{Re}_2(\text{CO})_{10}$ catalyzed hydrosilylation of esters



$\text{Mn}_2(\text{CO})_{10}$  (9.7 mg, 5.0 mol%) (method **A**) or  $\text{Re}_2(\text{CO})_{10}$  (1.6 mg, 0.5 mol%) (method **B**) was charged in a 20 mL Schlenk tube under argon atmosphere, followed by toluene (1 mL), carboxylic ester **57** (0.5 mmol),  $\text{Et}_3\text{SiH}$  (88  $\mu\text{L}$ , 0.55 mmol, 1.1 equiv.), then the Schlenk tube was stirred at room temperature under UV-LED irradiation (395–400 nm, 45 W) for 9 h. The crude solution was then diluted with ethyl acetate (2.0 mL) and filtered through a small pad of celite (2 cm in a Pasteur pipette). The celite was washed with ethyl acetate (2 $\times$ 2.0 mL). The

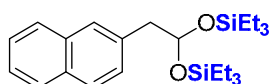
filtrate was evaporated and the crude residue was purified by column chromatography (SiO<sub>2</sub>, mixture of petroleum ether/ethyl acetate as eluent) to afford the desired product **58**.

### 7.7.5. Typical procedure for Mn<sub>2</sub>(CO)<sub>10</sub> or Re<sub>2</sub>(CO)<sub>10</sub> catalyzed hydrosilylation of amides

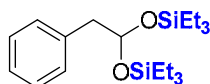


Mn<sub>2</sub>(CO)<sub>10</sub> (9.7 mg, 5.0 mol%) (method **A**) or Re<sub>2</sub>(CO)<sub>10</sub> (1.6 mg, 0.5 mol%) (method **B**) was charged in a 20 mL Schlenk tube under argon atmosphere, followed by toluene (1 mL), carboxylic amide **61** (0.5 mmol), Et<sub>3</sub>SiH (176 μL, 1.1 mmol, 2.2 equiv.), then the Schlenk tube was stirred at room temperature under UV (350 nm) irradiation for 9 h. The crude solution was then diluted with ethyl acetate (2.0 mL) and filtered through a small pad of celite (2 cm in a Pasteur pipette). The celite was washed with ethyl acetate (2×2.0 mL). The filtrate was evaporated and the crude residue was purified by column chromatography (SiO<sub>2</sub>, mixture of petroleum ether/ethyl acetate as eluent) to afford the desired product **62**.

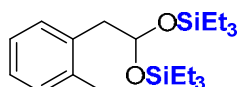
### 7.7.6. Characterization data for disilyl acetals



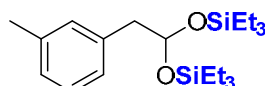
The compound **55a** was prepared as described in the general procedure (202 mg) in 97% yield. <sup>1</sup>H NMR (400 MHz, C<sub>6</sub>D<sub>6</sub>) δ 7.73 – 7.61 (m, 4H), 7.38 (dd, *J* = 8.4, 1.6 Hz, 1H), 7.31 – 7.21 (m, 2H), 5.50 (t, *J* = 5.3 Hz, 1H), 3.08 (d, *J* = 5.3 Hz, 2H), 0.97 (t, *J* = 7.9 Hz, 18H), 0.62 (q, *J* = 7.9 Hz, 12H). <sup>13</sup>C{<sup>1</sup>H} NMR (101 MHz, C<sub>6</sub>D<sub>6</sub>) δ 135.5, 134.1, 132.9, 128.9 (2C), 128.0, 127.92, 127.86, 126.2, 125.6, 94.6, 48.3, 7.2, 5.8. <sup>29</sup>Si{<sup>1</sup>H} NMR (79 MHz, C<sub>6</sub>D<sub>6</sub>) δ 15.78.



The compound **55b** was prepared as described in the general procedure in 96% yield (176.0 mg).<sup>[1]</sup> <sup>1</sup>H NMR (400 MHz, C<sub>6</sub>D<sub>6</sub>) δ 7.21 – 7.14 (m, 4H), 7.12 – 7.06 (m, 1H), 5.38 (t, *J* = 5.3 Hz, 1H), 2.90 (d, *J* = 5.3 Hz, 2H), 0.98 (t, *J* = 8.0 Hz, 18H), 0.61 (q, *J* = 8.0 Hz, 12H). <sup>13</sup>C{<sup>1</sup>H} NMR (101 MHz, C<sub>6</sub>D<sub>6</sub>) δ 138.0, 130.3, 128.4, 126.6, 94.6, 48.3, 7.2, 5.8. <sup>29</sup>Si{<sup>1</sup>H} NMR (79 MHz, C<sub>6</sub>D<sub>6</sub>) δ 15.64.

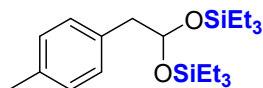


The compound **55c** was prepared as described in the general procedure in 62% yield (118.0 mg).<sup>[1]</sup> <sup>1</sup>H NMR (400 MHz, C<sub>6</sub>D<sub>6</sub>) δ 7.21 – 7.19 (m, 1H), 7.10 – 7.03 (m, 3H), 5.44 (t, *J* = 5.5 Hz, 1H), 2.97 (d, *J* = 5.5 Hz, 2H), 2.29 (s, 3H), 0.98 (t, *J* = 8.0 Hz, 18H), 0.62 (q, *J* = 8.0 Hz, 12H). <sup>13</sup>C{<sup>1</sup>H} NMR (101 MHz, C<sub>6</sub>D<sub>6</sub>) δ 137.0, 136.4, 131.1, 130.4, 126.8, 126.1, 94.3, 45.1, 20.1, 7.1, 5.7. <sup>29</sup>Si{<sup>1</sup>H} NMR (79 MHz, C<sub>6</sub>D<sub>6</sub>) δ 15.75.

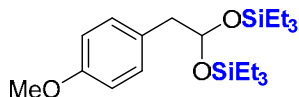


The compound **55d** was prepared as described in the general procedure in 86% yield (163.7 mg).<sup>[1]</sup> <sup>1</sup>H NMR (400 MHz, C<sub>6</sub>D<sub>6</sub>) δ 7.13 – 7.05 (m, 3H), 6.94 (d, *J* = 7.4 Hz, 1H), 5.42 (t, *J* = 5.3 Hz, 1H), 2.94 (d, *J* = 5.3 Hz, 2H), 2.19 (s, 3H), 1.00 (t, *J* = 7.9 Hz, 18H), 0.63 (q, *J*

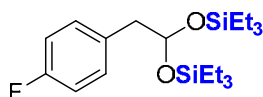
= 7.9 Hz, 12H).  $^{13}\text{C}\{^1\text{H}\}$  NMR (75 MHz,  $\text{C}_6\text{D}_6$ )  $\delta$  137.9, 137.6, 131.3, 127.4, 94.7, 48.2, 21.4, 7.2, 5.8.  $^{29}\text{Si}\{^1\text{H}\}$  NMR (79 MHz,  $\text{C}_6\text{D}_6$ )  $\delta$  15.60.



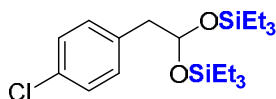
The compound **55e** was prepared as described in the general procedure in 90% yield (171.3 mg).  $^1\text{H}$  NMR (400 MHz,  $\text{C}_6\text{D}_6$ )  $\delta$  7.17 (d,  $J$  = 7.8 Hz, 2H), 7.02 (d,  $J$  = 7.8 Hz, 2H), 5.41 (t,  $J$  = 5.3 Hz, 1H), 2.93 (d,  $J$  = 5.3 Hz, 2H), 2.14 (s, 3H), 1.00 (t,  $J$  = 7.9 Hz, 18H), 0.65 (q,  $J$  = 8.0 Hz, 12H).  $^{13}\text{C}\{^1\text{H}\}$  NMR (75 MHz,  $\text{C}_6\text{D}_6$ )  $\delta$  135.9, 135.0, 130.2, 129.1, 94.8, 47.9, 21.1, 7.2, 5.8.  $^{29}\text{Si}\{^1\text{H}\}$  NMR (79 MHz,  $\text{C}_6\text{D}_6$ )  $\delta$  15.59.



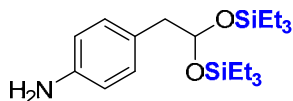
The compound **55f** was prepared as described in the general procedure (188.4 mg) in 95% yield.  $^1\text{H}$  NMR (400 MHz,  $\text{C}_6\text{D}_6$ )  $\delta$  7.16 (d,  $J$  = 8.5 Hz, 2H), 6.82 (d,  $J$  = 8.5 Hz, 2H), 5.40 (t,  $J$  = 5.2 Hz, 1H), 3.33 (s, 3H), 2.91 (d,  $J$  = 5.2 Hz, 2H), 1.01 (t,  $J$  = 8.0 Hz, 18H), 0.65 (q,  $J$  = 8.1 Hz, 12H).  $^{13}\text{C}\{^1\text{H}\}$  NMR (75 MHz,  $\text{C}_6\text{D}_6$ )  $\delta$  159.0, 131.2, 130.0, 114.0, 94.8, 54.8, 47.4, 7.2, 5.8.  $^{29}\text{Si}\{^1\text{H}\}$  NMR (79 MHz,  $\text{C}_6\text{D}_6$ )  $\delta$  15.60.



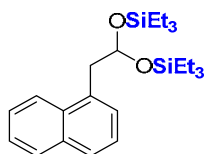
The compound **55g** was prepared as described in the general procedure (177.0 mg) in 92% yield.  $^1\text{H}$  NMR (400 MHz,  $\text{C}_6\text{D}_6$ )  $\delta$  6.99 (dd,  $J$  = 8.5, 5.6 Hz, 2H), 6.83 (t,  $J$  = 8.7 Hz, 2H), 5.29 (t,  $J$  = 5.2 Hz, 1H), 2.79 (d,  $J$  = 5.2 Hz, 2H), 0.97 (t,  $J$  = 7.9 Hz, 18H), 0.60 (q,  $J$  = 8.2 Hz, 12H).  $^{13}\text{C}\{^1\text{H}\}$  NMR (75 MHz,  $\text{C}_6\text{D}_6$ )  $\delta$  162.3 (d,  $J$  = 243.9 Hz), 133.6 (d,  $J$  = 3.2 Hz), 131.7 (d,  $J$  = 7.7 Hz), 115.1 (d,  $J$  = 21.0 Hz), 94.3, 47.2, 7.1, 5.7.  $^{19}\text{F}$  NMR (376 MHz,  $\text{C}_6\text{D}_6$ )  $\delta$  -116.76.  $^{29}\text{Si}\{^1\text{H}\}$  NMR (79 MHz,  $\text{C}_6\text{D}_6$ )  $\delta$  15.88.



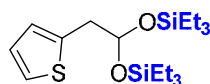
The compound **55h** was prepared as described in the general procedure (196.6 mg) in 98% yield.  $^1\text{H}$  NMR (400 MHz,  $\text{C}_6\text{D}_6$ )  $\delta$  7.16 – 7.13 (m, 2H), 6.94 (d,  $J$  = 8.3 Hz, 2H), 5.28 (t,  $J$  = 5.2 Hz, 1H), 2.75 (d,  $J$  = 5.2 Hz, 2H), 0.97 (t,  $J$  = 7.9 Hz, 18H), 0.59 (q,  $J$  = 8.2 Hz, 12H).  $^{13}\text{C}\{^1\text{H}\}$  NMR (101 MHz,  $\text{C}_6\text{D}_6$ )  $\delta$  136.4, 132.6, 131.7, 128.5, 94.1, 47.3, 7.1, 5.7.  $^{29}\text{Si}\{^1\text{H}\}$  NMR (79 MHz,  $\text{C}_6\text{D}_6$ )  $\delta$  15.98.



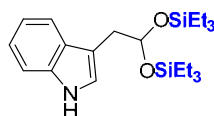
The compound **55j** was prepared as described in the general procedure (143.1 mg) in 75% yield.  $^1\text{H}$  NMR (400 MHz,  $\text{C}_6\text{D}_6$ )  $\delta$  7.07 (d,  $J$  = 8.3 Hz, 2H), 6.36 (d,  $J$  = 8.3 Hz, 2H), 5.39 (t,  $J$  = 5.3 Hz, 1H), 2.89 (d,  $J$  = 5.3 Hz, 2H), 2.77 (br, 2H), 1.02 (t,  $J$  = 7.9 Hz, 18H), 0.65 (q,  $J$  = 8.1 Hz, 12H).  $^{13}\text{C}\{^1\text{H}\}$  NMR (101 MHz,  $\text{C}_6\text{D}_6$ )  $\delta$  145.7, 131.0, 127.4, 114.9, 95.1, 47.5, 7.2, 5.8.  $^{29}\text{Si}\{^1\text{H}\}$  NMR (79 MHz,  $\text{C}_6\text{D}_6$ )  $\delta$  15.41.



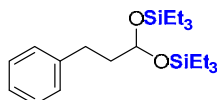
The compound **55l** was prepared as described in the general procedure (158.4 mg) in 75% yield.<sup>[1]</sup>  $^1\text{H}$  NMR (300 MHz,  $\text{C}_6\text{D}_6$ )  $\delta$  8.19 (d,  $J$  = 8.4 Hz, 1H), 7.67 (d,  $J$  = 8.2 Hz, 1H), 7.59 (d,  $J$  = 8.1 Hz, 1H), 7.38 – 7.32 (m, 2H), 7.29 – 7.24 (m, 2H), 5.63 (t,  $J$  = 5.4 Hz, 1H), 3.41 (d,  $J$  = 5.3 Hz, 2H), 0.93 (t,  $J$  = 7.9 Hz, 18H), 0.56 (q,  $J$  = 8.2 Hz, 12H).  $^{13}\text{C}\{^1\text{H}\}$  NMR (75 MHz,  $\text{C}_6\text{D}_6$ )  $\delta$  134.5, 134.4, 133.3, 129.0, 128.5, 127.6, 125.9, 125.7 (2C), 124.8, 94.2, 45.0, 7.1, 5.8.  $^{29}\text{Si}\{^1\text{H}\}$  NMR (79 MHz,  $\text{C}_6\text{D}_6$ )  $\delta$  15.84.



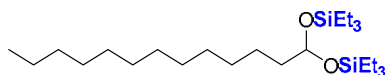
The compound **55m** was prepared as described in the general procedure (109.0 mg) in 59% yield.<sup>[1]</sup>  $^1\text{H}$  NMR (300 MHz,  $\text{C}_6\text{D}_6$ )  $\delta$  6.88 (dd,  $J$  = 4.8, 1.5 Hz, 1H), 6.78 – 6.75 (m, 2H), 5.41 (t,  $J$  = 5.0 Hz, 1H), 3.09 (d,  $J$  = 4.9 Hz, 2H), 1.00 (t,  $J$  = 7.9 Hz, 18H), 0.64 (q,  $J$  = 8.0 Hz, 12H).  $^{13}\text{C}\{^1\text{H}\}$  NMR (75 MHz,  $\text{C}_6\text{D}_6$ )  $\delta$  139.5, 126.7, 126.5, 124.4, 93.9, 42.2, 7.2, 5.8.  $^{29}\text{Si}\{^1\text{H}\}$  NMR (79 MHz,  $\text{C}_6\text{D}_6$ )  $\delta$  16.16.



The compound **55n** was prepared as described in the general procedure (180.5 mg) in 89% yield.<sup>[1]</sup>  $^1\text{H}$  NMR (300 MHz,  $\text{C}_6\text{D}_6$ )  $\delta$  7.81 – 7.78 (m, 1H), 7.24 – 7.19 (m, 2H), 7.09 – 7.05 (m, 1H), 6.72 (s, 2H), 5.58 (t,  $J$  = 5.3 Hz, 1H), 3.18 (d,  $J$  = 5.3 Hz, 2H), 1.00 (t,  $J$  = 7.9 Hz, 18H), 0.65 (q,  $J$  = 8.0 Hz, 12H).  $^{13}\text{C}\{^1\text{H}\}$  NMR (75 MHz,  $\text{C}_6\text{D}_6$ )  $\delta$  136.6, 128.6, 123.0, 122.1, 119.6, 119.5, 112.0, 111.3, 94.2, 37.8, 7.2, 5.8.  $^{29}\text{Si}\{^1\text{H}\}$  NMR (79 MHz,  $\text{C}_6\text{D}_6$ )  $\delta$  15.52.

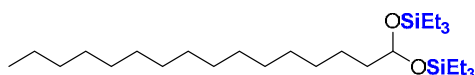


The compound **55o** was prepared as described in the general procedure (177.0 mg) in 93% yield.<sup>[1]</sup>  $^1\text{H}$  NMR (400 MHz,  $\text{C}_6\text{D}_6$ )  $\delta$  7.20 – 7.16 (m, 4H), 7.08 – 7.04 (m, 1H), 5.29 (t,  $J$  = 4.9 Hz, 1H), 2.84 – 2.80 (m, 2H), 2.00 – 1.95 (m, 2H), 1.03 (t,  $J$  = 7.9 Hz, 18H), 0.67 (q,  $J$  = 7.9 Hz, 12H).  $^{13}\text{C}\{^1\text{H}\}$  NMR (101 MHz,  $\text{C}_6\text{D}_6$ )  $\delta$  142.5, 128.8 (2C), 126.2, 93.2, 43.0, 31.4, 7.2, 5.9.  $^{29}\text{Si}\{^1\text{H}\}$  NMR (79 MHz,  $\text{C}_6\text{D}_6$ )  $\delta$  15.36.

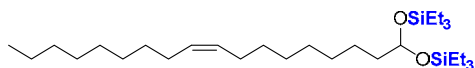


The compound **55p** was prepared as described in the general procedure (218.0 mg) in 98% yield.<sup>[1]</sup>  $^1\text{H}$  NMR (400 MHz,  $\text{C}_6\text{D}_6$ )  $\delta$  5.34 (t,  $J$  = 5.0 Hz, 1H), 1.75 – 1.70 (m, 2H), 1.59–1.53 (m, 2H), 1.37– 1.30 (m, 18H), 1.07 (t,  $J$  = 7.9 Hz, 18H), 0.92 (t,  $J$  = 16.4 Hz, 3H), 0.72 (q,  $J$  = 7.9 Hz, 12H).  $^{13}\text{C}\{^1\text{H}\}$  NMR (101 MHz,  $\text{C}_6\text{D}_6$ )  $\delta$  94.0, 41.4, 32.4, 30.22, 30.17, 30.14, 30.13, 30.10, 30.0, 29.8, 25.1, 23.1, 14.4, 7.3, 5.9.  $^{29}\text{Si}\{^1\text{H}\}$  NMR (79 MHz,  $\text{C}_6\text{D}_6$ )  $\delta$  14.94.

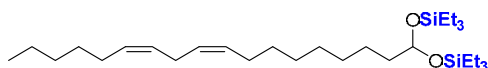




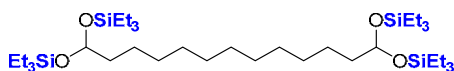
The compound **55q** was prepared as described in the general procedure (236.2 mg) in 97% yield.<sup>[1]</sup>  $^1\text{H NMR}$  (400 MHz,  $\text{C}_6\text{D}_6$ )  $\delta$  5.29 (t,  $J$  = 5.0 Hz, 1H), 1.69 – 1.64 (m, 2H), 1.53–1.50 (m, 2H), 1.34 – 1.30 (m, 24H), 1.04 (t,  $J$  = 8.0 Hz, 18H), 0.91 (t,  $J$  = 6.8 Hz, 3H), 0.68 (q,  $J$  = 7.9 Hz, 12H).  $^{13}\text{C}\{^1\text{H}\}$  NMR (101 MHz,  $\text{C}_6\text{D}_6$ )  $\delta$  94.0, 41.5, 32.4, 30.3, 30.23, 30.17, 30.1, 29.9, 25.2, 23.2, 14.4, 7.3, 6.0.  $^{29}\text{Si}\{^1\text{H}\}$  NMR (79 MHz,  $\text{C}_6\text{D}_6$ )  $\delta$  14.79.



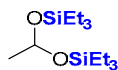
The compound **55r** was prepared as described in the general procedure (238.5 mg) in 93% yield.<sup>[1]</sup>  $^1\text{H NMR}$  (400 MHz,  $\text{C}_6\text{D}_6$ )  $\delta$  5.54 – 5.46 (m, 2H), 5.33 (t,  $J$  = 5.0 Hz, 1H), 2.13 – 2.08 (m, 4H), 1.74 – 1.69 (m, 2H), 1.56–1.53 (m, 2H), 1.42 – 1.21 (m, 20H), 1.07 (t,  $J$  = 7.9 Hz, 18H), 0.92 (t,  $J$  = 6.7 Hz, 3H), 0.72 (q,  $J$  = 8.0 Hz, 12H).  $^{13}\text{C}\{^1\text{H}\}$  NMR (126 MHz,  $\text{C}_6\text{D}_6$ )  $\delta$  130.3, 130.2, 93.9, 41.4, 32.3, 30.3, 30.2, 30.1, 30.00, 29.98, 29.79, 29.77, 29.69, 27.7, 25.1, 23.1, 14.4, 7.3, 5.9.  $^{29}\text{Si}\{^1\text{H}\}$  NMR (79 MHz,  $\text{C}_6\text{D}_6$ )  $\delta$  14.93.



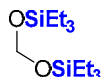
The compound **55s** was prepared as described in the general procedure (222.3 mg) in 87% yield.  $^1\text{H NMR}$  (400 MHz,  $\text{C}_6\text{D}_6$ )  $\delta$  5.53 – 5.43 (m, 4H), 5.32 (t,  $J$  = 5.0 Hz, 1H), 2.89 (t,  $J$  = 6.0 Hz, 2H), 2.11 – 2.05 (m, 4H), 1.73 – 1.68 (m, 2H), 1.50 – 1.25 (m, 16H), 1.07 (t,  $J$  = 7.9 Hz, 18H), 0.89 (t,  $J$  = 6.9 Hz, 3H), 0.71 (q,  $J$  = 7.9 Hz, 12H).  $^{13}\text{C}\{^1\text{H}\}$  NMR (101 MHz,  $\text{C}_6\text{D}_6$ )  $\delta$  130.4, 130.4, 128.5, 128.4, 93.9, 41.4, 31.9, 30.14, 30.12, 30.0, 29.8, 29.7, 27.71, 27.66, 26.2, 25.1, 23.0, 14.3, 7.3, 5.9.  $^{29}\text{Si}\{^1\text{H}\}$  NMR (79 MHz,  $\text{C}_6\text{D}_6$ )  $\delta$  14.92. HR-MS (ESI):  $m/z$  calcd for  $\text{C}_{30}\text{H}_{62}\text{O}_2\text{NaSi}_2$  ( $\text{M} + \text{Na}^+$ ) 533.41806, found 533.4176 (1 ppm).



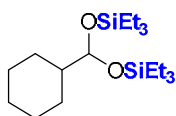
The compound **55t** was prepared as described in the general procedure (349.2 mg) in 99% yield.<sup>[1]</sup>  $^1\text{H NMR}$  (500 MHz,  $\text{C}_6\text{D}_6$ )  $\delta$  5.32 – 5.29 (m, 2H), 1.70 – 1.67 (m, 4H), 1.34 – 1.30 (m, 18H), 1.06 (t,  $J$  = 8.0 Hz, 36H), 0.70 (q,  $J$  = 7.9 Hz, 24H).  $^{13}\text{C}\{^1\text{H}\}$  NMR (126 MHz,  $\text{C}_6\text{D}_6$ )  $\delta$  94.0, 41.5, 30.2, 30.15, 30.13, 30.0, 25.1, 7.3, 6.0.  $^{29}\text{Si}\{^1\text{H}\}$  NMR (79 MHz,  $\text{C}_6\text{D}_6$ )  $\delta$  14.86.



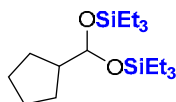
The compound **55u** was prepared as described in the general procedure (133.7 mg) in 92% yield.<sup>[1]</sup>  $^1\text{H NMR}$  (500 MHz,  $\text{C}_6\text{D}_6$ )  $\delta$  5.40 (q,  $J$  = 4.9 Hz, 1H), 1.33 (d,  $J$  = 4.9 Hz, 3H), 1.03 (t,  $J$  = 8.0 Hz, 18H), 0.66 (q,  $J$  = 8.0 Hz, 12H).  $^{13}\text{C}\{^1\text{H}\}$  NMR (126 MHz,  $\text{C}_6\text{D}_6$ )  $\delta$  90.9, 27.8, 7.2, 5.8.  $^{29}\text{Si}\{^1\text{H}\}$  NMR (79 MHz,  $\text{C}_6\text{D}_6$ )  $\delta$  14.83.



The compound **55v** was prepared as described in the general procedure (124.5 mg) in 90% yield.<sup>[1]</sup>  $^1\text{H NMR}$  (400 MHz,  $\text{C}_6\text{D}_6$ )  $\delta$  5.05 (s, 2H), 1.02 (t,  $J$  = 7.9 Hz, 18H), 0.64 (q,  $J$  = 8.0 Hz, 12H).  $^{13}\text{C}\{^1\text{H}\}$  NMR (101 MHz,  $\text{C}_6\text{D}_6$ )  $\delta$  84.5, 7.0, 5.3.  $^{29}\text{Si}\{^1\text{H}\}$  NMR (79 MHz,  $\text{C}_6\text{D}_6$ )  $\delta$  18.33.

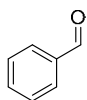


The compound **55w** was prepared as described in the general procedure (163.2 mg) in 91% yield.<sup>[2]</sup>  $^1\text{H NMR}$  (400 MHz,  $\text{C}_6\text{D}_6$ )  $\delta$  5.09 (d,  $J$  = 3.1 Hz, 1H), 1.89 – 1.66 (m, 5H), 1.47 – 1.21 (m, 6H), 1.05 (t,  $J$  = 7.9 Hz, 18H), 0.70 (q,  $J$  = 7.9 Hz, 12H).  $^{13}\text{C}\{^1\text{H}\}$  NMR (101 MHz,  $\text{C}_6\text{D}_6$ )  $\delta$  96.4, 47.7, 27.5, 27.2, 26.7, 7.3, 5.9.  $^{29}\text{Si}\{^1\text{H}\}$  NMR (79 MHz,  $\text{C}_6\text{D}_6$ )  $\delta$  14.71.

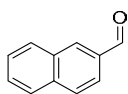


The compound **55x** was prepared as described in the general procedure (155.1 mg) in 90% yield.  $^1\text{H NMR}$  (400 MHz,  $\text{C}_6\text{D}_6$ )  $\delta$  5.21 (d,  $J$  = 4.1 Hz, 1H), 2.15 – 2.06 (m, 1H), 1.70 – 1.66 (m, 8H), 1.05 (t,  $J$  = 7.9 Hz, 18H), 0.69 (q,  $J$  = 7.9 Hz, 12H).  $^{13}\text{C}\{^1\text{H}\}$  NMR (75 MHz,  $\text{C}_6\text{D}_6$ )  $\delta$  95.9, 48.8, 27.8, 26.6, 7.3, 5.9.  $^{29}\text{Si}\{^1\text{H}\}$  NMR (79 MHz,  $\text{C}_6\text{D}_6$ )  $\delta$  14.69.

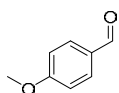
#### 7.7.7. Characterization data for aldehydes



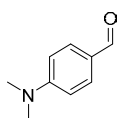
The compound **60a** was prepared as described in the general procedure (17.2 mg) in 65% yield.<sup>[3]</sup>  $^1\text{H NMR}$  (400 MHz,  $\text{CDCl}_3$ ) 10.02 (s, 1H), 7.90 – 7.87 (m, 2H), 7.66 – 7.61 (m, 1H), 7.55 – 7.51 (m, 2H).  $^{13}\text{C}\{^1\text{H}\}$  NMR (101 MHz,  $\text{CDCl}_3$ )  $\delta$  192.5, 136.6, 134.6, 129.9, 129.1.



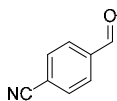
The compound **60b** was prepared as described in the general procedure (32.0 mg) in 82% yield.<sup>[3]</sup>  $^1\text{H NMR}$  (400 MHz,  $\text{CDCl}_3$ )  $\delta$  10.14 (s, 1H), 8.31 (s, 1H), 7.98 (d,  $J$  = 8.1 Hz, 1H), 7.96 – 7.87 (m, 3H), 7.65 – 7.61 (m, 1H), 7.60 – 7.56 (m, 1H).  $^{13}\text{C}\{^1\text{H}\}$  NMR (101 MHz,  $\text{CDCl}_3$ )  $\delta$  192.3, 136.5, 134.6, 134.2, 132.7, 129.6, 129.18, 129.15, 128.1, 127.2, 122.8.



The compound **60c** was prepared as described in the general procedure (26.9 mg) in 79% yield.<sup>[4]</sup>  $^1\text{H NMR}$  (400 MHz,  $\text{CDCl}_3$ )  $\delta$  9.88 (s, 1H), 7.83 (d,  $J$  = 8.8 Hz, 2H), 6.99 (d,  $J$  = 8.8 Hz, 2H), 3.88 (s, 3H).  $^{13}\text{C}\{^1\text{H}\}$  NMR (101 MHz,  $\text{CDCl}_3$ )  $\delta$  190.9, 164.7, 132.1, 130.1, 114.4, 55.7.



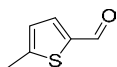
The compound **60d** was prepared as described in the general procedure (23.5 mg) in 63% yield.<sup>[5]</sup>  $^1\text{H NMR}$  (400 MHz,  $\text{CDCl}_3$ )  $\delta$  9.74 (s, 1H), 7.73 (d,  $J$  = 8.9 Hz, 2H), 6.70 (d,  $J$  = 8.9 Hz, 2H), 3.08 (s, 6H).  $^{13}\text{C}\{^1\text{H}\}$  NMR (101 MHz,  $\text{CDCl}_3$ )  $\delta$  190.4, 154.5, 132.1, 125.3, 111.1, 40.2.



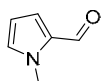
The compound **60g** was prepared as described in the general procedure (8.8 mg) in 27% yield.<sup>[6]</sup>  $^1\text{H NMR}$  (400 MHz,  $\text{CDCl}_3$ )  $\delta$  10.09 (s, 1H), 7.99 (d,  $J$  = 8.4 Hz, 2H), 7.84 (d,  $J$  = 8.2 Hz, 2H).  $^{13}\text{C}\{^1\text{H}\}$  NMR (101 MHz,  $\text{CDCl}_3$ )  $\delta$  190.7, 138.9, 133.0, 130.0, 117.8, 117.7.



The compound **60h** was prepared as described in the general procedure (13.9 mg) in 58% yield.<sup>[7]</sup>  $^1\text{H NMR}$  (400 MHz,  $\text{CDCl}_3$ )  $\delta$  9.65 (s, 1H), 7.68 – 7.68 (m, 1H), 7.24 (dd,  $J$  = 3.6, 0.8 Hz, 1H), 6.59 (dd,  $J$  = 3.6, 1.7 Hz, 1H).  $^{13}\text{C}\{^1\text{H}\}$  NMR (101 MHz,  $\text{CDCl}_3$ )  $\delta$  178.0, 153.1, 148.2, 121.1, 112.7.

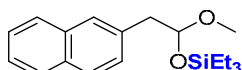


The compound **60i** was prepared as described in the general procedure (17.3 mg) in 55% yield.<sup>[8]</sup>  $^1\text{H NMR}$  (400 MHz,  $\text{CDCl}_3$ )  $\delta$  9.80 (s, 1H), 7.59 (d,  $J$  = 3.7 Hz, 1H), 6.88 (dd,  $J$  = 3.7, 0.8 Hz, 1H), 2.57 (s, 3H).  $^{13}\text{C}\{^1\text{H}\}$  NMR (101 MHz,  $\text{CDCl}_3$ )  $\delta$  182.7, 151.8, 142.1, 137.4, 127.2, 16.4.

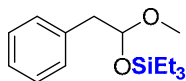


The compound **60j** was prepared as described in the general procedure (6.3 mg) in 23% yield.<sup>[9]</sup>  $^1\text{H NMR}$  (400 MHz,  $\text{CDCl}_3$ )  $\delta$  9.55 (d,  $J$  = 0.8 Hz, 1H), 6.91 (dd,  $J$  = 4.0, 1.7 Hz, 1H), 6.88 – 6.87 (m, 1H), 6.21 (dd,  $J$  = 4.0, 2.4 Hz, 1H), 3.95 (s, 3H).  $^{13}\text{C}\{^1\text{H}\}$  NMR (101 MHz,  $\text{CDCl}_3$ )  $\delta$  179.7, 132.15, 132.12, 124.2, 109.6, 36.6.

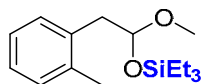
#### 7.7.8. Characterization data for the hydrosilylation products



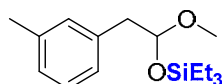
The compound **58a** was prepared as described in the general procedure (method A) (129.8 mg) in 82% yield.  $^1\text{H NMR}$  (400 MHz,  $\text{CDCl}_3$ )  $\delta$  7.82 – 7.76 (m, 3H), 7.67 (s, 1H), 7.47 – 7.40 (m, 2H), 7.38 (dd,  $J$  = 8.4, 1.6, 1H), 4.94 (ABX,  $J_{\text{AX}}$  = 6.1,  $J_{\text{BX}}$  = 4.7 Hz, 1H), 3.34 (s, 3H), 3.05 (ABX,  $J_{\text{AB}}$  = 13.7,  $J_{\text{AX}}$  = 6.1,  $J_{\text{BX}}$  = 4.7,  $\Delta\nu$  = 60.4 Hz, 2H), 0.94 (t,  $J$  = 7.9 Hz, 9H), 0.60 (q,  $J$  = 8.2 Hz, 6H).  $^{13}\text{C}\{^1\text{H}\}$  NMR (101 MHz,  $\text{CDCl}_3$ )  $\delta$  134.9, 133.6, 132.4, 128.4, 128.3, 127.8, 127.72, 127.68, 126.0, 125.4, 99.9, 54.1, 44.4, 6.9, 5.1.  $^{29}\text{Si}\{^1\text{H}\}$  NMR (80 MHz,  $\text{C}_6\text{D}_6$ )  $\delta$  16.8.



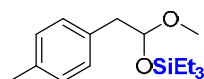
The compound **58b** was prepared as described in the general procedure (method B) (119.9 mg) in 92% yield.<sup>[10]</sup>  $^1\text{H NMR}$  (400 MHz,  $\text{C}_6\text{D}_6$ )  $\delta$  7.23 – 7.20 (m, 2H), 7.18 – 7.15 (m, 2H), 7.10 – 7.06 (m, 1H), 4.88 (ABX,  $J_{\text{AX}}$  = 5.7,  $J_{\text{BX}}$  = 5.0 Hz, 1H), 3.15 (s, 3H), 2.94 (ABX,  $J_{\text{AB}}$  = 13.5,  $J_{\text{AX}}$  = 5.7,  $J_{\text{BX}}$  = 5.0,  $\Delta\nu$  = 65.4 Hz, 2H), 0.96 (t,  $J$  = 7.9 Hz, 9H), 0.56 (q,  $J$  = 8.1 Hz, 6H).  $^{13}\text{C}\{^1\text{H}\}$  NMR (101 MHz,  $\text{C}_6\text{D}_6$ )  $\delta$  137.9, 130.2, 128.5, 126.6, 100.2, 53.3, 44.4, 7.1, 5.4.  $^{29}\text{Si}\{^1\text{H}\}$  NMR (79 MHz,  $\text{C}_6\text{D}_6$ )  $\delta$  16.68.



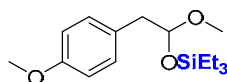
The compound **58c** was prepared as described in the general procedure (method B) (105.2 mg) in 75% yield.  $^1\text{H}$  NMR (300 MHz,  $\text{CDCl}_3$ )  $\delta$  7.20 – 7.10 (m, 4H), 4.87 (ABX,  $J_{\text{AX}} = 5.9$ ,  $J_{\text{BX}} = 5.2$  kHz, 1H), 3.33 (s, 3H), 2.92 (ABX,  $J_{\text{AB}} = 13.8$ ,  $J_{\text{AX}} = 5.9$ ,  $J_{\text{BX}} = 5.2$ ,  $\Delta\nu = 48.1$  Hz, 2H), 2.35 (s, 3H), 0.93 (t,  $J = 7.9$  Hz, 9H), 0.57 (q,  $J = 7.5$  Hz, 6H).  $^{13}\text{C}\{^1\text{H}\}$  NMR (75 MHz,  $\text{CDCl}_3$ )  $\delta$  136.9, 135.8, 130.6, 130.2, 126.6, 125.8, 99.5, 54.0, 41.2, 20.0, 6.9, 5.1.  $^{29}\text{Si}\{^1\text{H}\}$  NMR (80 MHz,  $\text{C}_6\text{D}_6$ )  $\delta$  16.7.



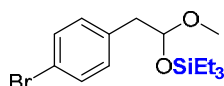
The compound **58d** was prepared as described in the general procedure (method B) (95.4 mg) in 68% yield.  $^1\text{H}$  NMR  $\delta$  7.13 – 7.11 (m, 1H), 7.08 – 7.06 (m, 2H), 6.93 (d,  $J = 7.2$  Hz, 1H), 4.91 (ABX,  $J_{\text{AX}} = 5.6$ ,  $J_{\text{BX}} = 5.1$  Hz, 1H), 3.17 (s, 3H), 2.95 (ABX,  $J_{\text{AB}} = 13.5$ ,  $J_{\text{AX}} = 5.6$ ,  $J_{\text{BX}} = 5.1$  kHz,  $\Delta\nu = 63.4$  Hz, 2H), 2.16 (s, 3H), 0.97 (t,  $J = 7.9$  Hz, 9H), 0.58 (t,  $J = 8.0$  Hz, 6H).  $^{13}\text{C}\{^1\text{H}\}$  NMR (101 MHz,  $\text{C}_6\text{D}_6$ )  $\delta$  137.8, 137.7, 131.1, 128.4, 127.4, 127.3, 100.3, 53.3, 44.4, 21.4, 7.1, 5.5.  $^{29}\text{Si}\{^1\text{H}\}$  NMR (80 MHz,  $\text{C}_6\text{D}_6$ )  $\delta$  16.55.



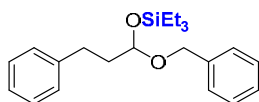
The compound **58e** was prepared as described in the general procedure (method A) (112.2 mg) in 80% yield.  $^1\text{H}$  NMR (300 MHz,  $\text{C}_6\text{D}_6$ )  $\delta$  7.17 (d,  $J = 7.8$  Hz, 2H), 7.01 (d,  $J = 7.8$  Hz, 2H), 4.90 (ABX,  $J_{\text{AX}} = 5.9$ ,  $J_{\text{BX}} = 4.9$  Hz, 1H), 3.17 (s, 3H), 2.95 (ABX,  $J_{\text{AB}} = 13.6$ ,  $J_{\text{AX}} = 5.9$ ,  $J_{\text{BX}} = 4.9$ ,  $\Delta\nu = 55.3$  Hz, 2H), 2.13 (s, 3H), 0.97 (t,  $J = 7.9$  Hz, 10H), 0.58 (q,  $J = 8.2$  Hz, 7H).  $^{13}\text{C}\{^1\text{H}\}$  NMR (75 MHz,  $\text{C}_6\text{D}_6$ )  $\delta$  135.8, 134.9, 130.1, 129.2, 100.4, 53.4, 44.1, 21.1, 7.1, 5.5.  $^{29}\text{Si}\{^1\text{H}\}$  NMR (80 MHz,  $\text{C}_6\text{D}_6$ )  $\delta$  16.54.



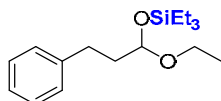
The compound **58f** was prepared as described in the general procedure (method A) (129.0 mg) in 87% yield.  $^1\text{H}$  NMR (300 MHz,  $\text{C}_6\text{D}_6$ )  $\delta$  7.17 – 7.14 (m, 2H), 6.83 – 6.79 (m, 2H), 4.87 (ABX,  $J_{\text{AX}} = 5.8$ ,  $J_{\text{BX}} = 4.9$  Hz, 1H), 3.32 (s, 3H), 3.18 (s, 3H), 2.93 (ABX,  $J_{\text{AB}} = 13.7$ ,  $J_{\text{AX}} = 5.8$ ,  $J_{\text{BX}} = 4.9$  kHz,  $\Delta\nu = 54.8$  Hz, 2H), 0.98 (t,  $J = 7.9$  Hz, 10H), 0.59 (q,  $J = 8.2$  Hz, 7H).  $^{13}\text{C}\{^1\text{H}\}$  NMR (75 MHz,  $\text{C}_6\text{D}_6$ )  $\delta$  159.0, 131.1, 129.9, 114.0, 100.4, 54.8, 53.4, 43.6, 7.1, 5.5.  $^{29}\text{Si}\{^1\text{H}\}$  NMR (80 MHz,  $\text{C}_6\text{D}_6$ )  $\delta$  16.5.



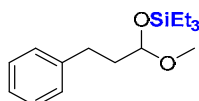
The compound **58g** was prepared as described in the general procedure (method A) (101.9 mg) in 59% yield.  $^1\text{H}$  NMR (300 MHz,  $\text{CDCl}_3$ )  $\delta$  7.42 – 7.37 (m, 2H), 7.12 – 7.08 (m, 2H), 4.81 (ABX,  $J_{\text{AX}} = 5.9$ ,  $J_{\text{BX}} = 4.6$  Hz, 1H), 3.31 (s, 3H), 2.83 (ABX,  $J_{\text{AB}} = 13.7$ ,  $J_{\text{AX}} = 5.9$ ,  $J_{\text{BX}} = 4.6$ ,  $\Delta\nu = 49.9$  Hz, 2H), 0.94 (t,  $J = 7.9$  Hz, 9H), 0.59 (q,  $J = 8.5$ , 8.0 Hz, 6H).  $^{13}\text{C}\{^1\text{H}\}$  NMR (75 MHz,  $\text{CDCl}_3$ )  $\delta$  136.3, 131.6, 131.3, 120.4, 99.4, 54.0, 43.5, 6.9, 5.1.  $^{29}\text{Si}\{^1\text{H}\}$  NMR (80 MHz,  $\text{C}_6\text{D}_6$ )  $\delta$  16.96.



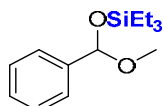
The compound **58h** was prepared as described in the general procedure (method B) (165.8 mg) in 93% yield.  $^1\text{H}$  NMR (300 MHz,  $\text{CDCl}_3$ )  $\delta$  7.40 – 7.36 (m, 4H), 7.35 – 7.26 (m, 3H), 7.23 – 7.16 (m, 3H), 4.93 (ABX,  $J_{\text{AX}} = 6.3$ ,  $J_{\text{BX}} = 4.0$  Hz, 1H), 4.77 (d,  $J = 11.8$  Hz, 1H), 4.49 (d,  $J = 11.8$  Hz, 1H), 2.86 – 2.65 (m, 2H), 2.12 – 1.83 (m, 2H), 1.00 (t,  $J = 7.9$  Hz, 9H), 0.67 (q,  $J = 7.8$  Hz, 6H).  $^{13}\text{C}\{^1\text{H}\}$  NMR (75 MHz,  $\text{CDCl}_3$ )  $\delta$  142.1, 138.6, 128.52, 128.49, 128.47, 127.8, 127.6, 125.9, 97.1, 68.3, 39.5, 30.9, 7.0, 5.3.  $^{29}\text{Si}\{^1\text{H}\}$  NMR (80 MHz,  $\text{C}_6\text{D}_6$ )  $\delta$  17.1.



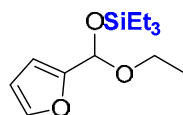
The compound **58i** was prepared as described in the general procedure (method A) (135.5 mg) in 92% yield.<sup>[10]</sup>  $^1\text{H}$  NMR (300 MHz,  $\text{C}_6\text{D}_6$ )  $\delta$  7.21 – 7.18 (m, 4H), 7.12 – 7.05 (m, 1H), 4.81 (ABX,  $J_{\text{AX}} = 5.9$ ,  $J_{\text{BX}} = 4.3$  Hz, 1H), 3.72 – 3.62 (m, 1H), 3.36 – 3.22 (m, 1H), 2.83 – 2.77 (m, 2H), 2.12 – 1.91 (m, 2H), 1.16 (t,  $J = 7.0$  Hz, 3H), 1.03 (t,  $J = 7.9$  Hz, 9H), 0.64 (q,  $J = 8.2$  Hz, 6H).  $^{13}\text{C}\{^1\text{H}\}$  NMR (75 MHz,  $\text{C}_6\text{D}_6$ )  $\delta$  142.5, 128.8, 128.7, 126.1, 97.7, 61.8, 39.8, 31.2, 15.6, 7.2, 5.7.  $^{29}\text{Si}\{^1\text{H}\}$  NMR (80 MHz,  $\text{C}_6\text{D}_6$ )  $\delta$  15.66.



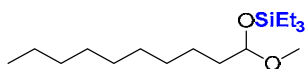
The compound **58j** was prepared as described in the general procedure (method B) (102.4 mg) in 73% yield.  $^1\text{H}$  NMR (300 MHz,  $\text{C}_6\text{D}_6$ )  $\delta$  7.21 – 7.18 (m, 4H), 7.11 – 7.05 (m, 1H), 4.72 (ABX,  $J_{\text{AX}} = 5.8$ ,  $J_{\text{BX}} = 4.4$  Hz, 1H), 3.22 (s, 3H), 2.78 (t,  $J = 8.0$  Hz, 2H), 2.10 – 1.89 (m, 2H), 1.02 (t,  $J = 7.9$  Hz, 9H), 0.64 (q,  $J = 8.2$  Hz, 6H).  $^{13}\text{C}\{^1\text{H}\}$  NMR (101 MHz,  $\text{C}_6\text{D}_6$ )  $\delta$  142.0, 128.4, 128.3, 125.7, 98.3, 52.9, 38.9, 30.8, 6.7, 5.2.  $^{29}\text{Si}\{^1\text{H}\}$  NMR (80 MHz,  $\text{C}_6\text{D}_6$ )  $\delta$  16.15.



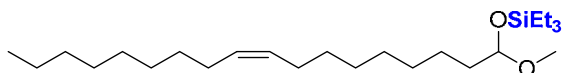
The compound **58l** was prepared as described in the general procedure (method A) (135.5 mg) in 86% yield.  $^1\text{H}$  NMR (400 MHz,  $\text{C}_6\text{D}_6$ )  $\delta$  7.57 – 7.55 (m, 2H), 7.22 – 7.17 (m, 2H), 7.13 – 7.09 (m, 1H), 5.81 (s, 1H), 3.15 (s, 3H), 0.98 (t,  $J = 7.9$  Hz, 9H), 0.63 (q,  $J = 8.0$  Hz, 6H).  $^{13}\text{C}\{^1\text{H}\}$  NMR (101 MHz,  $\text{C}_6\text{D}_6$ )  $\delta$  141.7, 128.5, 128.4, 126.9, 98.0, 51.6, 7.0, 5.4.  $^{29}\text{Si}\{^1\text{H}\}$  NMR (80 MHz,  $\text{C}_6\text{D}_6$ )  $\delta$  18.6.



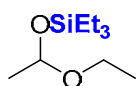
The compound **58p** was prepared as described in the general procedure (method A) (94.5 mg) in 78% yield.  $^1\text{H}$  NMR (400 MHz,  $\text{C}_6\text{D}_6$ )  $\delta$  7.09 (s, 1H), 6.38 (d,  $J = 3.0$  Hz, 1H), 6.09 – 6.08 (m, 1H), 5.90 (s, 1H), 3.60 – 3.48 (m, 2H), 1.11 (t,  $J = 7.0$  Hz, 3H), 1.00 (t,  $J = 7.9$  Hz, 9H), 0.65 (q,  $J = 7.9$  Hz, 6H).  $^{13}\text{C}\{^1\text{H}\}$  NMR (101 MHz,  $\text{C}_6\text{D}_6$ )  $\delta$  155.0, 142.0, 110.3, 107.5, 92.1, 60.6, 15.4, 7.0, 5.3.  $^{29}\text{Si}\{^1\text{H}\}$  NMR (79 MHz,  $\text{C}_6\text{D}_6$ )  $\delta$  19.10.



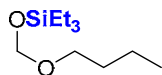
The compound **58s** was prepared as described in the general procedure (method B) (140.7 mg) in 93% yield.  $^1\text{H}$  NMR (400 MHz,  $\text{C}_6\text{D}_6$ )  $\delta$  4.76 (ABX,  $J_{\text{AX}} = 5.8$ ,  $J_{\text{BX}} = 4.6$  Hz, 1H), 3.23 (s, 3H), 1.83 – 1.64 (m, 2H), 1.31 – 1.26 (m, 14H), 1.04 (t,  $J = 7.9$  Hz, 9H), 0.90 (t,  $J = 6.8$  Hz, 3H), 0.67 (q,  $J = 7.9$  Hz, 6H).  $^{13}\text{C}\{^1\text{H}\}$  NMR (101 MHz,  $\text{C}_6\text{D}_6$ )  $\delta$  99.5, 53.1, 37.6, 32.3, 30.2, 30.1, 30.0, 29.8, 25.0, 23.1, 14.4, 7.2, 5.7.  $^{29}\text{Si}\{^1\text{H}\}$  NMR (80 MHz,  $\text{C}_6\text{D}_6$ )  $\delta$  15.7.



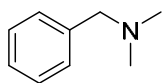
The compound **58t** was prepared as described in the general procedure (method B) (152.7 mg) in 74% yield.  $^1\text{H}$  NMR (400 MHz,  $\text{C}_6\text{D}_6$ )  $\delta$  5.53 – 5.43 (m, 2H), 4.75 (ABX,  $J_{\text{AX}} = 5.7$ ,  $J_{\text{BX}} = 4.6$  Hz, 1H), 3.23 (s, 3H), 2.1 – 2.05 (m, 4H), 1.80 – 1.62 (m, 2H), 1.39 – 1.28 (m, 22H), 1.04 (t,  $J = 7.9$  Hz, 9H), 0.91 (t,  $J = 6.8$  Hz, 3H), 0.66 (q,  $J = 7.9$  Hz, 6H).  $^{13}\text{C}\{^1\text{H}\}$  NMR (126 MHz,  $\text{C}_6\text{D}_6$ )  $\delta$  130.2, 99.5, 53.1, 37.6, 32.3, 32.33, 30.26, 30.23, 30.04, 30.02, 30.00, 29.8, 29.7, 27.7, 25.0, 23.1, 14.4, 7.2, 5.7.  $^{29}\text{Si}\{^1\text{H}\}$  NMR (79 MHz,  $\text{C}_6\text{D}_6$ )  $\delta$  15.70.



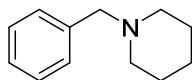
The compound **58q** was prepared as described in the general procedure (method A) (91.0 mg) in 89% yield.  $^1\text{H}$  NMR (400 MHz,  $\text{C}_6\text{D}_6$ )  $\delta$  4.91 (q,  $J = 5.1$  Hz, 1H), 3.71 – 3.64 (m, 1H), 3.32 – 3.24 (m, 1H), 1.33 (d,  $J = 4.8$  Hz, 3H), 1.14 (t,  $J = 7.0$  Hz, 3H), 1.01 (t,  $J = 7.9$  Hz, 9H), 0.62 (q,  $J = 9.6$ , 8.7 Hz, 6H).  $^{13}\text{C}\{^1\text{H}\}$  NMR (101 MHz,  $\text{C}_6\text{D}_6$ )  $\delta$  95.2, 61.6, 24.4, 15.6, 7.1, 5.6.  $^{29}\text{Si}\{^1\text{H}\}$  NMR (80 MHz,  $\text{C}_6\text{D}_6$ )  $\delta$  15.0.



The compound **58r** was prepared as described in the general procedure (method B) (99.4 mg) in 91% yield.  $^1\text{H}$  NMR (300 MHz,  $\text{CDCl}_3$ )  $\delta$  4.85 (s, 2H), 3.55 (t,  $J = 6.6$  Hz, 2H), 1.61 – 1.52 (m, 2H), 1.44 – 1.32 (m, 2H), 0.97 (t,  $J = 7.9$  Hz, 9H), 0.64 (q,  $J = 8.3$  Hz, 6H).  $^{13}\text{C}\{^1\text{H}\}$  NMR (75 MHz,  $\text{CDCl}_3$ )  $\delta$  90.0, 67.9, 32.0, 19.5, 14.1, 6.8, 4.8.  $^{29}\text{Si}\{^1\text{H}\}$  NMR (80 MHz,  $\text{CDCl}_3$ )  $\delta$  19.9.



The compound **62a** was prepared as described in the general procedure (method B) (55.4 mg) in 82% yield.  $^1\text{H}$  NMR (400 MHz,  $\text{C}_6\text{D}_6$ )  $\delta$  7.35 – 7.33 (m, 2H), 7.21 – 7.17 (m, 2H), 7.13 – 7.08 (m, 1H), 3.26 (s, 2H), 2.08 (s, 6H).  $^{13}\text{C}\{^1\text{H}\}$  NMR (101 MHz,  $\text{C}_6\text{D}_6$ )  $\delta$  140.0, 129.2, 128.5, 127.2, 64.6, 45.4.



The compound **62b** was prepared as described in the general procedure (method A) (78.9 mg) in 90% yield.  $^1\text{H}$  NMR (400 MHz,  $\text{CDCl}_3$ )  $\delta$  7.35 – 7.27 (m, 5H), 3.51 (s, br, 2H), 2.41 (s, br, 4H), 1.64 – 1.58 (m, 4H), 1.50 – 1.44 (m, 2H).  $^{13}\text{C}\{^1\text{H}\}$  NMR (101 MHz,  $\text{CDCl}_3$ )  $\delta$  138.8, 129.3, 128.2, 126.9, 64.0, 54.6, 26.1, 24.5.

## 7.8. References

- [1] J. Zheng, S. Chevance, C. Darcel, J.-B. Sortais, *Chem. Commun.* **2013**, 49, 10010-10012.
- [2] N. Buu-Hoï, F. Perin, P. Jacquignon, *J. Heterocycl. Chem.* **1965**, 2, 7-10.
- [3] B. Guan, D. Xing, G. Cai, X. Wan, N. Yu, Z. Fang, L. Yang, Z. Shi, *J. Am. Chem. Soc.* **2005**, 127, 18004-18005.
- [4] N. Jiang, A. J. Ragauskas, *Org. Lett.* **2005**, 7, 3689-3692.
- [5] J. Dorie, J.-P. Gouesnard, M. L. Martin, *J. Chem. Soc., Perkin Trans. 2* **1981**, 912-917.
- [6] B. R. Kim, H.-G. Lee, E. J. Kim, S.-G. Lee, Y.-J. Yoon, *J. Org. Chem.* **2010**, 75, 484-486.
- [7] M. Mascal, E. B. Nikitin, *ChemSusChem* **2009**, 2, 423-426.
- [8] D. L. Comins, M. O. Killpack, *J. Org. Chem.* **1987**, 52, 104-109.
- [9] M. L. Laurila, N. A. Magnus, M. A. Staszak, *Org. Process Res. Dev.* **2009**, 13, 1199-1201.
- [10] Y. Corre, V. Rysak, F. Capet, J.-P. Djukic, F. Agbossou-Niedercorn, C. Michon, *Chem. Eur. J.* **2016**, 22, 14036-14041.

## **Chapter IV - (Transfer)Hydrogenation Reactions Catalyzed by Mn(I) Bidentate Complexes**

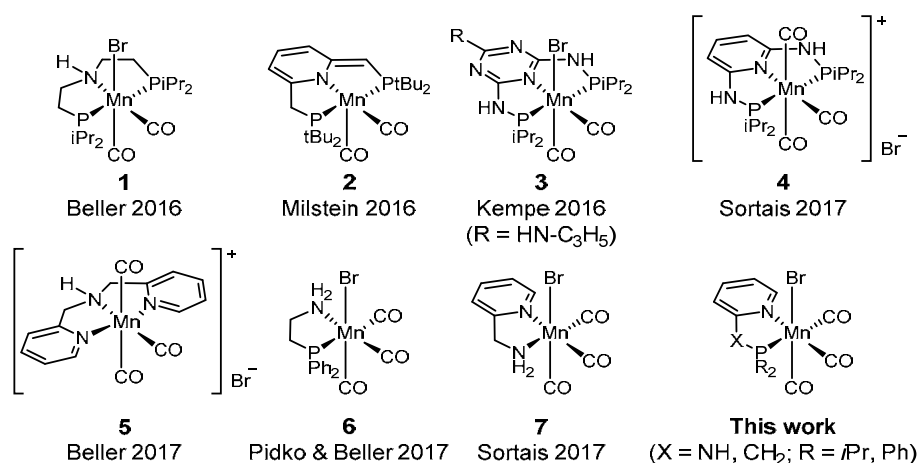




## Chapter IV - (Transfer)Hydrogenation Reactions Catalyzed by Mn(I) Bidentate Complexes

### Introduction

Hydrogenation with molecular dihydrogen is a clean, atom-economic and efficient reaction that has drawn a huge interest for more than a century from the Nobel Prize of Sabatier in 1912 for heterogeneous hydrogenation to the one of Noyori and Knowles in 2001 for asymmetric hydrogenation.<sup>[1]</sup> Homogeneous hydrogenation catalysts are usually complexes based on late transition metals including ruthenium, rhodium, iridium, nickel and palladium. In the last decade, iron has emerged as a powerful sustainable alternative candidate in catalyzed reduction reactions, as it is the most abundant and inexpensive transition metal.<sup>[2]</sup> Actually, the level of the activity, and chemo- and enantioselectivity of iron catalytic systems is now comparable to the ones involving noble transition metals.<sup>[3]</sup> Manganese, being the third most abundant transition metals after iron and titanium, has recently emerged as suitable transition metal for the design of efficient hydrogenation catalysts<sup>[4]</sup> starting with a seminal contribution of Beller in 2016 using the Mn(I) complex **1** featuring a tridentate bis(phosphino)amine ligand (Scheme 1).<sup>[5]</sup> Soon after, a series of parent Mn(I) complexes exhibiting a variety of tridentate ligands including nitrogen and phosphorus donor fragments has been successfully applied in hydrogenation<sup>[6]</sup> and related hydrogen borrowing reactions,<sup>[7]</sup> selected representative examples being shown in Scheme 1.



**Scheme 1.** Representative examples of manganese catalysts for redox reactions.

In the course of our investigations directed toward manganese catalyzed reduction reactions,<sup>[8]</sup> we first demonstrated that the PN<sup>3</sup>P manganese complex **4** bearing a 2,6-(diaminopyridinyl)-diphosphine ligand was suitable for the hydrogenation of carbonyl derivatives,<sup>[6c]</sup> yet with

moderate activity compared to  $\text{PN}^5\text{P}$  analogue **3** developed by Kempe<sup>[6a]</sup> and based on the 2,6-(diaminotriazinyl)-diphosphine ligand. Searching for simpler catalytic system, we found later that the manganese complex **7** featuring a bidentate 2-picolylamine ligand was significantly more active<sup>[6d]</sup> than Beller's tridentate dipicolylamine complex **5**<sup>[6b]</sup> in the case of hydrogen transfer reaction using 2-propanol as the reductant. In the meantime, Pidko and Beller showed that the manganese complex **6** bearing bidentate phosphinoamine ligand was as active as **1** for the hydrogenation of esters.<sup>[5b, 9]</sup>

## IV-1 Hydrogenation of carbonyl derivatives catalyzed by bidentate Mn complexes

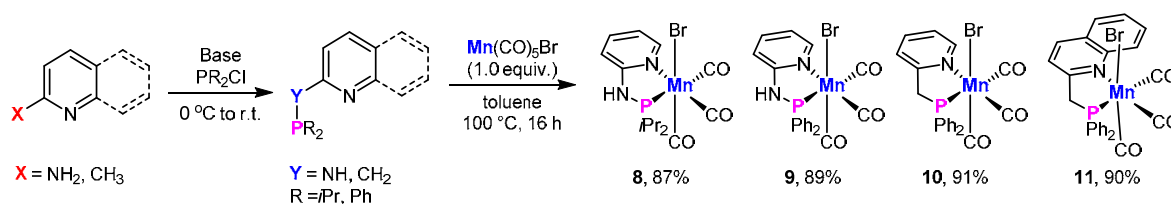
**Contributions in this part:** Synthesis of the complexes: Duo Wei, Antoine Bruneau-Voisine, Téo Chauvin; Optimization and Scope: Duo Wei.

**Publication:** D. Wei, A. Bruneau-Voisine, T. Chauvin, V. Dorcet, T. Roisnel, D. A. Valyaev, N. Lugan, J.-B. Sortais, *Adv. Synth. Catal.* **2018**, 360, 676-681.

Following the development of catalyst **7** bearing a bidentate picolylamine ligand which was proved to be more active than catalyst **5** supported by analogue tridentate dipicolylamine ligand, we wanted to explore simple Mn(I) complexes bearing readily available phosphino-pyridinyl PN bidentate ligands analogue to our pincer catalyst **4**.

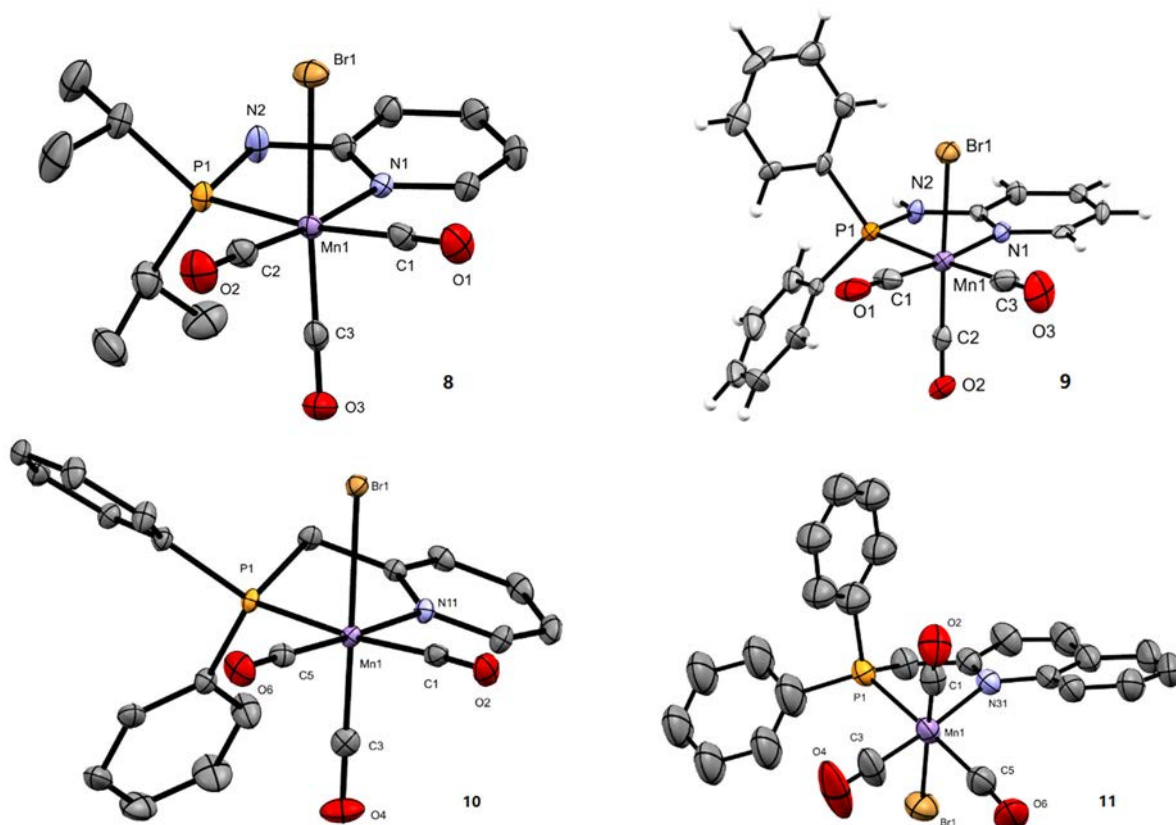
### 1.1. Results and discussions

#### 1.1.1. Ligand and complex synthesis



**Figure 1.** Manganese complexes synthesised for hydrogenation of carbonyl derivatives.

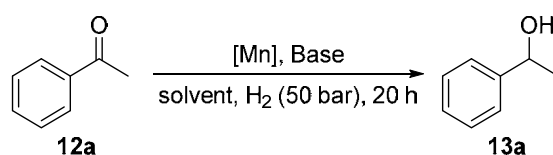
The ligands  $\text{R}_2\text{P-X-Py}$  (**L1**:  $\text{R} = i\text{Pr}$ ,  $\text{X} = \text{NH}$ ; **L2**:  $\text{R} = \text{Ph}$ ,  $\text{X} = \text{NH}$ ; **L3**:  $\text{R} = \text{Ph}$ ,  $\text{X} = \text{CH}_2$ ) and  $\text{Ph}_2\text{P-CH}_2\text{-Qn}$  (**L4**) were obtained in high yields starting from the appropriate chlorophosphines  $\text{R}_2\text{PCl}$  and 2-aminopyridine (for **L1**, **L2**),<sup>[10]</sup> 2-picoline (for **L3**),<sup>[11]</sup> or 2-methylquinoline (for **L4**),<sup>[12]</sup> respectively, according to literature procedures. The corresponding complexes  $\text{Mn}(\text{CO})_3\text{Br}(\kappa^2P,N\text{-L1-L4})$  (**8-11**) (Figure 1) were readily obtained in excellent yields (87-91%) upon simple heating of an equimolar mixture of  $\text{Mn}(\text{CO})_5\text{Br}$  and the given ligand in toluene at 100 °C overnight. They were fully characterised by IR and NMR spectroscopy, high-resolution mass spectrometry and elemental analysis. Their solid-state structures were determined by single-crystal X-ray diffraction. Perspective views of the complexes are displayed on Figure 2 for complexes **8-11**, respectively. All complexes show a typical octahedral environment for the Mn center, the **L1-L4** ligands being coordinated in a  $\kappa^2P,N$  mode and the three carbonyl ligands being in facial position (Figure 2).



**Figure 2.** Perspective views of complexes **8-11** with thermal ellipsoids drawn at the 50% probability level. Hydrogen atoms, except NH, were omitted for clarity.

### 1.1.2. Optimization of reaction conditions

The catalytic activity of the new complexes **8-11** was then evaluated for the reduction of ketones under hydrogenation conditions (Table 1). Under the previously optimized reaction conditions determined for the  $\text{PN}^3\text{P}$  catalyst **4**,<sup>[6c]</sup> *i.e.* complex **8** (5.0 mol%), *t*BuOK (10 mol%) as the base, toluene, 110°C,  $\text{H}_2$  (50 bar), 22 h, a full conversion of acetophenone **12a** to the corresponding alcohol **13a** was obtained (entry 1). The catalyst loading could be reduced to 1.0 mol% without any alteration of the activity (Table 1, entry 2). The performance of the four complexes was then compared at 80 °C (entries 3-6): the complex **8** exhibiting the amino-bridged diisopropylphosphino-pyridinyl bidentate ligand **L1** gave a moderate conversion (65%), whereas the diphenylphosphino derivative **9** gave the alcohol in 90% yield. Disappointingly, complexes **10** and **11** featuring the methylene-bridged PN bidentate ligands **L3** and **L4** led to the corresponding derivatives with low conversions (15 and 16% respectively, entries 5 and 6). The nature of the base was optimized using **9** as the pre-catalyst. KHMDS (potassium bis(trimethylsilyl)amide) appeared to be the best base leading to the alcohol with a full conversion with 1.0 mol% of complex **9** and 2.0 mol% of base at 80 °C in toluene (entry 7). With this base, the catalyst loading could be even decreased to 0.5 mol% (entries 8 and 12).

**Table 1.** Optimization of the reaction parameters<sup>[a]</sup>

Entry	Cat (mol%)	Base (mol%)	Temp. (°C)	Solvent	Yield(%) <sup>[b]</sup>
1	<b>8</b> (5.0)	<i>t</i> BuOK (10)	110	toluene	>98
2	<b>8</b> (1.0)	<i>t</i> BuOK (2.0)	110	toluene	>98
3	<b>8</b> (1.0)	<i>t</i> BuOK (2.0)	80	toluene	65
4	<b>9</b> (1.0)	<i>t</i> BuOK (2.0)	80	toluene	90
5	<b>10</b> (1.0)	<i>t</i> BuOK (2.0)	80	toluene	15
6	<b>11</b> (1.0)	<i>t</i> BuOK (2.0)	80	toluene	16
7	<b>9</b> (1.0)	KHMDS (2.0)	80	toluene	>98
8	<b>9</b> (0.5)	KHMDS (1.0)	80	toluene	81
9	<b>9</b> (0.5)	KHMDS (1.0)	80	<i>t</i> -amyl alcohol	76
10	<b>9</b> (0.5)	KHMDS (1.0)	80	1,4-dioxane	11
11	<b>9</b> (0.5)	KHMDS (1.0)	80	THF	2
12	<b>9</b> (0.5)	KHMDS (2.0)	80	toluene	95
13 <sup>[c]</sup>	<b>9</b> (0.5)	KHMDS (2.0)	80	toluene	87
14 <sup>[d]</sup>	<b>9</b> (0.5)	KHMDS (2.0)	80	toluene	7
15	<b>9</b> (0.1)	KHMDS (1.0)	80	toluene	43
16	<b>9</b> (0.5)	KHMDS (2.0)	50	toluene	93
17	<b>9</b> (0.5)	KHMDS (2.0)	50	<i>t</i> -amyl alcohol	51
18	<b>9</b> (0.5)	KHMDS (2.0)	30	toluene	44
19	-	KHMDS (2.0)	50	toluene	0
20	<b>9</b> (0.5)	-	50	toluene	0
21 <sup>[e]</sup>	<b>9</b> (0.5)	KHMDS (2.0)	80	toluene	93

<sup>[a]</sup> Typical conditions: in an autoclave, **9** (0.5 mol%), toluene (4 mL), ketone (2 mmol), KHMDS (2.0 mol%), H<sub>2</sub> (50 bar) were added in this order.

<sup>[b]</sup> Yield determined by GC and <sup>1</sup>H NMR.

<sup>[c]</sup> 30 bar of H<sub>2</sub>.

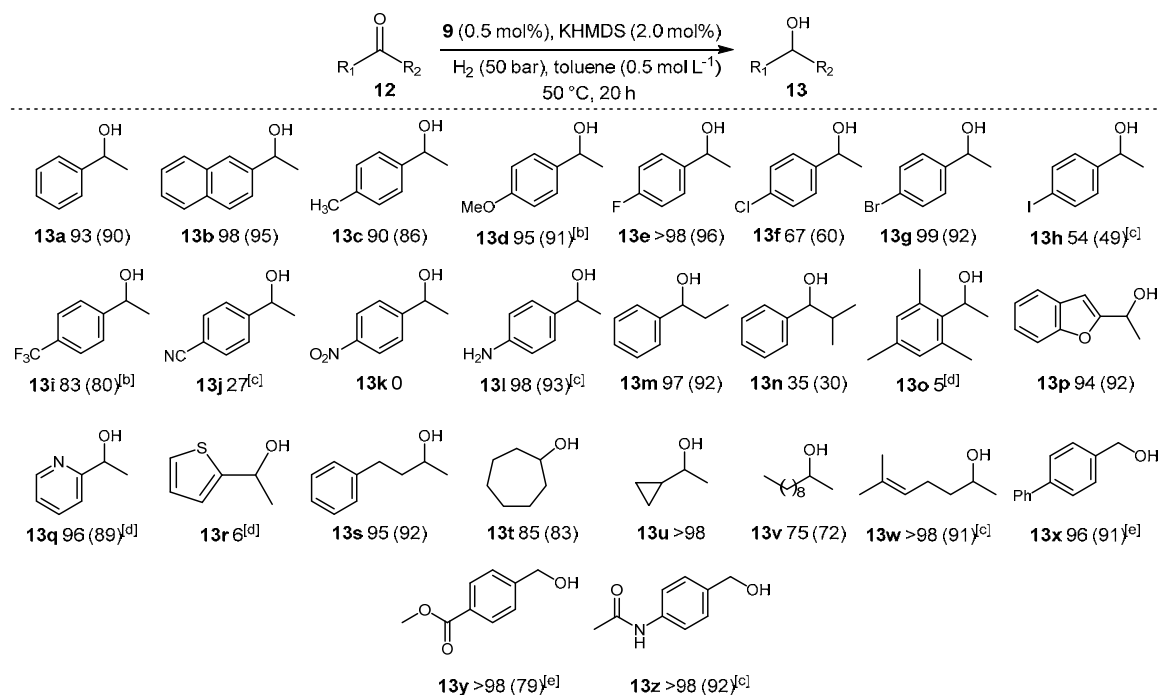
<sup>[d]</sup> 10 bar of H<sub>2</sub>.

<sup>[e]</sup> 300 equiv. of Hg (vs **9**) were added before H<sub>2</sub> in the reaction mixture.

The influence of the solvent and of the pressure was also evaluated. Notably, *tert*-amyl alcohol was found to be suitable for this reaction at 80 °C, as an alternative greener solvent (entries 9 and 17).<sup>[13]</sup> However, 1,4-dioxane and THF gave low yields of the alcohol **13a** (entries 10 and 11). 30 bar of H<sub>2</sub> led to a slightly low yield of **13a** (87%), while 10 bar of H<sub>2</sub> gave only 7% yield (entries 13 and 14). With 0.1 mol% of catalyst, a TON of 430 was achieved (entry 15). The temperature could also be lowered to 50 °C without significant loss of efficiency (entries 16-17). At 30 °C, however, the conversion dropped to 44% (entry 18). Control experiment showed that the presence of Hg has no influence on the reaction (entry 21 vs entry 12). Eventually, the optimal condition selected for the scope of the reaction were catalyst **9** (0.5 mol%), KHMDS (2.0 mol%), toluene, 50 bar of hydrogen, 20 h (entry 12).

### 1.1.3. Scope for hydrogenation of carbonyl derivatives

**Table 2.** Scope of the hydrogenation of carbonyl derivatives under the catalysis of **9**.<sup>[a]</sup>



<sup>[a]</sup> General conditions: ketone (2 mmol), H<sub>2</sub> (50 bar), **9** (0.5 mol%), KHMDS (2.0 mol%), toluene (4 mL, 0.5 mol·L<sup>-1</sup>), 50 °C, 20 h. Conversion determined by <sup>1</sup>H NMR, isolated yield in parentheses.

<sup>[b]</sup> **9** (0.5 mol%), KHMDS (2.0 mol%), 80 °C.

<sup>[c]</sup> **9** (1.0 mol%), *t*BuOK (2.0 mol%), 80 °C.

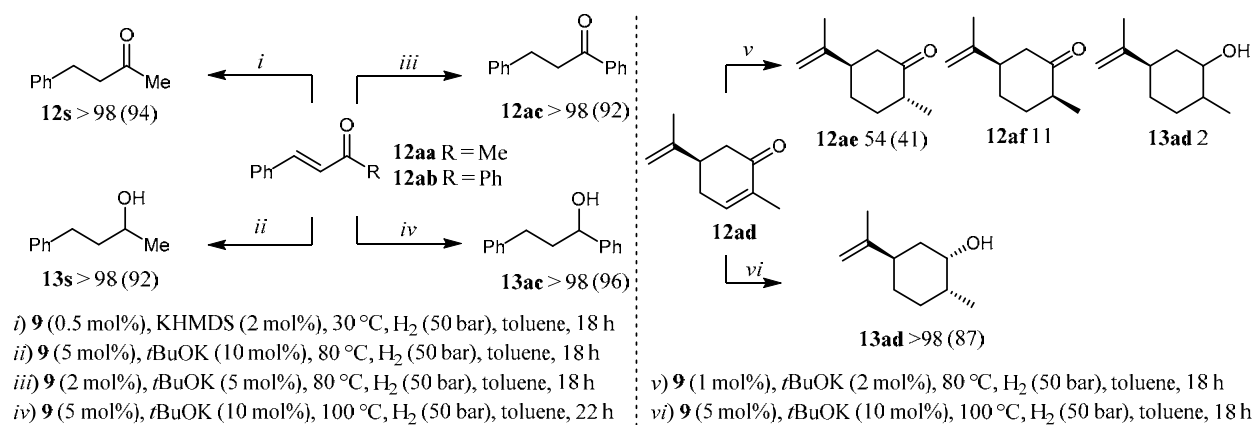
<sup>[d]</sup> **9** (5.0 mol%), *t*BuOK (10 mol%), 80 °C.

<sup>[e]</sup> **9** (1.0 mol%), *t*BuOK (2.0 mol%), 50 °C.

Next, we explored the substrates scope amenable for the PN manganese precatalyst **9** in hydrogenation (Table 2). In general, arylketones bearing both electron withdrawing and electron donating substituents were reduced in very good yields. In the case of *p*-halogenated ketones, fluoro- and bromo-derivatives (**12e** and **12g**) were well tolerated with low catalyst loading, whereas chloro- and iodo-substituted ketones (**12f** and **12h**) were not fully reduced, even under slightly forcing conditions. Steric hindrance had a noticeable influence as increasing the length and the branching of the alkyl chains of the ketone from methyl (**12a**), ethyl (**12m**) to isopropyl (**13n**) induced a significant drop in the conversion (93% for **13a**, 97% for **13m** to 35% for **13n**). In line with these observations, 2',4',6'-trimethylacetophenone **12o** was not reduced with this system. Among the various coordinating functional groups, primary amine (**13l**), benzofuran (**13p**), and pyridine (**13q**) were tolerated, but a higher catalyst loading was required to reach good conversions. Conversely, the cyano derivative (**13j**) was reduced

in very low yield, and nitro (**13k**) and thiophene (**13r**) moieties completely inhibited the reaction. (see also Table 3 for competitive experiments)

Additionally, it must be underlined that the reduction of acetophenone in the presence of 4-nitrotoluene, in a competitive experiment, was completely inhibited (Table 3, entry 4), which underlined that the nitro moiety should coordinate the manganese complex. A series of aliphatic and cyclic ketones was reduced smoothly (**13s-13w**). Isolated tri-substituted C=C double bond in **13w** remained completely intact during the hydrogenation process. In order to confirm this selectivity, a series of competitive reduction of acetophenone, in the presence of 1-decene, 5-decene and 5-decyne, respectively, were conducted (Table 3, entries 1-3). Finally, *para*-substituted benzaldehydes (**12x-12z**) were also reduced to the corresponding benzylic alcohols in high yields showing the tolerance toward ester (**13y**) and amide (**13z**) groups.



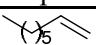
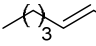
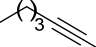
**Scheme 2.** Selective reduction of conjugated enones.

In the case of  $\alpha,\beta$ -unsaturated 4-phenylbut-3-en-2-one **12aa**, under the standard conditions (50 bar H<sub>2</sub>, 0.5 mol% **9**, 2 mol% KHMDS, 50 °C, 20 h), a 13:87 mixture of fully reduced product **13s** and ketone **12s** was obtained. Interestingly, under milder conditions, at 30 °C for 18 h, the saturated ketone **12s** was obtained selectively in 94% isolated yield, while under harsher ones (50 bar H<sub>2</sub>, 5.0 mol% **9**, 10 mol% *t*-BuOK, 80 °C, 18 h), the saturated alcohol **13s** was obtained quantitatively in 92% yield (Scheme 2, *i* and *ii*). Similarly, chalcone **12ab** could be reduced selectively to 1,3-diphenylpropan-1-one **12ac** or to 1,3(diphenylpropan-1-ol **13ac** (Scheme 2, *iii* and *iv*). The reduction of (*R*)-carvone **12ad**, bearing both a conjugated and a non-conjugated C=C bond, under mild conditions (50 bar H<sub>2</sub>, 1.0 mol% **9**, 2 mol% *t*-BuOK, 80 °C, 18 h), led to the formation of a mixture of isomer of dihydrocarvone<sup>[14]</sup> **12ae** and **12af**. Under harsher conditions (5.0 mol% **9**, 100 °C), dihydrocarveol<sup>[15]</sup> **13ad** was obtained in high yield (87%). In both cases, the non-conjugated C=C bond remained intact. Compared to the



reduction of  $\alpha,\beta$ -unsaturated aldehydes by aliphatic PNP manganese catalysts **1**,<sup>[5a]</sup> where the unsaturated alcohols were produced selectively, and to the reduction of  $\alpha,\beta$ -unsaturated esters,<sup>[5b]</sup> where solely saturated alcohols were obtained, the present catalytic system allows to reduce exclusively the conjugated C=C double bond, supplementing the previously described ones.

**Table 3.** Competition reactions<sup>a</sup>

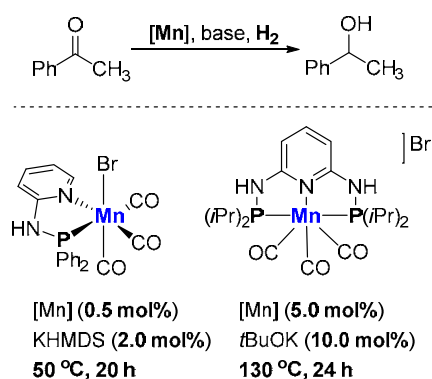
Entry	Substrate mixture		9 [mol%]	Base [mol%]	Temp. [°C]	Conv. [%] <sup>b</sup> 12a/14
	Ketone	Competition substrate				
1	Acetophenone	 <b>14a</b>	5.0	tBuOK [10]	110	92/0
2	Acetophenone	 <b>14b</b>	5.0	tBuOK [10]	110	99/0
3	Acetophenone	 <b>14c</b>	0.5	KHMDS [2.0]	50	97/0
4	Acetophenone	<i>p</i> -Me-C <sub>6</sub> H <sub>4</sub> -NO <sub>2</sub> <b>14d</b>	0.5	KHMDS [2.0]	80	0/0

<sup>[a]</sup> Acetophenone **12a** (2 mmol), competition substrate **14** (2 mmol), toluene (0.5 M), H<sub>2</sub> (50 bar), 18 h.

<sup>[b]</sup> Conversion by <sup>1</sup>H NMR.

In order to evaluate additional functional group tolerance, competition reactions were also performed. In all the cases, the reduction of the ketone proceeded without the reduction of the unsaturated C-C bond (Table 3, entries 1-3). However, the presence of nitro group inhibited the reduction of acetophenone (entry 4).

## 1.2. Conclusion



**Scheme 3.** Comparison of tridentate/bidentate catalytic systems for hydrogenation of ketones.

In conclusion of this first paragraph, a series four new Mn(I) complexes bearing readily available phosphino-pyridinyl PN bidentate ligands have been prepared, fully characterized, and their catalytic activity was evaluated in the hydrogenation of aldehydes and ketones. The complex Mn(CO)<sub>3</sub>Br( $\kappa^2P,N$ -Ph<sub>2</sub>PN(H)Py) **9** exhibited good performances for the

hydrogenation of carbonyl derivatives under mild conditions with low catalyst loading and satisfying functional group tolerance, compared to the most active catalytic systems.<sup>[6a, 6c]</sup>

In terms of catalyst design and taking the  $\text{PN}^3\text{P}$  Mn(I) complex **4** as a reference,<sup>[6c]</sup> it appears that simplifying the ancillary tridentate ligand to a bidentate ligand by removing one of its wingtip led to a dramatic increase of the activity of resulting catalytic system. Indeed, the use of the  $\text{PN}$  Mn(I) complex **9** allowed reducing the catalyst loading by a factor of ten, and lowering the temperature from 130 °C to 50 °C, still keeping the same level of activity and chemoselectivity (Scheme 3).<sup>[6c]</sup>



## IV-2 Reductive amination of aldehydes with H<sub>2</sub> catalyzed by bidentate Mn complexes

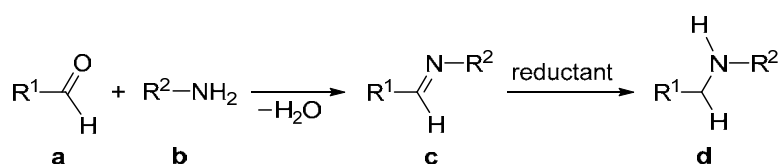
**Contributions in this part:** Synthesis of the complexes: Duo Wei, Antoine Bruneau-Voisine; Optimization: Duo Wei; Scope: Duo Wei, Antoine Bruneau-Voisine.

**Publication:** D. Wei, A. Bruneau-Voisine, D. A. Valyaev, N. Lugan, J.-B. Sortais, *Chem. Commun.* **2018**, 54, 4302-4305.

### 2.1. Introduction

Having developed efficient catalysts for the hydrogenation of aldehydes and ketones, we continued to explore the potential of these catalysts in the hydrogenation of related imines C=N bonds. With manganese based catalysts, at the time, the access to various higher amine derivatives using alcohols as alkylating reagents was developed,<sup>[5c]</sup> including the *N*-monomethylation of amines,<sup>[5c, 7e, 7f]</sup> aminomethylation of (hetero)arenes with methanol/ amines,<sup>[7j]</sup> and multi-component synthesis of quinolines,<sup>[7b]</sup> pyrroles<sup>[7i]</sup> and pyrimidines.<sup>[7h]</sup>

Reductive amination<sup>[16]</sup> is one of the chemical reaction in the chemist tool-box for the preparation of amines.<sup>[17]</sup> It relies on the *in situ* condensation of a ketone or aldehyde with an amine to form the corresponding imine, which is subsequently reduced to the desired amine (Scheme 4), as already described for the iron catalyzed reductive amination reactions to synthesize cyclic amines in the presence of hydrosilanes as the reductants in Chapter III, Part 1. When using molecular hydrogen as reductant, it appears that the key step in the reaction sequence is the hydrogenation of the intermediate imine.



**Scheme 4.** Synthesis of amines *via* reductive amination.

### 2.2. Results and discussions

The same bidentate catalysts **8-11** as the one studied in hydrogenation of ketones (§ 2.1.) were further explored for the hydrogenation of imines (Figure 1).

#### 2.2.1. Optimization of reaction conditions

We initially focused on the direct hydrogenation of *N*-benzylideneaniline **15a** as model substrate, using the catalyst **9** and a base, under 50 bar of H<sub>2</sub>, based on previously optimized conditions for the hydrogenation of ketones. First, we found that alcohols, including *t*-amyl

alcohol, *n*-BuOH, methanol and notably ethanol, were suitable solvents for the hydrogenation step (Table 4, entries 2, 9-11) as a green solvent alternative to toluene.

**Table 4.** Hydrogenation of benzylideneaniline **15a**: influence of the solvent.<sup>[a]</sup>

Entry	Temp. (°C)	Solvent	Yield (%)
1	130	Toluene	48
2	130	<i>t</i> -amyl alcohol	81
3	130	Dimethyl carbonate	84
4	130	THF	95
5	130	1,4-dioxane	40
6	130	CPME	43
7	100	THF	71
8	100	<i>t</i> -amyl alcohol	28
9	100	EtOH	98
10	100	<i>n</i> -BuOH	95
11	100	MeOH	84

<sup>[a]</sup> Conditions: An autoclave was charged in a glovebox with, in this order, **15a** (45.3 mg, 0.25 mmol), solvent (2.0 mL), **9** (6.2 mg, 5.0 mol%), *t*BuOK (2.8 mg, 10 mol%), and then pressurized with H<sub>2</sub> (50 bar) and heated at the indicated temperature. Yields determined by GC and by <sup>1</sup>H NMR spectroscopy.

It then appeared that the nature of the base had little influence on the reaction: *t*BuONa, *t*BuOK, KHMDS, or Cs<sub>2</sub>CO<sub>3</sub> led to satisfactory yields: **9** (1.0 mol%), base (2.0 mol%), 100 °C, EtOH, 22 h, 41% to 64% yield, Table 5.

**Table 5.** Hydrogenation of benzylideneaniline **15a**: influence of the base.<sup>[a]</sup>

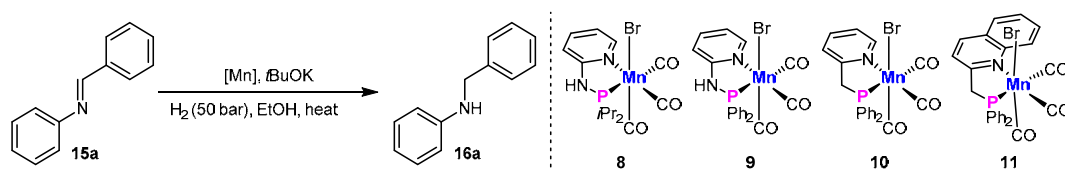
Entry	Base (mol%)	Yield (%)
1	<i>t</i> BuOK (2.0)	64
2	<i>t</i> BuONa (2.0)	50
3	Cs <sub>2</sub> CO <sub>3</sub> (2.0)	57
4	KHMDS (2.0)	41

<sup>[a]</sup> Conditions: An autoclave was charged in a glovebox with, in this order, **15a** (90.6 mg, 0.5 mmol), anhydrous ethanol (2.0 mL), **9** (2.5 mg, 1.0 mol%), base (2.0 mol%), and then pressurized with H<sub>2</sub> (50 bar) and heated at 100 °C. Yield determined by GC and by <sup>1</sup>H NMR spectroscopy.

The activity of complexes **8-11** was compared under the following conditions, at 80 °C with 1.0 mol% catalyst and 2.0 mol% of *t*BuOK (Table 6, entries 1-4) and the complex **9**

appeared to be the most active one. Increasing the catalyst loading of **9** to 2.0 mol% led to a full conversion (entry 5). Interestingly, the temperature could be decreased to 50 °C without any detrimental effect on activity (entry 6), and even to 30 °C where a decent conversion still occurred (76%, entry 7). Controlled experiments were performed in the absence of Mn-complex (entry 8) or base (entry 9), where nearly no amine **16a** was detected. With lower hydrogen pressure (30 bar), slightly lower yield of **16a** (87%) was obtained (entry 10).

**Table 6.** Optimization of the reactions conditions of the hydrogenation of benzylideneaniline **15a** with manganese catalysts **8-11**.



Entry <sup>[a]</sup>	Catalyst (mol%)	T (°C)	Time (h)	Yield (%) <sup>[c]</sup>
1 <sup>[a]</sup>	<b>8</b> (1.0)	80	19	40
2 <sup>[a]</sup>	<b>9</b> (1.0)	80	24	74
3 <sup>[a]</sup>	<b>10</b> (1.0)	80	19	17
4 <sup>[a]</sup>	<b>11</b> (1.0)	80	19	1
5 <sup>[b]</sup>	<b>9</b> (2.0)	80	17	>98
6 <sup>[b]</sup>	<b>9</b> (2.0)	50	17	>98
7 <sup>[b]</sup>	<b>9</b> (2.0)	30	24	76
8 <sup>[b,d]</sup>	-	50	22	<1
9 <sup>[b,e]</sup>	<b>9</b> (2.0)	50	22	3
10 <sup>[b,f]</sup>	<b>9</b> (2.0)	50	22	87

<sup>[a]</sup> Conditions: an autoclave was charged in a glovebox with, in this order, **15a** (181 mg, 1.0 mmol), EtOH (4.0 mL), Mn-complex (1.0 mol%), *t*BuOK (2.2 mg, 2.0 mol%), and then pressurized with H<sub>2</sub> (50 bar) and heated;

<sup>[b]</sup> **15a** (91 mg, 0.5 mmol), EtOH (2.0 mL), **9** (5.0 mg, 2.0 mol%), *t*BuOK (2.8 mg, 5.0 mol%);

<sup>[c]</sup> Yield was determined by <sup>1</sup>H NMR spectroscopy and by GC on the crude mixture;

<sup>[d]</sup> Without Mn-complex in the presence of the base.

<sup>[e]</sup> With **9** and without *t*BuOK;

<sup>[f]</sup> 30 bar H<sub>2</sub>.

Although promising results were obtained for the hydrogenation of the aldimine **15a**, the more challenging reduction of ketimines was not found to be efficient under the catalysis of Mn complex **9** (Table 7). Even under harsher conditions (**9** (5.0 mol%), *t*BuOK (10 mol%), 100 °C, 24 h), the corresponding amines were not detected, demonstrating that this catalytic system is not suitable for the reduction of ketimines.

**Table 7.** Hydrogenation of the ketimine **17a**.

Entry <sup>[a]</sup>	<b>9</b> (mol%)	<i>t</i> BuOK (mol%)	Temp. (°C)	Yield <b>18a</b> (%)
1	2.0	5.0	50	<1
2	5.0	10	100	<1

<sup>[a]</sup> Conditions: an autoclave was charged in a glovebox with, in this order, ketimine **17a** (119.7 mg, 0.5 mmol), anhydrous ethanol (2.0 mL), **9** (2.0 or 5.0 mol%), *t*BuOK (5.0 or 10 mol%), pressurized with H<sub>2</sub> (50 bar), then heated at the indicated temperature.

In terms of practical and economical synthesis, the direct reductive amination of aldehydes is more desirable than hydrogenation of corresponding isolated imines. Hence, we turned our attention towards the direct synthesis of benzylaniline **16a** from benzaldehyde **19a** and aniline **20a**. In a first attempt, all the components, *i.e.* **9**, **19a**, **20a**, *t*BuOK, and H<sub>2</sub>, were introduced in an autoclave being heated at 80 °C overnight (Scheme 5, conditions A). Disappointingly, a mixture of benzylalcohol **21a** (44%), imine **15a** (38%), and the desired amine **16a** (18%) was obtained, showing that the hydrogenation of benzaldehyde occurred faster than the condensation with aniline **20a**.

	<b>15a</b>	<b>16a</b>	<b>21a</b>
<b>Conditions A:</b>	38	18	44
<b>Conditions B:</b>	29	7	61
<b>Conditions C:</b>	2	87	11

**Scheme 5.** Optimization of the procedure for reductive amination of benzaldehyde with aniline under the catalysis of manganese complex **9**.

**Conditions A:** an autoclave was charged with **9** (5.0 mg, 2.0 mol%), anhydrous ethanol (2.0 mL), aniline **20a** (46 µL, 0.5 mmol), benzaldehyde **19a** (51.0 µL, 0.5 mmol), *t*BuOK (2.8 mg, 5.0 mol%) and H<sub>2</sub> (50 bar) and heated at 80 °C for 20 h.

**Conditions B:** an autoclave was charged with **9** (5.0 mg, 2.0 mol%), anhydrous ethanol (2.0 mL), aniline **20a** (46 µL, 0.5 mmol), benzaldehyde **19a** (51.0 µL, 0.5 mmol) and *t*BuOK (2.8 mg, 5.0 mol%). After heating at 80 °C for 5 h, H<sub>2</sub> (50 bar) was charged and the mixture heated at 80 °C for 20 h.

**Conditions C:** in a 20 mL Schlenk tube aniline **20a** (46 µL, 0.5 mmol) and benzaldehyde **19a** (51.0 µL, 0.5 mmol) in anhydrous ethanol (2.0 mL) were heated at 100 °C for 24 h. The reaction mixture was transferred into an autoclave followed by **9** (5.0 mg, 2.0 mol%), *t*BuOK (2.8 mg, 5.0 mol%) and H<sub>2</sub> (50 bar), then heated at 80 °C for 20 h.

In a second strategy, the condensation step was carried out in the presence of the catalyst and the base at 80 °C for 5 h, then the reaction mixture was pressurized under H<sub>2</sub> and stirred at 80 °C overnight (conditions B). Unfortunately, the main products were again alcohol **21a** (61%) and imine **15a** (29%). Finally, the condensation was first performed by reaction of the aldehyde with the amine in EtOH, leading to the imine **15a** in 90% yield after 24 h at 100 °C, and then the addition of the precatalyst, the base, and H<sub>2</sub> was done to the crude imine before heating under stirring at 80 °C overnight (Conditions C). To our delight, under these conditions, the desired *N*-benzylaniline **16a** was obtained in high yield (87%). Hereafter, to probe the scope of this first manganese catalyzed reductive amination system, 1.2 equiv. of amines **20** were used to ensure the full conversion of the aldehyde **19** into the imines **15** before the hydrogenation step (Table 8).

### 2.2.2. Scope of the reductive amination of aldehydes

In general, as far as the formation of the imines is not a limiting step, the subsequent hydrogenation proceeds well for a wide variety of aldehydes and amines (Table 8). Notably, for benzaldehyde derivatives with anilines, the condensation takes place at r.t. in typically 1 hour (Table 8, entry 4). First, benzaldehyde derivatives bearing either electron donating or electron withdrawing groups both react with anilines to afford *in fine* the corresponding amines in good yields (entries 1-16). Noticeably, halogen substituents (**16f-16j**), including iodo substituent, were well tolerated with less than 10% deiodination in the cases of **16i** and **16j**. Noticeably, esters and amides moieties were not reduced under these conditions (**16l-16m**). Interestingly, starting from 4-formylacetophenone **19o** in the presence of 2.2 equiv. of aniline **20a**, only the aldimine moieties was reduced in the transient di-imine intermediate affording the corresponding amino-ketimine **16n** (88%, entry 14) while in the presence of 1 equiv. of **20a**, amino-ketone **16o** was obtained in good yield (73%, entry 15). In the same vein, the reductive amination of benzaldehyde **19a** with 4-acetyl-aniline **20p** led selectively to the corresponding 4-acetylamine **16p** (96% yield) leaving the ketone functionality untouched (entry 16). Organometallic ferrocenylcarboxaldehyde **19q** was also suitable for this protocol leading **16q** in 98% yield (entry 17). Several heterocycles, including pyrrole, furane, pyridine, thiophene, and thiazole were well tolerated by the catalytic system (entries 18-23).



**Table 8.** Scope of the reductive amination of aldehydes with amines in presence of **9** as precatalyst.<sup>[a]</sup>

Entry	Product	Temp. (°C)	Time (h)	Yield (%) <sup>[b]</sup>	Entry	Product	Temp. (°C)	Time (h)	Yield (%) <sup>[b]</sup>		
1		16a	50	18	93	21		16u	80	48	55
2		16b	100	36	94	22		16v	80	48	90
3		16c	100	48	72	23		16w	80	48	92
4		16d	100	24	78 <sup>[c]</sup>	24		16x	80	48	93
5		16e	50	48	87	25		16y	100	48	90
6		16f	100	48	28	26		16z	80	18	95
7		16g	80	36	90	27		16aa	80	48	94
8		16h	50	48	80	28		16ab	80	36	96
9		16i	100	36	98 <sup>[d]</sup>	29		16ac	80	36	94
10		16j	100	36	98 <sup>[d]</sup>	30		16ad	80	36	93
11		16k	80	36	97	31 <sup>[f]</sup>		16ae	100	48	95
12		16l	80	48	92	32		16af	100	24	86
13		16m	100	48	95	33		16ag	100	24	83
14 <sup>[e]</sup>		16n	80	36	88	34		16ah	100	18	97
15		16o	50	18	73	35 <sup>[g]</sup>		16ai	100	18	90
16		16p	50	18	96	36 <sup>[g]</sup>		16aj	100	36	91
17		16q	80	48	98	37		16ak	50	48	96
18		16r	100	48	97	38		16al	50	48	95
19		16s	100	48	90	39		16am	50	36	96
20		16t	80	36	68	40 <sup>[g]</sup>		16an	100	48	93

- [a] Typical reaction conditions: a solution of aldehyde **19** (0.5 mmol), amine **20** (0.6 mmol) and anhydrous EtOH (2.0 mL) was stirred at 100 °C for 24 h, then transferred to a 20 mL autoclave followed by **9** (5.0 mg, 2.0 mol%) and *t*BuOK (2.8 mg, 5.0 mol%). The autoclave was subsequently charged with H<sub>2</sub> (50 bar) and heated.
- [b] Isolated yield after purification.
- [c] Benzaldehyde **19a** (4.3 mmol), condensation: 2 h, r.t.
- [d] *c.a.* 10% of deiodination product.
- [e] Aniline **20a** (100 μL, 1.1 mmol, 2.2 equiv.).
- [f] Benzaldehyde **19a** (122 μL, 1.2 mmol).
- [g] **9** (5 %mol), *t*BuOK (10 mol%).

It is noteworthy that this reductive amination protocol is not limited to aniline derivatives, as benzenesulfonylamide **20x** (entry 24) as well as aliphatic primary **20y-20z** and secondary amines **20aa-20ad** (entries 25-30) were also successfully coupled. Ethylenediamine **20ae** afforded the *N,N'*-dibenzylethylenediamine **16ae** in 95% yield, without formation of imidazolines (entry 31).<sup>[18]</sup> Remarkably, the amino-alcohols **20af-20ah** were alkylated to afford selectively the corresponding hydroxyamines **16af-16ah** in 83-97% yields, the pending hydroxy group not entering into a potentially competitive *N*-alkylation process (entries 32-34).<sup>[5c]</sup> To complete the series of amines amenable for this transformation, α-amino-esters **16ai-16aj** were also alkylated with success when increasing the catalytic amount of **9** to 5.0 mol% (entries 35 and 36). A series of aliphatic aldehydes **19ak-19an**, including butanal **19ak**, readily available by hydroformylation, or bio-sourced aldehydes such as cinnamaldehyde **19an**, were also successfully engaged in the present reductive amination protocol (entries 37-40). Non-conjugated C=C were typically not reduced in the course of the reaction (entries 38 and 39), while the conjugated C=C bond in cinnamaldehyde **19an** was reduced under harsher conditions (100 °C, 48 h, entry 40), *e.g.* under standard conditions, *c.a.* 10% of α,β-unsaturated amine **16an'** was identified in the crude mixture, which is in line with the selectivity observed for the reduction of α,β-unsaturated ketones.<sup>[19]</sup> Finally, it has to be noted that a few functional groups such as terminal alkyne, nitro group, or unprotected pyrrole were not tolerated.

## 2.3. Conclusion

In conclusion, we have shown in this paragraph that a well-defined manganese pre-catalyst featuring a readily available bidendate diphenyl-(2-aminopyridinyl)-phosphine ligand such as **9** catalyzes efficiently the reductive amination of aldehydes with a wide variety of amines using H<sub>2</sub> as reductant with a wide functional group tolerance. This higher amine synthesis protocol significantly enlarges the scope of reactions catalyzed by manganese complexes and nicely complements a previous approach based on alkylation of amines with alcohols.



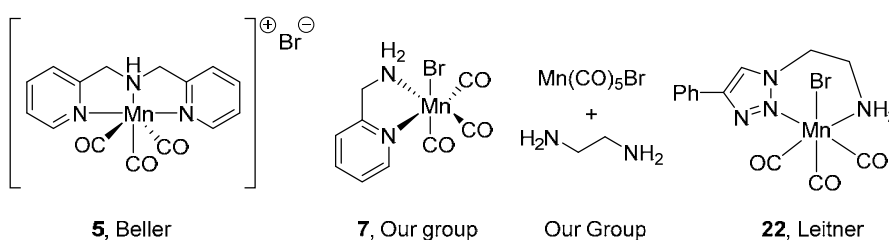
## IV-3 Transfer hydrogenation of aldimines catalyzed by bidentate Mn complexes

**Contributions in this part:** Synthesis of the complex: Antoine Bruneau-Voisine; Optimization and scope: Duo Wei, Antoine Bruneau-Voisine, Maxime Dubois.

**Publication:** D. Wei,<sup>+</sup> A. Bruneau-Voisine,<sup>+</sup> M. Dubois, S. Bastin, J.-B. Sortais, *ChemCatChem*. 2019, in press, doi: 10.1002/cctc.201900314. <sup>+</sup>equal contributions

### 3.1. Introduction

#### Transfer hydrogenation



#### Asymmetric transfer hydrogenation

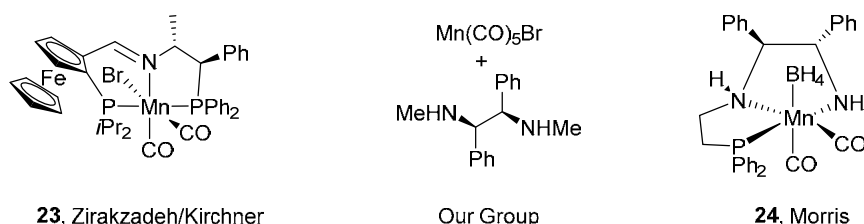


**Figure 3.** Manganese catalysts used in transfer hydrogenation.

Compared to hydrogenation, only a few catalytic systems based on manganese were developed for transfer hydrogenation reactions, including the asymmetric version (Figure 3).<sup>[6b, 6d, 6e, 6g, 20]</sup> The first system **5** was developed by the group of Beller, with a tridentate ligand, namely dipicolamine, for the reduction of ketones.<sup>[6b]</sup> Zirakzadeh and Kirchner reported the application of a chiral catalyst **23** supported by a tridentate PNP ligand bearing a ferrocenyl moiety for the enantioselective production of alcohols.<sup>[6g]</sup> Similar catalytic system, developed by Clarke, performed the reduction of ketones in the presence of alcohols, but required hydrogen pressure to exhibit enantioselectivity.<sup>[6e]</sup> More recently, the groups of Leitner<sup>[20a]</sup> and Morris,<sup>[20b]</sup> reported respectively an aminotriazole **22** and a chiral tridentate manganese catalysts **24** efficient in transfer hydrogenation reactions. Our group demonstrated that simple manganese complex based on a bidentate aminomethylpyridine ligand could perform with high efficiency the reduction of ketones and aldehydes, even at room temperature.<sup>[6d]</sup> We also showed that the combination of  $\text{Mn}(\text{CO})_5\text{Br}$ , as a commercial manganese precursor, and a diamine ligand, for

example ethylenediamine or a chiral diamine, namely (1*R*,2*R*)-*N,N*-dimethyl-1,2-diphenylethane-1,2-diamine, could promote the (asymmetric-) transfer hydrogen of carbonyl compound.<sup>[20c]</sup>

So, to date, manganese-catalyzed transfer hydrogenation reactions were limited to the reduction of ketones and aldehydes. Furthermore, examples of reduction of imines *via* this methodology involving non-noble metals such as iron,<sup>[3b, 21]</sup> nickel,<sup>[22]</sup> and cobalt<sup>[23]</sup>, are quite scarce. Starting from this statement, and taking into account the importance of amines in organic synthesis,<sup>[17b]</sup> we found relevant to explore the manganese-catalyzed reduction of imines by hydrogen transfer<sup>[24]</sup> as a complementary method in the chemist tool box to hydrogenation,<sup>[1]</sup> hydrosilylation<sup>[17a]</sup> or hydrogen borrowing,<sup>[25]</sup> for example.

### 3.2. Results and discussions

We have selected the well-defined Mn(I) complex **7** (Figure 3) featuring an 2-(aminomethyl)-pyridine ligand for this study as it was the most efficient catalyst for the reduction of carbonyl derivatives.<sup>[6d]</sup> Besides, the synthesis of this complex is very straightforward, as **7** can be obtained in high yield in only one step from commercially available reactants.<sup>[6d]</sup>

#### 3.2.1. Optimization of reaction conditions

The conditions of the reaction were optimized for the reduction of *N*-benzylidene-4-methylaniline **15d** in 2-propanol as the solvent (Table 9). At 80 °C, in the presence of *t*BuOK (2.0 mol%) and manganese complex **7** (1.0 mol%), the corresponding amine **16d**, namely *N*-benzyl-4-methylaniline, was formed in 77% yield. Various bases were first screened (entries 1-6), showing that *t*BuOK and KHMDS gave the best results (77%, entries 1 and 3). Interestingly, the common base KOH could also be used, albeit affording a slightly lower conversion than the former bases (65%, entry 4). The concentration of the reaction mixture is often crucial for the reduction of carbonyl derivatives, as transfer hydrogenation is a reversible reaction. Therefore, the influence of the concentration of **15d** was examined ranging from 0.5 to 0.05 mol.L<sup>-1</sup>. An optimal concentration of 0.1 mol.L<sup>-1</sup> (entries 1, 7-9) was identified. With 1.0 mol% catalyst, lengthen the reaction time (3 h) allowed to improve the conversion to 88% (entry 10). However, lowering the temperature had a detrimental effect on the activity as the conversion dropped to 39% at 50 °C and to 7% at 30 °C (entries 11 and 12). A satisfying yield (93%) was obtained using 2.0 mol% of catalyst **7** and 4.0 mol% of *t*BuOK at 80 °C after 3 h (entry 13). Finally, lowering the catalyst loading to 0.5 mol% resulted in a moderate TON of 120 (**7**, 3 h, 60% conversion, entry 14).

**Table 9.** Optimization of the parameters of the reduction of imine with the catalyst **23**.<sup>[a]</sup>

Cc1ccc(cc1)/C=C/c2ccccc2
 $\xrightarrow[\text{heat, } i\text{PrOH}]{\text{Complex 7, Base}}$ 
Cc1ccc(cc1)NCc2ccccc2

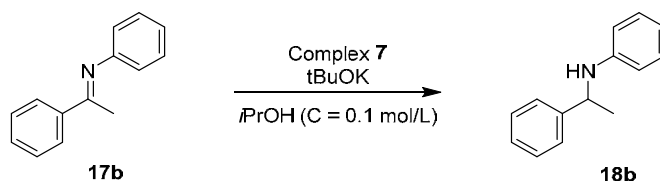
**15d**  **16d**

Entry	Cat (mol%)	Base (mol%)	Conc. (mol·L <sup>-1</sup> )	T (°C)	Time(h)	Conv. (%)
1	1.0	<i>t</i> BuOK (2.0)	0.16	80	1.5	77
2	1.0	<i>t</i> BuONa (2.0)	0.16	80	1.5	63
3	1.0	KHMDS (2.0)	0.16	80	1.5	77
4	1.0	KOH (2.0)	0.16	80	1.5	65
5	1.0	Na <sub>2</sub> CO <sub>3</sub> (2.0)	0.16	80	1.5	15
6	1.0	K <sub>3</sub> PO <sub>4</sub> (2.0)	0.16	80	1.5	12
7	1.0	<i>t</i> BuOK (2.0)	0.5	80	1.5	58
8	1.0	<i>t</i> BuOK (2.0)	0.1	80	1.5	82
9	1.0	<i>t</i> BuOK (2.0)	0.05	80	1.5	83
10	1.0	<i>t</i> BuOK (2.0)	0.1	80	3	88
11	1.0	<i>t</i> BuOK (2.0)	0.1	50	3	29
12	1.0	<i>t</i> BuOK (2.0)	0.1	30	3	7
13	2.0	<i>t</i> BuOK (4.0)	0.1	80	3	93
14	0.5	<i>t</i> BuOK (2.0)	0.1	80	3	60

<sup>[a]</sup> Reaction conditions: Under inert atmosphere, a 20 mL Schlenk tube was filled sequentially with the imine **15d** (0.5 mmol), anhydrous 2-propanol, complex **7**, and the base. The reaction was heated in an oil bath. Conversion was determined by <sup>1</sup>H NMR spectroscopy

Given the promising activity of the catalyst **7** for the reduction of aldimine **15d**, we then investigated its potential for the more challenging reduction of ketimines, with *N*-(1-phenylethylidene)-aniline **17b** as a model substrate (Table 10). In a disappointing way, even under harsh conditions: **7** (5.0 mol%), *t*BuOK (10 mol%), 130 °C, 18 h, the corresponding amine **18b** was obtained in low yield (20%), demonstrating that this catalytic system is not suitable for the reduction of ketimines.

**Table 10.** Optimization of the parameters of the reduction of the ketimine **17b** with the catalyst **23**.<sup>[a]</sup>



Entry	Complex 23 (mol%)	<i>t</i> BuOK (mol%)	T (°C)	Time(h)	Conv. (%)
1	1.0	2.0	80	3	5
2	2.0	4.0	80	18	17
3	5.0	10	100	18	23
4	5.0	50	100	18	22
5	5.0	10	130	18	20
6	5.0	50	130	18	18

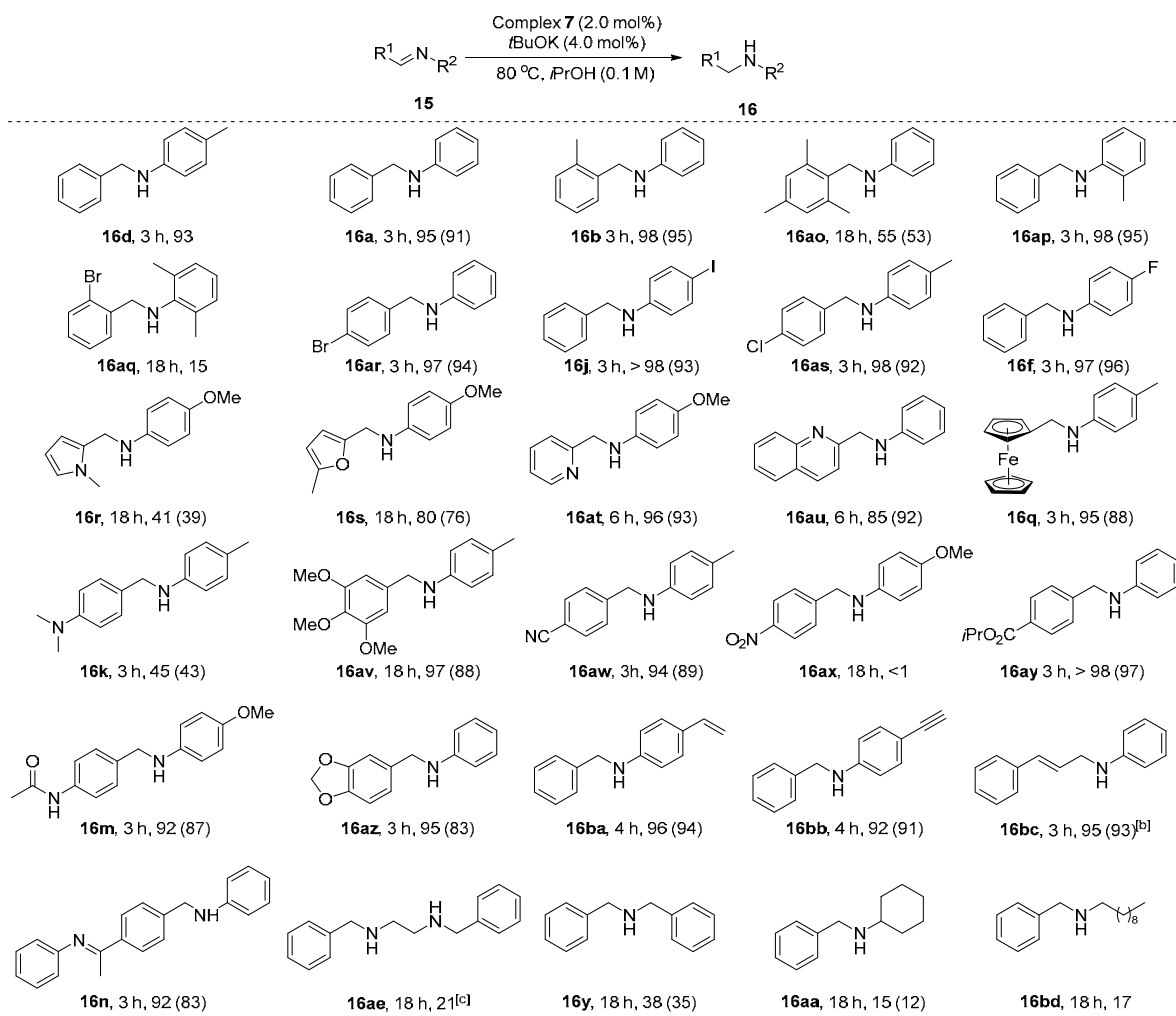
<sup>[a]</sup> Reaction conditions: a 20 mL Schlenk tube was charged with the ketimine **17b** (0.5 mmol), anhydrous isopropanol (5.0 mL), Mn complex **7** and *t*BuOK under argon. Then the mixture was stirred at indicated temperature in an oil bath. After cooling to room temperature, the solution was diluted with ethyl acetate (2 mL) and filtered through a small pad of celite (2 cm in a Pasteur pipette). The celite was washed with ethyl acetate (2×2 mL). The filtrate was evaporated and the conversion were determined by <sup>1</sup>H NMR of the crude mixture.

### 3.2.2. Scope for the reduction of aldimines

Having optimized the conditions for the reduction of aldimines: complex **7** (2.0 mol%), *t*BuOK (4.0 mol%), *i*PrOH (C = 0.1 mol·L<sup>-1</sup>), 80 °C, 3 h, we then explored the scope of this transformation (Table 11). In general, a large variety of aldimines, prepared by the condensation of benzaldehyde with aniline derivatives, was reduced in high yields. Steric hindrance has an influence as increasing the number of *ortho* substituents on both the benzaldehyde (**16b**, **16ao**) or the aniline (**16ap**, **16aq**) moieties, led to the sterically hindered amines **16ao** and **16aq** in lower yields than **16b** and **16ap**. Halogen substituents (F, Cl, Br, I) were well tolerated (**16ar**, **16j**, **16as**, **16f**, isolated yields >90%), and no product resulting from dehalogenation was detected. Interestingly, heteroaromatic imines (**15r**, **15s**, **15t**, **15au**) affording *N*-substituted-aminomethylheterocycles (**16r**, **16s**, **16t**, **16au**) were also surprisingly reduced without significant loss of activity (39-93% yields). It should be noticed that the structures of the reaction products are very similar to the ones of the ligand used to coordinate the manganese center, namely 2-(aminomethyl)-pyridine. Under the conditions of the catalysis, a dynamic exchange of ligands cannot be ruled out. Since diverse diamines proved to be active ligands in transfer hydrogenation of ketones, such an exchange may not alter the reduction.<sup>[20c]</sup> Likewise, organometallic 4-methyl-*N*-(ferrocenylmethylidene)-aniline **15q** was totally reduced and led to the corresponding amine **16q** in good isolated yield (88%). The tolerance toward various functional groups such as amino (**16k**), methoxy (**16av**), cyano (**16aw**), ester (**16ay**),

amido (**16m**), acetal (**16az**), vinyl (**16ba**) and alkynyl (**16bb**) groups was evaluated and it was shown that they did not affect the catalytic system and remained intact after the reduction. Only with the nitro-substituted imine **15ax**, no reaction occurred. In the case of the conjugated imine **15bc**, the unsaturated amine **16bc** was obtained as major product (80%) along with 20% of the corresponding saturated amine **16am**.

**Table 11.** Generality of the reduction of aldimines **15** catalyzed by the complex **7** <sup>[a]</sup>



<sup>[a]</sup> Reaction conditions: Under inert atmosphere, a 20 mL Schlenk tube was filled sequentially with the imine (0.5 mmol), anhydrous 2-propanol (5 mL), complex **7** (3.3 mg, 2.0 mol%), and *t*BuOK (2.2 mg, 4.0 mol%). The reaction was heated in an oil bath at 80 °C for 3 h. Conversion was determined by <sup>1</sup>H NMR spectroscopy. Isolated yield in parenthesis.

<sup>[b]</sup> Isolated as mixture containing 20% of saturated amine **16am**.

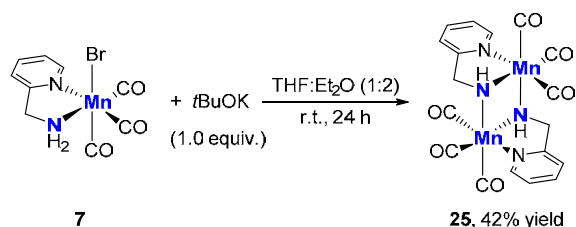
<sup>[c]</sup> complex **7** (6.6 mg, 4.0 mol%), *t*BuOK (4.4 mg, 8.0 mol%).

The inability of our catalytic system to reduce ketimines can appear to be an advantage for the selective reduction of substrates displaying both ketimine and aldimine moieties. Gratifyingly, for the diimine **15n** derived from 4-formylacetophenone, only the aldimine moiety was reduced affording the corresponding amino-ketimine **16n** in 83% isolated yield. Finally, imines bearing



aliphatic substituents were difficult to convert to the desired amines which were obtained in low yields (**16ae**, **16y**, **16aa** and **16bd**, 17%-38% yields).

### 3.3. Mechanistic insights



**Scheme 6.** Synthesis of the dimer Mn complex **24**.

Then, to gain insight into the nature of the catalytic active species, we performed stoichiometric reactions between complex **7** and 1 equiv. of *t*-BuOK. After 24 h at r.t., the dimeric manganese complex **25**, resulting from the deprotonation of the NH moieties, could be isolated in 42% yield (Scheme 6). Unfortunately, further reactions of **25** with 2-propanol or **7** with NaBH<sub>4</sub> did not allow the characterization of any manganese hydride intermediate.<sup>[6d]</sup>

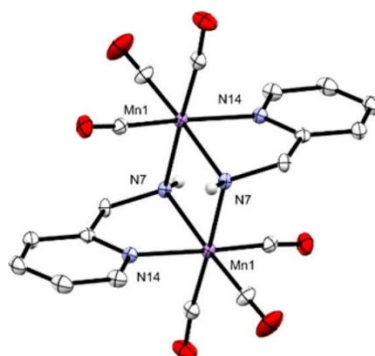
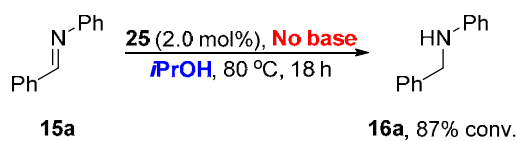


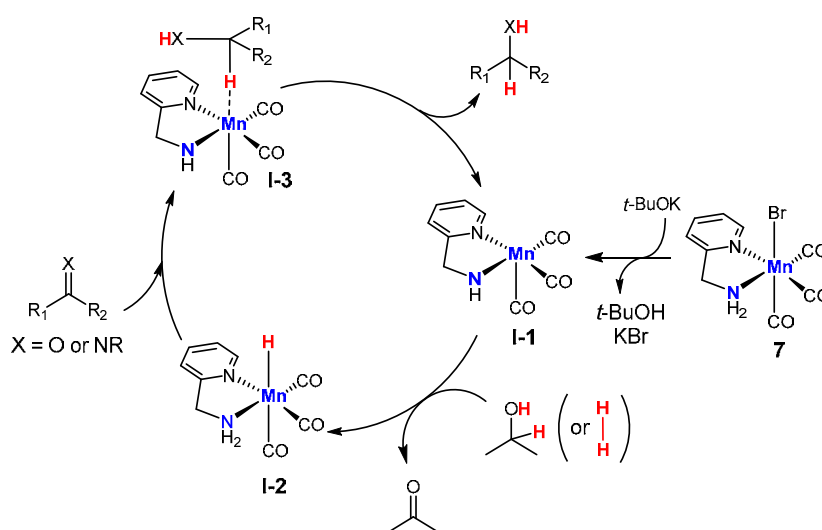
**Figure 4.** Perspective view of the molecular structure of the dimer Mn complex **25** with thermal ellipsoids drawn at 50% probability. Hydrogens, except the NH, were omitted for clarity.

The molecular structure of **25** was confirmed by X-ray diffraction studies (Figure 4).<sup>[6d]</sup> Finally, the dimeric complex **25** was tested as a catalyst (2.0 mol%) for the transfer hydrogenation of the aldimine **15a**, under base-free conditions and 87% of conversion were achieved (Scheme 7). The corresponding deprotonated monomer, formed by the dissociation of the dimer, is likely the intermediate of the catalytic cycle, which is in line with the mechanism of ligand-assisted hydrogen-transfer reactions.



**Scheme 7.** Transfer hydrogenation of the aldimine **15a** under base-free conditions catalyzed by **25**.

Based on our mechanistic study above and the previous works of other groups on related complexes with Mn<sup>[9]</sup> we propose the following mechanism (Scheme 8). In a first step, the base activated the precatalyst by deprotonation of the NH moieties to give the 16 electrons intermediate **I-1**. This 16 electrons species then dehydrogenated isopropanol forming acetone and the amino-hydride intermediate **I-2** (or by heterolytic splitting of dihydrogen in the case of hydrogenation). The C=X (X = O or NR) reduction was a two-steps process with first hydride transfer from Mn to C, followed by proton transfer from N-H of the ligand to X, regenerating the active species **I-1**.



**Scheme 8.** Proposed mechanism for (transfer)hydrogenation of carbonyl compounds catalyzed by bidentate Mn complex.

### 3.4. Conclusion

In conclusion, we reported in this paragraph the first application of Mn-based catalyst in transfer hydrogenation of imines. We have shown that manganese(I) pre-catalyst **23** bearing a 2-aminomethylpyridine ligand catalyzed efficiently the transfer hydrogenation of aldimines in the presence of *i*PrOH as reductant under mild conditions (2.0 mol% catalyst, 4.0 mol% base, 80 °C, 3 to 18 h). The catalytic process displayed a high tolerance towards a large variety of functional groups. This protocol enlarges the scope of reaction catalyzed by manganese, highlighting the rising potential of this transition metal in homogeneous catalysis.

## IV-4 Conclusion of Chapter IV

In this chapter, we have explored the application of a series of well-defined manganese pre-catalysts featuring readily available bidendate pyridinyl-phosphine and 2-picolylamine ligands in hydrogenation type reactions, namely

- 1) hydrogenation of carbonyl derivatives with molecular hydrogen,
- 2) reductive amination of aldehydes under hydrogenation conditions and
- 3) transfer hydrogenation of aldimines in the presence of *i*PrOH.

Those bidendate Mn complexes showed good catalytic performances under mild conditions with low catalyst loading and exhibited a good functional group tolerance. Those protocols enlarge the scope of reactions catalyzed by manganese, highlighting the rising potential of this transition metal in homogeneous catalysis.

## IV-5 References

- [1] J. G. De Vries, C. J. Elsevier, *The Handbook of Homogeneous Hydrogenation*, WILEY-VCH, Weinheim, **2007**.
- [2] a) S. Gaillard, J.-L. Renaud, *ChemSusChem* **2008**, *1*, 505-509; b) R. H. Morris, *Chem. Soc. Rev.* **2009**, *38*, 2282-2291; c) R. H. Morris, *Acc. Chem. Res.* **2015**, *48*, 1494-1502; d) L. C. Misal Castro, H. Li, J.-B. Sortais, C. Darcel, *Green Chem.* **2015**, *17*, 2283-2303; e) D. S. Mérel, M. L. T. Do, S. Gaillard, P. Dupau, J.-L. Renaud, *Coord. Chem. Rev.* **2015**, *288*, 50-68; f) I. Bauer, H.-J. Knölker, *Chem. Rev.* **2015**, *115*, 3170-3387.
- [3] a) R. M. Bullock, *Science* **2013**, *342*, 1054-1055; b) W. Zuo, A. J. Lough, Y. F. Li, R. H. Morris, *Science* **2013**, *342*, 1080-1083.
- [4] a) R. I. Khusnutdinov, A. R. Bayguzina, U. M. Dzhemilev, *Russ. J. Org. Chem.* **2012**, *48*, 309-348; b) R. J. Trovitch, *Synlett* **2014**, *25*, 1638-1642; c) D. A. Valyaev, G. Lavigne, N. Lugan, *Coord. Chem. Rev.* **2016**, *308*, 191-235.
- [5] a) S. Elangovan, C. Topf, S. Fischer, H. Jiao, A. Spannenberg, W. Baumann, R. Ludwig, K. Junge, M. Beller, *J. Am. Chem. Soc.* **2016**, *138*, 8809-8814; b) S. Elangovan, M. Garbe, H. Jiao, A. Spannenberg, K. Junge, M. Beller, *Angew. Chem. Int. Ed.* **2016**, *55*, 15364-15368; c) S. Elangovan, J. Neumann, J.-B. Sortais, K. Junge, C. Darcel, M. Beller, *Nat. Commun.* **2016**, *7*, 12641; d) M. Peña-López, P. Piehl, S. Elangovan, H. Neumann, M. Beller, *Angew. Chem. Int. Ed.* **2016**, *55*, 14967-14971; e) M. Andérez-Fernández, L. K. Vogt, S. Fischer, W. Zhou, H. Jiao, M. Garbe, S. Elangovan, K. Junge, H. Junge, R. Ludwig, M. Beller, *Angew. Chem. Int. Ed.* **2017**, *56*, 559-562.
- [6] a) F. Kallmeier, T. Irrgang, T. Dietel, R. Kempe, *Angew. Chem. Int. Ed.* **2016**, *55*, 11806-11809; b) M. Perez, S. Elangovan, A. Spannenberg, K. Junge, M. Beller, *ChemSusChem* **2017**, *10*, 83-86; c) A. Bruneau-Voisine, D. Wang, T. Roisnel, C. Darcel, J.-B. Sortais, *Catal. Commun.* **2017**, *92*, 1-4; d) A. Bruneau-Voisine, D. Wang, V. Dorcet, T. Roisnel, C. Darcel, J.-B. Sortais, *Org. Lett.* **2017**, *19*, 3656-3659; e) M. B. Widegren, G. J. Harkness, A. M. Z. Slawin, D. B. Cordes, M. L. Clarke, *Angew. Chem. Int. Ed.* **2017**, *56*, 5825-5828; f) F. Bertini, M. Glatz, N. Gorgas, B. Stöger, M. Peruzzini, L. F. Veiros, K. Kirchner, L. Gonsalvi, *Chem. Sci.* **2017**, *8*, 5024-5029; g) A. Zirakzadeh, S. R. M. M. de Aguiar, B. Stöger, M. Widhalm, K. Kirchner, *ChemCatChem* **2017**, *9*, 1744-1748; h) N. A. Espinosa-Jalapa, A. Nerush, L. J. W. Shimon, G. Leitius, L. Avram, Y. Ben-David, D. Milstein, *Chem. Eur. J.* **2017**, *23*, 5934-5938; i) A. M. Tondreau, J. M. Boncella, *Organometallics* **2016**, *35*, 2049-2052; j) A. M. Tondreau, J. M. Boncella, *Polyhedron* **2016**, *116*, 96-104; k) A. Dubey, L. Nencini, R. R. Fayzullin, C. Nervi, J. R. Khusnutdinova, *ACS Catal.* **2017**, *7*, 3864-3868; l) V. Papa, J. R. Cabrero-Antonino, E. Alberico, A. Spanneberg, K. Junge, H. Junge, M. Beller, *Chem. Sci.* **2017**, *8*, 3576-3585.
- [7] a) M. Mastalir, M. Glatz, N. Gorgas, B. Stöger, E. Pittenauer, G. Allmaier, L. F. Veiros, K. Kirchner, *Chem. Eur. J.* **2016**, *22*, 12316-12320; b) M. Mastalir, M. Glatz, E. Pittenauer, G. Allmaier, K. Kirchner, *J. Am. Chem. Soc.* **2016**, *138*, 15543-15546; c) A. Mukherjee, A. Nerush, G. Leitius, L. J. W. Shimon, Y. Ben David, N. A. Espinosa Jalapa, D. Milstein, *J. Am. Chem. Soc.* **2016**, *138*, 4298-4301; d) A. Nerush, M. Vogt, U. Gellrich, G. Leitius, Y. Ben-David, D. Milstein, *J. Am. Chem. Soc.* **2016**, *138*, 6985-6997; e) J. Neumann, S. Elangovan, A. Spannenberg, K. Junge, M. Beller, *Chem. Eur. J.* **2017**, *23*, 5410-5413; f) A. Bruneau-Voisine, D. Wang, V. Dorcet, T. Roisnel, C. Darcel, J.-B. Sortais, *J. Catal.* **2017**, *347*, 57-62; g) D. H. Nguyen, X. Trivelli, F. Capet, J.-F. Paul, F. Dumeignil, R. M. Gauvin, *ACS Catal.* **2017**, *7*, 2022-2032; h) N. Deibl, R. Kempe, *Angew. Chem. Int. Ed.* **2017**, *56*, 1663-1666; i) F. Kallmeier, B. Dudziec, T. Irrgang, R. Kempe, *Angew. Chem. Int. Ed.* **2017**, *56*, 7261-7265; j) M. Mastalir, E. Pittenauer, G. Allmaier, K. Kirchner, *J. Am. Chem. Soc.* **2017**, *139*, 8812-8815; k) J. O. Bauer, S. Chakraborty, D. Milstein, *ACS Catal.* **2017**, *7*, 4462-4466; l) S. Chakraborty, U. Gellrich, Y. Diskin-Posner, G. Leitius, L. Avram, D. Milstein, *Angew. Chem. Int. Ed. Engl.* **2017**, *56*, 4229-4233.
- [8] a) J. Zheng, S. Chevance, C. Darcel, J.-B. Sortais, *Chem. Commun.* **2013**, *49*, 10010-10012; b) J. Zheng, S. Elangovan, D. A. Valyaev, R. Brousses, V. César, J.-B. Sortais, C. Darcel, N. Lugan, G. Lavigne, *Adv. Synth. Catal.* **2014**, *356*, 1093-1097; c) D. A. Valyaev, D. Wei, S.

- Elangovan, M. Cavailles, V. Dorcet, J.-B. Sortais, C. Darcel, N. Lugan, *Organometallics* **2016**, *35*, 4090-4098.
- [9] R. van Putten, E. A. Uslamin, M. Garbe, C. Liu, A. Gonzalez-de-Castro, M. Lutz, K. Junge, E. J. M. Hensen, M. Beller, L. Lefort, E. A. Pidko, *Angew. Chem. Int. Ed.* **2017**, *56*, 7531-7534.
- [10] a) S. M. Aucott, A. M. Z. Slawin, J. D. Woollins, *J. Chem. Soc., Dalton Trans.* **2000**, 2559-2575; b) D. Benito-Garagorri, K. Mereiter, K. Kirchner, *Collect. Czech. Chem. Commun.* **2007**, *72*, 527-540.
- [11] M. Alvarez, N. Lugan, R. Mathieu, *J. Chem. Soc., Dalton Trans.* **1994**, 2755-2760.
- [12] E. Mothes, S. Sentets, M. A. Luquin, R. Mathieu, N. Lugan, G. Lavigne, *Organometallics* **2008**, *27*, 1193-1206.
- [13] a) R. K. Henderson, C. Jimenez-Gonzalez, D. J. C. Constable, S. R. Alston, G. G. A. Inglis, G. Fisher, J. Sherwood, S. P. Binks, A. D. Curzons, *Green Chem.* **2011**, *13*, 854-862; b) S. D. Ramgren, L. Hie, Y. Ye, N. K. Garg, *Org. Lett.* **2013**, *15*, 3950-3953.
- [14] T. Hirata, A. Matsushima, Y. Sato, T. Iwasaki, H. Nomura, T. Watanabe, S. Toyoda, S. Izumi, *J. Mol. Catal. B: Enzym.* **2009**, *59*, 158-162.
- [15] X. Chen, X. Gao, Q. Wu, D. Zhu, *Tetrahedron: Asymmetry* **2012**, *23*, 734-738.
- [16] S. Gomez, J. A. Peters, T. Maschmeyer, *Adv. Synth. Catal.* **2002**, *344*, 1037-1057.
- [17] a) B. Li, J.-B. Sortais, C. Darcel, *RSC Adv.* **2016**, *6*, 57603-57625; b) S. A. Lawrence, *Amines: Synthesis, Properties and Applications*, Cambridge University Press, Cambridge, **2004**.
- [18] M. Ishihara, H. Togo, *Tetrahedron* **2007**, *63*, 1474-1480.
- [19] D. Wei, A. Bruneau-Voisine, T. Chauvin, V. Dorcet, T. Roisnel, D. Valyaev, N. Lugan, J.-B. Sortais, *Adv. Synth. Catal.* **2018**, *360*, 676-681.
- [20] a) O. Martínez-Ferraté, C. Werlé, G. Franciò, W. Leitner, *ChemCatChem* **2018**, *10*, 4514-4518; b) K. Z. Demmans, M. E. Olson, R. H. Morris, *Organometallics* **2018**, *37*, 4608-4618; c) D. Wang, A. Bruneau-Voisine, J.-B. Sortais, *Catal. Commun.* **2018**, *105*, 31-36.
- [21] a) M. Cettolin, X. Bai, D. Lübken, M. Gatti, S. V. Facchini, U. Piarulli, L. Pignataro, C. Gennari, *Eur. J. Org. Chem.* **2019**, *2019*, 647-654; b) S. Zhou, S. Fleischer, K. Junge, S. Das, D. Addis, M. Beller, *Angew. Chem. Int. Ed.* **2010**, *49*, 8121-8125; c) A. A. Mikhailine, M. I. Maishan, R. H. Morris, *Org. Lett.* **2012**, *14*, 4638-4641; d) H.-J. Pan, T. W. Ng, Y. Zhao, *Org. Biomol. Chem.* **2016**, *14*, 5490-5493; e) S. V. Facchini, M. Cettolin, X. Bai, G. Casamassima, L. Pignataro, C. Gennari, U. Piarulli, *Adv. Synth. Catal.* **2018**, *360*, 1054-1059.
- [22] a) S. Kuhl, R. Schneider, Y. Fort, *Organometallics* **2003**, *22*, 4184-4186; b) F. Alonso, P. Riente, M. Yus, *Synlett* **2008**, *2008*, 1289-1292; c) H. Xu, P. Yang, P. Chuanprasit, H. Hirao, J. Zhou, *Angew. Chem. Int. Ed.* **2015**, *54*, 5112-5116.
- [23] a) G. Zhang, S. K. Hanson, *Chem. Commun.* **2013**, *49*, 10151-10153; b) J. R. Cabrero-Antonino, R. Adam, K. Junge, R. Jackstell, M. Beller, *Catal. Sci. Technol.* **2017**, *7*, 1981-1985.
- [24] a) M. Wills, *Top. Curr. Chem.* **2016**, *374*, 14; b) M. Wills, *Imino Reductions by Transfer Hydrogenation in Modern Reduction Methods* (Eds.: P. G. Andersson, I. J. Munslow), Wiley-VCH, Weinheim, **2008**, pp. 271-296; c) P.-G. Echeverria, T. Ayad, P. Phansavath, V. Ratovelomanana-Vidal, *Synthesis* **2016**, *48*, 2523-2539.
- [25] T. Irrgang, R. Kempe, *Chem. Rev.* **2019**, *119*, 2524-2549.

## IV-6 Experimental data

### 6.1. General information

Manganese pentacarbonyl bromide, min. 98%, were purchased from Strem Chemicals.

Magnetic stirred Parr autoclaves (22 mL) were used for the hydrogenation reactions.

$^1\text{H}$ ,  $^{13}\text{C}$ ,  $^{19}\text{F}$  and  $^{31}\text{P}$  NMR spectra were recorded in  $\text{CDCl}_3$ , acetone- $d_6$ , or  $\text{CD}_3\text{OD}$  at 298 K, on Bruker, AVANCE 400 and AVANCE 300 spectrometers at 400.1, and 300.1 MHz, respectively.  $^1\text{H}$  and  $^{13}\text{C}$  NMR spectra were calibrated using the residual solvent signal at the corresponding central peak ( $^1\text{H}$ :  $\text{CDCl}_3$  7.26 ppm, acetone- $d_6$  2.05 ppm,  $\text{CD}_3\text{OD}$  3.31 ppm;  $^{13}\text{C}$ :  $\text{CDCl}_3$  77.16 ppm, acetone- $d_6$  29.84 ppm,  $\text{CD}_3\text{OD}$  49.0 ppm).  $^{19}\text{F}$  and  $^{31}\text{P}$  NMR spectra calibrated against  $\text{CFCl}_3$  and 85%  $\text{H}_3\text{PO}_4$  internal standard, respectively. Chemical shift ( $\delta$ ) and coupling constants ( $J$ ) are given in ppm and in Hz, respectively. The peak patterns are indicated as follows: (s, singlet; d, doublet; t, triplet; q, quartet; quin, quintet; m, multiplet, and br. for broad).

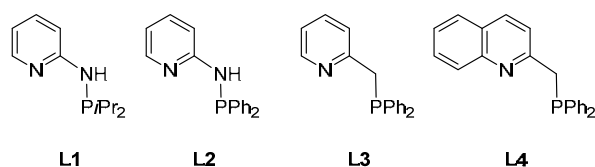
IR spectra were measured in  $\text{CH}_2\text{Cl}_2$  solution with a Shimadzu IR-Affinity 1 instrument and given in  $\text{cm}^{-1}$  with a relative intensity in the parenthesis (vs, very strong; s, strong; m, medium). HR-MS spectra (ESI positive mode) and microanalysis were carried out by the corresponding facilities at the CRMPO (Centre Régional de Mesures Physiques de l'Ouest), Université de Rennes 1.

GC analyses were performed with GC-2014 (Shimadzu) 2010 equipped with a 30 m capillary column (Supelco, SPBTM-20, fused silica capillary column, 30 m  $\times$  0.25 mm  $\times$  0.25 mm film thickness).

Specific rotations were measured in a 1 dm thermostated quartz cell on a Jasco-P1010 polarimeter.

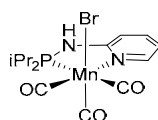
### 6.2. Part IV-1- Hydrogenation of Carbonyl Derivatives

#### 6.2.1. Synthesis of PN ligands L1-L4



The ligands **L1**,<sup>[1]</sup> **L2**,<sup>[2]</sup> **L3**<sup>[3]</sup> and **L4**<sup>[4]</sup> were synthesized according to the literature procedures.

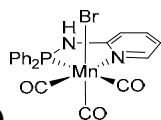
#### 6.2.2. Synthesis of Manganese Complexes 8-11



**Mn(CO)<sub>3</sub>Br(L1) (8).**

**L1** (210 mg, 0.365 mmol) was added to a solution of  $\text{Mn(CO)}_5\text{Br}$  (100 mg, 0.365 mmol, 1.0 equiv.) in anhydrous toluene (6 mL). The mixture was stirred at 100 °C overnight, then cooled to r.t. and toluene was evaporated under vacuum. The crude residue was dissolved in dichloromethane (1 mL) and then pentane (5 mL) was added to afford yellow needle crystals. The supernatant was removed and the crystals were washed with pentane (3 $\times$ 2 mL) and dried under vacuum to afford pure compound **8** (136 mg, 87%). Single crystals suitable for X-Ray diffraction studies were grown by slow diffusion of pentane into a  $\text{CH}_2\text{Cl}_2$  solution at r.t.

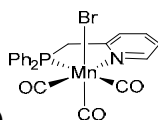
**<sup>1</sup>H NMR** (400.1 MHz, acetone-*d*<sub>6</sub>) δ 8.68 – 8.44 (m, 1H, Py), 7.77 (br. d, *J*<sub>HH</sub> = 5.0 Hz, 1H, *NH*), 7.63 (t, *J*<sub>HH</sub> = 7.7 Hz, 1H, Py), 7.02 (d, *J*<sub>HH</sub> = 8.4 Hz, 1H, Py), 6.81 (t, *J*<sub>HH</sub> = 6.5 Hz, 1H), 3.57 – 3.24 (m, 1H, CH(CH<sub>3</sub>)<sub>2</sub>), 2.98 – 2.66 (m, 1H, CH(CH<sub>3</sub>)<sub>2</sub>), 1.58 – 1.33 (m, 9H, CH(CH<sub>3</sub>)<sub>2</sub>), 1.27 (dd, *J*<sub>PH</sub> = 15.0, *J*<sub>HH</sub> = 7.2 Hz, 3H, CH(CH<sub>3</sub>)<sub>2</sub>). **<sup>13</sup>C{<sup>1</sup>H} NMR** (100.6 MHz, acetone-*d*<sub>6</sub>) δ 224.1 (br. s, CO), 216.6 (br. s, CO), 162.9 (d, <sup>2</sup>*J*<sub>PC</sub> = 12.6 Hz, C<sub>Py</sub>), 154.0 (d, *J* = 4.4 Hz, CH<sub>Py</sub>), 140.2 (s, CH<sub>Py</sub>), 116.6 (s, CH<sub>Py</sub>), 111.9 (d, *J*<sub>PC</sub> = 6.9 Hz, CH<sub>Py</sub>), 28.7 (d, <sup>1</sup>*J*<sub>PC</sub> = 24.3 Hz, CH(CH<sub>3</sub>)<sub>2</sub>), 27.6 (d, <sup>1</sup>*J*<sub>PC</sub> = 22.6 Hz, CH(CH<sub>3</sub>)<sub>2</sub>), 19.4 (d, <sup>3</sup>*J*<sub>PC</sub> = 7.7 Hz, CH(CH<sub>3</sub>)<sub>2</sub>), 19.0 (d, <sup>3</sup>*J*<sub>PC</sub> = 6.2 Hz, CH(CH<sub>3</sub>)<sub>2</sub>), 18.4 (s, CH(CH<sub>3</sub>)<sub>2</sub>), 17.3 (d, <sup>3</sup>*J*<sub>PC</sub> = 4.6 Hz, CH(CH<sub>3</sub>)<sub>2</sub>). **<sup>31</sup>P{<sup>1</sup>H} NMR** (162.0 MHz, acetone-*d*<sub>6</sub>) δ 125.5. **IR (CH<sub>2</sub>Cl<sub>2</sub>):** ν<sub>CO</sub> 2021 (s), 1936 (m), 1911 (s), 1884 (vs) cm<sup>-1</sup>. **Anal. Calcd.** (%) for C<sub>14</sub>H<sub>19</sub>BrMnN<sub>2</sub>O<sub>3</sub>P: C, 39.18; H, 4.46; N, 6.53. Found: C, 39.12; H, 4.44; N, 6.40. **HR-MS (ESI):** *m/z* calcd for C<sub>14</sub>H<sub>19</sub><sup>79</sup>BrMnN<sub>2</sub>NaO<sub>3</sub>P (M + Na<sup>+</sup>) 450.9589, found 450.9587 (0 ppm).



**Mn(CO)<sub>3</sub>Br(L2) (9)**

Following the general procedure employed for the synthesis of **8**, starting from **L2** (101 mg, 0.365 mmol) and Mn(CO)<sub>5</sub>Br (100 mg, 0.365 mmol) the product **9** (161 mg, 89%) was obtained as yellow crystals.

**<sup>1</sup>H NMR** (400.1 MHz, acetone-*d*<sub>6</sub>) δ 8.86 (d, *J*<sub>HH</sub> = 5.3 Hz, 1H, *NH*), 8.63 (d, *J*<sub>HH</sub> = 5.6 Hz, 1H, Py), 7.97 – 7.81 (m, 2H, Ph), 7.78 – 7.70 (m, 3H, Ph), 7.63 – 7.38 (m, 6H, Ph + Py), 7.27 (br d, *J*<sub>HH</sub> = 6.5 Hz, 1H, Py), 6.92 (t, *J*<sub>HH</sub> = 6.4 Hz, 1H, Py). **<sup>13</sup>C{<sup>1</sup>H} NMR** (100.6 MHz, acetone-*d*<sub>6</sub>) δ 224.1 (br. s, CO), 221.9 (br. s, CO), 217.0 (br. s, CO), 162.1 (d, <sup>2</sup>*J*<sub>PC</sub> = 15.9 Hz, C<sub>Py</sub>), 154.1 (d, *J*<sub>PC</sub> = 4.5 Hz, CH<sub>Py</sub>), 140.6 (s, CH<sub>Py</sub>), 138.0 (d, <sup>1</sup>*J*<sub>PC</sub> = 47.4 Hz, *C*<sub>ipso</sub> Ph), 133.5 (d, <sup>1</sup>*J*<sub>PC</sub> = 48.9 Hz, *C*<sub>ipso</sub> Ph), 133.2 (d, *J*<sub>PC</sub> = 11.2 Hz, CH<sub>Ph</sub>), 131.5 (d, *J*<sub>PC</sub> = 4.7 Hz, CH<sub>Ph</sub>), 131.45 (d, *J*<sub>PC</sub> = 4.2 Hz, CH<sub>Ph</sub>), 130.8 (d, *J*<sub>PC</sub> = 12.3 Hz, CH<sub>Ph</sub>), 129.6 (d, *J*<sub>PC</sub> = 9.9 Hz, CH<sub>Ph</sub>), 128.8 (d, *J*<sub>PC</sub> = 10.6 Hz, CH<sub>Ph</sub>), 117.4 (s, CH<sub>Py</sub>), 112.6 (d, *J*<sub>PC</sub> = 8.1 Hz, CH<sub>Py</sub>). **<sup>31</sup>P{<sup>1</sup>H} NMR** (162.0 MHz, acetone-*d*<sub>6</sub>) δ 101.9. **IR (CH<sub>2</sub>Cl<sub>2</sub>):** ν<sub>CO</sub> 2023 (s), 1948 (s), 1917 (s) cm<sup>-1</sup>. **Anal. Calcd.** (%) for C<sub>20</sub>H<sub>15</sub>BrMnN<sub>2</sub>O<sub>3</sub>P: C, 48.32; H, 3.04; N, 5.63. Found: C, 47.98; H, 3.10; N, 5.61. **HR-MS (ESI):** *m/z* calcd for C<sub>17</sub>H<sub>15</sub>MnN<sub>2</sub>P (M<sup>+</sup>–3CO–Br) 333.03478, found 333.0345 (1 ppm).

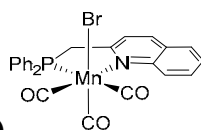


**Mn(CO)<sub>3</sub>Br(L3) (10)**

Following the general procedure employed for the synthesis of **8**, starting from **L3** (101 mg, 0.365 mmol) and Mn(CO)<sub>5</sub>Br (100 mg, 0.364 mmol), the product **10** (164.5 mg, 91%) was obtained as yellow crystals.

**<sup>1</sup>H NMR** (400.1 MHz, acetone-*d*<sub>6</sub>) δ 9.11 (d, *J*<sub>HH</sub> = 5.0 Hz, 1H, Py), 8.14 – 7.95 (m, 3H, Ph), 7.90 (d, *J* = 7.1 Hz, 1H, Py), 7.63 – 7.49 (m, 3H, Ph), 7.48 – 7.40 (m, 6H, Ph + Py), 4.79 – 4.53 (m, 2H, PCH<sub>2</sub>). **<sup>13</sup>C{<sup>1</sup>H} NMR** (100.6 MHz, acetone-*d*<sub>6</sub>) δ 225.1 (br. s, CO), 223.1 (br. s, CO), 217.4 (br. s, CO), 162.8 (d, <sup>2</sup>*J*<sub>PC</sub> = 7.6 Hz, C<sub>Py</sub>), 156.2 (d, *J*<sub>PC</sub> = 3.8 Hz, CH<sub>Py</sub>), 140.3 (s, CH<sub>Py</sub>), 135.7 (d, <sup>1</sup>*J*<sub>PC</sub> = 39.2 Hz, *C*<sub>ipso</sub> Ph), 134.9 (d, *J*<sub>PC</sub> = 9.7 Hz, CH<sub>Ph</sub>), 132.0 (d, *J*<sub>PC</sub> = 2.5 Hz, CH<sub>Ph</sub>), 131.6 (d, *J*<sub>PC</sub> = 10.0 Hz, CH<sub>Ph</sub>), 131.1 (d, *J*<sub>PC</sub> = 2.1 Hz, CH<sub>Ph</sub>), 131.1 (d, *J*<sub>PC</sub> = 44.1 Hz, *C*<sub>ipso</sub> Ph), 129.8 (d, *J*<sub>PC</sub> = 9.2 Hz, CH<sub>Ph</sub>), 129.5 (d, *J*<sub>PC</sub> = 10.0 Hz, CH<sub>Ph</sub>), 125.8 (d, *J*<sub>PC</sub> = 9.6 Hz, CH<sub>Py</sub>), 124.4 (s, CH<sub>Py</sub>), 41.1 (d, <sup>1</sup>*J*<sub>PC</sub> = 25.4 Hz, PCH<sub>2</sub>). **<sup>31</sup>P{<sup>1</sup>H} NMR** (162.0 MHz, acetone-*d*<sub>6</sub>) δ

57.3. **IR** ( $\text{CH}_2\text{Cl}_2$ ):  $\nu_{\text{CO}}$  2021 (s), 1939 (m), 1915 (vs)  $\text{cm}^{-1}$ . **Anal. Calcd** (%). for  $\text{C}_{21}\text{H}_{16}\text{BrNO}_3\text{PMn}$ : C, 50.83; H, 3.25; N, 2.82. Found: C, 50.64; H, 3.23; N, 2.78. **HR-MS (ESI)**:  $m/z$  calcd for  $\text{C}_{18}\text{H}_{16}\text{MnNP}$  ( $\text{M}^+ - 3\text{CO} - \text{Br}$ ) 332.03953, found 332.0404 (3 ppm).



### **Mn(CO)<sub>3</sub>Br(L4) (11)**

Following the general procedure employed for the synthesis of **8**, starting from **L4** (119 mg, 0.365 mmol) and  $\text{Mn(CO)}_5\text{Br}$  (100 mg, 0.365 mmol), the product **11** (179 mg, 90%) was obtained as yellow crystals.

**<sup>1</sup>H NMR** (400.1 MHz, acetone- $d_6$ )  $\delta$  9.00 (d,  $J_{\text{HH}} = 8.8$  Hz, 1H, Py), 8.56 (s, 1H, Ar), 8.20 – 7.84 (m, 5H, Ph + Ar), 7.74 (t,  $J_{\text{HH}} = 6.3$  Hz, 1H, Ar), 7.68 – 7.50 (m, 3H, Ph + Ar), 7.46 – 7.33 (m, 5H, Ph + Ar), 5.30 (dd,  $^2J_{\text{HH}} = 16.5$  Hz,  $^2J_{\text{PH}} = 6.7$  Hz, 1H,  $\text{PCH}_2$ ), 4.90 (t,  $^2J_{\text{PH}} = ^2J_{\text{HH}} = 16.0$  Hz, 1H,  $\text{PCH}_2$ ). **<sup>13</sup>C{<sup>1</sup>H} NMR** (100.6 MHz, acetone- $d_6$ )  $\delta$  225.9 (br. s, CO), 223.9 (br. s, CO), 217.7 (br. s, CO), 166.8 (d,  $J_{\text{PC}} = 6.9$  Hz,  $\text{C}_{\text{Py}}$ ), 150.3 (d,  $J_{\text{PC}} = 1.9$  Hz,  $\text{CH}_{\text{Py}}$ ), 141.1 (d,  $J_{\text{PC}} = 1.7$  Hz,  $\text{CH}_{\text{Ph}}$ ), 134.9 (d,  $J_{\text{PC}} = 9.8$  Hz,  $\text{CH}_{\text{Ph}}$ ), 134.8 (d,  $^1J_{\text{PC}} = 39.7$  Hz,  $\text{C}_{\text{ipso Ph}}$ ), 134.0 (s,  $\text{C}_{\text{Ar}}$ ), 132.2 (d,  $J_{\text{PC}} = 2.4$  Hz,  $\text{CH}_{\text{Ph}}$ ), 132.0 (s,  $\text{CH}_{\text{Ar}}$ ), 131.7 (d,  $J_{\text{PC}} = 10.0$  Hz,  $\text{CH}_{\text{Ph}}$ ), 131.1 (d,  $J_{\text{PC}} = 2.2$  Hz,  $\text{CH}_{\text{Ph}}$ ), 130.6 (d,  $J_{\text{PC}} = 46.1$  Hz,  $\text{C}_{\text{ipso Ph}}$ ), 130.3 (s,  $\text{CH}_{\text{Ar}}$ ), 130.25 (s,  $\text{CH}_{\text{Ar}}$ ), 129.8 (d,  $J_{\text{PC}} = 9.2$  Hz,  $\text{CH}_{\text{Ph}}$ ), 129.6 (d,  $J_{\text{PC}} = 10.1$  Hz,  $\text{CH}_{\text{Ph}}$ ), 129.2 (s,  $\text{C}_{\text{Ar}}$ ), 128.7 (s,  $\text{CH}_{\text{Ar}}$ ), 127.9 (s,  $\text{CH}_{\text{Ph}}$ ), 123.3 (d,  $J_{\text{PC}} = 9.7$  Hz,  $\text{CH}_{\text{Py}}$ ), 44.7 (d,  $^1J_{\text{PC}} = 26.8$  Hz,  $\text{PCH}_2$ ). **<sup>31</sup>P{<sup>1</sup>H} NMR** (162.0 MHz, acetone- $d_6$ )  $\delta$  55.4. **IR** ( $\text{CH}_2\text{Cl}_2$ ):  $\nu_{\text{CO}}$  2015 (s), 1934 (m), 1915 (vs)  $\text{cm}^{-1}$ . **Anal. Calc** (%). for  $(\text{C}_{25}\text{H}_{18}\text{BrMnNO}_3\text{P}) \cdot (\text{CH}_2\text{Cl}_2)$ : C, 49.48; H, 3.19; N, 2.22. Found: C, 49.43; H, 3.30; N, 2.44. **HR-MS (ESI)**:  $m/z$  calcd for  $\text{C}_{22}\text{H}_{18}\text{MnNP}$  ( $\text{M}^+ - 3\text{CO} - \text{Br}$ ) 382.05518, found 382.0545 (2 ppm).

### **6.2.3. General procedure for hydrogenation reactions**

In an argon filled glove box, an autoclave was charged with complex **9** (5.0 mg, 0.5 mol%) and anhydrous toluene (4.0 mL), followed by ketone (2.0 mmol) and potassium bis(trimethylsilyl)amide (KHMDs, 8.0 mg, 2.0 mol%), in this order. The autoclave is then charged  $\text{H}_2$  (50 bar). The mixture was stirred for 20 hours at 50 °C in an oil bath. The solution was then diluted with ethyl acetate (2.0 mL) and filtered through a small pad of silica (2 cm in a Pasteur pipette). The silica was washed with ethyl acetate. The filtrate was evaporated and the crude residue was purified by column chromatography ( $\text{SiO}_2$ , mixture of petroleum ether/ethyl acetate as eluent).

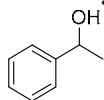
### **6.2.4. Mercury test**

In an argon filled glove box, an autoclave was charged with complex **9** (0.5 mol%, 5.0 mg), KHMDs (2.0 mol%, 8.0 mg) and anhydrous toluene (4.0 mL), followed by Hg (1.5 mmol, 602 mg) and acetophenone (234  $\mu\text{L}$ , 2.0 mmol) in this order. The autoclave is then charged  $\text{H}_2$  (50 bar). The mixture was stirred for 18 hours at 80 °C in an oil bath. The solution was then diluted with ethyl acetate (2.0 mL) and filtered through a small pad of silica (2 cm in a Pasteur pipette). The silica was washed with ethyl acetate (2.0 mL  $\times$  2). The filtrate was evaporated to provide the crude NMR in  $\text{CDCl}_3$  (93 % conversion).



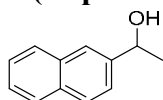
## 6.2.5. Characterization of the products of the catalysis

### 1-Phenylethanol **13a**<sup>[5]</sup>



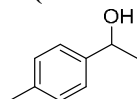
According to general procedure, acetophenone **12a** (234  $\mu$ L, 2.0 mmol) gave the title compound **13a** as a colorless oil (220 mg, 90%). <sup>1</sup>H NMR (400.1 MHz, CDCl<sub>3</sub>):  $\delta$  7.38 – 7.25 (m, 5H), 4.88 (q,  $J_{\text{HH}}$  = 6.5 Hz, 1H), 1.95 (s, br, 1H), 1.49 (d,  $J_{\text{HH}}$  = 6.5 Hz, 3H). <sup>13</sup>C{<sup>1</sup>H} NMR (100.6 MHz, CDCl<sub>3</sub>):  $\delta$  145.9, 128.6, 127.6, 125.5, 70.5, 25.3.

### 1-(Naphthalen-2-yl)ethanol **13b**<sup>[5]</sup>



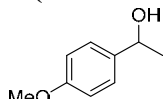
According to general procedure, 1-(naphthalen-2-yl)ethan-1-one **12b** (340 mg, 2.0 mmol) gave the title compound **13b** as a white solid (330.5 mg, 95%). <sup>1</sup>H NMR (400.1 MHz, CDCl<sub>3</sub>):  $\delta$  7.85 – 7.81 (m, 4H), 7.52 – 7.45 (m, 3H), 5.07 (q,  $J_{\text{HH}}$  = 6.5 Hz, 1H), 1.91 (br. s, 1H), 1.59 (d,  $J_{\text{HH}}$  = 6.5 Hz, 3H). <sup>13</sup>C{<sup>1</sup>H} NMR (100.6 MHz, CDCl<sub>3</sub>):  $\delta$  143.3, 133.5, 133.1, 128.4, 128.1, 127.8, 126.3, 125.9, 123.95, 123.93, 70.7, 25.3.

### 1-(4-Methylphenyl)ethanol **13c**<sup>[5]</sup>



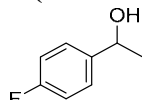
According to general procedure, 4'-methylacetophenone **12c** (267  $\mu$ L, 2.0 mmol) gave the title compound **13c** as a colorless oil (234 mg, 86%). <sup>1</sup>H NMR (400.1 MHz, CDCl<sub>3</sub>):  $\delta$  7.27 (d,  $J_{\text{HH}}$  = 8.0 Hz, 2H), 7.16 (d,  $J_{\text{HH}}$  = 8.0 Hz, 2H), 4.87 (q,  $J_{\text{HH}}$  = 6.5 Hz, 1H), 2.35 (s, 3H), 1.49 (br. s, 1H), 1.47 (d,  $J_{\text{HH}}$  = 6.5 Hz, 3H). <sup>13</sup>C{<sup>1</sup>H} NMR (100.6 MHz, CDCl<sub>3</sub>):  $\delta$  143.0, 137.3, 129.3, 125.5, 70.4, 25.2, 21.2.

### 1-(4-Methoxyphenyl)ethanol **13d**<sup>[5]</sup>



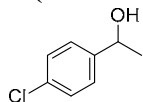
According to general procedure, 4'-methoxyacetophenone **12d** (300 mg, 2.0 mmol) gave the title compound **13d** as a colorless oil (277 mg, 91%). <sup>1</sup>H NMR (400.1 MHz, CDCl<sub>3</sub>):  $\delta$  7.30 (d,  $J_{\text{HH}}$  = 8.7 Hz, 2H), 6.88 (d,  $J_{\text{HH}}$  = 8.7 Hz, 2H), 4.85 (q,  $J_{\text{HH}}$  = 6.5 Hz, 1H), 3.80 (s, 3H), 1.79 (br. s, 3H), 1.48 (d,  $J_{\text{HH}}$  = 6.5 Hz, 3H). <sup>13</sup>C{<sup>1</sup>H} NMR (100.6 MHz, CDCl<sub>3</sub>):  $\delta$  159.1, 138.1, 126.8, 114.0, 70.1, 55.4, 25.1.

### 1-(4-Fluorophenyl)ethanol **13e**<sup>[5]</sup>



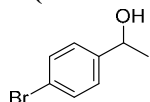
According to general procedure, 4'-fluoroacetophenone **12e** (244  $\mu$ L, 2.0 mmol) gave the title compound **13e** as a pale yellow oil (269 mg, 96%). <sup>1</sup>H NMR (400.1 MHz, CDCl<sub>3</sub>):  $\delta$  7.35 – 7.32 (m, 2H), 7.05 – 7.00 (m, 2H), 4.88 (q,  $J_{\text{HH}}$  = 6.5 Hz, 1H), 1.84 (br. s, 1H), 1.48 (d,  $J_{\text{HH}}$  = 6.5 Hz, 3H). <sup>13</sup>C{<sup>1</sup>H} NMR (100.6 MHz, CDCl<sub>3</sub>):  $\delta$  162.2 (d,  $J_{\text{CF}}$  = 245 Hz), 141.6 (d,  $J_{\text{CF}}$  = 3 Hz), 127.2 (d,  $J_{\text{CF}}$  = 8 Hz), 115.4 (d,  $J_{\text{CF}}$  = 21 Hz), 69.9, 25.4. <sup>19</sup>F{<sup>1</sup>H} NMR (376.5 MHz, CDCl<sub>3</sub>):  $\delta$  -115.37.

### 1-(4-Chlorophenyl)ethanol **13f**<sup>[5]</sup>



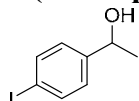
According to general procedure, 4'-chloroacetophenone **12f** (259.5  $\mu$ L, 2.0 mmol) gave the title compound **13f** as a pale yellow oil (188 mg, 60%). <sup>1</sup>H NMR (400.1 MHz, CDCl<sub>3</sub>):  $\delta$  7.37 – 7.24 (m, 4H), 4.88 (q,  $J_{\text{HH}}$  = 6.5 Hz, 1H), 1.90 (br. s, 1H), 1.47 (d,  $J_{\text{HH}}$  = 6.5 Hz, 3H). <sup>13</sup>C{<sup>1</sup>H} NMR (100.6 MHz, CDCl<sub>3</sub>):  $\delta$  144.4, 133.2, 128.7, 126.9, 69.9, 25.4.

### 1-(4-Bromophenyl)ethanol **13g**



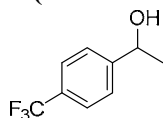
According to general procedure, 4'-bromoacetophenone **12g** (398 mg, 2.0 mmol) gave the title compound **13g** as a pale yellow oil (370 mg, 92%). <sup>1</sup>H NMR (400.1 MHz, CDCl<sub>3</sub>):  $\delta$  7.49 (d,  $J$  = 8.4 Hz, 2H), 7.27 (d,  $J_{\text{HH}}$  = 8.4 Hz, 2H), 4.89 (q,  $J_{\text{HH}}$  = 6.5 Hz, 1H), 1.89 (br. s, 1H), 1.49 (d,  $J_{\text{HH}}$  = 6.5 Hz, 3H). <sup>13</sup>C{<sup>1</sup>H} NMR (100.6 MHz, CDCl<sub>3</sub>):  $\delta$  144.7, 131.4, 127.1, 121.0, 69.5, 25.1.

### 1-(4-Iodophenyl)ethanol **13h**<sup>[5]</sup>



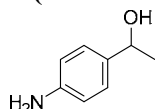
According to general procedure, 4'-iodoacetophenone **12h** (246 mg, 1.0 mmol) gave the title compound **13h** as a brown oil (122 mg, 49%). <sup>1</sup>H NMR (400.1 MHz, CDCl<sub>3</sub>):  $\delta$  7.66 (d,  $J_{\text{HH}}$  = 8.3 Hz, 1H), 7.10 (d,  $J_{\text{HH}}$  = 8.2 Hz, 1H), 4.82 (q,  $J_{\text{HH}}$  = 6.2 Hz, 1H), 2.12 (br. s, 1H), 1.45 (d,  $J_{\text{HH}}$  = 6.2 Hz, 3H). <sup>13</sup>C{<sup>1</sup>H} NMR (100.6 MHz, CDCl<sub>3</sub>):  $\delta$  145.6, 137.6, 127.5, 92.8, 69.9, 25.3.

### 1-(4-Trifluoromethylphenyl)ethanol **13i**<sup>[5]</sup>



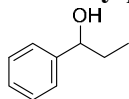
According to general procedure, 4'-trifluoromethylacetophenone **12i** (376 mg, 2.0 mmol) gave the title compound **13i** as a colorless oil (304 mg, 80%). <sup>1</sup>H NMR (400.1 MHz, CDCl<sub>3</sub>):  $\delta$  7.61 (d,  $J_{\text{HH}}$  = 8.1 Hz, 2H), 7.49 (d,  $J_{\text{HH}}$  = 8.1 Hz, 2H), 4.97 (q,  $J_{\text{HH}}$  = 6.5 Hz, 1H), 1.90 (s, br, 1H), 1.51 (d,  $J_{\text{HH}}$  = 6.5 Hz, 3H). <sup>13</sup>C{<sup>1</sup>H} NMR (100.6 MHz, CDCl<sub>3</sub>):  $\delta$  149.8, 129.8 (q,  $J_{\text{CF}}$  = 33 Hz), 125.8, 125.6 (q,  $J_{\text{CF}}$  = 4 Hz), 124.3 (q,  $J_{\text{CF}}$  = 270 Hz), 70.0, 25.5. <sup>19</sup>F {<sup>1</sup>H} NMR (376.5 MHz, CDCl<sub>3</sub>):  $\delta$  -62.5.

### 1-(4-Aminophenyl)ethanol **13l**<sup>[5]</sup>



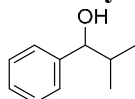
According to general procedure, 4'-aminoacetophenone **12l** (135 mg, 1.0 mmol) gave the title compound **13l** as a yellowish brown solid (128 mg, 93%). <sup>1</sup>H NMR (400.1 MHz, CDCl<sub>3</sub>):  $\delta$  7.14 (d,  $J_{\text{HH}}$  = 8.4 Hz, 2H), 6.63 (d,  $J_{\text{HH}}$  = 8.4 Hz, 2H), 4.75 (q,  $J_{\text{HH}}$  = 6.5 Hz, 1H), 3.65 (s, 2H), 2.27 (s, 1H), 1.44 (d,  $J_{\text{HH}}$  = 6.5 Hz, 3H). <sup>13</sup>C{<sup>1</sup>H} NMR (100.6 MHz, CDCl<sub>3</sub>):  $\delta$  145.7, 136.1, 126.7, 115.2, 70.0, 24.9.

### 1-Phenylpropanol **13m**<sup>[5]</sup>



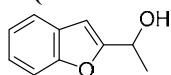
According to general procedure, propiophenone **12m** (266  $\mu$ L, 2.0 mmol) gave the title compound **13m** as a colorless oil (251 mg, 92%). <sup>1</sup>H NMR (400.1 MHz, CDCl<sub>3</sub>):  $\delta$  7.40 – 7.28 (m, 5H), 4.62 (t,  $J_{\text{HH}}$  = 6.8 Hz, 1H), 1.89 – 1.74 (m, 3H, CH<sub>2</sub>+OH), 0.95 (t,  $J_{\text{HH}}$  = 7.5 Hz, 3H). <sup>13</sup>C{<sup>1</sup>H} NMR (100.6 MHz, CDCl<sub>3</sub>):  $\delta$  144.7, 128.5, 127.6, 126.1, 76.2, 32.0, 10.3.

### 2-Methyl-1-phenylpropanol **13n**<sup>[5]</sup>



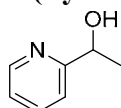
According to general procedure, 2-methyl-1-phenylpropanone **12n** (300  $\mu$ L, 2.0 mmol) gave the title compound **13n** as a colorless oil (90 mg, 30%). <sup>1</sup>H NMR (400.1 MHz, CDCl<sub>3</sub>):  $\delta$  7.39 – 7.27 (m, 5H), 4.38 (d,  $J_{\text{HH}}$  = 6.9 Hz, 1H), 2.05 – 1.93 (m, 2H, CH+OH), 1.03 (d,  $J_{\text{HH}}$  = 6.7 Hz, 3H), 0.83 (d,  $J_{\text{HH}}$  = 6.7 Hz, 3H). <sup>13</sup>C{<sup>1</sup>H} NMR (100.6 MHz, CDCl<sub>3</sub>):  $\delta$  143.8, 128.3, 127.5, 126.7, 80.2, 35.4, 19.1, 18.4.

### 1-(Benzofuran-2-yl)ethan-1-ol **13p**<sup>[5]</sup>



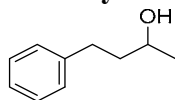
According to general procedure, 1-(benzofuran-2-yl)ethan-1-one **12p** (321 mg, 2.0 mmol) gave the title compound **13p** as a brown oil (299 mg, 92%). <sup>1</sup>H NMR (400.1 MHz, CDCl<sub>3</sub>):  $\delta$  7.57 (d,  $J_{\text{HH}}$  = 7.7 Hz, 1H), 7.48 (d,  $J_{\text{HH}}$  = 7.8 Hz, 1H), 7.31 – 7.22 (m, 2H), 6.63 (s, 1H), 5.05 (q,  $J_{\text{HH}}$  = 6.5 Hz, 1H), 2.19 (br. s, 1H), 1.67 (d,  $J_{\text{HH}}$  = 6.5 Hz, 3H). <sup>13</sup>C{<sup>1</sup>H} NMR (100.6 MHz, CDCl<sub>3</sub>):  $\delta$  160.3, 154.9, 128.3, 124.3, 122.9, 121.2, 111.3, 101.9, 64.3, 21.6.

### 1-(Pyridin-2-yl)ethan-1-ol **13q**<sup>[5]</sup>



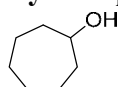
According to general procedure, 1-(pyridin-2-yl)ethan-1-one **12q** (28  $\mu$ L, 0.25 mmol) gave the title compound **13q** as a dark-red oil (28 mg, 89%). <sup>1</sup>H NMR (400.1 MHz, CDCl<sub>3</sub>):  $\delta$  8.54 (br. s, 1H), 7.70 (t,  $J_{\text{HH}}$  = 7.6 Hz, 1H), 7.29 (d,  $J_{\text{HH}}$  = 8.3 Hz, 1H), 7.22 – 7.19 (m, 1H), 4.91 – 4.89 (br. m, 1H), 1.51 (d,  $J_{\text{HH}}$  = 6.6 Hz, 3H). <sup>13</sup>C{<sup>1</sup>H} NMR (100.6 MHz, CDCl<sub>3</sub>):  $\delta$  163.1, 148.3, 137.0, 122.4, 120.0, 68.9, 24.4.

### 4-Phenylbutan-2-ol **13s**<sup>[6]</sup>



According to general procedure, 4-phenyl-2-butanone **12s** (293  $\mu$ L, 2.0 mmol) gave the title compound **13s** as a pale yellow oil (277 mg, 92%). <sup>1</sup>H NMR (400.1 MHz, CDCl<sub>3</sub>):  $\delta$  7.33 – 7.28 (m, 2H), 7.24 – 7.19 (m, 3H), 3.89 – 3.83 (m, 1H), 2.83 – 2.66 (m, 2H), 1.84 – 1.77 (m, 2H), 1.34 (br. s, 1H), 1.26 (d,  $J_{\text{HH}}$  = 6.1 Hz, 3H). <sup>13</sup>C{<sup>1</sup>H} NMR (100.6 MHz, CDCl<sub>3</sub>):  $\delta$  142.2, 128.5, 125.9, 67.7, 41.0, 32.3, 23.8.

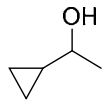
### Cycloheptanol **13t**<sup>[5]</sup>



According to general procedure, cycloheptanone **12t** (256  $\mu$ L, 2.0 mmol) gave the title compound **13t** as a pale yellow oil (190 mg, 83%). <sup>1</sup>H NMR (400.1 MHz, CDCl<sub>3</sub>):  $\delta$  3.86 –

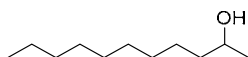
3.80 (m, 1H), 1.94 – 1.87 (m, 2H), 1.67 – 1.50 (m, 8H), 1.43 – 1.33 (m, 3H).  $^{13}\text{C}\{^1\text{H}\}$  NMR (100.6 MHz,  $\text{CDCl}_3$ )  $\delta$  72.9, 37.7, 28.2, 22.8.

#### Cyclopropylethan-1-ol **13u**<sup>[5]</sup>



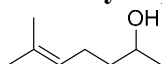
According to general procedure, cyclopropylethan-1-one **12u** (186  $\mu\text{L}$ , 2.0 mmol) gave the title compound **13u** as a pale yellow oil (98% NMR yield).  $^1\text{H}$  NMR (400.1 MHz,  $\text{CDCl}_3$ ):  $\delta$  3.10 – 3.02 (m, 1H), 1.73 (s, 1H), 1.27 (d,  $J_{\text{HH}} = 6.2$  Hz, 3H), 0.94 – 0.85 (m, 1H), 0.52 – 0.44 (m, 2H), 0.31 – 0.12 (m, 2H).  $^{13}\text{C}\{^1\text{H}\}$  NMR (100.6 MHz,  $\text{CDCl}_3$ ):  $\delta$  73.1, 22.6, 19.4, 3.1, 2.4.

#### Undecan-2-ol **13v**<sup>[5]</sup>



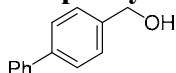
According to general procedure, 2-undecanone **12v** (413  $\mu\text{L}$ , 2.0 mmol) gave the title compound **13v** as a pale yellow oil (248 mg, 72%).  $^1\text{H}$  NMR (400.1 MHz,  $\text{CDCl}_3$ ):  $\delta$  3.83 – 3.75 (m, 1H), 1.48 – 1.23 (m, 17H), 1.11 (d,  $J_{\text{HH}} = 6.1$  Hz, 3H), 0.88 (t,  $J_{\text{HH}} = 6.8$  Hz, 3H).  $^{13}\text{C}\{^1\text{H}\}$  NMR (100.6 MHz,  $\text{CDCl}_3$ ):  $\delta$  68.4, 39.5, 32.0, 29.79, 29.78, 29.71, 29.5, 25.9, 23.6, 22.8, 14.3.

#### 6-Methylhept-5-en-2-ol **13w**<sup>[5]</sup>



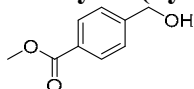
According to general procedure, 6-methylhept-5-en-2-one **12w** (148  $\mu\text{L}$ , 1.0 mmol) gave the title compound **13w** as a pale yellow oil (117 mg, 91%).  $^1\text{H}$  NMR (400.1 MHz,  $\text{CDCl}_3$ ):  $\delta$  5.12 (t,  $J_{\text{HH}} = 7.2$  Hz, 1H), 3.83 – 3.76 (m, 1H), 2.12 – 1.99 (m, 2H), 1.68 (s, 3H), 1.61 (s, 3H), 1.51 – 1.44 (m, 3H), 1.18 (d,  $J_{\text{HH}} = 6.2$  Hz, 3H).  $^{13}\text{C}\{^1\text{H}\}$  NMR (100.6 MHz,  $\text{CDCl}_3$ ):  $\delta$  132.2, 124.2, 68.1, 39.3, 25.8, 24.6, 23.6, 17.8.

#### 4-Biphenylmethanol **13x**<sup>[5]</sup>



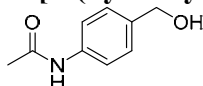
According to general procedure, 4-biphenylmethanal **12x** (182 mg, 1.0 mmol) gave the title compound **13x** as a white solid (168 mg, 91%).  $^1\text{H}$  NMR (400.1 MHz,  $\text{CDCl}_3$ ):  $\delta$  7.63 – 7.59 (m, 4H), 7.48 – 7.43 (m, 4H), 7.40 – 7.36 (m, 1H), 4.73 (s, 2H), 2.08 (br. s, 1H).  $^{13}\text{C}\{^1\text{H}\}$  NMR (100.6 MHz,  $\text{CDCl}_3$ ):  $\delta$  140.9, 140.7, 140.0, 128.9, 127.56, 127.42, 127.39, 127.2, 65.1.

#### Methyl-4-(hydroxymethyl)benzoate **13y**<sup>[7]</sup>



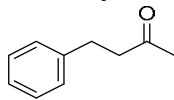
According to general procedure, methyl-4-formylbenzoate **12y** (164 mg, 1.0 mmol) gave the title compound **13y** as a white solid (131 mg, 79%).  $^1\text{H}$  NMR (400.1 MHz,  $\text{CDCl}_3$ ):  $\delta$  7.97 (d,  $J_{\text{HH}} = 8.2$  Hz, 2H), 7.38 (d,  $J_{\text{HH}} = 8.2$  Hz, 2H), 4.71 (s, 2H), 3.88 (s, 3H), 2.56 (br. s, 1H).  $^{13}\text{C}\{^1\text{H}\}$  NMR (100.6 MHz,  $\text{CDCl}_3$ ):  $\delta$  167.2, 146.3, 129.8, 129.2, 126.5, 64.5, 52.2.

#### N-[4-(hydroxymethyl)phenyl]-acetamide **13z**<sup>[5, 8]</sup>



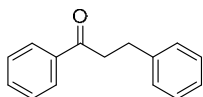
According to general procedure, 4-acetamido-benzaldehyde **12z** (163 mg, 1.0 mmol) gave the title compound **13z** as a pale yellow solid (152 mg, 92%).  $^1\text{H}$  NMR (400.1 MHz,  $\text{CD}_3\text{OD}$ ):  $\delta$  7.51 (d,  $J_{\text{HH}} = 8.5$  Hz, 2H), 7.28 (d,  $J_{\text{HH}} = 8.5$  Hz, 2H), 4.86 (br. s, 2H), 4.55 (s, 2H), 2.10 (s, 3H).  $^{13}\text{C}\{^1\text{H}\}$  NMR (100.6 MHz,  $\text{CD}_3\text{OD}$ ):  $\delta$  171.7, 138.9, 138.4, 128.5, 121.1, 64.8, 23.8.

#### 4-Phenyl-2-butanone **12s**<sup>[9]</sup>



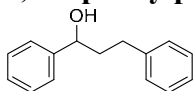
According to general procedure, 4-phenyl-3-buten-2-one **12aa** (293  $\mu$ L, 2.0 mmol) gave the title compound **12s** as a colorless oil (279 mg, 94%). <sup>1</sup>H NMR (400.1 MHz, CDCl<sub>3</sub>):  $\delta$  7.33 – 7.28 (m, 2H), 7.24 – 7.20 (m, 3H), 2.93 (t,  $J_{\text{HH}}$  = 7.6 Hz, 2H), 2.79 (t,  $J_{\text{HH}}$  = 7.5 Hz, 2H), 2.17 (s, 3H). <sup>13</sup>C{<sup>1</sup>H} NMR (100.6 MHz, CDCl<sub>3</sub>):  $\delta$  207.9, 141.1, 128.6, 128.4, 126.2, 45.2, 30.1, 29.8.

#### 1,3-Diphenylpropan-1-one **12ac**



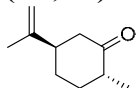
According to general procedure, (*E*)-chalcone **12ab** (104 mg, 0.5 mmol) gave the title compound **12ac** as a white solid (97 mg, 92%). <sup>1</sup>H NMR (400.1 MHz, CDCl<sub>3</sub>):  $\delta$  8.01 (d,  $J_{\text{HH}}$  = 7.4 Hz, 2H), 7.60 (t,  $J_{\text{HH}}$  = 7.4 Hz, 1H), 7.50 (t,  $J_{\text{HH}}$  = 7.6 Hz, 2H), 7.41 – 7.20 (m, 5H), 3.35 (t,  $J_{\text{HH}}$  = 7.7 Hz, 2H), 3.13 (t,  $J_{\text{HH}}$  = 7.7 Hz, 2H). <sup>13</sup>C{<sup>1</sup>H} NMR (100.6 MHz, CDCl<sub>3</sub>):  $\delta$  199.2, 141.3, 136.9, 133.1, 128.6, 128.6, 128.5, 128.1, 126.2, 40.5, 30.2.

#### 1,3-diphenylpropan-1-ol **13ac**



According to general procedure, (*E*)-chalcone **12ab** (52 mg, 0.25 mmol) gave the title compound **13ac** as a pale yellow liquid (51 mg, 96%). <sup>1</sup>H NMR (400.1 MHz, CDCl<sub>3</sub>):  $\delta$  7.36 (d,  $J_{\text{HH}}$  = 4.4 Hz, 4H), 7.32 – 7.24 (m, 3H), 7.20 (d,  $J_{\text{HH}}$  = 7.4 Hz, 3H), 4.70 (m, 1H), 2.84 – 2.62 (m, 2H), 2.22 – 1.98 (m, 2H), 1.85 (s, 1H). <sup>13</sup>C{<sup>1</sup>H} NMR (100.6 MHz, CDCl<sub>3</sub>):  $\delta$  144.7, 141.9, 128.7, 128.6, 128.5, 127.8, 126.1, 126.0, 74.0, 40.6, 32.2.

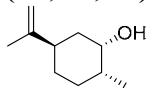
#### (1*R*,4*R*)-Dihydrocarvone **12ae**<sup>[10]</sup>



According to general procedure, (*R*)-(-)-Carvone **12ad** (157  $\mu$ L, 1 mmol) gave the title compound **12ae** as a colorless oil (63 mg, 41%).

<sup>1</sup>H NMR (400.1 MHz, CDCl<sub>3</sub>):  $\delta$  4.74 (d,  $J_{\text{HH}}$  = 10.6 Hz, 2H), 2.55 – 2.20 (m, 4H), 2.13 (ddt,  $J_{\text{HH}}$  = 12.9, 6.3, 3.3 Hz, 1H), 2.01 – 1.88 (m, 1H), 1.74 (s, 3H), 1.70 – 1.55 (m, 1H), 1.49 – 1.31 (m, 1H), 1.03 (d,  $J_{\text{HH}}$  = 6.5 Hz, 3H). <sup>13</sup>C{<sup>1</sup>H} NMR (100.6 MHz, CDCl<sub>3</sub>):  $\delta$  212.8, 147.8, 109.7, 47.2, 47.0, 44.9, 35.1, 30.9, 20.6, 14.5.

#### (1*S*,2*R*,5*R*)-Dihydrocarveol **13ad**<sup>[11]</sup>



According to general procedure, (*R*)-(-)-Carvone **12ad** (39.2  $\mu$ L, 0.25 mmol) gave the title compound **13ad** as a colorless oil (33 mg, 87%). <sup>1</sup>H NMR (400.1 MHz, CDCl<sub>3</sub>):  $\delta$  4.69 (s, 2H), 3.89 (q,  $J$  = 2.8 Hz, 1H), 2.37 – 2.17 (m, 1H), 1.98 – 1.86 (m, 1H), 1.82 – 1.67 (m, 4H), 1.66 – 1.27 (m, 5H), 1.27 – 1.10 (m, 1H), 0.97 (d,  $J$  = 6.7 Hz, 3H). <sup>13</sup>C{<sup>1</sup>H} NMR (100.6 MHz, CDCl<sub>3</sub>):  $\delta$  150.4, 108.5, 71.1, 38.8, 37.9, 36.2, 31.5, 28.3, 21.1, 18.4.

## 6.2.6. X-ray data

CCDC-1565260-1565263 contains the supplementary crystallographic data for complexes **1**, **2**, **3** and **4**. These data can be obtained free of charge from The Cambridge Crystallographic Data Centre via [www.ccdc.cam.ac.uk/data\\_request/cif](http://www.ccdc.cam.ac.uk/data_request/cif).

### X-ray data for the complex **8**

X-ray diffraction data were collected on a D8 VENTURE Bruker AXS diffractometer equipped with a PHOTON 100 CMOS detector, using multilayers monochromated Mo-K $\alpha$  radiation ( $\lambda = 0.71073$  Å) at  $T = 150(2)$  K. The structure was solved by dual-space algorithm using the *SHELXT* program,<sup>[12]</sup> and then refined with full-matrix least-square methods based on  $F^2$  (*SHELXL-2014*).<sup>[13]</sup> All non-hydrogen atoms were refined with anisotropic atomic displacement parameters. H atoms were finally included in their calculated positions. A final refinement on  $F^2$  with 4024 unique intensities and 203 parameters converged at  $\omega R(F^2) = 0.0805$  ( $R(F) = 0.0408$ ) for 3315 observed reflections with  $I > 2\sigma(I)$ .

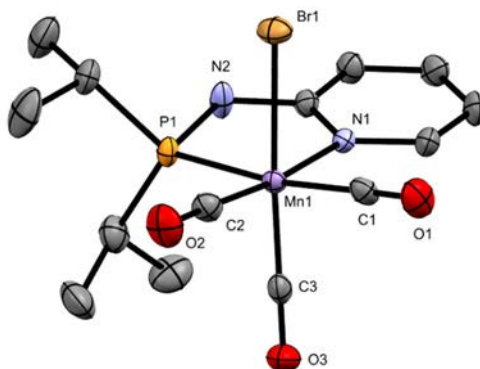


**Figure S1:** Perspective view of the molecular structure of the complex **8** with thermal ellipsoids drawn at 50% probability. Hydrogens atoms were omitted for clarity.

**Table S1.** Crystal data and structure refinement for the complex **8**.

Empirical formula	C <sub>14</sub> H <sub>19</sub> Br Mn N <sub>2</sub> O <sub>3</sub> P
Formula weight	429.13
Temperature	150(2) K
Wavelength	0.71073 Å
Crystal system, space group	orthorhombic, <i>P b c n</i>
Unit cell dimensions	$a = 29.2332(11)$ Å, $\alpha = 90^\circ$ $b = 9.9889(4)$ Å, $\beta = 90^\circ$ $c = 12.0827(4)$ Å, $\gamma = 90^\circ$
Volume	$3528.2(2)$ Å <sup>3</sup>
<i>Z</i> , Calculated density	8, 1.616 (g.cm <sup>-3</sup> )
Absorption coefficient	$3.115$ mm <sup>-1</sup>
<i>F</i> (000)	1728
Crystal size	$0.600 \times 0.100 \times 0.060$ mm
Crystal color	yellow
Theta range for data collection	$2.920$ to $27.473^\circ$
<i>h</i> <sub>min</sub> , <i>h</i> <sub>max</sub>	$-37, 37$
<i>k</i> <sub>min</sub> , <i>k</i> <sub>max</sub>	$-12, 12$
<i>l</i> <sub>min</sub> , <i>l</i> <sub>max</sub>	$-15, 13$
Reflections collected / unique	20407 / 4024 [ $R(\text{int})^a = 0.0477$ ]
Reflections [ $I > 2\sigma$ ]	3315
Completeness to theta <sub>max</sub>	0.997
Absorption correction type	multi-scan

Max. and min. transmission	0.830 , 0.608
Refinement method	Full-matrix least-squares on $F^2$
Data / restraints / parameters	4024 / 0 / 203
<sup>b</sup> Goodness-of-fit	1.099
Final $R$ indices [ $I > 2\sigma$ ]	$R1^c = 0.0408$ , $wR2^d = 0.0805$
$R$ indices (all data)	$R1^c = 0.0539$ , $wR2^d = 0.0847$
Largest diff. peak and hole	0.605 and $-0.881 \text{ e}^- \cdot \text{\AA}^{-3}$
$^a R_{int} = \sum  F_o^2 - \langle F_o^2 \rangle  / \sum [F_o^2]$	
$^b S = \{ \sum [w(F_o^2 - F_c^2)^2] / (n - p) \}^{1/2}$	
$^c R1 = \sum    F_o  -  F_c    / \sum  F_o $	
$^d wR2 = \{ \sum [w(F_o^2 - F_c^2)^2] / \sum [w(F_o^2)^2] \}^{1/2}$	
$w = 1 / [\sigma(F_o^2) + aP^2 + bP] \text{ where } P = [2F_c^2 + \text{MAX}(F_o^2, 0)] / 3$	

### X-ray data for the complex 9

X-ray diffraction data were collected on a APEXII Bruker AXS diffractometer equipped with a CCD detector, using graphite-monochromated Mo-K $\alpha$  radiation ( $\lambda = 0.71073 \text{ \AA}$ ) at  $T = 150 (2) \text{ K}$ . The structure was solved by dual-space algorithm using the *SHELXT* program,<sup>[12]</sup> and then refined with full-matrix least-square methods based on  $F^2$  (*SHELXL-2014*).<sup>[13]</sup> All non-hydrogen atoms were refined with anisotropic atomic displacement parameters. H atoms were finally included in their calculated positions. A final refinement on  $F^2$  with 4664 unique intensities and 253 parameters converged at  $\omega R(F^2) = 0.0966$  ( $R(F) = 0.0729$ ) for 2438 observed reflections with  $I > 2\sigma(I)$ .

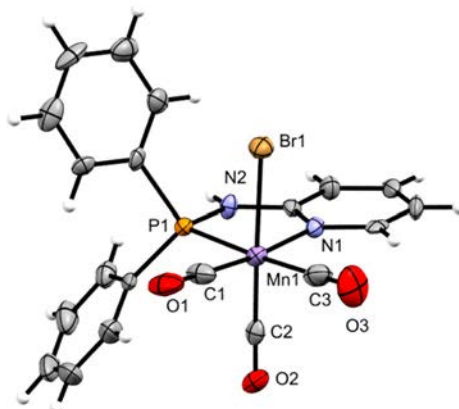


**Figure S2:** Perspective view of the molecular structure of the complex **9** with thermal ellipsoids drawn at 50% probability.

**Table S2.** Crystal data and structure refinement for the complex **9**.

Empirical formula	$\text{C}_{20} \text{H}_{15} \text{Br Mn N}_2 \text{O}_3 \text{P}$
Formula weight	497.16
Temperature	$150(2) \text{ K}$
Wavelength	$0.71073 \text{ \AA}$
Crystal system, space group	monoclinic, $P 2_1/c$
Unit cell dimensions	$a = 10.298(2) \text{ \AA}$ , $\alpha = 90^\circ$ $b = 12.401(2) \text{ \AA}$ , $\beta = 105.890(7)^\circ$ $c = 16.675(4) \text{ \AA}$ , $\gamma = 90^\circ$
Volume	$2048.0(8) \text{ \AA}^3$
$Z$ , Calculated density	4, $1.612 \text{ (g.cm}^{-3}\text{)}$
Absorption coefficient	$2.696 \text{ mm}^{-1}$

$F(000)$	992
Crystal size	0.250 x 0.200 x 0.110 mm
Crystal color	colourless
Theta range for data collection	3.025 to 27.482 °
$h_{\min}$ , $h_{\max}$	-13, 13
$k_{\min}$ , $k_{\max}$	-15, 15
$l_{\min}$ , $l_{\max}$	-21, 21
Reflections collected / unique	13584 / 4664 [ $R(\text{int})^a = 0.1067$ ]
Reflections [ $I > 2\sigma$ ]	2438
Completeness to $\theta_{\max}$	0.994
Absorption correction type	multi-scan
Max. and min. transmission	0.743 , 0.633
Refinement method	Full-matrix least-squares on $F^2$
Data / restraints / parameters	4664 / 0 / 253
$^b$ Goodness-of-fit	0.989
Final $R$ indices [ $I > 2\sigma$ ]	$R1^c = 0.0729$ , $wR2^d = 0.0966$
$R$ indices (all data)	$R1^c = 0.1610$ , $wR2^d = 0.1225$
Largest diff. peak and hole	0.750 and -0.616 $\text{e}^- \cdot \text{\AA}^{-3}$

$$^a R_{\text{int}} = \sum |F_o^2 - \langle F_o^2 \rangle| / \sum [F_o^2]$$

$$^b S = \{ \sum [w(F_o^2 - F_c^2)^2] / (n - p) \}^{1/2}$$

$$^c R1 = \sum | |F_o| - |F_c| | / \sum |F_o|$$

$$^d wR2 = \{ \sum [w(F_o^2 - F_c^2)^2] / \sum [w(F_o^2)^2] \}^{1/2}$$

$$w = 1 / [\sigma(F_o^2) + aP^2 + bP] \text{ where } P = [2F_c^2 + \text{MAX}(F_o^2, 0)] / 3$$

### X-ray data for the complex 10

X-ray diffraction data were collected on a D8 VENTURE Bruker AXS diffractometer equipped with a PHOTON 100 CMOS detector, using multilayers monochromated Mo-K $\alpha$  radiation ( $\lambda = 0.71073 \text{ \AA}$ ) at  $T = 150(2) \text{ K}$ . The structure was solved by dual-space algorithm using the *SHELXT* program,<sup>[12]</sup> and then refined with full-matrix least-square methods based on  $F^2$  (*SHELXL-2014*).<sup>[13]</sup> All non-hydrogen atoms were refined with anisotropic atomic displacement parameters. H atoms were finally included in their calculated positions. A final refinement on  $F^2$  with 4688 unique intensities and 253 parameters converged at  $\omega R(F^2) = 0.0508$  ( $R(F) = 0.0214$ ) for 4340 observed reflections with  $I > 2\sigma(I)$ .

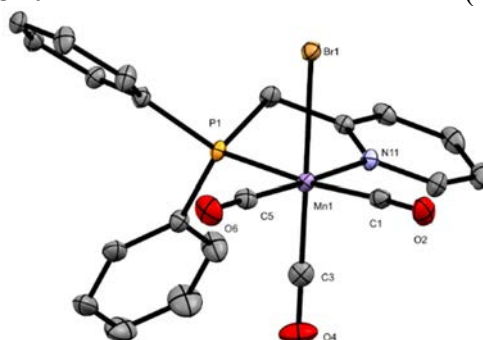


**Figure S3:** Perspective view of the molecular structure of complex **10** with thermal ellipsoids drawn at 50% probability. Hydrogens atoms were omitted for clarity.

**Table S3.** Crystal data and structure refinement for complex **10**.

Empirical formula	$\text{C}_{21} \text{H}_{16} \text{Br Mn N O}_3 \text{P}$
Formula weight	496.17
Temperature	150 K



Wavelength	0.71073 Å
Crystal system, space group	monoclinic, $P 2_1/c$
Unit cell dimensions	$a = 9.2456(5)$ Å, $\alpha = 90^\circ$ $b = 8.5879(3)$ Å, $\beta = 90.599(3)^\circ$ $c = 25.8035(10)$ Å, $\gamma = 90^\circ$
Volume	$2048.69(15)$ Å <sup>3</sup>
$Z$ , Calculated density	4, 1.609 (g.cm <sup>-3</sup> )
Absorption coefficient	2.694 mm <sup>-1</sup>
$F(000)$	992
Crystal size	0.280 x 0.180 x 0.150 mm
Crystal color	yellow
Theta range for data collection	3.158 to 27.482 °
$h_{\min}$ , $h_{\max}$	-12, 12
$k_{\min}$ , $k_{\max}$	-11, 11
$l_{\min}$ , $l_{\max}$	-33, 33
Reflections collected / unique	22344 / 4688 [ $R(\text{int})^a = 0.0259$ ]
Reflections [ $I > 2\sigma$ ]	4340
Completeness to $\theta_{\max}$	0.999
Absorption correction type	multi-scan
Max. and min. transmission	0.668 , 0.584
Refinement method	Full-matrix least-squares on $F^2$
Data / restraints / parameters	4688 / 0 / 253
$\chi^2$ (Goodness-of-fit)	1.071
Final $R$ indices [ $I > 2\sigma$ ]	$R1^c = 0.0214$ , $wR2^d = 0.0508$
$R$ indices (all data)	$R1^c = 0.0244$ , $wR2^d = 0.0520$
Largest diff. peak and hole	0.314 and -0.516 e <sup>-</sup> .Å <sup>-3</sup>

$$^a R_{\text{int}} = \sum |F_o^2 - \langle F_o^2 \rangle| / \sum [F_o^2]$$

$$^b S = \{ \sum [w(F_o^2 - F_c^2)^2] / (n - p) \}^{1/2}$$

$$^c R1 = \sum | |F_o| - |F_c| | / \sum |F_o|$$

$$^d wR2 = \{ \sum [w(F_o^2 - F_c^2)^2] / \sum [w(F_o^2)^2] \}^{1/2}$$

$$w = 1 / [\sigma(F_o^2) + aP^2 + bP] \text{ where } P = [2F_c^2 + \text{MAX}(F_o^2, 0)] / 3$$

## X-ray data for the complex 11

X-ray diffraction data were collected on a APEXII Bruker AXS diffractometer equipped with a CCD detector, using graphite-monochromated Mo-K $\alpha$  radiation ( $\lambda = 0.71073$  Å) at  $T = 295$  K. The structure was solved by dual-space algorithm using the *SHELXT* program,<sup>[12]</sup> and then refined with full-matrix least-square methods based on  $F^2$  (*SHELXL-2014*).<sup>[13]</sup> The contribution of the disordered solvents to the structure factors was calculated by the *PLATON SQUEEZE* procedure<sup>[14]</sup> and then taken into account in the final *SHELXL-2014* least-square refinement. All non-hydrogen atoms were refined with anisotropic atomic displacement parameters. H atoms were finally included in their calculated positions. A final refinement on  $F^2$  with 6433 unique intensities and 217 parameters converged at  $\omega R(F^2) = 0.1417$  ( $R(F) = 0.0601$ ) for 4884 observed reflections with  $I > 2\sigma(I)$ .

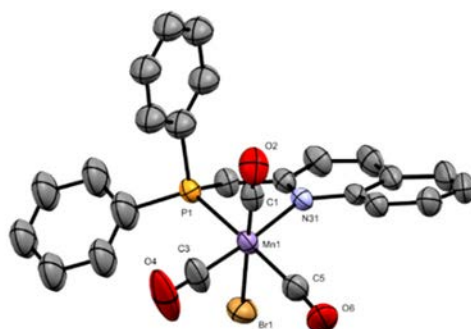


**Figure S4:** Perspective view of the molecular structure of complex **11** with thermal ellipsoids drawn at 50% probability. Hydrogens atoms were omitted for clarity.

**Table S4.** Crystal data and structure refinement for complex **11**.

Empirical formula	C <sub>25</sub> H <sub>18</sub> Br Mn N O <sub>3</sub> P
Formula weight	546.22
Temperature	295 K
Wavelength	0.71073 Å
Crystal system, space group	triclinic, <i>P</i> -1
Unit cell dimensions	<i>a</i> = 10.966(4) Å, $\alpha$ = 72.966(11) ° <i>b</i> = 11.067(4) Å, $\beta$ = 81.251(11) ° <i>c</i> = 13.178(4) Å, $\gamma$ = 67.615(11) °
Volume	1412.4(8) Å <sup>3</sup>
<i>Z</i> , Calculated density	2, 1.284 (g.cm <sup>-3</sup> )
Absorption coefficient	1.961 mm <sup>-1</sup>
<i>F</i> (000)	548
Crystal size	0.580 x 0.360 x 0.140 mm
Crystal color	yellow
Theta range for data collection	2.929 to 27.484 °
<i>h</i> <sub>min</sub> , <i>h</i> <sub>max</sub>	-14, 14
<i>k</i> <sub>min</sub> , <i>k</i> <sub>max</sub>	-13, 14
<i>l</i> <sub>min</sub> , <i>l</i> <sub>max</sub>	-17, 16
Reflections collected / unique	35439 / 6433 [R(int) <sup>a</sup> = 0.0281]
Reflections [I>2σ]	4884
Completeness to theta <sub>max</sub>	0.993
Absorption correction type	multi-scan
Max. and min. transmission	0.760 , 0.573
Refinement method	Full-matrix least-squares on <i>F</i> <sup>2</sup>
Data / restraints / parameters	6433 / 0 / 217
<sup>b</sup> <i>S</i> (Goodness-of-fit)	1.022
Final <i>R</i> indices [I>2σ]	<i>R</i> <sub>1</sub> <sup>c</sup> = 0.0601, <i>wR</i> <sub>2</sub> <sup>d</sup> = 0.1417
<i>R</i> indices (all data)	<i>R</i> <sub>1</sub> <sup>c</sup> = 0.0840, <i>wR</i> <sub>2</sub> <sup>d</sup> = 0.1617
Largest diff. peak and hole	2.149 and -1.171 e <sup>-</sup> .Å <sup>-3</sup>

$$^a R_{int} = \sum |F_o^2 - \langle F_o^2 \rangle| / \sum [F_o^2]$$

$$^b S = \{ \sum [w(F_o^2 - F_c^2)^2] / (n - p) \}^{1/2}$$

$$^c R_1 = \sum | |F_o| - |F_c| | / \sum |F_o|$$

$$^d wR_2 = \{ \sum [w(F_o^2 - F_c^2)^2] / \sum [w(F_o^2)^2] \}^{1/2}$$

$$w = 1 / [\sigma(F_o^2) + aP^2 + bP] \text{ where } P = [2F_c^2 + \text{MAX}(F_o^2, 0)] / 3$$

### 6.3. Part IV-2- Reductive amination of aldehydes with H<sub>2</sub>

#### 6.3.1. General procedure for reductive amination reaction.

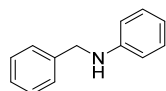
In an argon filled glove box, a 20 mL Schlenk tube was charged with aldehyde **18** (0.5 mmol), amine **19** (0.6 mmol) and anhydrous ethanol (2.0 mL). The reaction mixture was stirred at 100 °C (or at room temperature for aldehyde containing  $\alpha$ -protons) for 24 h. After cooling to room temperature, the mixture was transferred to a 20 mL autoclave followed by manganese complex **9** (5.0 mg, 2.0 mol%) and *t*BuOK (2.8 mg, 5.0 mol%). The autoclave was charged with H<sub>2</sub> (50 bar) and the mixture was stirred at indicated temperature in an oil bath (see Table 8, § 2.2.1). After cooling to room temperature, the solution was diluted with ethyl acetate (2 mL) and filtered through a small pad of celite (2 cm in a Pasteur pipette). The celite was washed with ethyl acetate (2×2 mL). The filtrate was evaporated and the crude residue was purified by column chromatography (SiO<sub>2</sub>, mixture of petroleum ether/ethyl acetate as eluent).

#### III-2. Specific procedure for reductive amination reaction on large scale (Table 8, entry 4).

A 50 mL Maximator autoclave (“Réacteur à ouverture rapide”) was purged with N<sub>2</sub> and then charged with a solution of benzaldehyde (475  $\mu$ L, 4.3 mmol) and *p*-toluidine (500 mg, 4.6 mmol, 1.08 equiv.) in EtOH (10 mL). After stirring for 2 h at r.t., a solution of complex **9** (43 mg, 2.0 mol%) in EtOH (4 mL) and a solution of *t*BuOK (28 mg, 5.0 mol%) in EtOH (4 mL) were added under N<sub>2</sub> flow. The autoclave was charged with H<sub>2</sub> (50 bar) and the mixture was stirred at 100 °C for 24 h. The solution was concentrated under reduced pressure, and the crude residue was purified by column chromatography (SiO<sub>2</sub>, mixture of petroleum ether/ethyl acetate as eluent). *N*-benzyl-4-methylaniline **16d** was obtained as pale yellow oil (663 mg, 78%).

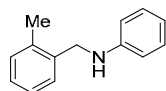
#### III-3. Characterization of the products of the catalysis

##### *N*-Benzylaniline **16a**<sup>[15]</sup>



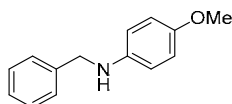
Following the general procedure, benzaldehyde (51.0  $\mu$ L, 0.5 mmol) and aniline (54.8  $\mu$ L, 0.6 mmol) gave the title compound **16a** as a brown liquid (85.2 mg, 93% yield). <sup>1</sup>H NMR (400.1 MHz, CDCl<sub>3</sub>)  $\delta$  7.43 – 7.36 (m, 4H), 7.34 – 7.28 (m, 1H), 7.23 – 7.19 (m, 2H), 6.76 (td, *J* = 7.3, 1.1 Hz, 1H), 6.68 (d, *J* = 7.7 Hz, 2H), 4.36 (s, 2H), 4.08 (br, 1H). <sup>13</sup>C{<sup>1</sup>H} NMR (100.6 MHz, CDCl<sub>3</sub>)  $\delta$  148.2, 139.5, 129.4, 128.7, 127.6, 127.3, 117.7, 113.0, 48.5.

##### *N*-(2-Methylbenzyl)aniline **16b**<sup>[16]</sup>



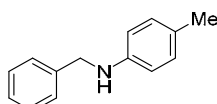
Following the general procedure, 2-methylbenzaldehyde (57.8  $\mu$ L, 0.5 mmol) and aniline (54.8  $\mu$ L, 0.6 mmol) gave the title compound **16b** as a dark brown liquid (52.7 mg, 94% yield). <sup>1</sup>H NMR (400.1 MHz, CDCl<sub>3</sub>)  $\delta$  7.35 (d, *J* = 6.7 Hz, 1H), 7.26 – 7.17 (m, 5H), 6.74 (tt, *J* = 7.3, 1.1 Hz, 1H), 6.67 – 6.64 (m, 2H), 4.29 (s, 2H), 3.84 (s, 1H), 2.39 (s, 3H). <sup>13</sup>C{<sup>1</sup>H} NMR (100.6 MHz, CDCl<sub>3</sub>)  $\delta$  148.4, 137.1, 136.5, 130.5, 129.4, 128.4, 127.6, 126.3, 117.6, 112.8, 46.5, 19.1.

### ***N*-Benzyl-4-methoxyaniline 16c<sup>[15]</sup>**



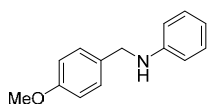
Following the general procedure, benzaldehyde (51.0  $\mu$ L, 0.5 mmol) and 4-methoxyaniline (73.9 mg, 0.6 mmol) gave the title compound **16c** as a brown solid (76.8 mg, 72% yield). **<sup>1</sup>H NMR** (400.1 MHz, CDCl<sub>3</sub>)  $\delta$  7.40 – 7.33 (m, 4H), 7.29 (d,  $J$  = 7.1 Hz, 1H), 6.81 – 6.77 (m, 2H), 6.64 – 6.60 (m, 2H), 4.30 (s, 2H), 3.75 (s, 3H). **<sup>13</sup>C{<sup>1</sup>H} NMR** (100.6 MHz, CDCl<sub>3</sub>)  $\delta$  152.4, 142.5, 139.8, 128.7, 127.7, 127.3, 115.0, 114.3, 55.9, 49.4.

### ***N*-Benzyl-4-methylaniline 16d<sup>[15]</sup>**



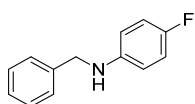
Following the specific procedure, benzaldehyde (475.0  $\mu$ L, 4.3 mmol) and 4-methylaniline (500.0 mg, 4.6 mmol) gave the title compound **16d** as a pale yellow oil (663 mg, 78% yield). **<sup>1</sup>H NMR** (400.1 MHz, CDCl<sub>3</sub>)  $\delta$  7.50 – 7.21 (m, 5H), 7.14 – 6.96 (m, 2H), 6.68 – 6.57 (m, 2H), 4.36 (s, 2H), 3.94 (s, 1H), 2.31 (s, 3H). **<sup>13</sup>C{<sup>1</sup>H} NMR** (100.6 MHz, CDCl<sub>3</sub>)  $\delta$  146.0, 139.8, 129.9, 128.7, 127.6, 127.2, 126.8, 113.1, 48.7, 20.5.

### ***N*-(4-Methoxybenzyl)aniline 16e<sup>[15]</sup>**



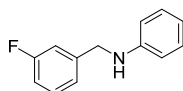
Following the general procedure, 4-methoxybenzaldehyde (60.8  $\mu$ L, 0.5 mmol) and aniline (54.8  $\mu$ L, 0.6 mmol) gave the title compound **16e** as a yellow liquid (92.8 mg, 87% yield). **<sup>1</sup>H NMR** (400.1 MHz, CDCl<sub>3</sub>)  $\delta$  7.30 (d,  $J$  = 8.6, 2H), 7.21 – 7.16 (m, 2H), 6.89 (d,  $J$  = 8.6 Hz, 2H), 6.73 (t,  $J$  = 7.3 Hz, 1H), 6.66 (dd,  $J$  = 7.7, 1.1 Hz, 2H), 4.27 (s, 2H), 3.81 (s, 3H). **<sup>13</sup>C{<sup>1</sup>H} NMR** (100.6 MHz, CDCl<sub>3</sub>)  $\delta$  = 159.0, 148.2, 131.4, 129.4, 129.0, 117.8, 114.2, 113.1, 55.4, 48.0.

### ***N*-Benzyl-4-fluoroaniline 16f<sup>[15]</sup>**



Following the general procedure, benzaldehyde (51.0  $\mu$ L, 0.5 mmol) and 4-fluoroaniline (57.6  $\mu$ L, 0.6 mmol) gave the title compound **16f** as a brown solid (28.2 mg, 28% yield). **<sup>1</sup>H NMR** (400.1 MHz, CDCl<sub>3</sub>)  $\delta$  7.39 – 7.26 (m, 5H), 6.89 (t,  $J$  = 8.7, 2H), 6.60 – 6.55 (m, 2H), 4.30 (s, 2H), 3.94 (br, 1H). **<sup>13</sup>C{<sup>1</sup>H} NMR** (100.6 MHz, CDCl<sub>3</sub>)  $\delta$  156.0 (d,  $^1J_{CF}$  = 235.0), 144.6 (d,  $J_{CF}$  = 1.5 Hz), 139.4, 128.8, 127.6, 127.4, 115.8 (d,  $J_{CF}$  = 22.3 Hz), 113.8 (d,  $J_{CF}$  = 7.4 Hz), 49.1. **<sup>19</sup>F NMR** (376.5 MHz, CDCl<sub>3</sub>)  $\delta$  -127.91.

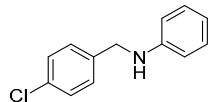
### ***N*-(3-Fluorobenzyl)aniline 16g<sup>[17]</sup>**



Following the general procedure, 3-fluorobenzaldehyde (53.0  $\mu$ L, 0.5 mmol) and aniline (54.8  $\mu$ L, 0.6 mmol) gave the title compound **16g** as a pale yellow solid (90.6 mg, 90% yield). **<sup>1</sup>H NMR** (400.1 MHz, CDCl<sub>3</sub>)  $\delta$  7.30 (td,  $J$  = 7.9, 7.3 Hz, 1H), 7.20–7.14 (m, 3H), 7.09 (dt,  $J$  = 9.8, 2.0 Hz, 1H), 6.96 (td,  $J$  = 8.4, 2.6 Hz, 1H), 6.74 (t,  $J$  = 7.3 Hz, 1H), 6.62 (d,  $J$  = 7.9 Hz,

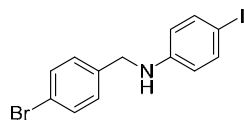
2H), 4.35 (s, 2H), 4.09 (br, 1H).  $^{13}\text{C}\{^1\text{H}\}$  NMR (75 MHz,  $\text{CDCl}_3$ )  $\delta$  163.2 (d,  $^1J_{\text{CF}} = 246.2$  Hz), 147.9, 142.4 (d,  $J_{\text{CF}} = 6.8$  Hz), 130.2 (d,  $J_{\text{CF}} = 8.2$  Hz), 129.4, 122.9 (d,  $J_{\text{CF}} = 2.8$  Hz), 117.9, 114.4 (d,  $J_{\text{CF}} = 8.3$  Hz), 114.1 (d,  $J_{\text{CF}} = 7.9$  Hz), 113.0, 47.9.  $^{19}\text{F}$  NMR (376 MHz,  $\text{CDCl}_3$ )  $\delta$  -113.00. GC-MS,  $m/z$  (%) = 201 ( $[\text{M}]^+$ , 100), 109 (100), 77 (57), 65 (18), 51 (20).

#### *N*-(4-Chlorobenzyl)aniline **16h**<sup>[18]</sup>



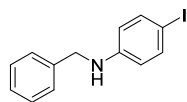
Following the general procedure, 4-chlorobenzaldehyde (70.3 mg, 0.5 mmol) and aniline (54.8  $\mu\text{L}$ , 0.6 mmol) gave the title compound **16h** as a pale yellow liquid (87.1 mg, 80% yield).  $^1\text{H}$  NMR (400.1 MHz,  $\text{CDCl}_3$ )  $\delta$  7.31 (s, 4H), 7.18 (t,  $J = 7.9$  Hz, 2H), 6.74 (t,  $J = 7.3$  Hz, 1H), 6.62 (d,  $J = 7.8$  Hz, 2H), 4.32 (s, 2H), 4.06 (br, 1H).  $^{13}\text{C}\{^1\text{H}\}$  NMR (100.6 MHz,  $\text{CDCl}_3$ )  $\delta$  147.9, 138.1, 133.0, 129.4, 128.9, 128.8, 117.9, 113.0, 47.8.

#### *N*-(4-Bromobenzyl)-4-iodoaniline **16i**



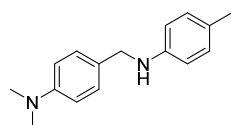
Following the general procedure, 4-bromobenzaldehyde (92.5 mg, 0.5 mmol) and 4-iodoaniline (131.4 mg, 0.6 mmol) gave the title compound **16i** as a white solid (190.1 mg, 98% yield). The isolated product contains about 13% of 4-bromobenzylaniline resulting from deiodination.  $^1\text{H}$  NMR (400.1 MHz,  $\text{CDCl}_3$ )  $\delta$  7.46 (d,  $J = 7.9$ , 2H), 7.41 (d,  $J = 8.1$ , 2H), 7.21 (d,  $J = 8.1$ , 2H), 6.38 (d,  $J = 8.2$ , 2H), 4.26 (s, 2H), 4.12 (br, 1H).  $^{13}\text{C}\{^1\text{H}\}$  NMR (100.6 MHz,  $\text{CDCl}_3$ )  $\delta$  147.4, 138.03, 137.99, 131.9, 129.1, 121.3, 115.2, 78.6, 47.6. GC-MS,  $m/z$  (%) = 389 ( $[\text{M}]^+$ , 67), 308 (8), 169 (100), 90 (53), 76 (18), 63 (11), 50 (10).

#### *N*-Benzyl-4-iodoaniline **16j**<sup>[19]</sup>



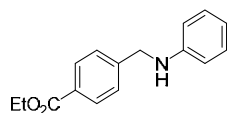
Following the general procedure, benzaldehyde (51.0  $\mu\text{L}$ , 0.5 mmol) and 4-iodoaniline (131.4 mg, 0.6 mmol) gave the title compound **16j** as a brown liquid (149.9 mg, 97% yield). The isolated product contains about 10% of benzylaniline resulting from deiodination.  $^1\text{H}$  NMR (400.1 MHz,  $\text{CDCl}_3$ )  $\delta$  7.41 (d,  $J = 8.6$  Hz, 2H), 7.37 – 7.34 (m, 5H), 6.42 (d,  $J = 8.6$  Hz, 2H), 4.30 (d,  $J = 3.9$  Hz, 2H), 4.10 (br, 1H).  $^{13}\text{C}\{^1\text{H}\}$  NMR (100.6 MHz,  $\text{CDCl}_3$ )  $\delta$  147.8, 139.0, 137.9, 128.8, 127.6, 127.5, 115.2, 78.3, 48.2.

#### *N,N*-Dimethyl-4-((*p*-tolylamino)methyl)aniline **16k**<sup>[20]</sup>



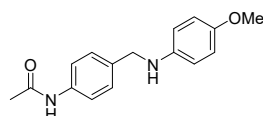
Following the general procedure, 4-(dimethylamino)benzaldehyde (74.6 mg, 0.5 mmol) and *p*-toluidine (64.3 mg, 0.6 mmol) gave the title compound **16k** as a colorless solid (117.8 mg, 97% yield).  $^1\text{H}$  NMR (400.1 MHz,  $\text{CDCl}_3$ )  $\delta$  7.25 (d,  $J = 8.8$  Hz, 2H), 6.99 (d,  $J = 7.9$  Hz, 2H), 6.73 (d,  $J = 8.2$  Hz, 2H), 6.58 (d,  $J = 8.0$  Hz, 2H), 4.19 (s, 2H), 3.76 (br, 1H), 2.94 (s, 6H), 2.25 (s, 3H).  $^{13}\text{C}\{^1\text{H}\}$  NMR (100.6 MHz,  $\text{CDCl}_3$ )  $\delta$  150.1, 146.4, 129.8, 128.8, 127.5, 126.6, 113.1, 112.9, 48.4, 40.9, 20.5.

### Ethyl 4-((phenylamino)methyl)benzoate **16l**



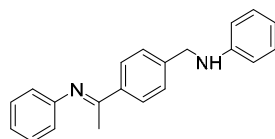
Following the general procedure, methyl 4-formylbenzoate (82.1 mg, 0.5 mmol) and aniline (54.8  $\mu$ L, 0.6 mmol) gave the title compound **16l** as a pale yellow liquid (117.4 mg, 92% yield).  $^1\text{H NMR}$  (400.1 MHz,  $\text{CDCl}_3$ )  $\delta$  8.02 (d,  $J$  = 8.2 Hz, 1H), 7.44 (d,  $J$  = 8.1 Hz, 2H), 7.17 (t,  $J$  = 7.9 Hz, 2H), 6.73 (t,  $J$  = 7.3 Hz, 1H), 6.61 (d,  $J$  = 8.1 Hz, 2H), 4.41 – 4.34 (m, 5H,  $N\text{-CH}_2\text{+CH}_2\text{+NH}$ ), 1.39 (t,  $J$  = 7.1 Hz, 3H).  $^{13}\text{C}\{^1\text{H}\}$  NMR (100.6 MHz,  $\text{CDCl}_3$ )  $\delta$  166.6, 147.9, 145.0, 130.0, 129.4, 127.2, 118.0, 113.0, 61.1, 48.1, 14.5. GC-MS,  $m/z(\%)$  = 255 ( $[\text{M}]^+$ , 100), 226(24), 210(28), 182(49), 163(100), 135(60), 106(51), 89(34), 77(40), 65(10), 51(8).

### *N*-(4-(((4-Methoxyphenyl)amino)methyl)phenyl)acetamide **16m**<sup>[15]</sup>



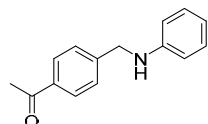
Following the general procedure, *N*-(4-formylphenyl)acetamide (81.6 mg, 0.5 mmol) and 4-methoxyaniline (73.9, 0.6 mmol) gave the title compound **16m** as a pale yellow solid (128.4 mg, 95% yield).  $^1\text{H NMR}$  (400.1 MHz,  $\text{CDCl}_3$ )  $\delta$  7.45 (d,  $J$  = 8.3 Hz, 2H), 7.31 (d,  $J$  = 8.2 Hz, 2H), 6.77 (d,  $J$  = 8.9 Hz, 2H), 6.59 (d,  $J$  = 8.9 Hz, 2H), 4.24 (s, 2H), 3.74 (s, 3H), 2.16 (s, 3H), 1.67 (br, 1H).  $^{13}\text{C}\{^1\text{H}\}$  NMR (100.6 MHz,  $\text{CDCl}_3$ )  $\delta$  168.4, 152.3, 142.5, 137.0, 135.8, 128.3, 120.3, 115.0, 114.3, 56.0, 48.9, 24.7.

### *N*-(4-(1-(Phenylimino)ethyl)benzyl)aniline **16n**



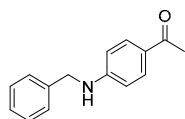
Following the general procedure, 4-acetylbenzaldehyde (74.1 mg, 0.5 mmol) and aniline (100.4  $\mu$ L, 1.1 mmol) gave the title compound **16n** as a dark brown liquid (132.2 mg, 88% yield, 95% purity).  $^1\text{H NMR}$  (400.1 MHz,  $\text{CDCl}_3$ )  $\delta$  7.96 (d,  $J$  = 8.3 Hz, 2H), 7.45 (d,  $J$  = 8.1 Hz, 2H), 7.36 (t,  $J$  = 7.8 Hz, 2H), 7.18 (t,  $J$  = 7.3 Hz, 2H), 7.09 (t,  $J$  = 7.3 Hz, 1H), 6.80 (d,  $J$  = 7.3 Hz, 2H), 6.74 (t,  $J$  = 7.3 Hz, 1H), 6.64 (d,  $J$  = 7.8 Hz, 2H), 4.41 (s, 2H), 4.12 (br, 1H), 2.23 (s, 3H).  $^{13}\text{C}\{^1\text{H}\}$  NMR (100.6 MHz,  $\text{CDCl}_3$ )  $\delta$  165.3, 151.8, 148.1, 142.3, 138.7, 129.4, 129.1, 127.7, 127.4, 123.3, 119.5, 117.9, 113.1, 48.1, 17.5. GC-MS,  $m/z(\%)$  = 300 ( $[\text{M}]^+$ , 100), 285(23), 208(68), 193(33), 143(17), 116(15), 105(88), 90(30), 77(55), 51(14).

### 1-(4-((Phenylamino)methyl)phenyl)ethan-1-one **16o**<sup>[21]</sup>



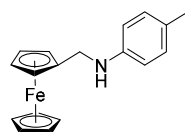
Following the general procedure, 4-acetylbenzaldehyde (74.1 mg, 0.5 mmol) and aniline (54.8  $\mu$ L, 0.6 mmol) gave the title compound **16o** as a pale yellow solid (82.2 mg, 73% yield).  $^1\text{H NMR}$  (400.1 MHz,  $\text{CDCl}_3$ )  $\delta$  7.93 (d,  $J$  = 8.2 Hz, 2H), 7.47 (d,  $J$  = 8.2 Hz, 2H), 7.17 (dd,  $J$  = 8.6, 7.2 Hz, 2H), 6.73 (t,  $J$  = 7.3 Hz, 1H), 6.61 (d,  $J$  = 7.7 Hz, 2H), 4.42 (s, 2H), 4.19 (s, br, 1H), 2.59 (s, 3H).  $^{13}\text{C}\{^1\text{H}\}$  NMR (100.6 MHz,  $\text{CDCl}_3$ )  $\delta$  197.9, 147.8, 145.3, 136.3, 129.4, 128.9, 127.4, 118.0, 113.1, 48.1, 26.7.

### 1-(4-(Benzylamino)phenyl)ethan-1-one **16p**<sup>[22]</sup>



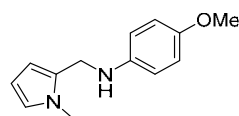
Following the general procedure, benzaldehyde (51.0  $\mu$ L, 0.5 mmol) and 4-aminoacetophenone (67.6 mg, 0.5 mmol) gave the title compound **16p** as a pale yellow solid (108.1 mg, 96% yield). <sup>1</sup>H NMR (400.1 MHz, CDCl<sub>3</sub>)  $\delta$  7.82 (d,  $J$  = 8.6 Hz, 2H), 7.38 – 7.30 (m, 5H), 6.60 (d,  $J$  = 8.6 Hz, 2H), 4.58 (br, 1H), 4.41 (d,  $J$  = 5.5 Hz, 2H), 2.49 (s, 3H). <sup>13</sup>C{<sup>1</sup>H} NMR (100.6 MHz, CDCl<sub>3</sub>)  $\delta$  196.5, 152.1, 138.4, 130.9, 128.9, 127.6, 127.4, 127.0, 111.7, 47.6, 26.1.

### *N*-(Ferrocenylmethyl)-4-methylaniline **16q**<sup>[20]</sup>



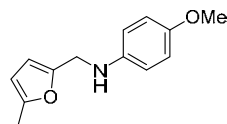
Following the general procedure, ferrocenecarboxaldehyde (107.0 mg, 0.5 mmol) and *p*-toluidine (64.3 mg, 0.6 mmol) gave the title compound **16q** as a dark brown liquid (149.5 mg, 98% yield). <sup>1</sup>H NMR (400.1 MHz, CDCl<sub>3</sub>)  $\delta$  7.02 (d,  $J$  = 8.1 Hz, 2H), 6.60 (d,  $J$  = 8.3 Hz, 2H), 4.24 (t,  $J$  = 1.9 Hz, 2H), 4.18 (s, 5H), 4.14 (t,  $J$  = 1.8 Hz, 2H), 3.94 (s, 2H), 3.75 (br, 1H), 2.26 (s, 3H). <sup>13</sup>C{<sup>1</sup>H} NMR (100.6 MHz, CDCl<sub>3</sub>)  $\delta$  146.3, 129.9, 126.9, 113.2, 86.9, 68.6, 68.2, 68.0, 43.9, 20.6.

### 4-Methoxy-*N*-((1-methyl-1*H*-pyrrol-2-yl)methyl)aniline **16r**<sup>[20]</sup>



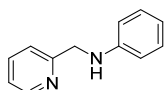
Following the general procedure, 1-methyl-1*H*-pyrrole-2-carbaldehyde (53.7  $\mu$ L, 0.5 mmol) and 4-methoxyaniline (73.9 mg, 0.6 mmol) gave the title compound **16r** as a dark brown liquid (104.9 mg, 97% yield). <sup>1</sup>H NMR (400.1 MHz, CDCl<sub>3</sub>)  $\delta$  6.84 – 6.79 (m, 2H), 6.67 – 6.66 (m, 2H), 6.63 – 6.62 (m, 1H), 6.12 – 6.11 (m, 1H), 6.08 (t,  $J$  = 3.1 Hz, 1H), 4.17 (s, 2H), 3.76 (s, 3H), 3.64 (s, 3H), 3.41 (br, 1H). <sup>13</sup>C{<sup>1</sup>H} NMR (100.6 MHz, CDCl<sub>3</sub>)  $\delta$  152.5, 142.6, 130.1, 122.9, 115.1, 114.4, 108.5, 106.9, 56.0, 41.5, 33.9.

### 4-Methoxy-*N*-((5-methylfuran-2-yl)methyl)aniline **16s**<sup>[20]</sup>



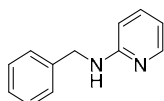
Following the general procedure, 5-methylfuran-2-carbaldehyde (50.1  $\mu$ L, 0.5 mmol) and 4-methoxyaniline (73.9 mg, 0.6 mmol) gave the title compound **16s** as a brown solid (97.8 mg, 90% yield). <sup>1</sup>H NMR (400.1 MHz, CDCl<sub>3</sub>)  $\delta$  6.79 (d,  $J$  = 8.9 Hz, 2H), 6.65 (d,  $J$  = 8.8 Hz, 2H), 6.09 (d,  $J$  = 3.0 Hz, 1H), 5.98 (d,  $J$  = 2.5 Hz, 1H), 4.21 (s, 2H), 3.75 (s, 4H, OCH<sub>3</sub>+NH), 2.28 (s, 3H). <sup>13</sup>C{<sup>1</sup>H} NMR (100.6 MHz, CDCl<sub>3</sub>)  $\delta$  152.7, 151.7, 151.2, 142.1, 115.0, 114.8, 107.9, 106.2, 55.9, 42.7, 13.7.

### *N*-(Pyridin-2-ylmethyl)aniline **16t**<sup>[16]</sup>



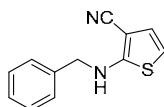
Following the general procedure, pyridine-2-carboxaldehyde (47.6  $\mu$ L, 0.5 mmol) and aniline (54.8  $\mu$ L, 0.6 mmol) gave the title compound **16t** as a brown liquid (62.6 mg, 68% yield, 90% purity by  $^1\text{H}$  NMR).  $^1\text{H}$  NMR (400.1 MHz,  $\text{CDCl}_3$ )  $\delta$  8.59 (d,  $J$  = 4.8 Hz, 1H), 7.63 (td,  $J$  = 7.7, 1.8 Hz, 1H), 7.34 (d,  $J$  = 7.8 Hz, 1H), 7.21 – 7.16 (m, 3H), 6.73 (tt,  $J$  = 7.4, 1.1 Hz, 1H), 6.69 – 6.66 (m, 2H), 4.84 (br, 1H), 4.47 (s, 2H).  $^{13}\text{C}\{^1\text{H}\}$  NMR (100.6 MHz,  $\text{CDCl}_3$ )  $\delta$  158.6, 149.2, 147.9, 136.7, 129.3, 122.2, 121.7, 117.6, 113.1, 49.3.

### *N*-Benzylpyridin-2-amine **16u**<sup>[18]</sup>



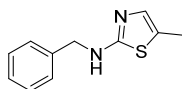
Following the general procedure, benzaldehyde (51.0  $\mu$ L, 0.5 mmol) and 2-aninopyridine (56.5 mg, 0.6 mmol) gave the title compound **16u** as a colorless solid (50.7 mg, 55% yield).  $^1\text{H}$  NMR (400.1 MHz,  $\text{CDCl}_3$ )  $\delta$  8.12 (ddd,  $J$  = 5.0, 2.0, 0.9 Hz, 1H), 7.44 – 7.34 (m, 5H), 7.32–7.28 (m, 1H), 6.61 (ddd,  $J$  = 7.1, 5.0, 0.9 Hz, 1H), 6.39 (dt,  $J$  = 8.3, 1.0 Hz, 1H), 5.05 (s, 1H), 4.53 (d,  $J$  = 5.8 Hz, 2H).  $^{13}\text{C}\{^1\text{H}\}$  NMR (100.6 MHz,  $\text{CDCl}_3$ )  $\delta$  158.8, 148.3, 139.3, 137.6, 128.7, 127.5, 127.3, 113.2, 106.9, 46.4.

### 2-(Benzylamino)thiophene-3-carbonitrile **16v**



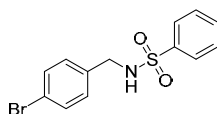
Following the general procedure, benzaldehyde (51.0  $\mu$ L, 0.5 mmol) and 2-aminothiophene-3-carbonitrile (74.5 mg, 0.6 mmol) gave the title compound **16v** as a dark green solid (96.4 mg, 90% yield).  $^1\text{H}$  NMR (400.1 MHz,  $\text{CDCl}_3$ )  $\delta$  7.41 – 7.30 (m, 5H), 6.78 (d,  $J$  = 5.7 Hz, 1H), 6.29 (d,  $J$  = 5.7 Hz, 1H), 5.57 (br, 1H), 4.41 (s, 2H).  $^{13}\text{C}\{^1\text{H}\}$  NMR (100.6 MHz,  $\text{CDCl}_3$ )  $\delta$  165.3, 136.6, 128.9, 128.2, 127.8, 126.1, 116.4, 108.7, 84.5, 51.8. GC-MS,  $m/z$ (%) = 214 ( $[\text{M}]^+$ , 19), 91(100), 65(15).

### *N*-Benzyl-5-methylthiazol-2-amine **16w**<sup>[23]</sup>



Following the general procedure, benzaldehyde (51.0  $\mu$ L, 0.5 mmol) and 5-methylthiazol-2-amine (68.5 mg, 0.6 mmol) gave the title compound **16w** as a colorless solid (94.0 mg, 92% yield, 95% purity).  $^1\text{H}$  NMR (400.1 MHz,  $\text{CDCl}_3$ )  $\delta$  7.38 – 7.26 (m, 5H), 6.65 (s, 1H), 6.28 (br, 1H), 4.42 (s, 2H), 2.26 (s, 3H).  $^{13}\text{C}\{^1\text{H}\}$  NMR (100.6 MHz,  $\text{CDCl}_3$ )  $\delta$  169.2, 138.0, 135.3, 128.7, 127.74, 127.66, 121.0, 49.9, 12.1.

### *N*-(4-Bromobenzyl)benzenesulfonamide **16x**

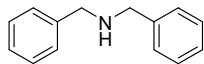


Following the general procedure, 4-bromobenzaldehyde (92.5 mg, 0.5 mmol) and benzenesulfonamide (94.3 mg, 0.6 mmol) gave the title compound **16x** as a white solid (151.7 mg, 93% yield, 90% purity).  $^1\text{H}$  NMR (400.1 MHz,  $\text{CDCl}_3$ )  $\delta$  7.81 (d,  $J$  = 7.6 Hz, 2H), 7.57 (t,



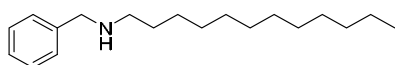
$J = 7.4$  Hz, 1H), 7.47 (t,  $J = 7.7$  Hz, 2H), 7.34 (d,  $J = 8.3$  Hz, 2H), 7.04 (d,  $J = 8.2$  Hz, 2H), 5.43 (t,  $J = 6.4$  Hz, 1H), 4.06 (d,  $J = 5.8$  Hz, 2H).  $^{13}\text{C}\{^1\text{H}\}$  NMR (100.6 MHz,  $\text{CDCl}_3$ )  $\delta$  139.9, 135.5, 132.9, 131.9, 129.6, 129.3, 127.2, 121.9, 46.7. GC-MS,  $m/z(\%) = 325$  ( $[\text{M}]^+$ , 0.5), 246(0.5), 184(100), 157(10), 143(20), 125(11), 104(10), 90(13), 77(91), 51(31).

### Dibenzylamine **16y**<sup>[15]</sup>



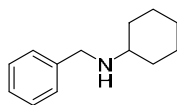
Following the general procedure, benzaldehyde (51.0  $\mu\text{L}$ , 0.5 mmol) and benzylamine (65.5  $\mu\text{L}$ , 0.6 mmol) gave the title compound **16y** as a pale yellow liquid (88.8 mg, 90% yield).  $^1\text{H}$  NMR (400.1 MHz,  $\text{CDCl}_3$ )  $\delta$  7.38 – 7.26 (m, 10H), 3.84 (s, 4H), 1.91 (br, 1H).  $^{13}\text{C}\{^1\text{H}\}$  NMR (100.6 MHz,  $\text{CDCl}_3$ )  $\delta$  140.4, 128.5, 128.3, 127.1, 53.3.

### *N*-Benzylododecan-1-amine **16z**<sup>[24]</sup>



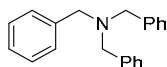
Following the general procedure, benzaldehyde (51.0  $\mu\text{L}$ , 0.5 mmol) and dodecylamine (111.2 mg, 0.6 mmol) gave the title compound **16z** as a pale yellow liquid (130.9 mg, 95% yield).  $^1\text{H}$  NMR (400.1 MHz,  $\text{CDCl}_3$ )  $\delta$  7.37 – 7.22 (m, 5H), 3.79 (s, 2H), 2.63 (t,  $J = 7.0$  Hz, 2H), 1.58 – 1.47 (m, 2H), 1.35 – 1.26 (m, 20H), 0.88 (t,  $J = 6.8$  Hz, 3H).  $^{13}\text{C}\{^1\text{H}\}$  NMR (100.6 MHz,  $\text{CDCl}_3$ )  $\delta$  140.7, 128.5, 128.3, 127.0, 54.2, 49.7, 32.1, 30.3, 29.81, 29.79, 29.76, 29.72, 29.5, 27.5, 22.8, 14.3.

### *N*-Benzylcyclohexanamine **16aa**<sup>[25]</sup>



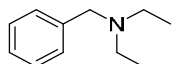
Following the general procedure, benzaldehyde (51.0  $\mu\text{L}$ , 0.5 mmol) and cyclohexylamine (68.8  $\mu\text{L}$ , 0.6 mmol) gave the title compound **16aa** as a pale yellow liquid (89.0 mg, 94% yield).  $^1\text{H}$  NMR (400.1 MHz,  $\text{CDCl}_3$ )  $\delta$  7.35 – 7.22 (m, 5H), 3.82 (s, 2H), 2.52 – 2.47 (m, 1H), 1.93 – 1.91 (m, 2H), 1.76 – 1.71 (m, 2H), 1.64 – 1.59 (m, 1H), 1.42 (br, 1H), 1.31 – 1.08 (m, 5H).  $^{13}\text{C}\{^1\text{H}\}$  NMR (100.6 MHz,  $\text{CDCl}_3$ )  $\delta$  141.1, 128.5, 128.2, 126.9, 56.3, 51.2, 33.7, 26.3, 25.2.

### Tribenzylamine **16ab**<sup>[26]</sup>



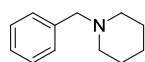
Following the general procedure, benzaldehyde (51.0  $\mu\text{L}$ , 0.5 mmol) and dibenzylamine (116.1  $\mu\text{L}$ , 0.6 mmol) gave the title compound **16ab** as a pale yellow solid (138.0 mg, 96% yield).  $^1\text{H}$  NMR (400.1 MHz,  $\text{CDCl}_3$ )  $\delta$  7.47 (d,  $J = 7.5$  Hz, 6H), 7.37 (t,  $J = 7.4$  Hz, 6H), 7.29 (d,  $J = 7.2$  Hz, 3H), 3.62 (s, 6H).  $^{13}\text{C}\{^1\text{H}\}$  NMR (100.6 MHz,  $\text{CDCl}_3$ )  $\delta$  139.8, 128.9, 128.3, 127.0, 58.1.

### *N*-Benzyl-*N*-ethylethanamine **16ac**<sup>[27]</sup>



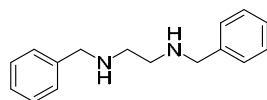
Following the general procedure, benzaldehyde (51.0  $\mu\text{L}$ , 0.5 mmol) and diethylamine (61.8  $\mu\text{L}$ , 0.6 mmol) gave the title compound **16ac** as a pale yellow liquid (76.7 mg, 94% yield).  $^1\text{H}$  NMR (400.1 MHz,  $\text{CDCl}_3$ )  $\delta$  7.38 – 7.21 (m, 5H), 3.57 (s, 2H), 2.52 (q,  $J = 7.1$  Hz, 4H), 1.04 (t,  $J = 7.1$  Hz, 6H).  $^{13}\text{C}\{^1\text{H}\}$  NMR (100.6 MHz,  $\text{CDCl}_3$ )  $\delta$  138.8, 129.3, 128.3, 127.1, 57.2, 46.5, 11.4.

### 1-Benzylpiperidine **16ad**<sup>[26]</sup>



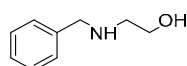
Following the general procedure, benzaldehyde (51.0  $\mu$ L, 0.5 mmol) and piperidine (59.3  $\mu$ L, 0.6 mmol) gave the title compound **16ad** as a pale yellow liquid (81.5 mg, 93% yield).  $^1\text{H}$  NMR (400.1 MHz,  $\text{CDCl}_3$ )  $\delta$  7.39 – 7.28 (m, 5H), 3.53 (s, 2H), 2.50 – 2.41 (m, 4H), 1.63 – 1.57 (m, 4H), 1.45 – 1.43 (m, 2H).  $^{13}\text{C}\{^1\text{H}\}$  NMR (100.6 MHz,  $\text{CDCl}_3$ )  $\delta$  138.0, 129.6, 128.3, 127.2, 63.7, 54.4, 25.9, 24.4.

### *N,N'*-Dibenzylethane-1,2-diamine **16ae**<sup>[28]</sup>



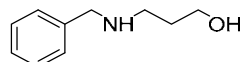
Following the general procedure, benzaldehyde (122.4  $\mu$ L, 1.2 mmol) and ethane-1,2-diamine (33.5  $\mu$ L, 0.5 mmol) gave the title compound **16ae** as a pale yellow solid (114.2 mg, 95% yield).  $^1\text{H}$  NMR (400.1 MHz,  $\text{CDCl}_3$ )  $\delta$  7.37–7.25 (m, 10H), 3.81 (s, 4H), 2.79 (s, 4H), 1.86 (s, 2H, NH).  $^{13}\text{C}\{^1\text{H}\}$  NMR (100.6 MHz,  $\text{CDCl}_3$ )  $\delta$  140.5, 128.5, 128.2, 127.0, 54.0, 48.8.

### 2-(Benzylamino)ethan-1-ol **16af**<sup>[29]</sup>



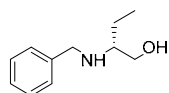
Following the general procedure, benzaldehyde (51.0  $\mu$ L, 0.5 mmol) and 2-aminoethan-1-ol (30.0  $\mu$ L, 0.5 mmol) gave the title compound **16af** as a pale yellow liquid (65.0 mg, 86% yield).  $^1\text{H}$  NMR (400.1 MHz,  $\text{CDCl}_3$ )  $\delta$  7.35 – 7.23 (m, 5H), 3.81 (s, 2H), 3.65 (t,  $J$  = 5.2 Hz, 2H), 2.80 (t,  $J$  = 5.2 Hz, 2H), 2.07 (br, 2H, NH + OH +  $\text{H}_2\text{O}$ ).  $^{13}\text{C}\{^1\text{H}\}$  NMR (100.6 MHz,  $\text{CDCl}_3$ )  $\delta$  140.1, 128.6, 128.3, 127.2, 61.1, 53.6, 50.7.

### 3-(Benzylamino)propan-1-ol **16ag**



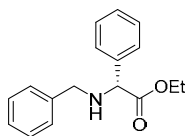
Following the general procedure, benzaldehyde (51.0  $\mu$ L, 0.5 mmol) and 3-aminopropan-1-ol (38.2  $\mu$ L, 0.5 mmol) gave the title compound **16ag** as a colorless liquid (68.6 mg, 83% yield).  $^1\text{H}$  NMR (400.1 MHz,  $\text{CDCl}_3$ )  $\delta$  = 7.35 – 7.23 (m, 5H), 3.81 (t,  $J$  = 5.2, 2H), 3.79 (s, 2H), 2.89 (t,  $J$  = 5.8 Hz, 2H), 2.81 (br, 2H), 1.72 (quint.,  $J$  = 5.5 Hz, 2H).  $^{13}\text{C}\{^1\text{H}\}$  NMR (100.6 MHz,  $\text{CDCl}_3$ )  $\delta$  = 139.7, 128.6, 128.3, 127.3, 64.4, 54.1, 49.5, 30.9. GC-MS,  $m/z$ (%) = 165([M]<sup>+</sup>, 2), 120(50), 106(19), 91(100), 77(3), 65(9).

### (*R*)-2-(Benzylamino)butan-1-ol **16ah**<sup>[30]</sup>



Following the general procedure, benzaldehyde (51.0  $\mu$ L, 0.5 mmol) and (*R*)-2-amino-1-butanol (CAS: 5856-63-3, 47.5  $\mu$ L, 0.5 mmol) gave the title compound **16ah** as a white solid (86.9 mg, 97% yield).  $^1\text{H}$  NMR (400.1 MHz,  $\text{CDCl}_3$ )  $\delta$  7.37 – 7.24 (m, 5H), 3.91 – 3.79 (m, 2H), 3.67 – 3.65 (m, 1H), 3.34 (br, 1H), 2.64 (br, 1H), 1.56 – 1.42 (m, 2H), 0.93 (t,  $J$  = 6.8, 3H).  $^{13}\text{C}\{^1\text{H}\}$  NMR (100.6 MHz,  $\text{CDCl}_3$ )  $\delta$  140.5, 128.6, 128.2, 127.2, 62.7, 59.8, 51.2, 24.5, 10.5.  $[\alpha]_{\text{D}}^{20}$  = -30.61 ( $C$  = 0.5,  $\text{CH}_2\text{Cl}_2$ ).

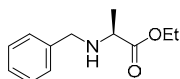
### Ethyl (*R*)-2-(benzylamino)-2-phenylacetate **16ai**<sup>[31]</sup>



(*R*)-2-Phenylglycinemethyl ester hydrochloride (CAS: 19883-41-1, 121.0 mg, 0.6 mmol) was added into an Et<sub>3</sub>N (111.5  $\mu$ L, 0.8 mmol) solution in THF (5.0 mL) and stirred for 2 h. The solution was filtered through celite then washed with ethyl acetate (3 $\times$ 2.0 mL). The filtrate was evaporated to dryness to afford (*R*)-2-phenylglycinemethyl ester, which was used for the following step without further purification.

Following the general procedure, benzaldehyde (51.0  $\mu$ L, 0.5 mmol) and (*R*)-2-phenylglycinemethyl ester hydrochloride (121.0 mg, 0.6 mmol) gave the title compound **16ai** as a pale yellow liquid (121.2 mg, 90% yield). <sup>1</sup>H NMR (400.1 MHz, CDCl<sub>3</sub>)  $\delta$  7.41 – 7.24 (m, 10H), 4.39 (s, 1H), 4.24 – 4.09 (m, 2H), 3.75 (s, 2H), 1.21 (t, *J* = 7.0 Hz, 3H). <sup>13</sup>C{<sup>1</sup>H} NMR (100.6 MHz, CDCl<sub>3</sub>)  $\delta$  173.1, 139.6, 138.3, 128.7, 128.5, 128.4, 128.1, 127.6, 127.2, 64.5, 61.2, 51.5, 14.2. [ $\alpha$ ]<sub>D</sub><sup>20</sup> = -4.98 (*C* = 1.2, CH<sub>2</sub>Cl<sub>2</sub>)

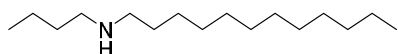
### Ethyl benzyl-L-alaninate **16aj**<sup>[32]</sup>



L-Alanine ethyl ester hydrochloride (CAS: 1115-59-9, 92.2 mg, 0.6 mmol) was added into an Et<sub>3</sub>N (111.5  $\mu$ L, 0.8 mmol) solution in THF (5.0 mL) and stirred for 2 h. The solution was filtered through celite then washed with ethyl acetate (3 $\times$ 2.0 mL). The filtrate was evaporated to dryness to afford L-alanine ethyl ester, which was used for the following step without further purification.

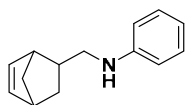
Following the general procedure, benzaldehyde (51.0  $\mu$ L, 0.5 mmol) and L-alanine ethyl ester hydrochloride (92.2 mg, 0.6 mmol) gave the title compound **16aj** as a pale yellow liquid (94.3 mg, 91% yield). <sup>1</sup>H NMR (400.1 MHz, CDCl<sub>3</sub>)  $\delta$  = 7.34– 7.22 (m, 5H), 4.19 (q, *J* = 7.1, 2H), 3.83 – 3.66 (m, 2H), 3.40 – 3.38 (m, 1H), 2.10 (br, 1H), 1.32 (d, *J* = 6.3, 3H), 1.29 (t, *J* = 7.0, 4H). <sup>13</sup>C{<sup>1</sup>H} NMR (100.6 MHz, CDCl<sub>3</sub>)  $\delta$  = 175.9, 139.7, 128.5, 128.4, 127.2, 60.8, 56.0, 52.2, 19.2, 14.4. [ $\alpha$ ]<sub>D</sub><sup>20</sup> = + 3.17 (*C* = 0.9, CH<sub>2</sub>Cl<sub>2</sub>)

### *N*-Butyldodecan-1-amine **16ak**



Following the general procedure, butyraldehyde (45.1  $\mu$ L, 0.5 mmol) and dodecylamine (111.2 mg, 0.6 mmol) gave the title compound **16ak** as a yellow-green liquid (115.9 mg, 96% yield). This compound was further purified by bulb to bulb distillation. <sup>1</sup>H NMR (400.1 MHz, CDCl<sub>3</sub>)  $\delta$  2.59 (m, 4H), 1.70 – 1.12 (m, 25H), 0.93 – 0.86 (m, 6H). <sup>13</sup>C{<sup>1</sup>H} NMR (100.6 MHz, CDCl<sub>3</sub>)  $\delta$  50.3, 49.9, 32.4, 32.1, 30.2, 29.82, 29.79, 29.77, 29.74, 29.5, 27.6, 22.8, 20.7, 14.27, 14.18. GC-MS, *m/z*(%) = 241 ([*M*]<sup>+</sup>, 25), 198(100), 184(9), 142(9), 87(100), 70(11), 57(27).

### *N*-(Bicyclo[2.2.1]hept-5-en-2-ylmethyl)aniline **16al**

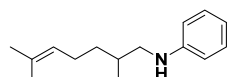


Following the general procedure, 5-norbornene-2-carboxaldehyde (52.6  $\mu$ L, 0.5 mmol) and aniline (54.8  $\mu$ L, 0.6 mmol) gave the title compound **16al** as mixture of *endo/exo* isomers as a brown liquid (94.7mg, 95% yield).

*M* = Major isomer *endo*, *m* = minor isomer *exo*, ratio *M*:*m* = 60:40

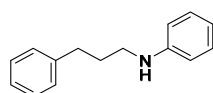
**<sup>1</sup>H NMR** (400.1 MHz, CDCl<sub>3</sub>) δ 7.20–7.16 (m, 2H, *M* + *m*, CH<sub>Ar</sub>), 6.75 – 6.66 (m, 1H, *M* + *m*, CH<sub>Ar</sub>), 6.64 – 6.58 (m, 2H, CH<sub>Ar</sub>), 6.19 (dd, *J* = 5.7, 3.0 Hz, 1H, *M*, CH=CH), 6.15 – 6.02 (m, 2H, *m*, CH=CH), 5.97 (dd, *J* = 5.8, 2.9 Hz, 1H, *M*, CH=CH), 3.18 (dd, *J* = 11.9, 6.9 Hz, 1H, *m*, CH<sub>2</sub>N), 3.09 (dd, *J* = 11.9, 8.3 Hz, 1H, *m*, CH<sub>2</sub>N), 2.92 (br s, 1H, *M*, CH), 2.90 – 2.76 (m, 4H, *M*, CH<sub>2</sub>N + CH, *m*, CH), 2.73 (br s, 1H, *m*, CH), 2.36 (m, 1H, *M*, CH), 1.92 (ddd, *J* = 11.5, 9.1, 3.9 Hz, 1H, *M*, CH<sub>2</sub>), 1.76 – 1.64 (m, 1H, *m*, CH), 1.47 (dd, *J* = 8.2, 2.2 Hz, 1H, *M*, CH<sub>2</sub>), 1.44 – 1.33 (m, 3H, *m*, CH<sub>2</sub>), 1.28 (dt, *J* = 8.3, 1.6 Hz, 1H, *M*, CH<sub>2</sub>), 1.23 (dt, *J* = 11.6, 3.8 Hz, 1H, *m*, CH<sub>2</sub>), 0.64 (ddd, *J* = 11.5, 4.4, 2.6 Hz, 1H, *M*, CH<sub>2</sub>). **<sup>13</sup>C{<sup>1</sup>H} NMR** (100.6 MHz, CDCl<sub>3</sub>) δ 148.69 (C<sub>qAr</sub>, *M*), 148.63 (C<sub>qAr</sub>, *m*), 137.76 (*M*, CH=CH), 136.91 (*m*, CH=CH), 136.56 (*m*, CH=CH), 132.19 (*M*, CH=CH), 129.37 (*m*, CH<sub>Ar</sub>), 129.34 (*M*, CH<sub>Ar</sub>), 117.24 (*m*, CH<sub>Ar</sub>), 117.20 (*M*, CH<sub>Ar</sub>), 112.83 (*M*, CH<sub>Ar</sub>), 112.78 (*m*, CH<sub>Ar</sub>), 49.72 (*m*, CH<sub>2</sub>), 49.70 (*M*, CH<sub>2</sub>), 48.33 (*M*, CH<sub>2</sub>), 45.39 (*m*, CH<sub>2</sub>), 44.63 (*m*, CH), 44.38 (*M*, CH), 42.53 (*M*, CH), 41.83 (*m*, CH), 39.14 (*m*, CH), 38.87 (*M*, CH), 31.41 (*m*, CH<sub>2</sub>), 30.59 (*M*, CH<sub>2</sub>). **GC-MS**, *m/z*(%) = 199([M]<sup>+</sup>, 47), 158(12), 132(88), 106(100), 91(13), 77(42), 65(13), 51(13)

#### *N*-(2,6-Dimethylhept-5-en-1-yl)aniline **16am**



Following the general procedure, 2,6-dimethyl-5-heptenal (84.2 μL, 0.5 mmol) and aniline (54.8 μL, 0.6 mmol) gave the title compound **16am** as a brown liquid (104.3 mg, 96% yield). **<sup>1</sup>H NMR** (400.1 MHz, CDCl<sub>3</sub>) δ 7.17 (td, *J* = 7.4, 1.8 Hz, 2H), 6.68 (tt, *J* = 7.3, 1.1 Hz, 1H), 6.60 (dd, *J* = 8.6, 1.1 Hz, 2H), 5.11 (m, 1H), 3.70 (br, 1H), 3.06 (dd, *J* = 12.2, 5.9 Hz, 1H), 2.89 (dd, *J* = 12.2, 7.3 Hz, 1H), 2.14 – 1.94 (m, 2H), 1.82 – 1.72 (m, 1H), 1.69 (s, 3H), 1.62 (s, 3H), 1.54 – 1.42 (m, 1H), 1.32 – 1.08 (m, 1H), 0.99 (d, *J* = 6.7, 3H). **<sup>13</sup>C{<sup>1</sup>H} NMR** (100.6 MHz, CDCl<sub>3</sub>) δ 148.77, 131.71, 129.35, 124.64, 117.07, 112.77, 50.40, 35.02, 32.70, 25.87, 25.59, 18.17, 17.85. **GC-MS**, *m/z*(%) = 217([M]<sup>+</sup>, 60), 146(100), 133(10), 106(95), 93(20), 77(35), 69(9), 51(9).

#### *N*-(3-Phenylpropyl)aniline **16an**<sup>[33]</sup>

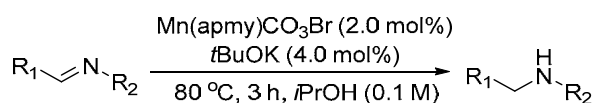


Following the general procedure cinnamaldehyde (62.9 μL, 0.5 mmol) and aniline (54.8 μL, 0.6 mmol) gave the title compound **16an** as pale yellow liquid (98.3 mg, 93% yield). **<sup>1</sup>H NMR** (400.1 MHz, CDCl<sub>3</sub>) δ 7.36 – 7.11 (m, 7H), 6.70 (t, *J* = 7.3 Hz, 1H), 6.59 (d, *J* = 7.9 Hz, 2H), 3.62 (s, 1H), 3.16 (t, *J* = 7.0 Hz, 2H), 2.75 (t, *J* = 7.5 Hz, 2H), 1.97 (p, *J* = 7.2 Hz, 2H). **<sup>13</sup>C{<sup>1</sup>H} NMR** (100.6 MHz, CDCl<sub>3</sub>) δ 148.5, 141.8, 129.4, 128.6, 128.5, 126.1, 117.3, 112.9, 43.6, 33.5, 31.2.

### 6.4. Part IV-3- Transfer hydrogenation of aldimines

The manganese complex **23** was synthesized according to the literature procedure.<sup>[34]</sup>

#### 6.4.1. Typical procedure for transfer hydrogenation of imines

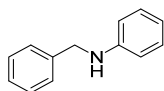


A 20 mL Schlenk tube was charged with imine (0.5 mmol), anhydrous isopropanol (5.0 mL), Mn complex **23** (2.0 mol%), and *t*-BuOK (4.0 mol%) under argon. Then the mixture was stirred at 80 °C in an oil bath for 3 h. After cooling to room temperature, the solution was diluted with

ethyl acetate (2 mL) and filtered through a small pad of celite (2 cm in a Pasteur pipette). The celite was washed with ethyl acetate (2×2 mL). The filtrate was evaporated and the crude residue was purified by column chromatography (SiO<sub>2</sub>, mixture of petroleum ether/ethyl acetate as eluent) to afford the desired product.

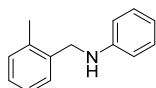
#### 6.4.2. Characterization data for amines

##### *N*-Benzylaniline **16a**<sup>[35]</sup>



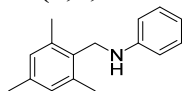
The compound **16a** was prepared as described in the general procedure (83.3 mg) in 91% yield. <sup>1</sup>H NMR (400 MHz, CDCl<sub>3</sub>) δ 7.41 – 7.34 (m, 4H), 7.32 – 7.28 (m, 1H), 7.22 – 7.18 (m, 2H), 6.76 – 6.72 (m, 1H), 6.67 – 6.65 (m, 2H), 4.35 (s, 2H), 4.04 (br, 1H). <sup>13</sup>C NMR (101 MHz, CDCl<sub>3</sub>) δ 148.3, 139.6, 129.4, 128.8, 127.6, 127.4, 117.7, 113.0, 48.5.

##### *N*-(2-Methylbenzyl)aniline **16b**<sup>[16]</sup>



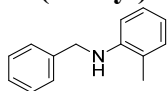
The compound **16b** was prepared as described in the general procedure (91.7 mg) in 95% yield. <sup>1</sup>H NMR (400 MHz, CDCl<sub>3</sub>) δ 7.34 (d, *J* = 6.8 Hz, 1H), 7.22 – 7.18 (m, 5H), 6.73 (t, *J* = 7.3 Hz, 1H), 6.65 (d, *J* = 7.9 Hz, 2H), 4.28 (d, *J* = 5.0 Hz, 2H), 3.84 (br, 1H), 2.38 (s, 3H). <sup>13</sup>C NMR (101 MHz, CDCl<sub>3</sub>) δ 148.5, 137.1, 136.5, 130.6, 129.4, 128.4, 127.6, 126.3, 117.6, 112.8, 46.5, 19.1.

##### *N*-(2,4,6-Trimethylbenzyl)aniline **16ao**<sup>[36]</sup>



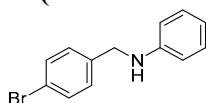
The compound **16ao** was prepared as described in the general procedure (59.7 mg) in 53% yield. <sup>1</sup>H NMR (400 MHz, CDCl<sub>3</sub>) δ 7.35 – 7.18 (m, 2H), 6.96 (s, 2H), 6.79 (td, *J* = 7.3, 1.3 Hz, 1H), 6.72 (d, *J* = 8.4 Hz, 2H), 4.25 (s, 2H), 3.46 (s, 1H), 2.41 (s, 6H), 2.36 (s, 3H). <sup>13</sup>C NMR (101 MHz, CDCl<sub>3</sub>) δ 148.7, 137.6, 137.4, 132.3, 129.4, 129.2, 117.3, 112.5, 42.5, 21.1, 19.5.

##### *N*-(benzyl)-2-methyl-aniline **16ap**<sup>[37]</sup>



The compound **16ap** was prepared as described in the general procedure (93.7 mg) in 95% yield. <sup>1</sup>H NMR (300 MHz, CDCl<sub>3</sub>) δ 7.36 (dt, *J* = 21.3, 7.4 Hz, 5H), 7.17 – 7.05 (m, 2H), 6.69 (td, *J* = 7.4, 1.2 Hz, 2H), 6.63 (d, *J* = 7.9 Hz, 1H), 4.39 (d, *J* = 5.4 Hz, 2H), 3.87 (t, *J* = 5.4 Hz, 1H), 2.19 (s, 3H). <sup>13</sup>C NMR (101 MHz, CDCl<sub>3</sub>) δ 146.2, 139.6, 130.2, 128.8, 127.7, 127.4, 127.3, 122.1, 117.3, 110.1, 48.5, 17.7.

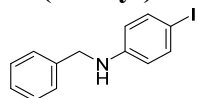
##### *N*-(4-Bromobenzyl)aniline **16ar**<sup>[38]</sup>



The compound **16ar** was prepared as described in the general procedure (123.2 mg) in 94% yield. <sup>1</sup>H NMR (400 MHz, CDCl<sub>3</sub>) δ 7.48 – 7.43 (m, 2H), 7.25 – 7.23 (m, 1H), 7.20 – 7.15 (m,

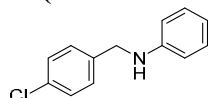
2H), 6.75 – 6.70 (m, 1H), 6.63 – 6.59 (m, 2H), 4.30 (d,  $J = 5.7$  Hz, 2H), 4.05 (br, 1H).  $^{13}\text{C}$  NMR (101 MHz,  $\text{CDCl}_3$ )  $\delta$  147.9, 138.7, 131.8, 129.4, 129.2, 121.1, 118.0, 113.0, 47.8.

#### *N*-(Benzyl)-4-iodo-aniline **16j**<sup>[19,35]</sup>



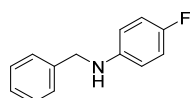
The compound **16j** was prepared as described in the general procedure (143.8 mg) in 93% yield.  $^1\text{H}$  NMR (400 MHz,  $\text{CDCl}_3$ )  $\delta$  7.42 – 7.39 (m, 2H), 7.35 – 7.26 (m, 5H), 6.43 – 6.40 (m, 2H), 4.30 (d,  $J = 5.6$  Hz, 2H), 4.10 (br, 1H).  $^{13}\text{C}$  NMR (101 MHz,  $\text{CDCl}_3$ )  $\delta$  147.8, 139.0, 137.9, 128.8, 127.6, 127.5, 115.2, 78.3, 48.2.

#### *N*-(4-Chlorobenzyl)aniline **16as**<sup>[35]</sup>



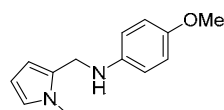
The compound **16as** was prepared as described in the general procedure (106.6 mg) in 92% yield.  $^1\text{H}$  NMR (400 MHz,  $\text{CDCl}_3$ )  $\delta$  7.30 (s, 4H), 6.99 (d,  $J = 8.1$  Hz, 2H), 6.54 (d,  $J = 8.4$  Hz, 2H), 4.29 (s, 2H), 3.93 (s, 1H), 2.24 (s, 3H).  $^{13}\text{C}$  NMR (101 MHz,  $\text{CDCl}_3$ )  $\delta$  145.7, 138.4, 132.9, 129.9, 128.8, 128.8, 127.2, 113.2, 48.1, 20.5.

#### *N*-Benzyl-4-fluoroaniline **16f**<sup>[15]</sup>



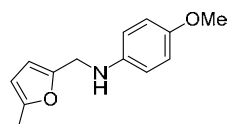
The compound **16f** was prepared as described in the general procedure (96.6 mg) in 96% yield.  $^1\text{H}$  NMR (400 MHz,  $\text{CDCl}_3$ )  $\delta$  7.40 – 7.27 (m, 5H), 6.92 – 6.86 (m, 2H), 6.59 – 6.56 (m, 2H), 4.30 (d,  $J = 5.7$  Hz, 2H), 3.93 (t,  $J = 5.7$  Hz, 1H).  $^{13}\text{C}$  NMR (101 MHz,  $\text{CDCl}_3$ )  $\delta$  156.0 (d,  $J = 235.0$  Hz), 144.6 (d,  $J = 1.9$  Hz), 139.4, 128.8, 127.6, 127.4, 115.8 (d,  $J = 22.3$  Hz), 113.8 (d,  $J = 7.3$  Hz), 49.1.  $^{19}\text{F}$  NMR (376 MHz,  $\text{CDCl}_3$ )  $\delta$  -127.92.

#### 4-Methoxy-*N*-((1-methyl-1*H*-pyrrol-2-yl)methyl)aniline **16r**<sup>[20]</sup>



The compound **16r** was prepared as described in the general procedure (42.2 mg) in 39% yield.  $^1\text{H}$  NMR (400 MHz,  $\text{CDCl}_3$ )  $\delta$  6.83 – 6.79 (m, 2H), 6.66 – 6.62 (m, 3H), 6.11 – 6.08 (m, 1H), 6.09 – 6.07 (m, 1H), 4.17 (s, 2H), 3.76 (s, 3H), 3.64 (s, 3H), 3.41 (br, 1H).  $^{13}\text{C}$  NMR (101 MHz,  $\text{CDCl}_3$ )  $\delta$  152.5, 142.6, 130.1, 122.9, 115.1, 114.4, 108.5, 106.9, 56.0, 41.5, 33.9.

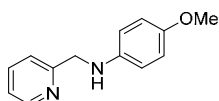
#### 4-Methoxy-*N*-((5-methylfuran-2-yl)methyl)aniline **16s**<sup>[20]</sup>



The compound **16s** was prepared as described in the general procedure (82.6 mg) in 76% yield.  $^1\text{H}$  NMR (400 MHz,  $\text{CDCl}_3$ )  $\delta$  6.83 – 6.73 (m, 2H), 6.70 – 6.61 (m, 2H), 6.09 (d,  $J = 3.1$  Hz, 1H), 5.88 (d,  $J = 3.1$  Hz, 1H), 4.20 (s, 2H), 3.75 (s, 3H), 2.27 (s, 3H).

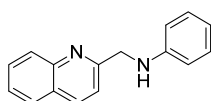
$^{13}\text{C}$  NMR (101 MHz,  $\text{CDCl}_3$ )  $\delta$  152.7, 151.7, 151.2, 142.1, 114.9, 114. , 107.9, 106.2, 55.9, 42.7, 13.7.

#### *N*-(Pyridin-2-ylmethyl)aniline **16t**<sup>[16]</sup>



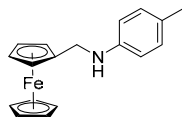
The compound **16t** was prepared as described in the general procedure (99.6 mg) in 93% yield.  $^1\text{H}$  NMR (400 MHz,  $\text{CDCl}_3$ )  $\delta$  8.58 (d,  $J$  = 4.4 Hz, 1H), 7.64 (td,  $J$  = 7.7, 1.7 Hz, 1H), 7.34 (d,  $J$  = 7.8 Hz, 1H), 7.17 (dd,  $J$  = 7.0, 5.2 Hz, 1H), 6.79 – 6.77 (m, 2H), 6.66 – 6.63 (m, 2H), 4.48 (br, 1H), 4.42 (d,  $J$  = 5.5 Hz, 2H), 3.74 (s, 3H).  $^{13}\text{C}$  NMR (101 MHz,  $\text{CDCl}_3$ )  $\delta$  159.0, 152.4, 149.4, 142.3, 136.7, 122.2, 121.8, 115.0, 114.5, 55.9, 50.4.

#### *N*-(Quinolin-2-ylmethyl)aniline **16au**<sup>[16]</sup>



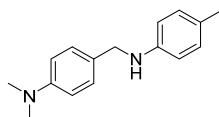
The compound **16au** was prepared as described in the general procedure (107.8 mg) in 92% yield.  $^1\text{H}$  NMR (400 MHz,  $\text{CDCl}_3$ )  $\delta$  8.12 (d,  $J$  = 8.4 Hz, 2H), 7.81 (dd,  $J$  = 8.1, 1.2 Hz, 1H), 7.73 (ddd,  $J$  = 8.4, 6.8, 1.3 Hz, 1H), 7.54 (ddd,  $J$  = 8.1, 6.9, 1.2 Hz, 1H), 7.45 (d,  $J$  = 8.5 Hz, 1H), 7.23 – 7.19 (m, 2H), 6.76 – 6.74 (m, 3H), 5.15 (t,  $J$  = 5.2 Hz, 1H), 4.64 (d,  $J$  = 5.2 Hz, 2H).  $^{13}\text{C}$  NMR (101 MHz,  $\text{CDCl}_3$ )  $\delta$  158.8, 148.1, 147.8, 136.8, 129.8, 129.4, 129.1, 127.8, 127.5, 126.4, 119.9, 117.7, 113.2, 49.9.

#### *N*-(Ferrocenylmethyl)-4-methylaniline **16q**<sup>[20]</sup>



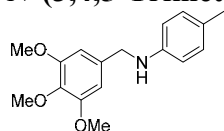
The compound **16q** was prepared as described in the general procedure (134.3 mg) in 88% yield.  $^1\text{H}$  NMR (400 MHz,  $\text{CDCl}_3$ )  $\delta$  7.02 (d,  $J$  = 8.1 Hz, 2H), 6.60 (d,  $J$  = 8.1 Hz, 2H), 4.25 (t,  $J$  = 1.8 Hz, 2H), 4.18 (s, 5H), 4.14 (t,  $J$  = 1.8 Hz, 2H), 3.95 (s, 2H), 3.75 (br, 1H), 2.26 (s, 3H).  $^{13}\text{C}$  NMR (101 MHz,  $\text{CDCl}_3$ )  $\delta$  146.3, 129.9, 126.9, 113.2, 86.9, 68.6, 68.2, 68.0, 43.9, 20.5.

#### *N,N*-Dimethyl-4-((*p*-tolylamino)methyl)aniline **16k**<sup>[20]</sup>



The compound **16k** was prepared as described in the general procedure (51.7 mg) in 43% yield.  $^1\text{H}$  NMR (400 MHz,  $\text{CDCl}_3$ )  $\delta$  7.25 (d,  $J$  = 8.6 Hz, 2H), 6.99 (d,  $J$  = 8.3 Hz, 2H), 6.73 (d,  $J$  = 8.6 Hz, 2H), 6.58 (d,  $J$  = 8.3 Hz, 2H), 4.19 (s, 2H), 3.75 (br, 1H), 2.95 (s, 6H), 2.25 (s, 3H).  $^{13}\text{C}$  NMR (101 MHz,  $\text{CDCl}_3$ )  $\delta$  150.2, 146.4, 129.8, 128.8, 127.5, 126.6, 113.1, 112.9, 48.4, 40.9, 20.5.

### *N*-(3,4,5-Trimethoxybenzyl)4-methyl-aniline **16ao**<sup>[19]</sup>

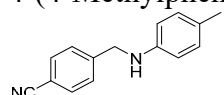


The compound was prepared as described in the general procedure (126.4 mg) in 88% yield.

**<sup>1</sup>H NMR** (400 MHz, CDCl<sub>3</sub>) δ 7.01 (d, *J* = 8.2 Hz, 2H), 6.63 (s, 2H), 6.59 (d, *J* = 8.3 Hz, 2H), 4.24 (d, *J* = 5.5 Hz, 2H), 3.92 (t, *J* = 5.7 Hz, 1H), 3.86 (s, 9H), 3.85 (s, 9H), 2.26 (s, 3H).

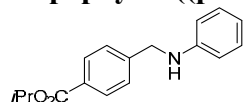
**<sup>13</sup>C NMR** (101 MHz, CDCl<sub>3</sub>) δ 153.4, 146.0, 137.0, 135.5, 129.8, 126.9, 113.1, 104.4, 60.9, 56.1, 49.1, 20.4.

### 4-(4-Methylphenylamino)methylbenzonitrile **16aw**<sup>[39]</sup>



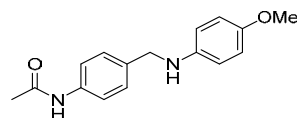
The compound **16aw** was prepared as described in the general procedure (98.9 mg) in 89% yield. **<sup>1</sup>H NMR** (400 MHz, CDCl<sub>3</sub>) δ 7.62 (d, *J* = 8.2 Hz, 2H), 7.47 (d, *J* = 8.2 Hz, 2H), 6.98 (d, *J* = 8.1 Hz, 2H), 6.50 (d, *J* = 8.4 Hz, 2H), 4.41 (d, *J* = 5.6 Hz, 2H), 4.07 (t, *J* = 5.6 Hz, 1H), 2.23 (s, 3H). **<sup>13</sup>C NMR** (101 MHz, CDCl<sub>3</sub>) δ 145.8, 145.3, 132.6, 130.0, 127.8, 127.5, 119.0, 113.1, 111.0, 48.2, 20.5.

### Isopropyl 4-((phenylamino)methyl)benzoate **16ay**



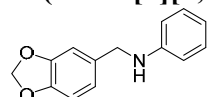
The compound **16ay** was prepared as described in the general procedure (130.6 mg) in 97% yield. **<sup>1</sup>H NMR** (300 MHz, CDCl<sub>3</sub>) δ 8.01 (d, *J* = 8.2 Hz, 2H), 7.43 (d, *J* = 8.1 Hz, 2H), 7.20 – 7.13 (m, 2H), 6.72 (t, *J* = 7.3 Hz, 1H), 6.61 (d, *J* = 7.8 Hz, 2H), 5.25 (hept, *J* = 6.2 Hz, 1H), 4.41 (d, *J* = 5.8 Hz, 2H), 4.13 (t, *J* = 5.8 Hz, 1H), 1.36 (d, *J* = 6.2 Hz, 6H). **<sup>13</sup>C NMR** (101 MHz, CDCl<sub>3</sub>) δ 166.1, 147.9, 144.8, 130.0, 129.4, 127.2, 118.0, 113.0, 68.4, 48.1, 22.1.

### *N*-(4-(((4-Methoxyphenyl)amino)methyl)phenyl)acetamide **16m**<sup>[15]</sup>



The compound **16m** was prepared as described in the general procedure (117.6 mg) in 87% yield. **<sup>1</sup>H NMR** (400 MHz, CDCl<sub>3</sub>) δ 7.46 (d, *J* = 8.0 Hz, 2H), 7.32 (d, *J* = 8.1 Hz, 2H), 6.77 (d, *J* = 8.8 Hz, 2H), 6.59 (d, *J* = 8.8 Hz, 2H), 4.24 (s, 2H), 3.74 (s, 3H), 2.17 (s, 3H), 1.52 (d, *J* = 50.9 Hz, 1H). **<sup>13</sup>C NMR** (101 MHz, CDCl<sub>3</sub>) δ 168.7, 152.3, 142.5, 137.1, 135.7, 128.2, 120.3, 115.0, 114.2, 55.9, 48.8, 24.6.

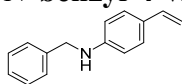
### *N*-(benzo[*d*][1,3]dioxol-5-ylmethyl)aniline **16az**<sup>[40]</sup>



The compound **16az** was prepared as described in the general procedure (94.3 mg) in 83% yield. **<sup>1</sup>H NMR** (300 MHz, CDCl<sub>3</sub>) δ 7.29 – 7.23 (m, 2H), 6.94 – 6.78 (m, 4H), 6.71 – 6.68 (m, 2H), 5.99 (s, 2H), 4.29 (s, 2H), 4.05 (br, 1H). **<sup>13</sup>C NMR** (75 MHz, CDCl<sub>3</sub>) δ 148.1, 148.0, 146.8, 133.4, 129.3, 120.6, 117.6, 112.9, 108.3, 108.1, 101.0, 48.1.

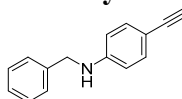


### *N*-benzyl-4-vinylaniline **16ba**<sup>[41]</sup>



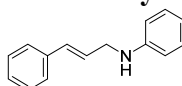
The compound **16ba** was prepared as described in the general procedure (98.4 mg) in 94% yield. <sup>1</sup>H NMR (400 MHz, CDCl<sub>3</sub>) δ 7.38 – 7.33 (m, 4H), 7.30 – 7.24 (m, 3H), 6.65 – 6.58 (m, 3H), 5.53 (dd, *J* = 17.5, 1.1 Hz, 1H), 5.02 (dd, *J* = 10.9, 1.1 Hz, 1H), 4.35 (s, 3H), 4.12 (br, 1H). <sup>13</sup>C NMR (101 MHz, CDCl<sub>3</sub>) δ 148.0, 139.4, 136.8, 128.8, 127.6, 127.6, 127.5, 127.4, 112.9, 109.7, 48.4.

### *N*-benzyl-4-ethynylaniline **16bb**<sup>[42]</sup>

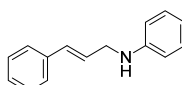


The compound **16bb** was prepared as described in the general procedure (94.3 mg) in 91% yield. <sup>1</sup>H NMR (400 MHz, CDCl<sub>3</sub>) δ 7.37 – 7.26 (m, 7H), 6.57 – 6.54 (m, 2H), 4.35 (d, *J* = 5.5 Hz, 2H), 4.24 (br, 1H), 2.97 (s, 1H). <sup>13</sup>C NMR (101 MHz, CDCl<sub>3</sub>) δ 148.5, 138.9, 133.6, 128.9, 127.6, 114.7, 112.5, 110.4, 84.8, 74.9, 48.1. GC-MS, *m/z*(%) = 269([M]<sup>+</sup>, 99), 210(18), 182(29), 135(100), 106(34), 89(27), 77(28).

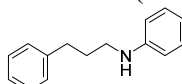
### *N*-cinnamylaniline **16bc**<sup>[S2, S14]</sup>



The compound **16bc** was prepared as described in the general procedure (97.3 mg) in 93% yield, and was isolated as 80:20 mixture of *N*-cinnamylaniline and *N*-3-phenylpropyl-aniline. Characteristic signals are listed below.

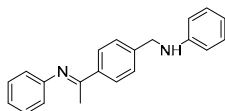


<sup>1</sup>H NMR (400.1 MHz, CDCl<sub>3</sub>) δ 6.34 (dt, *J* = 15.9, 5.7 Hz, 1H), 3.95 (d, *J* = 5.4 Hz, 2H),



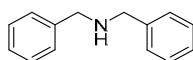
<sup>1</sup>H NMR (400.1 MHz, CDCl<sub>3</sub>) δ 3.16 (t, *J* = 7.0 Hz, 2H), 2.75 (t, *J* = 7.5 Hz, 2H), 1.97 (p, *J* = 7.2 Hz, 2H).

### *N*-(4-(1-(Phenylimino)ethyl)benzyl)aniline **16n**<sup>[35]</sup>



The compound **16n** was prepared as described in the general procedure (124.7 mg) in 83% yield. <sup>1</sup>H NMR (400 MHz, CDCl<sub>3</sub>) δ 7.96 (d, *J* = 8.1 Hz, 2H), 7.45 (d, *J* = 8.0 Hz, 2H), 7.35 (t, *J* = 7.6 Hz, 2H), 7.18 (t, *J* = 7.6 Hz, 2H), 7.09 (t, *J* = 7.3 Hz, 1H), 6.80 (d, *J* = 7.7 Hz, 2H), 6.73 (t, *J* = 7.3, 6.9 Hz, 1H), 6.64 (d, *J* = 8.0 Hz, 2H), 4.41 (d, *J* = 5.7 Hz, 2H), 4.12 (br, 1H), 2.23 (s, 3H). <sup>13</sup>C NMR (101 MHz, CDCl<sub>3</sub>) δ 165.3, 151.8, 148.1, 142.3, 138.7, 129.4, 129.1, 127.7, 127.4, 123.4, 119.5, 117.9, 113.1, 48.1, 17.5.

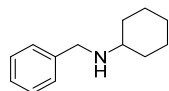
### Dibenzylamine **16y**<sup>[15]</sup>



The compound **16y** was prepared as described in the general procedure (34.5 mg) in 35% yield.

**<sup>1</sup>H NMR** (400 MHz, CDCl<sub>3</sub>) δ 7.37 – 7.26 (m, 10H), 3.87 (s, 4H), 1.71 (br, 1H).  
**<sup>13</sup>C NMR** (101 MHz, CDCl<sub>3</sub>) δ 140.5, 128.5, 128.3, 127.1, 53.3.

### **N-Benzylcyclohexanamine 16aa**<sup>[25]</sup>



The compound **16aa** was prepared as described in the general procedure (11.4 mg) in 12% yield. **<sup>1</sup>H NMR** (400 MHz, CDCl<sub>3</sub>) δ 7.43 – 7.14 (m, 5H), 3.82 (s, 2H), 2.49 (tt, *J* = 10.1, 3.8 Hz, 1H), 2.11 – 0.69 (m, 11H). **<sup>13</sup>C NMR** (101 MHz, CDCl<sub>3</sub>) δ 141.0, 128.5, 128.2, 126.9, 56.3, 51.1, 33.7, 26.3, 25.1.

## **6.5. References**

- [1] D. Benito-Garagorri, K. Mereiter, K. Kirchner, *Collect. Czech. Chem. Commun.* **2007**, 72, 527-540.
- [2] S. M. Aucott, A. M. Z. Slawin, J. D. Woollins, *J. Chem. Soc., Dalton Trans.* **2000**, 2559-2575.
- [3] M. Alvarez, N. Lugan, R. Mathieu, *J. Chem. Soc., Dalton Trans.* **1994**, 2755-2760.
- [4] E. Mothes, S. Sentets, M. A. Luquin, R. Mathieu, N. Lugan, G. Lavigne, *Organometallics* **2008**, 27, 1193-1206.
- [5] D. Wei, T. Roisnel, C. Darcel, E. Clot, J.-B. Sortais, *ChemCatChem* **2017**, 9, 80-83.
- [6] L. Shi, Y.-Q. Tu, M. Wang, F.-M. Zhang, C.-A. Fan, Y.-M. Zhao, W.-J. Xia, *J. Am. Chem. Soc.* **2005**, 127, 10836-10837.
- [7] K. Miyamoto, N. Tada, M. Ochiai, *J. Am. Chem. Soc.* **2007**, 129, 2772-2773.
- [8] B. T. Cho, S. K. Kang, M. S. Kim, S. R. Ryu, D. K. An, *Tetrahedron* **2006**, 62, 8164-8168.
- [9] D. J. Fox, D. S. Pedersen, S. Warren, *Org. Biomol. Chem.* **2006**, 4, 3102-3107.
- [10] T. Hirata, A. Matsushima, Y. Sato, T. Iwasaki, H. Nomura, T. Watanabe, S. Toyoda, S. Izumi, *J. Mol. Catal. B: Enzym.* **2009**, 59, 158-162.
- [11] X. Chen, X. Gao, Q. Wu, D. Zhu, *Tetrahedron: Asymmetry* **2012**, 23, 734-738.
- [12] G. M. Sheldrick, *Acta Cryst.* **2015**, A71, 3-8.
- [13] G. M. Sheldrick, *Acta Cryst.* **2015**, C71, 3-8.
- [14] A. Spek, *Acta Cryst.* **2015**, C71, 9-18.
- [15] J. Zheng, T. Roisnel, C. Darcel, J.-B. Sortais, *ChemCatChem* **2013**, 5, 2861-2864.
- [16] M. Zhang, H. Yang, Y. Zhang, C. Zhu, W. Li, Y. Cheng, H. Hu, *Chem. Commun.* **2011**, 47, 6605-6607.
- [17] P. Liu, R. Liang, L. Lu, Z. Yu, F. Li, *J. Org. Chem.* **2017**, 82, 1943-1950.
- [18] D. B. Bagal, R. A. Watile, M. V. Khedkar, K. P. Dhake, B. M. Bhanage, *Catal. Sci. Technol.* **2012**, 2, 354-358.
- [19] M. Yang, F. Liu, *J. Org. Chem.* **2007**, 72, 8969-8971.
- [20] L. P. Bheeter, M. Henrion, M. J. Chetcuti, C. Darcel, V. Ritleng, J.-B. Sortais, *Catal. Sci. Technol.* **2013**, 3, 3111-3116.
- [21] R. Cano, M. Yus, D. J. Ramón, *Tetrahedron* **2011**, 67, 8079-8085.
- [22] C. T. Yang, Y. Fu, Y. B. Huang, J. Yi, Q. X. Guo, L. Liu, *Angew. Chem.* **2009**, 121, 7534-7537.
- [23] R. Cano, D. J. Ramon, M. Yus, *J. Org. Chem.* **2011**, 76, 5547-5557.
- [24] P. R. Likhar, R. Arundhathi, M. L. Kantam, P. S. Prathima, *Eur. J. Org. Chem.* **2009**, 2009, 5383-5389.
- [25] L. C. M. Castro, J.-B. Sortais, C. Darcel, *Chem. Commun.* **2012**, 48, 151-153.
- [26] T. Dombray, C. Helleu, C. Darcel, J.-B. Sortais, *Adv. Synth. Catal.* **2013**, 355, 3358-3362.
- [27] L. Blackburn, R. J. K. Taylor, *Org. Lett.* **2001**, 3, 1637-1639.
- [28] S. Lateef, S. Reddy Krishna Mohan, S. Reddy Jayarama Reddy, *Tetrahedron Lett.* **2007**, 48, 77-80.
- [29] M. Largeron, M.-B. Fleury, *Org. Lett.* **2009**, 11, 883-886.

- [30] a) Y. Turgut, N. Demirel, H. Hoşgören, *J. Inclusion Phenom. Macrocyclic Chem.* **2006**, *1*, 29-33; b) H. Bräuner-Osborne, L. Bunch, N. Chopin, F. Couty, G. Evano, A. A. Jensen, M. Kusk, B. Nielsen, N. Rabasso, *Org. Biomol. Chem.* **2005**, *3*, 3926-3936.
- [31] Q.-H. Deng, H.-W. Xu, A. W.-H. Yuen, Z.-J. Xu, C.-M. Che, *Org. Lett.* **2008**, *10*, 1529-1532.
- [32] B. T. Cho, S. K. Kang, *Tetrahedron* **2005**, *61*, 5725-5734.
- [33] R. Kubiak, I. Prochnow, S. Doye, *Angew. Chem. Int. Ed.* **2010**, *49*, 2626-2629.
- [34] A. Bruneau-Voisine, D. Wang, V. Dorcet, T. Roisnel, C. Darcel, J.-B. Sortais, *Org. Lett.* **2017**, *19*, 3656-3659.
- [35] D. Wei, A. Bruneau-Voisine, D. A. Valyaev, N. Lugan, J.-B. Sortais, *Chem. Commun.* **2018**, *54*, 4302-4305.
- [36] J. R. Miecznikowski, R. H. Crabtree, *Polyhedron* **2004**, *23*, 2857-2872.
- [37] C.-T. Yang, Y. Fu, Y.-B. Huang, J. Yi, Q.-X. Guo, L. Liu, *Angew. Chem. Int. Ed.* **2009**, *48*, 7398-7401.
- [38] R. Kawahara, K.-i. Fujita, R. Yamaguchi, *Adv. Synth. Catal.* **2011**, *353*, 1161-1168.
- [39] B. Li, J.-B. Sortais, C. Darcel, P. H. Dixneuf, *ChemSusChem* **2012**, *5*, 396-399.
- [40] M. Mastalir, G. Tomsu, E. Pittenauer, G. Allmaier, K. Kirchner, *Org. Lett.* **2016**, *18*, 3462-3465.
- [41] S. Elangovan, J. Neumann, J.-B. Sortais, K. Junge, C. Darcel, M. Beller, *Nat. Commun.* **2016**, *7*, 12641.
- [42] T. Mizutani, C. Yoshimura, H. Kondo, M. Kitade, S. Ohkubo (L. TAIHO PHARMACEUTICAL CO.), WO2015199136A1, **2015**.

## **Chapter V - (De)Hydrogenative Synthesis Catalyzed by Rhenium**



## Chapter V - (De)Hydrogenative Synthesis Catalyzed by Rhenium

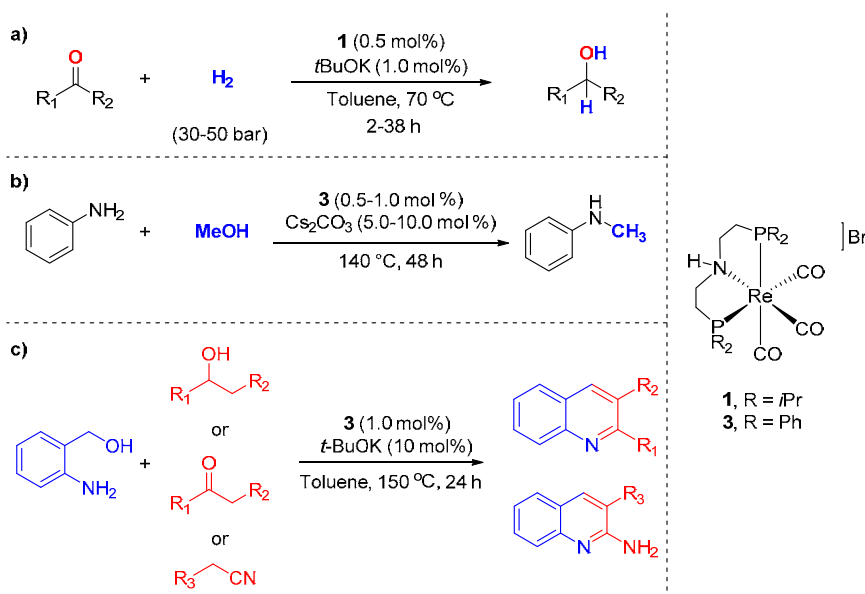
### Introduction

Hydrogenation reactions have been of central importance in chemistry for more than a century.<sup>[1]</sup> Nevertheless, it remains an important field of investigation, notably with the current challenge of the transformation of highly oxygenated biomass-resources into less functionalized chemical building blocks.<sup>[2]</sup> Compared to the transition metals of groups 8, 9, and 10 (Fe, Co, Ni) which are classical in reduction area, group 7 transition metals have been scarcely applied in hydrogenation or related reduction reactions<sup>[3]</sup> Nevertheless, since few years, manganese has been proved to be a suitable transition metal for the design of efficient hydrogenation and hydrogen borrowing catalysts (see introduction in Chapter IV for more details).<sup>[3a, 4]</sup> In the case of rhenium, after the seminal work of Ephritikhine on dehydrogenation of alkanes to alkenes,<sup>[5]</sup> rare examples of stoichiometric<sup>[6]</sup> and catalytic<sup>[7]</sup> hydrogenation of alkenes have been described with rhenium nitrosyl hydride complexes mainly by Berke, and a single example of the hydrogenation of acetophenone is reported.<sup>[7b]</sup> Interestingly, Berke has also developed a bifunctional rhenium complex, bearing a non-innocent cyclopentadienol ligand, as hydrogen transfer catalyst for the reduction of ketones and imines.<sup>[7f, 8]</sup> Due to the importance of cooperative metal-ligand complexes in hydrogenation,<sup>[9]</sup> notably through the so-called NH-effect,<sup>[10]</sup> we became interested in the preparation of well-defined rhenium PN(H)P pincer complexes as catalysts for reduction reactions. The first part of this chapter will focus on the hydrogenation of carbonyl derivatives catalyzed by Re PN(H)P pincer complex (Scheme 1a).

In the context of green and sustainable development, the utilization of non-toxic, inexpensive, renewable and readily available reagents is highly desirable. As such, the replacement of hazardous and waste-generating reactants embraces several of the 12 principles of green chemistry, especially when coupled with catalysis.<sup>[11]</sup>

In this respect and considering the importance of *N*-methylated amines as key intermediates and building blocks in synthetic chemistry, the development of methylation reagents greener than the classical formaldehyde, methyl iodide, methyl triflate, or dimethyl sulfate is a topical challenge. For selective mono *N*-methylation of amines, sustainable sources of “methyl” group were investigated,<sup>[12]</sup> including carbon dioxide,<sup>[13]</sup> dialkylcarbonate<sup>[14]</sup> and formic acid.<sup>[15]</sup> Methanol, the simplest alcohol, can also be used as a green and renewable C1 source for methylation reactions<sup>[16]</sup> using the hydrogen borrowing methodology.<sup>[17]</sup> Actually, “Methanol

Economy” identifies and promotes methanol as a substitute for petroleum oil in the field of energy and chemistry.<sup>[18]</sup> Methanol is a biodegradable liquid, easy to handle and a safe chemical to produce, for example, formaldehyde, acetic acid, or ethylene.<sup>[19]</sup> In addition, due to the plurality of its supplies including from renewable sources,<sup>[20]</sup> methanol is a sustainable building block. Therefore, in the second part of this chapter, we will describe the mono *N*-methylation of anilines with methanol catalyzed by Re PN(H)P pincer complexes (Scheme 1b).



**Scheme 1.** (De)Hydrogenative synthesis catalyzed by rhenium.

On the other hand, *N*-heterocycles are ubiquitous skeleton in natural products and biologically active molecules.<sup>[21]</sup> Among this family, substituted quinolines are extensively used in pharmaceuticals, medicinal chemistry,<sup>[22]</sup> agrochemicals, and functional materials.<sup>[23]</sup> Accordingly, new synthetic protocols are continuously needed to access a large diversity of functionalized quinolines. Conventional routes for the access of quinolines,<sup>[21]</sup> such as Skraup<sup>[24]</sup>, Camps<sup>[25]</sup> and Knorr<sup>[26]</sup> synthesis, have been reported over a century ago. However most of these methods suffer from multiple steps synthesis, harsh conditions (high temperature, excess of bases or acids), low chemoselectivity leading to overall low yields and poor atom economy.<sup>[27]</sup> Among those synthetic approaches, the Friedländer reaction has been proven to be one of the simplest and most efficient methods.<sup>[28]</sup> Although the Friedländer method is quite versatile, the primary limitation of this approach is the preparation and stability of the starting materials, *i.e.* 2-aminobenzaldehyde derivatives, since these compounds undergo easily self-condensation. To overcome these limitations, the indirect Friedländer reaction, involving the oxidative annulation of stable 2-aminobenzylalcohols with either readily available secondary alcohols or ketones, *via* hydrogen auto-transfer reactions, is a powerful and sustainable way to

access quinolines.<sup>[17g, 29]</sup> The synthesis of quinolines through acceptorless dehydrogenative coupling catalyzed by the same type of rhenium complexes will be depicted in the third part of this chapter (Scheme 1c).





## V-1 Hydrogenation of carbonyl derivatives catalyzed by Re PN(H)P complexes

**Contributions in this part:** Synthesis of the complexes, optimization, scope and mechanistic studies: Duo Wei; X-ray diffraction studies: Thierry Roisnel; DFT calculations: Eric Clot.

**Publication:** D. Wei, T. Roisnel, C. Darcel, E. Clot, J.-B. Sortais, *ChemCatChem*, **2017**, 9, 80-83

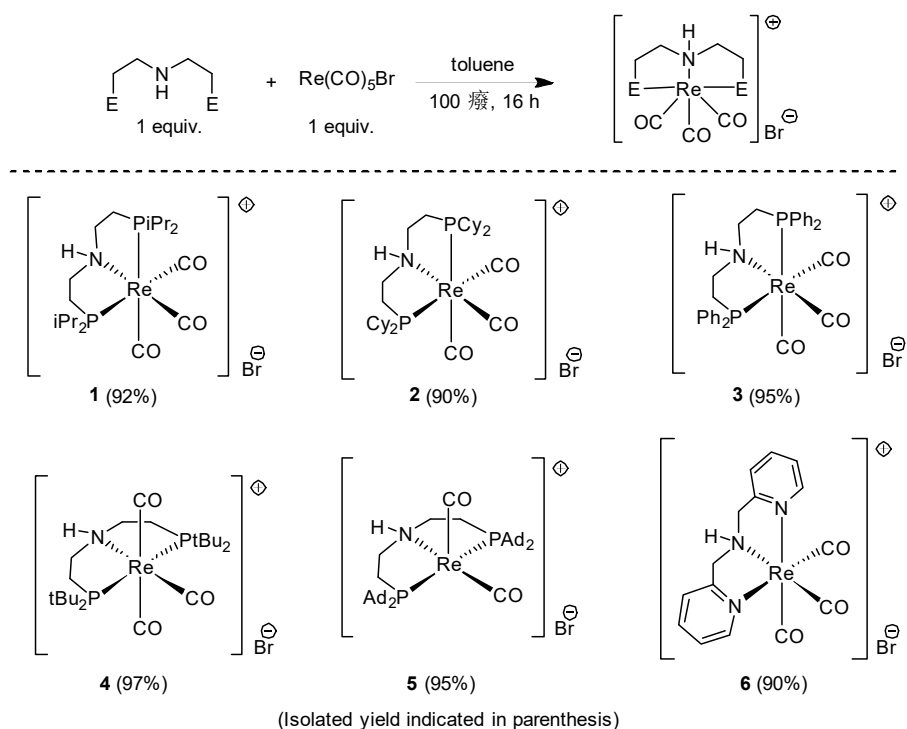
In the field of hydrogenation reactions, until now, rhenium PNP pincer type complexes have been sparsely discussed in the literature.<sup>[7f, 30]</sup> We report in this first paragraph the first efficient and broad scope hydrogenation of carbonyl derivatives with a well-defined rhenium complex based on a PN(H)P ligand.

### 1.1. Results and discussions

#### 1.1.1. Rhenium complex synthesis

A new series of cationic tricarbonyl Re(I) complexes bearing tridentate PNP<sup>[7f, 30b-d, 30f-l, 31]</sup> based on  $\text{NH}(\text{CH}_2\text{CH}_2\text{PR}_2)_2$  ligands with different alkyl or aryl substituents on the phosphorus atoms (**1**, R = *i*Pr; **2**, R = Cy; **3**, R = Ph; **4**, R = *t*Bu; **5**, R = Ad), was prepared upon reaction of one equivalent of ligand with one equivalent of  $\text{ReBr}(\text{CO})_5$  in toluene at 100 °C overnight. For comparative purpose, the **1-5** series of complexes was complemented with the dipicolylamine analogue **6**, prepared following the same procedure from  $\text{ReBr}(\text{CO})_5$  and dipicolylamine. Complexes **1-6** were thus obtained in excellent yields (90-97% yields, Scheme 2). It must be noted that the complex **6** has been previously prepared starting from the  $[\text{NEt}_4]_2[\text{Re}(\text{CO})_3\text{Br}_3]$  cationic precursor.<sup>[32]</sup>

All the new complexes **1-5** were characterized by NMR, elemental analysis, IR, HR-MS and X-ray diffraction studies (Figures 1, 2 and 3). Surprisingly, the coordination mode of the tridentate ligands in **1**, **2** and **3** adopted a facial coordination at Re contrary to other octahedral complexes with Mn,<sup>[4h]</sup> Fe,<sup>[33]</sup> Ru<sup>[34]</sup> or Os<sup>[35]</sup> that exhibit a meridional coordination mode of the ligand (Figures 1 and 2). While for the complexes **4** and **5**, meridional coordination modes were observed when the size of the substituents on the phosphorus atom increased (Figure 3). According to our calculations (Scheme 4, in mechanistic studies), *mer*-isomers correspond to a thermodynamic stable geometry, and thus isolated *fac*-isomers are the kinetic products of the reaction.



**Scheme 2.** Synthesis and structures of the rhenium complexes **1-6**.

In the case of the bulkiest adamantyl derivative, the complex **5** was obtained as an orange solid, in sharp contrast with the white color of all the other complexes. The  $^{13}\text{C}\{^1\text{H}\}$  NMR displayed only two signals of seemingly equal intensity for the carbonyl ligands, while complexes **1-4** and **6** typically displayed three distinct signals. In the IR spectrum, only two equally intense CO stretching bands were present, while three were present for complexes **1-4** and **6** (Table 1). Finally, the X-ray structure confirmed the sole presence of two carbonyl coordinated to the rhenium center (Figure 3, right), along with the PNP ligand, thus highlighting the unsaturated coordination sphere of the metal.

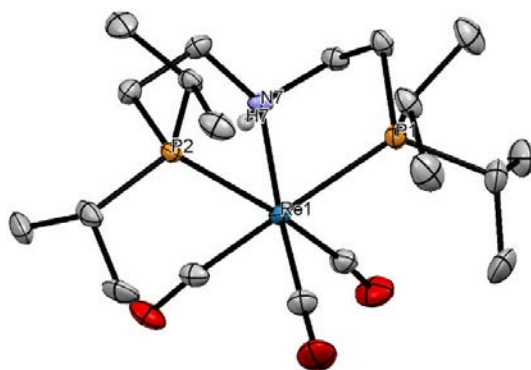


**Figure 1.** Perspective view of the cationic part of complex **1** (thermal ellipsoids drawn at the 50% probability level, hydrogen atoms, except NH, were omitted for clarity).

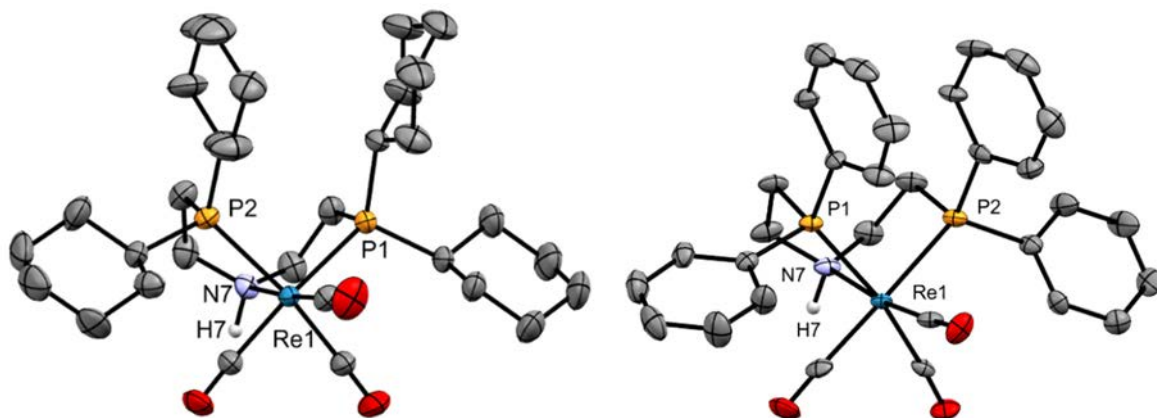


**Figure 2.** Perspective view of the cationic part of the complexes **2** (left) and **3** (right) (thermal ellipsoids drawn at the 50% probability level, hydrogen atoms, except NH, were omitted for clarity).

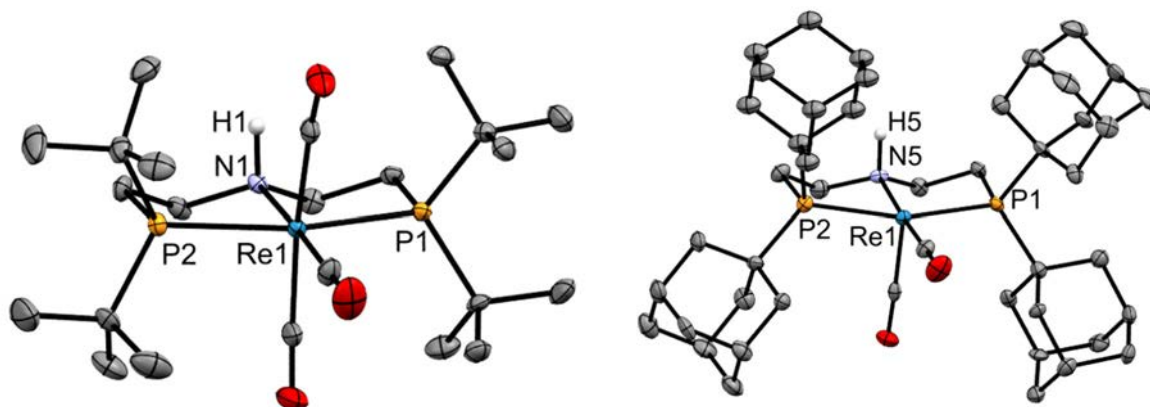


**Figure 3.** Perspective view of the cationic part of the complexes **4** (left) and **5** (right) (thermal ellipsoids drawn at the 50% probability level, hydrogen atoms, except NH, were omitted for clarity).

**Table 1.** Stretching frequencies of carbonyl ligands in IR for complexes **1-6**<sup>[a]</sup>

Complex	$\nu_{\text{CO}}$ ( $\text{cm}^{-1}$ )
<b>1</b>	2031, 1944, 1921
<b>2</b>	2029, 1940, 1919
<b>3</b>	2042, 1967, 1923
<b>4</b>	2027, 1923, 1913
<b>5</b>	1925, 1838
<b>6</b>	2033, 1935, 1911

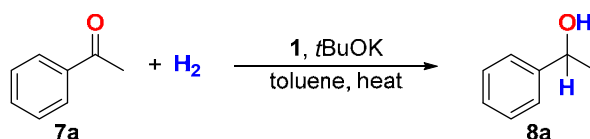
<sup>[a]</sup>  $\nu_{\text{CO}}$  ( $\text{cm}^{-1}$ )  $\text{CH}_2\text{Cl}_2$  solution.

### 1.1.2. Optimization of the reaction conditions for the hydrogenation of acetophenone

In our first attempt, we investigated only the activity of the complex **1** in hydrogenation reactions. The 5 others complexes **2-6** were mainly used for the mono *N*-methylation of anilines and the acceptorless dehydrogenative synthesis of quinolines (see § 5.2 and 5.3).

Aiming at probing the hydrogenation catalytic activity of the complex **1**, the initial investigations were carried out on acetophenone **7a** (Table 2). Full reduction of **7a** to the corresponding 1-phenylethanol **8a** was achieved in the presence of 5.0 mol% of the complex **1**, 10 mol% *t*-BuOK, 50 bar of H<sub>2</sub> at 110 °C for 16 h (entry 1). Interestingly, these conditions resulted in full conversion already after 2 hours (entry 2). Using only Re(CO)<sub>5</sub>Br precursor, without any ligand, resulted in no hydrogenation activity (entry 3). The same lack of reactivity was also observed in the absence of a base (entry 4).

**Table 2.** Optimization of the reaction parameters<sup>[a]</sup>



Entry	Complex (mol%)	<i>t</i> -BuOK (mol%)	H <sub>2</sub> (bar)	T (°C)	t (h)	Yield (%)
1	<b>1</b> (5.0)	10	50	110	16	>98
2	<b>1</b> (5.0)	10	50	110	2	>98
3	Re(CO) <sub>5</sub> Br (5.0)	10	50	110	2	<3
4	<b>1</b> (5.0)	-	50	110	2	<3
5	<b>1</b> (5.0)	10	50	70	16	>98
6	<b>1</b> (5.0)	10	50	30	16	<3
7	<b>1</b> (0.5)	1.0	50	70	16	>98
8	<b>1</b> (0.1)	5.0	50	70	18	63
9	<b>1</b> (0.5)	1.0	30	70	16	>98
10	<b>1</b> (1.0)	2.0	10	70	18	90
11	<b>1</b> (5.0)	10	1	110	16	85
12	<b>1</b> (5.0)	10	1 <sup>[b]</sup>	110	16	81

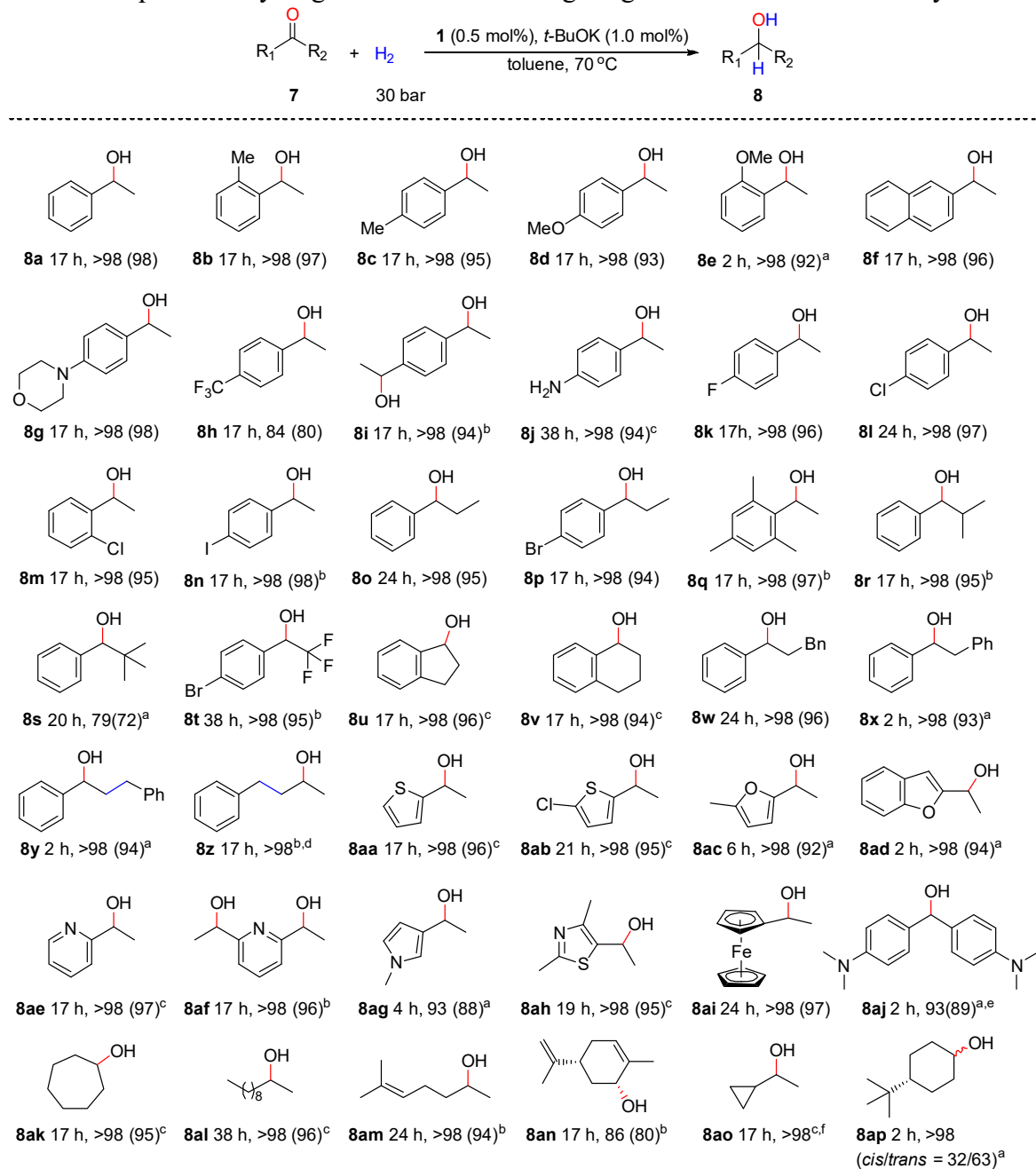
<sup>[a]</sup> Reaction conditions: in a glove box, an autoclave is filled with 1) complex **1**, 2) toluene, 3) acetophenone **7a** 4) *t*-BuOK, then pressurized with H<sub>2</sub>. The reaction was heated in an oil bath.

<sup>[b]</sup> A balloon of H<sub>2</sub> was used.

The influence of reaction parameters such as temperature, catalyst loading and pressure was then investigated. At 70 °C, full conversion of **7a** was still observed after 16 hours (entry 5), but lowering the temperature to 30 °C completely shuts down the catalytic activity (entry 6). Under 50 bar of H<sub>2</sub>, at 70 °C, the catalyst loading could be decreased to 0.5 mol% without losing any activity, however, with only 0.1 mol% of **1**, the conversion dropped to 63% (TON 630, entries 7-8). The pressure of hydrogen can be lowered to 30 bar in the presence of 0.5 mol% of catalyst (entry 9). Ketone hydrogenation still takes place with lower pressure, down to 1 bar, even with a balloon of H<sub>2</sub>, although at the expense of the charge of catalyst and temperature (entries 10-12). The optimal conditions selected to probe the substrate scope of the reaction were 0.5 mol% **1**, 1.0 mol% base, 30 bar H<sub>2</sub>, 70°C, 16 h (Table 3).

### 1.1.3. Scope for rhenium-catalyzed hydrogenation of ketones

**Table 3.** Scope of the hydrogenation of ketones **7** giving alcohols **8** under the catalysis of **1**.



General conditions: ketone **7** (2.5 mmol), H<sub>2</sub> (30 bar), **1** (0.5 mol%), *t*-BuOK (1.0 mol%), toluene, 70 °C; Isolated yields of **8** in parentheses;

[a] H<sub>2</sub> (50 bar), **1** (5.0 mol%), *t*-BuOK (10 mol%), 110 °C;

[b] H<sub>2</sub> (50 bar), **1** (1.0 mol%), *t*-BuOK (2.0 mol%), 110 °C;

[c] H<sub>2</sub> (30 bar), **1** (0.5 mol%), *t*-BuOK (1.0 mol%), 110 °C;

[d] 10% of the unsaturated alcohol was detected in the crude mixture;

[e] Isolated yield with 3% of starting material;

[f] THF as the solvent.

In general, ketones bearing electron-donating and electron-withdrawing substituents, e.g. *o*- and *p*-methyl (**7b**, **7c**), *p*- and *o*-methoxy (**7d**, **7e**), *p*-morpholinyl (**7g**), *p*-fluoro (**7k**), *p*- and *o*-chloro (**7l**, **7m**), *p*-bromide (**7p**, **7t**), *p*-trifluoromethyl (**7h**), *p*-amino (**7j**) and the more reactive

*p*-iodo (**7n**) groups were reduced without alteration of the functional groups. Harsher conditions were needed for the hydrogenation of *o*-methoxy- acetophenone **7e** (H<sub>2</sub> (50 bar), **1** (5.0 mol%), *t*-BuOK (10 mol%), 110 °C). In addition, 2'-acetonaphthone **7f** and di- ketones (**7i**) were also reduced with good yields.

Next, we explored the activity of the rhenium catalyst **1** towards a collection of more sterically hindered ketones **7o-7t**, **7w**, **7x**. As a representative example, pivalophenone **7s** was successfully hydrogenated to the corresponding alcohol **8s** in 72% isolated yield. 1-Indanone **7u**,  $\alpha$ -tetralone **7v** could be converted to the corresponding alcohols when the reaction was performed at 110 °C. Noteworthy, the  $\alpha,\beta$ -unsaturated chalcone afforded selectively the saturated alcohol **8y** in good yield, and the reduction of benzylideneacetone led to 4-phenylbutan-2-ol **8z** as the major product, contaminated with unsaturated alcohol, 4-phenylbut-3-en-2-ol (ratio 90:10). Additionally, the heteroaromatic ketones (**7aa-7ah**) based on thiophene, furane, pyridine, pyrrole and thiazole were smoothly converted into the corresponding alcohols (88-97% isolated yields).

Even the challenging di(*p*-dimethylaminophenyl)methanone **7aj** can be hydrogenated in 89% yield with this catalytic system. Then, we explored the scope of aliphatic ketones (**7ak-7ap**). Under these conditions, the rhenium-based catalyst **1** tolerated cyclic, long-chain and remote C=C bond (**8ak-8an**). Starting from the enantiopure (*R*)-carvone **7an**, (-)-*cis*-carveol was obtained as a single diastereoisomer **8an** in 80% yield. Besides, the internal tri-substituted conjugated C=C in **7an** was not reduced. Notably, the cyclopropyl-substituted ketone **7ao** furnished a quantitative yield of the alcohol **8ao** indicating that the reaction does not proceed *via* stable radical intermediates. Hydrogenation of 4-(*tert*- butyl)cyclohexanone **7ap** gave full conversion and a mixture of alcohols **8ap** was obtained with a *cis/trans* ratio of 32:63.

#### 1.1.4. Scope for the hydrogenation of aldehydes

Aldehydes can also be reduced to the corresponding alcohols with this catalytic system (Figure 4). For example, 4-biphenylaldehyde **9a** was hydrogenated to the corresponding primary alcohol smoothly in 2 h. Noticeably, internal C-C triple bond and amide moieties were tolerated (**10b-10c**).

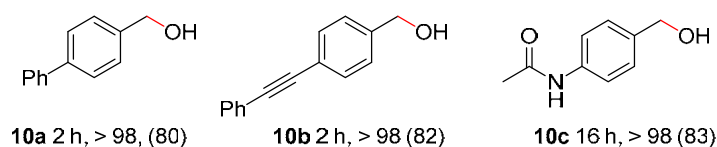
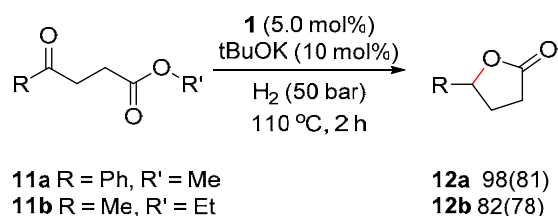


**Figure 4.** Scope of the hydrogenation of aldehydes leading to the corresponding alcohols under the catalysis of **1**. [General conditions: H<sub>2</sub> (50 bar), **1** (5.0 mol%), *t*-BuOK (10 mol%), 110 °C, toluene.]

### 1.1.5. Scope for the hydrogenation of $\gamma$ -keto-esters

Next,  $\gamma$ -keto-esters, such as methyl 3-benzoylpropionate **11a** were subjected to the reductive conditions in the presence of **1**. To our delight,  $\gamma$ -phenyl  $\gamma$ -butyrolactone **12a** was obtained in high conversion and 81% isolated yield, showing the tolerance toward ester/lactone functional groups. Interestingly, starting from the biomass derived ethyl levunilate **11b**,  $\gamma$ -valerolactone **12b**, which can be used as liquid fuel, additive, solvent or intermediate for organic synthesis,<sup>[16]</sup> was obtained in good yield (78%) using standard conditions, *i.e.* 5.0 mol% of **1**, 50 bar of H<sub>2</sub>, at 110 °C for 2 h (Scheme 3).<sup>[17]</sup>



**Scheme 3.** Synthesis of  $\gamma$ -lactones from  $\gamma$ -keto esters. Yields of the isolated products are given in parentheses.

Finally, despite this significant scope and functional group tolerance, a few limitations also need to be noted (Figure 5). No conversion was detected with acetophenone derivatives containing *p*-groups such as coordinating cyano, acidic phenolic and boric acid as well as chelating  $\beta$ -ester (e.g. ethyl 3-oxo-3-phenylpropanoate) and  $\beta$ -acetyl substituents (e.g. 1-phenylbutane-1,3-dione).

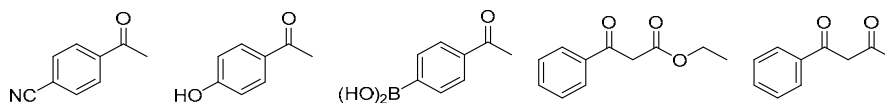
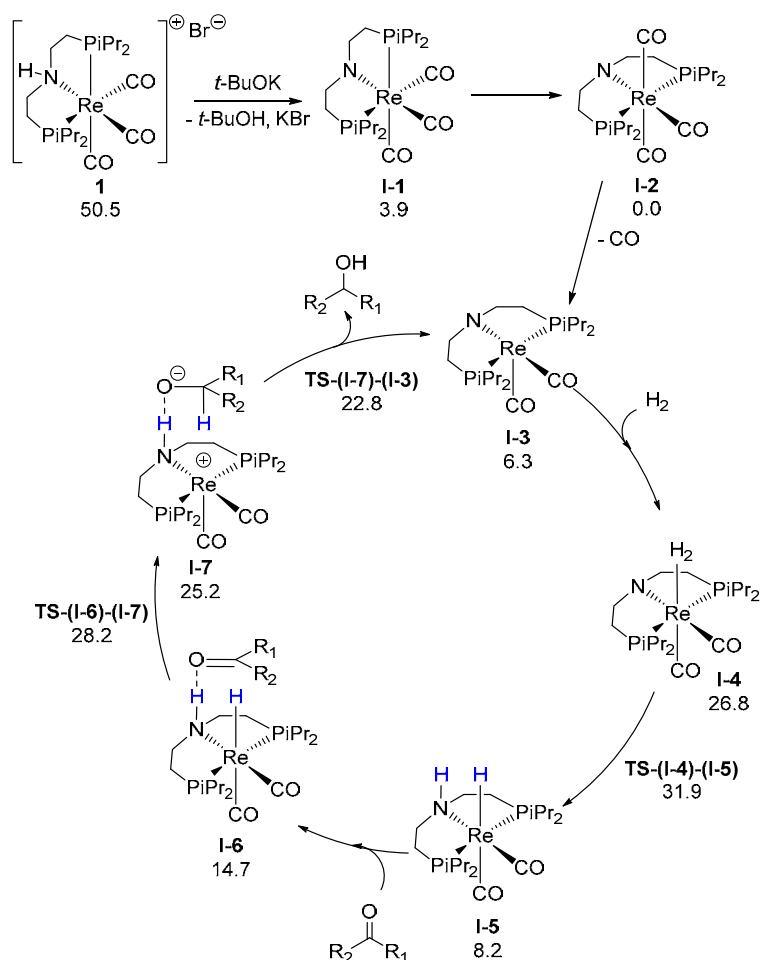


**Figure 5.** Non-working substrates

## 1.2. Mechanistic insights

On the basis of previous works of other groups on related complexes with Fe and Ru,<sup>[36]</sup> as well as our DFT(PBE0-D3) calculations, we propose the following mechanism (Scheme 4).





**Scheme 4.** Proposed catalytic cycle for the rhenium hydrogenation of ketones to give alcohols based on PBE0-D3 calculations. DFT computed Gibbs free energies ( $\text{kcal}\cdot\text{mol}^{-1}$ ) relative to **I-2** are shown.

In a first step, the base activates the precatalyst **1** by exoergic deprotonation of the NH moieties to form **I-1** ( $\Delta G = -46.6 \text{ kcal}\cdot\text{mol}^{-1}$ ), followed by the isomerisation to the more stable *mer*-[Re(P(N)P)(CO)<sub>3</sub>] complex **I-2** ( $\Delta G = -3.9 \text{ kcal}\cdot\text{mol}^{-1}$ ). Dissociation of CO from **I-2** is slightly uphill ( $\Delta G = 6.3 \text{ kcal}\cdot\text{mol}^{-1}$ ) and forms the 16-electron dicarbonyl complex **I-3** that is the active form of the catalyst. Endoergic coordination of H<sub>2</sub> to form **I-4** ( $\Delta G = 20.5 \text{ kcal}\cdot\text{mol}^{-1}$ ) is followed by facile heterolytic splitting of dihydrogen ( $\Delta G^\ddagger = 5.1 \text{ kcal}\cdot\text{mol}^{-1}$ ) to yield the amino-hydride intermediate **I-5**, only slightly less stable than **I-3** ( $\Delta G = 1.9 \text{ kcal}\cdot\text{mol}^{-1}$ ). Acetophenone forms an adduct with **I-5** essentially upon interaction of the carbonyl oxygen with the N-H proton ( $\Delta G = 6.5 \text{ kcal}\cdot\text{mol}^{-1}$ ). The carbonyl reduction is a two-steps process with first hydride transfer from Re to C ( $\Delta G^\ddagger = 13.5 \text{ kcal}\cdot\text{mol}^{-1}$  and  $\Delta G = 10.5 \text{ kcal}\cdot\text{mol}^{-1}$ ), followed by proton transfer from N-H to O, regenerating the active species **I-3**. Although TS-(**I-7**)-(**I-3**) is computed at higher electronic energy than **I-7**, this energy difference is reversed when Gibbs free energies are considered. Overall, the rate-determining step is the H<sub>2</sub> heterolytic splitting with an activation barrier of  $\Delta G^\ddagger = 31.9 \text{ kcal}\cdot\text{mol}^{-1}$  from **I-2**.

For the kinetic modeling, the Copasi software<sup>[37]</sup> was used and three reactions were considered to represent the catalytic transformation:

- 1) CO dissociation from I-2:  $\text{I-2} = \text{I-3} + \text{CO}$ . For this reaction, the reverse rate constant  $k_{-1}$  was considered to result from a diffusion limited coordination of CO and a value of  $1.2 \cdot 10^{10} \text{ mL}/(\text{mmol} \cdot \text{s})$  was used. This corresponds to an activation barrier  $\Delta G^\ddagger = 4.5 \text{ kcal} \cdot \text{mol}^{-1}$  at 353 K. The forward reaction rate constant  $k_1$  was thus the sum of the thermodynamic energy difference  $\Delta G = 6.3$  and this 4.5 value, resulting in  $k_1 = 1.6 \cdot 10^6 \text{ s}^{-1}$ .
- 2) H<sub>2</sub> splitting on I-3:  $\text{I-3} + \text{H}_2 = \text{I-5}$ . The forward rate constant  $k_2$  is associated to the energy difference between **TS-(I-4)-(I-5)** and **I-3**. With  $\Delta G^\ddagger = 25.6 \text{ kcal} \cdot \text{mol}^{-1}$ , this translates to  $k_2 = 9.65 \cdot 10^{-4} \text{ mL}/(\text{mmol} \cdot \text{s})$  at 353 K. For the forward reaction, the rate constant  $k_{-2}$  is obtained using the energy difference between **TS-(I-4)-(I-5)** and **I-5**. A value of  $k_{-2} = 0.0145 \text{ s}^{-1}$  is obtained at 353 K.
- 3) Ketone hydrogenation:  $\text{I-5} + \text{PhC(O)CH}_3 = \text{I-3} + \text{PhCH(OH)(CH}_3\text{)}$ . For this last step, the forward reaction is associated to a rate constant  $k_3$  obtained using the energy difference between **TS-(I-6)-(I-7)** and **I-5**,  $\Delta G^\ddagger = 20 \text{ kcal} \cdot \text{mol}^{-1}$ . A value of  $k_3 = 3.07 \text{ mL}/(\text{mmol} \cdot \text{s})$  is obtained at 353 K. For the reverse reaction, it is necessary to include the thermodynamic of the reaction,  $\Delta G = -2.8$  in the new energy of the active species **I-3**. Consequently the value of the reverse rate constant at 353 K is  $k_{-3} = 3.93 \cdot 10^{-3} \text{ mL}/(\text{mmol} \cdot \text{s})$ .

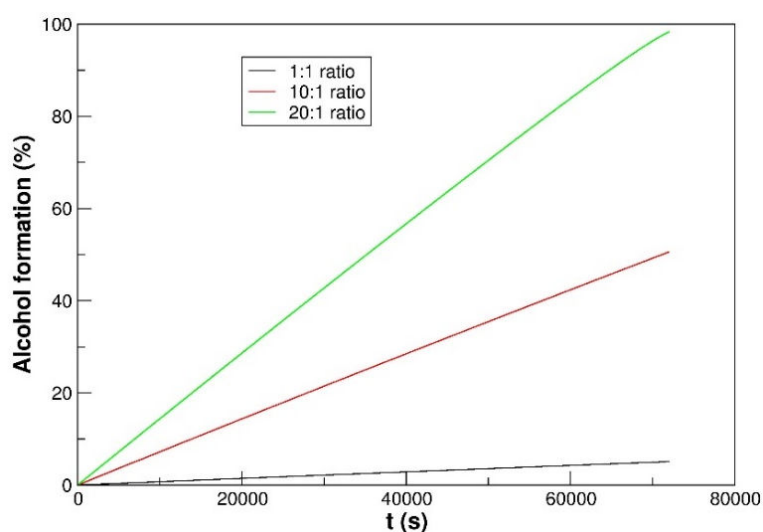


**Figure 6.** Rate of product of 1-phenylethanol depending on the concentration of H<sub>2</sub> using the kinetic modelling with Copasi with the calculated activation barriers.

With all these values for the various rate constants and using the initial concentration of **I-2**<sub>0</sub> = 0.005 mmol/mL, [H<sub>2</sub>]<sub>0</sub> = [PhC(O)(CH<sub>3</sub>)]<sub>0</sub> = 1 mmol/mL, the time evolution of the concentration in alcohol formed is shown in Figure 6 (black curve). This result indicated that with 0.5 mol% **I-2** and an equimolar ratio of acetophenone and H<sub>2</sub>, the yield in alcohol after 20 h is only approximately 5%. Changing the initial ration [H<sub>2</sub>]<sub>0</sub>/[PhC(O)(CH<sub>3</sub>)]<sub>0</sub> to 10:1 and 20:1 resulted in higher conversion to the alcohol (red and green curves, respectively). The conversion evolves from 5% in 20 hours (1:1) to 50% (10:1) and 98% (20:1). This qualitatively shows the importance of using significantly high pressure of H<sub>2</sub> and good stirring to facilitate the energy-demanding first step of the reaction by increasing the concentration of H<sub>2</sub>.

### 1.3. Conclusion

In conclusion, we have developed an efficient and general hydrogenation of carbonyl derivatives using a well-defined rhenium PN(H)P complex **1**. Of notable interest, the reduction proceeded well for a large range of substrates with low catalyst loading (0.5 mol%) under mild conditions (70 °C) and 30 bar of H<sub>2</sub>.

DFT calculations suggested that the hydrogen transfer from the catalyst to the ketone is a two-step process with first a hydride transfer from Re to C followed by proton transfer from N to O. However, the rate-determining step of the transformation has been found to be the heterotypic cleavage of H<sub>2</sub> across the Re-N bond. Kinetic modeling highlighted the importance of the actual value of the concentration of H<sub>2</sub> to induce full conversion.

## V-2 Mono *N*-methylation of anilines with methanol catalyzed by Re PN(H)P complexes

**Contributions in this part:** Synthesis of the complexes, optimization, and mechanistic studies: Duo Wei; Scope: Duo Wei, Omar Sadek; X-ray diffraction studies: Vincent Dorcet, Thierry Roisnel; DFT calculations: Eric Clot.

**Publication:** D. Wei, O. Sadek, V. Dorcet, T. Roisnel, C. Darcel, E. Gras, E. Clot, J.-B. Sortais, *J. Catal.* **2018**, *366*, 300-309.

### 2.1. Introduction

The first methylations of amines with methanol as alkylating reagent were developed using group 8-10 transition metal-based catalysts.<sup>[38]</sup> By contrast, group 7 transition metals remained in the shadow for designing catalysts for hydrogen borrowing reactions and related hydrogenations.<sup>[3]</sup> In particular, the activation of methanol<sup>[39]</sup> allowed mono *N*-methylation of amines,<sup>[40]</sup> formylation of amines,<sup>[41]</sup> and amino-methylation of aromatic compounds.<sup>[42]</sup>

With rhenium-based catalysts, hydrogen auto-transfer reactions are quite rare. Rhenium polyhydride phosphine complexes catalyzed acceptorless deshydrogenative coupling of alcohols with carbonyl derivatives,<sup>[43]</sup> amines or alcohols,<sup>[44]</sup> and amination of alcohols.<sup>[45]</sup> Heterogeneous rhenium catalysts promoted the *N*-methylation of amines with CO<sub>2</sub> and H<sub>2</sub>.<sup>[46]</sup>

In the course of the present study, Beller's group independently reported hydrogen autotransfer and related dehydrogenative coupling reactions to form  $\alpha$ -alkylated ketones and substituted pyrroles, using the rhenium PN(H)P pincer complex **1**.<sup>[47]</sup>

### 2.2. Results and discussions

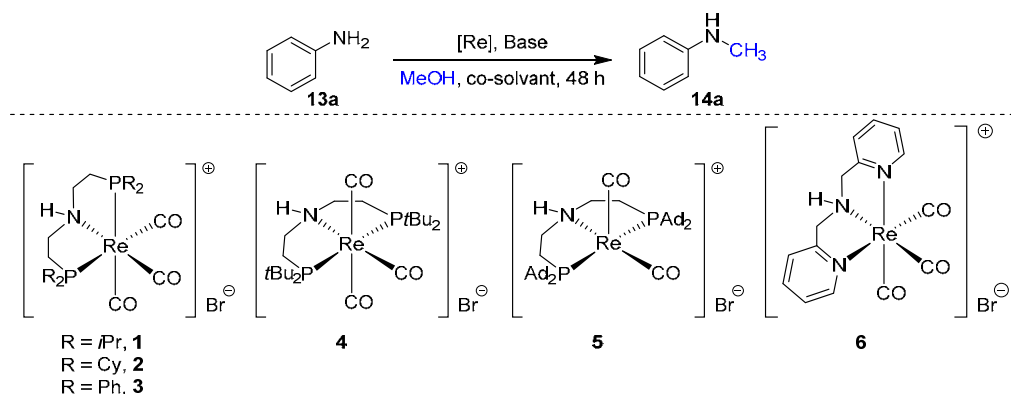
#### 2.2.1. Optimization of the reaction conditions for the mono *N*-methylation of aniline

In the previous part, we have demonstrated that the complex **1** efficiently promotes the hydrogenation of carbonyl derivatives with low catalyst loading.<sup>[48]</sup> Pursuing our investigations of this class of rhenium complexes, we decided to investigate the challenging methylation of amines with MeOH as alkylation agent. Hereafter, we describe the first example of methylation of aromatic amines with methanol catalyzed by rhenium catalysts with the exclusive formation of the mono *N*-methylated products.

Initial screening of the catalytic activity of the complexes **1-6** focused on the methylation of aniline **13a** with methanol (Table 4), using similar conditions as those optimized for manganese catalysts,<sup>[40b]</sup> *i.e.* in the presence of *t*BuOK (25 mol%) as the base, at 130 °C for 48 h (entries

1-7), and in a 1:1 (v:v) mixture of methanol and toluene as solvent. Gratifyingly, catalysts **1-3** were active, **3** giving the highest conversion (75%), whereas the complexes **4-6** and  $\text{Re}(\text{CO})_5\text{Br}$  were totally inactive (entries 4-7). It is worth noting that in all the reactions, the mono-methylated product **14a** was obtained nearly exclusively and that *N,N*-dimethylaniline was not detected by GC or NMR.

**Table 4.** Optimisation of the reaction parameters for *N*-methylation of aniline **13a** with methanol<sup>[a]</sup>



Entry	Catalyst (mol%)	Base (mol%)	T (°C)	Yield (%)
1 <sup>[b]</sup>	<b>1</b> (5.0)	<i>t</i> BuOK (25)	130	70
2 <sup>[b]</sup>	<b>2</b> (5.0)	<i>t</i> BuOK (25)	130	56
3 <sup>[b]</sup>	<b>3</b> (5.0)	<i>t</i> BuOK (25)	130	75
4 <sup>[b]</sup>	<b>4</b> (5.0)	<i>t</i> BuOK (25)	130	1
5 <sup>[b]</sup>	<b>5</b> (5.0)	<i>t</i> BuOK (25)	130	0
6 <sup>[b]</sup>	<b>6</b> (5.0)	<i>t</i> BuOK (25)	130	0
7 <sup>[b]</sup>	$\text{Re}(\text{CO})_5\text{Br}$ (5.0)	<i>t</i> BuOK (25)	130	0
8 <sup>[b]</sup>	<b>3</b> (1.0)	<i>t</i> BuOK (10)	140	87
9 <sup>[c]</sup>	<b>3</b> (1.0)	<i>t</i> BuOK (10)	140	85
10 <sup>[c]</sup>	<b>3</b> (1.0)	KOH (10)	140	47
11 <sup>[c]</sup>	<b>3</b> (1.0)	$\text{K}_2\text{CO}_3$ (10)	140	72
12 <sup>[c]</sup>	<b>3</b> (1.0)	$\text{Cs}_2\text{CO}_3$ (10)	140	96
13 <sup>[c]</sup>	<b>3</b> (1.0)	No base	140	0
14 <sup>[c]</sup>	No catalyst	$\text{Cs}_2\text{CO}_3$ (10)	140	1
15 <sup>[c]</sup>	<b>3</b> (1.0)	$\text{Cs}_2\text{CO}_3$ (5)	140	97
16 <sup>[c]</sup>	<b>3</b> (0.5)	$\text{Cs}_2\text{CO}_3$ (5)	140	96
17 <sup>[c]</sup>	<b>3</b> (0.5)	$\text{Cs}_2\text{CO}_3$ (1)	140	32

<sup>[a]</sup> General conditions: an ACE® pressure tube was charged in a glovebox with rhenium catalyst, aniline **13a**, base, and solvent, in that order. The tube was heated in an oil bath for 48 h. The yield was determined by GC and <sup>1</sup>H NMR of the crude mixture;

<sup>[b]</sup> 0.25 mmol scale, MeOH / toluene (0.5 mL / 0.5 mL) as solvent;

<sup>[c]</sup> 0.5 mmol scale, MeOH (2 mL) as solvent.

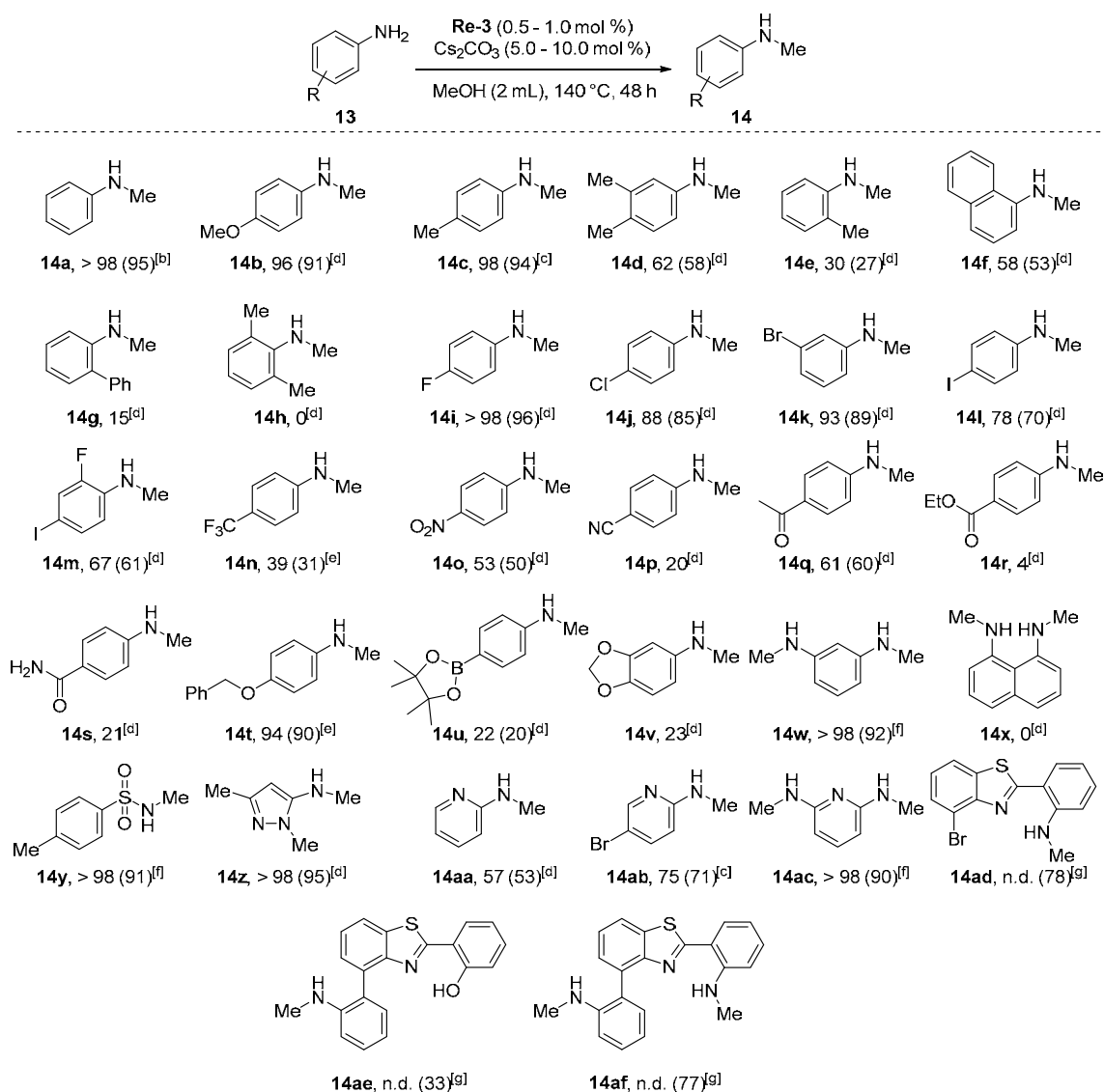
The reaction conditions were further optimized with the catalyst **3** at 140 °C, various bases were tested (entries 8-12),  $\text{Cs}_2\text{CO}_3$  being identified as the best one. The loading of catalyst was decreased to 0.5 mol% and the quantity of base could be lowered to 5.0 mol% without

significant loss of activity (entry 16). Blank reactions carried out in the absence of the catalyst **3** or a base demonstrated that both components were crucial, as no conversion was detected in each case (entries 13 and 14). Finally, the reaction could be performed directly in methanol acting as sole solvent and reactant. Compared to the parent manganese system (3.0 mol%, 100 mol% *t*BuOK, 100 °C, 24 h),<sup>[40a]</sup> the present rhenium system is more robust as the reaction proceeds well with both a lower catalyst loading and a lower amount of base, but displays a lower activity as 48 h at 140 °C are required to reach full conversions.

### 2.2.2. Scope for the mono *N*-methylation of anilines with methanol

With the optimized conditions in hand, we then evaluated the catalytic performance of **3** in the methylation of other aniline derivatives (Table 5). Almost quantitative conversions were obtained starting with *p*-methoxy- and *p*-methyl-aniline **13b** and **13c**. On the opposite, the conversion decreased as the hindrance of the anilines increased (**14d-14h**, 0-58% conversion). This behavior is in line with the trend observed in the case of the hydrogenation of ketones with the catalyst **1**, where slightly harsher conditions were required to convert sterically hindered ketones to the corresponding alcohols.<sup>[48]</sup> Halogenated anilines **13i-13n** were smoothly mono-methylated, even if the iodo substituted anilines led to lower performance. The tolerance toward various reducible and chelating functional groups was next evaluated. *p*-Nitro- (**13o**), *p*-acetyl- (**13q**) and *p*-benzyloxy-aniline (**13t**) were converted with moderate to good yields (50-90%) while anilines bearing a nitrile (**13p**), an ester (**13r**), a boronic ester (**13u**) or an primary amide (**13s**) groups were methylated in low conversions (4-21%).<sup>[48]</sup> Interestingly, each amino group of 1,3-diaminobenzene (**13w**) was methylated leading to **14w** in 92% isolated yield. On the opposite, the chelating 1,8-diaminonaphtalene (**13x**) poisoned the catalyst and no conversion was detected, in contrast with manganese catalyzed reaction for which 1*H*-perimidine was obtained.<sup>[40b]</sup> Tolylsulfonamide **13y** can be also methylated efficiently using 1 equiv. of base. Finally, heteroaromatic amines (**13z-13af**) such as pyrazolyl-amine, pyridinyl-amine, and benzothiazolyl-derivatives were successfully converted to the corresponding mono *N*-methylamine in 53-95% yields. Notably, 2,6-diaminopyridine **13ac** was fully converted selectively to the corresponding *N,N'*-dimethyl-2,6-diaminopyridine **14ac** in 90% yield. It is worth noting that aliphatic amines, such as dodecylamine or benzylamine, were not methylated even under forcing conditions (conditions d, Table 5).

**Table 5.** Scope of the reaction of methylation of aniline derivatives<sup>[a]</sup>



<sup>[a]</sup> General conditions: an ACE® pressure tube was charged in a glovebox with the rhenium catalyst **3**, aniline **13** (0.5 mmol), base, and solvent (2 mL), in that order. The tube was heated in an oil bath. Conversion was determined by <sup>1</sup>H NMR (isolated yield in parentheses);

<sup>[b]</sup> **3** (0.5 mol%), Cs<sub>2</sub>CO<sub>3</sub> (5.0 mol%);

<sup>[c]</sup> **3** (1.0 mol%), Cs<sub>2</sub>CO<sub>3</sub> (5.0 mol%);

<sup>[d]</sup> **3** (1.0 mol%), Cs<sub>2</sub>CO<sub>3</sub> (10.0 mol%);

<sup>[e]</sup> Starting material aniline was neutralized with 1 equiv. *t*-BuOK;

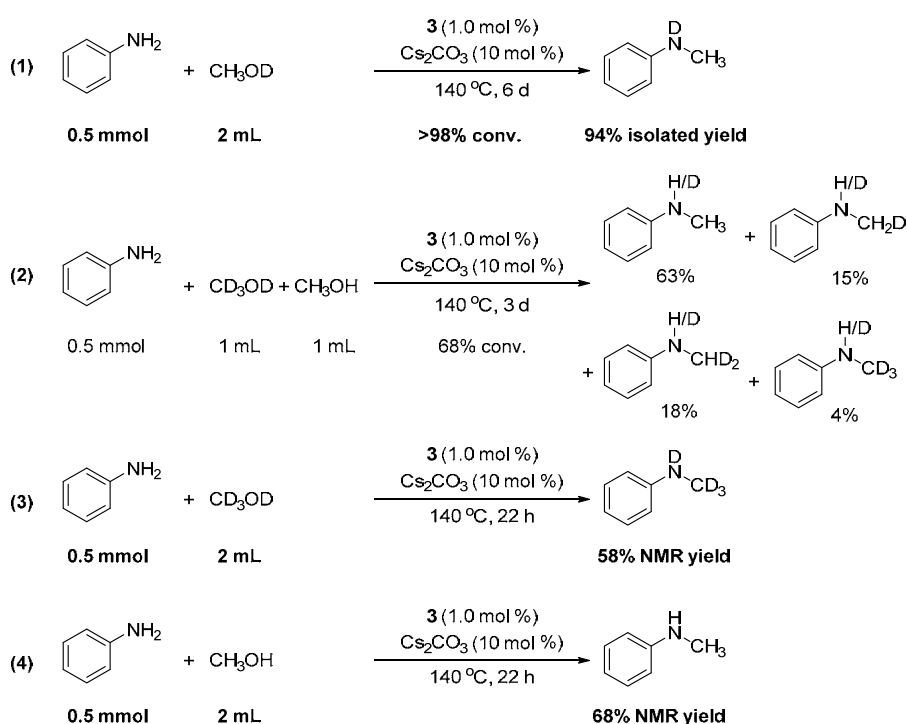
<sup>[f]</sup> **3** (1.0 mol%), Cs<sub>2</sub>CO<sub>3</sub> (100 mol%);

<sup>[g]</sup> **3** (5.0 mol%), Cs<sub>2</sub>CO<sub>3</sub> (100 mol%); 5 days.

### 2.3. Mechanistic insights

In order to get insight in the reaction mechanism, we have performed a series of experiments with deuterated methanol (Scheme 5).<sup>[49]</sup> In the presence of methanol-*d*<sup>1</sup>, *N*-methylaniline was obtained with no incorporation of deuterium on the methyl-group (Scheme 5, equation 1). This experiment suggests that during the reaction, H-D is not released as a gas, and that the protic deuterium O-D is selectively transferred to the nitrogen of the product *via* the catalyst. In a

second step, a mixture of CD<sub>3</sub>OD/CH<sub>3</sub>OH (1:1, v:v) was used in a competitive experiment (Scheme 5, equation 2): by analysis of the <sup>1</sup>H NMR of the crude mixture, we observed the incorporation of zero, one, two or three deuterium on the methyl of the product. The distribution of the product is in line with (i) the formation of methyldine-aniline Ph-N=CH<sub>2</sub> (78%) and deuterated methyldine-aniline-d<sup>2</sup> Ph-N=CD<sub>2</sub> (22%) and the corresponding hydrido-rhenium complexes, then (ii) the reduction of the mixture of imines statistically by the mixture of hydrido- and deuterio-rhenium complexes. Finally, we have checked the conversion after 22 h in parallel experiments: the conversion was 68% for CH<sub>3</sub>OH and 58% for CD<sub>3</sub>OD leading to a kinetic isotope effect of 1.17.



**Scheme 5.** Labelling experiments with deuterated methanol.

In order to rationalize the mechanism of this reaction, DFT (PBE0-D3) calculations have been carried out for the reaction of methanol with aniline catalyzed by **1**<sup>+</sup>. The active form of the catalyst was considered to be the neutral complex **II-2** resulting from deprotonation by the strong base of the nitrogen atom on the PNP ligand. That later adopts in **II-2** a meridional geometry (Figure 7). Dissociation of CO from **II-2** to yield **II-3** is computed to be slightly endergonic in methanol as a solvent ( $\Delta G = 0.8\text{ kcal}\cdot\text{mol}^{-1}$ ). The same process was computed to be more demanding energetically in toluene ( $\Delta G = 6.3\text{ kcal}\cdot\text{mol}^{-1}$ ).<sup>[48]</sup> All Gibbs free energy values given are referenced with respect to **II-3** + CH<sub>3</sub>OH + PhNH<sub>2</sub>. Creation of a hydrogen bond between methanol and the nitrogen atom of the PNP ligand leads to complex **II-8**



computed to lie at  $\Delta G = 9.0 \text{ kcal}\cdot\text{mol}^{-1}$  above **II-3** (Figure 7). A transition state structure, **TS-(II-8)-(II-9)**, could be located on the potential energy surface at  $\Delta G^\ddagger = 29.8 \text{ kcal}\cdot\text{mol}^{-1}$  with respect to **II-3**. In **TS-(II-8)-(II-9)**, formaldehyde, the product of methanol dehydrogenation, is interacting through a hydrogen bond with the protonated nitrogen ( $\text{N-H}\cdots\text{O} = 1.954 \text{ \AA}$ ). The distance between the carbonyl carbon and the hydride is long at  $2.7 \text{ \AA}$ . The geometry of the hydride rhenium complex **II-9** after dissociation of formaldehyde is almost identical to that of the corresponding fragment in **TS-(II-8)-(II-9)**. Thus dehydrogenation of methanol to formaldehyde catalyzed by **1** is computed to be an endergonic process ( $\Delta G = 19.5 \text{ kcal}\cdot\text{mol}^{-1}$ ) with an activation barrier of  $\Delta G^\ddagger = 29.8 \text{ kcal}\cdot\text{mol}^{-1}$  associated to a late TS structure.

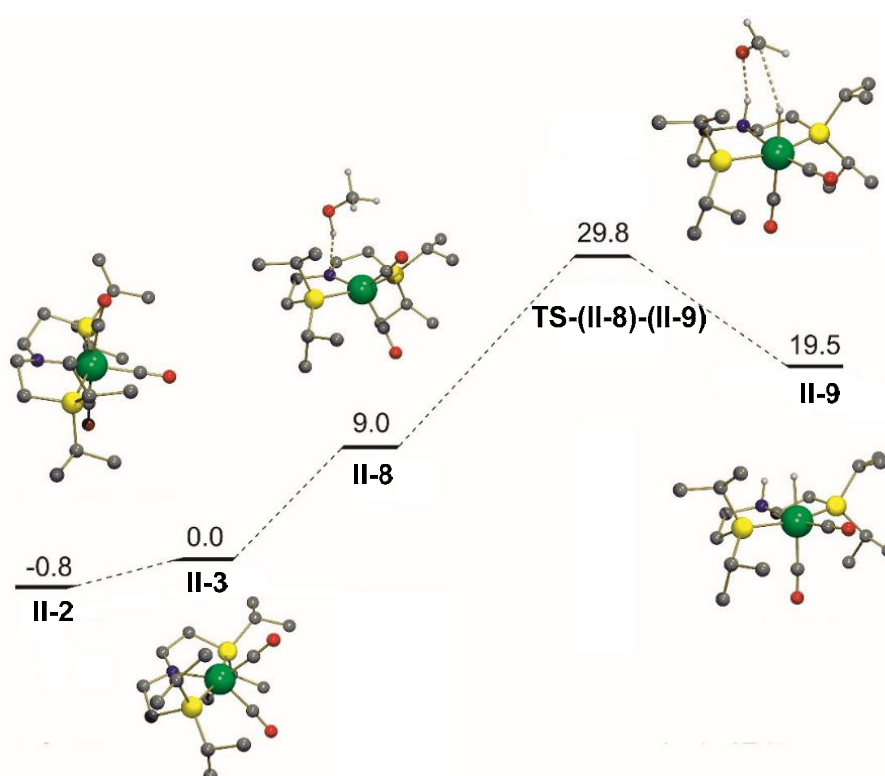


**Figure 7.** Computed reaction mechanism (Gibbs free energies in  $\text{kcal}\cdot\text{mol}^{-1}$  relative to **II-3** + MeOH + PhNH<sub>2</sub>) for the dehydrogenation of methanol. Most H atoms omitted for clarity.

Once formaldehyde is formed from methanol, it is considered to react easily with an amine to form an imine, with the formation of an hemiaminal as an intermediate. The hemiaminal is computed to be  $\Delta G = 0.4 \text{ kcal}\cdot\text{mol}^{-1}$  less stable than formaldehyde + amine, whereas the water + imine system is computed to lie at  $\Delta G = -3.7 \text{ kcal}\cdot\text{mol}^{-1}$  [The numbers in Figure 7 are for a reaction forming  $\text{H}_2\text{C}=\text{O}$  from MeOH and thus the free molecules in the evaluation of the energy of **II-9** are  $\text{H}_2\text{C}=\text{O}$ , CO and PhNH<sub>2</sub>. On Figure 8, the transformation is for the hydrogenation of the imine that was considered to be formed independently. Therefore, there is a shift in energy of  $3.7 \text{ kcal}\cdot\text{mol}^{-1}$  corresponding to the reaction energy of the transformation

$\text{PhNH}_2 + \text{H}_2\text{CO} = \text{H}_2\text{O} + \text{PhNCH}_2$ ]. Therefore, the imine formation is thermodynamically favored. Contrary to the case of methanol dehydrogenation, where no adduct could be found between formaldehyde and the hydride complex **II-9**, the adduct **II-10** between **II-11** and the imine is located at  $\Delta G = 25.8 \text{ kcal}\cdot\text{mol}^{-1}$  above **II-3** (Figure 8). From **II-10**, hydride transfer from Re to C, through **TS-(II-10)-(II-11)**, leads directly to **II-11** with  $\Delta G^\ddagger = 5.7 \text{ kcal}\cdot\text{mol}^{-1}$  and  $\Delta G = -26.4 \text{ kcal}\cdot\text{mol}^{-1}$  with respect to **II-10**. The dissociation of the amine from **II-11** regenerating the active catalyst **II-3** is favored thermodynamically with  $\Delta G = -8.3 \text{ kcal}\cdot\text{mol}^{-1}$ .

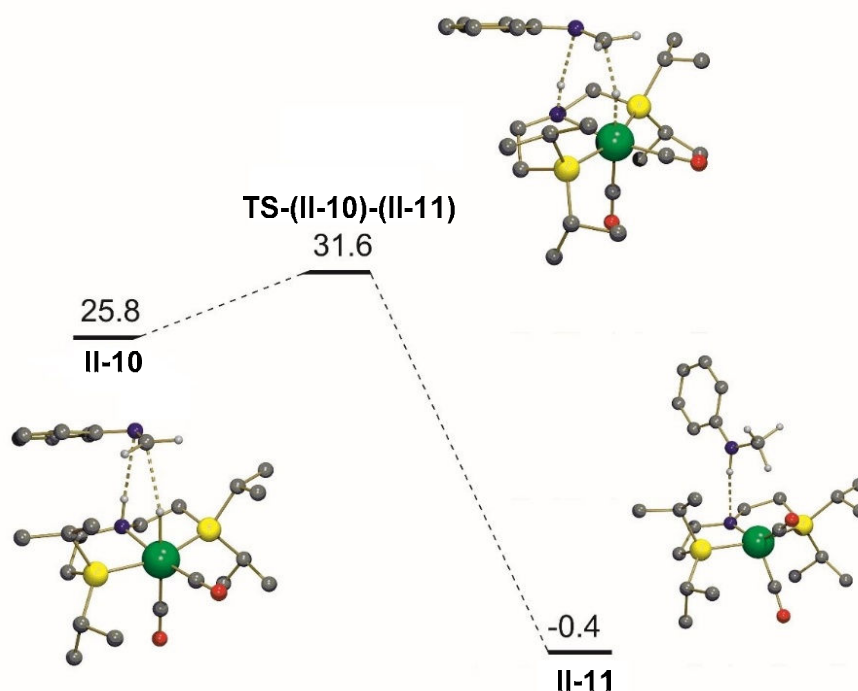
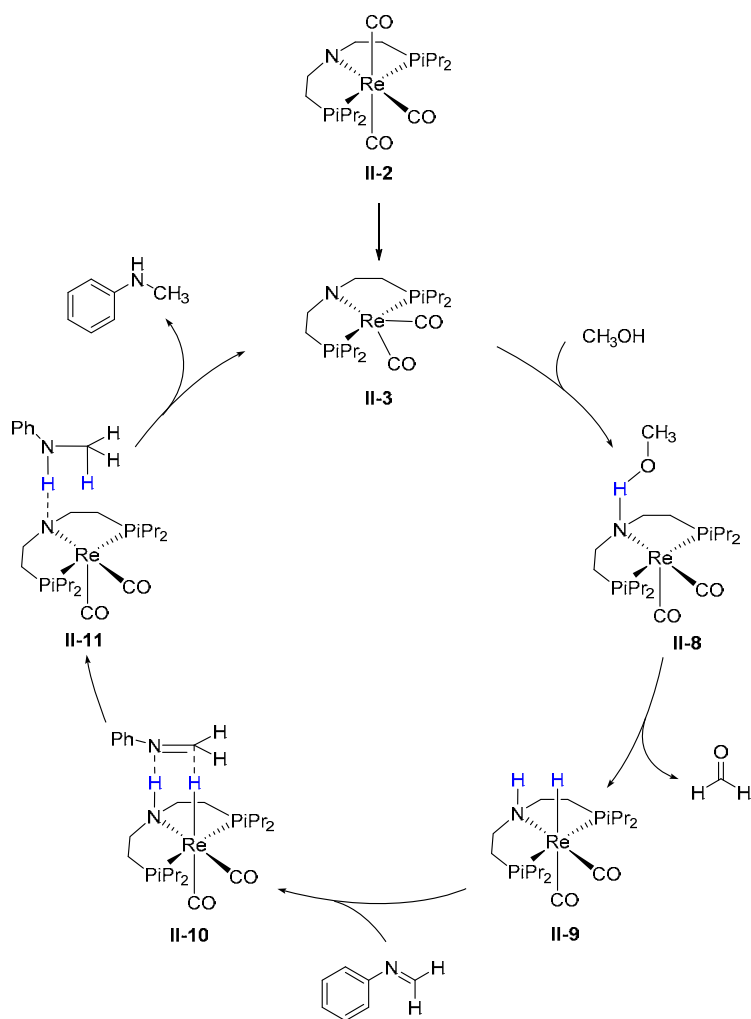


**Figure 8.** Computed reaction mechanism (Gibbs free energies in  $\text{kcal}\cdot\text{mol}^{-1}$  relative to **II-3**<sup>+</sup> + MeOH + PhNH<sub>2</sub>) for the hydrogenation of imine. Most H atoms omitted for clarity.

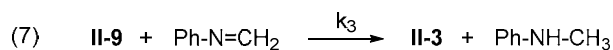
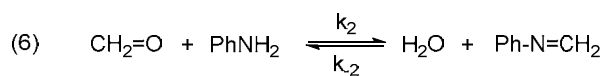
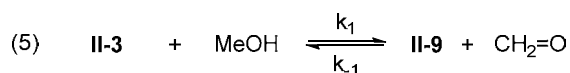
Overall, when the rhenium-dihydride **II-9** and imine are considered as the origin of energy, hydrogenation is associated to an activation barrier of  $\Delta G^\ddagger = 15.8 \text{ kcal}\cdot\text{mol}^{-1}$  and is favored thermodynamically with  $\Delta G = -24.8 \text{ kcal}\cdot\text{mol}^{-1}$ . This is to be compared with the hydrogenation of formaldehyde that has an activation barrier of  $\Delta G^\ddagger = 10.3 \text{ kcal}\cdot\text{mol}^{-1}$  and is favored thermodynamically by  $\Delta G = -19.5 \text{ kcal}\cdot\text{mol}^{-1}$  (see Figure 7). So once formaldehyde and imine are both present, hydrogenation by the rhenium-dihydride is kinetically preferred, while hydrogenation of the later is thermodynamically preferred. In comparison to the two aforementioned hydrogenation processes, formation of H<sub>2</sub> from **II-9** to regenerate **II-3** is computed to have an activation barrier of  $\Delta G^\ddagger = 28.6 \text{ kcal}\cdot\text{mol}^{-1}$  and is slightly exergonic ( $\Delta G = -2.4 \text{ kcal}\cdot\text{mol}^{-1}$ ). Therefore, the formation of H<sub>2</sub> from **II-9** is not a competitive pathway with

the hydrogenation processes to recover methanol from aldehyde or to form amine from imine. A simplified catalytic cycle is depicted on Scheme 6<sup>[50]</sup>.



**Scheme 6.** Simplified catalytic cycle.

A simplified kinetic model to describe the transformation from methanol to amine is given below (eq. 5-7, Scheme 7). The rate constants  $k_1$ ,  $k_{-1}$  and  $k_3$  can be estimated, using Eyring equation, from the computed values shown in Figures 7 and 8. The ratio  $k_2/k_{-2}$  is known from the computed value of the imine formation ( $\Delta G = -3.7 \text{ kcal}\cdot\text{mol}^{-1}$ ). The only unknown is the value of the activation barrier for the imine formation from nucleophilic attack of the amine on the aldehyde.



**Scheme 7.** Simplified kinetic model.

The experimental conditions shown in Scheme 5 equation (1) correspond to a ratio of 100:1:0.01 between methanol, aniline and catalyst initial concentrations. Figure 9 represents the evolution with time of the amine product concentration computed with the Copasi software using the kinetic model above and initial concentrations of the reactants in the same ratio as that of the actual experiments.<sup>[37]</sup> The different curves correspond to different values, ranging from 15 kcal•mol<sup>-1</sup> to 25 kcal•mol<sup>-1</sup>, for the activation barrier for the imine formation.

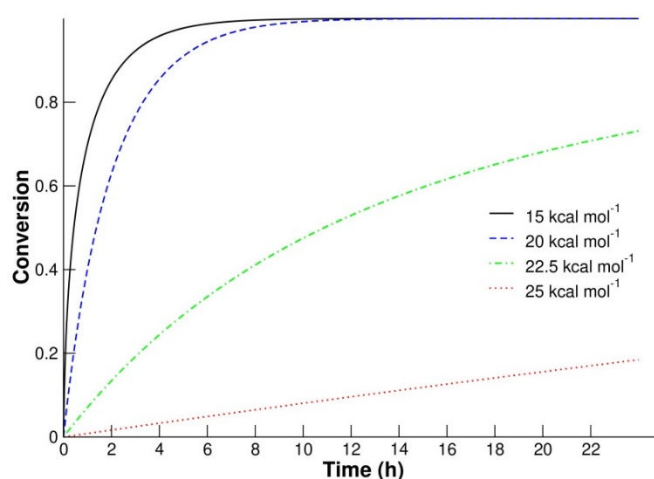


**Figure 9.** Time evolution of the concentration of the amine product Ph-NH-CH<sub>3</sub> using the kinetic model described by eq. 5-7 for different values of the rate constant  $k_2$ .

The results clearly illustrate the critical influence of the actual kinetics of imine formation on the overall reaction time. For a fast formation of imine from aldehyde, the reaction should be complete in less than 6 hours. The experimental observation of ca. 70% NMR yield after 22 hours (Scheme 5, eq. 4) is more in agreement with a significantly slow imine formation from aldehyde ( $\Delta G^\ddagger = 22.5$  kcal•mol<sup>-1</sup>, see Figure 9). Concentrating on the reactions occurring in the coordination sphere of the transition metal complex is not necessarily enough to fully understand the reactivity, and in particular the kinetics, of a catalytic system. Using an activation barrier of  $\Delta G^\ddagger = 22.5$  kcal•mol<sup>-1</sup> for the imine formation, the time evolution of the concentration of Ph-ND-CD<sub>3</sub> and Ph-NH-CH<sub>3</sub> are compared in Figure 10. The conversions after 22 hours are 70.8 and 58% for Ph-NH-CH<sub>3</sub> and Ph-ND-CD<sub>3</sub>, respectively. These results are in excellent agreement with the experimental observations for the parallel experiment. In addition, the ratio between the values of  $k_1$  for the dehydrogenation of CH<sub>3</sub>OH and CD<sub>3</sub>OD is computed to be 3.8, in very good agreement with the value of 3.54 deduced from the ratio of the different products observed in the competitive experiment [Scheme 5, eq. 2, ratio Ph-N=CH<sub>2</sub>:Ph-N=CD<sub>2</sub> = (63+15)/(18+4) = 78/22].

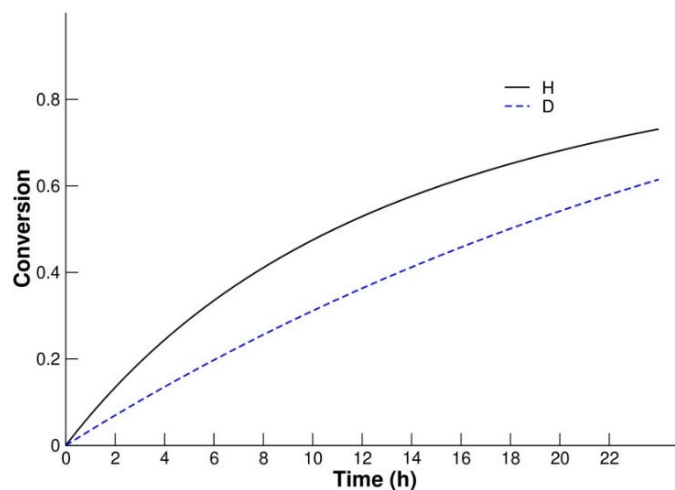


**Figure 10.** Time evolution of the concentration of Ph-NH-CH<sub>3</sub> and Ph-ND-CD<sub>3</sub> with an assumed activation barrier of  $\Delta G^\ddagger = 22.5 \text{ kcal}\cdot\text{mol}^{-1}$ .

## 2.4. Conclusion

In conclusion, a series of new rhenium complexes bearing aliphatic tridentate PNP ligands with various substituents on the phosphorus atom was proven to catalyze efficiently the selective *N*-methylation of aromatic amines with methanol with low amount of both catalyst (0.5 mol%) and base (5.0 mol%). The reaction proceeds well for a large range of substrates. The mechanism of the reaction was investigated by DFT calculations, showing the importance not only of the metal catalyzed processes on the kinetics but also the role of the formation of the organic intermediate, namely the imine.

## V-3 Synthesis of quinolines through acceptorless dehydrogenative coupling catalyzed by Re PN(H)P complexes

**Contributions in this part:** Synthesis of the complexes, optimization and scope: Duo Wei; X-ray diffraction studies: Vincent Dorcet.

**Publication:** D. Wei, V. Dorcet, C. Darcel, J.-B. Sortais, *ChemSusChem* **2019**, *12*, 3078-3082.

### 3.1. Introduction

For the indirect Friedländer reaction, several catalytic systems based on group 8 to 10 transition metals (Ru,<sup>[51]</sup> Rh,<sup>[52]</sup> Pd,<sup>[53]</sup> Ir,<sup>[54]</sup> Au<sup>[55]</sup>, Cu,<sup>[56]</sup> Co<sup>[57]</sup>) have been developed. In particular, our group reported the first non-noble metal catalyzed Friedländer annulation reaction using iron Knölker-type complexes.<sup>[58]</sup> It is also worth noting that stoichiometric amount of bases are also able to promote metal-free indirect Friedländer reactions.<sup>[59]</sup>

By contrast, group 7 transition metals based catalysts have just emerged very recently as suitable metals for promoting hydrogen borrowing reactions.<sup>[3]</sup> Manganese catalysis for (de)-hydrogenation reactions has grown exponentially over the last two years.<sup>[4c, 4h-j, 40a, 40c, 60]</sup> Nevertheless, to date, only three catalytic systems are reported for the synthesis of quinolines, two of which are using over-stoichiometric amount of bases.<sup>[61]</sup> On the opposite, hydrogen auto-transfer reactions catalyzed by rhenium are still quite rare.<sup>[43-46]</sup> Interestingly, an efficient synthesis of quinolines, pyrimidines, quinoxalines, pyrroles, and aminomethylated aromatic compounds catalyzed by a Re(I) PN<sup>3</sup>P pincer complex was described by the group of Kirchner, in succession of this current study.<sup>[62]</sup> In the last two parts of this chapter, we have developed a series of rhenium complexes with the tridentate PN(H)P ligands (Scheme 2, **1-5**), which are efficiently employed in the hydrogenation of carbonyl derivatives<sup>[48]</sup> and mono *N*-methylation of anilines with methanol as C1 source *via* hydrogen auto-transfer.<sup>[63]</sup>

### 3.2. Results and discussions

Inspired by these recent developments in the area of synthesis of *N*-heterocycles and following our interest in hydrogenation<sup>[60g, 64]</sup> and hydrogenation borrowing reactions<sup>[40b]</sup> based on group 7 transition metal complexes, we described herein the first example synthesis of quinolines *via* acceptorless dehydrogenative coupling catalyzed by rhenium catalysts in the presence of a catalytic amount of base.

### 3.2.1. Optimization of reaction conditions of the quinoline synthesis

Initially, we selected 2-aminobenzyl alcohol (**15a**, 1.0 equiv.) and 1-phenylethanol (**16a**, 1.0equiv.) as a benchmark system for the dehydrogenative cross-coupling formation of 2-phenylquinoline (Table 6). All reactions were performed with a stoichiometric ratio between the two coupling partners. Complexes **1**, **2** and **3** showed excellent reactivity (entries 1-3) at a catalyst loading of 5.0 mol% in toluene at 140 °C for 24 h in the presence of catalytic amount of *t*-BuOK (10 mol%), giving respectively 88%, 87% and, 90% yields. Not surprisingly, complexes **4** and **5**, bearing the more steric hindered PNP ligands, and the precursor Re(CO)<sub>5</sub>Br were not active, (entries 4-6) which is in line with the reactivity already observed for the mono *N*-methylation of anilines.<sup>[63]</sup>

**Table 6.** Optimization of the parameters of the reaction.<sup>[a]</sup>

Nc1ccccc1CO (**15a**) + c1ccccc1C(O)C (**16a**)  $\xrightarrow[\text{Toluene, 24 h}]{\text{cat. base}}$  c1ccc(cc1)-c2ccccc2n3ccccc13 (**17a**)

**1**: R = *i*Pr, **2**: R = Cy, **3**: R = Ph  
**4**: R = *t*Bu  
**5**: R = Ad

Entry	Cat.(mol%)	Base (mol%)	Temp. (°C)	Yield (%)
1	<b>1</b> (5.0)	<i>t</i> -BuOK (10)	140	88
2	<b>2</b> (5.0)	<i>t</i> -BuOK (10)	140	87
3	<b>3</b> (5.0)	<i>t</i> -BuOK (10)	140	90
4	<b>4</b> (5.0)	<i>t</i> -BuOK (10)	140	7
5	<b>5</b> (5.0)	<i>t</i> -BuOK (10)	140	5
6	Re(CO) <sub>5</sub> Br (5.0)	<i>t</i> -BuOK (10)	140	0
7	<b>3</b> (1.0)	<i>t</i> -BuOK (10)	150	87
8	<b>3</b> (1.0)	KOH (10)	150	70
9	<b>3</b> (1.0)	Cs <sub>2</sub> CO <sub>3</sub> (10)	150	58
10	<b>3</b> (1.0)	K <sub>2</sub> CO <sub>3</sub> (10)	150	3
11	<b>3</b> (1.0)	None	150	0
12	No catalyst	<i>t</i> -BuOK (10)	150	3
13	<b>3</b> (1.0)	<i>t</i> -BuOK (5.0)	150	74
14	<b>3</b> (1.0)	<i>t</i> -BuOK (2.0)	150	50

<sup>[a]</sup> General conditions: in an argon-filled glovebox, a Schlenk tube was charged with rhenium catalyst, **15a**, **16a**, base and solvent, in that order. The reaction was heated in an oil bath with argon stream. The yield of **17a** was determined by <sup>1</sup>H NMR.

The conditions of the reaction were further optimized with catalyst **3** (1.0 mol%) at 150 °C: various bases were tested (entries 7-10), showing that *t*-BuOK was the best candidate, giving 87% yield. Further decreasing of the amount of base to 5.0 or 2.0 mol% led to lower yields, 74% and 54% respectively (entries 13 and 14). Two blank reactions, in the absence of catalyst or base, gave no detectable conversion, demonstrating that the presence of both components is important in this protocol (entries 11 and 12).

### 3.2.2 Scope for synthesis of quinolines

With our optimized conditions in hands, we then explored the substrates amenable for this transformation (Tables 7, 8 and 9).

**Table 7.** Synthesis of quinolines *via* the annulation of 2-aminobenzyl alcohol with aromatic alcohols and ketones under the catalysis of rhenium complex **3**.

Entry	16	18	Conv./% (Yield /%)	Entry	16	18	Conv./% (Yield /%)
1			90 (87)	13 <sup>[c]</sup>			93 (91)
2 <sup>[b]</sup>			>98 (91)				
3			>98 (93)	14			>98 (92)
4			18c R = F 95 (80)	15			>98 (95)
5			18d R = Cl 97 (92)				
6			18e R = Br 93 (89)				
7			18f R = I 81 (75)				
8			18g R = OMe 85 (79)				
9			18h R = CF <sub>3</sub> 90 (85)				
10			87 (79)	16 <sup>[d]</sup>			>98 (95)
11			86 (80)	17 <sup>[d]</sup>			97 (86)
12			96 (91)	18 <sup>[d]</sup>			>98 (96)

<sup>[a]</sup> General reaction conditions: **15a** (0.5 mmol), **16** or **17** (0.5 mmol), catalyst **3** (1.0 mol%), toluene (2 mL), *t*-BuOK (10 mol%) at 150 °C with argon stream for 24 h; isolated yield in parenthesis.

<sup>[b]</sup> Acetophenone was used instead of 1-phenylethanol.

<sup>[c]</sup> Yield of isolated product with 7% of starting material **16l**.

<sup>[d]</sup> 1.0 mmol of **15a** was used.

Firstly, with 2-aminobenzyl alcohol **15a**, a series of secondary aromatic alcohols or ketones were engaged as coupling partners (Table 7). The reaction proceeded well for various



substituted 1-phenylethanol derivatives. (Table 7, entries 1-9). 1-(naphthalen-2-yl)ethanol (**16b**) gave full conversion and **18b** was isolated with an excellent isolated yield (93%). Halide substituents, such as fluoro, chloro, bromo and even iodo groups at the *para*-position of the phenyl ring were well-tolerated (**18c-18f**, 75-92% isolated yields, entries 4-7).

Substrates bearing electron-donating and electron-withdrawing groups, such as *p*-methoxy-1-phenylethanol **16g**, *p*-trifluoromethyl-1-phenylethanol **16h**, were well tolerated, affording the products **18g** and **18h** in 79% and 85% isolated yields, respectively (entries 7 and 8). It should be noted that starting from acetophenone instead of 1-phenylethanol (Table 7 entry 1 vs entry 2), slightly higher conversion and isolated yield were obtained (>98 vs 90% conversion), as the dehydrogenation reaction step is not needed when using ketones. 1-Phenylpropanol **16i** and 1-tetralol **16j** gave the corresponding 2,3-disubstituted quinolines **18i** and **18j** in good isolated yields (entries 10 and 11). Interestingly, heteroaromatic alcohols (**16k**, **16m** and **16n**) or ketones (**17l**, **17o-q**), based on pyridine, thiophene and benzofuran core, were smoothly converted into corresponding 2-heteroaryl quinolines. In particular, 1,2 or 1,3-diketones, such **17o**, **17p** and **17q**, gave di-quinolinyl (hetero)-arene products in quantitative yields, which could be further employed in coordination chemistry as polydentate ligands (entries 16-18).

Then, aliphatic and cyclic alcohols were engaged in this acceptorless dehydrogenative coupling. Disappointingly, the coupling of cyclohexanol, used as the model aliphatic secondary alcohols, did not proceed (4% yield, Table 8, entry 1), even if **15a** was fully consumed yielding mostly 2-aminobenzaldehyde. It is likely that the dehydrogenative oxidation of aliphatic alcohol is more difficult than the one of 1-phenylethanol derivatives leading to relatively stable arylketone intermediates. Therefore, we continued to explore the scope with aliphatic ketones. Under our standard conditions, starting from cyclic substrates and aliphatic ketones **17r-17v**, the corresponding quinolines **17r-17v** were obtained in good isolated yields (up to 96%). Notably, a cyclopropyl-substituted ketone **17u** furnished **18u** in quantitative yield, which indicated that the reaction did not proceed *via* stable radical intermediates. The reaction of phenylacetaldehyde (**17w**) with **15a** led to 3-phenylquinoline **18w** in moderate yield (63%, entry 7). Finally, 2-aminoacetophenone **15b** can be converted smoothly into 2-phenyl-4-methylquinoline **18x** by coupling with **16a** (entry 8).

**Table 8.** Scope of the synthesis of quinoline derivatives with aliphatic ketones and aldehydes.

Entry	15	17	18	Conv./% (Yield /%)
1 <sup>[b]</sup> 2				>98 (4) >98 (86)
	15a	17r	18r	
3 <sup>[c]</sup>				>98 (88)
	15a	17s	18s	
4				80 (76)
	15a	17t	18t	
5				92 (89)
	15a	17u	18u	
6 <sup>[d]</sup>				>98 (96)
	15a	17v	18v	
7 <sup>[e]</sup>				95 (63)
	15a	17w	18w	
8				>98 (89)
	15b	16a	18x	

<sup>[a]</sup> General reaction conditions: catalyst **3** (1.0 mmol%), **15** (0.5 mmol), **16** or **17** (0.5 mmol), toluene (2 mL), *t*-BuOK (10 mol%) at 150 °C under argon stream for 24 h; isolated yield in parenthesis.

<sup>[b]</sup> Cyclohexanol was used instead of cyclohexanone and NMR yield is shown in parentheses.

<sup>[c]</sup> Yield of isolated product with 8% of starting material **15a**.

<sup>[d]</sup> 1.0 mL of acetone was used.

<sup>[e]</sup> 130 °C

Interestingly, 2-phenylacetonitrile **19a** has been recently proven to be an effective annulation partner in the synthesis of 2-alkylaminoquinolines.<sup>[65]</sup> To our delight, **19a** could also be smoothly converted to 2-amino-3-phenylquinoline **20a** with our catalytic system at 140 °C (Table 9). The molecular structure of **20a** (as well as **20b**) were confirmed by X-Ray diffraction studies (Figure 11).

As shown in Table 9, all the reactions proceeded smoothly and gave the desired products in moderate to good isolated yields. In particular, bromo-substituted 2-phenylacetonitriles **19b**

and **19c** gave the corresponding products **20b** and **20c**, in 67% and 33% yield respectively (entries 2 and 3). Interestingly, halogen-containing products, such as **19b** and **19c**, can be further converted into more complex molecules *via* cross-coupling reactions. 2-(2-thiophenyl)acetonitrile **19d** afforded the corresponding product in high yield (90%, entry 4) while, unexpectedly, the parent 2-(3-thiophenyl)acetonitrile **19e** led to moderate conversion (42%) (entries 4 and 5). Eventually, aliphatic butyronitrile **19f** gave 2-amino-3-ethylquinoline **20f** in good yield 80%.

**Table 9.** Scope of the synthesis of 2-amino-quinoline derivatives with nitriles.

Entry	19	9	Conv./% (Yield %)
1			70 (67)
2			67 (52)
3			33
4			95 (90)
5			42
6 <sup>[b]</sup>			93 (80)

<sup>[a]</sup> General reaction conditions: catalyst **3** (1.0 mmol%), **15a** (0.5 mmol), **19** (0.5 mmol), *t*-BuOK (10 mol%), toluene (2 mL) at 140 °C for 24 h; isolated yield in parenthesis.

<sup>[b]</sup> 2.0 equiv. of **19f** was used

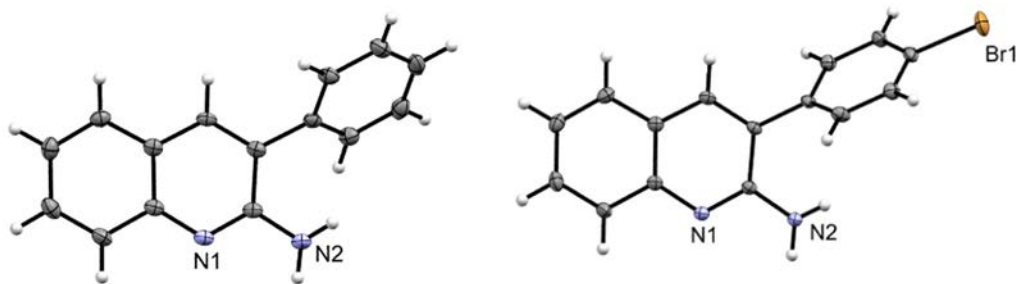


**Figure 11.** Perspective view of the products **20a** (left) and **20b** (right), thermal ellipsoids drawn at the 50% probability level.

### 3.3. Conclusion

In summary, a practical and sustainable synthesis of substituted quinolines was achieved *via* the annulation of 2-aminobenzyl alcohol with a variety of secondary alcohols, ketones, aldehyde or nitriles. The reaction proceeds with a high atom efficiency *via* a sequence of dehydrogenation and condensation steps that give rise to selective C–C and C–N bond formations. The key to develop this first rhenium catalyzed acceptorless dehydrogenative coupling was the use of a well-defined complex bearing a tridentate diphosphinoamino ligand as the catalyst (1.0 mol%) in the presence of *t*-BuOK (10 mol%) at 150 °C.

## V-4 Conclusion of Chapter V

In this chapter, we have described that a series of amino-bisphosphino ligands coordinated rhenium catalysts (synthesized and fully characterized) can efficiently promote the:

- 1) hydrogenation of carbonyl derivatives with a general substrate scope. DFT calculations suggested that the rate-determining step of the transformation is the heterotypic cleavage of H<sub>2</sub> across the Re-N bond.
- 2) mono *N*-methylation of anilines using methanol with low amount of both catalyst (0.5 mol%) and base (5.0 mol%). The reaction proceeds well for a large range of substrates. The mechanism of the reaction was also investigated by DFT calculations, showing the importance not only of the metal catalyzed processes on the kinetics but also the role of the formation of the organic intermediate: imine.
- 3) practical and sustainable synthesis of quinolines derivatives through acceptorless dehydrogenative coupling with low catalyst loading (1.0 mol%) in the presence of *t*-BuOK (10 mol%) and broad substrates scope were developed thereafter.

## V-5 References

- [1] J. G. De Vries, C. J. Elsevier, *The Handbook of Homogeneous Hydrogenation*, WILEY-VCH, Weinheim, **2007**.
- [2] a) J. G. de Vries, P. J. Deuss, K. Barta, *Catal. Sci. Technol.* **2014**, *4*, 1174-1196; b) G. W. Huber, S. Iborra, A. Corma, *Chem. Rev.* **2006**, *106*, 4044-4098; c) C.-H. Zhou, X. Xia, C.-X. Lin, D.-S. Tong, J. Beltramini, *Chem. Soc. Rev.* **2011**, *40*, 5588-5617; d) P. N. R. Vennestrøm, C. M. Osmundsen, C. H. Christensen, E. Taarning, *Angew. Chem. Int. Ed.* **2011**, *50*, 10502-10509.
- [3] a) D. A. Valyaev, G. Lavigne, N. Lugan, *Coord. Chem. Rev.* **2016**, *308*, 191-235; b) Y. Kuninobu, K. Takai, *Chem. Rev.* **2011**, *111*, 1938-1953.
- [4] a) R. I. Khusnutdinov, A. R. Bayguzina, U. M. Dzhemilev, *Russ. J. Org. Chem.* **2012**, *48*, 309-348; b) M. Garbe, K. Junge, M. Beller, *Eur. J. Org. Chem.* **2017**, 4344-4362; c) B. Maji, M. K. Barman, *Synthesis* **2017**, *49*, 3377-3393; d) F. Kallmeier, R. Kempe, *Angew. Chem. Int. Ed.* **2018**, *57*, 46-60; e) N. Gorgas, K. Kirchner, *Acc. Chem. Res.* **2018**, *51*, 1558-1569; f) G. A. Filonenko, R. van Putten, E. J. M. Hensen, E. A. Pidko, *Chem. Soc. Rev.* **2018**, *47*, 1459-1483; g) T. Zell, R. Langer, *ChemCatChem* **2018**, *10*, 1930-1940; h) S. Elangovan, C. Topf, S. Fischer, H. Jiao, A. Spannenberg, W. Baumann, R. Ludwig, K. Junge, M. Beller, *J. Am. Chem. Soc.* **2016**, *138*, 8809-8814; i) A. Mukherjee, A. Nerush, G. Leitus, L. J. W. Shimon, Y. Ben David, N. A. Espinosa Jalapa, D. Milstein, *J. Am. Chem. Soc.* **2016**, *138*, 4298-4301; j) F. Kallmeier, R. Kempe, *Angew. Chem. Int. Ed.* **2018**, *57*, 46-60.
- [5] a) D. Baudry, M. Ephritikhine, H. Felkin, R. Holmes-Smith, *J. Chem. Soc., Chem. Commun.* **1983**, 788-789; b) D. Baudry, M. Ephritikhine, H. Felkin, *J. Chem. Soc., Chem. Commun.* **1980**, 1243-1244.
- [6] D. G. DeWit, K. Folting, W. E. Streib, K. G. Caulton, *Organometallics* **1985**, *4*, 1149-1153.
- [7] a) Y. Jiang, H. Berke, *Chem. Commun.* **2007**, 3571-3573; b) A. Choualeb, E. Maccaroni, O. Blacque, H. W. Schmalle, H. Berke, *Organometallics* **2008**, *27*, 3474-3481; c) B. Dudle, K. Rajesh, O. Blacque, H. Berke, *J. Am. Chem. Soc.* **2011**, *133*, 8168-8178; d) Y. Jiang, B. Schirmer, O. Blacque, T. Fox, S. Grimme, H. Berke, *J. Am. Chem. Soc.* **2013**, *135*, 4088-4102; e) Y. Jiang, W. Huang, H. W. Schmalle, O. Blacque, T. Fox, H. Berke, *Organometallics* **2013**, *32*, 7043-7052; f) A. Choualeb, A. J. Lough, D. G. Gusev, *Organometallics* **2007**, *26*, 3509-3515; g) K. Rajesh, B. Dudle, O. Blacque, H. Berke, *Adv. Synth. Catal.* **2011**, *353*, 1479-1484.
- [8] A. Landwehr, B. Dudle, T. Fox, O. Blacque, H. Berke, *Chem. Eur. J.* **2012**, *18*, 5701-5714.
- [9] a) H. Grützmacher, *Angew. Chem. Int. Ed.* **2008**, *47*, 1814-1818; b) W. Kuriyama, T. Matsumoto, O. Ogata, Y. Ino, K. Aoki, S. Tanaka, K. Ishida, T. Kobayashi, N. Sayo, T. Saito, *Org. Process Res. Dev.* **2012**, *16*, 166-171.
- [10] a) H. Doucet, T. Ohkuma, K. Murata, T. Yokozawa, M. Kozawa, E. Katayama, A. F. England, T. Ikariya, R. Noyori, *Angew. Chem. Int. Ed.* **1998**, *37*, 1703-1707; b) R. Noyori, T. Ohkuma, *Angew. Chem. Int. Ed.* **2001**, *40*, 40-73; c) S. E. Clapham, A. Hadzovic, R. H. Morris, *Coord. Chem. Rev.* **2004**, *248*, 2201-2237; d) B. Zhao, Z. Han, K. Ding, *Angew. Chem. Int. Ed.* **2013**, *52*, 4744-4788.
- [11] a) P. T. Anastas, J. C. Warner, *Green Chemistry: Theory and Practice*, Oxford University Press, New York, **1998**; b) P. T. Anastas, M. M. Kirchhoff, *Acc. Chem. Res.* **2002**, *35*, 686-694.
- [12] a) G. Yan, A. J. Borah, L. Wang, M. Yang, *Adv. Synth. Catal.* **2015**, *357*, 1333-1350; b) B. Li, J.-B. Sortais, C. Darcel, *RSC Adv.* **2016**, *6*, 57603-57625.
- [13] a) O. Jacquet, X. Frogneux, C. Das Neves Gomes, T. Cantat, *Chem. Sci.* **2013**, *4*, 2127-2131; b) E. Blondiaux, J. Pouessel, T. Cantat, *Angew. Chem. Int. Ed.* **2014**, *53*, 12186-12190; c) X. Frogneux, O. Jacquet, T. Cantat, *Catal. Sci. Technol.* **2014**, *4*, 1529-1533; d) A. Tlili, X. Frogneux, E. Blondiaux, T. Cantat, *Angew. Chem. Int. Ed.* **2014**, *53*, 2543-2545; e) A. Tlili, E. Blondiaux, X. Frogneux, T. Cantat, *Green Chem.* **2015**, *17*, 157-168; f) K. Beydoun, T. vom Stein, J. Klankermayer, W. Leitner, *Angew. Chem. Int. Ed.* **2013**, *52*, 9554-9557; g) S. Das, F. D. Bobbink, G. Laurenczy, P. J. Dyson, *Angew. Chem. Int. Ed.* **2014**, *53*, 12876-12879; h) G. Jin, C. G. Werncke, Y. Escudié, S. Sabo-Etienne, S. Bontemps, *J. Am. Chem. Soc.* **2015**, *137*, 9563-9566; i) Y. Li, I. Sorribes, T. Yan, K. Junge, M. Beller, *Angew. Chem. Int. Ed.* **2013**, *52*, 12156-12160; j) Q. Liu, L. Wu, R. Jackstell, M. Beller, *Nat. Commun.* **2015**, *6*, 5933; k) K.

- Beydoun, G. Ghattas, K. Thenert, J. Klankermayer, W. Leitner, *Angew. Chem. Int. Ed.* **2014**, *53*, 11010-11014.
- [14] a) J. Zheng, C. Darcel, J.-B. Sortais, *Chem. Commun.* **2014**, *50*, 14229-14232; b) Y. Li, I. Sorribes, C. Vicent, K. Junge, M. Beller, *Chem. Eur. J.*, **2015**, *21*, 16759-16763; c) J. R. Cabrero-Antonino, R. Adam, K. Junge, M. Beller, *Catal. Sci. Technol.* **2016**, *6*, 7956-7966.
- [15] a) S. Savourey, G. Lefevre, J.-C. Berthet, T. Cantat, *Chem. Commun.* **2014**, *50*, 14033-14036; b) L. Zhu, L.-S. Wang, B. Li, W. Li, B. Fu, *Catal. Sci. Technol.* **2016**, *6*, 6172-6176; c) I. Sorribes, K. Junge, M. Beller, *Chem. Eur. J.* **2014**, *20*, 7878-7883.
- [16] K. Natte, H. Neumann, M. Beller, R. V. Jagadeesh, *Angew. Chem. Int. Ed.* **2017**, *56*, 6384-6394.
- [17] a) T. D. Nixon, M. K. Whittlesey, J. M. J. Williams, *Dalton Trans.* **2009**, 753-762; b) C. Gunanathan, D. Milstein, *Science* **2013**, *341*, 1229712; c) S. Bähn, S. Imm, L. Neubert, M. Zhang, H. Neumann, M. Beller, *ChemCatChem* **2011**, *3*, 1853-1864; d) D. Hollmann, *ChemSusChem* **2014**, *7*, 2411-2413; e) M. Pera-Titus, F. Shi, *ChemSusChem* **2014**, *7*, 720-722; f) G. E. Dobereiner, R. H. Crabtree, *Chem. Rev.* **2010**, *110*, 681-703; g) G. Guillena, D. J. Ramón, M. Yus, *Chem. Rev.* **2010**, *110*, 1611-1641; h) A. J. A. Watson, J. M. J. Williams, *Science* **2010**, *329*, 635-636; i) M. H. S. A. Hamid, P. A. Slatford, J. M. J. Williams, *Adv. Synth. Catal.* **2007**, *349*, 1555-1575; j) Q. Yang, Q. Wang, Z. Yu, *Chem. Soc. Rev.* **2015**, *44*, 2305-2329; k) F. Huang, Z. Liu, Z. Yu, *Angew. Chem. Int. Ed.* **2016**, *55*, 862-875; l) Y. Obora, *ACS Catal.* **2014**, *4*, 3972-3981; m) A. M. Faisca Phillips, A. J. L. Pombeiro, M. N. Kopylovich, *ChemCatChem* **2017**, *9*, 217-246.
- [18] a) G. A. Olah, *Angew. Chem. Int. Ed.* **2005**, *44*, 2636-2639; b) G. A. Olah, *Angew. Chem. Int. Ed.* **2013**, *52*, 104-107.
- [19] <http://www.methanol.org/> as of Jul. 2019
- [20] a) M. Usman, W. M. A. W. Daud, *RSC Adv.* **2015**, *5*, 21945-21972; b) Y.-N. Li, R. Ma, L.-N. He, Z.-F. Diao, *Catal. Sci. Technol.* **2014**, *4*, 1498-1512; c) I. Ganesh, *Renew. Sust. Energ. Rev.* **2014**, *31*, 221-257; d) K. A. Ali, A. Z. Abdullah, A. R. Mohamed, *Renew. Sust. Energ. Rev.* **2015**, *44*, 508-518; e) N. S. Shamsul, S. K. Kamarudin, N. A. Rahman, N. T. Kofli, *Renew. Sust. Energ. Rev.* **2014**, *33*, 578-588; f) B. Sam, B. Breit, M. J. Krische, *Angew. Chem. Int. Ed.* **2015**, *54*, 3267-3274; g) C. Chauvier, T. Cantat, *ACS Catal.* **2017**, *7*, 2107-2115.
- [21] J. A. Joule, K. Mills, *Heterocyclic Chemistry*, 5<sup>th</sup> Edition, Wiley-Blackwell, Chichester, **2010**.
- [22] a) J. P. Michael, *Nat. Prod. Rep.* **1999**, *16*, 697-709; b) J. P. Michael, *Nat. Prod. Rep.* **2002**, *19*, 742-760.
- [23] a) M. Krishnamurthy, B. D. Gooch, P. A. Beal, *Org. Lett.* **2004**, *6*, 63-66; b) J. B. Chaires, J. Ren, M. Henary, O. Zegrocka, G. R. Bishop, L. Strekowski, *J. Am. Chem. Soc.* **2003**, *125*, 7272-7283; c) A. Wissner, E. Overbeek, M. F. Reich, M. B. Floyd, B. D. Johnson, N. Mamuya, E. C. Rosfjord, C. Discafani, R. Davis, X. Shi, S. K. Rabindran, B. C. Gruber, F. Ye, W. A. Hallett, R. Nilakantan, R. Shen, Y.-F. Wang, L. M. Greenberger, H.-R. Tsou, *J. Med. Chem.* **2003**, *46*, 49-63; d) N. Kaila, K. Janz, S. DeBernardo, P. W. Bedard, R. T. Camphausen, S. Tam, D. H. H. Tsao, J. C. Keith, C. Nickerson-Nutter, A. Shilling, R. Young-Sciame, Q. Wang, *J. Med. Chem.* **2007**, *50*, 21-39; e) B. D. Lindner, Y. Zhang, S. Höfle, N. Berger, C. Teusch, M. Jesper, K. I. Hardcastle, X. Qian, U. Lemmer, A. Colsmann, U. H. F. Bunz, M. Hamburger, *J. Mater. Chem. C* **2013**, *1*, 5718-5724; f) S. A. Lawrence, *Amines: Synthesis, Properties and Applications*, Cambridge University Press, Cambridge U.K., **2004**.
- [24] Z. H. Skraup, *Monatsh. Chem. Verw. Teile. Anderer Wiss.* **1880**, *1*, 316-318.
- [25] R. Camps, *Arch. Pharm.* **1899**, *237*, 659-691.
- [26] L. Knorr, *Justus Liebigs Ann. Chem.*, **1886**, *236*, 69-115.
- [27] P. A. Keller, 7.05 - Pyridines and their Benzo Derivatives: Synthesis in *Comprehensive Heterocyclic Chemistry III* (Eds.: A. R. Katritzky, C. A. Ramsden, E. F. V. Scriven, R. J. K. Taylor), Elsevier, Oxford, **2008**, pp. 217-308.
- [28] J. Marco-Contelles, E. Pérez-Mayoral, A. Samadi, M. d. C. Carreiras, E. Soriano, *Chem. Rev.* **2009**, *109*, 2652-2671.
- [29] A. Corma, J. Navas, M. J. Sabater, *Chem. Rev.* **2018**, *118*, 1410-1459.

- [30] a) H.-F. Lang, P. E. Fanwick, R. A. Walton, *Inorg. Chim. Acta* **2002**, 329, 1-8; b) O. V. Ozerov, J. C. Huffman, L. A. Watson, K. G. Caulton, *Organometallics* **2003**, 22, 2539-2541; c) O. V. Ozerov, L. A. Watson, M. Pink, K. G. Caulton, *J. Am. Chem. Soc.* **2004**, 126, 6363-6378; d) O. V. Ozerov, L. A. Watson, M. Pink, K. G. Caulton, *J. Am. Chem. Soc.* **2007**, 129, 6003-6016; e) T. J. Korstanje, M. Lutz, J. T. B. H. Jastrzebski, R. J. M. Klein Gebbink, *Organometallics* **2014**, 33, 2201-2209; f) A. T. Radosevich, J. G. Melnick, S. A. Stoian, D. Bacciu, C.-H. Chen, B. M. Foxman, O. V. Ozerov, D. G. Nocera, *Inorg. Chem.* **2009**, 48, 9214-9221; g) M. Porchia, F. Tisato, F. Refosco, C. Bolzati, M. Cavazza-Ceccato, G. Bandoli, A. Dolmella, *Inorg. Chem.* **2005**, 44, 4766-4776; h) F. Tisato, F. Refosco, M. Porchia, C. Bolzati, G. Bandoli, A. Dolmella, A. Duatti, A. Boschi, C. M. Jung, H.-J. Pietzsch, W. Kraus, *Inorg. Chem.* **2004**, 43, 8617-8625; i) C. Bolzati, F. Refosco, A. Cagnolini, F. Tisato, A. Boschi, A. Duatti, L. Uccelli, A. Dolmella, E. Marotta, M. Tubaro, *Eur. J. Inorg. Chem.* **2004**, 1902-1913; j) Y.-S. Kim, Z. Hea, R. Schibli, S. Liu, *Inorg. Chim. Acta* **2006**, 359, 2479-2488; k) I. Klopsch, M. Kinauer, M. Finger, C. Würtele, S. Schneider, *Angew. Chem. Int. Ed.* **2016**, 55, 4786-4789; l) I. Klopsch, M. Finger, C. Würtele, B. Milde, D. B. Werz, S. Schneider, *J. Am. Chem. Soc.* **2014**, 136, 6881-6883; m) M. Vogt, A. Nerush, Y. Diskin-Posner, Y. Ben-David, D. Milstein, *Chem. Sci.* **2014**, 5, 2043-2051; n) M. Vogt, A. Nerush, M. A. Iron, G. Leituss, Y. Diskin-Posner, L. J. W. Shimon, Y. Ben-David, D. Milstein, *J. Am. Chem. Soc.* **2013**, 135, 17004-17018.
- [31] N. S. Lambic, R. D. Sommer, E. A. Ison, *Dalton Trans.* **2018**, 47, 758-768.
- [32] S. R. Banerjee, M. K. Levadala, N. Lazarova, L. Wei, J. F. Valliant, K. A. Stephenson, J. W. Babich, K. P. Maresca, J. Zubietta, *Inorg. Chem.* **2002**, 41, 6417-6425.
- [33] E. Alberico, P. Sponholz, C. Cordes, M. Nielsen, H.-J. Drexler, W. Baumann, H. Junge, M. Beller, *Angew. Chem. Int. Ed.* **2013**, 52, 14162-14166.
- [34] M. Käß, A. Friedrich, M. Drees, S. Schneider, *Angew. Chem. Int. Ed.* **2009**, 48, 905-907.
- [35] M. Bertoli, A. Choualeb, A. J. Lough, B. Moore, D. Spasyuk, D. G. Gusev, *Organometallics* **2011**, 30, 3479-3482.
- [36] a) S. Chakraborty, P. O. Lagaditis, M. Förster, E. A. Bielinski, N. Hazari, M. C. Holthausen, W. D. Jones, S. Schneider, *ACS Catal.* **2014**, 4, 3994-4003; b) R. Xu, S. Chakraborty, S. M. Bellows, H. Yuan, T. R. Cundari, W. D. Jones, *ACS Catal.* **2016**, 6, 2127-2135; c) X. Yang, *ACS Catal.* **2013**, 3, 2684-2688.
- [37] S. Hoops, S. Sahle, R. Gauges, C. Lee, J. Pahle, N. Simus, M. Singhal, L. Xu, P. Mendes, U. Kummer, *Bioinformatics* **2006**, 22, 3067-3074.
- [38] a) R. Grigg, T. R. B. Mitchell, S. Sutthivaiyakit, N. Tongpenyai, *J. Chem. Soc., Chem. Commun.* **1981**, 611-612; b) H. Keun-Tae, T. Yasushi, K. Masanobu, O. Fumio, W. Yoshihisa, *Chem. Lett.* **1988**, 17, 449-452; c) S. Naskar, M. Bhattacharjee, *Tetrahedron Lett.* **2007**, 48, 3367-3370; d) F. Li, J. Xie, H. Shan, C. Sun, L. Chen, *RSC Adv.* **2012**, 2, 8645-8652; e) J. Campos, L. S. Sharninghausen, M. G. Manas, R. H. Crabtree, *Inorg. Chem.* **2015**, 54, 5079-5084; f) T. T. Dang, B. Ramalingam, A. M. Seayad, *ACS Catal.* **2015**, 5, 4082-4088; g) V. N. Tsarev, Y. Morioka, J. Caner, Q. Wang, R. Ushimaru, A. Kudo, H. Naka, S. Saito, *Org. Lett.* **2015**, 17, 2530-2533; h) L. Zhang, Y. Zhang, Y. Deng, F. Shi, *RSC Adv.* **2015**, 5, 14514-14521; i) C.-P. Xu, Z.-H. Xiao, B.-Q. Zhuo, Y.-H. Wang, P.-Q. Huang, *Chem. Commun.* **2010**, 46, 7834-7836; j) T. Oku, Y. Arita, H. Tsuneki, T. Ikariya, *J. Am. Chem. Soc.* **2004**, 126, 7368-7377; k) A. Del Zotto, W. Baratta, M. Sandri, G. Verardo, P. Rigo, *Eur. J. Inorg. Chem.* **2004**, 2004, 524-529; l) K. Chakrabarti, M. Maji, D. Panja, B. Paul, S. Shee, G. K. Das, S. Kundu, *Org. Lett.* **2017**; m) B. Paul, S. Shee, K. Chakrabarti, S. Kundu, *ChemSusChem* **2017**, 10, 2370-2374.
- [39] M. Andérez-Fernández, L. K. Vogt, S. Fischer, W. Zhou, H. Jiao, M. Garbe, S. Elangovan, K. Junge, H. Junge, R. Ludwig, M. Beller, *Angew. Chem. Int. Ed.* **2017**, 56, 559-562.
- [40] a) S. Elangovan, J. Neumann, J.-B. Sortais, K. Junge, C. Darcel, M. Beller, *Nat. Commun.* **2016**, 7, 12641; b) A. Bruneau-Voisine, D. Wang, V. Dorcet, T. Roisnel, C. Darcel, J.-B. Sortais, *J. Catal.* **2017**, 347, 57-62; c) J. Neumann, S. Elangovan, A. Spannenberg, K. Junge, M. Beller, *Chem. Eur. J.* **2017**, 23, 5410-5413.
- [41] S. Chakraborty, U. Gellrich, Y. Diskin-Posner, G. Leituss, L. Avram, D. Milstein, *Angew. Chem. Int. Ed.* **2017**, 56, 4229-4233.
- [42] M. Mastalir, E. Pittenauer, G. Allmaier, K. Kirchner, *J. Am. Chem. Soc.* **2017**, 139, 8812-8815.



- [43] H. Jin, J. Xie, C. Pan, Z. Zhu, Y. Cheng, C. Zhu, *ACS Catal.* **2013**, *3*, 2195-2198.
- [44] P. P. M. Schlekter, R. Honeker, J. Klankermayer, W. Leitner, *ChemCatChem* **2013**, *5*, 1762-1764.
- [45] A. Abdulkader, H. Jin, Y. Cheng, C. Zhu, *Tetrahedron Lett.* **2014**, *55*, 4172-4174.
- [46] T. Toyao, S. M. A. H. Siddiki, Y. Morita, T. Kamachi, A. S. Touchy, W. Onodera, K. Kon, S. Furukawa, H. Ariga, K. Asakura, K. Yoshizawa, K. i. Shimizu, *Chem. Eur. J.*, **2017**, *23*, 14848-14859.
- [47] P. Piehl, M. Pena-Lopez, A. Frey, H. Neumann, M. Beller, *Chem. Commun.* **2017**, *53*, 3265-3268.
- [48] D. Wei, T. Roisnel, C. Darcel, E. Clot, J.-B. Sortais, *ChemCatChem* **2017**, *9*, 80-83.
- [49] E. M. Simmons, J. F. Hartwig, *Angew. Chem. Int. Ed.* **2012**, *51*, 3066-3072.
- [50] Z. Wei, A. de Aguirre, K. Junge, M. Beller, H. Jiao, *Catal. Sci. Technol.* **2018**, *8*, 3649-3665.
- [51] a) C. S. Cho, B. T. Kim, T.-J. Kim, S. C. Shim, *Chem. Commun.* **2001**, 2576-2577; b) C. S. Cho, B. T. Kim, H.-J. Choi, T.-J. Kim, S. C. Shim, *Tetrahedron* **2003**, *59*, 7997-8002; c) R. Martínez, D. J. Ramón, M. Yus, *Tetrahedron* **2006**, *62*, 8982-8987; d) R. Martinez, D. J. Ramon, M. Yus, *Eur. J. Org. Chem.* **2007**, *2007*, 1599-1605; e) H. Vander Mierde, N. Ledoux, B. Allaert, P. Van Der Voort, R. Drozdak, D. De Vos, F. Verpoort, *New J. Chem.* **2007**, *31*, 1572-1574; f) H. Vander Mierde, P. Van Der Voort, D. De Vos, F. Verpoort, *Eur. J. Org. Chem.* **2008**, *2008*, 1625-1631; g) D. Srimani, Y. Ben-David, D. Milstein, *Chem. Commun.* **2013**, *49*, 6632-6634; h) B. Pan, B. Liu, E. Yue, Q. Liu, X. Yang, Z. Wang, W.-H. Sun, *ACS Catal.* **2016**, *6*, 1247-1253; i) S. Michlik, R. Kempe, *Angew. Chem. Int. Ed.* **2013**, *52*, 6326-6329; j) M. Maji, K. Chakrabarti, B. Paul, B. C. Roy, S. Kundu, *Adv. Synth. Catal.* **2018**, *360*, 722-729.
- [52] C. S. Cho, H. J. Seok, S. O. Shim, *J. Heterocycl. Chem.* **2005**, *42*, 1219-1222.
- [53] a) C. S. Cho, W. X. Ren, S. C. Shim, *Bull. Korean Chem. Soc.* **2005**, *26*, 1286; b) C. S. Cho, W. X. Ren, *J. Organomet. Chem.* **2007**, *692*, 4182-4186; c) B. W. J. Chen, L. L. Chng, J. Yang, Y. Wei, J. Yang, J. Y. Ying, *ChemCatChem* **2013**, *5*, 277-283.
- [54] a) K. Taguchi, S. Sakaguchi, Y. Ishii, *Tetrahedron Lett.* **2005**, *46*, 4539-4542; b) X. Yu, W. Yao, W. Hu, D. Wang, *Russ. J. Gen. Chem.* **2016**, *86*, 376-379; c) S. Ruch, T. Irrgang, R. Kempe, *Chem. Eur. J.* **2014**, *20*, 13279-13285; d) R. Wang, H. Fan, W. Zhao, F. Li, *Org. Lett.* **2016**, *18*, 3558-3561; e) S. Michlik, R. Kempe, *Nat. Chem.* **2013**, *5*, 140-144.
- [55] S. Atechian, N. Nock, R. D. Norcross, H. Ratni, A. W. Thomas, J. Verron, R. Masciadri, *Tetrahedron* **2007**, *63*, 2811-2823.
- [56] C. S. Cho, W. X. Ren, N. S. Yoon, *J. Mol. Catal. A: Chem.* **2009**, *299*, 117-120.
- [57] S. Shee, K. Ganguli, K. Jana, S. Kundu, *Chem. Commun.* **2018**, *54*, 6883-6886.
- [58] S. Elangovan, J.-B. Sortais, M. Beller, C. Darcel, *Angew. Chem. Int. Ed.* **2015**, *54*, 14483-14486.
- [59] a) H. V. Mierde, P. V. D. Voort, F. Verpoort, *Tetrahedron Lett.* **2008**, *49*, 6893-6895; b) N. Anand, S. Koley, B. J. Ramulu, M. S. Singh, *Org. Biomol. Chem.* **2015**, *13*, 9570-9574; c) H. V. Mierde, P. V. D. Voort, F. Verpoort, *Tetrahedron Lett.* **2009**, *50*, 201-203; d) Y.-F. Liang, X.-F. Zhou, S.-Y. Tang, Y.-B. Huang, Y.-S. Feng, H.-J. Xu, *RSC Adv.* **2013**, *3*, 7739-7742; e) Y. Zhu, C. Cai, *RSC Adv.* **2014**, *4*, 52911-52914; f) R. Martínez, D. J. Ramón, M. Yus, *J. Org. Chem.* **2008**, *73*, 9778-9780.
- [60] a) M. Peña-López, P. Piehl, S. Elangovan, H. Neumann, M. Beller, *Angew. Chem. Int. Ed.* **2016**, *55*, 14967-14971; b) F. Kallmeier, T. Irrgang, T. Dietel, R. Kempe, *Angew. Chem. Int. Ed.* **2016**, *55*, 11806-11809; c) M. Mastalir, M. Glatz, N. Gorgas, B. Stöger, E. Pittenauer, G. Allmaier, L. F. Veiros, K. Kirchner, *Chem. Eur. J.* **2016**, *22*, 12316-12320; d) M. B. Widegren, G. J. Harkness, A. M. Z. Slawin, D. B. Cordes, M. L. Clarke, *Angew. Chem. Int. Ed.* **2017**, *56*, 5825-5828; e) V. Papa, J. R. Cabrero-Antonino, E. Alberico, A. Spanneberg, K. Junge, H. Junge, M. Beller, *Chem. Sci.* **2017**, *8*, 3576-3585; f) M. Perez, S. Elangovan, A. Spannenberg, K. Junge, M. Beller, *ChemSusChem* **2017**, *10*, 83-86; g) A. Bruneau-Voisine, D. Wang, V. Dorcet, T. Roisnel, C. Darcel, J.-B. Sortais, *Org. Lett.* **2017**, *19*, 3656-3659; h) N. Deibl, R. Kempe, *Angew. Chem. Int. Ed.* **2017**, *56*, 1663-1666; i) F. Kallmeier, B. Dudziec, T. Irrgang, R. Kempe, *Angew. Chem. Int. Ed.* **2017**, *56*, 7261-7265; j) N. A. Espinosa-Jalapa, A. Kumar, G. Leitius, Y. Diskin-Posner, D. Milstein, *J. Am. Chem. Soc.* **2017**, *139*, 11722-11725; k) N. A. Espinosa-Jalapa, A. Nerush, L. J. W. Shimon, G. Leitius, L. Avram, Y. Ben-David, D. Milstein, *Chem. Eur. J.* **2017**,

- 23, 5934-5938; l) A. Kumar, N. A. Espinosa-Jalapa, G. Leitus, Y. Diskin-Posner, L. Avram, D. Milstein, *Angew. Chem. Int. Ed.* **2017**, *56*, 14992-14996; m) B. M. K., W. Satyadeep, M. Biplab, *Angew. Chem. Int. Ed.* **2018**, *57*, 9126-9130; n) R. Fertig, T. Irrgang, F. Freitag, J. Zander, R. Kempe, *ACS Catal.* **2018**, *8*, 8525-8530; o) M. Glatz, B. Stöger, D. Himmelbauer, L. F. Veiros, K. Kirchner, *ACS Catal.* **2018**, *8*, 4009-4016.
- [61] a) M. Mastalir, M. Glatz, E. Pittenauer, G. Allmaier, K. Kirchner, *J. Am. Chem. Soc.* **2016**, *138*, 15543-15546; b) B. M. K., J. Akash, M. Biplab, *Adv. Synth. Catal.* **2018**, *0*; c) K. Das, A. Mondal, D. Srimani, *Chem. Commun.* **2018**, *54*, 10582-10585.
- [62] M. Mastalir, M. Glatz, E. Pittenauer, G. Allmaier, K. Kirchner, *Org. Lett.* **2019**, *21*, 1116-1120.
- [63] D. Wei, O. Sadek, V. Dorcet, T. Roisnel, C. Darcel, E. Gras, E. Clot, J.-B. Sortais, *J. Catal.* **2018**, *366*, 300-309.
- [64] a) H. Li, D. Wei, A. Bruneau-Voisine, M. Ducamp, M. Henrion, T. Roisnel, V. Dorcet, C. Darcel, J.-F. Carpentier, J.-F. Soulé, J.-B. Sortais, *Organometallics* **2018**, *37*, 1271-1279; b) A. Bruneau-Voisine, D. Wang, T. Roisnel, C. Darcel, J.-B. Sortais, *Catal. Commun.* **2017**, *92*, 1-4; c) D. Wei, A. Bruneau-Voisine, T. Chauvin, V. Dorcet, T. Roisnel, D. A. Valyaev, N. Lugan, J.-B. Sortais, *Adv. Synth. Catal.* **2018**, *360*, 676-681; d) D. Wei, A. Bruneau-Voisine, D. A. Valyaev, N. Lugan, J.-B. Sortais, *Chem. Commun.* **2018**, *54*, 4302-4305; e) D. Wang, A. Bruneau-Voisine, J.-B. Sortais, *Catal. Commun.* **2018**, *105*, 31-36.
- [65] W. Lv, B. Xiong, H. Jiang, M. Zhang, *Adv. Synth. Catal.* **2017**, *359*, 1202-1207.

## V-6 Experimental data

### 6.1. General information

All reactions were carried out with oven-dried glassware using standard Schlenk techniques under an inert atmosphere of dry argon or in an argon-filled glove-box. Toluene, THF, diethyl ether (Et<sub>2</sub>O), and CH<sub>2</sub>Cl<sub>2</sub> were dried over Braun MB-SPS-800 solvent purification system and degassed by thaw-freeze cycles. Technical grade petroleum ether, diethyl ether were used for chromatography column. Analytical TLC was performed on Merck 60F<sub>254</sub> silica gel plates (0.25 mm thickness). Column chromatography was performed on Across Organics Ultrapure silica gel (mesh size 40-60 μm, 60 Å). All reagents were obtained from commercial sources and liquid reagents were dried on 4 Å molecular sieves and degassed prior to use.

Rhenium pentacarbonyl bromide, min. 98%, and PN(H)P ligands were purchased from Strem Chemicals. Bis[(2-di-*alkyl*-phosphino)ethyl]amine ligands were purchased from Strem Chemicals Inc.

<sup>1</sup>H, <sup>13</sup>C and <sup>31</sup>P NMR spectra were recorded in CDCl<sub>3</sub>, C<sub>6</sub>D<sub>6</sub>, C<sub>7</sub>D<sub>8</sub> at 298 K unless otherwise stated, on Bruker, AVANCE 400 and AVANCE 300 spectrometers at 400.1 and 300.1 MHz, respectively. <sup>1</sup>H and <sup>13</sup>C NMR spectra were calibrated using the residual solvent signal as internal standard (<sup>1</sup>H: CDCl<sub>3</sub> 7.26 ppm, C<sub>6</sub>D<sub>6</sub> 7.16 ppm, C<sub>7</sub>H<sub>8</sub> 2.08 ppm, <sup>13</sup>C: CDCl<sub>3</sub>, central peak is 77.16 ppm, C<sub>6</sub>D<sub>6</sub>, central peak is 128.1 ppm, C<sub>7</sub>D<sub>8</sub>, central peak is 20.4 ppm). <sup>31</sup>P NMR spectra were calibrated against an external H<sub>3</sub>PO<sub>4</sub> standard. Chemical shift (δ) and coupling constants (*J*) are given in ppm and in Hz, respectively. The peak patterns are indicated as follows: (s, singlet; d, doublet; t, triplet; q, quartet; quin, quintet; m, multiplet, and br. for broad).

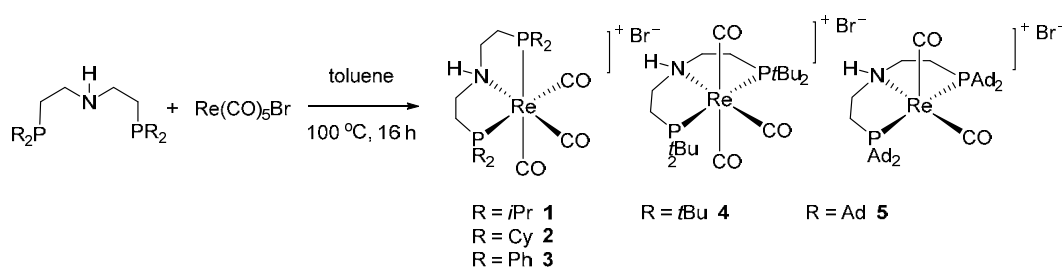
HR-MS spectra and microanalysis were carried out by the corresponding facilities at the CRMPO (Centre Régional de Mesures Physiques de l'Ouest), Université de Rennes 1

Magnetic stirred Parr autoclaves (22 mL) were used for the hydrogenation.

ACE pressure tubes (sealed tube) (15 mL) were used for the methylation reactions.

### 6.2. Synthesis of rhenium complexes 1-5

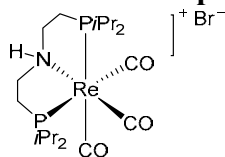
#### 6.2.1. General procedure for synthesis of rhenium complexes 1-5



Bis[(2-di-*alkyl*-phosphino)ethyl]amine (0.492 mmol) was added to a solution of Re(CO)<sub>5</sub>Br (0.492 mmol, 200 mg, 1.0 equiv.) in anhydrous toluene (8 mL). The mixture was stirred at 100 °C overnight. Toluene was then evaporated. The crude residue was then recrystallized from dichloromethane (1 mL) and pentane (5 mL) to afford crystals. The solid was washed with pentane (2 mL × 2) to afford pure compound.

## 6.2.2. Characterization of Re PN(H)P complexes 1-5 and the Re NN(H)N complex 6.

### Rhenium complex 1:



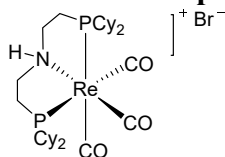
According to the general procedure, bis[(2-di-*iso*-propylphosphino)ethyl]amine (0.492 mmol, 1.7 mL, 10 wt% in THF, 1.0 equiv.) gave the title complex as white needle crystals (297 mg, 92%). Single crystals suitable for X-Ray diffraction studies have been grown by slow diffusion of pentane into a CH<sub>2</sub>Cl<sub>2</sub> solution at r.t. **<sup>1</sup>H NMR** (400 MHz, CDCl<sub>3</sub>) δ = 7.88 (s, 1H, NH), 3.04 – 3.00 (m, 4H, NH-CH<sub>2</sub>), 2.46 – 2.41 (m, 2H, CH), 2.10 – 2.03 (m, 6H, CH + CH<sub>2</sub>-P), 1.38 – 1.24 (m, 24H, CH<sub>3</sub>). **<sup>13</sup>C{<sup>1</sup>H} NMR** (101 MHz, CDCl<sub>3</sub>) δ = 195.0 (t, *J* = 7 Hz, CO), 190.1 (t, *J* = 19 Hz, CO), 189.6 (t, *J* = 18 Hz, CO), 53.9 (br., NH-CH<sub>2</sub>), 30.2 – 29.7 (m, CH), 27.2 – 26.7 (m, CH<sub>2</sub>-P), 26.2 – 25.7 (m, CH), 21.9 (CH<sub>3</sub>), 20.1 (CH<sub>3</sub>), 19.5 (CH<sub>3</sub>), 18.2 (t, *J* = 3 Hz, CH<sub>3</sub>). **<sup>31</sup>P{<sup>1</sup>H} NMR** (162 MHz, CDCl<sub>3</sub>) δ = 38.0.

**<sup>1</sup>H NMR** (400 MHz, CD<sub>2</sub>Cl<sub>2</sub>) δ 8.20 (s, 1H, NH), 3.10 – 2.82 (m, 4H, NH-CH<sub>2</sub>), 2.55 – 2.41 (m, 2H, CH), 2.21 – 2.10 (m, 2H, CH<sub>2</sub>), 2.08 – 1.97 (m, 2H, CH), 1.94 – 1.84 (m, 2H, CH<sub>2</sub>), 1.44 – 1.25 (m, 24H, CH<sub>3</sub>). **<sup>13</sup>C{<sup>1</sup>H} NMR** (101 MHz, CD<sub>2</sub>Cl<sub>2</sub>) δ = 195.4 (t, *J* = 6 Hz, CO), 190.7 (t, *J* = 17 Hz, CO), 190.3 (t, *J* = 18 Hz, CO), 54.2 (NH-CH<sub>2</sub>)\*, 54.1 (br, NH-CH<sub>2</sub>)\*, 30.7-30.2 (m, CH), 27.6-27.1 (m, CH<sub>2</sub>-P), 26.6-26.1 (m, CH), 22.0 (CH<sub>3</sub>), 20.2 (CH<sub>3</sub>), 19.6 (CH<sub>3</sub>), 18.1 (t, *J* = 3 Hz, CH<sub>3</sub>). **<sup>31</sup>P{<sup>1</sup>H} NMR** (162 MHz, CD<sub>2</sub>Cl<sub>2</sub>) δ = 38.0.

\*= overlapping with the solvent residual signal

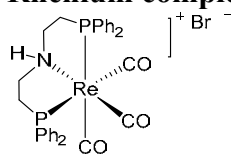
**Anal. Calc** (%). for (C<sub>19</sub>H<sub>37</sub>NO<sub>3</sub>BrP<sub>2</sub>Re): C, 34.81; H, 5.69; N, 2.14. Found: C, 34.79; H, 5.63; N, 2.00. **HR-MS** (ESI): *m/z* [M]<sup>+</sup> calcd for C<sub>19</sub> H<sub>37</sub> N O<sub>3</sub> P<sub>2</sub> <sup>187</sup>Re 576.18009, found 576.1806 (1 ppm); *m/z* [M-CO]<sup>+</sup> calcd for C<sub>18</sub> H<sub>37</sub> N O<sub>2</sub> P<sub>2</sub> <sup>187</sup>Re 546.18517 *m/z* found 548.1858 (1 ppm); *m/z* [2M<sup>+</sup>, Br-]<sup>+</sup> calcd for C<sub>38</sub> H<sub>74</sub> N<sub>2</sub> O<sub>6</sub> <sup>79</sup>Br P<sub>4</sub> <sup>187</sup>Re<sub>2</sub> 1231.27906 *m/z* found 1231.2782 (1 ppm). **IR** (ν, cm<sup>-1</sup>, CH<sub>2</sub>Cl<sub>2</sub>): 2031, 1944, 1921.

### Rhenium complex 2:



According to the general procedure, bis[(2-di-cyclohexylphosphino)ethyl]amine (229 mg, 0.492 mmol) gave the title complex as white crystals (361.2 mg, 90%). Single crystals suitable for X-Ray diffraction studies have been grown by slow diffusion of pentane into a CH<sub>2</sub>Cl<sub>2</sub> solution at r.t. **<sup>1</sup>H NMR** (400 MHz, CD<sub>2</sub>Cl<sub>2</sub>): δ 8.25 (s, 1H), 3.07 – 2.98 (m, 2H), 2.89 – 2.81 (m, 2H), 2.19 – 2.05 (m, 4H), 1.96 – 1.30 (m, 44H). **<sup>13</sup>C{<sup>1</sup>H} NMR** (101 MHz, CD<sub>2</sub>Cl<sub>2</sub>): δ 195.4 (t, *J* = 6.5 Hz, CO), 190.9 (t, *J* = 19.1 Hz, CO), 190.4 (t, *J* = 17.1 Hz, CO), 53.1 (t, *J* = 2.8 Hz, CH<sub>2</sub>), 41.3 – 39.7 (m, CH), 38.9 – 37.5 (m, CH), 32.7 (CH<sub>2</sub>), 30.0 (CH<sub>2</sub>), 29.7 (CH<sub>2</sub>), 28.3 (t, *J* = 3.6 Hz, CH<sub>2</sub>), 27.9 – 27.5 (m, CH<sub>2</sub>), 27.3 (t, *J* = 3.9 Hz, CH<sub>2</sub>), 26.2 (d, *J* = 10.5 Hz, CH<sub>2</sub>), 25.8 – 25.1 (m, CH<sub>2</sub>). **<sup>31</sup>P{<sup>1</sup>H} NMR** (162 MHz, CD<sub>2</sub>Cl<sub>2</sub>): δ 28.7. **Anal. Calc** (%). for (C<sub>31</sub>H<sub>53</sub>NO<sub>3</sub>BrP<sub>2</sub>Re): C, 45.64; H, 6.55; N, 1.72. Found: C, 45.56; H, 6.63; N, 1.63. **HR-MS** (ESI): *m/z* [M]<sup>+</sup> calcd for C<sub>31</sub>H<sub>53</sub>NO<sub>3</sub>P<sub>2</sub> <sup>187</sup>Re 736.3053, found 736.3051 (0 ppm). **IR** (ν, cm<sup>-1</sup>, CH<sub>2</sub>Cl<sub>2</sub>): 2029, 1940, 1919.

### Rhenium complex 3:

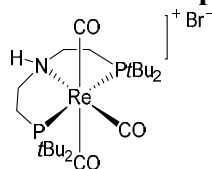


To a 20 mL round-bottomed flask were added bis[2-(di-phenylphosphino)ethyl]amine hydrochloride (191 mg, 0.40 mmol), 10% NaOH aq. (2 mL), and toluene (4 mL). The mixture was stirred at room temperature until all the solids dissolved. After decantation of the solution, the organic layer was washed with H<sub>2</sub>O (2 mL  $\times$  3), dried over Na<sub>2</sub>SO<sub>4</sub>, and then concentrated under reduced pressure.<sup>[1]</sup> The resulting bis[2-(di-phenylphosphino)ethyl]amine ligand was directly used for the coordination with Re(CO)<sub>5</sub>Br (163 mg, 0.4 mmol) following the general procedure, giving the title complex as white crystals (300.8 mg, 95%). Single crystals suitable for X-Ray diffraction studies have been grown by slow evaporation from MeOH at r.t. **<sup>1</sup>H NMR** (400 MHz, CD<sub>3</sub>OD):  $\delta$  7.75 – 7.69 (m, 4H), 7.52 – 7.43 (m, 6H), 7.19 – 7.13 (m, 6H), 7.03 – 6.99 (m, 4H), 3.71 – 3.57 (m, 2H), 3.29 – 3.19\* (m, 2H), 3.11 – 3.03 (m, 2H), 2.89 – 2.80 (m, 2H). **<sup>13</sup>C{<sup>1</sup>H} NMR** (101 MHz, CD<sub>3</sub>OD):  $\delta$  196.3 (t,  $J$  = 7.2 Hz, CO), 191.0 (t,  $J$  = 18.8 Hz, CO), 190.5 (d,  $J$  = 17.2 Hz, CO), 135.8-135.2 (m, C<sub>qAr</sub>), 132.5-132.4 (m, CH<sub>Ar</sub>), 132.2, 131.8-131.7 (m, CH<sub>Ar</sub>), 130.4-130.2 (m, CH<sub>Ar</sub>), 56.2-56.0 (m, CH<sub>2</sub>), 29.0 (m, CH<sub>2</sub>), 28.8 (m, CH<sub>2</sub>). **<sup>31</sup>P{<sup>1</sup>H} NMR** (162 MHz, CD<sub>3</sub>OD):  $\delta$  24.1.

\*= overlapping with the solvent residual signal.

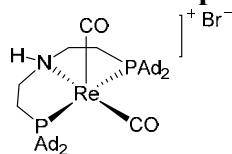
**Anal. Calc** (%). for (C<sub>31</sub>H<sub>29</sub>NO<sub>3</sub>BrP<sub>2</sub>Re): C, 47.03; H, 3.69; N, 1.77. Found: C, 47.18; H, 3.76; N, 1.77. **HR-MS** (ESI):  $m/z$  [M]<sup>+</sup> calcd for C<sub>31</sub>H<sub>29</sub>NO<sub>3</sub>P<sub>2</sub><sup>187</sup>Re 712.1175, found 712.1178 (0 ppm). **IR** ( $\nu$ , cm<sup>-1</sup>, CH<sub>2</sub>Cl<sub>2</sub>): 2042, 1967, 1923.

### Rhenium complex 4:



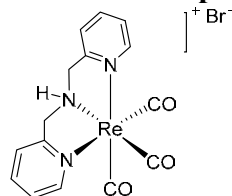
According to the general procedure, bis[(2-di-*t*-butylphosphino)ethyl]amine (10 wt% in hexanes, 178 mg, 0.492 mmol) gave the title complex as white crystals (418.0 mg, 97%). Single crystals suitable for X-Ray diffraction studies have been grown by slow diffusion of pentane into a CH<sub>2</sub>Cl<sub>2</sub> solution at r.t. **<sup>1</sup>H NMR** (400 MHz, CD<sub>2</sub>Cl<sub>2</sub>):  $\delta$  7.23 (br. s, 1H, NH), 3.74 (t,  $J$  = 13.7 Hz, 2H, CH<sub>2</sub>), 2.25 (s, 6H, CH<sub>2</sub>), 1.50 (s, 18H, *t*Bu), 1.44 (s, 18H, *t*Bu). **<sup>13</sup>C{<sup>1</sup>H} NMR** (101 MHz, CD<sub>2</sub>Cl<sub>2</sub>):  $\delta$  200.7 (t,  $J$  = 8.0 Hz, CO), 197.8 (t,  $J$  = 8.3 Hz, CO), 195.9 (t,  $J$  = 3 Hz, CO), 58.4 (t,  $J$  = 2.8 Hz, CH<sub>2</sub>), 38.8 (t,  $J$  = 9.1 Hz, C(CH<sub>3</sub>)<sub>3</sub>), 38.5 (t,  $J$  = 10.8 Hz, C(CH<sub>3</sub>)<sub>3</sub>), 31.5 (CH<sub>3</sub>), 30.9 (CH<sub>3</sub>), 25.1 (t,  $J$  = 10.1 Hz, CH<sub>2</sub>). **<sup>31</sup>P{<sup>1</sup>H} NMR** (162 MHz, CD<sub>2</sub>Cl<sub>2</sub>):  $\delta$  74.9. **Anal. Calc** (%). for (C<sub>23</sub>H<sub>45</sub>NO<sub>3</sub>BrP<sub>2</sub>Re): C, 38.82; H, 6.37; N, 1.97. Found: C, 38.59; H, 6.45; N, 2.01. **HR-MS** (ESI):  $m/z$  [M]<sup>+</sup> calcd for C<sub>23</sub>H<sub>45</sub>NO<sub>3</sub>P<sub>2</sub><sup>187</sup>Re 632.2427, found 632.2434 (1 ppm);  $m/z$  [M-CO]<sup>+</sup> calcd for C<sub>22</sub>H<sub>45</sub>NO<sub>2</sub>P<sub>2</sub><sup>187</sup>Re 604.2478  $m/z$  found 604.2473 (1 ppm). **IR** ( $\nu$ , cm<sup>-1</sup>, CH<sub>2</sub>Cl<sub>2</sub>): 2027, 1923, 1913.

### Rhenium complex 5:



According to the general procedure, bis[(2-di-1-adamantylphosphino)ethyl]amine (332 mg, 0.492 mmol) gave the title complex as orange crystals (465.6 mg, 95%). Single crystals suitable for X-Ray diffraction studies have been grown by slow diffusion of pentane into a  $\text{CH}_2\text{Cl}_2$  solution at r.t.  **$^1\text{H}$  NMR** (400 MHz,  $\text{CD}_2\text{Cl}_2$ ):  $\delta$  7.18 (br. s, 1H), 3.93 – 3.82 (m, 2H), 2.60 – 2.34 (m, 12H), 2.19 – 1.98 (m, 24H), 1.80 – 1.68 (m, 24H), 1.41 – 1.18 (m, 6H).  **$^{13}\text{C}\{^1\text{H}\}$  NMR** (101 MHz,  $\text{CD}_2\text{Cl}_2$ ):  $\delta$  211.0 (t,  $J = 4.5$  Hz, CO), 199.9 (t,  $J = 6.5$  Hz, CO), 57.0 (t,  $J = 3.6$  Hz,  $\text{CH}_2$ ), 44.6 (t,  $J = 10.2$  Hz,  $\text{C}_q$ ), 41.2 (t,  $J = 9.7$  Hz,  $\text{C}_q$ ), 39.7 ( $\text{CH}_2$ ), 39.5 ( $\text{CH}_2$ ), 36.7 ( $\text{CH}_2$ ), 36.7 ( $\text{CH}_2$ ), 29.0 (t,  $J = 4.4$  Hz, CH), 28.8 (t,  $J = 4.4$  Hz, CH), 21.0 (t,  $J = 10.2$  Hz,  $\text{CH}_2$ ).  **$^{31}\text{P}\{^1\text{H}\}$  NMR** (162 MHz,  $\text{CD}_2\text{Cl}_2$ ):  $\delta$  73.6. **Anal. Calc** (%). for  $(\text{C}_{46}\text{H}_{69}\text{NO}_2\text{BrP}_2\text{Re})$ : C, 55.47; H, 6.98; N, 1.41. Found: C, 55.55; H, 7.11; N, 1.31. **HR-MS** (ESI):  $m/z$   $[\text{M}]^+$  calcd for  $\text{C}_{46}\text{H}_{69}\text{NO}_2\text{P}_2^{187}\text{Re}$  916.4356, found 916.4356 (0 ppm). **IR** ( $\nu$ ,  $\text{cm}^{-1}$ ,  $\text{CH}_2\text{Cl}_2$ ): 1925, 1838.

### Rhenium complex 6:



Complex **6** has been already prepared in the literature starting from  $[\text{NEt}_4]_2[\text{ReBr}_3(\text{CO})_3]$ .<sup>[2]</sup> As an alternative, following the general procedure, at 100 °C, after 70 h, dipicolylamine (50 mg, 0.25 mmol) and  $\text{Re}(\text{CO})_5\text{Br}$  (101.5 mg, 0.25 mmol) gave rhenium complex **6** in 90 % yield (124 mg) as a white solid. Single crystals suitable for X-Ray diffraction studies have been grown by slow diffusion of pentane into a  $\text{CH}_2\text{Cl}_2$  solution at r.t. X-Ray diffraction studies on single crystals confirmed the *fac*-geometry of the  $\text{Re}(\text{CO})_3$  fragment.<sup>[2]</sup>  **$^1\text{H}$  NMR** (400 MHz,  $\text{CD}_2\text{Cl}_2$ )  $\delta$  8.80 (d,  $J = 5.3$  Hz, 2H), 8.54 (t,  $J = 6.2$  Hz, 1H), 7.82 (td,  $J = 7.8, 1.4$  Hz, 2H), 7.58 (d,  $J = 7.9$  Hz, 2H), 7.25 (t,  $J = 6.5$  Hz, 2H), 5.05 (dd,  $J = 17.6, 6.8$  Hz, 2H), 4.75 (d,  $J = 17.7$  Hz, 2H).  **$^{13}\text{C}\{^1\text{H}\}$  NMR** (101 MHz,  $\text{CD}_2\text{Cl}_2$ )  $\delta$  195.5, 161.9, 151.9, 140.1, 125.5, 123.7, 63.3. **IR** ( $\nu$ ,  $\text{cm}^{-1}$ ,  $\text{CH}_2\text{Cl}_2$ ): 2033, 1935, 1911.

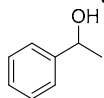
## 6.3. Part V-1- Hydrogenation of Carbonyl Derivatives

### 6.3.1. General procedure for hydrogenation reactions of ketones

In an argon filled glove box, an autoclave was charged with Re-PNP complex **1** (8.2 mg, 0.5 mol%) and toluene (2.5 mL), followed by ketone (2.5 mmol) and *t*-BuOK (2.8 mg, 1.0 mol%), in this order. The autoclave is then charged  $\text{H}_2$  (30 bar). The mixture was stirred for 17 hours at 70°C in an oil bath. The solution was then diluted with diethyl ether (2 mL) and filtered through a small pad of silica (2 cm in a Pasteur pipette). The silica was washed with diethyl ether. The filtrate was evaporated and the crude residue was purified by column chromatography ( $\text{SiO}_2$ , mixture of petroleum ether/ethyl acetate as eluent).

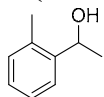
### 6.3.2. Characterization of the hydrogenated products

#### 1-Phenylethanol **8a**<sup>[3]</sup>



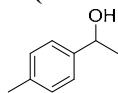
According to general procedure, acetophenone (293  $\mu$ L, 2.5 mmol) gave the title compound **8a** as a colourless oil (299.4 mg, 98%). <sup>1</sup>H NMR (400 MHz, CDCl<sub>3</sub>)  $\delta$  = 7.39 – 7.29 (m, 5H), 4.86 (q,  $J$  = 6.5 Hz, 1H), 3.00 (s, 1H), 1.50 (d,  $J$  = 6.5 Hz, 3H). <sup>13</sup>C{<sup>1</sup>H} NMR (101 MHz, CDCl<sub>3</sub>)  $\delta$  = 145.9, 128.4, 127.3, 125.4, 70.2, 25.1.

#### 1-(2-Methylphenyl)ethanol **8b**<sup>[4]</sup>



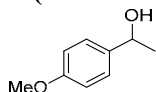
According to general procedure, 2'-methylacetophenone (327  $\mu$ L, 2.5 mmol) gave the title compound **8b** as a pale yellow oil (330.3 mg, 97%). <sup>1</sup>H NMR (400 MHz, CDCl<sub>3</sub>)  $\delta$  = 7.52 (d,  $J$  = 7.5 Hz, 1H), 7.28 – 7.22 (m, 1H), 7.21 – 7.10 (m, 2H), 5.13 (qd,  $J$  = 6.4 Hz,  $J$  = 3.6 Hz, 1H), 2.35 (s, 3H), 1.88 – 1.71 (m, 1H), 1.47 (d,  $J$  = 6.4, 3H). <sup>13</sup>C{<sup>1</sup>H} NMR (101 MHz, CDCl<sub>3</sub>)  $\delta$  = 143.9, 134.3, 130.5, 127.3, 126.5, 124.6, 67.0, 24.1, 19.0.

#### 1-(4-Methylphenyl)ethanol **8c**<sup>[3]</sup>



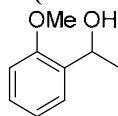
According to general procedure, 4'-methylacetophenone (334  $\mu$ L, 2.5 mmol) gave the title compound **8c** as a colourless oil (323.5 mg, 95%). <sup>1</sup>H NMR (400 MHz, CDCl<sub>3</sub>)  $\delta$  = 7.29 (d,  $J$  = 8.0 Hz, 2H), 7.20 (d,  $J$  = 7.9 Hz, 2H), 4.88 (qd,  $J$  = 6.5 Hz,  $J$  = 3.1 Hz, 1H), 2.38 (s, 3H), 2.05 (d,  $J$  = 3.1 Hz, 1H), 1.51 (d,  $J$  = 6.5 Hz, 3H). <sup>13</sup>C{<sup>1</sup>H} NMR (101 MHz, CDCl<sub>3</sub>)  $\delta$  = 143.0, 137.2, 129.2, 125.5, 70.3, 25.2, 21.2.

#### 1-(4-Methoxyphenyl)ethanol **8d**<sup>[3]</sup>



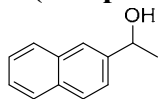
According to general procedure B, 4'-methoxyacetophenone (375.4 mg, 2.5 mmol) gave the title compound **8d** as a colourless oil (353.9 mg, 93%). <sup>1</sup>H NMR (300 MHz, CDCl<sub>3</sub>)  $\delta$  = 7.29 (d,  $J$  = 8.7 Hz, 2H), 6.89 (d,  $J$  = 8.7 Hz, 2H), 4.83 (q,  $J$  = 6.4 Hz, 1H), 3.81 (s, 3H), 2.35 (s, 1H), 1.47 (d,  $J$  = 6.4 Hz, 3H). <sup>13</sup>C{<sup>1</sup>H} NMR (75 MHz, CDCl<sub>3</sub>)  $\delta$  = 158.9, 138.2, 126.7, 113.9, 69.9, 55.3, 25.1.

#### 1-(2-Methoxyphenyl)ethanol **8e**<sup>[4]</sup>



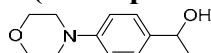
According to general procedure, 2'-methoxyacetophenone (34  $\mu$ L, 0.25 mmol) gave the title compound **8e** as a pale yellow oil (35.0 mg, 92%). <sup>1</sup>H NMR (300 MHz, CDCl<sub>3</sub>)  $\delta$  = 7.34 (dd,  $J$  = 7.5 Hz,  $J$  = 1.7 Hz, 1H), 7.25 (td,  $J$  = 7.9 Hz,  $J$  = 1.7 Hz, 1H), 6.97 (td,  $J$  = 7.5 Hz,  $J$  = 1.0 Hz, 1H), 6.89 (dd,  $J$  = 8.1 Hz,  $J$  = 0.7 Hz, 1H), 5.14 – 5.06 (m, 1H), 3.87 (s, 3H), 2.64 (d,  $J$  = 4.9 Hz, 1H), 1.51 (d,  $J$  = 6.5 Hz, 3H). <sup>13</sup>C{<sup>1</sup>H} NMR (75 MHz, CDCl<sub>3</sub>)  $\delta$  = 156.7, 133.6, 128.4, 126.2, 120.9, 110.6, 66.7, 55.4, 23.0.

### 1-(2-naphthyl)ethanol **8f**<sup>[5]</sup>



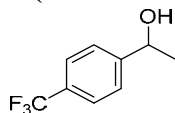
According to general procedure, 2'-acetonaphthone (425.5 mg, 2.5 mmol) gave the title compound **8f** as a white solid (413.3 mg, 96%). <sup>1</sup>H NMR (300 MHz, CDCl<sub>3</sub>) δ = 7.86 – 7.79 (m, 4H), 7.53 – 7.46 (m, 3H), 5.03 (qd, *J* = 6.5 Hz, *J* = 3.6 Hz, 1H), 2.38 (d, *J* = 3.6 Hz, 1H), 1.58 (d, *J* = 6.5 Hz, 3H). <sup>13</sup>C{<sup>1</sup>H} NMR (75 MHz, CDCl<sub>3</sub>) δ = 143.3, 133.4, 133.0, 128.3, 128.0, 127.7, 126.2, 125.8, 123.92, 123.88, 70.5, 25.2.

### 1-(4-Morpholinylphenyl)ethanol **8g**<sup>[4]</sup>



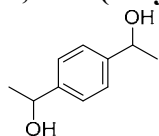
According to general procedure, 4'-morpholinoacetophenone (513.1 mg, 2.5 mmol) gave the title compound **8g** as a pale yellow solid (507.9 mg, 98%). <sup>1</sup>H NMR (400 MHz, CDCl<sub>3</sub>) δ = 7.24 (d, *J* = 8.6 Hz, 2H), 6.84 (d, *J* = 8.6 Hz, 2H), 4.74 (qd, *J* = 6.4 Hz, *J* = 3.5 Hz, 1H), 3.78 (m, 4H), 3.27 (d, *J* = 3.5 Hz, 1H), 3.06 (m, 4H), 1.43 (d, *J* = 6.4 Hz, 3H). <sup>13</sup>C{<sup>1</sup>H} NMR (101 MHz, CDCl<sub>3</sub>) δ = 150.3, 137.6, 126.2, 115.5, 69.3, 66.6, 49.3, 24.9.

### 1-(4-Trifluoromethylphenyl)ethanol **8h**<sup>[6]</sup>



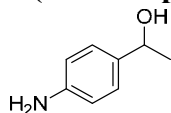
According to general procedure, 4'-trifluoromethylacetophenone (470.1 mg, 2.5 mmol) gave the title compound **8h** as a colourless oil (380.4 mg, 80%). <sup>1</sup>H NMR (300 MHz, CDCl<sub>3</sub>) δ = 7.60 (d, *J* = 8.2 Hz, 2H), 7.48 (d, *J* = 8.2 Hz, 2H), 4.96 (q, *J* = 6.1 Hz, 1H), 2.02 (s, 1H), 1.50 (d, *J* = 6.4 Hz, 3H). <sup>13</sup>C{<sup>1</sup>H} NMR (101 MHz, CDCl<sub>3</sub>) δ = 149.8, 129.8 (q, *J*<sub>C-F</sub> = 32 Hz), 125.8, 125.6 (q, *J*<sub>C-F</sub> = 4 Hz), 124.0 (q, *J*<sub>C-F</sub> = 271 Hz), 70.0, 25.5. <sup>19</sup>F NMR (376 MHz, CDCl<sub>3</sub>) δ = -62.48.

### 1,4-Bis(1-hydroxyethyl)benzene **8i**<sup>[7]</sup>



According to general procedure, 1,4-diacetylbenzene (203.0 mg, 1.25 mmol) gave the title compound **8i** as a pale yellow solid (195.3 mg, 94%). <sup>1</sup>H NMR (300 MHz, CDCl<sub>3</sub>) δ = 7.34 (s, 4H), 4.88 (q, *J* = 6.5 Hz, 2H), 1.99 (s, 2H), 1.48 (d, *J* = 6.5 Hz, 6H). <sup>13</sup>C{<sup>1</sup>H} NMR (75 MHz, CDCl<sub>3</sub>) δ = 145.2, 125.7, 70.3, 25.3.

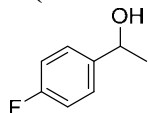
### 1-(4-Aminophenyl)ethanol **8j**<sup>[8]</sup>



According to general procedure, 4'-aminoacetophenone (338.0 mg, 2.5 mmol) gave the title compound **8j** as a yellowish brown solid (322.4 mg, 94%). <sup>1</sup>H NMR (400 MHz, CDCl<sub>3</sub>) δ = 7.14 (d, *J* = 7.8 Hz, 2H), 6.63 (d, *J* = 7.9 Hz, 2H), 4.76 (q, *J* = 5.9 Hz, 1H), 3.14 (br. s, 3H), 1.44 (d, *J* = 6.2 Hz, 3H). <sup>13</sup>C{<sup>1</sup>H} NMR (101 MHz, CDCl<sub>3</sub>) δ = 145.7, 136.1, 126.7, 115.2, 70.1, 24.9.

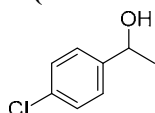


### 1-(4-Fluorophenyl)ethanol **8k**<sup>[3]</sup>



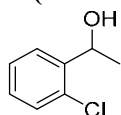
According to general procedure, 4'-fluoroacetophenone (324  $\mu$ L, 2.5 mmol) gave the title compound **8k** as a pale yellow oil (379.8 mg, 97%). <sup>1</sup>H NMR (400 MHz, CDCl<sub>3</sub>)  $\delta$  = 7.36 – 7.29 (m, 2H), 7.06–7.00 (m, 2H), 4.94 – 4.82 (m, 1H), 1.84 (br. s, 1H, OH), 1.47 (d,  $J$  = 6.4 Hz, 3H). <sup>13</sup>C{<sup>1</sup>H} NMR (101 MHz, CDCl<sub>3</sub>)  $\delta$  = 162.2 (d,  $J_{C-F}$  = 245 Hz), 141.6 (d,  $J_{C-F}$  = 3 Hz), 127.1 (d,  $J_{C-F}$  = 7 Hz), 115.3 (d,  $J_{C-F}$  = 21 Hz), 69.9, 25.4. <sup>19</sup>F NMR (376 MHz, CDCl<sub>3</sub>)  $\delta$  = -115.44.

### 1-(4-Chlorophenyl)ethanol **8l**<sup>[9]</sup>



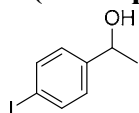
According to general procedure, 4'-chloroacetophenone (324  $\mu$ L, 2.5 mmol) gave the title compound **8l** as a pale yellow oil (379.8 mg, 97%). <sup>1</sup>H NMR (400 MHz, CDCl<sub>3</sub>)  $\delta$  = 7.31 (m, 4H), 4.88 (qd,  $J$  = 6.5 Hz,  $J$  = 3.6 Hz, 1H), 1.89 (d,  $J$  = 3.6 Hz, 1H), 1.47 (d,  $J$  = 6.5 Hz, 3H). <sup>13</sup>C{<sup>1</sup>H} NMR (101 MHz, CDCl<sub>3</sub>)  $\delta$  = 144.4, 133.2, 128.7, 126.9, 69.9, 25.4.

### 1-(2-Chlorophenyl)ethanol **8m**<sup>[10]</sup>



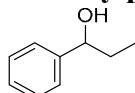
According to general procedure, 2'-chloroacetophenone (325  $\mu$ L, 2.5 mmol) gave the title compound **8m** as a pale yellow oil (371.9 mg, 95%). <sup>1</sup>H NMR (300 MHz, CDCl<sub>3</sub>)  $\delta$  = 7.59 (dd,  $J$  = 7.6 Hz,  $J$  = 1.7 Hz, 1H), 7.37 – 7.27 (m, 2H), 7.20 (td,  $J$  = 7.6 Hz,  $J$  = 1.8 Hz, 1H), 5.30 (qd,  $J$  = 6.4 Hz,  $J$  = 3.7 Hz, 1H), 2.02 (d,  $J$  = 3.7 Hz, 1H), 1.49 (d,  $J$  = 6.4 Hz, 3H). <sup>13</sup>C{<sup>1</sup>H} NMR (75 MHz, CDCl<sub>3</sub>)  $\delta$  = 143.2, 131.8, 129.5, 128.5, 127.3, 126.5, 67.1, 23.6.

### 1-(4-Iodophenyl)ethanol **8n**



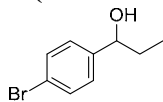
According to general procedure, 4'-iodoacetophenone (307.6 mg, 1.25 mmol) gave the title compound **8n** as a brown oil (303.9 mg, 98%). <sup>1</sup>H NMR (400 MHz, CDCl<sub>3</sub>)  $\delta$  = 7.66 (d,  $J$  = 8.3 Hz, 2H), 7.10 (d,  $J$  = 8.2 Hz, 2H), 4.81 (qd,  $J$  = 6.1 Hz,  $J$  = 3.3 Hz, 1H), 2.21 (br.s, 1H), 1.44 (d,  $J$  = 6.5 Hz, 3H). <sup>13</sup>C{<sup>1</sup>H} NMR (75 MHz, CDCl<sub>3</sub>)  $\delta$  = 145.6, 137.7, 127.5, 92.8, 70.0, 25.4.

### 1-Phenylpropanol **8o**



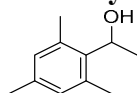
According to general procedure, propiophenone (332  $\mu$ L, 2.5 mmol) gave the title compound **8o** as a colourless oil (323.5 mg, 95%). <sup>1</sup>H NMR (400 MHz, CDCl<sub>3</sub>)  $\delta$  = 7.50 – 7.16 (m, 5H), 4.60 (td,  $J$  = 6.6 Hz,  $J$  = 3.4 Hz, 1H), 2.20 (d,  $J$  = 3.4 Hz, 1H), 1.92 – 1.70 (m, 2H), 0.94 (t,  $J$  = 7.4 Hz, 3H). <sup>13</sup>C{<sup>1</sup>H} NMR (101 MHz, CDCl<sub>3</sub>)  $\delta$  = 144.7, 128.5, 127.5, 126.1, 76.1, 32.0, 10.2.

### 1-(4-Bromophenyl)propanol **8p**



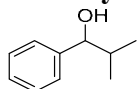
According to general procedure, 1-(4-bromophenyl)propanone (532.7 mg, 2.5 mmol) gave the title compound **8p** as a pale yellow oil (505.5 mg, 94%).  $^1\text{H NMR}$  (300 MHz,  $\text{CDCl}_3$ )  $\delta$  = 7.44 (d,  $J$  = 8.4 Hz, 2H), 7.16 (d,  $J$  = 8.4 Hz, 2H), 4.50 (td,  $J$  = 6.5 Hz,  $J$  = 3.5 Hz, 1H), 2.43 (d,  $J$  = 3.4 Hz, 1H), 1.87 – 1.56 (m, 2H), 0.87 (t,  $J$  = 7.4 Hz, 3H).  $^{13}\text{C}\{^1\text{H}\}$  NMR (75 MHz,  $\text{CDCl}_3$ )  $\delta$  = 143.6, 131.5, 127.8, 121.2, 75.3, 31.9, 10.0.

### 1-Mesitylethanol **8q**<sup>[4]</sup>



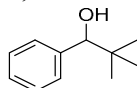
According to general procedure, 1-mesitylethanone (208  $\mu\text{L}$ , 1.25 mmol) gave the title compound **8q** as a white solid (199.1 mg, 97%).  $^1\text{H NMR}$  (400 MHz,  $\text{CDCl}_3$ )  $\delta$  = 6.84 (s, 2H), 5.36 (q,  $J$  = 6.8 Hz, 1H), 2.43 (s, 6H), 2.28 (s, 3H), 1.94 (br. s, 1H), 1.54 (d,  $J$  = 6.8 Hz, 3H).  $^{13}\text{C}\{^1\text{H}\}$  NMR (101 MHz,  $\text{CDCl}_3$ )  $\delta$  = 137.8, 136.5, 135.7, 130.2, 67.5, 21.7, 20.8, 20.6.

### 1-Phenyl-2-methylpropanol **8r**<sup>[3]</sup>



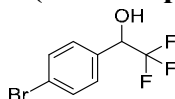
According to general procedure, isobutyrophenone (187  $\mu\text{L}$ , 1.25 mmol) gave the title compound **8r** as a colourless oil (178.4 mg, 95%).  $^1\text{H NMR}$  (400 MHz,  $\text{CDCl}_3$ )  $\delta$  = 7.44 – 7.24 (m, 5H), 4.39 (dd,  $J$  = 6.8 Hz,  $J$  = 3.2 Hz, 1H), 1.98 (oct,  $J$  = 6.8 Hz, 1H), 1.90 – 1.81 (br. s, 1H), 1.03 (d,  $J$  = 6.8 Hz, 3H), 0.83 (d,  $J$  = 6.8 Hz, 3H).  $^{13}\text{C}\{^1\text{H}\}$  NMR (101 MHz,  $\text{CDCl}_3$ )  $\delta$  = 143.8, 128.3, 127.5, 126.7, 80.2, 35.4, 19.2, 18.4.

### 2,2-Dimethyl-1-phenylpropanol **8s**<sup>[9]</sup>



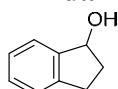
According to general procedure, pivalophenone (42  $\mu\text{L}$ , 0.25 mmol) gave the title compound **8s** as a colourless oil (29.6 mg, 72%).  $^1\text{H NMR}$  (400 MHz,  $\text{CDCl}_3$ )  $\delta$  = 7.34 – 7.28 (m, 5H), 4.42 (s, 1H), 1.90 (s, 1H), 0.95 (s, 9H).  $^{13}\text{C}\{^1\text{H}\}$  NMR (75 MHz,  $\text{CDCl}_3$ )  $\delta$  = 142.3, 127.7, 127.7, 127.4, 82.6, 35.8, 26.1.

### 1-(4-Bromophenyl)-2,2,2-trifluoroethanol **8t**<sup>[4]</sup>



According to general procedure, 4-bromo- $\alpha,\alpha,\alpha$ -trifluoroacetophenone (316.3 mg, 1.25 mmol) gave the title compound **8t** as a brown oil (302.8 mg, 95%).  $^1\text{H NMR}$  (400 MHz,  $\text{CDCl}_3$ )  $\delta$  = 7.55 (d,  $J$  = 8.3 Hz, 2H), 7.36 (d,  $J$  = 8.3 Hz, 2H), 5.00 (q,  $J$  = 6.6 Hz, 1H), 2.70 (s, 1H).  $^{13}\text{C}\{^1\text{H}\}$  NMR (101 MHz,  $\text{CDCl}_3$ )  $\delta$  = 132.9, 131.9, 129.2, 124.2 (q,  $J_{\text{C-F}}$  = 281 Hz), 123.9, 72.4 (q,  $J_{\text{C-F}}$  = 32 Hz).  $^{19}\text{F NMR}$  (376 MHz,  $\text{CDCl}_3$ )  $\delta$  = -78.53.

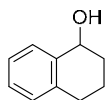
### 1-Indanol **8u**<sup>[3]</sup>



According to general procedure, 1-indanone (330.4 mg, 2.5 mmol) gave the title compound **8u** as a red oil (322.1 mg, 96%).  $^1\text{H NMR}$  (300 MHz,  $\text{CDCl}_3$ )  $\delta$  = 7.49 – 7.39 (m, 1H), 7.32 – 7.24

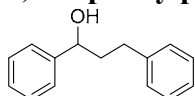
(m, 3H), 5.27 (q,  $J = 6.8$  Hz, 1H), 3.09 (ddd,  $J = 16.0$  Hz,  $J = 8.5$  Hz,  $J = 4.8$  Hz, 1H), 2.83 (m, 1H), 2.52 (m, 1H), 1.97 (m, 1H), 1.80 (d,  $J = 7.1$ , 1H).  $^{13}\text{C}\{^1\text{H}\}$  NMR (75 MHz,  $\text{CDCl}_3$ )  $\delta = 145.1, 143.5, 128.5, 126.9, 125.0, 124.3, 76.6, 36.1, 29.9$ .

### 1-Tetralol<sup>[4]</sup>



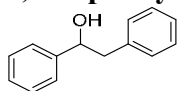
According to general procedure, 1-oxotetralin (333  $\mu\text{L}$ , 2.5 mmol) gave the title compound **2v** as a brown oil (348.3 mg, 94%).  $^1\text{H}$  NMR (300 MHz,  $\text{CDCl}_3$ )  $\delta = 7.49 - 7.39$  (m, 1H), 7.27 - 7.14 (m, 2H), 7.17 - 7.06 (m, 1H), 4.79 (q,  $J = 5.4$  Hz, 1H), 2.92 - 2.64 (m, 2H), 2.02 - 1.73 (m, 5H).  $^{13}\text{C}\{^1\text{H}\}$  NMR (75 MHz,  $\text{CDCl}_3$ )  $\delta = 139.0, 137.3, 129.2, 128.8, 127.7, 126.3, 68.3, 32.4, 29.4, 18.9$ .

### 1,3-Diphenylpropan-1-ol **8w**



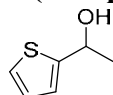
According to general procedure, 1,3-diphenylpropan-1-one (525.7 mg, 2.5 mmol) gave the title compound **8w** as a colourless oil (509.5 mg, 96%).  $^1\text{H}$  NMR (400 MHz,  $\text{CDCl}_3$ )  $\delta = 7.38 - 7.37$  (m, 4H), 7.33 - 7.29 (m, 3H), 7.23 - 7.20 (m, 3H), 4.72-4.68 (m, 1H), 2.82 - 2.65 (m, 2H), 2.20 - 2.04 (m, 2H), 2.03 (d,  $J = 3.5$ , 1H).  $^{13}\text{C}\{^1\text{H}\}$  NMR (101 MHz,  $\text{CDCl}_3$ )  $\delta = 144.7, 141.9, 128.61, 128.55, 128.49, 127.7, 126.04, 125.96, 74.0, 40.6, 32.2$ .

### 1,2-Diphenylethanol **8x**



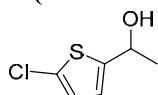
According to general procedure, 1,2-diphenylethanol (49.1 mg, 0.25 mmol) gave the title compound **8x** as a white solid (46.1 mg, 93%).  $^1\text{H}$  NMR (300 MHz,  $\text{CDCl}_3$ )  $\delta = 7.41 - 7.23$  (m, 10H), 4.96-4.90 (m, 1H), 3.13 - 3.02 (m, 2H), 2.11 (d,  $J = 2.7$  Hz, 1H).  $^{13}\text{C}\{^1\text{H}\}$  NMR (75 MHz,  $\text{CDCl}_3$ )  $\delta = 143.9, 138.2, 129.6, 128.6, 128.5, 127.7, 126.7, 126.0, 75.4, 46.2$ .

### 1-(Thiophen-2-yl)ethanol **8aa**



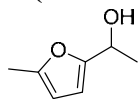
According to general procedure, 1-(thiophen-2-yl)ethanone (273  $\mu\text{L}$ , 2.5 mmol) gave the title compound **8aa** as an orange oil (307.7 mg, 96%).  $^1\text{H}$  NMR (300 MHz,  $\text{CDCl}_3$ )  $\delta = 7.31 - 7.21$  (m, 1H), 7.04 - 6.94 (m, 2H), 5.14 (br. q,  $J = 6.4$  Hz, 1H), 2.14 (br. s, 1H), 1.62 (d,  $J = 6.4$  Hz, 3H).  $^{13}\text{C}\{^1\text{H}\}$  NMR (75 MHz,  $\text{CDCl}_3$ )  $\delta = 150.0, 126.8, 124.5, 123.3, 66.4, 25.4$ .

### 1-(5-Chlorothiophen-2-yl)ethan-1-ol **8ab**



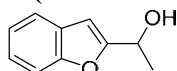
According to general procedure, 1-(5-chlorothiophen-2-yl)ethanone (401.6 mg, 2.5 mmol) gave the title compound **8ab** as an orange-red oil (386.2 mg, 95%).  $^1\text{H}$  NMR (400 MHz,  $\text{CDCl}_3$ )  $\delta = 6.75$  (d,  $J = 3.7$  Hz, 1H), 6.72 (d,  $J = 3.7$  Hz, 1H), 5.00 (m, 1H), 2.16 (d,  $J = 4.7$  Hz, 1H), 1.55 (d,  $J = 6.4$  Hz, 3H).  $^{13}\text{C}\{^1\text{H}\}$  NMR (101 MHz,  $\text{CDCl}_3$ )  $\delta = 148.7, 129.2, 125.7, 122.5, 66.6, 25.1$ .

### 1-(5-Methylfuran-2-yl)ethan-1-ol **8ac**



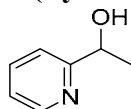
According to general procedure, 1-(5-methylfuran-2-yl)ethanone (29  $\mu$ L, 0.25 mmol) gave the title compound **8ac** as a brown oil (29.0 mg, 92%).  $^1\text{H}$  NMR (300 MHz,  $\text{CDCl}_3$ )  $\delta$  = 6.09 (d,  $J$  = 3.1 Hz, 1H), 5.90 – 5.88 (m, 1H), 4.86 – 4.78 (m, 1H), 2.28 (s, 3H), 1.93 (d,  $J$  = 4.4 Hz, 1H), 1.52 (d,  $J$  = 6.6 Hz, 3H).  $^{13}\text{C}\{^1\text{H}\}$  NMR (75 MHz,  $\text{CDCl}_3$ )  $\delta$  = 155.9, 151.8, 106.09, 106.07, 63.8, 21.3, 13.7.

### 1-(Benzofuran-2-yl)ethanol **8ad**



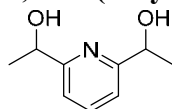
According to general procedure, 1-(benzofuran-2-yl)ethanone (40 mg, 0.25 mmol) gave the title compound **8ad** as a brown oil (38.1 mg, 94%).  $^1\text{H}$  NMR (400 MHz,  $\text{CDCl}_3$ )  $\delta$  = 7.57 (d,  $J$  = 7.7 Hz, 1H), 7.49 (d,  $J$  = 8.2 Hz, 1H), 7.32 – 7.22 (m, 2H), 6.64 (s, 1H), 5.08 – 5.02 (m, 1H), 2.17 (br. s, 1H), 1.67 (d,  $J$  = 6.6 Hz, 3H).  $^{13}\text{C}\{^1\text{H}\}$  NMR (101 MHz,  $\text{CDCl}_3$ )  $\delta$  = 160.3, 154.9, 128.3, 124.3, 122.9, 121.2, 111.3, 101.9, 64.3, 21.6.

### 1-(Pyridin-2-yl)ethanol **8ae**



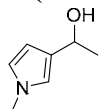
According to general procedure, 1-(pyridin-2-yl)ethanone (280.4  $\mu$ L, 2.5 mmol) gave the title compound **8ae** as a dark-red oil (298.8 mg, 97%).  $^1\text{H}$  NMR (400 MHz,  $\text{CDCl}_3$ )  $\delta$  = 8.55 (d,  $J$  = 4.7 Hz, 1H), 7.70 (td,  $J$  = 7.8 Hz,  $J$  = 1.6 Hz, 1H), 7.30 (d,  $J$  = 8.3 Hz, 1H), 7.21 (dd,  $J$  = 7.2 Hz,  $J$  = 5.0 Hz, 1H), 4.94 – 4.88 (m, 1H), 4.36 (d,  $J$  = 4.5 Hz, 1H), 1.52 (d,  $J$  = 6.6 Hz, 3H).  $^{13}\text{C}\{^1\text{H}\}$  NMR (101 MHz,  $\text{CDCl}_3$ )  $\delta$  = 163.2, 148.3, 136.9, 122.3, 119.9, 69.0, 24.4.

### 1,2-bis(1-hydroxyethyl)pyridine **8af**



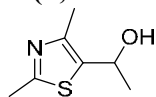
According to general procedure, 2,6-diacetylpyridine (204 mg, 1.25 mmol) gave the title compound **8af** as a pale yellow oil (200.6 mg, 96%, 1:1 mixture of *meso* and *rac*).  $^1\text{H}$  NMR (400 MHz,  $\text{CDCl}_3$ )  $\delta$  = 7.65 (t,  $J$  = 7.7 Hz, 1H), 7.18 (m, 2H), 4.85 (q,  $J$  = 6.5 Hz, 2H), 4.19 (s, 2H), 1.46 (d,  $J$  = 6.6 Hz, 6H).  $^{13}\text{C}\{^1\text{H}\}$  NMR (101 MHz,  $\text{CDCl}_3$ )  $\delta$  = 162.21, 162.18, 137.7, 118.32, 118.28, 69.3, 24.14, 24.10.

### 1-(*N*-methylpyrrol-3-yl)ethanol **8ag**



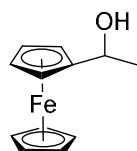
According to general procedure, 3-acetyl-*N*-methylpyrrole (31  $\mu$ L, 0.25 mmol) gave the title compound **8ag** as an orange-red solid (27.5 mg, 88%).  $^1\text{H}$  NMR (300 MHz,  $\text{CDCl}_3$ )  $\delta$  = 6.59 (t,  $J$  = 1.9 Hz, 1H), 6.55 (t,  $J$  = 2.4 Hz, 1H), 6.14 (t,  $J$  = 2.1 Hz, 1H), 4.85 (q,  $J$  = 6.4 Hz, 1H), 3.63 (s, 3H), 1.61 (br. s, 1H), 1.50 (d,  $J$  = 6.4 Hz, 3H).  $^{13}\text{C}\{^1\text{H}\}$  NMR (101 MHz,  $\text{CDCl}_3$ )  $\delta$  = 129.6, 122.1, 118.7, 106.2, 64.8, 36.3, 24.4.

### 1-(2,4-Dimethylthiazol-5-yl)ethanol **8ah**



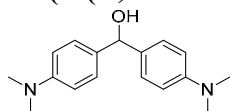
According to general procedure, 1-(2,4-dimethylthiazol-5-yl)ethanone (337  $\mu$ L, 2.5 mmol) gave the title compound **8ah** as a yellow oil (373.4 mg, 95%).  $^1\text{H}$  NMR (300 MHz,  $\text{CDCl}_3$ )  $\delta$  = 5.11 (qd,  $J$  = 6.4 Hz,  $J$  = 3.3 Hz, 1H), 2.60 (s, 3H), 2.30 (s, 3H), 1.87 (s, 1H), 1.50 (d,  $J$  = 6.4 Hz, 3H).  $^{13}\text{C}\{^1\text{H}\}$  NMR (75 MHz,  $\text{CDCl}_3$ )  $\delta$  = 163.6, 146.8, 136.6, 63.8, 25.7, 19.2, 15.1.

### 1-Ferrocenylethanol **8ai**<sup>[3]</sup>



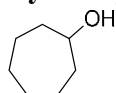
According to general procedure, acetylferrocene (570.0 mg, 2.5 mmol) gave the title compound **8ai** as an orange solid (558.0 mg, 97%).  $^1\text{H}$  NMR (400 MHz,  $\text{CDCl}_3$ )  $\delta$  = 4.56 – 4.54 (m, 1H), 4.22 – 4.16 (m, 9H), 1.87 (d,  $J$  = 4.7 Hz, 1H), 1.44 (d,  $J$  = 6.4 Hz, 3H).  $^{13}\text{C}\{^1\text{H}\}$  NMR (101 MHz,  $\text{CDCl}_3$ )  $\delta$  = 94.9, 68.4, 68.1, 68.0, 66.3, 66.2, 65.7, 23.9.

### Bis(4-(*N,N*-dimethylamino)phenyl)methanol **8aj**



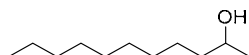
According to general procedure, bis(4-(dimethylamino)phenyl)methanone (67 mg, 0.25 mmol) gave the title compound **8aj** as a yellow-green solid (60 mg, 89%, isolated yield with 3 % of starting material).  $^1\text{H}$  NMR (400 MHz,  $\text{CDCl}_3$ )  $\delta$  = 7.23 (d,  $J$  = 8.7 Hz, 4H), 6.70 (d,  $J$  = 8.7 Hz, 4H), 5.69 (s, 1H), 2.92 (s, 12H), 2.25 (br. s, 1H).  $^{13}\text{C}\{^1\text{H}\}$  NMR (101 MHz,  $\text{CDCl}_3$ )  $\delta$  = 150.1, 132.7, 127.6, 112.6, 75.8, 40.8.

### Cycloheptanol **8ak**<sup>[3]</sup>



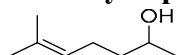
According to general procedure, cycloheptanone (295  $\mu$ L, 2.5 mmol) gave the title compound **8ak** as a pale yellow oil (271.2 mg, 95%).  $^1\text{H}$  NMR (300 MHz,  $\text{CDCl}_3$ )  $\delta$  = 3.89 – 3.79 (m, 1H), 1.95 – 1.87 (m, 2H), 1.70 – 1.49 (m, 8H), 1.44 – 1.35 (m, 3H).  $^{13}\text{C}\{^1\text{H}\}$  NMR (75 MHz,  $\text{CDCl}_3$ )  $\delta$  = 72.9, 37.8, 28.3, 22.8.

### Undecan-2-ol **8al**<sup>[3]</sup>



According to general procedure B, undecan-2-one (517  $\mu$ L, 2.5 mmol) gave the title compound **2al** as a pale yellow oil (413.5 mg, 96%).  $^1\text{H}$  NMR (400 MHz,  $\text{CDCl}_3$ )  $\delta$  = 3.82 – 3.74 (m, 1H), 1.47 – 1.26 (m, 17H), 1.18 (d,  $J$  = 6.1 Hz, 3H), 0.87 (t,  $J$  = 6.8 Hz, 3H).  $^{13}\text{C}\{^1\text{H}\}$  NMR (101 MHz,  $\text{CDCl}_3$ )  $\delta$  = 68.3, 39.5, 32.1, 29.8, 29.8, 29.7, 29.5, 25.9, 23.6, 22.8, 14.3.

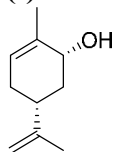
### 6-Methylhept-5-en-2-ol **8am**



According to general procedure, 6-methylhept-5-en-2-one (185  $\mu$ L, 1.25 mmol) gave the title compound **8am** as a pale yellow oil (150.6 mg, 94%).  $^1\text{H}$  NMR (400 MHz,  $\text{CDCl}_3$ )  $\delta$  = 5.13 (t,  $J$  = 7.1 Hz, 1H), 3.84 – 3.76 (m, 1H), 2.14 – 1.99 (m, 2H), 1.69 (s, 3H), 1.62 (s, 3H), 1.55 –

1.42 (m, 3H), 1.18 (d,  $J = 6.2$  Hz, 3H).  $^{13}\text{C}\{^1\text{H}\}$  NMR (101 MHz,  $\text{CDCl}_3$ )  $\delta = 132.2, 124.2, 68.1, 39.4, 25.9, 24.6, 23.6, 17.8$ .

#### (-)-*cis*-Carveol **8an**



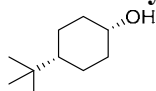
According to general procedure, (*R*)-(-)-carvone (196  $\mu\text{L}$ , 1.25 mmol) gave the title compound **8an** as a colourless oil (152.2 mg, 80%).  $^1\text{H}$  NMR (400 MHz,  $\text{CDCl}_3$ )  $\delta = 5.49$  (m, 1H), 4.72 (s, 2H), 4.18 (s, 1H), 2.30 – 2.22 (m, 1H), 2.18 – 2.12 (m, 1H), 2.10 – 2.07 (m, 1H), 1.99 – 1.89 (m, 1H), 1.75 – 1.73 (m, 6H), 1.65 (s, 1H), 1.50 (m, 1H).  $^{13}\text{C}\{^1\text{H}\}$  NMR (101 MHz,  $\text{CDCl}_3$ )  $\delta = 149.1, 136.3, 124.0, 109.3, 71.0, 40.6, 38.1, 31.2, 20.8, 19.1$ .

#### 1-Cyclopropylethan-1-ol **8ao**



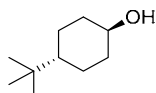
According to general procedure, cyclopropylethan-1-one (233  $\mu\text{L}$ , 2.5 mmol) gave the title compound **8ao** as a pale yellow oil (98% NMR yield).  $^1\text{H}$  NMR (300 MHz,  $\text{CDCl}_3$ )  $\delta = 3.1 - 3.02$  (m, 1H), 2.15 (s, 1H), 1.26 (d,  $J = 6.2$  Hz, 3H), 0.95 – 0.83 (m, 1H), 0.53 – 0.42 (m, 2H), 0.32 – 0.10 (m, 2H).  $^{13}\text{C}\{^1\text{H}\}$  NMR (75 MHz,  $\text{CDCl}_3$ )  $\delta = 73.1, 22.6, 19.3, 3.1, 2.3$ .

#### *cis*-4-*t*-Butyl-1-cyclohexanol **8ap-cis**



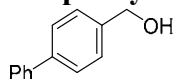
According to general procedure, 4-(*tert*-butyl)cyclohexan-1-one (38.6 mg, 0.25 mmol) gave the title compound **8ap-cis** as a white solid (12.5 mg, 32%).  $^1\text{H}$  NMR (400 MHz,  $\text{CDCl}_3$ )  $\delta = 4.04 - 4.03$  (m, 1H), 1.85 – 1.81 (m, 2H), 1.56 – 1.21 (m, 7H), 1.03 – 0.95 (m, 1H), 0.86 (s, 9H).  $^{13}\text{C}\{^1\text{H}\}$  NMR (101 MHz,  $\text{CDCl}_3$ )  $\delta = 66.1, 48.2, 33.5, 32.7, 27.6, 21.0$ .

#### *trans*-4-*t*-Butyl-1-cyclohexanol **8ap-trans**



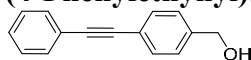
According to general procedure, 4-(*tert*-butyl)cyclohexan-1-one (38.6 mg, 0.25 mmol) gave the title compound **8ap-trans** as a white solid (24.6 mg, 63%).  $^1\text{H}$  NMR (400 MHz,  $\text{CDCl}_3$ )  $\delta = 3.55 - 3.47$  (m, 1H), 2.01 – 1.89 (m, 2H), 1.79 – 1.76 (m, 2H), 1.45 (s, 1H), 1.25 – 1.17 (m, 2H), 1.09 – 0.96 (m, 2H), 0.84 (s, 9H).  $^{13}\text{C}\{^1\text{H}\}$  NMR (101 MHz,  $\text{CDCl}_3$ )  $\delta = 71.4, 47.3, 36.3, 32.4, 27.8, 25.8$ .

#### 4-Biphenylmethanol **10a**<sup>[11]</sup>



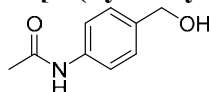
According to general procedure, 4-biphenylmethanal (46 mg, 0.25 mmol) gave the title compound **10a** as a white solid (36.8 mg, 80%).  $^1\text{H}$  NMR (400 MHz,  $\text{CDCl}_3$ )  $\delta = 7.60 - 7.60$  (m, 4H), 7.47 – 7.44 (m, 4H), 7.39 – 7.34 (m, 1H), 4.74 (s, 2H), 1.89 (s, 1H).  $^{13}\text{C}\{^1\text{H}\}$  NMR (101 MHz,  $\text{CDCl}_3$ )  $\delta = 140.9, 140.7, 140.0, 128.9, 127.6, 127.4, 127.2, 65.2$ .

### (4-Phenylethynyl)benzyl alcohol **10b**<sup>[12]</sup>



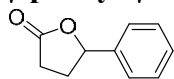
According to general procedure, 4-phenylethynyl-benzaldehyde (22 mg, 0.11 mmol) gave the title compound **10b** as a white solid (19 mg, 82%). <sup>1</sup>H NMR (300 MHz, CDCl<sub>3</sub>) δ = 7.55 – 7.52 (m, 4H), 7.37 – 7.33 (m, 5H), 4.71 (s, 2H). <sup>13</sup>C{<sup>1</sup>H} NMR (75 MHz, CDCl<sub>3</sub>) δ = 141.1, 131.9, 131.7, 128.5, 128.4, 127.0, 123.4, 122.7, 89.6, 89.3, 65.1.

### N-[4-(hydroxymethyl)phenyl]-acetamide **10c**<sup>[13]</sup>



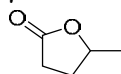
According to general procedure, 4-acetamido-benzaldehyde (40 mg, 0.25 mmol) gave the title compound **10c** as an orange solid (34 mg, 83%). <sup>1</sup>H NMR (400 MHz, CD<sub>2</sub>Cl<sub>2</sub>) δ = 7.47 (d, *J* = 8.4 Hz, 2H), 7.39 (br. s, 1H), 7.30 (d, *J* = 8.4 Hz, 2H), 4.61 (s, 2H), 2.12 (s, 3H), 1.91 (br. s, 1H). <sup>13</sup>C{<sup>1</sup>H} NMR (100 MHz, CD<sub>2</sub>Cl<sub>2</sub>) δ = 168.7, 137.9, 137.4, 128.0, 120.1, 65.0, 24.7.

### γ-phenyl-γ-butyrolactone **12a**<sup>[14]</sup>



According to general procedure, methyl 3-benzoylpropionate (44 μL, 0.25 mmol) gave the title compound **12a** as a colorless oil (32.8 mg, 81%). <sup>1</sup>H NMR (400 MHz, CDCl<sub>3</sub>) δ = 7.42 – 7.32 (m, 5H), 5.52 (dd, *J* = 8.1 Hz, *J* = 6.1 Hz, 1H), 2.71 – 2.62 (m, 3H), 2.26 – 2.14 (m, 1H). <sup>13</sup>C{<sup>1</sup>H} NMR (101 MHz, CDCl<sub>3</sub>) δ = 177.0, 139.5, 128.9, 128.6, 125.4, 81.4, 31.1, 29.1.

### γ-Valerolactone **12b**



According to general procedure, ethyl levulinate (71 μL, 0.5 mmol) gave the title compound **12b** as a colorless oil (39.0 mg, 78%). <sup>1</sup>H NMR (400 MHz, CDCl<sub>3</sub>) δ = 4.62 (m, 1H), 2.55 – 2.51 (m, 2H), 2.38 – 2.30 (m, 1H), 1.86 – 1.76 (m, 1H), 1.39 (d, *J* = 6.3 Hz, 3H). <sup>13</sup>C{<sup>1</sup>H} NMR (75 MHz, CDCl<sub>3</sub>) δ = 177.3, 77.4, 29.8, 29.2, 21.2.

## 6.3.3. Computational details for hydrogenation of carbonyl derivatives

Geometry optimizations have been performed with the Gaussian 09 package<sup>[15]</sup> at the PBE0 level of hybrid density functional theory,<sup>[16]</sup> with inclusion of D3(bj) corrections in the optimization process.<sup>[17]</sup> The geometry of all the structures optimized is available as a single xyz file in the Supporting Information. The atoms C, H, N, P, and O were represented by a def2-svp basis set.<sup>[18]</sup> The atom Re was represented by Dolg's pseudopotential and the associated basis set.<sup>[19]</sup> The solvent (toluene) influence was taken into consideration through single-point calculations on the gas-phase optimized geometry with SCRF calculations within the SMD model.<sup>[20]</sup> For the SCRF calculations, the atoms were treated with a def2-qzvpp basis set.<sup>[21]</sup> All energies reported in the present work are Gibbs free energies obtained by summing the SMD energy (including D3 corrections) and the gas-phase Gibbs contribution at 353 K and 1 atm. The calculated values are given below. Full details on calculated geometries are included in the file “Geom-Calculated.xyz” given as supporting materials.

	E(SMD/Def2QZVPP)	G(353)
Acetophenone	-384,6299778	0,09848
Alcohol	-385,8296481	0,120879
CO	-113,2326555	-0,018118
tBuOH	-233,5191922	0,099936

<b>tBuO</b>	-232,9508982	0,084046	
<b>H<sub>2</sub></b>	-1,168498115	-0,004306	
<b>Br</b>	-2574,042265	-0,019623	
<b>1</b>	-1786,940049	0,462872	<b>50,5</b>
<b>I-1</b>	-1786,450576	0,450682	<b>3,9</b>
<b>I-2</b>	-1786,453063	0,446871	<b>0,00</b>
<b>I-3</b>	-1673,185043	0,439705	<b>6,3</b>
<b>I-4</b>	-1674,342458	0,457344	<b>26,8</b>
<b>TS-(I-4)-(I-5)</b>	-1674,332497	0,455694	<b>31,9</b>
<b>I-6</b>	-1674,376136	0,461059	<b>8,2</b>
<b>I-6</b>	-2059,022653	0,586576	<b>14,7</b>
<b>TS-(I-6)-(I-7)</b>	-2059,007247	0,592893	<b>28,2</b>
<b>I-7</b>	-2059,013618	0,594566	<b>25,2</b>
<b>TS-(I-7)-I-3</b>	-2059,012493	0,589377	<b>22,8</b>

### 6.3.4. X-ray data

#### X-ray data for the complex 1

CCDC 1501902 contains the supplementary crystallographic data for this complex.

X-ray diffraction data were collected on a D8 VENTURE Bruker AXS diffractometer equipped with a PHOTON 100 CMOS detector, using multilayers monochromated Mo-K $\alpha$  radiation ( $\lambda = 0.71073$  Å) at T = 150(2) K. The structure was solved by direct methods using the *SHELXT* program,<sup>[22]</sup> and then refined with full-matrix least-square methods based on  $F^2$  (*SHELXL-2014*).<sup>[23]</sup> The contribution of the disordered solvents to the calculated structure factors was estimated following the *BYPASS* algorithm,<sup>[24]</sup> implemented as the *SQUEEZE* option in *PLATON*.<sup>[25]</sup> A new data set, free of solvent contribution, was then used in the final refinement. All non-hydrogen atoms were refined with anisotropic atomic displacement parameters. Except nitrogen linked hydrogen atoms that were introduced in the structural model through Fourier difference maps analysis, H atoms were finally included in their calculated positions. A final refinement on  $F^2$  with 13026 unique intensities and 536 parameters converged at  $\omega R(F^2) = 0.0557$  ( $R(F) = 0.0233$ ) for 11478 observed reflections with  $I > 2\sigma(I)$ .

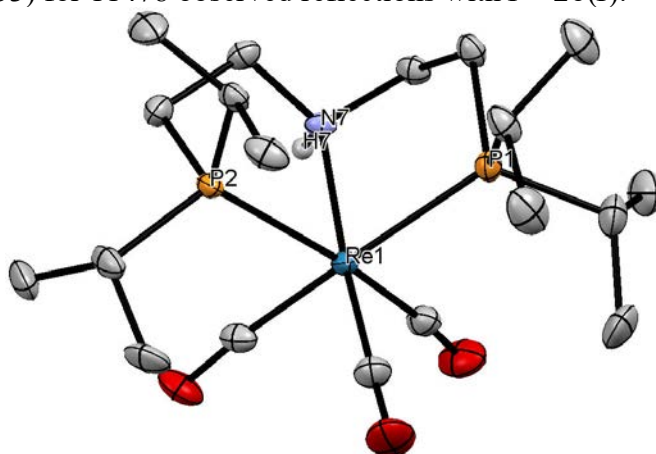


**Figure S1:** ORTEP view of the molecular structure of complex **1** with thermal ellipsoids drawn at 50% probability. Hydrogens atoms, except the NH, bromide, and one molecule of CH<sub>2</sub>Cl<sub>2</sub> were omitted for clarity.



**Table S1.** Crystal data and structure refinement for complex 1.

Empirical formula	C39 H76 Br2 Cl2 N2 O6 P4 Re2
Extended formula	2(C19 H37 N O3 P2 Re), 2(Br), CH <sub>2</sub> Cl <sub>2</sub>
Formula weight	1396.01
Temperature	150 K
Wavelength	0.71073 Å
Crystal system, space group	Triclinic, P $\bar{1}$
Unit cell dimensions	a = 12.0856(11) Å, $\alpha$ = 90.849(3) b = 13.3076(12) Å, $\beta$ = 99.415(3) c = 17.9259(17) Å, $\gamma$ = 91.802(3)
Volume	2842.2(5) Å <sup>3</sup>
Z, Calculated density	2, 1.631 (g.cm <sup>-3</sup> )
Absorption coefficient	5.906 mm <sup>-1</sup>
F(000)	1372
Crystal size	0.550 x 0.150 x 0.070 mm
Crystal color	colourless
Theta range for data collection	3.053 to 27.484 °
h_min, h_max	-15, 15
k_min, k_max	-17, 17
l_min, l_max	-23, 23
Reflections collected / unique	61025 / 13026 [R(int)a = 0.0464]
Reflections [ $I > 2\sigma$ ]	11478
Completeness to theta_max	0.998
Absorption correction type	multi-scan
Max. and min. transmission	0.661 , 0.315
Refinement method	Full-matrix least-squares on F <sup>2</sup>
Data / restraints / parameters	13026 / 0 / 536
bGoodness-of-fit	1.073
Final R indices [ $I > 2\sigma$ ]	R1c = 0.0233, wR2d = 0.0557
R indices (all data)	R1c = 0.0277, wR2d = 0.0574
Largest diff. peak and hole	0.813 and -1.364 e-Å <sup>-3</sup>

$$^a R_{int} = \sum |F_o^2 - \langle F_o^2 \rangle| / \sum [F_o^2]$$

$$^b S = \{ \sum [w(F_o^2 - F_c^2)^2] / (n - p) \}^{1/2}$$

$$^c R1 = \sum | |F_o| - |F_c| | / \sum |F_o|$$

$$^d wR2 = \{ \sum [w(F_o^2 - F_c^2)^2] / \sum [w(F_o^2)^2] \}^{1/2}$$

$$w = 1 / [\sigma(F_o^2) + aP^2 + bP] \text{ where } P = [2F_c^2 + \text{MAX}(F_o^2, 0)] / 3$$

## X-ray data for the complex 2

CCDC 1838314 contains the supplementary crystallographic data for this complex

X-ray diffraction data were collected on a D8 VENTURE Bruker AXS diffractometer equipped with a PHOTON 100 CMOS detector, using multilayers monochromated Mo-K $\alpha$  radiation ( $\lambda$  = 0.71073 Å) at T = 295 K. The structure was solved by dual-space algorithm using the

*SHELXT* program<sup>[22]</sup>, and then refined with full-matrix least-square methods based on  $F^2$  (*SHELXL-2014*).<sup>[23]</sup> All non-hydrogen atoms were refined with anisotropic atomic displacement parameters. H atoms were finally included in their calculated positions. A final refinement on  $F^2$  with 9370 unique intensities and 407 parameters converged at  $\omega R(F^2) = 0.0948$  ( $R(F) = 0.0413$ ) for 7939 observed reflections with  $I > 2\sigma(I)$ .

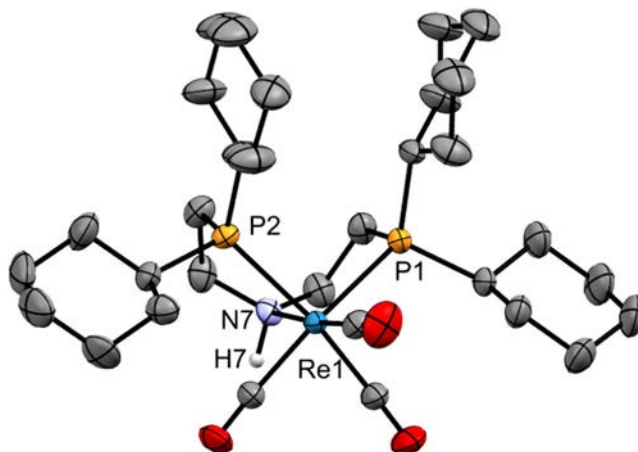


**Figure S2:** ORTEP view of the molecular structure of the complex **2** with thermal ellipsoids drawn at 50% probability. Hydrogen atoms, except *NH*, bromide, and two molecules of  $\text{CH}_2\text{Cl}_2$  were omitted for clarity.

**Table S2.** Crystal data and structure refinement for complex **2**.

Empirical formula	$\text{C}_{33} \text{H}_{57} \text{Br} \text{Cl}_4 \text{N} \text{O}_3 \text{P}_2 \text{Re}$
Extended formula	$\text{C}_{31} \text{H}_{53} \text{N} \text{O}_3 \text{P}_2 \text{Re}, 2(\text{C} \text{H}_2 \text{Cl}_2), \text{Br}$
Formula weight	985.64
Temperature	295 (2) K
Wavelength	0.71073 Å
Crystal system, space group	monoclinic, $P 2_1/c$
Unit cell dimensions	$a = 13.7303(8) \text{ Å}, \alpha = 90^\circ$ $b = 15.5912(7) \text{ Å}, \beta = 106.434(2)^\circ$ $c = 19.9472(11) \text{ Å}, \gamma = 90^\circ$
Volume	$4095.7(4) \text{ Å}^3$
$Z$ , Calculated density	4, $1.598 \text{ (g.cm}^{-3}\text{)}$
Absorption coefficient	$4.313 \text{ mm}^{-1}$
$F(000)$	1976
Crystal size	$0.480 \times 0.390 \times 0.300 \text{ mm}$
Crystal color	colourless
Theta range for data collection	$2.965 \text{ to } 27.483^\circ$
$h_{\text{min}}, h_{\text{max}}$	-17, 17
$k_{\text{min}}, k_{\text{max}}$	-17, 20
$l_{\text{min}}, l_{\text{max}}$	-25, 25
Reflections collected / unique	61054 / 9370 [ $R(\text{int})^a = 0.0658$ ]
Reflections [ $I > 2\sigma$ ]	7939
Completeness to $\theta_{\text{max}}$	0.999
Absorption correction type	multi-scan
Max. and min. transmission	0.274, 0.110
Refinement method	Full-matrix least-squares on $F^2$
Data / restraints / parameters	9370 / 0 / 407
<sup>b</sup> Goodness-of-fit	1.108
Final $R$ indices [ $I > 2\sigma$ ]	$R1^c = 0.0413, wR2^d = 0.0948$
$R$ indices (all data)	$R1^c = 0.0525, wR2^d = 0.1041$
Largest diff. peak and hole	2.275 and $-2.907 \text{ e}^- \cdot \text{Å}^{-3}$

$$^a R_{int} = \sum |F_o^2 - \langle F_o^2 \rangle| / \sum [F_o^2]$$

$$^b S = \{ \sum [w(F_o^2 - F_c^2)^2] / (n - p) \}^{1/2}$$

$$^c R1 = \sum | |F_o| - |F_c| | / \sum |F_o|$$

$$^d wR2 = \{ \sum [w(F_o^2 - F_c^2)^2] / \sum [w(F_o^2)^2] \}^{1/2}$$

$$w = 1 / [\sigma(F_o^2) + aP^2 + bP] \text{ where } P = [2F_c^2 + \text{MAX}(F_o^2, 0)] / 3$$

### X-ray data for the complex 3

CCDC 1838315 contains the supplementary crystallographic data for this complex

X-ray diffraction data were collected on a D8 VENTURE Bruker AXS diffractometer equipped with a PHOTON 100 CMOS detector, using multilayers monochromated Mo-K $\alpha$  radiation ( $\lambda$  = 0.71073 Å) at T = 150(2) K. The structure was solved by dual-space algorithm using the *SHELXT* program [1],[22] and then refined with full-matrix least-square methods based on  $F^2$  (*SHELXL-2014*) [2],[23]. The contribution of the disordered solvents to the structure factors was calculated by the *PLATON SQUEEZE* procedure[26] [3] and then taken into account in the final *SHELXL-2014* least-square refinement. All non-hydrogen atoms were refined with anisotropic atomic displacement parameters. H atoms were finally included in their calculated positions. A final refinement on  $F^2$  with 14407 unique intensities and 703 parameters converged at  $\omega R(F^2)$  = 0.0965 ( $R(F)$  = 0.0471) for 10227 observed reflections with  $I > 2\sigma(I)$ .

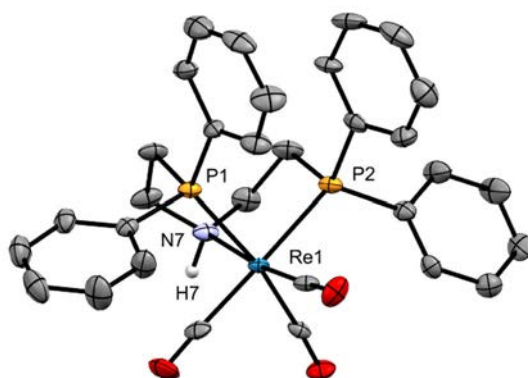


**Figure S3:** ORTEP view of the molecular structure of the complex **3** with thermal ellipsoids drawn at 50% probability. Hydrogen atoms, except NH, and bromide were omitted for clarity.

**Table S3.** Crystal data and structure refinement for complex **3**.

Empirical formula	C <sub>62</sub> H <sub>58</sub> Br <sub>2</sub> N <sub>2</sub> O <sub>6</sub> P <sub>4</sub> Re <sub>2</sub>
Extended formula	2(C <sub>31</sub> H <sub>29</sub> N O <sub>3</sub> P <sub>2</sub> Re), 2(Br)
Formula weight	1583.20
Temperature	150 (2) K
Wavelength	0.71073 Å
Crystal system, space group	monoclinic, <i>P</i> 2/ <i>n</i>
Unit cell dimensions	<i>a</i> = 18.6981(12) Å, $\alpha$ = 90 ° <i>b</i> = 13.0817(8) Å, $\beta$ = 91.262(3) ° <i>c</i> = 25.7348(17) Å, $\gamma$ = 90 °
Volume	6293.3(7) Å <sup>3</sup>
<i>Z</i> , Calculated density	4, 1.671 (g.cm <sup>-3</sup> )
Absorption coefficient	5.264 mm <sup>-1</sup>
<i>F</i> (000)	3088
Crystal size	0.290 x 0.180 x 0.030 mm
Crystal color	colourless
Theta range for data collection	3.023 to 27.484 °
<i>h</i> <sub>min</sub> , <i>h</i> <sub>max</sub>	-24, 23
<i>k</i> <sub>min</sub> , <i>k</i> <sub>max</sub>	-16, 16

l_min, l_max	-32, 33
Reflections collected / unique	43525 / 14407 [R(int) <sup>a</sup> = 0.0659]
Reflections [I>2σ]	10227
Completeness to theta_max	0.997
Absorption correction type	multi-scan
Max. and min. transmission	0.854 , 0.604
Refinement method	Full-matrix least-squares on F <sup>2</sup>
Data / restraints / parameters	14407 / 0 / 703
<sup>b</sup> Goodness-of-fit	1.019
Final R indices [I>2σ]	R1 <sup>c</sup> = 0.0471, wR2 <sup>d</sup> = 0.0965
R indices (all data)	R1 <sup>c</sup> = 0.0816, wR2 <sup>d</sup> = 0.1114
Largest diff. peak and hole	2.668 and -2.390 e <sup>-</sup> .Å <sup>-3</sup>

$$^a R_{int} = \sum |F_o^2 - \langle F_o^2 \rangle| / \sum [F_o^2]$$

$$^b S = \{ \sum [w(F_o^2 - F_c^2)^2] / (n - p) \}^{1/2}$$

$$^c R1 = \sum | |F_o| - |F_c| | / \sum |F_o|$$

$$^d wR2 = \{ \sum [w(F_o^2 - F_c^2)^2] / \sum [w(F_o^2)^2] \}^{1/2}$$

$$w = 1 / [\sigma(F_o^2) + aP^2 + bP] \text{ where } P = [2F_c^2 + \text{MAX}(F_o^2, 0)] / 3$$

### X-ray data for the complex 4

CCDC 1838317 contains the supplementary crystallographic data for this complex

X-ray diffraction data were collected on a APEXII Bruker AXS diffractometer equipped with an APEXII CCD detector, using graphite monochromated Mo-Kα radiation (λ = 0.71073 Å) at T = 150(2) K. The structure was solved by dual-space algorithm using the *SHELXT* program,<sup>[22]</sup> and then refined with full-matrix least-square methods based on F<sup>2</sup> (*SHELXL-2014*).<sup>[23]</sup> All non-hydrogen atoms were refined with anisotropic atomic displacement parameters. H atoms were finally included in their calculated positions. A final refinement on F<sup>2</sup> with 6379 unique intensities and 292 parameters converged at ωR(F<sup>2</sup>) = 0.0473 (R(F) = 0.0250) for 5482 observed reflections with I > 2σ(I).

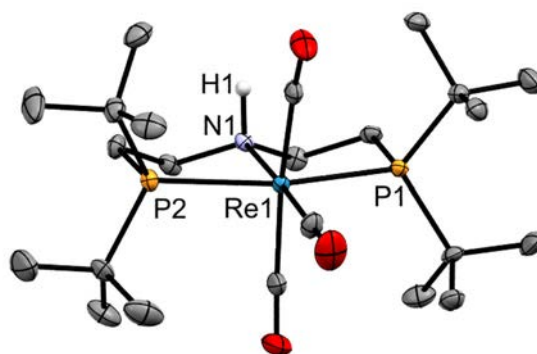


**Figure S4:** ORTEP view of the molecular structure of complex **4** with thermal ellipsoids drawn at 50% probability. Hydrogen atoms, except NH, and bromide were omitted for clarity.

**Table S4.** Crystal data and structure refinement for complex **4**.

Empirical formula	C <sub>23</sub> H <sub>45</sub> Br N O <sub>3</sub> P <sub>2</sub> Re
Extended formula	C <sub>23</sub> H <sub>45</sub> N O <sub>3</sub> P <sub>2</sub> Re, Br
Formula weight	711.65
Temperature	150(2) K
Wavelength	0.71073 Å
Crystal system, space group	monoclinic, <i>P</i> 2 <sub>1</sub> / <i>c</i>
Unit cell dimensions	$a = 14.3480(8) \text{ Å}, \alpha = 90^\circ$ $b = 13.1393(6) \text{ Å}, \beta = 110.032(2)^\circ$ $c = 15.7971(8) \text{ Å}, \gamma = 90^\circ$

Volume	2797.9(2) Å <sup>3</sup>
Z, Calculated density	4, 1.689 (g.cm <sup>-3</sup> )
Absorption coefficient	5.909 mm <sup>-1</sup>
F(000)	1416
Crystal size	0.560 x 0.500 x 0.480 mm
Crystal color	colourless
Theta range for data collection	3.022 to 27.481 °
h_min, h_max	-18, 15
k_min, k_max	-16, 17
l_min, l_max	-20, 19
Reflections collected / unique	18356 / 6379 [R(int) <sup>a</sup> = 0.0331]
Reflections [I>2σ]	5482
Completeness to theta_max	0.994
Absorption correction type	multi-scan
Max. and min. transmission	0.059 , 0.047
Refinement method	Full-matrix least-squares on F <sup>2</sup>
Data / restraints / parameters	6379 / 0 / 292
<sup>b</sup> Goodness-of-fit	1.043
Final R indices [I>2σ]	R1 <sup>c</sup> = 0.0250, wR2 <sup>d</sup> = 0.0473
R indices (all data)	R1 <sup>c</sup> = 0.0334, wR2 <sup>d</sup> = 0.0494
Largest diff. peak and hole	0.774 and -0.789 e <sup>-</sup> .Å <sup>-3</sup>
<sup>a</sup> R <sub>int</sub> = $\sum  F_o^2 - \langle F_o^2 \rangle  / \sum [F_o^2]$	
<sup>b</sup> S = $\{\sum [w(F_o^2 - F_c^2)^2] / (n - p)\}^{1/2}$	
<sup>c</sup> R1 = $\sum   F_o  -  F_c   / \sum  F_o $	
<sup>d</sup> wR2 = $\{\sum [w(F_o^2 - F_c^2)^2] / \sum [w(F_o^2)^2]\}^{1/2}$	
$w = 1 / [\sigma(F_o^2) + aP^2 + bP]$ where $P = [2F_c^2 + \text{MAX}(F_o^2, 0)] / 3$	

## X-ray data for the complex 5

CCDC 1838316 contains the supplementary crystallographic data for this complex. X-ray diffraction data were collected on an APEXII Bruker AXS diffractometer equipped with an APEXII CCD detector, using graphite monochromated Mo-Kα radiation ( $\lambda = 0.71073$  Å) at T = 150(2) K. The structure was solved by dual-space algorithm using the *SHELXT* program,<sup>[22]</sup> and then refined with full-matrix least-square methods based on  $F^2$  (*SHELXL-2014*) [2].<sup>[23]</sup> All non-hydrogen atoms were refined with anisotropic atomic displacement parameters. H atoms were finally included in their calculated positions. A final refinement on  $F^2$  with 20639 unique intensities and 929 parameters converged at  $\omega R(F^2) = 0.0647$  ( $R(F) = 0.0329$ ) for 18858 observed reflections with  $I > 2\sigma(I)$ .

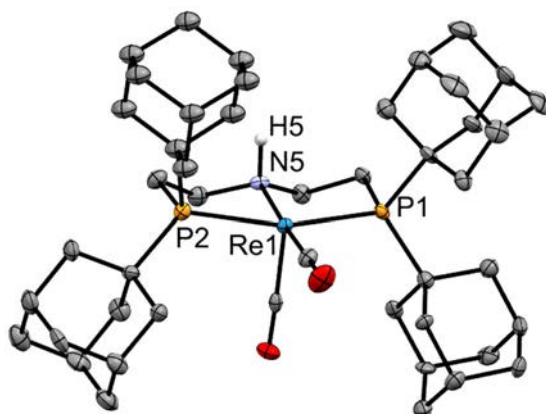


**Figure S5:** ORTEP view of the molecular structure of complex **5** with thermal ellipsoids drawn at 50% probability. Two molecules of **5** and 3 molecules of CH<sub>2</sub>Cl<sub>2</sub> are present in the crystal unit. Hydrogen atoms, except NH, bromide, and molecules of CH<sub>2</sub>Cl<sub>2</sub> were omitted for clarity.

**Table S5.** Crystal data and structure refinement for complex **5**.

Empirical formula	C <sub>95</sub> H <sub>144</sub> Br <sub>2</sub> Cl <sub>6</sub> N <sub>2</sub> O <sub>4</sub> P <sub>4</sub> Re <sub>2</sub>
Extended formula	2(C <sub>46</sub> H <sub>69</sub> N O <sub>2</sub> P <sub>2</sub> Re), 3(C H <sub>2</sub> Cl <sub>2</sub> ), 2(Br)
Formula weight	2246.91
Temperature	150 (2) K
Wavelength	0.71073 Å
Crystal system, space group	monoclinic, <i>P</i> 2 <sub>1</sub>
Unit cell dimensions	<i>a</i> = 16.1581(4) Å, α = 90 ° <i>b</i> = 19.2559(5) Å, β = 113.5370(10) ° <i>c</i> = 16.2039(4) Å, γ = 90 °
Volume	4622.2(2) Å <sup>3</sup>
<i>Z</i> , Calculated density	2, 1.614 (g.cm <sup>-3</sup> )
Absorption coefficient	3.776 mm <sup>-1</sup>
<i>F</i> (000)	2284
Crystal size	0.320 x 0.110 x 0.080 mm
Crystal color	orange
Theta range for data collection	2.939 to 27.484 °
<i>h</i> <sub>min</sub> , <i>h</i> <sub>max</sub>	-12, 20
<i>k</i> <sub>min</sub> , <i>k</i> <sub>max</sub>	-25, 25
<i>l</i> <sub>min</sub> , <i>l</i> <sub>max</sub>	-21, 21
Reflections collected / unique	50150 / 20639 [R(int) <sup>a</sup> = 0.0413]
Reflections [ <i>I</i> >2σ]	18858
Completeness to theta <sub>max</sub>	0.990
Absorption correction type	multi-scan
Max. and min. transmission	0.739 , 0.605
Refinement method	Full-matrix least-squares on <i>F</i> <sup>2</sup>
Data / restraints / parameters	20639 / 1 / 929
Flack parameter	0.487(5)
<sup>b</sup> Goodness-of-fit	1.032
Final <i>R</i> indices [ <i>I</i> >2σ]	<i>R</i> <sup>c</sup> = 0.0329, <i>wR</i> <sup>d</sup> = 0.0647
<i>R</i> indices (all data)	<i>R</i> <sup>c</sup> = 0.0388, <i>wR</i> <sup>d</sup> = 0.0672
Largest diff. peak and hole	0.941 and -0.932 e <sup>-</sup> .Å <sup>-3</sup>

$$^a R_{int} = \sum |F_o^2 - \langle F_o^2 \rangle| / \sum [F_o^2]$$

$$^b S = \{ \sum [w(F_o^2 - F_c^2)^2] / (n - p) \}^{1/2}$$

$$^c R_1 = \sum | |F_o| - |F_c| | / \sum |F_o|$$

$$^d wR_2 = \{ \sum [w(F_o^2 - F_c^2)^2] / \sum [w(F_o^2)^2] \}^{1/2}$$

$$w = 1 / [\sigma(F_o^2) + aP^2 + bP] \text{ where } P = [2F_c^2 + \text{MAX}(F_o^2, 0)] / 3$$

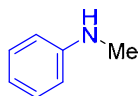
## 6.4. Part V-2- Mono *N*-methylation of anilines with methanol

### 6.4.1. General procedure for methylation reactions

In an argon filled glove box, an ACE pressure tube (15 mL) was charged with **3** (3.9 mg, 1.0 mol%) and methanol (2.0 mL), followed by aniline (0.5 mmol) and Cs<sub>2</sub>CO<sub>3</sub> (8.2 mg, 5.0 mol%), in this order. The mixture was then stirred for 48 hours at 140 °C in an oil bath. The solution was then diluted with ethyl acetate (2.0 mL) and filtered through a small pad of silica (2 cm in a Pasteur pipette). The silica was washed with ethyl acetate. The filtrate was evaporated and the crude residue was purified by column chromatography (SiO<sub>2</sub>, mixture of petroleum ether/ethyl acetate as eluent).

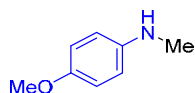
## 6.4.2. Characterization of the methylated products

### *N*-Methylaniline **14a**<sup>[27]</sup>



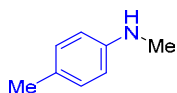
According to the general procedure, aniline (46  $\mu$ L, 0.5 mmol) gave the title compound **14a** as a colorless oil (51.0 mg, 95%). <sup>1</sup>H NMR (400 MHz, CDCl<sub>3</sub>):  $\delta$  7.24 – 7.19 (m, 2H), 6.76–6.71 (m, 1H), 6.66 – 6.62 (m, 2H), 3.70 (br, 1H), 2.85 (s, 3H). <sup>13</sup>C{<sup>1</sup>H} NMR (101 MHz, CDCl<sub>3</sub>):  $\delta$  149.5, 129.3, 117.4, 112.5, 30.9.

### 4-Methoxy-*N*-methylaniline **14b**<sup>[28]</sup>



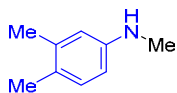
According to the general procedure, 4-methoxyaniline (62 mg, 0.5 mmol) gave the title compound **14b** as a colorless oil (62.4 mg, 91%). <sup>1</sup>H NMR (300 MHz, CDCl<sub>3</sub>):  $\delta$  6.86 – 6.81 (m, 2H), 6.63 – 6.58 (m, 2H), 3.77 (s, 3H), 3.38 (br, 1H), 2.82 (s, 3H). <sup>13</sup>C{<sup>1</sup>H} NMR (75 MHz, CDCl<sub>3</sub>):  $\delta$  152.1, 143.8, 115.0, 113.7, 55.9, 31.6.

### *N*-Methyl-4-methylaniline **14c**<sup>[27]</sup>



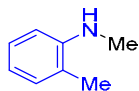
According to the general procedure, 4-methylaniline (54 mg, 0.5 mmol) gave the title compound **14c** as a colorless oil (57.0 mg, 94%). <sup>1</sup>H NMR (300 MHz, CDCl<sub>3</sub>):  $\delta$  7.04 (d,  $J$  = 8.2 Hz, 2H), 6.57 (d,  $J$  = 8.2 Hz, 2H), 3.56 (br s, 1H), 2.84 (d,  $J$  = 5.5 Hz, 3H), 2.28 (s, 3H).

### *N*-Methyl-3,4-dimethylaniline **14d**<sup>[29]</sup>



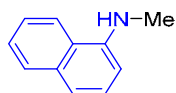
According to the general procedure, 3,4-dimethylaniline (61 mg, 0.5 mmol) gave the title compound **14d** as a colorless oil (39.2 mg, 58%). <sup>1</sup>H NMR (400 MHz, CDCl<sub>3</sub>):  $\delta$  6.96 (d,  $J$  = 8.1 Hz, 1H), 6.47 (d,  $J$  = 2.8 Hz, 1H), 6.41 (dd,  $J$  = 8.1, 2.7 Hz, 1H), 3.10 (br, 1H), 2.82 (s, 3H), 2.21 (s, 3H), 2.17 (s, 3H). <sup>13</sup>C{<sup>1</sup>H} NMR (101 MHz, CDCl<sub>3</sub>):  $\delta$  147.6, 137.4, 130.4, 125.5, 114.6, 110.2, 31.3, 20.2, 18.8.

### *N*-Methyl-2-methylaniline **14e**<sup>[27]</sup>



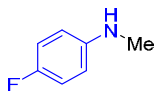
According to the general procedure, 2-methylaniline (54  $\mu$ L, 0.5 mmol) gave the title compound **14e** as a colorless oil (16.4 mg, 27%). <sup>1</sup>H NMR (400 MHz, CDCl<sub>3</sub>):  $\delta$  7.23 – 7.12 (m, 1H), 7.12 – 7.03 (m, 1H), 6.67 (td,  $J$  = 7.3, 1.3 Hz, 1H), 6.62 (dd,  $J$  = 8.0, 1.2 Hz, 1H), 3.55 (s, 1H), 2.90 (s, 3H), 2.14 (s, 3H).

### ***N*-Methyl-1-naphthylamine 14f<sup>[30]</sup>**



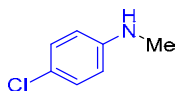
According to the general procedure, 1-naphthylamine (71 mg, 0.5 mmol) gave the title compound **14f** as a colorless oil (41.7 mg, 53%). <sup>1</sup>H NMR (300 MHz, CDCl<sub>3</sub>): δ 7.86 – 7.78 (m, 2H), 7.53 – 7.40 (m, 3H), 7.30 (d, *J* = 8.1 Hz, 1H), 6.64 (dd, *J* = 7.5, 1.1 Hz, 1H), 4.38 (br, 1H), 3.04 (s, 3H). <sup>13</sup>C{<sup>1</sup>H} NMR (75 MHz, CDCl<sub>3</sub>): δ 144.5, 134.3, 128.8, 126.8, 125.8, 124.8, 123.6, 119.9, 117.5, 104.1, 31.2.

### **4-Fluoro-*N*-methylaniline 14i<sup>[31]</sup>**



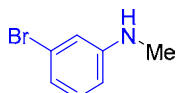
According to the general procedure, 4-fluoroaniline (48 μL, 0.5 mmol) gave the title compound **14i** as a colorless oil (60.0 mg, 96%). <sup>1</sup>H NMR (400 MHz, CDCl<sub>3</sub>): δ 6.94 – 6.87 (m, 2H), 6.57 – 6.52 (m, 2H), 3.55 (br, 1H), 2.81 (s, 3H). <sup>13</sup>C{<sup>1</sup>H} NMR (101 MHz, CDCl<sub>3</sub>): δ 155.9 (d, *J* = 234.3 Hz), 145.8 (d, *J* = 1.9 Hz), 115.7 (d, *J* = 22.3 Hz), 113.3 (d, *J* = 7.7 Hz), 31.5. <sup>19</sup>F NMR (376 MHz, CDCl<sub>3</sub>) δ -128.5.

### **4-Chloro-*N*-methylaniline 14j<sup>[27]</sup>**



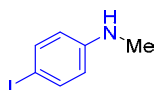
According to the general procedure, 4-chloroaniline (64 mg, 0.5 mmol) gave the title compound **14j** as a colorless oil (60.2 mg, 85%). <sup>1</sup>H NMR (300 MHz, CDCl<sub>3</sub>): δ 7.15 (d, *J* = 9.0 Hz, 2H), 6.53 (d, *J* = 8.9 Hz, 2H), 3.63 (br, 1H), 2.81 (s, 3H). <sup>13</sup>C{<sup>1</sup>H} NMR (75 MHz, CDCl<sub>3</sub>): δ 148.0, 129.1, 121.8, 113.5, 30.9.

### **3-Bromo-*N*-methylaniline 14k<sup>[28]</sup>**



According to the general procedure, 3-bromoaniline (55 μL, 0.5 mmol) gave the title compound **14k** as a colorless oil (82.8 mg, 89%). <sup>1</sup>H NMR (400 MHz, CDCl<sub>3</sub>) δ 7.02 (t, *J* = 8.0 Hz, 1H), 6.81 (d, *J* = 7.8 Hz, 1H), 6.74 (t, *J* = 2.1 Hz, 1H), 6.51 (dd, *J* = 8.2, 2.4 Hz, 1H), 3.76 (br, 1H), 2.82 (s, 3H). <sup>13</sup>C{<sup>1</sup>H} NMR (101 MHz, CDCl<sub>3</sub>): δ 150.7, 130.5, 123.4, 120.0, 114.9, 111.4, 30.6.

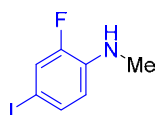
### **4-Iodo-*N*-methylaniline 14l<sup>[27]</sup>**



According to the general procedure, 4-iodoaniline (110 mg, 0.5 mmol) gave the title compound **14l** as a colorless oil (81.6 mg, 70%). <sup>1</sup>H NMR (400 MHz, CDCl<sub>3</sub>): δ 7.43 (d, *J* = 8.9 Hz, 1H), 6.39 (d, *J* = 8.9 Hz, 1H), 3.71 (br, 1H), 2.81 (s, 3H). <sup>13</sup>C{<sup>1</sup>H} NMR (101 MHz, CDCl<sub>3</sub>): δ 149.0, 137.9, 114.7, 77.8, 30.7.

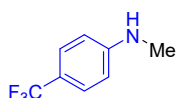


## 2-Fluoro-4-Iodo-*N*-methylaniline **14m**



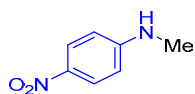
According to the general procedure, 2-fluoro-4-iodo-aniline (119 mg, 0.5 mmol) gave the title compound **14m** as a colorless oil (76.6 mg, 61%). <sup>1</sup>H NMR (400 MHz, CDCl<sub>3</sub>): δ 7.32 (dt, *J* = 8.4, 1.6 Hz, 1H), 7.27 (dd, *J* = 10.9, 2.0 Hz, 1H), 6.45 (t, *J* = 8.8 Hz, 1H), 3.98 (br, 1H), 2.87 (s, 3H). <sup>13</sup>C{<sup>1</sup>H} NMR (101 MHz, CDCl<sub>3</sub>): δ 151.4 (d, *J* = 243.9 Hz), 137.8 (d, *J* = 11.6 Hz), 133.6 (d, *J* = 3.5 Hz), 123.0 (d, *J* = 20.8 Hz), 113.2 (d, *J* = 3.9 Hz), 74.8 (d, *J* = 7.7 Hz), 30.1. <sup>19</sup>F NMR (376 MHz, CDCl<sub>3</sub>): δ -134.4. GC-MS, *m/z*(%) = 251([M]<sup>+</sup>, 100), 236(9), 209(10), 123(58), 109(10), 97(16), 77(38), 63(8), 50(10).

## *N*-Methyl-4-trifluoromethylaniline<sup>[28]</sup>



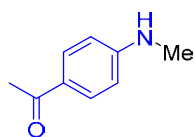
According to the general procedure, 4-trifluoromethylaniline hydrochloride, (99 mg, 0.5 mmol) gave the title compound **14n** as a colorless oil (27.2 mg, 31%). <sup>1</sup>H NMR (400 MHz, CDCl<sub>3</sub>): δ 7.42 (d, *J* = 8.5 Hz, 2H), 6.60 (d, *J* = 8.5 Hz, 2H), 4.04 (br, 1H), 2.87 (d, *J* = 5.1 Hz, 3H). <sup>13</sup>C{<sup>1</sup>H} NMR (101 MHz, CDCl<sub>3</sub>): δ 151.8, 126.7 (q, *J* = 3.9 Hz), 125.2 (q, *J* = 270 Hz), 118.7 (q, *J* = 32.6 Hz), 111.6, 30.4. <sup>19</sup>F NMR (376 MHz, CDCl<sub>3</sub>): δ -60.9.

## *N*-Methyl-4-nitroaniline **14o**<sup>[32]</sup>



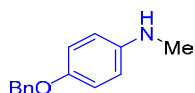
According to the general procedure, 4-nitroaniline (70 mg, 0.5 mmol) gave the title compound **14o** as a colorless oil (38.1 mg, 50%). <sup>1</sup>H NMR (400 MHz, CDCl<sub>3</sub>): δ 8.09 (d, *J* = 9.2 Hz, 2H), 6.52 (d, *J* = 9.3 Hz, 2H), 4.65 (br. s, 1H), 2.93 (d, *J* = 5.1 Hz, 3H). <sup>13</sup>C{<sup>1</sup>H} NMR (101 MHz, CDCl<sub>3</sub>): δ 154.3, 138.0, 126.5, 110.8, 30.3.

## 4-Acetyl-*N*-methylaniline **14q**<sup>[27]</sup>



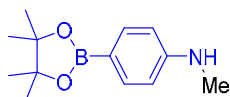
According to the general procedure, 4-aminoacetophenone (68 mg, 0.5 mmol) gave the title compound **14q** as a colorless oil (44.8 mg, 60%). <sup>1</sup>H NMR (400 MHz, CDCl<sub>3</sub>): δ 7.81 (d, *J* = 8.7 Hz, 2H), 6.53 (d, *J* = 8.7 Hz, 2H), 4.49 (br. s, 1H), 2.86 (d, *J* = 1.6 Hz, 3H), 2.48 (s, 3H). <sup>13</sup>C{<sup>1</sup>H} NMR (101 MHz, CDCl<sub>3</sub>) δ 196.5, 153.3, 130.8, 126.4, 111.0, 30.1, 26.0.

## *N*-Methyl-4-benzyloxyaniline **14t**



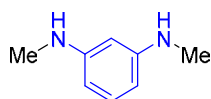
According to the general procedure, 4-(benzyloxy)aniline hydrochloride, (118 mg, 0.5 mmol) gave the title compound **14t** as a colorless oil (102.3 mg, 90%). <sup>1</sup>H NMR (400 MHz, CDCl<sub>3</sub>): δ 7.46-7.42 (m, 2H), 7.41 – 7.37 (m, 2H), 7.34 – 7.30 (m, 1H), 6.89 (d, *J* = 8.9 Hz, 2H), 6.60 (d, *J* = 8.8 Hz, 2H), 5.01 (s, 2H), 3.29 (br, 1H), 2.82 (s, 3H). <sup>13</sup>C{<sup>1</sup>H} NMR (101 MHz, CDCl<sub>3</sub>): δ 151.4, 144.1, 137.8, 128.6, 127.9, 127.6, 116.3, 113.7, 71.0, 31.7.

### *N*-Methyl-4-(4,4,5,5-tetramethyl-1,3,2-dioxaborolan-2-yl)-aniline **14u**



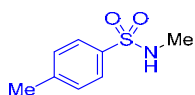
According to the general procedure, 4-(4,4,5,5-tetramethyl-1,3,2-dioxaborolan-2-yl)-aniline, (109 mg, 0.5 mmol) gave the title compound **14u** as a colorless oil (23.3 mg, 20%). <sup>1</sup>H NMR (400 MHz, CDCl<sub>3</sub>): δ 7.65 (d, *J* = 8.3 Hz, 2H), 6.58 (d, *J* = 8.4 Hz, 2H), 3.87 (br, 1H), 2.85 (s, 3H), 1.32 (s, 12H). <sup>13</sup>C{<sup>1</sup>H} NMR (101 MHz, CDCl<sub>3</sub>, the carbon attached to quadrupole B was not observed due to low intensity): δ 151.9, 136.4, 111.6, 83.3, 30.4, 25.0. <sup>11</sup>B{<sup>1</sup>H} NMR (128 MHz, CDCl<sub>3</sub>): δ 30.8. GC-MS, *m/z*(%) = 233([M]<sup>+</sup>, 100), 218(19), 175(22), 160(44), 147(25), 134(97), 119(8), 108(14), 77(13).

### *N,N'*-Dimethyl-1,3-diaminobenzene **14w**<sup>[33]</sup>



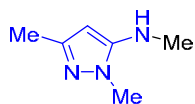
According to the general procedure, 1,3-diaminobenzene, (54 mg, 0.5 mmol) gave the title compound **14w** as a colorless oil (62.7 mg, 92%). <sup>1</sup>H NMR (300 MHz, CDCl<sub>3</sub>): δ 7.03 (t, *J* = 8.0 Hz, 1H), 6.05 (dd, *J* = 8.0, 2.2 Hz, 2H), 5.89 (t, *J* = 2.2 Hz, 1H), 3.53 (br. s, 2H), 2.83 (s, 6H). <sup>13</sup>C{<sup>1</sup>H} NMR (101 MHz, CDCl<sub>3</sub>): δ 150.7, 130.0, 102.6, 96.5, 30.9.

### *N*-Methyl-4-methylbenzenesulfonamide **14y**<sup>[27]</sup>



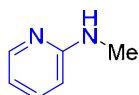
According to the general procedure, 4-methylbenzenesulfonamide, (86 mg, 0.5 mmol) gave the title compound **14y** as a colorless oil (77.0 mg, 91%). <sup>1</sup>H NMR (300 MHz, CDCl<sub>3</sub>): δ 7.74 (d, *J* = 8.2 Hz, 1H), 7.30 (d, *J* = 8.2 Hz, 1H), 4.85 (d, *J* = 5.3 Hz, 1H), 2.61 (d, *J* = 5.4 Hz, 3H), 2.41 (s, 3H). <sup>13</sup>C{<sup>1</sup>H} NMR (75 MHz, CDCl<sub>3</sub>): δ 143.6, 135.8, 129.8, 127.3, 29.4, 21.6.

### *N*-Methyl-1,3-dimethyl-1*H*-pyrazol-5-amine **14z**



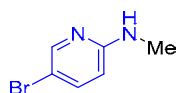
According to the general procedure, 1,3-dimethyl-1*H*-pyrazol-5-amine, (56 mg, 0.5 mmol) gave the title compound **14z** as a colorless oil (59.5 mg, 95%). <sup>1</sup>H NMR (400 MHz, CDCl<sub>3</sub>): δ 5.21 (s, 1H), 3.46 (s, 3H), 3.45 (br. s, 1H), 2.74 (d, *J* = 5.4 Hz, 3H), 2.12 (s, 3H). <sup>13</sup>C{<sup>1</sup>H} NMR (101 MHz, CDCl<sub>3</sub>): δ 149.9, 147.1, 87.1, 33.7, 32.4, 13.9. GC-MS, *m/z*(%) = 125([M]<sup>+</sup>, 100), 110(41), 95(10), 83(24), 66(18), 55(36).

### *N*-Methyl-2-aminopyridine **14aa**<sup>[34]</sup>



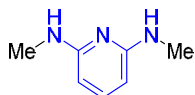
According to the general procedure, 2-aminopyridine, (47 mg, 0.5 mmol) gave the title compound **14aa** as a colorless oil (28.6 mg, 53%). <sup>1</sup>H NMR (400 MHz, CDCl<sub>3</sub>): δ 8.08 (ddd, *J* = 5.0, 2.0, 0.9 Hz, 1H), 7.42 (ddd, *J* = 8.8, 7.2, 1.9 Hz, 1H), 6.56 (ddd, *J* = 7.2, 5.0, 1.0 Hz, 1H), 6.37 (dt, *J* = 8.4, 1.0 Hz, 1H), 4.58 (br, 1H), 2.91 (d, *J* = 5.3 Hz, 3H). <sup>13</sup>C{<sup>1</sup>H} NMR (101 MHz, CDCl<sub>3</sub>): δ 159.7, 148.3, 137.5, 112.8, 106.3, 29.2.

### 5-Bromo-2-methylamino-pyridine<sup>[35]</sup>



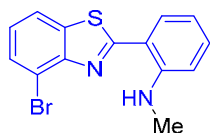
According to the general procedure, 2-amino-5-bromo-2-pyridine, (87 mg, 0.5 mmol) gave the title compound **14ab** as a colorless oil (66.4 mg, 71%). <sup>1</sup>H NMR (400 MHz, CDCl<sub>3</sub>): δ 8.09 (d, *J* = 2.7 Hz, 1H), 7.46 (dd, *J* = 8.9, 2.5 Hz, 1H), 6.27 (d, *J* = 8.8 Hz, 1H), 4.74 (br. s, 1H), 2.87 (d, *J* = 5.1 Hz, 3H). <sup>13</sup>C{<sup>1</sup>H} NMR (101 MHz, CDCl<sub>3</sub>): δ 158.2, 148.7, 139.8, 107.7, 106.9, 29.2.

### *N,N'*-Dimethyl-2,6-diaminopyridine **14ac**<sup>[33]</sup>



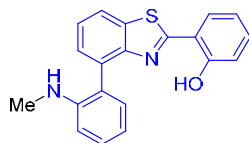
According to the general procedure, 2,6-diaminopyridine, (55 mg, 0.5 mmol) gave the title compound **14ac** as a colorless oil (28.6 mg, 90%). <sup>1</sup>H NMR (300 MHz, CDCl<sub>3</sub>): δ 7.28 (t, *J* = 7.9 Hz, 1H), 5.73 (d, *J* = 8.0 Hz, 2H), 4.28 (br. s, 2H), 2.85 (d, *J* = 5.2 Hz, 6H). <sup>13</sup>C{<sup>1</sup>H} NMR (75 MHz, CDCl<sub>3</sub>): δ 159.2, 139.2, 94.2, 29.3.

### 4-Bromo-2-(2-*N*-Methylaminophenyl)-benzothiazole **14ad**



An oven dried 10 mL Pyrex Wheaton vial was charged with a stir bar, **3** (23 mg, 0.025 mmol, 5.0 mol%), Cs<sub>2</sub>CO<sub>3</sub> (188.9 mg, 0.6 mmol, 100 mol%), 2-(2-aminophenyl)-4-bromobenzothiazole (174.5 mg, 0.6 mmol) and dry MeOH (2 mL). The vial was purged with Ar, then the reaction mixture degassed (3 cycles of freeze-pump-thaw) and left under an atmosphere of Ar before being sealed with a Teflon lined cap. The vial was then placed in an oil bath at 140 °C and reaction progress monitored by TLC (9:1 cyclohexane/EtOAc). After 5 days, the reaction mixture was cooled to rt, diluted with EtOAc and passed through a Silica plug in a Pasteur pipette and eluted with EtOAc. The residue was concentrated onto Celite and purified using Silica gel flash column chromatography using 100% cyclohexane to cyclohexane/CH<sub>2</sub>Cl<sub>2</sub> (7:3). Desired fractions were collected and concentrated under reduced pressure to furnish the desired product **14ad** as a yellow powder, which was further dried under high vacuum overnight (149.3 mg, 78%). <sup>1</sup>H NMR (400 MHz, CDCl<sub>3</sub>) δ 7.78 (dd, *J* = 7.9, 1.0 Hz), 7.68 (dd, *J* = 7.9, 1.5 Hz), 7.63 (dd, *J* = 7.8, 1.0 Hz), 7.36 (ddd, *J* = 8.6, 7.1, 1.5 Hz), 7.19 (t, *J* = 7.9 Hz), 6.80 (dd, *J* = 8.5, 1.1 Hz), 6.69 (ddd, *J* = 8.1, 7.1, 1.1 Hz), 3.08 (d, *J* = 4.4 Hz, 3H). <sup>13</sup>C{<sup>1</sup>H} NMR (101 MHz, CDCl<sub>3</sub>) δ 170.0, 151.8, 148.9, 134.0, 132.8, 130.6, 129.4, 125.7, 120.4, 115.8, 115.1, 114.2, 111.2, 30.0. HR-MS-ESI (*m/z*): found [M<sup>79</sup>Br+H]<sup>+</sup> 318.9892, calcd C<sub>14</sub>H<sub>12</sub>N<sub>2</sub>S<sup>79</sup>Br requires 318.9905.

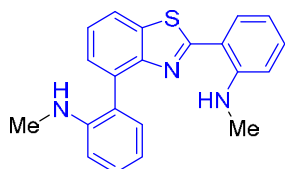
### 2-(2-Hydroxyphenyl)-4-(2-*N*-Methylaminophenyl)-benzothiazole **14ae**



An oven dried 10 mL Pyrex Wheaton vial was charged with a stir bar, **3** (21 mg, 0.025 mmol, 5.0 mol%), Cs<sub>2</sub>CO<sub>3</sub> (170 mg, 0.5 mmol, 100 mol%), 2-(2-hydroxyphenyl)-4-(2-aminophenyl)benzothiazole (156.7 mg, 0.5 mmol) and dry MeOH (2 mL). The vial was purged

with Ar, then the reaction mixture degassed (3 cycles of freeze-pump-thaw) and left under an atmosphere of Ar before being sealed with a Teflon lined cap. The vial was then placed in an oil bath at 140 °C and reaction progress monitored by TLC (9:1 cyclohexane/EtOAc). After 5 days, the reaction mixture was cooled to rt, diluted with EtOAc and passed through a Silica plug in a Pasteur pipette and eluted with EtOAc. The residue was concentrated onto Celite and purified using Silica gel flash column chromatography using 100% cyclohexane to cyclohexane/EtOAc (9:1). Desired fractions were collected and concentrated under reduced pressure to furnish the desired product **14ae** as a yellow powder, which was further dried under high vacuum overnight (54.7 mg, 33%). Starting material could be recovered from purification (75 mg, 48% recovery). <sup>1</sup>H NMR (400 MHz, CDCl<sub>3</sub>) δ 7.92 (dd, *J* = 7.7, 1.5 Hz, 1H), 7.68 (dd, *J* = 7.9, 1.6 Hz, 1H), 7.55 (dd, *J* = 7.4, 1.5 Hz, 1H), 7.50 (t, *J* = 7.6 Hz, 1H), 7.36 (dddd, *J* = 8.2, 7.2, 6.3, 1.6 Hz, 2H), 7.24 (dd, *J* = 7.5, 1.7 Hz, 1H), 7.03 (dd, *J* = 8.4, 1.1 Hz, 1H), 6.97 – 6.90 (m, 1H), 6.86 (td, *J* = 7.5, 1.2 Hz, 1H), 6.82 (d, *J* = 8.2 Hz, 1H), 2.82 (s, 3H). <sup>13</sup>C{<sup>1</sup>H} NMR (101 MHz, CDCl<sub>3</sub>) δ 169.1, 158.1, 150.3, 146.5, 133.6, 133.5, 133.0, 130.9, 129.7, 128.42, 128.39, 126.2, 124.2, 120.9, 119.5, 118.1, 117.0, 116.9, 110.4, 30.9. HR-MS-ESI (*m/z*): found [M+H]<sup>+</sup> 333.1062, calcd C<sub>20</sub>H<sub>17</sub>N<sub>2</sub>OS requires 333.1062.

## 2, 4-di-(2-*N*-Methylaminophenyl) benzothiazole **14af**



An oven dried 10 mL Pyrex Wheaton vial was charged with a stir bar, **3** (20 mg, 0.025 mmol, 5.0 mol%), Cs<sub>2</sub>CO<sub>3</sub> (190 mg, 0.6 mmol, 100 mol%), 2,2'-(benzo[d]thiazole-2,4-diyl)dianiline (180 mg, 0.6 mmol) and dry MeOH (2 mL). The vial was purged with Ar, then the reaction mixture degassed (3 cycles of freeze-pump-thaw) and left under an atmosphere of Ar before being sealed with a Teflon lined cap. The vial was placed in an oil bath at 140 °C for 5 days; reaction progress monitored by LCMS and TLC (4:1 cyclohexane/EtOAc). The reaction mixture was cooled to rt, and diluted with EtOAc (10 mL) and passed through a Silica plug, and the Silica washed with EtOAc. The organic phase was washed with saturated aqueous NaHCO<sub>3</sub> (1 x 25 mL) and brine (1 x 50 mL). The organic phase was dried over anhydrous MgSO<sub>4</sub>, then filtered and concentrated onto Celite and purified by Silica flash column chromatography (eluent: 100% cyclohexane to 9:1 cyclohexane/EtOAc). Desired fractions were combined and concentrated under reduced pressure to provide the product **14af** as a yellow foam (159.6 mg, 77%). <sup>1</sup>H NMR (400 MHz, CDCl<sub>3</sub>) δ 7.88 (dd, *J* = 7.8, 1.3 Hz, 1H), 7.71 (dd, *J* = 7.9, 1.5 Hz, 1H), 7.50 (dd, *J* = 7.4, 1.3 Hz, 1H), 7.44 (t, *J* = 7.6 Hz, 1H), 7.39 (td, *J* = 8.0, 1.6 Hz, 1H), 7.35 – 7.29 (m, 2H), 6.90 (t, *J* = 6.8 Hz, 2H), 6.74 – 6.64 (m, 2H), 2.83 (s, 3H), 2.81 (s, 3H). <sup>13</sup>C{<sup>1</sup>H} NMR (101 MHz, CDCl<sub>3</sub>) δ 169.3, 151.5, 148.6, 146.2, 133.8, 133.1, 132.4, 131.3, 130.4, 129.4, 127.6, 125.7, 125.5, 120.6, 117.5, 115.0, 114.5, 111.1, 110.8, 31.3, 29.8. HR-MS-ESI (*m/z*): found [M+H]<sup>+</sup> 346.1387, calc'd C<sub>21</sub>H<sub>20</sub>N<sub>3</sub>S requires 346.1378.

### 6.4.3. Computational details for *N*-methylation of anilines with methanol

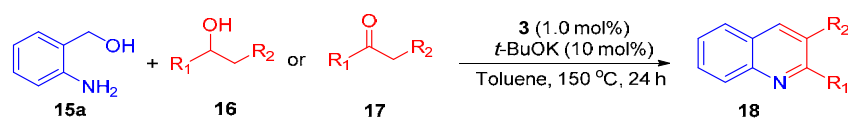
Geometry optimizations have been performed with the Gaussian 09 package<sup>[15]</sup> at the PBE0 level of hybrid density functional theory,<sup>[16]</sup> with inclusion of D3(bj) corrections in the optimization process.<sup>[17]</sup> The geometry of all the structures optimized is available as a single xyz file in the Supporting Information. The atoms C, H, N, P, and O were represented by a def2-svp basis set.<sup>[18]</sup> The atom Re was represented by Dolg's pseudopotential and the associated basis set.<sup>[19]</sup> The solvent (methanol) influence was taken into consideration through

single-point calculations on the gas-phase optimized geometry with SCRF calculations within the SMD model.<sup>[20]</sup> For the SCRF calculations, the atoms were treated with a def2-qzvpp basis set.<sup>[21]</sup> All energies reported in the present work are Gibbs free energies obtained by summing the SMD energy (including D3 corrections) and the gas-phase Gibbs contribution at 353 K and 1 atm. The calculated values are given below. Full details on calculated geometries are included in the file “Geom-Calculated.xyz” given as supporting materials.

	E(SMD/Def2QZVPP)		
	Methanol	G(413) H	G(413) D
H <sub>2</sub> O	-76,39832905	-0,005477	
H <sub>2</sub>	-1,168765243	-0,007457	
CH <sub>2</sub> =O	-114,4292551	-0,004923	-0,011576
PhNH <sub>2</sub>	-287,4096815	0,074144	
Hemiaminal	-401,8696272	0,100581	
CH <sub>3</sub> OH	-115,6557789	0,018135	0,003728
Ph-N=CH <sub>2</sub>	-325,4481097	0,076268	0,069396
Ph-NH-CH <sub>3</sub>	-326,6820497	0,098229	0,083876
CO	-113,2278569	-0,022797	
II-2	-1786,448498	0,423873	
II-3	-1673,190243	0,417468	
II-8	-1788,859659	0,463613	0,449152
TS-(II-8)-(II-9)	-1788,821375	0,458462	0,445821
II-9	-1674,383931	0,438776	0,432526
TS-(II-9)-H <sub>2</sub>	-1674,333164	0,433574	0,428831
II-10	-1999,844726	0,543823	0,530655
TS-(II-10)-(II-11)	-1999,838212	0,546365	0,533315
II-11	-1999,886788	0,543791	0,529415

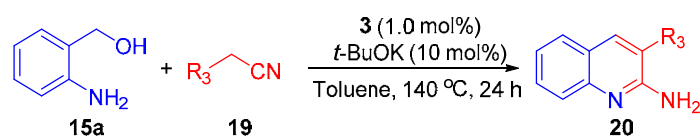
## 6.5. Part V-3- Synthesis of quinolines through acceptorless dehydrogenative coupling

### 6.5.1. General procedure for synthesis of quinolines using 2-aminobenzyl alcohol with alcohols or ketones



In an argon filled glove box, a 20 mL Schlenk tube was charged with 2-aminobenzyl alcohol **15a** (0.5 mmol), **16** or **17** (0.5 mmol), **3** (1.0 mol%), t-BuOK (10 mol%) and toluene (2 mL) in this order. Then the reaction mixture was heated at 150 °C with argon stream for 24 h. After cooling to room temperature, the solution was diluted with ethyl acetate (2 mL) and filtered through a small pad of silica (2 cm in a Pasteur pipette). The silica was washed with ethyl acetate. The filtrate was evaporated and the crude residue was purified by column chromatography (SiO<sub>2</sub>, mixture of petroleum ether/ethyl acetate as eluent).

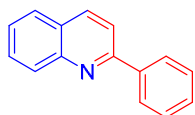
### 6.5.2. General procedure for synthesis of 2-amino quinolines with nitriles



In an argon filled glove box, a 20 mL Schlenk tube was charged with 2-aminobenzyl alcohol **15a** (0.5 mmol), **19** (0.5 mmol), **3** (1.0 mol%), *t*-BuOK (10 mol%) and toluene (2 mL) in this order. Then the reaction mixture was heated at 140 °C with argon stream for 24 h. After cooling to room temperature, the solution was diluted with ethyl acetate (2 mL) and filtered through a small pad of silica (2 cm in a Pasteur pipette). The silica was washed with ethyl acetate. The filtrate was evaporated and the crude residue was purified by column chromatography (SiO<sub>2</sub>, mixture of petroleum ether/ethyl acetate as eluent).

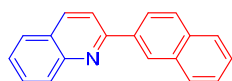
### 6.5.3. Characterization of quinolines

#### 2-Phenylquinoline **18a**<sup>[36]</sup>



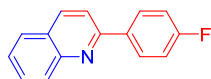
According to the general procedure, 2-(hydroxymethyl)aniline **15a** (62 mg, 0.5 mmol) and 1-phenylethanol **16a** (60  $\mu$ L, 0.5 mmol) gave the title compound **18a** as white solid (89 mg, 87%). According to the general procedure, 2-(hydroxymethyl)aniline **15a** (62 mg, 0.5 mmol) and acetophenone (60  $\mu$ L, 0.5 mmol) gave the title compound **18a** as white solid (93.3 mg, 91%). <sup>1</sup>H NMR (400 MHz, CDCl<sub>3</sub>):  $\delta$  8.23 (d, *J* = 8.7 Hz, 1H), 8.19 – 8.16 (m, 3H), 7.89 (d, *J* = 8.6 Hz, 1H), 7.84 (d, *J* = 8.1 Hz, 1H), 7.73 (ddd, *J* = 8.6, 6.8, 1.6 Hz, 1H), 7.56 – 7.51 (m, 3H), 7.49 – 7.45 (m, 1H). <sup>13</sup>C{<sup>1</sup>H} NMR (101 MHz, CDCl<sub>3</sub>)  $\delta$  157.5, 148.4, 139.8, 136.9, 129.9, 129.8, 129.5, 129.0, 127.7, 127.6, 127.3, 126.4, 119.2.

#### 2-(Naphthalen-2-yl)quinoline **18b**<sup>[37]</sup>



According to the general procedure, 2-(hydroxymethyl)aniline **15a** (62 mg, 0.5 mmol) and 1-(naphthalen-2-yl)ethanol **16b** (86 mg, 0.5 mmol) gave the title compound **18b** as colorless crystals (119 mg, 93%). <sup>1</sup>H NMR (400 MHz, CDCl<sub>3</sub>):  $\delta$  8.63 (d, *J* = 2.1 Hz, 1H), 8.39 (dd, *J* = 8.6, 1.9 Hz, 1H), 8.25 (t, *J* = 8.5 Hz, 2H), 8.08 – 7.97 (m, 3H), 7.93–7.89 (m, 1H), 7.85 (dd, *J* = 8.1, 1.5 Hz, 1H), 7.76 (ddd, *J* = 8.4, 6.8, 1.6 Hz, 1H), 7.58 – 7.49 (m, 3H). <sup>13</sup>C{<sup>1</sup>H} NMR (101 MHz, CDCl<sub>3</sub>):  $\delta$  157.3, 148.5, 137.1, 136.9, 134.0, 133.7, 129.9, 129.8, 129.0, 128.7, 127.9, 127.6, 127.4, 127.3, 126.8, 126.6, 126.5, 125.2, 119.3.

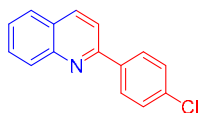
#### 2-(4-Fluorophenyl)quinoline **18c**<sup>[37-38]</sup>



According to the general procedure, 2-(hydroxymethyl)aniline **15a** (62 mg, 0.5 mmol) and 1-(4-fluorophenyl)ethanol **16c** (70 mg, 0.5 mmol) gave the title compound **18c** as colorless crystals (89 mg, 80%). <sup>1</sup>H NMR (400 MHz, CDCl<sub>3</sub>):  $\delta$  8.21 – 8.16 (m, 4H), 7.81 (t, *J* = 8.0 Hz, 2H), 7.78–7.73 (m, 1H), 7.54 (ddd, *J* = 8.1, 6.8, 1.3 Hz, 1H), 7.23 (t, *J* = 8.7 Hz, 2H). <sup>13</sup>C{<sup>1</sup>H} NMR (101 MHz, CDCl<sub>3</sub>):  $\delta$  163.8 (d, *J* = 248.9 Hz), 156.2, 148.3, 136.9, 135.8 (d, *J* = 3.1 Hz), 129.8, 129.7, 129.4 (d, *J* = 8.1 Hz), 127.5, 127.1, 126.4, 118.6, 115.8 (d, *J* = 21.6 Hz). <sup>19</sup>F{<sup>1</sup>H} NMR (376 MHz, CDCl<sub>3</sub>)  $\delta$  -112.39.



### 2-(4-Chlorophenyl)quinoline 18d<sup>[37]</sup>



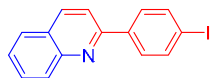
According to the general procedure, 2-(hydroxymethyl)aniline **15a** (62 mg, 0.5 mmol) and 1-(4-chlorophenyl)ethanol **16d** (78 mg, 0.5 mmol) gave the title compound **18d** as colorless crystals (110 mg, 92%). <sup>1</sup>H NMR (400 MHz, CDCl<sub>3</sub>): δ 8.20 (dd, *J* = 8.6, 2.1 Hz, 1H), 8.16 (d, *J* = 8.6 Hz, 1H), 8.14 – 8.09 (m, 2H), 7.82 (dd, *J* = 8.6, 2.0 Hz, 2H), 7.74 (ddd, *J* = 8.4, 6.9, 1.6 Hz, 1H), 7.53 (ddd, *J* = 8.1, 6.8, 1.3 Hz, 1H), 7.51 – 7.47 (m, 2H). <sup>13</sup>C{<sup>1</sup>H} NMR (101 MHz, CDCl<sub>3</sub>): δ 156.1, 148.3, 138.2, 137.0, 135.6, 129.9, 129.8, 129.1, 128.9, 127.6, 127.3, 126.6, 118.6.

### 2-(4-Bromophenyl)quinoline 18e<sup>[36]</sup>



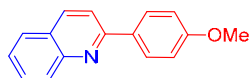
According to the general procedure, 2-(hydroxymethyl)aniline **15a** (62 mg, 0.5 mmol) and 1-(4-bromophenyl)ethanol **16e** (101 mg, 0.5 mmol) gave the title compound **18e** as colorless crystals (126 mg, 89%). <sup>1</sup>H NMR (400 MHz, CDCl<sub>3</sub>): δ 8.18 – 8.14 (m, 2H), 8.05 – 8.02 (m, 2H), 7.81 – 7.76 (m, 2H), 7.73 (ddd, *J* = 8.4, 6.9, 1.5 Hz, 1H), 7.65 – 7.62 (m, 2H), 7.52 (ddd, *J* = 8.1, 6.8, 1.2 Hz, 1H). <sup>13</sup>C{<sup>1</sup>H} NMR (101 MHz, CDCl<sub>3</sub>) δ 156.0, 148.3, 138.5, 137.0, 132.0, 129.9, 129.8, 129.1, 127.6, 127.3, 126.6, 124.0, 118.5.

### 2-(4-Iodophenyl)quinoline 18f<sup>[39]</sup>



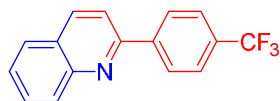
According to the general procedure, 2-(hydroxymethyl)aniline **15a** (62 mg, 0.5 mmol) and 1-(4-iodophenyl)ethanol **16f** (124 mg, 0.5 mmol) gave the title compound **18f** as colorless crystals (124 mg, 75%). <sup>1</sup>H NMR (400 MHz, CDCl<sub>3</sub>) δ 8.19-8.15 (m, 2H), 7.94 – 7.81 (m, 4H), 7.81-7.78 (m, 2H), 7.73 (ddd, *J* = 8.4, 6.8, 1.6 Hz, 1H), 7.53 (t, *J* = 7.2 Hz, 1H). <sup>13</sup>C{<sup>1</sup>H} NMR (101 MHz, CDCl<sub>3</sub>) δ 156.2, 148.3, 139.1, 138.0, 137.0, 129.9, 129.8, 129.3, 127.6, 127.4, 126.6, 118.5, 96.0.

### 2-(4-Methoxyphenyl)quinoline 18g<sup>[36]</sup>



According to the general procedure, 2-(hydroxymethyl)aniline **15a** (62 mg, 0.5 mmol) and 1-(4-methoxyphenyl)ethanol **16g** (76 mg, 0.5 mmol) gave the title compound **18g** as colorless crystals (93 mg, 79%). <sup>1</sup>H NMR (400 MHz, CDCl<sub>3</sub>) δ 8.17-8.13 (m, 4H), 7.82 (d, *J* = 8.6, 1H), 7.79 (d, *J* = 7.8 Hz, 1H), 7.71 (ddd, *J* = 8.4, 6.8, 1.6 Hz, 1H), 7.50 (t, *J* = 7.5 Hz, 1H), 7.05 (d, *J* = 8.9 Hz, 2H), 3.88 (s, 3H). <sup>13</sup>C{<sup>1</sup>H} NMR (101 MHz, CDCl<sub>3</sub>) δ 160.9, 157.0, 148.4, 136.7, 132.3, 129.7, 129.6, 129.0, 127.5, 127.0, 126.0, 118.6, 114.3, 55.5.

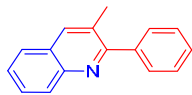
### 2-(4-(Trifluoromethyl)phenyl)quinoline 18h<sup>[36]</sup>



According to the general procedure, 2-(hydroxymethyl)aniline **15a** (62 mg, 0.5 mmol) and 1-(4-trifluoromethylphenyl)ethanol **16h** (95 mg, 0.5 mmol) gave the title compound **18h** as colorless crystals (116 mg, 85%). <sup>1</sup>H NMR (400 MHz, CDCl<sub>3</sub>) δ 8.27 (d, *J* = 7.9 Hz, 2H), 8.24

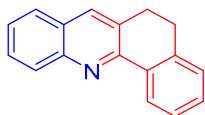
– 8.18 (m, 2H), 7.86 – 7.82 (m, 2H), 7.78 – 7.74 (m, 3H), 7.56 (ddd,  $J = 8.2, 6.8, 1.3$  Hz, 1H).  $^{13}\text{C}\{^1\text{H}\}$  NMR (101 MHz,  $\text{CDCl}_3$ )  $\delta$  155.7, 148.4, 143.0 (q,  $J = 1.1$  Hz), 137.2, 131.2 (q,  $J = 32.4$  Hz), 130.1, 130.0, 127.9, 127.6, 127.5, 127.0, 125.8 (q,  $J = 3.7$  Hz), 124.3 (q,  $J = 272.1$  Hz), 118.8.  $^{19}\text{F}\{^1\text{H}\}$  NMR (376 MHz,  $\text{CDCl}_3$ )  $\delta$  -62.5.

### 3-Methyl-2-phenylquinoline **18i**<sup>[36]</sup>



According to the general procedure, 2-(hydroxymethyl)aniline **15a** (62 mg, 0.5 mmol) and 1-phenylpropan-1-ol **16i** (68 mg, 0.5 mmol) gave the title compound **18i** as colorless crystals (87 mg, 79%).  $^1\text{H}$  NMR (400 MHz,  $\text{CDCl}_3$ ):  $\delta$  8.13 (d,  $J = 8.3$  Hz, 1H), 8.03 (s, 1H), 7.79 (d,  $J = 7.7$  Hz, 1H), 7.67 (ddd,  $J = 8.6, 7.0, 1.6$  Hz, 1H), 7.63 – 7.55 (m, 2H), 7.57 – 7.39 (m, 4H), 2.47 (d,  $J = 1.0$  Hz, 3H).  $^{13}\text{C}\{^1\text{H}\}$  NMR (101 MHz,  $\text{CDCl}_3$ ):  $\delta$  160.7, 146.8, 141.0, 136.9, 129.4, 129.4, 129.0, 128.9, 128.5, 128.3, 127.8, 126.8, 126.6, 20.8.

### 5,6-Dihydrobenzo[*c*]acridine **18j**<sup>[36]</sup>



According to the general procedure, 2-(hydroxymethyl)aniline **15a** (62 mg, 0.5 mmol) and 1-tetralol **16j** (74 mg, 0.5 mmol) gave the title compound **18j** as colorless crystals (92 mg, 80%).

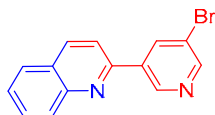
$^1\text{H}$  NMR (400 MHz,  $\text{CDCl}_3$ )  $\delta$  8.64 (dd,  $J = 7.7, 1.7$  Hz, 1H), 8.18 (d,  $J = 8.4$  Hz, 1H), 7.88 (s, 1H), 7.73 (d,  $J = 8.1$  Hz, 1H), 7.67 (ddd,  $J = 8.4, 6.8, 1.5$  Hz, 1H), 7.50 – 7.44 (m, 2H), 7.39 (td,  $J = 7.4, 1.5$  Hz, 1H), 7.29 (d,  $J = 7.5$  Hz, 1H), 3.13 – 3.08 (m, 2H), 3.04–2.99 (m, 2H).  $^{13}\text{C}\{^1\text{H}\}$  NMR (101 MHz,  $\text{CDCl}_3$ )  $\delta$  153.4, 147.7, 139.5, 134.8, 133.7, 130.6, 129.7, 129.5, 128.7, 128.0, 127.9, 127.4, 127.0, 126.1, 126.1, 28.9, 28.5.

### 2-(Pyridin-2-yl)quinoline **18k**<sup>[36]</sup>



According to the general procedure, 2-(hydroxymethyl)aniline **15a** (62 mg, 0.5 mmol) and 1-(2-pyridinyl)ethanol **16k** (62 mg, 0.5 mmol) gave the title compound **18k** as colorless crystals (94 mg, 91%).  $^1\text{H}$  NMR (400 MHz,  $\text{CDCl}_3$ ):  $\delta$  8.74 (ddd,  $J = 4.8, 1.9, 1.0$  Hz, 1H), 8.66 (dt,  $J = 8.1, 1.2$  Hz, 1H), 8.57 (d,  $J = 8.6$  Hz, 1H), 8.27 (d,  $J = 8.7$  Hz, 1H), 8.19 (d,  $J = 8.4$  Hz, 1H), 7.90 – 7.81 (m, 2H), 7.73 (ddd,  $J = 8.6, 7.0, 1.6$  Hz, 1H), 7.54 (ddd,  $J = 8.1, 6.8, 1.3$  Hz, 1H), 7.35 (ddd,  $J = 7.5, 4.8, 1.2$  Hz, 1H).  $^{13}\text{C}\{^1\text{H}\}$  NMR (101 MHz,  $\text{CDCl}_3$ ):  $\delta$  156.5, 156.3, 149.3, 148.1, 137.0, 136.9, 130.0, 129.7, 128.4, 127.7, 126.9, 124.1, 121.9, 119.1.

### 2-(5-Bromopyridin-3-yl)quinoline **18l**

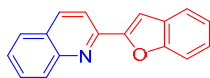


According to the general procedure, 2-(hydroxymethyl)aniline **15a** (62 mg, 0.5 mmol) and 5-bromo-3-acetylpyridine **17l** (100 mg, 0.5 mmol) gave the title compound **18l** as colorless crystals (130 mg, 91%, contaminated with 7% of **6l**).  $^1\text{H}$  NMR (400 MHz,  $\text{CDCl}_3$ ):  $\delta$  9.24 (s, 1H), 8.75 (s, 1H), 8.69 (s, 1H), 8.25 (d,  $J = 8.6$  Hz, 1H), 8.15 (d,  $J = 8.4$  Hz, 1H), 7.85–7.81 (m, 2H), 7.76 (ddd,  $J = 8.6, 6.8, 1.6$  Hz, 1H), 7.57 (m, 2H).  $^{13}\text{C}\{^1\text{H}\}$  NMR (101 MHz,  $\text{CDCl}_3$ ):



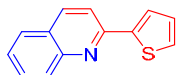
$\delta$  153.0, 151.2, 148.4, 146.8, 137.6, 137.5, 136.7, 130.3, 129.9, 127.7, 127.6, 127.3, 121.4, 118.4.

### 2-(Benzofuran-2-yl)quinoline **18m**<sup>[40]</sup>



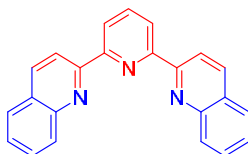
According to the general procedure, 2-(hydroxymethyl)aniline **15a** (62 mg, 0.5 mmol) and 1-(benzofuran-2-yl)ethanol **16m** (81 mg, 0.5 mmol) gave the title compound **18m** as colorless crystals (113 mg, 92%). <sup>1</sup>H NMR (400 MHz, CDCl<sub>3</sub>):  $\delta$  8.21 (d,  $J$  = 8.3 Hz, 2H), 8.00 (d,  $J$  = 8.6 Hz, 1H), 7.80 (dd,  $J$  = 8.2, 1.7 Hz, 1H), 7.74 (ddd,  $J$  = 8.4, 6.8, 1.5 Hz, 1H), 7.69 (d,  $J$  = 7.6 Hz, 1H), 7.65 (d,  $J$  = 8.2 Hz, 1H), 7.60 (d,  $J$  = 1.1 Hz, 1H), 7.53 (ddd,  $J$  = 8.1, 6.8, 1.2 Hz, 1H), 7.38 (ddd,  $J$  = 8.3, 7.2, 1.4 Hz, 1H), 7.29 (td,  $J$  = 7.5, 1.0 Hz, 1H). <sup>13</sup>C{<sup>1</sup>H} NMR (101 MHz, CDCl<sub>3</sub>):  $\delta$  155.7, 155.3, 149.1, 148.4, 136.9, 130.1, 129.7, 128.9, 127.7, 127.7, 126.8, 125.6, 123.4, 121.9, 118.2, 111.9, 106.3.

### 2-(Thiophen-2-yl)quinoline **18n**<sup>[41]</sup>



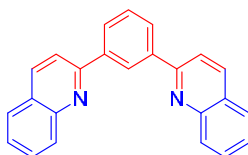
According to the general procedure, 2-(hydroxymethyl)aniline **15a** (62 mg, 0.5 mmol) and 1-(thiophen-2-yl)ethanol **16n** (64 mg, 0.5 mmol) gave the title compound **18n** as colorless crystals (100 mg, 95%). <sup>1</sup>H NMR (400 MHz, CDCl<sub>3</sub>):  $\delta$  8.12 (d,  $J$  = 8.6, 1H), 8.09 (d,  $J$  = 8.4 Hz, 1H), 7.78–7.68 (m, 4H), 7.54 – 7.40 (m, 2H), 7.16 (dd,  $J$  = 5.0, 3.7 Hz, 1H). <sup>13</sup>C{<sup>1</sup>H} NMR (101 MHz, CDCl<sub>3</sub>):  $\delta$  152.5, 148.3, 145.5, 136.7, 129.9, 129.4, 128.7, 128.2, 127.6, 127.3, 126.2, 126.0, 117.8.

### 2,6-Di(quinolin-2-yl)pyridine **18o**<sup>[42]</sup>



According to the general procedure, 2-(hydroxymethyl)aniline **15a** (123 mg, 1.0 mmol) and 2,5-diacetylpyridine **17o** (82 mg, 0.5 mmol) gave the title compound **18o** as colorless crystals (158 mg, 95%). <sup>1</sup>H NMR (400 MHz, CDCl<sub>3</sub>):  $\delta$  8.86 (d,  $J$  = 8.6 Hz, 2H), 8.78 (d,  $J$  = 7.8 Hz, 2H), 8.35 (d,  $J$  = 8.7 Hz, 2H), 8.22 (d,  $J$  = 8.4 Hz, 2H), 8.08 (t,  $J$  = 7.8 Hz, 1H), 7.89 (d,  $J$  = 8.1 Hz, 2H), 7.76 (ddd,  $J$  = 8.4, 6.9, 1.5 Hz, 2H), 7.58 (ddd,  $J$  = 8.2, 6.8, 1.2 Hz, 2H). <sup>13</sup>C{<sup>1</sup>H} NMR (101 MHz, CDCl<sub>3</sub>):  $\delta$  156.4, 155.7, 148.1, 138.1, 136.9, 130.0, 129.7, 128.5, 127.8, 126.9, 122.2, 119.2.

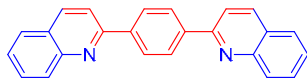
### 1,3-Di(quinolin-2-yl)benzene **18p**<sup>[43]</sup>



According to the general procedure, 2-(hydroxymethyl)aniline **15a** (123 mg, 1.0 mmol) and 1,3-diacetylbenzene **17p** (81 mg, 0.5 mmol) gave the title compound **18p** as colorless crystals (143 mg, 86%). <sup>1</sup>H NMR (400 MHz, CDCl<sub>3</sub>):  $\delta$  8.97 (t,  $J$  = 1.7 Hz, 1H), 8.30 (dd,  $J$  = 7.8, 1.9 Hz, 2H), 8.25 (t,  $J$  = 9.3 Hz, 4H), 8.03 (d,  $J$  = 8.6 Hz, 2H), 7.85 (d,  $J$  = 8.1 Hz, 2H), 7.75 (ddd,  $J$  = 8.6, 6.9, 1.5 Hz, 2H), 7.70 (t,  $J$  = 7.8 Hz, 1H), 7.55 (ddd,  $J$  = 8.1, 6.8, 1.2 Hz, 2H).

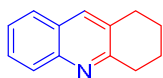
$^{13}\text{C}\{^1\text{H}\}$  NMR (101 MHz,  $\text{CDCl}_3$ )  $\delta$  157.2, 148.4, 140.4, 137.0, 129.9, 129.8, 129.5, 128.6, 127.6, 127.4, 126.9, 126.5, 119.3.

#### 1,4-Di(quinolin-2-yl)benzene **18q**<sup>[44]</sup>



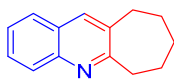
According to the general procedure, 2-(hydroxymethyl)aniline **15a** (123 mg, 1.0 mmol) and 1,4-diacetylbenzene **17q** (81 mg, 0.5 mmol) gave the title compound **18q** as colorless crystals (159 mg, 96%).  $^1\text{H}$  NMR (400 MHz,  $\text{CDCl}_3$ ):  $\delta$  8.36 (s, 4H), 8.26 (d,  $J$  = 8.6 Hz, 2H), 8.22 (d,  $J$  = 8.4 Hz, 2H), 7.98 (d,  $J$  = 8.6 Hz, 2H), 7.86 (d,  $J$  = 8.0 Hz, 2H), 7.76 (ddd,  $J$  = 8.4, 6.9, 1.5 Hz, 2H), 7.55 (ddd,  $J$  = 8.1, 6.8, 1.2 Hz, 2H).  $^{13}\text{C}\{^1\text{H}\}$  NMR (101 MHz,  $\text{CDCl}_3$ ):  $\delta$  156.9, 148.5, 140.5, 137.0, 130.0, 129.9, 128.1, 127.6, 127.5, 126.6, 119.2.

#### 1,2,3,4-Tetrahydroacridine **18r**<sup>[36]</sup>



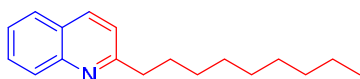
According to the general procedure, 2-(hydroxymethyl)aniline **15a** (62 mg, 0.5 mmol) and cyclohexanone **17r** (52  $\mu\text{L}$ , 0.5 mmol) gave the title compound **18r** as colorless crystals (79 mg, 86%).  $^1\text{H}$  NMR (400 MHz,  $\text{CDCl}_3$ )  $\delta$  7.98 (d,  $J$  = 8.4 Hz, 1H), 7.74 (s, 1H), 7.65 (d,  $J$  = 8.2 Hz, 1H), 7.58 (ddd,  $J$  = 8.4, 6.7, 1.5 Hz, 1H), 7.40 (m, 1H), 3.11 (t,  $J$  = 6.5 Hz, 2H), 2.92 (t,  $J$  = 6.3 Hz, 2H), 1.99 – 1.92 (m, 2H), 1.89 – 1.82 (m, 2H).  $^{13}\text{C}\{^1\text{H}\}$  NMR (101 MHz,  $\text{CDCl}_3$ ):  $\delta$  159.3, 146.5, 135.1, 131.0, 128.6, 128.2, 127.2, 126.9, 125.6, 33.5, 29.3, 23.2, 22.9.

#### 7,8,9,10-Tetrahydro-6H-cyclohepta[b]quinoline **18s**<sup>[45]</sup>



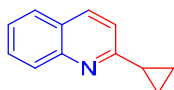
According to the general procedure, 2-(hydroxymethyl)aniline **15a** (62 mg, 0.5 mmol) and cycloheptanone **17s** (59  $\mu\text{L}$ , 0.5 mmol) gave the title compound **18s** as colorless crystals (87 mg, 88%, isolated with 8% of **5a**).  $^1\text{H}$  NMR (400 MHz,  $\text{CDCl}_3$ ):  $\delta$  8.04 (d,  $J$  = 8.4 Hz, 1H), 7.77 (s, 1H), 7.66 (d,  $J$  = 8.1 Hz, 1H), 7.59 (t,  $J$  = 7.2 Hz, 1H), 7.42 (t,  $J$  = 7.5 Hz, 1H), 3.22 – 3.19 (m, 2H), 2.90 – 2.87 (m, 2H), 1.87 – 1.68 (m, 6H).  $^{13}\text{C}\{^1\text{H}\}$  NMR (101 MHz,  $\text{CDCl}_3$ ):  $\delta$  164.5, 145.7, 136.6, 135.0, 128.7, 128.0, 127.3, 126.8, 125.9, 39.6, 35.4, 32.2, 28.8, 27.0.

#### 2-Nonylquinoline **18t**<sup>[46]</sup>



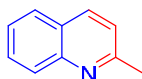
According to the general procedure, 2-(hydroxymethyl)aniline **15a** (62 mg, 0.5 mmol) and 2-undecanone **17t** (103  $\mu\text{L}$ , 0.5 mmol) gave the title compound **18t** as colorless crystals (97.0 mg, 76%).  $^1\text{H}$  NMR (400 MHz,  $\text{CDCl}_3$ )  $\delta$  8.05 (d,  $J$  = 8.4 Hz, 2H), 7.77 (d,  $J$  = 8.2 Hz, 1H), 7.68 (t,  $J$  = 7.7 Hz, 1H), 7.47 (t,  $J$  = 7.5 Hz, 1H), 7.29 (d,  $J$  = 8.4 Hz, 1H), 2.97 (t,  $J$  = 7.9 Hz, 2H), 1.85 – 1.77 (m, 2H), 1.44 – 1.22 (m, 12H), 0.87 (t,  $J$  = 6.9 Hz, 3H).  $^{13}\text{C}\{^1\text{H}\}$  NMR (101 MHz,  $\text{CDCl}_3$ )  $\delta$  163.3, 148.1, 136.3, 129.4, 129.0, 127.6, 126.8, 125.7, 121.5, 39.5, 32.0, 30.2, 29.7, 29.7, 29.7, 29.4, 22.8, 14.2.

## 2-Cyclopropylquinoline **18u**<sup>[47]</sup>



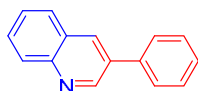
According to the general procedure, 2-(hydroxymethyl)aniline **15a** (62 mg, 0.5 mmol) and cyclopropylethan-1-one **17u** (47  $\mu$ L, 0.5 mmol) gave the title compound **18u** as colorless crystals (75 mg, 89%). <sup>1</sup>H NMR (400 MHz, CDCl<sub>3</sub>)  $\delta$  7.98 (t,  $J$  = 7.9 Hz, 2H), 7.73 (dd,  $J$  = 8.1, 1.7 Hz, 1H), 7.64 (ddd,  $J$  = 8.4, 6.8, 1.5 Hz, 1H), 7.43 (ddd,  $J$  = 8.1, 6.9, 1.3 Hz, 1H), 7.16 (d,  $J$  = 8.4 Hz, 1H), 2.28–2.21 (m, 1H), 1.19 – 1.13 (m, 2H), 1.13 – 1.07 (m, 2H). <sup>13</sup>C{<sup>1</sup>H} NMR (101 MHz, CDCl<sub>3</sub>):  $\delta$  163.5, 148.1, 135.9, 129.4, 128.8, 127.6, 126.9, 125.3, 119.5, 18.2, 10.4.

## 2-Methylquinoline **18v**<sup>[48]</sup>



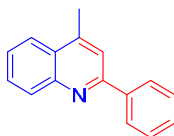
According to the general procedure, 2-(hydroxymethyl)aniline **15a** (62 mg, 0.5 mmol) and acetone **17v** (1 mL) gave the title compound **18v** as pale yellow oil (69 mg, 96%). <sup>1</sup>H NMR (400 MHz, CDCl<sub>3</sub>):  $\delta$  8.01 (d,  $J$  = 8.5 Hz, 1H), 7.97 (d,  $J$  = 8.5 Hz, 1H), 7.71 (d,  $J$  = 8.1 Hz, 1H), 7.64 (ddd,  $J$  = 8.6, 7.0, 1.6 Hz, 1H), 7.43 (t,  $J$  = 7.5 Hz, 1H), 7.22 (d,  $J$  = 8.4 Hz, 1H), 2.71 (s, 3H). <sup>13</sup>C{<sup>1</sup>H} NMR (75 MHz, CDCl<sub>3</sub>):  $\delta$  159.0, 147.9, 136.1, 129.4, 128.6, 127.5, 126.5, 125.7, 122.0, 25.4.

## 3-Phenylquinoline **18w**<sup>[49]</sup>



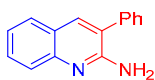
According to the general procedure, 2-(hydroxymethyl)aniline **15a** (62 mg, 0.5 mmol) and 2-phenylacetaldehyde **17w** (60 mg, 0.5 mmol) gave the title compound **18w** as yellow oil (65 mg, 63%, moderate purity see NMR Spectra). <sup>1</sup>H NMR (400 MHz, CDCl<sub>3</sub>):  $\delta$  9.20 (d,  $J$  = 2.4 Hz, 1H), 8.33 (d,  $J$  = 2.4 Hz, 1H), 8.17 (d,  $J$  = 8.4 Hz, 1H), 7.90 (dd,  $J$  = 8.2, 1.6 Hz, 1H), 7.76 – 7.72 (m, 3H), 7.59 (t,  $J$  = 7.6 Hz, 1H), 7.56 – 7.52 (m, 2H), 7.47 – 7.43 (m, 1H). <sup>13</sup>C{<sup>1</sup>H} NMR (101 MHz, CDCl<sub>3</sub>)  $\delta$  150.0, 147.4, 138.0, 134.0, 133.5, 129.6, 129.33, 129.29, 128.3, 128.19, 128.15, 127.6, 127.2.

## 4-Methyl-2-phenylquinoline **18x**<sup>[36]</sup>



According to the general procedure, 2-aminoacetophenone **15b** (68 mg, 0.5 mmol) and 1-phenylethanol **16a** (60  $\mu$ L, 0.5 mmol) gave the title compound **18x** as colorless crystals (98 mg, 89%). <sup>1</sup>H NMR (300 MHz, CDCl<sub>3</sub>)  $\delta$  8.20–8.04 (m, 3H), 8.00 (dd,  $J$  = 8.6, 1.6 Hz, 1H), 7.75 – 7.70 (m, 2H), 7.58 – 7.43 (m, 4H), 2.77 (d,  $J$  = 1.0 Hz, 3H). <sup>13</sup>C{<sup>1</sup>H} NMR (101 MHz, CDCl<sub>3</sub>)  $\delta$  157.2, 148.3, 144.9, 140.0, 130.4, 129.5, 129.3, 128.9, 127.7, 127.4, 126.2, 123.7, 119.9, 19.2.

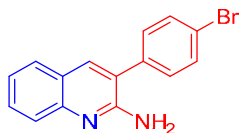
## 2-Amino-3-phenylquinoline **20a**<sup>[50]</sup>



According to the general procedure, 2-(hydroxymethyl)aniline **15a** (62 mg, 0.5 mmol) and 2-phenylacetonitrile **19a** (58  $\mu$ L, 0.5 mmol) gave the title compound **20a** as colorless crystals (74 mg, 67%). <sup>1</sup>H NMR (400 MHz, CDCl<sub>3</sub>):  $\delta$  7.81 (s, 1H), 7.72 (d,  $J$  = 8.4 Hz, 1H), 7.67 (dd,

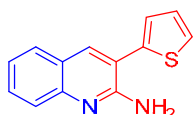
$J = 8.0, 1.7$  Hz, 1H), 7.61 – 7.43 (m, 6H), 7.31 – 7.27 (m, 1H), 5.07 (br s, 2H).  $^{13}\text{C}\{^1\text{H}\}$  NMR (101 MHz,  $\text{CDCl}_3$ ):  $\delta$  155.3, 147.3, 137.7, 137.4, 129.8, 129.3, 129.0, 128.4, 127.6, 125.7, 125.2, 124.3, 122.9.

### 2-Amino-3-(4-bromophenyl)quinoline 20b



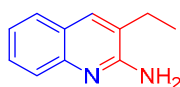
According to the general procedure, 2-(hydroxymethyl)aniline **15a** (62 mg, 0.5 mmol) and 2-(4-bromophenyl)acetonitrile **19b** (98 mg, 0.5 mmol) gave the title compound **20b** as pale yellow crystals (78 mg, 52%).  $^1\text{H}$  NMR (400 MHz,  $\text{CDCl}_3$ ):  $\delta$  = 7.79 (s, 1H), 7.71 (d,  $J = 8.4$  Hz, 1H), 7.67 – 7.63 (m, 3H), 7.60 (ddd,  $J = 8.4, 6.9, 1.5$  Hz, 1H), 7.42 – 7.39 (m, 2H), 7.30 (ddd,  $J = 8.1, 6.9, 1.2$  Hz, 1H), 5.03 (br, 2H).  $^{13}\text{C}\{^1\text{H}\}$  NMR (101 MHz,  $\text{CDCl}_3$ ):  $\delta$  = 154.8, 146.7, 137.8, 136.3, 132.6, 130.7, 130.3, 127.7, 125.5, 124.1, 124.0, 123.4, 122.8.

### 2-Amino-3-(Thiophen-2-yl)quinoline 20d<sup>[51]</sup>



According to the general procedure, 2-(hydroxymethyl)aniline **15a** (62 mg, 0.5 mmol) and 2-(2-thiophenyl)acetonitrile **19d** (62 mg, 0.5 mmol) gave the title compound **20d** as pale yellow crystals (102 mg, 90%).  $^1\text{H}$  NMR (400 MHz,  $\text{CDCl}_3$ ):  $\delta$  = 7.93 (s, 1H), 7.67 (d,  $J = 8.5$  Hz, 1H), 7.64 (d,  $J = 8.0$  Hz, 1H), 7.57 (ddd,  $J = 8.6, 6.9, 1.5$  Hz, 1H), 7.43 (dd,  $J = 5.1, 1.2$  Hz, 1H), 7.33 (dd,  $J = 3.5, 1.1$  Hz, 1H), 7.27 (ddd,  $J = 8.0, 6.8, 1.1$  Hz, 1H), 7.17 (dd,  $J = 5.1, 3.5$  Hz, 1H), 5.23 (br s, 2H).  $^{13}\text{C}\{^1\text{H}\}$  NMR (101 MHz,  $\text{CDCl}_3$ ):  $\delta$  = 155.1, 147.2, 139.0, 138.2, 130.2, 128.1, 127.7, 126.9, 126.6, 125.7, 124.0, 123.2, 117.9.

### 2-Amino-3-ethylquinoline 20f<sup>[50]</sup>



According to the general procedure, 2-(hydroxymethyl)aniline **15a** (62 mg, 0.5 mmol) and butyronitrile **19f** (69.1  $\mu\text{L}$ , 1.0 mmol, 2 equiv.) gave the title compound **20f** as pale yellow crystals (69 mg, 80%).  $^1\text{H}$  NMR (400 MHz,  $\text{CD}_2\text{Cl}_2$ ):  $\delta$  = 7.72 (s, 1H), 7.64 – 7.59 (m, 2H), 7.49 (ddd,  $J = 8.4, 6.9, 1.6$  Hz, 1H), 7.24 (ddd,  $J = 7.9, 6.8, 1.2$  Hz, 1H), 4.98 (s, 2H), 2.61 (q,  $J = 7.4, 2\text{H}$ ), 1.36 (t,  $J = 7.5, 3\text{H}$ ).  $^{13}\text{C}\{^1\text{H}\}$  NMR (101 MHz,  $\text{CD}_2\text{Cl}_2$ ):  $\delta$  = 156.7, 146.5, 134.5, 129.0, 127.3, 125.7, 125.5, 124.9, 122.8, 24.2, 12.4.

## 6.6. References

- [1] a) O. Ogata, Y. Nakayama, H. Nara, M. Fujiwhara, Y. Kayaki, *Org. Lett.* **2016**, *18*, 3894-3897; b) W. Kuriyama, T. Matsumoto, O. Ogata, Y. Ino, K. Aoki, S. Tanaka, K. Ishida, T. Kobayashi, N. Sayo, T. Saito, *Org. Process Res. Dev.* **2012**, *16*, 166-171.
- [2] S. R. Banerjee, M. K. Levadala, N. Lazarova, L. Wei, J. F. Valliant, K. A. Stephenson, J. W. Babich, K. P. Maresca, J. Zubietta, *Inorg. Chem.* **2002**, *41*, 6417-6425.
- [3] J. Zheng, C. Darcel, J.-B. Sortais, *Catal. Sci. Technol.* **2013**, *3*, 81-84.
- [4] L. C. Misal Castro, D. Bézier, J.-B. Sortais, C. Darcel, *Adv. Synth. Catal.* **2011**, *353*, 1279-1284.
- [5] J. Zheng, S. Elangovan, D. A. Valyaev, R. Brousses, V. César, J.-B. Sortais, C. Darcel, N. Lugan, G. Lavigne, *Adv. Synth. Catal.* **2014**, *356*, 1093-1097.
- [6] F. Jiang, D. Bézier, J.-B. Sortais, C. Darcel, *Adv. Synth. Catal.* **2011**, *353*, 239-244.
- [7] Y. Shimada, Y. Miyake, H. Matsuzawa, Y. Nishibayashi, *Chem. Asian J.* **2007**, *2*, 393-396.
- [8] Y. Motoyama, K. Kamo, H. Nagashima, *Org. Lett.* **2009**, *11*, 1345-1348.
- [9] A. Ouali, J.-P. Majoral, A.-M. Caminade, M. Taillefer, *ChemCatChem* **2009**, *1*, 504-509.
- [10] C. Azerraf, D. Gelman, *Organometallics* **2009**, *28*, 6578-6584.
- [11] L. Ford, F. Atefi, R. D. Singer, P. J. Scammells, *Eur. J. Org. Chem.* **2011**, 942-950.
- [12] D. Zhao, C. Gao, X. Su, Y. He, J. You, Y. Xue, *Chem. Commun.* **2010**, *46*, 9049-9051.
- [13] a) D. Das, S. Roy, P. K. Das, *Org. Lett.* **2004**, *6*, 4133-4136; b) B. T. Cho, S. K. Kang, M. S. Kim, S. R. Ryu, D. K. An, *Tetrahedron* **2006**, *62*, 8164-8168.
- [14] L. Huang, H. Jiang, C. Qi, X. Liu, *J. Am. Chem. Soc.* **2010**, *132*, 17652-17654.
- [15] M. J. Frisch, G. W. Trucks, H. B. Schlegel, G. E. Scuseria, M. A. Robb, J. R. Cheeseman, G. Scalmani, V. Barone, B. Mennucci, G. A. Petersson, H. Nakatsuji, M. Caricato, X. Li, H. P. Hratchian, A. F. Izmaylov, J. Bloino, G. Zheng, J. L. Sonnenberg, M. Hada, M. Ehara, K. Toyota, R. Fukuda, J. Hasegawa, M. Ishida, T. Nakajima, Y. Honda, O. Kitao, H. Nakai, T. Vreven, J. A. Montgomery Jr., J. E. Peralta, F. Ogliaro, M. Bearpark, J. J. Heyd, E. Brothers, K. N. Kudin, V. N. Staroverov, T. Keith, R. Kobayashi, J. Normand, K. Raghavachari, A. Rendell, J. C. Burant, S. S. Iyengar, J. Tomasi, M. Cossi, N. Rega, J. M. Millam, M. Klene, J. E. Knox, J. B. Cross, V. Bakken, C. Adamo, J. Jaramillo, R. Gomperts, R. E. Stratmann, O. Yazyev, A. J. Austin, R. Cammi, C. Pomelli, J. W. Ochterski, R. L. Martin, K. Morokuma, V. G. Zakrzewski, G. A. Voth, P. Salvador, J. J. Dannenberg, S. Dapprich, A. D. Daniels, O. Farkas, J. B. Foresman, J. V. Ortiz, J. Cioslowski, D. J. Fox, *Gaussian 09, Revision D.01*, Gaussian, Inc. Wallingford CT, **2009**.
- [16] C. Adamo, V. Barone, *J. Chem. Phys.* **1999**, *110*, 6158-6170.
- [17] a) S. Grimme, J. Antony, S. Ehrlich, H. Krieg, *J. Chem. Phys.* **2010**, *132*, 154104; b) S. Grimme, S. Ehrlich, L. Goerigk, *J. Comput. Chem.* **2011**, *32*, 1456-1465.
- [18] A. Schäfer, H. Horn, R. Ahlrichs, *J. Chem. Phys.* **1992**, *97*, 2571.
- [19] a) D. Andrae, U. Haussermann, M. Dolg, H. Stoll, H. Preuss, *Theor. Chim. Acta* **1990**, *77*, 123-141; b) K. A. Peterson, D. Figgen, E. Goll, H. Stoll, M. Dolg, *J. Chem. Phys.* **2003**, *119*, 11113-11123.
- [20] A. V. Marenich, C. J. Cramer, D. G. Truhlar, *J. Phys. Chem. B* **2009**, *113*, 6378-6396.
- [21] F. Weigend, R. Ahlrichs, *Phys. Chem. Chem. Phys.* **2005**, *7*, 3297-3305.
- [22] G. M. Sheldrick, *Acta Cryst.* **2015**, *A71*, 3-8.
- [23] G. M. Sheldrick, *Acta Cryst.* **2015**, *C71*, 3-8.
- [24] P. v.d. Sluis, A. L. Spek, *Acta Cryst.* **1990**, *A46*, 194-201.
- [25] A. L. Spek, *J. Appl. Cryst.* **2003**, *36*, 7-13.
- [26] A. Spek, *Acta Cryst.* **2015**, *C71*, 9-18.
- [27] T. T. Dang, B. Ramalingam, A. M. Seayad, *ACS Catal.* **2015**, *5*, 4082-4088.
- [28] I. González, J. Mosquera, C. Guerrero, R. Rodríguez, J. Cruces, *Org. Lett.* **2009**, *11*, 1677-1680.
- [29] Y. Imada, H. Iida, S. Ono, Y. Masui, S.-I. Murahashi, *Chem. Asian J.* **2006**, *1*, 136-147.
- [30] A. C. Kung, D. E. Falvey, *J. Org. Chem.* **2005**, *70*, 3127-3132.
- [31] a) N. Sun, S. Wang, W. Mo, B. Hu, Z. Shen, X. Hu, *Tetrahedron* **2010**, *66*, 7142-7148; b) M. Rueping, C. Vila, A. Szadkowska, R. M. Koenigs, J. Fronert, *ACS Catal.* **2012**, *2*, 2810-2815.
- [32] A. R. Katritzky, K. S. Laurenzo, *J. Org. Chem.* **1988**, *53*, 3978-3982.

- [33] I. Okamoto, M. Terashima, H. Masu, M. Nabeta, K. Ono, N. Morita, K. Katagiri, I. Azumaya, O. Tamura, *Tetrahedron* **2011**, *67*, 8536-8543.
- [34] A. T. Londregan, S. Jennings, L. Wei, *Org. Lett.* **2010**, *12*, 5254-5257.
- [35] V. Martínez-Barrasa, F. Delgado, C. Burgos, J. Luis García-Navío, M. Luisa Izquierdo, J. Alvarez-Builla, *Tetrahedron* **2000**, *56*, 2481-2490.
- [36] Y. Zhu, C. Cai, *RSC Adv.* **2014**, *4*, 52911-52914.
- [37] A. M. Berman, J. C. Lewis, R. G. Bergman, J. A. Ellman, *J. Am. Chem. Soc.* **2008**, *130*, 14926-14927.
- [38] Q. Wang, M. Wang, H.-J. Li, S. Zhu, Y. Liu, Y.-C. Wu, *Synthesis* **2016**, *48*, 3985-3995.
- [39] X. Chen, S. Qiu, S. Wang, H. Wang, H. Zhai, *Org. Biomol. Chem.* **2017**, *15*, 6349-6352.
- [40] T. Demaude, L. Knerr, P. Pasau, *J. Comb. Chem.* **2004**, *6*, 768-775.
- [41] M. Movassaghi, M. D. Hill, *J. Am. Chem. Soc.* **2006**, *128*, 4592-4593.
- [42] E. Largy, F. Hamon, F. Rosu, V. Gabelica, E. De Pauw, A. Guédin, J.-L. Mergny, M.-P. Teulade-Fichou, *Chem. Eur. J.* **2011**, *17*, 13274-13283.
- [43] C. S. Cho, *J. Organomet. Chem.* **2005**, *690*, 4094-4097.
- [44] a) N. P. Buu-Hoï, F. Périn, P. Jacquignon, *J. Heterocycl. Chem.* **1965**, *2*, 7-10; b) Z.-Q. Xiao, C. Xu, H.-M. Li, X. Han, Z.-Q. Wang, W.-J. Fu, X.-Q. Hao, M.-P. Song, *Transit. Met. Chem.* **2015**, *40*, 501-508.
- [45] D. Srimani, Y. Ben-David, D. Milstein, *Chem. Commun.* **2013**, *49*, 6632-6634.
- [46] T.-Y. Feng, H.-X. Li, D. J. Young, J.-P. Lang, *J. Org. Chem.* **2017**, *82*, 4113-4120.
- [47] G. A. Molander, P. E. Gormisky, *J. Org. Chem.* **2008**, *73*, 7481.
- [48] C. S. Cho, B. T. Kim, H.-J. Choi, T.-J. Kim, S. C. Shim, *Tetrahedron* **2003**, *59*, 7997-8002.
- [49] A.-M. L. Hogan, D. F. O'Shea, *Org. Lett.* **2006**, *8*, 3769-3772.
- [50] F. Kórodi, *Synth. Commun.* **1991**, *21*, 1841-1846.
- [51] R. Godemann, J. Madden, J. Krämer, M. Smith, U. Fritz, T. Hesterkamp, J. Barker, S. Höppner, D. Hallett, A. Cesura, A. Ebner, J. Kemp, *Biochemistry* **2009**, *48*, 10743-10751.



**Chapter VI - Mn-Catalyzed Imine and *N*-Heteroaromatic Compounds**  
**Synthesis *via* Aerobic Oxidation of Amines**





## Chapter VI - Mn-Catalyzed Imine and *N*-Heteroaromatic Compounds

### Synthesis *via* Aerobic Oxidation of Amines

**Contributions in this part:** Optimization, scope and mechanistic studies: Duo Wei.

#### 1. Introduction

Imines are important intermediates in organic synthesis. They can be used as electrophilic reagents in many transformations such as alkylations, condensations and cycloadditions including aza-Diels-Alder reactions.<sup>[1]</sup> Imines also serve as versatile starting materials for the synthesis of chiral amines, which are important intermediates in the preparation of biologically active compounds.<sup>[2]</sup> *N*-heteroaromatics (especially quinoline derivatives) are ubiquitous skeleton in natural products and biologically active molecules (see also Chapter V-3 for more details). The traditional protocol for the synthesis of imines involves the condensation of an amine with a carbonyl compound such as aldehyde or ketone but alternative routes are still desirable. Significant progress has been made in the development of mild and green methods for the synthesis of imines including metal-catalyzed dehydrogenation of amines.<sup>[3]</sup> Interestingly, the syntheses of some imines through the dehydrogenative coupling of alcohols and amines have been reported during the past two decades.<sup>[4]</sup> Recently, direct oxidations of amines to imines have attracted much attention.<sup>[5]</sup> A few examples of organic catalysts<sup>[6]</sup> and transition metal catalyzed oxidations of amines have also been reported with PhIO<sup>[7]</sup>, K<sub>2</sub>S<sub>2</sub>O<sub>8</sub><sup>[8]</sup>, MnO<sub>2</sub><sup>[9]</sup> and *t*BuOOH<sup>[10]</sup>, 4-*t*butylcatechol (TBC) as stoichiometric oxidants.<sup>[11]</sup>

Selective oxidation of organic compounds with O<sub>2</sub> (and more particularly air) as a sole oxidant is valuable from both environmental and economic points of view.<sup>[12]</sup> For these reasons, considerable efforts have been devoted in recent years to develop transition metal-catalyzed aerobic oxidation of amines using iron,<sup>[13]</sup> cobalt,<sup>[14]</sup> copper,<sup>[15]</sup> gold,<sup>[16]</sup> palladium,<sup>[17]</sup> ruthenium,<sup>[18]</sup> titanium,<sup>[19]</sup> or vanadium<sup>[20]</sup> compounds and also organic catalysts.<sup>[21]</sup> However, many of these catalytic systems have limited substrate scopes, some of them are only active for secondary amines and the use of stoichiometric amount of organic oxidants simultaneously is unavoidable in most cases.

It is also well-known since 1950's that activated manganese dioxide (MnO<sub>2</sub>)<sup>[22]</sup> is a powerful reagent for selective oxidation of alcohols to carbonyl compounds, amines to imines or nitriles, heterocycles to heteroaromatics.<sup>[23]</sup> Although several methods for preparation of activated MnO<sub>2</sub> have been reported, preparations are very tedious and sometimes the oxidation efficiency lacks of reproducibility and the utilization of stoichiometric amount of such reagent is widely

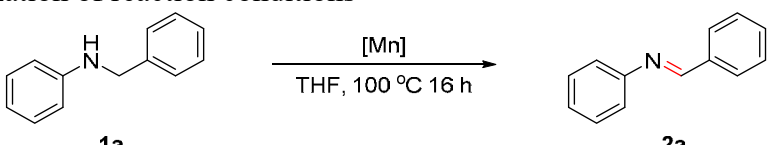
adopted. Commercially available activated MnO<sub>2</sub> can also be used, but again its activity varies widely. In 2011, an interesting example of MnO<sub>2</sub> catalyzed *N*-alkylation of sulfonamides and amines with alcohols under air was reported by Xu *et al.*<sup>[24]</sup> However base co-catalyst like K<sub>2</sub>CO<sub>3</sub> (up to 50 mol%) is required in this protocol. And yet it is comparatively rare that low oxidation state manganese were employed as catalysts in the oxidation of amines.<sup>[25]</sup> In this chapter, we report the first Mn(I)-catalyzed ligand- and additive-free aerobic oxidation of amines to prepare aldimines, *N*-heteroaromatics and also benzoimidazoles.

## 2. Results and discussions

### 2.1. Optimization of reaction conditions

*N*-benzylaniline **1a** was selected as the model substrate (Table 1) for the manganese catalyzed formation of aldimine. Firstly, blank reactions were performed in the absence of manganese precursors. *N*-benzylaniline **1a** remained intact after 16h in THF at 100 °C under argon atmosphere (entry 1). However, 9% of *N*-benzylideneaniline **2a** was detected when the reaction was set up under air atmosphere (entry 2). In the presence of Mn(CO)<sub>5</sub>Br as the catalyst (5.0 mol%), nearly no reaction occurred under argon or with argon stream (entries 3 and 4). The reactivity changed dramatically under normal air atmosphere, as *N*-benzylideneaniline **2a** was detected in 46% GC-yield (entry 5).

**Table 1.** Optimization of reaction conditions<sup>[a]</sup>



Entry	Mn [mol%]	Atmosphere	GC-yield of <b>2a</b> <sup>[b]</sup> [%]
1	None	argon	0
2	None	normal air	9 (10)
3	Mn(CO) <sub>5</sub> Br [5.0]	argon	3
4	Mn(CO) <sub>5</sub> Br [5.0]	argon stream	2
5	Mn(CO) <sub>5</sub> Br [5.0]	normal air	46 (47)

<sup>[a]</sup> The reaction was set up with **1a** (0.5 mmol), THF (1 mL) under indicated atmosphere in a closed Schlenk tube (20 mL) then heat at 100 °C for 16 h;

<sup>[b]</sup> NMR yield in parentheses;

Encouraged by this first result, different manganese precursors (all are commercially available) were then tested as catalysts under normal air atmosphere (Table 2): CpMn(CO)<sub>3</sub> gave a low yield of **1a** (29%). All the other precursors, such as Mn<sub>2</sub>(CO)<sub>10</sub>, MnF<sub>2</sub>, Mn(acac)<sub>3</sub>, Mn(OTf)<sub>2</sub>, MnO, MnO<sub>2</sub>, activated MnO<sub>2</sub> and KMnO<sub>4</sub> gave less than 10% yield of **2a** (entries 3-10). The

rhodium analogues such as  $\text{Re}(\text{CO})_5\text{Br}$  and  $\text{Re}_2(\text{CO})_{10}$  were inactive for the current reaction (entries 10 and 11).

**Table 2.** Evaluation of Mn salts and complexes in aerobic oxidation of amine<sup>[a]</sup>

Reaction scheme: **1a**  $\xrightarrow[\text{100 } ^\circ\text{C 16 h}]{\text{[Mn] (5.0 mol\%), normal air, THF (1 mL)}}$  **2a**

Entry	Mn [5.0 mol%]	GC-yield of <b>2a</b> [%]
1	$\text{Mn}(\text{CO})_5\text{Br}$	46
2	$\text{CpMn}(\text{CO})_3$	29
3	$\text{Mn}_2(\text{CO})_{10}$	7
4	$\text{MnF}_2$	5
5	$\text{Mn}(\text{acac})_3$	5
6	$\text{Mn}(\text{OTf})_2$	6
7	$\text{MnO}_2$	4
8	$\text{MnO}_2$ (activated)	6
9	$\text{KMnO}_4$	5
10	$\text{MnO}$	9
11	$\text{Re}(\text{CO})_5\text{Br}$	1
12	$\text{Re}_2(\text{CO})_{10}$	4

<sup>[a]</sup> The reaction was set up with **1a** (0.5 mmol), catalyst (5.0 mol%) and THF (1 mL) under normal air atmosphere (1 bar) in a closed Schlenk tube (20 mL) then heat at 100 °C for 16 h;

Then a screening of different solvents was performed (Table 3). The reaction proceeded well in *t*-amyl alcohol and ethyl acetate, leading to **2a** in 42% and 56% yield, respectively (entries 2 and 3). Other alcohol solvents like EtOH, MeOH, *i*PrOH and *n*BuOH, were less beneficial for the reaction (entries 4-7). In water, dimethyl carbonate, cyclopentyl methyl ether and 1,4-dioxane, the conversions were very low (entries 8-11). Further control experiments were conducted. The use of dry air (Alphagaz 1, Air Liquide,  $\text{O}_2 = 20 \text{ M\%}$ ,  $\text{N}_2 = 80 \text{ M\%}$ ,  $\text{CO}_2 < 1 \text{ PPM}$ ,  $\text{CO} < 1 \text{ ppm}$ ,  $\text{H}_2\text{O} < 3 \text{ ppm}$ , total  $\text{C}_n\text{H}_m < 100 \text{ ppb}$ ) instead of normal air (1 bar for both cases) led to the same conversion (entries 12 vs 1). The addition of 10 equiv. of  $\text{H}_2\text{O}$  to the THF solution quenched the reaction, as a low conversion of **1a** was detected (entries 13 vs 1).

**Table 3.** Evaluation of solvents<sup>[a]</sup>

c1ccccc1NCc2ccccc2
 $\xrightarrow[\text{normal air, solvent (1 mL)}]{\text{Mn(CO)}_5\text{Br (5.0 mol\%)}}$ 
c1ccccc1N=Cc2ccccc2

**1a**  **2a**

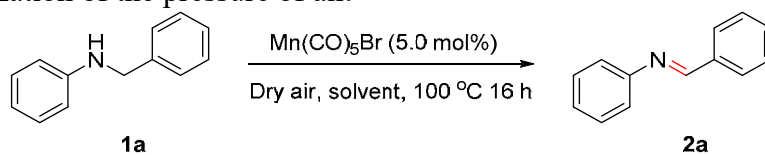
Entry	Solvent	GC-yield of <b>2a</b> [%]
1	<b>THF</b>	<b>46</b>
2	<b>Ethyl acetate</b>	<b>56</b>
3	<b><i>t</i>AmylOH</b>	<b>42</b>
4	EtOH	22
5	MeOH	20
6	<i>i</i> PrOH	32
7	<i>n</i> BuOH	34
8	H <sub>2</sub> O	9
9	DMC	7
10	CPME	<1
11	1,4-dioxane	8
12	THF	48 <sup>[b]</sup>
13	THF	<1 <sup>[c]</sup>

<sup>[a]</sup> The reaction was set up with **1a** (0.5 mmol), Mn(CO)<sub>5</sub>Br (5.0 mol%) and solvent (1 mL) under normal air atmosphere (1 bar) in a closed Schlenk tube (20 mL) then heat at 100 °C for 16 h;

<sup>[b]</sup> Under dry air atmosphere (1 bar). Dry air: (ALPHAGAZ 1 AIR) O<sub>2</sub> = 20 M%, N<sub>2</sub> = 80 M%, CO<sub>2</sub> < 1 ppm, CO < 1 ppm, H<sub>2</sub>O < 3 ppm, total C<sub>n</sub>H<sub>m</sub> < 100 ppb;

<sup>[c]</sup> With 10 equiv. H<sub>2</sub>O.

The influence of the pression of air was then evaluated using dry air as oxidant (Table 4). Surprisingly, a full conversion was obtained when charging 2 bar of dry air in the reaction Schlenk tube in THF (entry 1). The imine **2a** was isolated in 91% yield using bulb-to-bulb distillation. With CpMn(CO)<sub>3</sub> (5.0 mol%), using dry air (2 bar), the conversion was improved to 67%, without reaching the one obtained with Mn(CO)<sub>5</sub>Br (entry 2). Reaction in *t*-Amyl alcohol and ethyl acetate permitted to obtain **2a** in 71% and 88% yield under the same conditions (2 bar of dry air, entries 3 and 4). Full conversion could be obtained in *t*-amyl alcohol by increasing the pressure 50 bar of dry air in an autoclave (entry 5). In the absence of any manganese precursor, 10% of **2a** were observed in THF under 2 bar of dry air, while 50 bar of dry air led to 2% of **2a** in *t*-amyl alcohol (entries 6 and 7). The effect of water was also carefully analyzed: with 2 equiv. with respect to **1a**, low conversion was detected (15%, entry 8), while with 1 equiv. 85% of **2a** and 15% of benzaldehyde and aniline, resulting from hydrolysis of **2a**, were detected (entry 9).

**Table 4.** Optimization of the pressure of air.<sup>[a]</sup>

Entry	Solvent	Dry air <sup>[b]</sup> [bar]	GC-yield of 2a [%]
1	THF	2	>98 (91 <sup>[c]</sup> )
2 <sup>[d]</sup>	THF	2	67
3	<i>t</i> AmylOH	2	71
4	Ethyl acetate	2	88
5	<b><i>t</i>AmylOH</b>	<b>50</b>	<b>&gt;98</b>
6 <sup>[e]</sup>	THF	2	10
7 <sup>[e]</sup>	<i>t</i> AmylOH	50	2
8 <sup>[f]</sup>	THF	2	15
9 <sup>[g]</sup>	THF	2	85

<sup>[a]</sup> The reaction was set up with **1a** (0.5 mmol), Mn(CO)<sub>5</sub>Br (5.0 mol%) and solvent (1 mL) under dry air atmosphere (2 or 50 bar) in a closed Schlenk tube or autoclave (20 mL) then heat at 100 °C for 16 h;

<sup>[b]</sup> Dry air: (ALPHAGAZ 1 AIR) O<sub>2</sub> = 20 M%, N<sub>2</sub> = 80 M%, CO<sub>2</sub> < 1 ppm, CO < 1 ppm, H<sub>2</sub>O < 3 ppm, total C<sub>n</sub>H<sub>m</sub> < 100 ppb;

<sup>[c]</sup> Isolated yield after purification by bulb-to-bulb distillation;

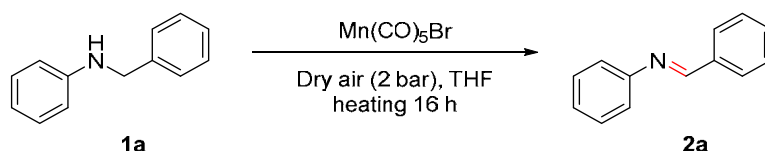
<sup>[d]</sup> With CpMn(CO)<sub>3</sub> (5.0 mol%), instead of MnBr(CO)<sub>5</sub>;

<sup>[e]</sup> Without any Mn;

<sup>[f]</sup> With 2 equiv. H<sub>2</sub>O with respect to **1a**;

<sup>[g]</sup> With 1 equiv. H<sub>2</sub>O with respect to **1a**, 15% of hydrolyzed product (benzaldehyde and aniline) was detected.

The modification of the temperature (100 to 30 °C) and catalyst loading (5.0 to 0.5 mol%) (Table 5) demonstrated that 100 °C and 5.0 mol% of Mn(CO)<sub>5</sub>Br were the optimal conditions.

**Table 5.** Optimization of the temperature and the catalyst loading.<sup>[a]</sup>

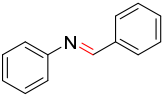
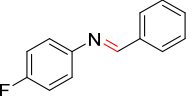
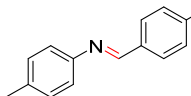
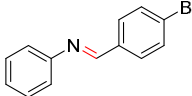
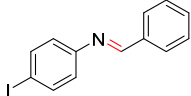
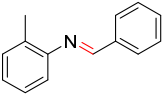
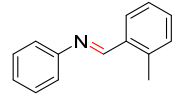
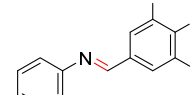
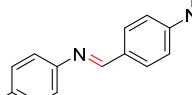
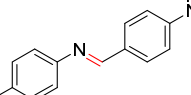
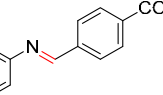
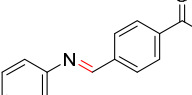
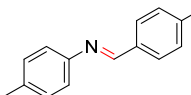
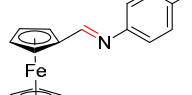
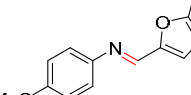
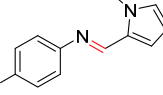
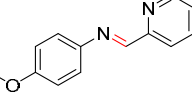
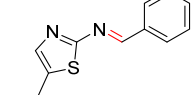
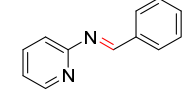
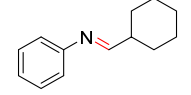
Entry	Mn(CO) <sub>5</sub> Br [mol%]	T [°C]	GC-yield 2a [%]
1	<b>5.0</b>	<b>100</b>	<b>&gt;98</b>
2	5.0	80	46
3	5.0	50	19
4	5.0	30	2
5	1.0	100	18
6	0.5	100	12

<sup>[a]</sup> The reaction was set up with **1a** (0.5 mmol), Mn(CO)<sub>5</sub>Br (0.5-5.0 mol%) and THF (1 mL) under dry air atmosphere (2 bar) in a closed Schlenk tube (20 mL) then heat at indicated temperature for 16 h.

## 2.2. Scope for the reaction of oxidation of amines to imines

With our optimized conditions in hand: 5.0 mol% of  $\text{Mn}(\text{CO})_5\text{Br}$ , dry air (2 bar), THF, 100 °C, 16 h, (Table 4, entry 1), we then explored the substrate scope for this catalytic oxidation of amines to imines (Table 6). In general, a large variety of aldimines was prepared *via* oxidation of *N*-benzylaniline derivatives in high yields. Halogen substituents (F, Cl, Br and I) were well tolerated (**2b-2e**, isolated yields >75%), although dehalogenation products (ca. 5%) were detected in the case of bromo and iodo derivatives **2d** and **2e**. Steric hindrance has little influence on both the aniline (**2f**) or benzaldehyde (**2g**) moieties. The tolerance toward various functional groups such as amino, amido, ester, acetyl, or cyano were tested and the corresponding imines **2i-2m** were obtained in good isolated yields. Likewise, organometallic 4-methyl-*N*-(ferrocenylmethylidene)-aniline **2n** was generated from the corresponding amine **1n** in lower isolated yield (38%).

**Table 6.** Scope of oxidation of amines to imines<sup>[a]</sup>

$  \begin{array}{c}  \text{R}_1\text{NHCH}_2\text{R}_2 \\  \mathbf{1}  \end{array}  \xrightarrow[\text{Dry air (2 bar), THF, 100 }^\circ\text{C}]{\text{Mn}(\text{CO})_5\text{Br (5.0 mol\%)}}  \begin{array}{c}  \text{R}_1\text{N}=\text{CHR}_2 \\  \mathbf{2}  \end{array}  $				
 <b>2a</b> , 16 h, >98 (91)	 <b>2b</b> , 18 h, >98 (98)	 <b>2c</b> , 18 h, >98 (90) <sup>[g]</sup>	 <b>2d</b> , 18 h, >98 (75) <sup>[c]</sup>	 <b>2e</b> , 18 h, 71 (66) <sup>[d]</sup>
 <b>2f</b> , 18 h, >98 (93) <sup>[e]</sup>	 <b>2g</b> , 18 h, >98 (98)	 <b>2h</b> , 18 h, >98 (83) <sup>[f]</sup>	 <b>2i</b> , 18 h, >98 (79) <sup>[f]</sup>	 <b>2j</b> , 20 h, >98 (78) <sup>[f]</sup>
 <b>2k</b> , 20 h, 87 (63) <sup>[g]</sup>	 <b>2l</b> , 18 h, >98 (83)	 <b>2m</b> , 20 h, >98 (94) <sup>[h]</sup>	 <b>2n</b> , 20 h, 53 (38)	 <b>2o</b> , 18 h, >98 (81)
 <b>2p</b> , 20 h, >98 (86) <sup>[f]</sup>	 <b>2q</b> , 18 h, 75 (70) <sup>[b]</sup>	 <b>2r</b> , 18 h, 5	 <b>2s</b> , 48 h, 3 18 h, 5 <sup>[b]</sup>	 <b>2t</b> , 18 h, 2 <sup>[b]</sup>

<sup>[a]</sup> General conditions: amine **1** (0.5 mmol),  $\text{Mn}(\text{CO})_5\text{Br}$  (6.9 mg, 5.0 mol%), THF (1.0 mL), dry air (2 bar), 100 °C; Conversion of the amine was detected by  $^1\text{H}$  NMR of the crude mixture; Isolated yield, shown in parentheses, was obtained after a bulb to bulb distillation.

<sup>[b]</sup> Dry air (50 bar), *t*-amyl alcohol (1.0 mL);

<sup>[c]</sup> ca. 5% debromination product was observed in the crude mixture;

<sup>[d]</sup> ca. 3% deiodination product was observed in the crude mixture;

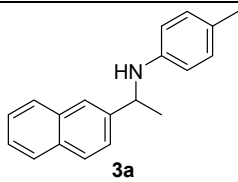
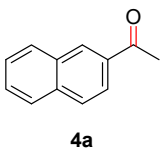
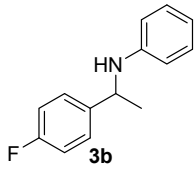
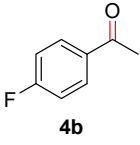
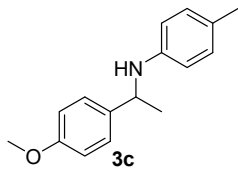
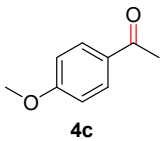
<sup>[e]</sup> Isolated with ca. 2% hydrolyzed product (corresponding amine and aldehyde);

<sup>[f]</sup> ca. 15%, <sup>g</sup> ca. 10%, <sup>h</sup> ca. 5% hydrolyzed product (aldehyde) was observed in the crude mixture.

Interestingly, *N*-substituted-aminomethylheterocycles **1o-1q** were also oxidized affording heteroaromatic imines **2o-2q** without significant loss of activity (81-86% yields). However, a strong chelate effect was observed with the amines **1r** and **1s** which inhibited the reaction. Unfortunately, *N*-alkylaniline like **1t** did not lead to the desired product.

However, the oxidation of  $\alpha$ -disubstituted amines such as 4-methyl-*N*-(1-(2-naphthalenyl)ethyl)aniline **3a** did not afford the corresponding ketimine, but the ketone **4a** in 54% NMR-yield, resulting from the hydrolysis of the desired ketimine product (Table 7). Similar results were observed for the other  $\alpha$ -disubstituted amines **3b** and **3c**.

**Table 7.** Ketone formation from oxidation of amines then hydrolysis<sup>[a]</sup>

$  \begin{array}{c}  \text{H} \\    \\  \text{R}_1\text{N} - \text{CH} - \text{R}_2 \\    \\  \text{3}  \end{array}  \xrightarrow[\substack{\text{Dry air (2 bar), THF (A)} \\ \text{or Dry air (50 bar), } t\text{AmylOH (B)} \\ 100\text{ }^\circ\text{C, 18 h}}]{\text{Mn(CO)}_5\text{Br (5.0 mol\%)}}  \begin{array}{c}  \text{O} \\     \\  \text{R}_2 \\  \text{4}  \end{array}  $				
Entry	Substrate	Product	Condition	Yield [%]
1	 <b>3a</b>	 <b>4a</b>	A	21
2			B	54
3	 <b>3b</b>	 <b>4b</b>	B	2
4	 <b>3c</b>	 <b>4c</b>	B	25

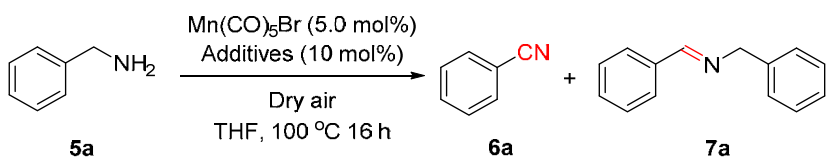
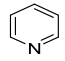
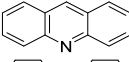
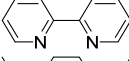
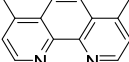
<sup>[a]</sup> General conditions: amine **3** (0.5 mmol), Mn(CO)<sub>5</sub>Br (6.9 mg, 5.0 mol%), condition A: Dry air (2 bar), THF (1 mL), or condition B: Dry air (50 bar), *t*AmylOH (1 mL), then heat at 100 °C for 18 h; Yield of **4** was determined by <sup>1</sup>H NMR of the crude mixture.

The oxidation of primary amines to nitrile compounds is another important target. Therefore, the oxidation of benzylamine **5a** to form benzonitrile **6a** was next investigated (Table 8). However, only homo coupling product **7a** was detected when the reaction was performed under 1 bar of normal air or 50 bar of dry air at 100 °C for 16 h (entries 1-3). It has shown that the employment of additives or ligands containing pyridine derivatives could promote the oxidation of benzylamine to benzonitrile.<sup>[18j, 26]</sup> Then, pyridine, acridine, 2,2'-bipyridine and 4,7-dimethyl-1,10-phenanthroline were selected as additives for this reaction. Although good



conversions of **5a** were achieved with those additives (entries 4-6), the formation of benzonitrile **6a** was not detected in all cases and only the homo coupling product **7a** was produced. However, a strong chelate effect was observed when adding 10 mol% of 4,7-dimethyl-1,10-phenanthroline, as it led to only 19% conversion of **5a** (entry 7).

**Table 8.** Optimization of the oxidation of benzylamine

					
Entry	Additives [10 mol%]	Dry air [bar]	Conv. [%]	GC-yield [%]	
				6a	7a
1	None	nomal air	42	0	39
2	None	50	>98	0	>98
3	None	50	>98 <sup>[b]</sup>	0	>98
4		50	>98	0	89
5		50	80	0	70
6		50	65	0	60
7		50	19	0	19

<sup>[a]</sup> The reaction was set up with **5a** (0.5 mmol), Mn(CO)<sub>5</sub>Br (5.0 mol%) and THF (1 mL) under dry air (50 bar) in an autoclave (20 mL) then heat at 100 °C for 16 h;

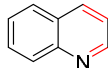
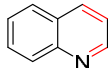
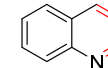
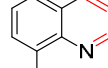
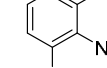
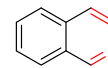
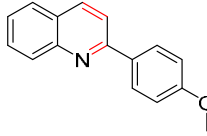
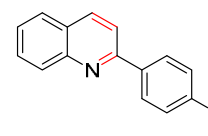
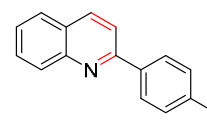
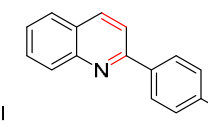
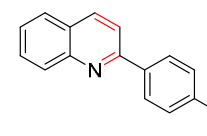
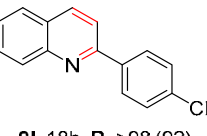
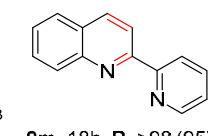
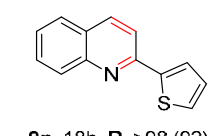
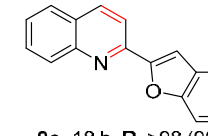
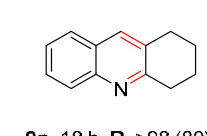
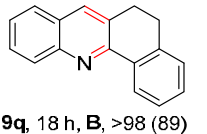
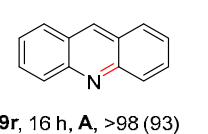
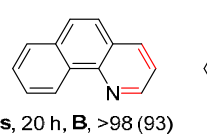
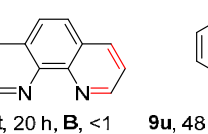
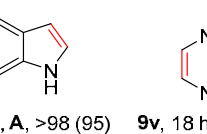
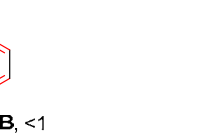
<sup>[b]</sup> *t*-amyl alcohol instead of THF.

### 2.3. Scope for the oxidation of cyclic amines to *N*-heteroaromatic derivatives

Aerobic oxidation of tetrahydroquinolines (THQs) is an other important route to prepare quinoline derivatives, complementary as a representative example to the rhenium promoted synthesis described in chapter V. Following the previous results on oxidation of amines, the oxidation of *N*-heterocycles **8** was investigated under similar conditions (Table 9). THQ **8a**, 2-MeTHQ **8b**, 3-MeTHQ **8c**, 8-MeTHQ **8d** and 8-BrTHQ **8e**, displayed excellent reaction efficiency and gave the quinoline derivatives **9a-9e** in up to 97% isolated yields, although **8b** and **8c** required harsher conditions (50 bar of dry air). Isotetrahydroquinoline **8f** was also converted into isoquinoline **9f** in 92% yield under 50 bar of dry air in *t*-amyl alcohol. The introduction of 2-aryl groups bearing methoxyl (**8g**), halogen (**8h-8k**) and trifluoromethyl (**8l**) in the *para* position did not influence the reactivity and the corresponding quinolines **9g-9l** were obtained in 90-98% isolated yields. Substrates with substituents at the position 2 with heteroaromatics, such as 2-(2-pyridyl)-THQ **8m**, 2-(2-thiophenyl)-THQ **8n**, and 2-(2-benzofuranyl)-THQ **8o** were also oxidized in excellent yields (90-95%) under 50 bar of dry air,

even the products could potentially act as bidentate ligands. 2,3-Disubstituted THQs **8p** and **8q** were also good partners in this transformation, as **9p** and **9q** were prepared in good yield, 80% and 89%, respectively.

**Table 9.** Scope of the oxidation of cyclic amines to *N*-heteroaromatic derivatives <sup>[a]</sup>

$  \begin{array}{c}  \text{R}_2 \\    \\  \text{C}_6\text{H}_4 \\    \\  \text{N} \\    \\  \text{R}_1 \\  \text{8}  \end{array}  \xrightarrow[\text{100 } ^\circ\text{C}]{\text{Mn(CO)}_5\text{Br (5.0 mol\%)}}  \begin{array}{c}  \text{R}_2 \\    \\  \text{C}_6\text{H}_4 \\    \\  \text{N} \\    \\  \text{R}_1 \\  \text{9}  \end{array}  $ <p style="text-align: center;">Dry air (2 bar), THF (A) or Dry air (50 bar), <i>t</i>AmylOH (B)</p>					
					
<b>9a</b> , 16 h, A, 83 (79)	<b>9b</b> , 48 h, B, >98 (97)	<b>9c</b> , 18 h, A, 49 18 h, B, >98 (94)	<b>9d</b> , 16 h, A, >98 (90)	<b>9e</b> , 48 h, A, >98 (87)	<b>9f</b> , 48 h, B, >98 (92)
					
<b>9g</b> , 18 h, B, >98 (92)	<b>9h</b> , 18 h, B, >98 (93)	<b>9i</b> , 18 h, B, >98 (98)	<b>9j</b> , 18 h, B, >98 (91) <sup>b</sup>	<b>9k</b> , 18 h, B, >98 (90) <sup>c</sup>	
					
<b>9l</b> , 18 h, B, >98 (92)	<b>9m</b> , 18 h, B, >98 (95)	<b>9n</b> , 18 h, B, >98 (92)	<b>9o</b> , 18 h, B, >98 (90)	<b>9p</b> , 18 h, B, >98 (80)	
					
<b>9q</b> , 18 h, B, >98 (89)	<b>9r</b> , 16 h, A, >98 (93)	<b>9s</b> , 20 h, B, >98 (93)	<b>9t</b> , 20 h, B, <1	<b>9u</b> , 48 h, A, >98 (95)	<b>9v</b> , 18 h, B, <1

<sup>[a]</sup> General conditions: *N*-heterocycle substrate **8** (0.5 mmol), Mn(CO)<sub>5</sub>Br (6.9 mg, 5.0 mol%), condition A: Dry air (2 bar), THF (1 mL), or condition B: Dry air (50 bar), *t*-amylOH. (1 mL), then heat at 100 °C, for the indicated time; Conversion of the amine substrate was detected by <sup>1</sup>H NMR of the crude mixture; Isolated yield shown in parentheses obtained by purification using bulb to bulb distillation apparatus;

<sup>[b]</sup> ca. 5% debromination product was observed in the crude mixture;

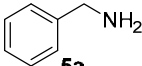
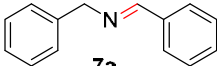
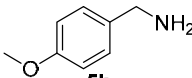
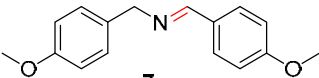
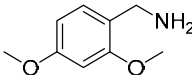
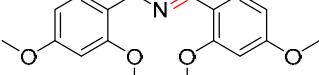
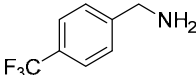
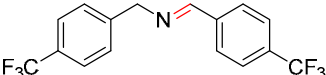
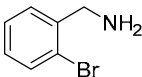
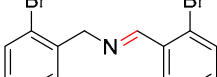
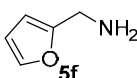
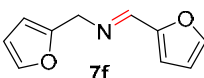
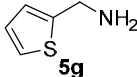

<sup>[c]</sup> ca. 3% deiodination product was observed in the crude mixture.

Additionally, 9,10-dihydroacridine **8r** was oxidized into acridine **9r** smoothly in 93% yield. Similarly, 1,2,3,4-tetrahydrobenzo[*h*]quinoline **8s** can be transformed into benzo[*h*]quinoline **9s** in 93% yield, while 1,10-phenanthroline **9t** was not detected when 1,2,3,4-tetrahydro-1,10-phenanthroline **8t** was used as the substrate, which contrasts with the case of 2-(2-pyridyl)-quinoline **9m** as both are polypyridinyl compound. The developed method was also applied to the oxidation of indoline to afford 1*H*-indole **9u** in excellent yield (95%). However, piperazine **8v** gave no reaction.

## 2.4. Scope for the oxidative homo-coupling of benzylamines

We then enlarged the oxidative homo-coupling of benzylamines to the imines. As revealed in Table 10, primary benzylic amines **5** were smoothly oxidized into the corresponding benzylidenebenzylamines **10** with very high conversions and yields. Beside benzylamine **5a**, benzylamines bearing methoxyl, *para*-trifluoromethyl and *ortho*-bromo groups **5b-5e** are all tolerated. To our delight, furfurylamine **5f** and 2-thiophenemethylamine **5g** shown also good reactivity (Table 10).

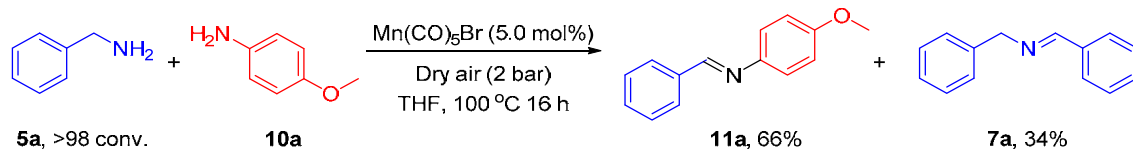
**Table 10.** Scope of the oxidative homo coupling of benzylamines<sup>[a]</sup>

Entry	Substrate	Product	Conv. (Yield) [%]
1	 <b>5a</b>	 <b>7a</b>	>98 (96)
2	 <b>5b</b>	 <b>7</b>	>98 (90)
3	 <b>5c</b>	 <b>7c</b>	92 (82)
4	 <b>5d</b>	 <b>7d</b>	>98 (68) >98 (90) <sup>b</sup>
5	 <b>5e</b>	 <b>7e</b>	>98 (87)
6	 <b>5f</b>	 <b>7f</b>	>98
7	 <b>5g</b>	 <b>7g</b>	>98 (89)

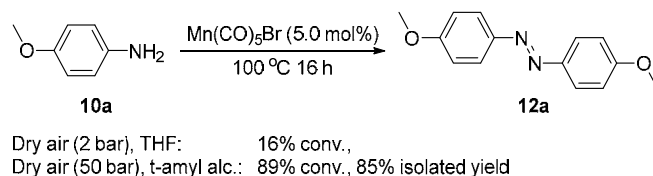
[a] General conditions: benzylamine derivative (0.5 mmol),  $\text{Mn}(\text{CO})_5\text{Br}$  (6.9 mg, 5.0 mol%), THF (1.0 mL), dry air (2 bar), 100 °C; Conversion of the amine substrate was detected by  $^1\text{H}$  NMR of the crude mixture; Isolated yield shown in parentheses obtained by purification by using bulb to bulb distillation apparatus;

[b] Dry air (50 bar), *t*-amyl alc. (1.0 mL).

The cross coupling of amines was also tested (Scheme 1). By reaction with *p*-methoxylaniline **10a**, benzylamine **5a** was converted in 66% to the imine **11a** (resulting for the cross coupling), although 34% of the homo coupling imine product **7a** was also detected. Homo-coupling of *p*-methoxylaniline **10a** to azo compound 1,2-bis(4-methoxyphenyl)diazene **12a** was next performed under 50 bar of dry air as shown in Scheme 2 and **12a** was obtained in 85% yield, while 2 bar of dry air led to 16% conversion of **10a**.

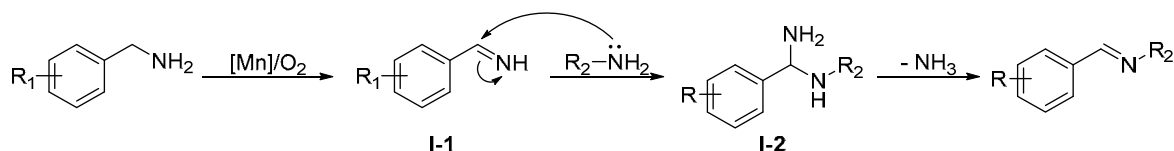


**Scheme 1.** Cross coupling of primary amines



**Scheme 2.** Homo-coupling of *p*-methoxyaniline to the azo compound **12a**.

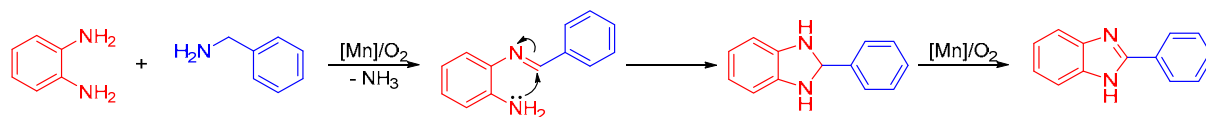
Accordingly, a reaction pathway can be proposed in Scheme 3 based on published results.<sup>[26]</sup> The transformation occurs *via* the formation of benzylamine **I-1**, which will then react with another amine leading to intermediate **I-2**. The coupled product was formed after releasing of  $\text{NH}_3$ .



**Scheme 3.** Proposed reaction pathway for the coupling of amines to prepare imines.

## 2.5. Scope for the synthesis of benzimidazoles

The oxidative cross-coupling reaction between benzylamine and *o*-phenylenediamine as the substrates to synthesise 2-phenyl-benzimidazole was already described.<sup>[3j]</sup> To our delight, benzylamine **5a** and *o*-phenylenediamine **13a** could also be fully converted to 2-phenyl-benzimidazole **14a** as the main product (91% selectivity) with 9 % of *N*-benzyl-1-phenylmethanimine **7a** as a by-product resulting from the homo-coupling of **5a**. The generation of the benzimidazole can be rationalized by a one-pot cascade reaction through dehydrogenation, cyclization and aromatization (Scheme 4).<sup>[13c]</sup>

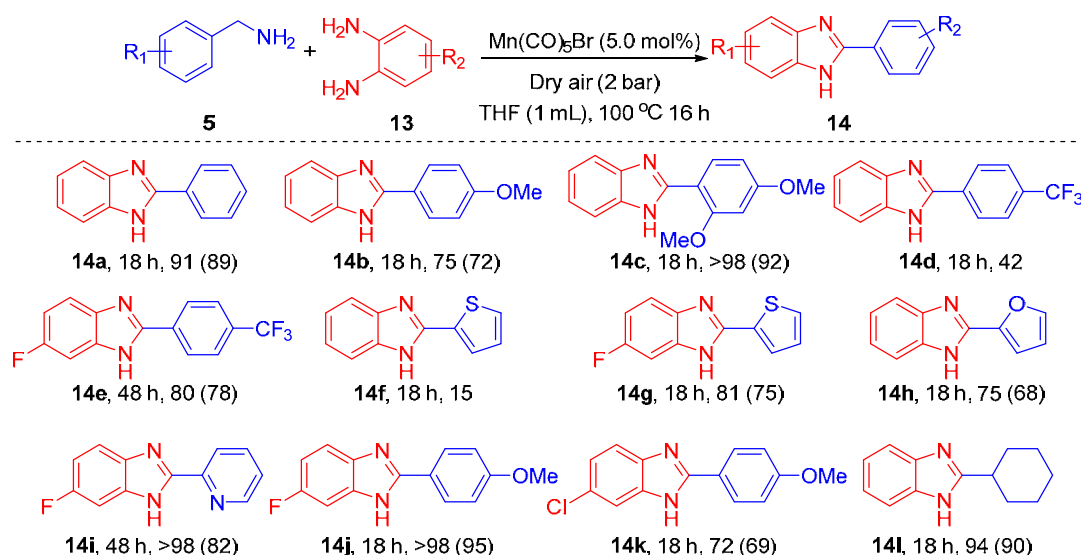


**Scheme 4.** Proposed reaction pathway for the oxidative synthesis of benzimidazoles.

Then different benzylamines and substituted *o*-phenylenediamine were combined to prepare benzimidazole derivatives (Table 11). It is noteworthy that in all reactions, we could detect the imine by-products **7** resulting from the homo-coupling reaction. *p*-Methoxybenzylamine and 2,4-dimethoxybenzylamine reacted with *o*-phenylenediamine giving **14b** and **14c** in 72% and

92% isolated yield, respectively. The combination of *p*-trifluoromethylbenzylamine and *o*-phenylenediamine gave moderate conversion (**14d**, 42%). By contrast, the utilization of electro-deficient 4-fluorobenzene-1,2-diamine as partner with *p*-trifluoromethylbenzylamine permitted to reach better conversion (**14e**, 80%). Similar trend was observed with 2-thiophenylmethanamine (**14f**, 15% conversion vs **14g**, 81% conversion).

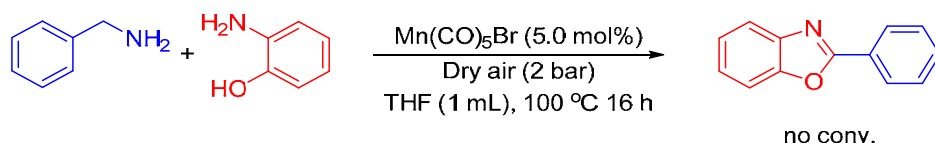
**Table 11.** One-pot synthesis of benzimidazoles<sup>[a]</sup>



<sup>[a]</sup> General conditions: benzylamine derivative (0.5 mmol), *o*-phenylenediamine **13** (0.5 mmol), Mn(CO)<sub>5</sub>Br (6.9 mg, 5.0 mol%), THF (1.0 mL), dry air (2 bar), 100 °C; Full conversion of the benzylamines were reached in all cases after 16 h; Selectivity of benzoimidazole (**14**) are shown; Isolated yield shown in parentheses after purification by chromatographic column;

By reaction with *o*-phenylenediamine, furfurylamine was converted into the corresponding benzoimidazole **14h** in 68% yield. 4-Fluorobenzene-1,2-diamine was shown after to be reactive in the presence of 2-pyridinylmethanamine and *p*-methoxybenzylamine substrates and led to **14i** and **14j** in 82 and 95% yield, respectively. 4-Chlorobenzene-1,2-diamine, on one side, and cyclohexylmethanamine, on the other side, were also active in such reactions giving **14k** and **14l**.

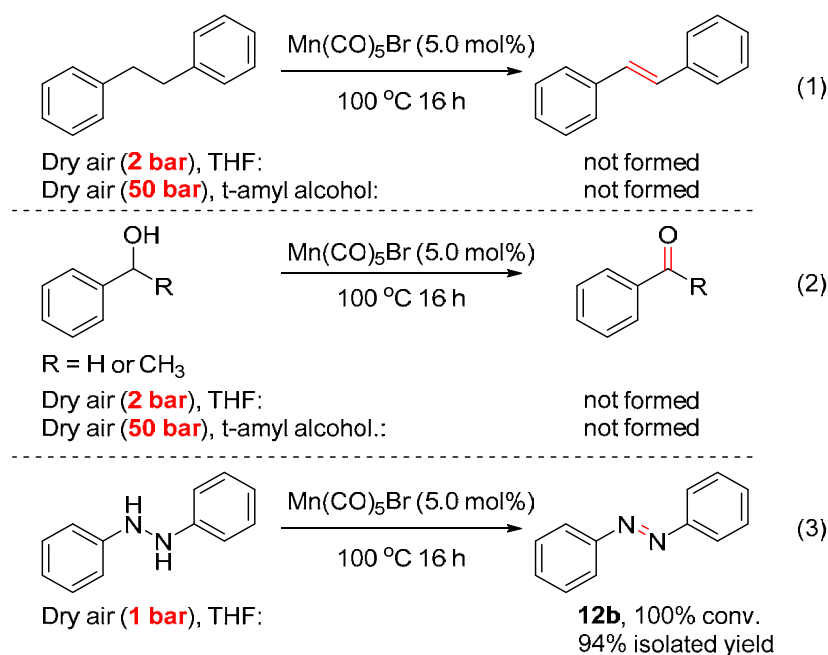
Although a wide functional group tolerance was achieved for the synthesis of benzoimidazole, benzylamine by reaction with 2-aminophenol was not capable to generate any benzoxazole product as no conversion of benzylamine was detected (Scheme 5). It is likely that the phenol group present in *o*-aminophenol has a negative effect on the oxidation procedure. Anyway, further controlled experiments like competitive experiments in the presence of phenol should be done in the future to verify this hypothesis.



**Scheme 5.** Non-working *o*-aminophenol substrate in this protocol.

### 3. Mechanistic insights

To gain some insight into the mechanism, we then carried out the oxidation reactions of the following substrates: **i)** bibenzyl, **ii)** benzyl alcohol and 1-phenylethanol, **iii)** 1,2-diphenylhydrazine (Scheme 6). For the bibenzyl substrate, no oxidation activity was observed under either 2 bar or 50 bar of dry air (eq. 1), suggesting the direct alkane oxidation pathway is unlikely to occur in this system. For the second two substrates, no carbonyl compounds were detected (eq. 2). However, when 1,2-diphenylhydrazine was subjected to catalytic reaction conditions, the fully oxidized product, 1,2-diphenyldiazene **12b**, was formed as the sole product even under 1 bar of dry air (eq. 3). This result demonstrates that the presence of the nitrogen atom in substrates is critical for the success of the catalysis.



**Scheme 6.** Oxidation reactions in the presence of bibenzyl (Eq. 1), benzyl alcohol and 1-phenylethanol (Eq. 2), and 1,2-diphenylhydrazine (Eq. 3).

A Kinetic study was also carried out for the oxidation of *N*-benzylaniline **1a** by Mn(CO)<sub>5</sub>Br performed under 2 bar of dry air at 100 °C in THF (black square) or *t*-amyl alcohol (red round). In fact, we observed that in *t*-amyl alcohol, the rate of the reaction was slower than in THF: ca. 30% less yield was observed after 2 h (Figure 1).

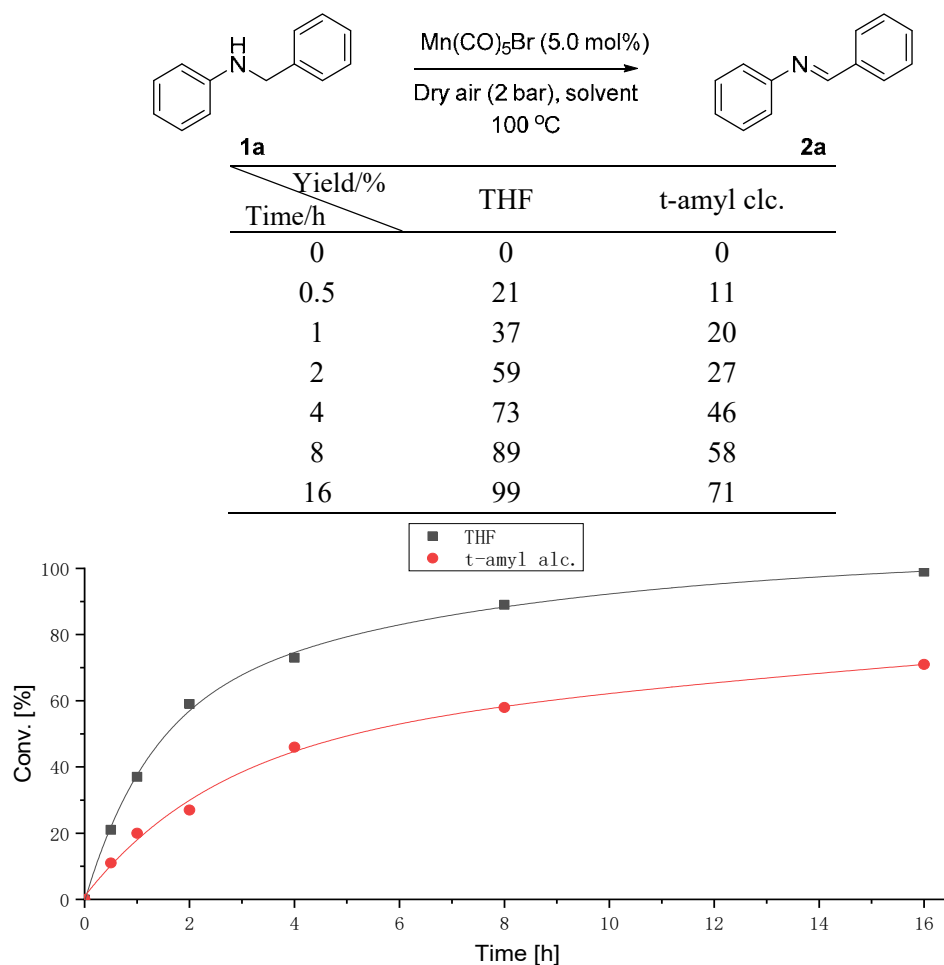
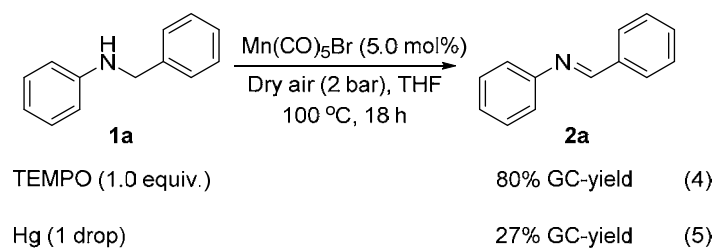


**Figure 1.** Kinetic profiles of the oxidation of *N*-benzylaniline **1a** by  $\text{Mn}(\text{CO})_5\text{Br}$  performed under 2 bar of dry air at 100 °C in THF (**black square**) or *t*-amyl alcohol (**red round**).

When adding 1 equiv. of TEMPO (2,2,6,6-tetramethylpiperidine-1-oxyl) into the reaction mixture, slightly lower yield was observed (Scheme 7, eq. 4) but no intermediate was observed *via* GC-MS, demonstrating that the radical process is unlikely happening in this reaction. Importantly, in the mercury test, one drop of Hg decreased the reaction yield to 27% (eq. 5), which seems to indicate that the catalytic active species might be a sort of soluble nanoparticles.



**Scheme 7.** Oxidation reactions in the presence of TEMPO (Eq. 4) and Hg (Eq. 5).

### Catalyst recycling tests

Next, the reusability of the catalyst was evaluated with two different reaction time, 18 h and 48 h. In both cases, excellent yields were obtained in a second run (91% and 98% respectively). The isolated yield dropped to 87% until the fifth run with 48 h reaction time. However, 72% yield was obtained with 18 h reaction time in the third run (Figure 2).

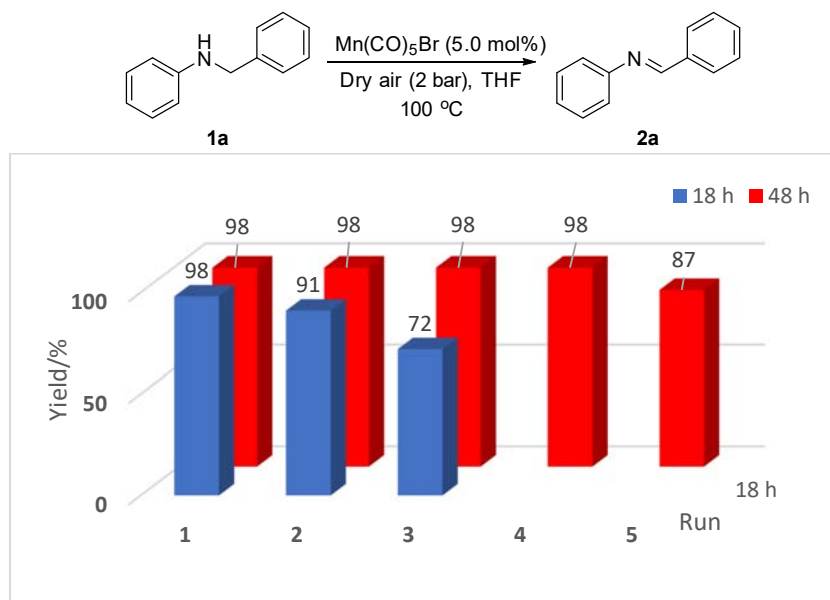


**Figure 2.** Catalyst recycling tests for the oxidation of *N*-benzylaniline by  $\text{Mn}(\text{CO})_5\text{Br}$  performed under 2 bar of dry air, THF, at 100 °C for 18 h (blue) and 48 h (red).

**Procedure for catalyst recycling tests:** after the first run (after 18 h or 48 h), the reactor was slowly depressurized and the reaction media was removed carefully by distillation with heat gun. The reactor was then reloaded with *N*-benzylaniline (0.5 mmol), fresh THF, and pressurized with 2 bar of dry air. After 18 h (or 48 h) at 100 °C, the reaction yields were determined by GC-MS analysis.

## 4. Conclusion of Chapter VI

In summary, we demonstrate here the first Mn(I)-catalyzed ligand- and additive-free aerobic oxidation of amines to selectively access aldimines, *N*-heteroaromatics and also benzoimidazoles. The catalytic process displayed a high tolerance towards a large variety of functional groups. Controlled experiments demonstrated that the presence of the nitrogen atom in substrates is critical for the success of the oxidation reactions. The formation of nanoparticles is likely to occur, and deeper mechanistic studies, for example Transmission Electron Microscopy (TEM) analysis of the reaction mixture to identify the formation of nanoparticles, would be needed to fully understand the pathway of this transformation.



## 5. References

- [1] J. P. Adams, *J. Chem. Soc., Perkin Trans. I* **2000**, 125-139.
- [2] a) R. Bloch, *Chem. Rev.* **1998**, 98, 1407-1438; b) S. Kobayashi, H. Ishitani, *Chem. Rev.* **1999**, 99, 1069-1094; c) O. Pàmies, A. H. Éll, J. S. M. Samec, N. Hermanns, J.-E. Bäckvall, *Tetrahedron Lett.* **2002**, 43, 4699-4702; d) N. Hermanns, S. Dahmen, C. Bolm, S. Bräse, *Angew. Chem. Int. Ed.* **2002**, 41, 3692-3694; e) B. Török, G. K. Surya Prakash, *Adv. Synth. Catal.* **2003**, 345, 165-168.
- [3] a) X.-Q. Gu, W. Chen, D. Morales-Morales, C. M. Jensen, *J. Mol. Catal. A: Chem.* **2002**, 189, 119-124; b) R. Yamaguchi, C. Ikeda, Y. Takahashi, K.-i. Fujita, *J. Am. Chem. Soc.* **2009**, 131, 8410-8412; c) A. Prades, E. Peris, M. Albrecht, *Organometallics* **2011**, 30, 1162-1167; d) D. Ainembabazi, N. An, J. C. Manayil, K. Wilson, A. F. Lee, A. M. Voutchkova-Kostal, *ACS Catal.* **2019**, 9, 1055-1065; e) Z. Wang, I. Tonks, J. Belli, C. M. Jensen, *J. Organomet. Chem.* **2009**, 694, 2854-2857; f) J. Wu, D. Talwar, S. Johnston, M. Yan, J. Xiao, *Angew. Chem. Int. Ed.* **2013**, 52, 6983-6987; g) S. Muthaiah, S. H. Hong, *Adv. Synth. Catal.* **2012**, 354, 3045-3053; h) S. Chakraborty, W. W. Brennessel, W. D. Jones, *J. Am. Chem. Soc.* **2014**, 136, 8564-8567; i) K.-H. He, F.-F. Tan, C.-Z. Zhou, G.-J. Zhou, X.-L. Yang, Y. Li, *Angew. Chem. Int. Ed.* **2017**, 56, 3080-3084; j) X. Jin, Y. Liu, Q. Lu, D. Yang, J. Sun, S. Qin, J. Zhang, J. Shen, C. Chu, R. Liu, *Org. Biomol. Chem.* **2013**, 11, 3776-3780; k) S. Wang, H. Huang, C. Bruneau, C. Fischmeister, *ChemSusChem* **2019**, 12, 2350-2354; l) Q. Wang, H. Chai, Z. Yu, *Organometallics* **2018**, 37, 584-591; m) Á. Vivancos, M. Beller, M. Albrecht, *ACS Catal.* **2018**, 8, 17-21; n) M. Mastalir, M. Glatz, E. Pittenauer, G. Allmaier, K. Kirchner, *Org. Lett.* **2019**, 21, 1116-1120.
- [4] a) L. Blackburn, R. J. K. Taylor, *Org. Lett.* **2001**, 3, 1637-1639; b) M. S. Kwon, S. Kim, S. Park, W. Bosco, R. K. Chidrala, J. Park, *J. Org. Chem.* **2009**, 74, 2877-2879; c) B. Gnanaprakasam, J. Zhang, D. Milstein, *Angew. Chem. Int. Ed.* **2010**, 49, 1468-1471; d) S. Kegnæs, J. Mielby, U. V. Mentzel, C. H. Christensen, A. Riisager, *Green Chem.* **2010**, 12, 1437-1441; e) M. A. Esteruelas, N. Honczek, M. Oliván, E. Oñate, M. Valencia, *Organometallics* **2011**, 30, 2468-2471; f) Q. Kang, Y. Zhang, *Green Chem.* **2012**, 14, 1016-1019; g) L. Han, P. Xing, B. Jiang, *Org. Lett.* **2014**, 16, 3428-3431; h) R. R. Donthiri, R. D. Patil, S. Adimurthy, *Eur. J. Org. Chem.* **2012**, 2012, 4457-4460; i) J. Xu, R. Zhuang, L. Bao, G. Tang, Y. Zhao, *Green Chem.* **2012**, 14, 2384-2387; j) R. Fertig, T. Irrgang, F. Freitag, J. Zander, R. Kempe, *ACS Catal.* **2018**, 8, 8525-8530; k) Simone V. Samuelsen, C. Santilli, M. S. G. Ahlquist, R. Madsen, *Chem. Sci.* **2019**, 10, 1150-1157; l) A. Mukherjee, A. Nerush, G. Leitus, L. J. W. Shimon, Y. Ben David, N. A. Espinosa Jalapa, D. Milstein, *J. Am. Chem. Soc.* **2016**, 138, 4298-4301; m) M. L. Buil, M. A. Esteruelas, M. P. Gay, M. Gómez-Gallego, A. I. Nicasio, E. Oñate, A. Santiago, M. A. Sierra, *Organometallics* **2018**, 37, 603-617.
- [5] a) E. Zhang, H. Tian, S. Xu, X. Yu, Q. Xu, *Org. Lett.* **2013**, 15, 2704-2707; b) R. D. Patil, S. Adimurthy, *Adv. Synth. Catal.* **2011**, 353, 1695-1700; c) B. Chen, L. Wang, S. Gao, *ACS Catal.* **2015**, 5, 5851-5876; d) Z. Hu, F. M. Kerton, *Org. Biomol. Chem.* **2012**, 10, 1618-1624.
- [6] a) T. Mukaiyama, A. Kawana, Y. Fukuda, J.-i. Matsuo, *Chem. Lett.* **2001**, 30, 390-391; b) O. R. Luca, T. Wang, S. J. Konezny, V. S. Batista, R. H. Crabtree, *New J. Chem.* **2011**, 35, 998-999.
- [7] a) P. Müller, D. M. Gilabert, *Tetrahedron* **1988**, 44, 7171-7175; b) F. Porta, C. Crotti, S. Cenini, G. Palmisano, *J. Mol. Catal.* **1989**, 50, 333-341.
- [8] S. Yamazaki, *Chem. Lett.* **1992**, 21, 823-826.
- [9] A. H. Éll, J. S. M. Samec, C. Brasse, J.-E. Bäckvall, *Chem. Commun.* **2002**, 1144-1145.
- [10] a) S.-I. Murahashi, T. Naota, H. Taki, *J. Chem. Soc., Chem. Commun.* **1985**, 613-614; b) H. Choi, M. P. Doyle, *Chem. Commun.* **2007**, 745-747; c) P. K. Khatri, S. L. Jain, L. N. Sivakumar K, B. Sain, *Org. Biomol. Chem.* **2011**, 9, 3370-3374; d) K. Maruyama, T. Kusukawa, Y. Higuchi, A. Nishinaga, *Cobalt-Schiff Base Complex Catalyzed Dehydrogenation of Amines with T-Butyl Hydroperoxide in Stud. Surf. Sci. Catal., Vol. 66* (Ed.: L. I. Simándi), Elsevier, **1991**, pp. 489-495; e) D. Ge, G. Qu, X. Li, K. Geng, X. Cao, H. Gu, *New J. Chem.* **2016**, 40, 5531-5536.

- [11] D. V. Jawale, E. Gravel, N. Shah, V. Dauvois, H. Li, I. N. N. Namboothiri, E. Doris, *Chem. Eur. J.* **2015**, *21*, 7039-7042.
- [12] a) E. Boring, Y. V. Geletii, C. L. Hill, *Catalysts for Selective Aerobic Oxidation under Ambient Conditions in Advances in Catalytic Activation of Dioxygen by Metal Complexes*, Springer, **2003**, pp. 227-264; b) T. Punniyamurthy, S. Velusamy, J. Iqbal, *Chem. Rev.* **2005**, *105*, 2329-2364; c) D. Wang, A. B. Weinstein, P. B. White, S. S. Stahl, *Chem. Rev.* **2018**, *118*, 2636-2679; d) S. E. Allen, R. R. Walvoord, R. Padilla-Salinas, M. C. Kozlowski, *Chem. Rev.* **2013**, *113*, 6234-6458.
- [13] a) X. Cui, Y. Li, S. Bachmann, M. Scalone, A.-E. Surkus, K. Junge, C. Topf, M. Beller, *J. Am. Chem. Soc.* **2015**, *137*, 10652-10658; b) A. Dhakshinamoorthy, M. Alvaro, H. Garcia, *ChemCatChem* **2010**, *2*, 1438-1443; c) J. Yu, Y. Xia, M. Lu, *Synth. Commun.* **2014**, *44*, 3019-3026.
- [14] a) A. Nishinaga, S. Yamazaki, T. Matsuura, *Tetrahedron Lett.* **1988**, *29*, 4115-4118; b) W. Zhou, D. Chen, F. a. Sun, J. Qian, M. He, Q. Chen, *Tetrahedron Lett.* **2018**, *59*, 949-953; c) P. A. Ganeshpure, A. Sudalai, S. Satish, *Proc. Indian Acad. Sci. (Chem. Sci.)* **1991**, *103*, 741-745.
- [15] a) M. Shimizu, H. Orita, T. Hayakawa, K. Suzuki, K. Takehira, *Heterocycles* **1995**, *4*, 773-779; b) M. Satoshi, O. Yasuhito, T. Akihiro, R. Ilhyong, K. Mitsuo, O. Yoshiki, *Chem. Lett.* **1997**, *26*, 311-312; c) M. Yasunari, N. Takahiro, U. Sakae, *Bull. Chem. Soc. Jpn.* **2003**, *76*, 2399-2403; d) Y. F. Wang, J. H. Zeng, X. R. Cui, *Org. Commun.* **2013**, *6*, 68-77; e) D. Jung, M. H. Kim, J. Kim, *Org. Lett.* **2016**, *18*, 6300-6303; f) J. Wang, S. Lu, X. Cao, H. Gu, *Chem. Commun.* **2014**, *50*, 5637-5640.
- [16] a) B. Zhu, R. J. Angelici, *Chem. Commun.* **2007**, 2157-2159; b) M.-H. So, Y. Liu, C.-M. Ho, C.-M. Che, *Chem. Asian J.* **2009**, *4*, 1551-1561; c) L. Aschwanden, B. Panella, P. Rossbach, B. Keller, A. Baiker, *ChemCatChem* **2009**, *1*, 111-115; d) A. Grirrane, A. Corma, H. Garcia, *J. Catal.* **2009**, *264*, 138-144; e) B. Zhu, M. Lazar, B. G. Trewyn, R. J. Angelici, *J. Catal.* **2008**, *260*, 1-6; f) P. Sudarsanam, B. Mallesham, A. Rangaswamy, B. G. Rao, S. K. Bhargava, B. M. Reddy, *J. Mol. Catal. A: Chem.* **2016**, *412*, 47-55; g) H. Miyamura, M. Morita, T. Inasaki, S. Kobayashi, *Bull. Chem. Soc. Jpn.* **2011**, *84*, 588-599.
- [17] a) J.-R. Wang, Y. Fu, B.-B. Zhang, X. Cui, L. Liu, Q.-X. Guo, *Tetrahedron Lett.* **2006**, *47*, 8293-8297; b) S. Furukawa, A. Suga, T. Komatsu, *Chem. Commun.* **2014**, *50*, 3277-3280; c) Y. Wang, C. Li, J. Huang, *Asian J. Org. Chem.* **2017**, *6*, 44-46; d) Y. Wang, C. Li, J. Huang, *Asian J. Org. Chem.* **2017**, *6*, 44-46.
- [18] a) J. S. M. Samec, A. H. Éll, J.-E. Bäckvall, *Chem. Eur. J.* **2005**, *11*, 2327-2334; b) K. Yamaguchi, N. Mizuno, *Chem. Eur. J.* **2003**, *9*, 4353-4361; c) K. Yamaguchi, N. Mizuno, *Angew. Chem. Int. Ed.* **2003**, *42*, 1480-1483; d) A. Taketoshi, T.-a. Koizumi, T. Kanbara, *Tetrahedron Lett.* **2010**, *51*, 6457-6459; e) S.-I. Murahashi, Y. Okano, H. Sato, T. Nakae, N. Komiya, *Synlett* **2007**, 1675-1678; f) S. Chen, Q. Wan, A. K. Badu-Tawiah, *Angew. Chem. Int. Ed.* **2016**, *55*, 9345-9349; g) N. Mizuno, K. Yamaguchi, *Catal. Today* **2008**, *132*, 18-26; h) F. Li, J. Chen, Q. Zhang, Y. Wang, *Green Chem.* **2008**, *10*, 553-562; i) Y. Zhang, F. Lu, R. Huang, H. Zhang, J. Zhao, *Catal. Commun.* **2016**, *81*, 10-13; j) R. Ray, S. Chandra, V. Yadav, P. Mondal, D. Maiti, G. K. Lahiri, *Chem. Commun.* **2017**, *53*, 4006-4009.
- [19] X. Lang, H. Ji, C. Chen, W. Ma, J. Zhao, *Angew. Chem. Int. Ed.* **2011**, *50*, 3934-3937.
- [20] S. Kodama, J. Yoshida, A. Nomoto, Y. Ueta, S. Yano, M. Ueshima, A. Ogawa, *Tetrahedron Lett.* **2010**, *51*, 2450-2452.
- [21] a) H. Huang, J. Huang, Y.-M. Liu, H.-Y. He, Y. Cao, K.-N. Fan, *Green Chem.* **2012**, *14*, 930-934; b) T. Sonobe, K. Oisaki, M. Kanai, *Chem. Sci.* **2012**, *3*, 3249-3255; c) F. Su, S. C. Mathew, L. Möhlmann, M. Antonietti, X. Wang, S. Blechert, *Angew. Chem. Int. Ed.* **2011**, *50*, 657-660; d) A. E. Wendlandt, S. S. Stahl, *J. Am. Chem. Soc.* **2014**, *136*, 11910-11913; e) M. K. Sahoo, G. Jaiswal, J. Rana, E. Balaraman, *Chem. Eur. J.* **2017**, *23*, 14167-14172.
- [22] For the discussion of activated MnO<sub>2</sub> see: <http://reag.paperplane.io/00001793.htm#13>.
- [23] a) M. Hirano, S. Yakabe, H. Chikamori, J. H. Clark, T. Morimoto, *J. Chem. Res., Synop.* **1998**, 770-771; b) Y. Hamada, M. Shibata, T. Sugiura, S. Kato, T. Shioiri, *J. Org. Chem.* **1987**, *52*, 1252-1255; c) J. Matsubara, K. Nakao, Y. Hamada, T. Shioiri, *Tetrahedron Lett.* **1992**, *33*, 4187-4190; d) N. Irako, Y. Hamada, T. Shioiri, *Tetrahedron* **1992**, *48*, 7251-7264; e) A. J.

- Fatiadi, *Synthesis* **1976**, 1976, 65-104; f) T. Aoyama, N. Sonoda, M. Yamauchi, K. Toriyama, M. Anzai, A. Ando, T. Shioiri, *Synlett* **1998**, 35-36; g) A. J. Fatiadi, *Synthesis* **1976**, 65-104; h) M. Z. Barakat, M. F. Abdel-Wahab, M. M. El-Sadr, *J. Chem. Soc.* **1956**, 4685-4687; i) Y. H. Kim, S. k. Hwang, Y. S. Lee, J. W. Kim, *Appl. Chem. Eng.* **2014**, 25, 215-221.
- [24] X. Yu, C. Liu, L. Jiang, Q. Xu, *Org. Lett.* **2011**, 13, 6184-6187.
- [25] a) C. Wang, J. Yang, X. Meng, Y. Sun, X. Man, J. Li, F. Sun, *Dalton Trans.* **2019**, 48, 4474-4478; b) M. F. Pinto, M. Olivares, Á. Vivancos, G. Guisado-Barrios, M. Albrecht, B. Royo, *Catal. Sci. Technol.* **2019**, 9, 2421-2425.
- [26] J. Wang, S. Lu, X. Cao, H. Gu, *Chem. Commun.* **2014**, 50, 5637-5640.

## 6. Experimental data

### 6.1. General information

**Table S1.** Commercial sources of manganese and rhenium precursors

Mn precursors	Commercial sources
Mn(CO) <sub>5</sub> Br	Strem Chemicals
CpMn(CO) <sub>3</sub>	Sigma-Aldrich
Mn <sub>2</sub> (CO) <sub>10</sub>	Strem Chemicals
MnF <sub>2</sub>	Strem Chemicals
Mn(acac) <sub>3</sub>	Sigma-Aldrich
Mn(OTf) <sub>2</sub>	Sigma-Aldrich
MnO <sub>2</sub>	Sigma-Aldrich
MnO <sub>2</sub> (activated)	Fluka
KMnO <sub>4</sub>	Sigma-Aldrich
MnO	Sigma-Aldrich
Re(CO) <sub>5</sub> Br	Strem Chemicals
Re <sub>2</sub> (CO) <sub>10</sub>	Strem Chemicals

Magnetic stirred Parr autoclaves (22 mL) were used for the oxidation.

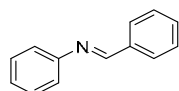
### 6.2. General procedure A for the oxidation of amines.

A 20 mL Schlenk tube was charged with amine (0.5 mmol), Mn(CO)<sub>5</sub>Br (6.9 mg, 5.0 mol%), and THF (1.0 mL), dry air (2 bar). The reaction mixture was stirred at 100 °C for indicated time. After cooling to r.t., the reactor was slowly depressurized and the reaction mixture was dried and the desired imine was isolated by bulb-to-bulb distillation. Benzimidazole products were purified by column chromatography (SiO<sub>2</sub>, mixture of petroleum ether/ethyl acetate as eluent).

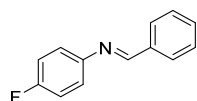
### 6.3. General procedure B for the oxidation of amines.

A 22 mL autoclave was charged with amine (0.5 mmol), Mn(CO)<sub>5</sub>Br (6.9 mg, 5.0 mol%), and *t*-amyl alcohol (1.0 mL), dry air (50 bar). The reaction mixture was stirred at 100 °C for indicated time. After cooling to room temperature, the reactor was slowly depressurized and the reaction mixture was dried and the desired imine was isolated by bulb-to-bulb distillation. Benzimidazole products were purified by column chromatography (SiO<sub>2</sub>, mixture of petroleum ether/ethyl acetate as eluent).

### 6.4. Characterization data for products

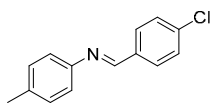


The compound **2a** was prepared as described in the general procedure A (82.5 mg) in 91% yield. <sup>1</sup>H NMR (400 MHz, CDCl<sub>3</sub>) δ 8.48 (s, 1H), 7.94 (dd, *J* = 6.6, 3.1 Hz, 2H), 7.51 – 7.49 (m, 3H), 7.43 (t, *J* = 7.8 Hz, 2H), 7.28 – 7.24 (m, 3H). <sup>13</sup>C NMR (101 MHz, CDCl<sub>3</sub>) δ 160.5, 152.2, 136.4, 131.5, 129.3, 128.9, 128.9, 126.0, 121.0.

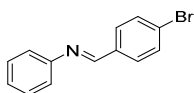


The compound **2b** was prepared as described in the general procedure A (97.6 mg) in 98%

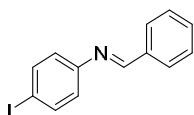
yield. **<sup>1</sup>H NMR** (400 MHz, CDCl<sub>3</sub>) δ 8.45 (s, 1H), 7.90 – 7.89 (m, 2H), 7.49 – 7.46 (m, 3H), 7.21 (dd, *J* = 8.6, 5.0 Hz, 2H), 7.08 (t, *J* = 8.5 Hz, 2H). **<sup>13</sup>C NMR** (101 MHz, CDCl<sub>3</sub>) δ 161.4 (d, *J* = 244.6 Hz), 160.3, 160.3, 148.2, 136.2, 131.6, 128.9 (d, *J* = 3.0 Hz), 122.4 (d, *J* = 8.3 Hz), 116.0 (d, *J* = 22.5 Hz). **<sup>19</sup>F NMR** (376 MHz, CDCl<sub>3</sub>) δ -117.3.



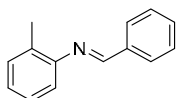
The compound **2c** was prepared as described in the general procedure **A** (103.4 mg) in 90% yield. **<sup>1</sup>H NMR** (400 MHz, CDCl<sub>3</sub>) δ 8.43 (s, 1H), 7.85 – 7.82 (m, 2H), 7.46 – 7.43 (m, 2H), 7.21 (d, *J* = 8.1 Hz, 2H), 7.15 – 7.12 (m, 2H), 2.38 (s, 3H). **<sup>13</sup>C NMR** (75 MHz, CDCl<sub>3</sub>) δ 158.1, 149.2, 137.3, 136.3, 135.0, 130.0, 130.0, 129.2, 120.9, 21.2.



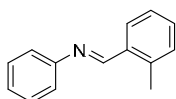
The compound **2d** was prepared as described in the general procedure **A** (97.5 mg) in 75% yield. **<sup>1</sup>H NMR** (400 MHz, CDCl<sub>3</sub>) δ 8.41 (s, 1H), 7.80 – 7.76 (m, 2H), 7.63 – 7.60 (m, 2H), 7.43 – 7.38 (m, 2H), 7.28 – 7.25 (m, 1H), 7.24 – 7.20 (m, 2H). **<sup>13</sup>C NMR** (101 MHz, CDCl<sub>3</sub>) δ 159.0, 151.8, 135.3, 132.2, 130.3, 129.3, 126.4, 126.0, 121.0.



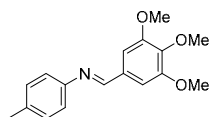
The compound **2e** was prepared as described in the general procedure **A** (101.4 mg) in 66% yield. **<sup>1</sup>H NMR** (400 MHz, CDCl<sub>3</sub>) δ 8.42 (s, 1H), 7.92 – 7.88 (m, 2H), 7.72 – 7.69 (m, 2H), 7.53 – 7.45 (m, 3H), 6.99 – 6.95 (m, 2H). **<sup>13</sup>C NMR** (75 MHz, CDCl<sub>3</sub>) δ 160.9, 151.8, 138.3, 136.1, 131.8, 129.0, 129.0, 123.1, 90.4.



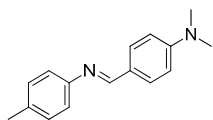
The compound **2f** was prepared as described in the general procedure **A** (90.8 mg) in 93% yield. **<sup>1</sup>H NMR** (300 MHz, CDCl<sub>3</sub>) δ 8.39 (s, 1H), 7.96 – 7.92 (m, 2H), 7.51 – 7.49 (m, 3H), 7.26 – 7.20 (m, 2H), 7.17 – 7.12 (m, 1H), 6.95 (d, *J* = 8.0 Hz, 1H), 2.39 (s, 3H). **<sup>13</sup>C NMR** (101 MHz, CDCl<sub>3</sub>) δ 159.5, 151.3, 136.6, 132.0, 131.3, 130.4, 128.9, 126.8, 125.8, 117.8, 18.0.



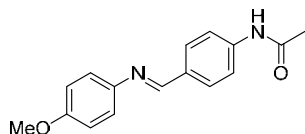
The compound **2g** was prepared as described in the general procedure **A** (95.7 mg) in 98% yield. **<sup>1</sup>H NMR** (300 MHz, CDCl<sub>3</sub>) δ 8.76 (s, 1H), 8.08 (dd, *J* = 7.4, 1.1 Hz, 1H), 7.43 – 7.31 (m, 4H), 7.29 – 7.19 (m, 4H), 2.60 (s, 3H). **<sup>13</sup>C NMR** (75 MHz, CDCl<sub>3</sub>) δ 159.3, 152.9, 138.7, 134.3, 131.2, 131.1, 129.3, 128.0, 126.5, 125.9, 121.0, 19.5.



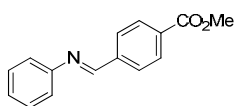
The compound **2h** was prepared as described in the general procedure **A** (118.4 mg) in 83% yield. **<sup>1</sup>H NMR** (400 MHz, CDCl<sub>3</sub>) δ 8.36 (s, 1H), 7.19 (d, *J* = 8.1 Hz, 2H), 7.15 – 7.12 (m, 4H), 3.94 (s, 6H), 3.92 (s, 3H), 2.37 (s, 3H). **<sup>13</sup>C NMR** (101 MHz, CDCl<sub>3</sub>) δ 159.1, 153.6, 149.5, 141.0, 135.8, 132.0, 129.9, 120.9, 105.8, 61.1, 56.4, 21.1.



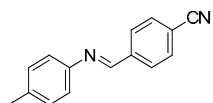
The compound **2i** was prepared as described in the general procedure **A** (94.1 mg) in 79% yield.  $^1\text{H NMR}$  (400 MHz,  $\text{CDCl}_3$ )  $\delta$  8.34 (s, 1H), 7.80 – 7.76 (m, 2H), 7.19 – 7.17 (m, 2H), 7.14 – 7.11 (m, 2H), 6.74 (d,  $J$  = 9.0 Hz, 2H), 3.05 (s, 6H), 2.37 (s, 3H).  $^{13}\text{C NMR}$  (101 MHz,  $\text{CDCl}_3$ )  $\delta$  159.7, 152.5, 150.5, 134.8, 130.4, 129.8, 124.7, 120.9, 111.7, 40.3, 21.1.



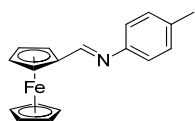
The compound **2j** was prepared as described in the general procedure **A** (104.6 mg) in 78% yield.  $^1\text{H NMR}$  (400 MHz,  $\text{CDCl}_3$ )  $\delta$  8.42 (s, 1H), 7.84 (d,  $J$  = 8.5 Hz, 2H), 7.62 (d,  $J$  = 8.2 Hz, 2H), 7.47 (s, 1H), 7.24 – 7.20 (m, 2H), 6.94 – 6.90 (m, 2H), 3.83 (s, 3H), 2.20 (s, 3H).  $^{13}\text{C NMR}$  (75 MHz,  $\text{CDCl}_3$ )  $\delta$  168.5, 158.3, 157.7, 145.1, 140.5, 132.6, 129.7, 122.3, 119.6, 114.5, 55.6, 24.9.



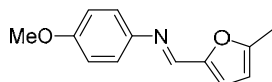
The compound **2k** was prepared as described in the general procedure **A** (75.4 mg) in 63% yield.  $^1\text{H NMR}$  (400 MHz,  $\text{CDCl}_3$ )  $\delta$  8.52 (s, 1H), 8.15 – 8.13 (m, 2H), 7.99 – 7.97 (m, 2H), 7.43 – 7.39 (m, 2H), 7.29 – 7.23 (m, 3H), 3.96 (s, 3H).  $^{13}\text{C NMR}$  (75 MHz,  $\text{CDCl}_3$ )  $\delta$  166.7, 159.2, 151.7, 140.2, 132.5, 130.1, 129.4, 128.8, 126.6, 121.0, 52.5.



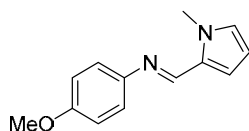
The compound **2m** was prepared as described in the general procedure **A** (103.5 mg) in 94% yield.  $^1\text{H NMR}$  (400 MHz,  $\text{CDCl}_3$ )  $\delta$  8.51 (s, 1H), 8.01 – 7.99 (m, 2H), 7.76 – 7.74 (m, 2H), 7.24 – 7.22 (m, 2H), 7.19 – 7.16 (m, 2H), 2.39 (s, 3H).  $^{13}\text{C NMR}$  (75 MHz,  $\text{CDCl}_3$ )  $\delta$  157.0, 148.5, 140.3, 137.2, 132.6, 130.1, 129.1, 121.1, 118.6, 114.3, 21.2.



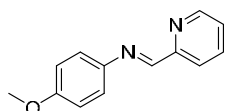
The compound **2n** was prepared as described in the general **A** procedure (57.6 mg) in 38% yield.  $^1\text{H NMR}$  (400 MHz,  $\text{CDCl}_3$ )  $\delta$  8.33 (s, 1H), 7.19 – 7.06 (m, 4H), 4.80 (s, 2H), 4.48 (s, 2H), 4.24 (s, 5H), 2.36 (s, 3H).  $^{13}\text{C NMR}$  (75 MHz,  $\text{CDCl}_3$ )  $\delta$  160.7, 150.5, 135.0, 129.8, 120.6, 80.8, 71.3, 69.4, 69.1, 21.1.



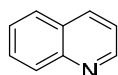
The compound **2o** was prepared as described in the general procedure **A** (102.9 mg) in 81% yield.  $^1\text{H NMR}$  (400 MHz,  $\text{CDCl}_3$ )  $\delta$  8.18 (s, 1H), 7.26 – 7.21 (m, 2H), 6.92 – 6.88 (m, 2H), 6.77 (d,  $J$  = 3.3 Hz, 1H), 6.14 (dd,  $J$  = 3.3, 0.9 Hz, 1H), 3.80 (s, 3H), 2.41 (s, 3H).  $^{13}\text{C NMR}$  (101 MHz,  $\text{CDCl}_3$ )  $\delta$  158.3, 156.5, 151.0, 145.9, 144.8, 122.3, 118.1, 114.4, 108.8, 55.6, 14.1.



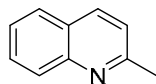
The compound **2p** was prepared as described in the general procedure **A** (92.1 mg) in 86% yield.  $^1\text{H NMR}$  (400 MHz,  $\text{CDCl}_3$ )  $\delta$  8.32 (s, 1H), 7.17 – 7.13 (m, 2H), 6.94 – 6.90 (m, 2H), 6.79 (t,  $J = 2.1$  Hz, 1H), 6.66 (dd,  $J = 3.9, 1.8$  Hz, 1H), 6.21 (dd,  $J = 3.8, 2.6$  Hz, 1H), 4.06 (s, 3H), 3.83 (s, 3H).  $^{13}\text{C NMR}$  (75 MHz,  $\text{CDCl}_3$ )  $\delta$  157.7, 149.6, 146.1, 130.6, 128.8, 121.9, 118.1, 114.5, 108.8, 55.6, 36.9.



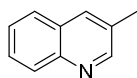
The compound **2q** was prepared as described in the general procedure **A** (74.3 mg) in 70% yield.  $^1\text{H NMR}$  (400 MHz,  $\text{CDCl}_3$ )  $\delta$  8.68 (ddd,  $J = 4.8, 1.8, 1.0$  Hz, 1H), 8.62 (s, 1H), 8.17 (dt,  $J = 7.9, 1.1$  Hz, 1H), 7.78 (td,  $J = 7.6, 1.3$  Hz, 1H), 7.34 – 7.31 (m, 3H), 6.96 – 6.92 (m, 2H), 3.82 (s, 3H).  $^{13}\text{C NMR}$  (101 MHz,  $\text{CDCl}_3$ )  $\delta$  159.1, 158.3, 155.0, 149.7, 143.8, 136.7, 124.9, 122.8, 121.7, 114.6, 55.6.



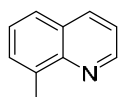
The compound **9a** was prepared as described in the general procedure **A** (51.0 mg) in 79% yield.  $^1\text{H NMR}$  (400 MHz,  $\text{CDCl}_3$ )  $\delta$  8.90 (dd,  $J = 4.3, 1.7$  Hz, 1H), 8.13 – 8.09 (m, 2H), 7.79 (dd,  $J = 8.2, 1.4$  Hz, 1H), 7.70 (ddd,  $J = 8.5, 6.8, 1.5$  Hz, 1H), 7.52 (ddd,  $J = 8.1, 6.8, 1.2$  Hz, 1H), 7.36 (dd,  $J = 8.3, 4.2$  Hz, 1H).  $^{13}\text{C NMR}$  (101 MHz,  $\text{CDCl}_3$ )  $\delta$  150.5, 148.4, 136.1, 129.6, 129.5, 128.4, 127.9, 126.6, 121.1.



The compound **9b** was prepared as described in the general procedure **B** (69.4 mg) in 97% yield.  $^1\text{H NMR}$  (400 MHz,  $\text{CDCl}_3$ )  $\delta$  8.02 (dd,  $J = 8.3, 3.7$  Hz, 2H), 7.76 (dd,  $J = 8.1, 1.4$  Hz, 1H), 7.67 (ddd,  $J = 8.5, 6.9, 1.5$  Hz, 1H), 7.47 (ddd,  $J = 8.1, 6.9, 1.2$  Hz, 1H), 7.27 (d,  $J = 8.4$  Hz, 1H), 2.74 (s, 3H).  $^{13}\text{C NMR}$  (101 MHz,  $\text{CDCl}_3$ )  $\delta$  159.1, 148.0, 136.3, 129.5, 128.8, 127.6, 126.6, 125.8, 122.1, 25.5.

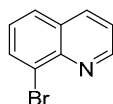


The compound **9c** was prepared as described in the general procedure **B** (67.3 mg) in 94% yield.  $^1\text{H NMR}$  (400 MHz,  $\text{CDCl}_3$ )  $\delta$  8.76 (d,  $J = 2.2$  Hz, 1H), 8.06 (d,  $J = 8.4$  Hz, 1H), 7.89 – 7.88 (m, 1H), 7.72 (dd,  $J = 8.1, 1.5$  Hz, 1H), 7.63 (ddd,  $J = 8.4, 6.8, 1.5$  Hz, 1H), 7.49 (ddd,  $J = 8.1, 6.8, 1.2$  Hz, 1H), 2.50 (s, 3H).  $^{13}\text{C NMR}$  (101 MHz,  $\text{CDCl}_3$ )  $\delta$  152.5, 146.7, 134.8, 130.6, 129.3, 128.5, 128.2, 127.2, 126.6, 18.8.

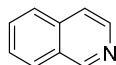


The compound **9d** was prepared as described in the general procedure **A** (64.4 mg) in 90% yield.  $^1\text{H NMR}$  (400 MHz,  $\text{CDCl}_3$ )  $\delta$  8.95 (dd,  $J = 4.2, 1.8$  Hz, 1H), 8.12 (dd,  $J = 8.2, 1.8$  Hz, 1H), 7.66 (d,  $J = 8.2$  Hz, 1H), 7.56 (d,  $J = 6.9$  Hz, 1H), 7.45 – 7.41 (m, 1H), 7.39 (dd,  $J = 8.2, 4.2$  Hz, 1H), 2.83 (s, 3H).  $^{13}\text{C NMR}$  (101 MHz,  $\text{CDCl}_3$ )  $\delta$  149.4, 147.5, 137.2, 136.4, 129.7,

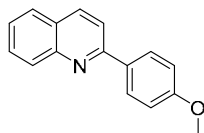
128.4, 126.4, 126.0, 121.0, 18.3.



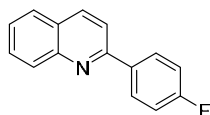
The compound **9e** was prepared as described in the general procedure **A** (90.5 mg) in 87% yield. **<sup>1</sup>H NMR** (400 MHz, CDCl<sub>3</sub>) δ 9.05 (d, *J* = 2.9 Hz, 1H), 8.16 (d, *J* = 8.0 Hz, 1H), 8.05 (d, *J* = 7.4 Hz, 1H), 7.78 (d, *J* = 8.1 Hz, 1H), 7.46 (dd, *J* = 8.2, 4.2 Hz, 1H), 7.39 (t, *J* = 7.8 Hz, 1H). **<sup>13</sup>C NMR** (101 MHz, CDCl<sub>3</sub>) δ 151.4, 145.4, 136.8, 133.3, 129.7, 127.9, 127.1, 124.9, 122.0.



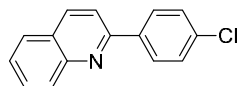
The compound **9f** was prepared as described in the general procedure **B** (59.4 mg) in 92% yield. **<sup>1</sup>H NMR** (400 MHz, CDCl<sub>3</sub>) δ 9.26 (s, 1H), 8.53 (d, *J* = 5.7 Hz, 1H), 7.96 (d, *J* = 8.2 Hz, 1H), 7.82 (d, *J* = 8.2 Hz, 1H), 7.71 – 7.67 (m, 1H), 7.64 (d, *J* = 5.7 Hz, 1H), 7.60 (ddd, *J* = 8.2, 6.8, 1.2 Hz, 1H). **<sup>13</sup>C NMR** (101 MHz, CDCl<sub>3</sub>) δ 152.7, 143.2, 135.9, 130.4, 128.8, 127.7, 127.3, 126.6, 120.6.



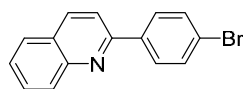
The compound **9g** was prepared as described in the general procedure **B** (108.2 mg) in 92% yield. **<sup>1</sup>H NMR** (300 MHz, CDCl<sub>3</sub>) δ 8.20 – 8.12 (m, 4H), 7.85 – 7.79 (m, 2H), 7.71 (ddd, *J* = 8.5, 6.9, 1.5 Hz, 1H), 7.50 (ddd, *J* = 8.1, 6.9, 1.1 Hz, 1H), 7.08 – 7.03 (m, 2H), 3.89 (s, 3H). **<sup>13</sup>C NMR** (75 MHz, CDCl<sub>3</sub>) δ 161.0, 157.0, 148.4, 136.8, 132.3, 129.8, 129.6, 129.1, 127.6, 127.1, 126.1, 118.7, 114.4, 55.6.



The compound **9h** was prepared as described in the general procedure **B** (103.8 mg) in 93% yield. **<sup>1</sup>H NMR** (400 MHz, CDCl<sub>3</sub>) δ 8.20 – 8.14 (m, 4H), 7.83 – 7.80 (m, 2H), 7.73 (ddd, *J* = 8.4, 6.8, 1.5 Hz, 1H), 7.53 (ddd, *J* = 8.1, 6.9, 1.2 Hz, 1H), 7.24 – 7.18 (m, 2H). **<sup>13</sup>C NMR** (101 MHz, CDCl<sub>3</sub>) δ 163.9 (d, *J* = 249.0 Hz), 156.3, 148.3, 137.0, 135.9 (d, *J* = 3.2 Hz), 129.9, 129.7, 129.5 (d, *J* = 8.4 Hz), 127.6, 127.2, 126.5, 118.7, 115.9 (d, *J* = 21.6 Hz). **<sup>19</sup>F NMR** (376 MHz, CDCl<sub>3</sub>) δ -112.41.



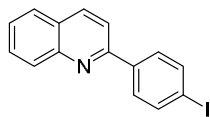
The compound **9i** was prepared as described in the general procedure **B** (117.4 mg) in 98% yield. **<sup>1</sup>H NMR** (400 MHz, CDCl<sub>3</sub>) δ 8.20 – 8.16 (m, 2H), 8.13 – 8.10 (m, 2H), 7.82 – 7.79 (m, 2H), 7.76 – 7.71 (m, 1H), 7.55 – 7.48 (m, 3H). **<sup>13</sup>C NMR** (101 MHz, CDCl<sub>3</sub>) δ 156.1, 148.3, 138.1, 137.0, 135.6, 129.9, 129.8, 129.1, 128.9, 127.6, 127.3, 126.6, 118.6.



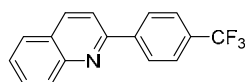
The compound **9j** was prepared as described in the general procedure **B** (129.3 mg) in 91% yield. **<sup>1</sup>H NMR** (400 MHz, CDCl<sub>3</sub>) δ 8.19 – 8.16 (m, 2H), 8.07 – 8.03 (m, 2H), 7.82 – 7.71 (m,



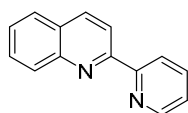
3H), 7.67 – 7.63 (m, 2H), 7.56 – 7.51 (m, 1H).  $^{13}\text{C}$  NMR (101 MHz,  $\text{CDCl}_3$ )  $\delta$  156.0, 148.3, 138.6, 137.0, 132.0, 129.9, 129.8, 129.2, 127.6, 127.3, 126.6, 124.0, 118.5.



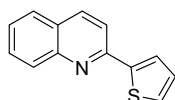
The compound **9k** was prepared as described in the general procedure **B** (149.0 mg) in 90% yield.  $^1\text{H}$  NMR (400 MHz,  $\text{CDCl}_3$ )  $\delta$  8.22 (d,  $J$  = 8.6 Hz, 1H), 8.16 (d,  $J$  = 8.5 Hz, 1H), 7.94 – 7.91 (m, 2H), 7.88 – 7.82 (m, 4H), 7.74 (ddd,  $J$  = 8.4, 6.9, 1.5 Hz, 1H), 7.54 (ddd,  $J$  = 8.1, 6.9, 1.2 Hz, 1H).  $^{13}\text{C}$  NMR (101 MHz,  $\text{CDCl}_3$ )  $\delta$  156.3, 148.4, 139.2, 138.1, 137.1, 130.0, 129.9, 129.4, 127.6, 127.4, 126.7, 118.6, 96.0.



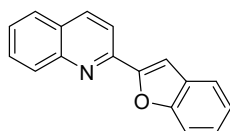
The compound **9l** was prepared as described in the general procedure **B** (125.7 mg) in 92% yield.  $^1\text{H}$  NMR (400 MHz,  $\text{CDCl}_3$ )  $\delta$  8.31 – 8.18 (m, 4H), 7.90 – 7.74 (m, 5H), 7.60 – 7.55 (m, 1H).  $^{13}\text{C}$  NMR (101 MHz,  $\text{CDCl}_3$ )  $\delta$  155.8, 148.4, 143.1, 137.3, 131.2 (q,  $J$  = 32.4 Hz), 130.1, 130.0, 128.0, 127.7, 127.6, 127.0, 125.9 (q,  $J$  = 3.8 Hz), 124.4 (q,  $J$  = 272.1 Hz), 118.9.  $^{19}\text{F}$  NMR (376 MHz,  $\text{CDCl}_3$ )  $\delta$  -62.56.



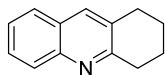
The compound **9m** was prepared as described in the general procedure **B** (98.0 mg) in 95% yield.  $^1\text{H}$  NMR (400 MHz,  $\text{CDCl}_3$ )  $\delta$  8.74 (d,  $J$  = 4.3 Hz, 1H), 8.66 (d,  $J$  = 8.0 Hz, 1H), 8.57 (d,  $J$  = 8.6 Hz, 1H), 8.27 (d,  $J$  = 8.6 Hz, 1H), 8.19 (d,  $J$  = 8.5 Hz, 1H), 7.88 – 7.83 (m, 2H), 7.73 (ddd,  $J$  = 8.4, 6.8, 1.5 Hz, 1H), 7.54 (ddd,  $J$  = 8.0, 6.8, 1.1 Hz, 1H), 7.34 (ddd,  $J$  = 7.5, 4.8, 1.2 Hz, 1H).  $^{13}\text{C}$  NMR (101 MHz,  $\text{CDCl}_3$ )  $\delta$  156.5, 156.3, 149.3, 148.0, 137.0, 136.9, 129.9, 129.7, 128.4, 127.7, 126.9, 124.1, 121.9, 119.1.



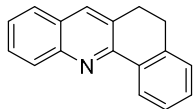
The compound **9n** was prepared as described in the general procedure **B** (97.2 mg) in 92% yield.  $^1\text{H}$  NMR (400 MHz,  $\text{CDCl}_3$ )  $\delta$  8.12 (d,  $J$  = 8.5 Hz, 1H), 8.09 (d,  $J$  = 8.7 Hz, 1H), 7.77 – 7.72 (m, 4H), 7.50 – 7.46 (m, 2H), 7.16 (dd,  $J$  = 5.1, 3.7 Hz, 1H).  $^{13}\text{C}$  NMR (101 MHz,  $\text{CDCl}_3$ )  $\delta$  152.5, 148.3, 145.6, 136.7, 130.0, 129.4, 128.7, 128.2, 127.6, 127.3, 126.2, 126.0, 117.8.



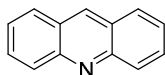
The compound **9o** was prepared as described in the general procedure **B** (110.4 mg) in 90% yield.  $^1\text{H}$  NMR (300 MHz,  $\text{CDCl}_3$ )  $\delta$  8.22 (dd,  $J$  = 8.5, 5.6 Hz, 2H), 8.02 (d,  $J$  = 8.6 Hz, 1H), 7.81 (d,  $J$  = 8.1 Hz, 1H), 7.74 (ddd,  $J$  = 8.5, 6.9, 1.5 Hz, 1H), 7.70 – 7.61 (m, 3H), 7.54 (ddd,  $J$  = 8.1, 6.8, 1.2 Hz, 1H), 7.38 (ddd,  $J$  = 8.2, 7.2, 1.4 Hz, 1H), 7.29 (td,  $J$  = 7.6, 0.9 Hz, 1H).  $^{13}\text{C}$  NMR (75 MHz,  $\text{CDCl}_3$ )  $\delta$  155.7, 155.3, 149.2, 148.4, 136.9, 130.2, 129.7, 128.9, 127.7, 127.7, 126.8, 125.7, 123.4, 121.9, 118.3, 112.0, 106.4.



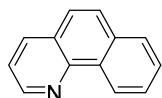
The compound **9p** was prepared as described in the general procedure **B** (73.3 mg) in 80% yield.  $^1\text{H NMR}$  (400 MHz,  $\text{CDCl}_3$ )  $\delta$  8.01 (d,  $J = 8.5$  Hz, 1H), 7.82 (s, 1H), 7.70 (d,  $J = 7.8$  Hz, 1H), 7.61 (ddd,  $J = 8.5, 6.8, 1.5$  Hz, 1H), 7.43 (ddd,  $J = 8.1, 6.8, 1.1$  Hz, 1H), 3.15 (t,  $J = 6.5$  Hz, 2H), 2.97 (t,  $J = 6.3$  Hz, 2H), 2.02 – 1.95 (m, 2H), 1.93 – 1.86 (m, 2H).  $^{13}\text{C NMR}$  (101 MHz,  $\text{CDCl}_3$ )  $\delta$  159.4, 146.3, 135.5, 131.2, 128.8, 128.1, 127.3, 127.0, 125.8, 33.4, 29.3, 23.3, 23.0.



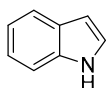
The compound **9q** was prepared as described in the general procedure **B** (102.9 mg) in 89% yield.  $^1\text{H NMR}$  (400 MHz,  $\text{CDCl}_3$ )  $\delta$  8.62 (dd,  $J = 7.8, 1.0$  Hz, 1H), 8.17 (d,  $J = 8.4$  Hz, 1H), 7.90 (s, 1H), 7.74 (d,  $J = 8.1$  Hz, 1H), 7.67 (ddd,  $J = 8.4, 6.9, 1.5$  Hz, 1H), 7.50 – 7.43 (m, 2H), 7.39 (td,  $J = 7.4, 1.5$  Hz, 1H), 7.29 (d,  $J = 7.4$  Hz, 1H), 3.14 – 3.08 (m, 2H), 3.04 – 2.99 (m, 2H).  $^{13}\text{C NMR}$  (101 MHz,  $\text{CDCl}_3$ )  $\delta$  153.5, 147.7, 139.5, 134.8, 133.8, 130.7, 129.8, 129.5, 128.7, 128.0, 128.0, 127.4, 127.0, 126.2, 126.1, 28.9, 28.5.



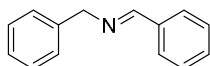
The compound **9r** was prepared as described in the general procedure **A** (88.3 mg) in 93% yield.  $^1\text{H NMR}$  (400 MHz,  $\text{CDCl}_3$ )  $\delta$  8.72 (s, 1H), 8.24 (dd,  $J = 8.8, 0.4$  Hz, 2H), 7.97 (d,  $J = 8.5$  Hz, 2H), 7.77 (ddd,  $J = 8.7, 6.6, 1.4$  Hz, 2H), 7.51 (ddd,  $J = 8.2, 6.6, 1.1$  Hz, 2H).  $^{13}\text{C NMR}$  (101 MHz,  $\text{CDCl}_3$ )  $\delta$  149.2, 136.1, 130.4, 129.5, 128.3, 126.7, 125.8.



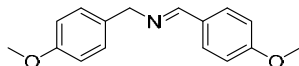
The compound **9s** was prepared as described in the general procedure **B** (83.3 mg) in 93% yield.  $^1\text{H NMR}$  (400 MHz,  $\text{CDCl}_3$ )  $\delta$  9.31 (d,  $J = 8.0$  Hz, 1H), 9.01 (dd,  $J = 4.4, 1.8$  Hz, 1H), 8.19 – 8.15 (m, 1H), 7.92 (d,  $J = 7.6$  Hz, 1H), 7.82 (dd,  $J = 8.8, 2.0$  Hz, 1H), 7.78 – 7.66 (m, 3H), 7.54 – 7.50 (m, 1H).  $^{13}\text{C NMR}$  (101 MHz,  $\text{CDCl}_3$ )  $\delta$  149.0, 146.7, 135.9, 133.7, 131.6, 128.3, 127.9, 127.9, 127.2, 126.5, 125.5, 124.5, 121.9.



The compound **9u** was prepared as described in the general procedure **A** (55.6 mg) in 95% yield.  $^1\text{H NMR}$  (400 MHz,  $\text{CDCl}_3$ )  $\delta$  8.05 (br, 1H), 7.71 (dd,  $J = 7.9, 3.0$  Hz, 1H), 7.41 (d,  $J = 8.1$  Hz, 1H), 7.28 – 7.23 (m, 1H), 7.21 – 7.16 (m, 2H), 6.61 – 6.60 (m, 1H).  $^{13}\text{C NMR}$  (101 MHz,  $\text{CDCl}_3$ )  $\delta$  135.9, 128.0, 124.3, 122.1, 120.9, 119.9, 111.2, 102.7.

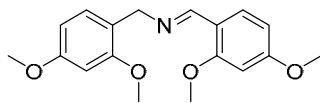


The compound **7a** was prepared as described in the general procedure **A** (93.7 mg) in 96% yield.  $^1\text{H NMR}$  (400 MHz,  $\text{CDCl}_3$ )  $\delta$  8.41 (s, 1H), 7.81 – 7.78 (m, 2H), 7.46 – 7.41 (m, 3H), 7.38 – 7.34 (m, 4H), 7.30 – 7.25 (m, 1H), 4.84 (d,  $J = 1.9$  Hz, 2H).  $^{13}\text{C NMR}$  (101 MHz,  $\text{CDCl}_3$ )  $\delta$  162.1, 139.4, 136.3, 130.9, 128.7, 128.6, 128.4, 128.1, 127.1, 65.2.

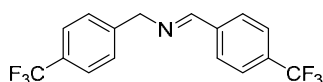


The compound **7b** was prepared as described in the general procedure **A** (114.9 mg) in 90%

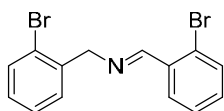
yield. **<sup>1</sup>H NMR** (300 MHz, CDCl<sub>3</sub>) δ 8.30 (s, 1H), 7.74 – 7.70 (m, 2H), 7.28 – 7.23 (m, 2H), 6.95 – 6.86 (m, 4H), 4.73 (s, 2H), 3.84 (s, 3H), 3.80 (s, 3H). **<sup>13</sup>C NMR** (126 MHz, CDCl<sub>3</sub>) δ 161.8, 161.0, 158.8, 131.8, 129.9, 129.3, 129.3, 114.1, 114.0, 64.5, 55.5, 55.4.



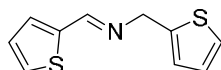
The compound **7c** was prepared as described in the general procedure **A** (129.3 mg) in 82% yield. **<sup>1</sup>H NMR** (300 MHz, CDCl<sub>3</sub>) δ 8.71 (s, 1H), 7.96 (d, *J* = 8.6 Hz, 1H), 7.18 (d, *J* = 8.9 Hz, 1H), 6.51 (dd, *J* = 8.6, 2.4 Hz, 1H), 6.50 – 6.43 (m, 3H), 4.72 (s, 2H), 3.84 (s, 3H), 3.83 (s, 3H), 3.81 (s, 3H), 3.79 (s, 3H). **<sup>13</sup>C NMR** (126 MHz, CDCl<sub>3</sub>) δ 163.0, 160.2, 160.0, 158.3, 157.5, 129.9, 128.8, 121.0, 118.4, 105.4, 104.2, 98.6, 98.2, 59.3, 55.7, 55.5, 55.5.



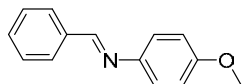
The compound **7d** was prepared as described in the general procedure **A** (149.1 mg) in 90% yield. **<sup>1</sup>H NMR** (300 MHz, CDCl<sub>3</sub>) δ 8.47 (s, 1H), 7.91 (d, *J* = 8.1 Hz, 2H), 7.69 (d, *J* = 8.2 Hz, 2H), 7.62 (d, *J* = 8.1 Hz, 2H), 7.47 (d, *J* = 8.1 Hz, 2H), 4.90 (s, 2H). **<sup>13</sup>C NMR** (101 MHz, CDCl<sub>3</sub>) δ 161.2, 143.1, 139.1, 132.7 (q, *J* = 32.4 Hz), 129.6 (q, *J* = 32.4 Hz), 128.7, 128.3, 125.8 (q, *J* = 3.8 Hz), 125.6 (q, *J* = 3.8 Hz), 124.03 (q, *J* = 272.4 Hz), 124.36 (q, *J* = 271.9 Hz), 64.6. **<sup>19</sup>F NMR** (376 MHz, CDCl<sub>3</sub>) δ -62.45, -62.83.



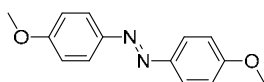
The compound **7e** was prepared as described in the general procedure **A** (153.6 mg) in 87% yield. **<sup>1</sup>H NMR** (300 MHz, CDCl<sub>3</sub>) δ 8.81 (s, 1H), 8.12 (dd, *J* = 7.7, 2.0 Hz, 1H), 7.59 (dd, *J* = 7.8, 0.8 Hz, 2H), 7.43 (dd, *J* = 7.6, 1.8 Hz, 1H), 7.38 – 7.26 (m, 3H), 7.15 (td, *J* = 7.7, 1.8 Hz, 1H), 4.94 (s, 2H). **<sup>13</sup>C NMR** (126 MHz, CDCl<sub>3</sub>) δ 162.1, 138.6, 134.7, 133.2, 132.8, 132.1, 129.9, 129.1, 128.7, 127.8, 127.7, 125.4, 123.8, 64.5.



The compound **7g** was prepared as described in the general procedure **A** (92.3 mg) in 89% yield. **<sup>1</sup>H NMR** (400 MHz, CDCl<sub>3</sub>) δ 8.42 (s, 1H), 7.42 (d, *J* = 5.0 Hz, 1H), 7.33 (d, *J* = 3.4 Hz, 1H), 7.24 (dd, *J* = 4.9, 1.4 Hz, 1H), 7.08 (dd, *J* = 5.1, 3.6 Hz, 1H), 7.00 – 6.96 (m, 2H), 4.95 (s, 2H). **<sup>13</sup>C NMR** (126 MHz, CDCl<sub>3</sub>) δ 155.6, 142.3, 141.7, 131.1, 129.5, 127.5, 127.0, 125.5, 125.0, 58.7.

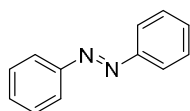


The compound **11a** was prepared as described in the general procedure **A** (69.7 mg) in 66% yield. **<sup>1</sup>H NMR** (400 MHz, CDCl<sub>3</sub>) δ 8.51 (s, 1H), 7.94 – 7.91 (m, 2H), 7.50 – 7.48 (m, 3H), 7.30 – 7.26 (m, 2H), 6.99 – 6.95 (m, 2H), 3.86 (s, 3H). **<sup>13</sup>C NMR** (101 MHz, CDCl<sub>3</sub>) δ 158.5, 158.4, 145.0, 136.6, 131.1, 128.8, 128.7, 122.3, 114.5, 55.6.

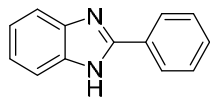


The compound **12a** was prepared as described in the general procedure **B** (107.8 mg) in 89% yield. **<sup>1</sup>H NMR** (500 MHz, CDCl<sub>3</sub>) δ 7.90 – 7.87 (m, 4H), 7.02 – 6.99 (m, 4H), 3.89 (s, 6H).

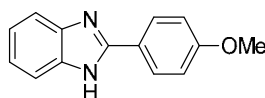
**<sup>13</sup>C NMR** (126 MHz, CDCl<sub>3</sub>) δ 161.7, 147.2, 124.5, 114.3, 55.7.



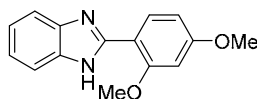
The compound **12b** was prepared as described in the general procedure **A** with 1 bar of dry air (85.6 mg) in 94% yield. **<sup>1</sup>H NMR** (400 MHz, CDCl<sub>3</sub>) δ 7.97 – 7.94 (m, 4H), 7.56 – 7.47 (m, 6H). **<sup>13</sup>C NMR** (101 MHz, CDCl<sub>3</sub>) δ 152.8, 131.1, 129.2, 123.0.



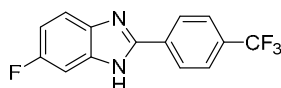
The compound **14a** was prepared as described in the general procedure **A** (86.4 mg) in 89% yield. **<sup>1</sup>H NMR** (500 MHz, d<sup>6</sup>-DMSO) δ 12.94 (br, 1H), 8.19 – 8.17 (m, 2H), 7.61 (br, 2H), 7.56 – 7.53 (m, 2H), 7.51 – 7.47 (m, 1H), 7.23 – 7.19 (m, 2H). **<sup>13</sup>C NMR** (126 MHz, d<sup>6</sup>-DMSO) δ 151.4, 130.2, 130.0, 129.1, 126.6.



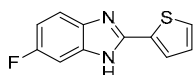
The compound **14b** was prepared as described in the general procedure **A** (80.7 mg) in 72% yield. **<sup>1</sup>H NMR** (400 MHz, d<sup>6</sup>-DMSO) δ 8.14 – 8.11 (m, 2H), 7.58 – 7.54 (m, 2H), 7.19 – 7.15 (m, 2H), 7.13 – 7.09 (m, 2H), 3.84 (s, 3H). **<sup>13</sup>C NMR** (101 MHz, d<sup>6</sup>-DMSO) δ 160.6, 151.3, 128.0, 122.7, 121.8, 114.4, 55.3.



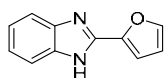
The compound **14c** was prepared as described in the general procedure **A** (117.0 mg) in 92% yield. **<sup>1</sup>H NMR** (400 MHz, d<sup>6</sup>-DMSO) δ 11.96 (br, 1H), 8.27 (d, *J* = 8.6 Hz, 1H), 7.61 – 7.57 (m, 2H), 7.18 – 7.13 (m, 2H), 6.76 (d, *J* = 2.3 Hz, 1H), 6.72 (dd, *J* = 8.7, 2.4 Hz, 1H), 4.02 (s, 3H), 3.85 (s, 3H). **<sup>13</sup>C NMR** (101 MHz, d<sup>6</sup>-DMSO) δ 162.0, 158.1, 149.2, 130.9, 121.4, 111.0, 106.2, 98.6, 55.8, 55.5.



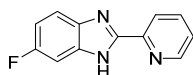
The compound **14e** was prepared as described in the general procedure **A** (109.3 mg) in 78% yield. **<sup>1</sup>H NMR** (400 MHz, d<sup>6</sup>-DMSO) δ 13.29 (br, 1H), 8.36 (d, *J* = 8.1 Hz, 2H), 7.92 (d, *J* = 8.2 Hz, 2H), 7.64 (s, 1H), 7.43 (s, 1H), 7.13 – 7.08 (m, 1H). **<sup>13</sup>C NMR** (101 MHz, d<sup>6</sup>-DMSO) δ 133.7, 130.3, 129.9, 129.6, 129.3, 128.2, 128.1, 127.9, 127.1, 126.0 (q, *J* = 3.8 Hz), 125.4, 122.7, 120.0. **<sup>19</sup>F NMR** (376 MHz, d<sup>6</sup>-DMSO) δ -61.3.



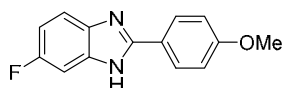
The compound **14g** was prepared as described in the general procedure **A** (81.8 mg) in 75% yield. **<sup>1</sup>H NMR** (400 MHz, d<sup>6</sup>-DMSO) δ 13.07 (br, 1H), 7.83 (dd, *J* = 3.7, 1.2 Hz, 1H), 7.73 (dd, *J* = 5.1, 1.2 Hz, 1H), 7.56 – 7.53 (m, 1H), 7.36 (d, *J* = 9.4 Hz, 1H), 7.23 (dd, *J* = 5.0, 3.6 Hz, 1H), 7.05 (td, *J* = 10.0, 2.5 Hz, 1H). **<sup>13</sup>C NMR** (101 MHz, d<sup>6</sup>-DMSO) δ 159.9, 157.5, 148.4, 133.3, 129.0, 128.3, 126.9, 110.3, 110.1. **<sup>19</sup>F NMR** (376 MHz, d<sup>6</sup>-DMSO) δ -119.5, -121.2.



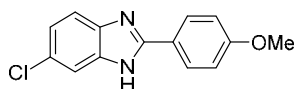
The compound **14h** was prepared as described in the general procedure **A** (62.6 mg) in 68% yield.  $^1\text{H NMR}$  (300 MHz,  $\text{d}^6\text{-DMSO}$ )  $\delta$  12.91 (br, 1H), 7.94 (d,  $J = 1.3$  Hz, 1H), 7.57 – 7.54 (m, 2H), 7.22 – 7.17 (m, 3H), 6.73 (dd,  $J = 3.5, 1.8$  Hz, 1H).  $^{13}\text{C NMR}$  (75 MHz,  $\text{d}^6\text{-DMSO}$ )  $\delta$  145.5, 144.6, 143.6, 122.2, 112.3, 110.4.



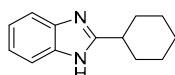
The compound **14i** was prepared as described in the general procedure **A** (87.4 mg) in 82% yield.  $^1\text{H NMR}$  (400 MHz,  $\text{d}^6\text{-DMSO-5\%TFA}$ )  $\delta$  8.88 – 8.86 (m, 1H), 8.39 (d,  $J = 7.9$  Hz, 1H), 8.18 (td,  $J = 7.8, 1.7$  Hz, 1H), 7.83 (dd,  $J = 9.0, 4.6$  Hz, 1H), 7.74 – 7.70 (m, 1H), 7.62 (dd,  $J = 8.6, 2.4$  Hz, 1H), 7.39 (td,  $J = 9.4, 2.5$  Hz, 1H).  $^{13}\text{C NMR}$  (101 MHz,  $\text{d}^6\text{-DMSO-5\%TFA}$ )  $\delta$  161.5, 159.2, 159.1, 158.8, 158.5, 158.1, 150.4, 149.6, 149.6, 143.2, 138.6, 134.1, 134.0, 130.4, 127.3, 123.2, 119.7, 116.8, 116.4, 116.3, 114.6, 114.3, 113.9, 111.0, 101.3, 101.0.  $^{19}\text{F NMR}$  (376 MHz,  $\text{d}^6\text{-DMSO-5\%TFA}$ )  $\delta$  -75.4.



The compound **14j** was prepared as described in the general procedure **A** (115.1 mg) in 95% yield.  $^1\text{H NMR}$  (300 MHz,  $\text{d}^6\text{-DMSO}$ )  $\delta$  12.86 (br, 1H), 8.10 (d,  $J = 8.7$  Hz, 2H), 7.54 (dd,  $J = 8.7, 4.9$  Hz, 1H), 7.35 (dd,  $J = 9.5, 2.5$  Hz, 1H), 7.11 (d,  $J = 8.8$  Hz, 2H), 7.06 – 6.99 (m, 1H), 3.84 (s, 3H).  $^{13}\text{C NMR}$  (75 MHz,  $\text{d}^6\text{-DMSO}$ )  $\delta$  160.7, 160.0, 156.9, 152.8, 128.0, 122.4, 114.4, 109.8, 109.5, 55.3.  $^{19}\text{F NMR}$  (376 MHz,  $\text{d}^6\text{-DMSO}$ )  $\delta$  -121.1.



The compound **14k** was prepared as described in the general procedure **A** (89.3 mg) in 69% yield.  $^1\text{H NMR}$  (500 MHz,  $\text{CDCl}_3$ )  $\delta$  10.54 (br, 1H), 8.06 (d,  $J = 8.6$  Hz, 2H), 7.47 – 7.47 (m, 1H), 7.42 (d,  $J = 8.6$  Hz, 1H), 7.16 (dd,  $J = 8.6, 1.9$  Hz, 1H), 6.87 (d,  $J = 8.8$  Hz, 2H), 3.78 (s, 3H).  $^{13}\text{C NMR}$  (126 MHz,  $\text{CDCl}_3$ )  $\delta$  161.6, 153.8, 139.9, 138.1, 128.6, 128.3, 123.3, 122.0, 115.8, 114.8, 55.5.



The compound **14l** was prepared as described in the general procedure **A** (90.1 mg) in 90% yield.  $^1\text{H NMR}$  (400 MHz,  $\text{CDCl}_3$ )  $\delta$  7.58 – 7.53 (m, 2H), 7.23 – 7.19 (m, 2H), 2.97 – 2.89 (m, 1H), 2.19 – 2.14 (m, 2H), 1.90 – 1.62 (m, 5H), 1.47 – 1.24 (m, 3H).  $^{13}\text{C NMR}$  (126 MHz,  $\text{d}^6\text{-DMSO}$ )  $\delta$  158.8, 134.9, 125.6, 121.1, 37.6, 31.2, 25.5, 25.5.

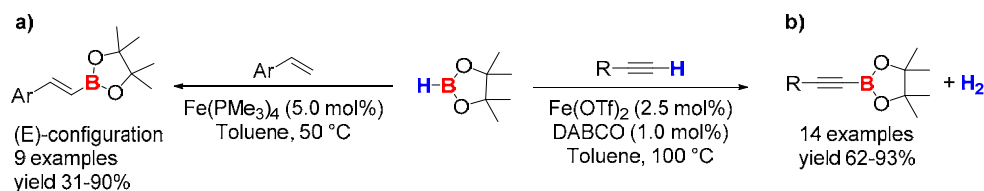
## **General Conclusion**



## General Conclusion

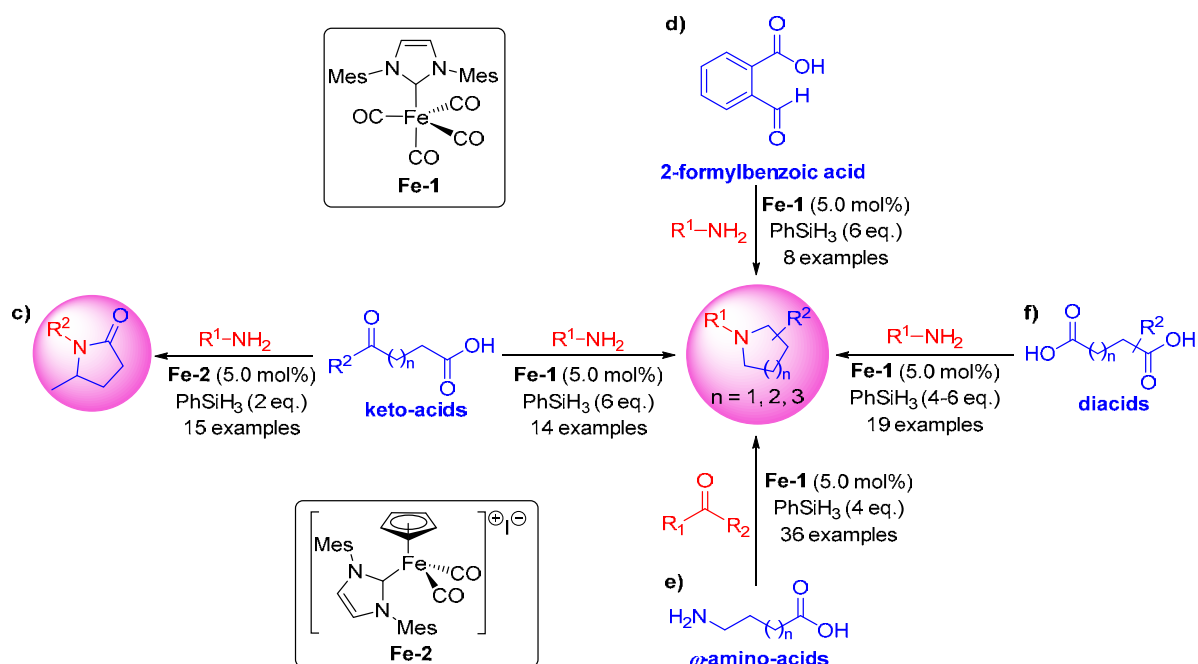
In summary, the research results presented in this thesis aimed at developing advanced eco-friendly methodologies in the area of iron, manganese and rhenium-catalyzed (de)hydrogenation and hydroelementation reactions. To achieve such goals, innocent as well as non-innocent redox-active (tri- or bi-dentate cooperative) ligands have been shown impressive and promising results. NHC, cyclopentadienyl and organophosphorus based complexes have also reveals outstanding activities and selectivities. Notably, in-depth mechanistic studies will be crucial to elucidate reaction pathways, important steps in the elaboration of well-defined as well as *in situ* generated catalysts able to reach the best activity and selectivity.

Initially, we reported the first examples of highly selective catalytic direct C-H borylation of **a)** styrene derivatives and **b)** terminal alkynes with pinacolborane (1.0 equiv.), using  $\text{Fe}(\text{PMe}_3)_4$  and  $\text{Fe}(\text{OTf})_2/\text{DABCO}$  as catalyst systems, respectively. Both aryl and alkyl substituted alkynes were applied in the C-H borylation reactions. Noticeably, the mechanism study (involving DFT calculations) of the dehydrogenative borylation of styrene shows that dehydroborylation is kinetically more favorable than hydroboration.

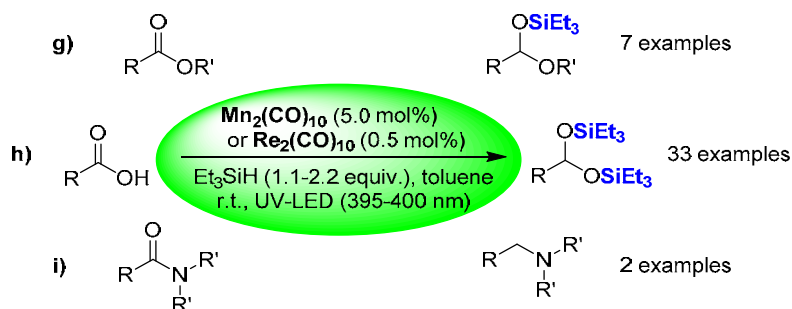


Afterwards, *N*-heterocyclic carbene (NHC) based iron complexes  $\text{Fe}(\text{CO})_4(\text{IMes})$  and  $[\text{CpFe}(\text{CO})_2(\text{IMes})][\text{I}]$  have been efficiently employed in the catalytic reductive amination reactions with hydrosilanes to access cyclic amines, including reductive amination of **c)** keto acids (particularly levulinic acid derivatives) with amines, **d)** 2-formylbenzoic acid with amines, **e)** carbonyl derivatives with  $\omega$ -amino fatty acids and **f)** dicarboxylic acids in the presence of amines. Broad substrate scopes have been achieved with a remarkable functional group tolerance as reducible groups such as carboxylic ester, amide, cyano and even acetyl, were well tolerated. The notable features of this protocol include the use of an Earth-abundant, nontoxic metal iron complex bearing *N*-heterocyclic carbene (NHC) ligand as the catalyst (5.0 mol%) in the presence of phenylsilane (2-6 equiv.) as the reducing agent at 100 °C and visible-light activation of the catalyst.



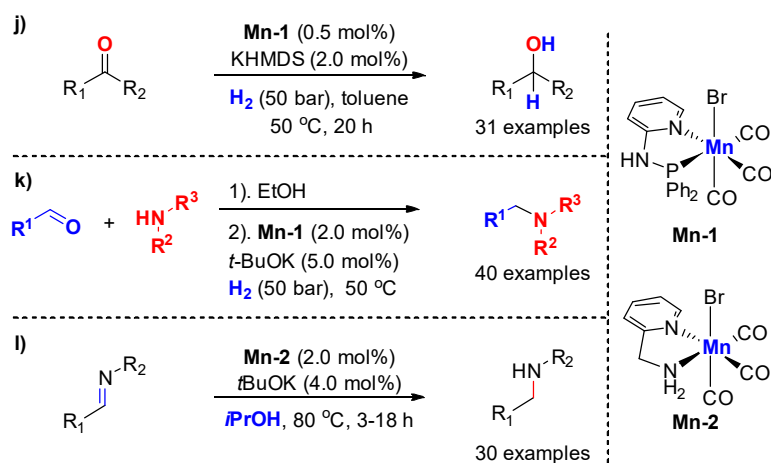


Manganese, the third most abundant transition metals after iron and titanium, could also be efficiently used in hydrosilylation reactions. Interestingly, with the commercially available  $\text{Mn}_2(\text{CO})_{10}$  (5.0 mol%) or its group 7 congener  $\text{Re}_2(\text{CO})_{10}$  (0.5 mol%) as catalysts and  $\text{Et}_3\text{SiH}$  as an inexpensive silane source, three substrates: **g**) carboxylic esters, **h**) carboxylic acids and **i**) carboxamides can be chemospecifically reduced leading directly to the corresponding protected aldehydes, namely acetals, and amines, in moderate to good yields by reaction at room temperature, under UV-LED irradiation ( $\lambda = 395\text{-}400\text{ nm}$ ). Functional groups, such as halides, amino, furyl, thienyl, pyridyl and internal  $\text{C}=\text{C}$  double bond, can be well tolerated.

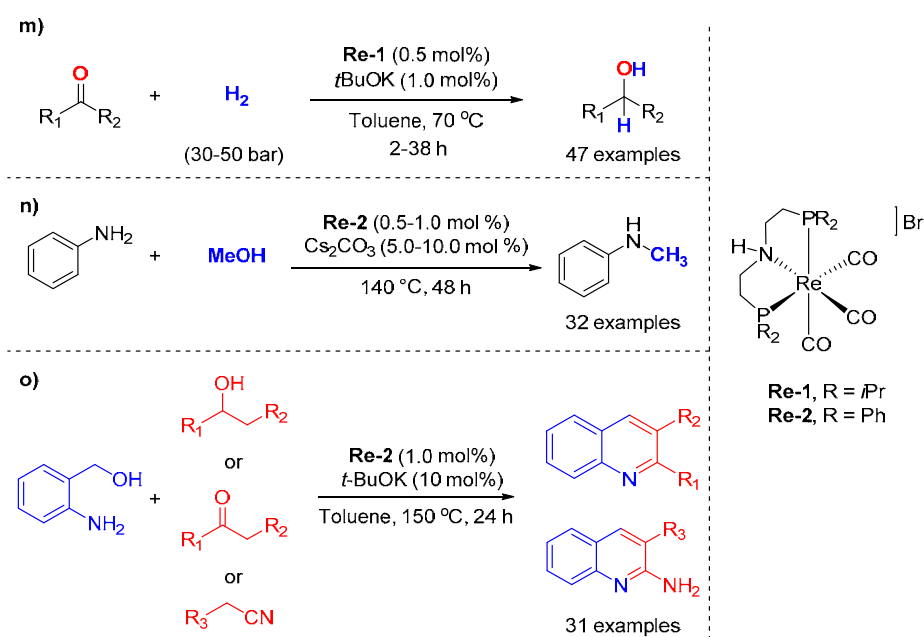


Besides hydrosilylation, we also explored the application of a series of well-defined manganese pre-catalysts featuring readily available bidendate pyridinyl-phosphine and 2-picolyamine ligands in hydrogenation type reactions, namely **j**) hydrogenation of carbonyl derivatives, **k**) reductive amination of aldehydes with molecular hydrogen and **l**) transfer hydrogenation of aldimines in the presence of *i*PrOH. Those bidendate Mn complexes exhibited good catalytic performances under mild conditions with low catalyst loading and good functional group tolerance. Those protocols enlarged the scope of reactions catalyzed by manganese,

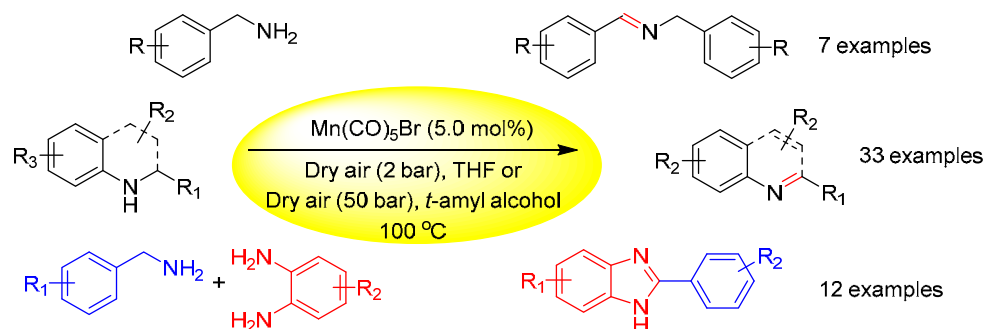
highlighting the rising potential of this non noble and Earth abundant transition metal in homogeneous catalysis.



In line with our interest in developing group 7 metals based catalysts, we have demonstrated that a series of new well-defined rhenium catalysts coordinated to amino-bisphosphino ligands can efficiently promote the **m)** hydrogenation of carbonyl derivatives, **n)** mono *N*-methylation of anilines with methanol, and **o)** synthesis of quinoline derivatives through acceptorless dehydrogenative coupling reaction with low catalyst loading and general substrate scope.



On the other hand, efforts were also devoted to develop the Mn-catalyzed ligand- and additive-free aerobic oxidation of amines to prepare aldimines, *N*-heteroaromatics and benzoimidazole derivatives. The catalytic process displayed a high tolerance towards a large variety of functional groups.



To conclude, catalysts based on inexpensive and abundant transition metals such as iron and manganese, as well as its related Group 7 rhenium can be efficiently applied in (de)hydrogenation and hydroelementation reactions, including:

- 1) dehydrogenative borylation of styrenes and terminal alkynes;
- 2) reductive amination reactions with hydrosilanes, hydrosilylation of carboxylic acids, esters and amides;
- 3) hydrogenation of carbonyl derivatives, transfer hydrogenation of aldimines, reductive amination of aldehydes with  $\text{H}_2$ ;
- 4) synthesis of mono *N*-methylated anilines with methanol *via* hydrogen borrowing reactions, and substituted quinolines, as well as
- 5) aerobic oxidation of amines to prepare aldimines, *N*-heteroaromatics under ligand- and additive-free conditions.

From a sustainable development point of view, the results summarized in this thesis clearly reveal that an accurate design of the catalytic system is crucial to perform highly chemoselective and efficient transformations. The initial achievements should stimulate the utilization of these methodologies in large-scale synthesis and fine chemistry.

In terms of catalytic reactions, several challenging transformations still have to be developed in years to come: **i)** the use of carbon dioxide as a C1 building block for catalytic methylation reactions and the efficient formation of formic acid, methanol and methane **ii)** the development of highly efficient and general asymmetric reduction of  $\text{C}=\text{C}$  and  $\text{C}=\text{O}$  moieties.

## Annex

### List of publications

- [1] **“Rhenium-Catalyzed Reduction of Carboxylic Acids with Hydrosilanes”**.  
D. Wei, R. Buhaibeh, Y. Canac, J.-B. Sortais, *Org. Lett.* **2019**, in press, doi: 10.1021/acs.orglett.9b02449.
- [2] **“Synthesis of Quinolines Through Acceptorless Dehydrogenative Coupling Catalyzed by Rhenium PN(H)P Complexes”**.  
D. Wei, V. Dorcet, C. Darcel, J.-B. Sortais, *ChemSusChem* **2019**, 12, 3078-3082.
- [3] **“Iron-Catalyzed Reductive Amination of Carbonyl Derivatives with  $\omega$ -Amino Fatty Acids to Access Cyclic Amines”**.  
D. Wei, C. Netkaew, V. Carré, C. Darcel, *ChemSusChem* **2019**, 12, 3008-3012.
- [4] **“Iron Catalysis in Reduction and Hydrometalation Reactions”**.  
D. Wei, C. Darcel, *Chem. Rev.* **2019**, 119, 2550-2610.
- [5] **“Iron-Catalyzed Switchable Synthesis of Pyrrolidines vs Pyrrolidinones by Reductive Amination of Levulinic Acid Derivatives via Hydrosilylation”**.  
D. Wei, C. Netkaew, C. Darcel, *Adv. Synth. Catal.* **2019**, 361, 1781-1786.
- [6] **“Manganese-Catalyzed Transfer Hydrogenation of Aldimines”**.  
D. Wei,<sup>+</sup> A. Bruneau-Voisine,<sup>+</sup> M. Dubois, S. Bastin, J.-B. Sortais, *ChemCatChem* **2019**, in press, doi: 10.1002/cctc.201900314. <sup>+</sup>equal contributions
- [7] **“Multi-Step Reactions Involving Iron-Catalyzed Reduction and Hydrogen Borrowing Reactions”**.  
D. Wei, C. Netkaew, C. Darcel, *Eur. J. Inorg. Chem.* **2019**, 20, 2471-2487.
- [8] **“Selective Mono *N*-Methylation of Anilines with Methanol Catalyzed by Rhenium Complexes: An Experimental and Theoretical Study”**.  
D. Wei, O. Sadek, V. Dorcet, T. Roisnel, C. Darcel, E. Gras, E. Clot, J.-B. Sortais, *J. Catal.* **2018**, 366, 300-309.
- [9] **“Manganese Catalyzed Reductive Amination of Aldehydes using Hydrogen as a Reductant”**.  
D. Wei, A. Bruneau-Voisine, D. A. Valyaev, N. Lugan, J.-B. Sortais, *Chem. Commun.* **2018**, 54, 4302-4305.
- [10] **“Iron-Catalyzed Dehydrogenative Borylation of Terminal Alkynes”**.  
D. Wei, B. Carboni, J.-B. Sortais, C. Darcel, *Adv. Synth. Catal.* **2018**, 360, 3649-3654.
- [11] **“Hydrogenation of Carbonyl Derivatives Catalyzed by Manganese Complexes Bearing Bidentate Pyridinyl-Phosphine Ligands”**.  
D. Wei, A. Bruneau-Voisine, T. Chauvin, V. Dorcet, T. Roisnel, D. A. Valyaev, N. Lugan, J.-B. Sortais, *Adv. Synth. Catal.* **2018**, 360, 676-681.
- [12] **“Hydrogenation of Carbonyl Derivatives with a Well-defined Rhenium Precatalyst”**.  
D. Wei, T. Roisnel, C. Darcel, E. Clot, J.-B. Sortais, *ChemCatChem* **2017**, 9, 80-83.
- [13] **“Rhenium and Manganese Complexes Bearing Amino-Bis(phosphinite) Ligands: Synthesis, Characterization, and Catalytic Activity in Hydrogenation of Ketones”**.  
H. Li, D. Wei, A. Bruneau-Voisine, M. Ducamp, M. Henrion, T. Roisnel, V. Dorcet, C. Darcel, J.-F. Carpentier, J.-F. Soulé, J.-B. Sortais, *Organometallics* **2018**, 37, 1271-1279.

**Titre : Réactions de (Dé)Hydrogénation et d'Hydroélémentation Catalysées par le Fer, le Manganèse et le Rhénium**

**Mots clés :** Catalyse; Fer; Manganèse; Rhénium; (Dé)Hydrogénation; Hydroélémentation

**Résumé :** L'objectif de ce travail doctoral a été de développer de nouvelles méthodes éco-compatibles pour réaliser efficacement des réactions de (dé)hydrogénation et d'hydroélémentation catalysées par des catalyseurs bien définis de fer, de manganèse et également de rhénium.

La première partie de ce travail porte sur le développement des premiers exemples de réaction de borylation de dérivés styrènes et acétyléniques terminaux avec le pinacolborane *via* une réaction d'activation de liaison C-H catalysée par des systèmes à base de  $\text{Fe}(\text{PMe}_3)_4$  ou de  $\text{Fe}(\text{OTf})_2/\text{DABCO}$ .

Dans une seconde partie, des complexes de fer à base de ligands carbènes *N*-hétérocycliques (NHC) tels que  $\text{Fe}(\text{CO})_4(\text{IMes})$  et  $[\text{CpFe}(\text{CO})_2(\text{IMes})][\text{I}]$  ont été efficacement utilisés pour la synthèse d'une grande variété d'amines cycliques (pyrrolidines, pipéridines et azépanes) *via* une réaction d'amination réductrice catalytique en présence d'hydrosilanes. De façon très intéressante, les catalyseurs commerciaux  $\text{Mn}_2(\text{CO})_{10}$  et  $\text{Re}_2(\text{CO})_{10}$  en présence de triéthylsilane, ont permis de réduire sélectivement les esters, acides carboxyliques et amides en acétals, alcools et amines

correspondants.

En complément de l'hydrosilylation, l'hydrogénation d'aldéhydes, cétones et aldimines a pu être efficacement menée grâce à l'utilisation de nouveaux précatalyseurs bien définis de manganèse à base de ligands bidentes facilement accessibles tels que la pyridinyl-phosphine et la 2-picolylamine.

Dans la continuité de notre intérêt pour le développement de nouveaux catalyseurs à base de métaux du groupe 7, une série de complexes de rhénium coordonnés à des ligands amino-bisphosphino a montré une excellente aptitude à promouvoir l'hydrogénation de composés carbonylés (aldéhydes, cétones), la mono-méthylation sélective d'amines avec le méthanol comme agent de méthylant durable et la synthèse quinolines substituées.

La dernière partie de ce travail décrit le développement d'oxydations aérobies d'amines pour préparer des aldimines, des composés *N*-hétéroaromatiques et des dérivés de type benzoimidazole *via* une catalyse au manganèse en l'absence de ligands ou d'additifs.

**Title : Iron, Manganese and Rhenium-Catalyzed (De)Hydrogenation and Hydroelementation Reactions**

**Keywords :** Catalysis; Iron; Manganese; Rhenium; (De)Hydrogenation; Hydroelementation

**Abstract :** This research work is aimed at developing advanced eco-friendly methodologies in the area of iron, manganese and rhenium-catalyzed (de)hydrogenation and hydroelementation reactions. Initially, we reported the first examples of highly selective catalytic direct C-H borylation of styrene derivatives and terminal alkynes with pinacolborane using  $\text{Fe}(\text{PMe}_3)_4$  and  $\text{Fe}(\text{OTf})_2/\text{DABCO}$  as catalyst systems, respectively.

Afterwards, *N*-heterocyclic carbene (NHC) based iron complexes  $\text{Fe}(\text{CO})_4(\text{IMes})$  and  $[\text{CpFe}(\text{CO})_2(\text{IMes})][\text{I}]$  were efficiently employed in the catalytic reductive amination reactions with hydrosilanes to access a large variety of cyclic amines (pyrrolidines, piperidines and azepanes). Interestingly, with the commercially available  $\text{Mn}_2(\text{CO})_{10}$  or  $\text{Re}_2(\text{CO})_{10}$  as catalyst and  $\text{Et}_3\text{SiH}$  as an inexpensive hydrosilane source, carboxylic esters, acids and amides can be chemospecifically reduced to the corresponding

acetals, alcohols and amines.

Besides hydrosilylation, we also explored the application of a series of well-defined manganese pre-catalysts featuring readily available bidentate pyridinyl-phosphine and 2-picolylamine ligands in hydrogenation reactions of aldehydes, ketones and aldimines.

In line with our interest in developing group 7 metals based catalysts, we have also demonstrated that a series of amino-bisphosphino ligands coordinated rhenium catalysts can efficiently promote the hydrogenation of carbonyl derivatives, the mono *N*-methylation of anilines with methanol and the dehydrogenative synthesis of substituted quinolines.

Lastly we also developed the Mn-catalysed ligand- and additive-free aerobic oxidation of amines to prepare aldimines, *N*-heteroaromatics and benzoimidazole derivatives.